

VOL. **609** NOS. **1 + 2** SEPTEMBER 18, 1992

COMPLETE IN ONE ISSUE

JOURNAL OF

CHROMATOGRAPHY

INCLUDING ELECTROPHORESIS AND OTHER SEPARATION METHODS

EDITORS

U. A. Th. Brinkman (Amsterdam)
 R. W. Giese (Boston, MA)
 J. K. Haken (Kensington, N.S.W.)
 K. Macek (Prague)
 L. R. Snyder (Orinda, CA)

EDITORS, SYMPOSIUM VOLUMES,

E. Heftmann (Orinda, CA), Z. Deyl (Prague)

EDITORIAL BOARD

D. W. Armstrong (Rolla, MO)
 W. A. Aue (Halifax)
 P. Boček (Brno)
 A. A. Boulton (Saskatoon)
 P. W. Carr (Minneapolis, MN)
 N. H. C. Cooke (San Ramon, CA)
 V. A. Davankov (Moscow)
 Z. Deyl (Prague)
 S. Dilli (Kensington, N.S.W.)
 F. Erni (Basle)
 M. B. Evans (Hatfield)
 J. L. Glajch (N. Billerica, MA)
 G. A. Guiochon (Knoxville, TN)
 P. R. Haddad (Hobart, Tasmania)
 I. M. Hais (Hradec Králové)
 W. S. Hancock (San Francisco, CA)
 S. Hjertén (Uppsala)
 S. Honda (Higashi-Osaka)
 Cs. Horváth (New Haven, CT)
 J. F. K. Huber (Vienna)
 K.-P. Hupe (Waldbronn)
 T. W. Hutchens (Houston, TX)
 J. Janák (Brno)
 P. Jandera (Pardubice)
 B. L. Karger (Boston, MA)
 J. J. Kirkland (Newport, DE)
 E. sz. Kováts (Lausanne)
 A. J. P. Martin (Cambridge)
 L. W. McLaughlin (Chestnut Hill, MA)
 E. D. Morgan (Keele)
 J. D. Pearson (Kalamazoo, MI)
 H. Poppe (Amsterdam)
 F. E. Regnier (West Lafayette, IN)
 P. G. Righetti (Milan)
 P. Schoenmakers (Eindhoven)
 R. Schwarzenbach (Dübendorf)
 R. E. Shoup (West Lafayette, IN)
 R. P. Singhal (Wichita, KS)
 A. M. Siouffi (Marseille)
 Ö. J. Strydom (Boston, MA)
 N. Tanaka (Kyoto)
 S. Terabe (Hyogo)
 K. K. Unger (Mainz)
 R. Verpoorte (Leiden)
 Gy. Vigh (College Station, TX)
 J. T. Watson (East Lansing, MI)
 B. D. Westerlund (Uppsala)

EDITORS, BIBLIOGRAPHY SECTION

Z. Deyl (Prague), J. Janák (Brno), V. Schwarz (Prague)

ELSEVIER

JOURNAL OF CHROMATOGRAPHY

INCLUDING ELECTROPHORESIS AND OTHER SEPARATION METHODS

Scope. The *Journal of Chromatography* publishes papers on all aspects of **chromatography, electrophoresis** and related methods. Contributions consist mainly of research papers dealing with chromatographic theory, instrumental developments and their applications. The section *Biomedical Applications*, which is under separate editorship, deals with the following aspects: developments in and applications of chromatographic and electrophoretic techniques related to clinical diagnosis or alterations during medical treatment; screening and profiling of body fluids or tissues related to the analysis of active substances and to metabolic disorders; drug level monitoring and pharmacokinetic studies; clinical toxicology; forensic medicine; veterinary medicine; occupational medicine; results from basic medical research with direct consequences in clinical practice. In *Symposium volumes*, which are under separate editorship, proceedings of symposia on chromatography, electrophoresis and related methods are published.

Submission of Papers. The preferred medium of submission is on disk with accompanying manuscript (see *Electronic manuscripts* in the Instructions to Authors, which can be obtained from the publisher, Elsevier Science Publishers B.V., P.O. Box 330, 1000 AH Amsterdam, Netherlands). Manuscripts (in English; *four* copies are required) should be submitted to: Editorial Office of *Journal of Chromatography*, P.O. Box 681, 1000 AR Amsterdam, Netherlands, Telefax (+31-20) 5862 304, or to: The Editor of *Journal of Chromatography, Biomedical Applications*, P.O. Box 681, 1000 AR Amsterdam, Netherlands. Review articles are invited or proposed in writing to the Editors who welcome suggestions for subjects. An outline of the proposed review should first be forwarded to the Editors for preliminary discussion prior to preparation. Submission of an article is understood to imply that the article is original and unpublished and is not being considered for publication elsewhere. For copyright regulations, see below.

Publication. The *Journal of Chromatography* (incl. *Biomedical Applications*) has 39 volumes in 1992. The subscription prices for 1992 are:

J. Chromatogr. (incl. *Cum. Indexes, Vols. 551-600*) + *Biomed. Appl.* (Vols. 573-611):

Dfl. 7722.00 plus Dfl. 1209.00 (p.p.h.) (total ca. US\$ 5380.00)

J. Chromatogr. (incl. *Cum. Indexes, Vols. 551-600*) only (Vols. 585-611):

Dfl. 6210.00 plus Dfl. 837.00 (p.p.h.) (total ca. US\$ 4245.25)

Biomed. Appl. only (Vols. 573-584):

Dfl. 2760.00 plus Dfl. 372.00 (p.p.h.) (total ca. US\$ 1886.75)

Subscription Orders. The Dutch guilder price is definitive. The US\$ price is subject to exchange-rate fluctuations and is given as a guide. Subscriptions are accepted on a prepaid basis only, unless different terms have been previously agreed upon. Subscriptions orders can be entered only by calendar year (Jan.-Dec.) and should be sent to Elsevier Science Publishers, Journal Department, P.O. Box 211, 1000 AE Amsterdam, Netherlands, Tel. (+31-20) 5803 642, Telefax (+31-20) 5803 598, or to your usual subscription agent. Postage and handling charges include surface delivery except to the following countries where air delivery via SAL (Surface Air Lift) mail is ensured: Argentina, Australia, Brazil, Canada, China, Hong Kong, India, Israel, Japan*, Malaysia, Mexico, New Zealand, Pakistan, Singapore, South Africa, South Korea, Taiwan, Thailand, USA. *For Japan air delivery (SAL) requires 25% additional charge of the normal postage and handling charge. For all other countries airmail rates are available upon request. Claims for missing issues must be made within three months of our publication (mailing) date, otherwise such claims cannot be honoured free of charge. Back volumes of the *Journal of Chromatography* (Vols. 1-572) are available at Dfl. 217.00 (plus postage). Customers in the USA and Canada wishing information on this and other Elsevier journals, please contact Journal Information Center, Elsevier Science Publishing Co. Inc., 655 Avenue of the Americas, New York, NY 10010, USA, Tel. (+1-212) 633 3750, Telefax (+1-212) 633 3990.

Abstracts/Contents Lists published in Analytical Abstracts, Biochemical Abstracts, Biological Abstracts, Chemical Abstracts, Chemical Titles, Chromatography Abstracts, Clinical Chemistry Lookout, Current Contents/Life Sciences, Current Contents/Physical, Chemical & Earth Sciences, Deep-Sea Research/Part B: Oceanographic Literature Review, Excerpta Medica, Index Medicus, Mass Spectrometry Bulletin, PASCAL-CNRS, Pharmaceutical Abstracts, Referativnyi Zhurnal, Research Alert, Science Citation Index and Trends in Biotechnology.

US Mailing Notice. *Journal of Chromatography* (main section ISSN 0021-9673, *Biomedical Applications* section ISSN 0378-4347) is published (78 issues/year) by Elsevier Science Publishers (Sara Burgerhartstraat 25, P.O. Box 211, 1000 AE Amsterdam, Netherlands). Annual subscription price in the USA US\$ 5380.00 (subject to change), including air speed delivery. Application to mail at second class postage rate is pending at Jamaica, NY 11431. **USA POSTMASTERS:** Send address changes to *Journal of Chromatography*, Publications Expediting, Inc., 200 Meacham Avenue, Elmont, NY 11003. Airfreight and mailing in the USA by Publication Expediting.

See inside back cover for Publication Schedule, Information for Authors and information on Advertisements.

© 1992 ELSEVIER SCIENCE PUBLISHERS B.V. All rights reserved.

0021-9673/92/\$05.00

No part of this publication may be reproduced, stored in a retrieval system or transmitted in any form or by any means, electronic, mechanical, photocopying, recording or otherwise, without the prior written permission of the publisher, Elsevier Science Publishers B.V., Copyright and Permissions Department, P.O. Box 521, 1000 AM Amsterdam, Netherlands.

Upon acceptance of an article by the journal, the author(s) will be asked to transfer copyright of the article to the publisher. The transfer will ensure the widest possible dissemination of information.

Special regulations for readers in the USA. This journal has been registered with the Copyright Clearance Center, Inc. Consent is given for copying of articles for personal or internal use, or for the personal use of specific clients. This consent is given on the condition that the copier pays through the Center the per-copy fee stated in the code on the first page of each article for copying beyond that permitted by Sections 107 or 108 of the US Copyright Law. The appropriate fee should be forwarded with a copy of the first page of the article to the Copyright Clearance Center, Inc., 27 Congress Street, Salem, MA 01970, USA. If no code appears in an article, the author has not given broad consent to copy and permission to copy must be obtained directly from the author. All articles published prior to 1980 may be copied for a per-copy fee of US\$ 2.25, also payable through the Center. This consent does not extend to other kinds of copying, such as for general distribution, resale, advertising and promotion purposes, or for creating new collective works. Special written permission must be obtained from the publisher for such copying.

No responsibility is assumed by the Publisher for any injury and/or damage to persons or property as a matter of products liability, negligence or otherwise, or from any use or operation of any methods, products, instructions or ideas contained in the materials herein. Because of rapid advances in the medical sciences, the Publisher recommends that independent verification of diagnoses and drug dosages should be made.

Although all advertising material is expected to conform to ethical (medical) standards, inclusion in this publication does not constitute a guarantee or endorsement of the quality or value of such product or of the claims made of it by its manufacturer.

This issue is printed on acid-free paper.

Printed in the Netherlands

CONTENTS

(Abstracts/Contents Lists published in Analytical Abstracts, Biochemical Abstracts, Biological Abstracts, Chemical Abstracts, Chemical Titles, Chromatography Abstracts, Current Awareness In Biological Sciences (CABS), Current Contents/Life Sciences, Current Contents/Physical, Chemical & Earth Sciences, Deep-Sea Research/Part B: Oceanographic Literature Review, Excerpta Medica, Index Medicus, Mass Spectrometry Bulletin, PASCAL-CNRS, Referativnyi Zhurnal, Research Alert and Science Citation Index)

REVIEW

Chiral separation by analytical electromigration methods

by J. Snopek (Prague, Czechoslovakia), I. Jelínek (Bloomington, IN, USA) and E. Smolková-Keulemansová (Prague, Czechoslovakia) (Received March 18th, 1992) 1

REGULAR PAPERS

Column Liquid Chromatography

Shock layer thickness in the case of wide bands of single components and binary mixtures in non-linear liquid chromatography
by Z. Ma and G. Guiochon (Knoxville and Oak Ridge, TN, USA) (Received May 21st, 1992) 19

Optimization of the experimental conditions and the column design parameters in displacement chromatography
by A. Felinger and G. Guiochon (Knoxville and Oak Ridge, TN, USA) (Received May 14th, 1992) 35

Application of non-porous silica ultramicrospheres to high-performance liquid chromatographic column packings
by F. Honda, H. Honda and M. Koishi (Hokkaido, Japan) (Received April 29th, 1992) 49

Short fibrous supports for preparative chromatographic separations of biomolecules
by J.-K. King and N. G. Pinto (Cincinnati, OH, USA) (Received June 1st, 1992) 61

Mechanism of retention of benzodiazepines in affinity, reversed-phase and adsorption high-performance liquid chromatography
in view of quantitative structure-retention relationships
by R. Kaliszan, A. Kaliszan and T. A. G. Noctor (Montreal, Canada), W. P. Purcell (Memphis, TN, USA) and I. W. Wainer (Montreal, Canada) (Received June 2nd, 1992) 69

Gel chromatographic evaluation of the binding constant for the interaction of thiamin diphosphate with magnesium ion
by C. K. Booth, P. F. Nixon and D. J. Winzor (Brisbane, Australia) (Received May 27th, 1992) 83

Progress in the design of selectors for buckminsterfullerene
by C. J. Welch and W. H. Pirkle (Urbana, IL, USA) (Received June 16th, 1992) 89

9-Fluoreneacetyl-tagged, solid-phase reagent for derivatization in direct plasma injection
by F.-X. Zhou and I. S. Krull (Boston, MA, USA) and B. Feibush (Bellefonte, PA, USA) (Received May 13th, 1992) 103

Liquid chromatography-electrochemistry procedure for the determination of chlorophenolic compounds in pulp mill effluents
and receiving waters
by E. C. V. Butler and G. Dal Pont (Hobart, Australia) (Received April 13th, 1992) 113

High-performance liquid chromatography of oligosaccharide alditols and glycopeptides on a graphitized carbon column
by M. Davies, K. D. Smith, A.-M. Harbin and E. F. Hounsell (Harrow, UK) (Received June 12th, 1992) 125

Silver ion high-performance liquid chromatography of derivatives of isomeric fatty acids
by B. Nikolova-Damyanova (Ayr, UK), B. G. Herslof (Stockholm, Sweden) and W. W. Christie (Ayr, UK) (Received
April 21st, 1992) 133

Rapid method for the determination of glutathione transferase isoenzymes in crude extracts
by E. Martínez-Lara, P. Pascual, F. Toribio, J. López-Barea and J. A. Bárcena (Córdoba, Spain) (Received June 9th,
1992) 141

Separation of dideoxyribonucleosides in trace amounts by automated liquid chromatography and capillary electrophoresis
by R. P. Singhal, D. Hughbanks and J. Xian (Wichita, KS, USA) (Received May 5th, 1992) 147

Chiral high-performance liquid chromatographic separation of vinca alkaloid analogues on α_1 -acid glycoprotein and human
serum albumin columns
by I. Fitos, J. Visy and M. Simonyi (Budapest, Hungary) and J. Hermansson (Norsborg, Sweden) (Received May 7th,
1992) 163

(Continued overleaf)

Contents (continued)

Enhancement of detection sensitivity and cleanup selectivity for tobramycin through pre-column derivatization by F. Lai and T. Sheehan (Walnut Creek, CA, USA) (Received June 9th, 1992)	173
Column liquid chromatography and microbiological assay compared for determination of cefadroxil preparations by M.-C. Hsu, Y.-W. Chang and Y.-T. Lee (Taipei, Taiwan) (Received May 18th, 1992)	181
Chiral separation of nipecotic acid amides by Z. Feng, R. Gollamudi and G. Han (Memphis, TN, USA) and Y. Tang and D. W. Armstrong (Rolla, MO, USA) (Received May 14th, 1992)	187
Normal-phase high-performance liquid chromatography with UV irradiation, morin complexation and fluorescence detection for the determination of organotin pesticides by J. A. Stäb, M. J. M. Rozing, B. van Hattum, W. P. Cofino and U. A. Th. Brinkman (Amsterdam, Netherlands) (Received June 1st, 1992)	195
Determination of <i>Penicillium roqueforti</i> toxin by reversed-phase high-performance liquid chromatography by K. Siemens and J. Zawistowski (Winnipeg, Canada) (Received April 24th, 1992)	205
Automated analyses of non-ionic surfactants in terms of hydrophobic and polyoxyethylated chain lengths by T. Okada (Shizuoka, Japan) (Received May 13th, 1992)	213
Erythrocyte partitioning in dextran-poly(ethylene glycol) aqueous phase systems. Events in phase and cell separation by H. Walter (Long Beach, CA, USA) and F. D. Raymond and D. Fisher (London, UK) (Received May 26th, 1992)	219
<i>Gas Chromatography</i>	
Pair-wise interactions by gas chromatography. I. Interaction free enthalpies of solutes with non-associated primary alcohol groups by K. S. Reddy, J.-Cl. Dutoit and E. sz. Kováts (Lausanne, Switzerland) (Received March 11th, 1992)	229
Factor analysis and experimental design in high-performance liquid chromatography. XIII. Correspondence factor analysis of the heterogeneity of the behaviour of congeneric solutes series studied on homogeneous OV phases in gas chromatography by J. R. Chrétien (Orléans and Paris, France), M. Righezza (Orléans, France) and A. Hassani and B. Y. Meklati (Algiers, Algeria) (Received March 13th, 1992)	261
Liquid jet evolution from a gas chromatographic injector by J. Qian, C.E. Polymeropoulos and R. Ulisse (Piscataway, NJ, USA) (Received March 6th, 1992)	269
Investigation of a scyllitol-derived (saturated) disc-shaped liquid crystal stationary phase in capillary gas chromatography by A. Kraus, U. Schumann and G. Kraus (Halle/Saale, Germany) and B. Kohne and K. Praefcke (Berlin, Germany) (Received April 23rd, 1992)	277
Separation and identification of all isomeric <i>n</i> -nonadecenes by capillary gas chromatography on a mesogenic stationary phase with Fourier transform infrared and mass spectrometric detection by L. Šoják, I. Ostrovský and R. Kubišec (Bratislava, Czechoslovakia) and G. Kraus and A. Kraus (Halle/Saale, Germany) (Received February 24th, 1992)	283
Gas chromatographic identification of halogenated hydrocarbons by using the correlation between their retention and boiling points by T. C. Gerbino, G. Castello and G. D'Amato (Genova, Italy) (Received May 18th, 1992)	289
Determination of trace amounts of carboxylic acids in ambient air by capillary gas chromatography-mass spectrometry by S. Sollinger, K. Levsen and M. Emmrich (Hannover, Germany) (Received April 23rd, 1992)	297
Determination of sulphurated compounds in <i>Tagetes patula</i> cv. <i>nana</i> essential oil by gas chromatography with mass spectro- metric, Fourier transform infrared and atomic emission spectrometric detection by C. Bicchì, C. Frattini, G. Pellegrino and P. Rubiolo (Turin, Italy) and V. Raverdino and G. Tsoupras (Geneva, Switzerland) (Received May 5th, 1992)	305
Chromatographic analysis of <i>cis</i> - and <i>trans</i> -mevinphos in poisoned wildlife by W. J. Allender (Rydalmere, Australia) and J. Keegan (Broadway, Australia) (Received May 19th, 1992)	315
<i>Supercritical Fluid Chromatography</i>	
Comparison of methods to prevent restrictor plugging during off-line supercritical extraction by M. D. Burford, S. B. Hawthorne and D. J. Miller (Grand Forks, ND, USA) and T. Braggins (Hamilton, New Zealand) (Received May 26th, 1992)	321

Supercritical fluid extraction of nitrated polycyclic aromatic hydrocarbons and polycyclic aromatic hydrocarbons from diesel exhaust particulate matter by T. Paschke, S. B. Hawthorne and D. J. Miller (Grand Forks, ND, USA) and B. Wenclawiak (Siegen, Germany) (Received June 9th, 1992)	333
--	-----

Planar Chromatography

High-performance thin-layer chromatographic mobility of porphyrins and their copper complexes on different adsorbents by K. Saitoh, R. Kashiwa, R. Tada, C. Kiyohara and N. Suzuki (Miyagi, Japan) (Received April 23rd, 1992)	341
Identification and determination of mellein in cultures of the fungus <i>Septoria nodorum</i> (Berk.) by thin-layer and high-performance liquid chromatography by J. Sachse (Zurich, Switzerland) (Received May 19th, 1992)	349
Critical thin-layer chromatography as a novel method for the determination of the molecular weight and compositional inhomogeneity of block copolymers by B. G. Belenkii, E. S. Gankina, V. N. Zgonnik, I. I. Malchova and E. U. Melenevskaya (St. Petersburg, Russia) (Received March 5th, 1992)	355

Electrophoresis

Theoretical aspects of chiral separation in capillary electrophoresis. II. The role of organic solvent by S. A. C. Wren and R. C. Rowe (Macclesfield, UK) (Received June 15th, 1992)	363
Effect of addition of glucose on micellar electrokinetic capillary chromatography with sodium dodecyl sulphate by T. Kaneta, S. Tanaka, M. Taga and H. Yoshida (Sapporo, Japan) (Received April 28th, 1992)	369
Capillary electrophoretic analysis of oxindole alkaloids from <i>Uncaria tomentosa</i> by H. Stuppner, S. Sturm and G. Konwalinka (Innsbruck, Austria) (Received June 9th, 1992)	375
Determination of C ₈ -C ₂₀ saturated anionic and cationic surfactant mixtures by capillary isotachopheresis with conductivity detection by C. Tribet, R. Gaboriaud and P. Gareil (Paris, France) (Received April 22nd, 1992)	381

SHORT COMMUNICATIONS

Column Liquid Chromatography

Reversed-phase high-performance liquid chromatographic and derivative UV spectrometric determination of -phenylethylamine in phosphomycin by G. Gazzani, G. Stoppini and C. Gandini (Pavia, Italy) and A. Bettero (Milan, Italy) (Received May 12th, 1992)	391
High-performance liquid chromatographic method for the enantiomeric separation of the chiral metabolites of midazolam by J. Drewe and E. Küsters (Basle, Switzerland) (Received June 19th, 1992)	395
Determination of folic acid in an elemental diet by high-performance liquid chromatography with UV detection by H. Iwase (Kawasaki, Japan) (Received June 3rd, 1992)	399
Isolation and identification via high-performance liquid chromatography and thin-layer chromatography of benzoxazolinone precursors from <i>Consolida orientalis</i> flowers by S. Özden, T. Özden, I. Attila, M. Küçükislamoglu and A. Okatan (Söğütlü/Trabzon, Turkey) (Received June 30th, 1992)	402
Application of two rapid techniques of column chromatography to separate the pungent principles of ginger, <i>Zingiber officinale</i> Roscoe by R. Zarate, Sukrasno and M. M. Yeoman (Edinburgh, UK) (Received June 1st, 1992)	407

Gas Chromatography

Gas chromatographic separation of polycyclic aromatic hydrocarbons on a mesomorphic copolysiloxane stationary phase by H. Wang, T. Gen, R. Fu, J. Zhu, X. Wei, H. Li and J. Liu (Beijing, China) (Received May 26th, 1992)	414
---	-----

Planar Chromatography

Thin-layer chromatography on polyacrylonitrile. V. Consideration of separation mechanisms of some aliphatic and aromatic amines by T. J. Janjić, D. M. Milojković, A. Broćović, Ž. J. Arbutina and M. B. Čelap (Belgrade, Yugoslavia) (Received June 11th, 1992)	419
---	-----

(Continued overleaf)

Contents (continued)

Determination of hypericin and pseudohypericin by thin-layer chromatography-densitometry by Th. Kartnig and I. Göbel (Graz, Austria) (Received June 26th, 1992)	423
Salting-out thin-layer chromatography of transition metal complexes. I. Investigation of the behaviour of mixed aminocarboxylato cobalt(III) complexes in silica gel by G. Vučković, D. Miljević, T. J. Janjić and M. B. Čelap (Belgrade, Yugoslavia) (Received July 1st, 1992)	427
BOOK REVIEW:	
High-performance liquid chromatography (by S. Lindsay), reviewed by V. R. Meyer (Berne, Switzerland)	432
AUTHOR INDEX	433
ERRATA	436
INSTRUCTIONS TO AUTHORS	437

JOURNAL OF CHROMATOGRAPHY

VOL. 609 (1992)

JOURNAL of CHROMATOGRAPHY

INCLUDING ELECTROPHORESIS AND OTHER SEPARATION METHODS

EDITORS

U. A. Th. BRINKMAN (Amsterdam), R. W. GIESE (Boston, MA), J. K. HAKEN (Kensington, N.S.W.), K. MACEK (Prague),
L. R. SNYDER (Orinda, CA)

EDITORS, SYMPOSIUM VOLUMES

E. HEFTMANN (Orinda, CA), Z. DEYL (Prague)

EDITORIAL BOARD

D. W. Armstrong (Rolla, MO), W. A. Aue (Halifax), P. Boček (Brno), A. A. Boulton (Saskatoon), P. W. Carr (Minneapolis, MN),
N. H. C. Cooke (San Ramon, CA), V. A. Davankov (Moscow), Z. Deyl (Prague), S. Dilli (Kensington, N.S.W.), F. Erni (Basle), M.
B. Evans (Hatfield), J. L. Glajch (N. Billerica, MA), G. A. Guiochon (Knoxville, TN), P. R. Haddad (Hobart, Tasmania), I. M. Hais
(Hradec Králové), W. S. Hancock (San Francisco, CA), S. Hjertén (Uppsala), S. Honda (Higashi-Osaka), Cs. Horváth (New
Haven, CT), J. F. K. Huber (Vienna), K.-P. Hupe (Waldbronn), T. W. Hutchens (Houston, TX), J. Janák (Brno), P. Jandera
(Pardubice), B. L. Karger (Boston, MA), J. J. Kirkland (Newport, DE), E. sz. Kováts (Lausanne), A. J. P. Martin (Cambridge), L.
W. McLaughlin (Chestnut Hill, MA), E. D. Morgan (Keele), J. D. Pearson (Kalamazoo, MI), H. Poppe (Amsterdam), F. E. Regnier
(West Lafayette, IN), P. G. Righetti (Milan), P. Schoenmakers (Eindhoven), R. Schwarzenbach (Dübendorf), R. E. Shoup (West
Lafayette, IN), R. P. Singhal (Wichita, KS), A. M. Siouffi (Marseille), D. J. Strydom (Boston, MA), N. Tanaka (Kyoto), S. Terabe
(Hyogo), K. K. Unger (Mainz), R. Verpoorte (Leiden), Gy. Vigh (College Station, TX), J. T. Watson (East Lansing, MI), B. D.
Westerlund (Uppsala)

EDITORS, BIBLIOGRAPHY SECTION

Z. Deyl (Prague), J. Janák (Brno), V. Schwarz (Prague)



ELSEVIER

AMSTERDAM — LONDON — NEW YORK — TOKYO

J. Chromatogr., Vol. 609 (1992)

ห้องสมุดกรมวิทยาศาสตร์บริการ

© 1992 ELSEVIER SCIENCE PUBLISHERS B.V. All rights reserved.

0021-9673/92/\$05.00

No part of this publication may be reproduced, stored in a retrieval system or transmitted in any form or by any means, electronic, mechanical, photocopying, recording or otherwise, without the prior written permission of the publisher, Elsevier Science Publishers B.V., Copyright and Permissions Department, P.O. Box 521, 1000 AM Amsterdam, Netherlands.

Upon acceptance of an article by the journal, the author(s) will be asked to transfer copyright of the article to the publisher. The transfer will ensure the widest possible dissemination of information.

Special regulations for readers in the USA. This journal has been registered with the Copyright Clearance Center, Inc. Consent is given for copying of articles for personal or internal use, or for the personal use of specific clients. This consent is given on the condition that the copier pays through the Center the per-copy fee stated in the code on the first page of each article for copying beyond that permitted by Sections 107 or 108 of the US Copyright Law. The appropriate fee should be forwarded with a copy of the first page of the article to the Copyright Clearance Center, Inc., 27 Congress Street, Salem, MA 01970, USA. If no code appears in an article, the author has not given broad consent to copy and permission to copy must be obtained directly from the author. All articles published prior to 1980 may be copied for a per-copy fee of US\$ 2.25, also payable through the Center. This consent does not extend to other kinds of copying, such as for general distribution, resale, advertising and promotion purposes, or for creating new collective works. Special written permission must be obtained from the publisher for such copying.

No responsibility is assumed by the Publisher for any injury and/or damage to persons or property as a matter of products liability, negligence or otherwise, or from any use or operation of any methods, products, instructions or ideas contained in the materials herein. Because of rapid advances in the medical sciences, the Publisher recommends that independent verification of diagnoses and drug dosages should be made.

Although all advertising material is expected to conform to ethical (medical) standards, inclusion in this publication does not constitute a guarantee or endorsement of the quality or value of such product or of the claims made of it by its manufacturer.

This issue is printed on acid-free paper.

Printed in the Netherlands

Review

Chiral separation by analytical electromigration methods

Jiří Snopek

Institute of Biotechnology, Charles University, Viničná 5, CS-128 44 Prague 2 (Czechoslovakia)

Ivan Jelínek[☆]

Department of Chemistry, Indiana University, Bloomington, IN 47405 (USA)

Eva Smolková-Keulemansová

Department of Analytical Chemistry, Charles University, Albertov 2030, CS-128 43 Prague 2 (Czechoslovakia)

(First received January 22nd, 1992; revised manuscript received March 18th, 1992)

ABSTRACT

An overview of important trends in electrophoretic methods for the direct separation of optical isomers is presented. The fundamental characteristics of electromigration techniques, the phenomena of molecular chirality and approaches to chiral separations by electrophoretic methods are discussed. The advantages of these techniques are demonstrated with numerous practical examples of electrophoretic enantioseparations.

CONTENTS

1. Introduction	2
2. Chirality and approach to chiral separation	2
3. Basics of electrophoretic methods	3
4. General aspects of chiral separation in electromigration methods	6
5. Chiral ligand-exchange mechanism	6
6. Chiral micellar mechanism	8
7. Chiral inclusion mechanism	9
8. Protein-based enantioselection mechanism	14
9. Conclusions	14
10. Addendum	15
References	15

Correspondence to: Dr. J. Snopek, Institute of Biotechnology, Charles University, Viničná 5, 128 44 Prague 2, Czechoslovakia.

[☆] On leave from the Department of Analytical Chemistry, Charles University, Albertov 2030, CS-128 43 Prague 2, Czechoslovakia.

1. INTRODUCTION

During the last decade, high-performance capillary electromigration methods (EMM) have become a subject of considerable importance to modern separation science. While the displacement form of the electrophoretic process, the so-called isotachopheresis (ITP), has steadily grown in application since the significant investigations made by Everaerts and co-workers [1,2], the recent progress in capillary zone electrophoresis (CZE) has been nearly explosive. The major reasons for this situation are: (a) unprecedented separation performance by CZE at high voltages; (b) wide choice of quantitative detection techniques; (c) automation possibilities; (d) small sample capabilities; and (e) recent successful coupling of CZE with mass spectrometry.

While the pioneering studies of Hjerten [3] and Mikkers *et al.* [4] on CZE indirectly pointed at some of these analytical advantages, investigation by Jorgenson and Lukacs [5–8] established clearly its potential for biological compounds and laid the foundation for the further development of related capillary techniques (capillary gel electrophoresis, isoelectric focusing, electrochromatography, micellar electrokinetic chromatography, etc.). The high separation efficiency of CZE is a fairly direct consequence of the utilization of high voltages in narrow capillaries that facilitate effective heat dissipation [9,10]; this process is generally favoured for macromolecular ions with small diffusion coefficients. This does not necessarily facilitate the separation of molecular entities with minor differences in their chemical structures, such as various isomeric compounds. Especially the direct determination of the optical purity and separation of enantiomers has long been a challenge to chemists. Various gas and liquid chromatographic methods [11–17] have recently been utilized to resolve numerous enantiomeric mixtures, both on a large scale and analytically.

The importance of chirality in biological phenomena, chemical synthesis and the design of pharmaceutical agents will likely accelerate a further search for new and effective means to resolve enantiomeric mixtures. There are numerous indications in the recent literature that the modern electromigration methods will soon join the already powerful arsenal of chemical separation approaches to chirality. A

very promising approach is the application of various chiral selectors or pseudo-phases [18], which substantially extend the application of electrophoretic methods towards various types of chiral compounds.

The aim of this review is to cover the recent promising developments in the electrophoretic separation of optically active substances. After a brief introduction into the fundamentals of chiral resolution and the principles of electromigration, we shall concentrate on various mechanisms utilized for enantiomeric separation in an electric field. These will include chiral ligand-exchange mechanisms, uses of chiral micelles, inclusion complexes and protein-based enantioselectors. Finally, future directions in this field will be discussed.

2. CHIRALITY AND APPROACH TO CHIRAL SEPARATION

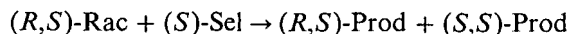
The symmetry arguments required for a proper understanding of molecular chirality go beyond the purely spatial aspects with which most chemists are familiar. The natural optical activity phenomena supported by chiral molecules are characterized by time-even pseudo-scalar observables such as optical rotation angle, rotation strength and Raman circular intensity difference. However, it is important to realize that optical activity is not necessarily the hallmark of chirality. True chirality is exhibited by systems that exist in two distinct enantiomeric states that are interconverted by space inversion, but not by time reversal combined with any proper spatial rotation. Space inversion is a more fundamental operation than the mirror reflection traditionally invoked but provides equivalent results. The second part of the definition is irrelevant for a stationary object. The above definition enables chirality to be distinguished from other types of dissymmetry [19–24]. It is possible to find the true enantiomer of a chiral object in the anti-world. The molecule with the opposite absolute configuration but composed of antiparticles will have exactly the same energy as the original [19,20,25]. This follows from the $\hat{C}\hat{P}\hat{T}$ theorem (\hat{C} = operator which interconverts particles and antiparticles; \hat{P} = parity operator which inverts the system through the origin of the space-fixed axes; and \hat{T} = time reversal operator, reversing the motion of all the particles in the system) and the

assumption that \hat{T} is not violated. So true enantiomers are interconverted by $\hat{C}\hat{P}$. It is intriguing to note that invariance under the combined operation of $\hat{C}\hat{P}\hat{T}$ is in fact the quantal and relativistic extension of \hat{T} invariance [26], which serves to emphasize the essential unity of space, time and matter.

A tiny energy difference exists between the enantiomers of a chiral molecule that both exist in our world. They are chiral, meaning that they possess “handedness”. The pair of enantiomers of a chiral substance react in a roughly equal manner, and are almost identical in their physical and chemical properties, such as melting points, heats of combustion and formation and reaction rates with achiral reagents in comparison with other types of isomers and/or structurally closely related compounds. Their behaviours, however, are significantly different in a chiral environment, being influenced, *e.g.*, by polarized light, optically active reagents and solvents or biological (enantiospecific) systems.

While it is feasible in principle to analyse the individual enantiomers spectroscopically in a mixture, their physical separation before a measurement is preferable in trace analysis. Such separations are due to a differential stereoselective interaction with a suitable chiral environment. Whether permanently induced by reaction with a chiral reagent or through a temporary complexation, such an association leads to preferential interactions of *R* or *S* antipodes

with the separation environment and their subsequent differentiation:



where Rac = a racemate separated, (*S*)-Sel = *S*-enantiomer of selector forming a chiral environment and Prod = products of interaction (= diastereoisomers).

Since optical isomers have a three-dimensional spatial character, at least three-point simultaneous interactions are generally needed between a chiral selector and an enantiomer (analyte) to cause physical separation. Further, at least one of these interactions must be stereochemically dependent. This “three-point” Dalglish rule [27] is illustrated in Fig. 1. The range of such simultaneous stereospecific interactions involved in enantiomeric separations is relatively broad, including (a) electrostatic interactions, (b) dipole–dipole and/or ion–dipole interactions, (c) inductive effects, (d) hydrogen bonding, (e) hydrophobic interactions and (f) Van der Waals interaction.

Advances in modern liquid chromatography (LC) during the last two decades have stimulated considerable progress in chiral separations. Sophisticated designs of chiral bonded phases [13,16,17] and addition of various chiral selectors to the liquid mobile phase [14] emphasize the importance of the “three-point rule”. The possibilities of chromatographing various racemic mixtures in the liquid phase are virtually unlimited, provided that the right combination of solute–solvent characteristics is found. However, certain adverse effects of a siliceous surface in LC (non-specific adsorption) still need additional work. While further developments in chiral LC separations will undoubtedly continue, electromigration methods, especially capillary high-performance techniques, provide additional opportunities for the separation of optical isomers.

3. BASICS OF ELECTROPHORETIC METHODS

Electrophoretic separation processes are generally based on the differential migration of electrically charged particles in an electric field. The transport of each component of a solution can be described by using the basic equation of transport phenomena, *i.e.*, the continuity equation [28] (eqn. 1). For a

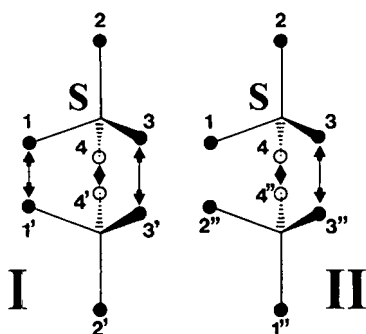


Fig. 1. The Dalglish model of three-point interaction for chiral recognition. S = Chiral selector; 1, 3 and 4 = selector's points of interaction; 1', 3', 4', 3'' and 4'' = chiral analyte's points of interaction; \leftrightarrow = interaction, I = faster interaction, II = weaker interaction (the distance $1 \leftrightarrow 1''$ is greater than $1 \leftrightarrow 1'$; point 1'' is sterically non-accessible for interaction with point 1).

substance particle with concentration c_z and charge z ,

$$\partial c_z / \partial t = -\text{div } J_z \quad (1)$$

where J_z is the substance (component) flow-rate, which is determined by

$$J_z = c_z v \quad (2)$$

where v is the vector of the rate of movement of a component at a given location in the solution, or

$$J = (J_z)_{\text{mig}} + (J_z)_{\text{dif}} + (J_z)_{\text{conv}} + (J_z)_{\text{therm}} \quad (3)$$

where the terms on the right-hand side represent for migration, diffusion, convection and thermal components of the substance flow, respectively.

The migration term of the substance flow characterizes the movement induced by an external force, the intensity of the electric field:

$$E = -\text{grad } \varphi \quad (4)$$

where φ is the electric potential, or, for one dimension ($x = L =$ length of separation environment),

$$E = V/L \quad (5)$$

where V is the voltage applied across the separation media. When the electric field acts on particles with charge z , the particles move with a velocity, $(v_e)_{\text{mig}}$, proportional to E :

$$(v_e)_{\text{mig}} = \mu_e E \quad (6)$$

where μ_e is the electrophoretic mobility.

The next fundamental process in capillary zone electrophoresis and some of its modifications is electroosmosis, the flow of solvent in an applied potential field. Under the influence of the field the spatial charge of the diffusive part of the electric double layer moves to the oppositely charged electrode, and a one-sided flow of ions originates near the wall. The whole solution then moves together with these ions. The linear velocity of the electroosmotic flow, v_{eo} , can be expressed as

$$v_{eo} = (\varepsilon/4 \pi \eta) E \zeta \quad (7)$$

where ζ is the zeta potential:

$$\zeta = (4 \pi \eta \mu_{eo} / \varepsilon) \quad (8)$$

η is viscosity, ε is the dielectric constant of the solution and μ_{eo} is the coefficient for electroosmotic flow [29].

In the presence of electroosmotic flow, the migration velocity from eqn. 6 can be rewritten as

$$(v)_{\text{mig}} = (\mu_e + \mu_{eo}) E \quad (9)$$

In zone electrophoresis, ionic species are resolved on the basis of differential electrophoretic migration. Similarly to classical chromatography, the selectivity can be related to the relative retention of two solutes (*e.g.*, enantiomers) and is defined as the resolution, R_s , between two peaks:

$$R_s = 2 \Delta t_R / (w_1 + w_2) \quad (10)$$

where Δt_R is the difference in migration times and w is the peak width at the peak base, usually determined by drawing tangent lines along the slopes of the peaks. It should be noted that R_s is a dimensionless quantity and that the Δt_R and w values should be expressed in the same units, *e.g.*, seconds or millimetres on a record trace.

The next possibility for the expression of the resolution of two zones in electrophoresis is given by

$$R = 0.25 N^{1/2} \Delta v / \bar{v} \quad (11)$$

where N is the average number of theoretical plates, Δv is the difference in zone velocities and \bar{v} is the average zone velocity [30], or

$$R = (1/4) 2^{1/2} (\mu_{e,1} - \mu_{e,2}) [V/D(\bar{\mu}_e + \mu_{eo})]^{1/2} \quad (12)$$

where $\mu_{e,1}$ and $\mu_{e,2}$ are the electrophoretic mobilities for the two solutes, *e.g.*, R and S enantiomers, $\bar{\mu}_e$ is the average electrophoretic mobility and D is the diffusion coefficient [5,8].

The modification of CZE which utilizes a quasi-stationary phase consisting of micelles is called (micellar) electrokinetic (capillary) chromatography (MECC or EKC) [31,32]. In this method a surfactant is added to the buffer solution above its critical

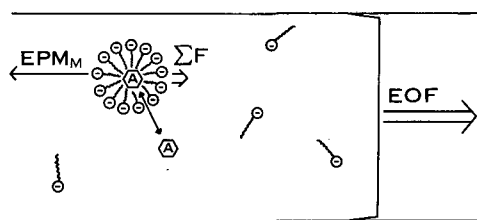


Fig. 2. Schematic representation of a system for EKC showing amphiphilic monomers, micelle and flow profile. A = Analyte; EPM_M = electrophoretic effective mobility of micelle; EOF = electroosmotic flow factor; $\Sigma F = (EOF) - (FPM_M)$.

micellar concentration, thereby affording an effective mechanism for the separation of both neutral and ionic substances. The separation of neutral solutes is based simply on their differential partitioning between the electroosmotically pumped aqueous mobile phase and the hydrophobic interior of the micelles which are charged and moving at a slower speed than the mobile phase owing to electrophoretic effects (see Fig. 2).

The fundamental equation to describe the resolution of a pair of neutral solutes in EKC is

$$R = \frac{\sqrt{N}}{4} \cdot \frac{\alpha - 1}{\alpha} \cdot \frac{k'_2}{k'_2 + 1} \cdot \frac{1 - t_0}{1 + \frac{t_0 k'_1}{t_m}} \quad (13)$$

where the selectivity factor and the capacity factor, α and k' , respectively, are given by

$$\alpha = k'_2/k'_1 \quad (14)$$

and

$$k' = (t_R - t_0) / t_0 (1 - t_R/t_m) \quad (15)$$

where t_R is the migration time of a solute that interacts with micelles, t_0 is the migration time of a solute that has no (or little) interaction with the micelles and t_m is the migration time of a solute that is totally solubilized by the micelles.

A major advantage of EKC over high-performance liquid chromatography (HPLC) is its separation efficiency. Whereas HPLC separations typically exhibit 5000-25 000 theoretical plates, EKC systems often generate efficiencies of 50 000-500 000 plates and higher. Fast, efficient separations are obtained in EKC because of three important phenomena [33]: (1) the flat flow profile of electroosmotic flow minimizes resistance to mass transfer in the mobile phase, (2) fused-silica capillaries dissipate heat efficiently, thereby minimizing thermal effects, and (3) micelles are dynamic structures, allowing for fast solute entrance/exit kinetics.

Charged solutes are not only distributed between the micellar and liquid phase but are also simultaneously separated electrophoretically according to their effective mobilities. The superposition of the two phenomena may either enhance or deteriorate the separation efficiency. If the velocity vectors of electrophoretic migration of particles and electroosmotic flow have opposite directions, the electro-

phoretic velocity of charged species must be smaller than the electroosmotic flow in the opposite direction, otherwise there is no possibility of detecting and thus quantifying the moving zone.

The next high-performance analytical technique belonging to the group of electrophoretic techniques is capillary isotachopheresis (ITP) [2,34]. Its characteristic feature is that it cannot be used to separate simultaneously samples that contain both positively and negatively charged ions. The mixture of substances to be separated is introduced between the so-called leading (LE) and terminating (TE) electrolytes. The LE contains an ion with an effective mobility higher than that of any of the ions in the sample mixture and the TE contains an ion with an effective mobility lower than that of any ion in the sample mixture. On application of an electric field, migration proceeds until a steady state is established. Its essential feature is the presence of sharp boundaries between the separated zones of the individual components of the sample. The zones migrate in close contact with each other, with the same velocity (hence the name "iso + tacho"), and their migration sequence is determined by the electrophoretic mobilities of the separated substances.

The solution of the equations for electrophoretic separation in the steady ITP state leads to certain important conclusions. First, the potential gradient in the i th zone is determined by the effective mobility of ions in this zone, as

$$v = \mu_{e,1}E_1 = \mu_{e,2}E_2 = \mu_{e,i}E_i = \text{constant} \quad (16)$$

where v is the velocity of movement of zone boundaries. Second, the concentration of any separated ion, S, with charge $z(S)$, is determined by the concentration of the LE ion, L, with charge $z(L)$, by the mobilities of both ions and by the mobility of a counter ion, C. This relationship is expressed by means of the Kohlraush regulating function [35]

$$\sum_i \sum_z |z| c_{i,z} / \mu_{i,z} = \text{constant} \quad (17)$$

in the form

$$c_{S,z(S)} = c_{L,z(L)} [\mu_{L,z(L)} + \mu_{C,z(C)}] \mu_{S,z(S)} |z_L| \cdot \{ [\mu_{S,z(S)} + \mu_{C,z(C)}] \mu_{L,z(L)} |z_S| \}^{-1} \quad (18)$$

This feature of isotachopheresis is particularly important for dilute solutions, where the concentration corresponds to eqn. 18, and distinguishes it from zone electrophoresis.

As with other separation techniques, electrophoretic separations can be optimized with respect to efficiency, selectivity and time. Variables such as buffer type and both its ionic strength and pH, specific additives to the electrolyte systems, operating voltage, solid support material as part of the migration channel or, in the case of the microchannel of a capillary, the column dimensions, and its inner surface chemical modification must be considered and will affect both efficiency and selectivity.

4. GENERAL ASPECTS OF CHIRAL SEPARATION IN ELECTROMIGRATION METHODS

There are two possible solutions to the problem of chiral resolution in electromigration methods: (1) a pre-separation derivatization of chiral compounds separated with appropriate chiral reagents and (2) direct chiral separation.

Pre-separation derivatization produces diastereomers, which can be separated by "non-chiral" electromigration techniques. There are, however, four major disadvantages with this method. First, it is difficult to obtain appropriate chiral derivatizing reagents of absolute enantiomeric purity, contamination with the unwanted isomer leading to spurious determinations. Second, as the resulting diastereomers have differing physico-chemical properties, their rates of formation will also differ (kinetic resolution). The final ratio of diastereomers will not therefore necessarily reflect the exact ratio of the starting enantiomers. Third, the diastereomers may have different detector responses. Fourth, the derivatization step is time consuming.

An example of this type of "chiral" analysis is the separation of chiral amino acids and peptides derivatized with Marfey's reagent (1-fluoro-2,4-dinitrophenyl-5-L-alaninamide) [36,37] and/or tetra-O-acetyl- β -D-glucopyranosyl isothiocyanate [38].

Considering that the above-mentioned separations are "non-chiral" from the electromigration point of view, we shall not concern ourselves with this subject here.

Depending on the type of selector and hence the type of chiral interaction, different separation mechanisms are observed in the case of direct chiral separation. They can be generally classified as a chiral ligand exchange mechanism, chiral micellar

mechanism, chiral inclusion (or "micromicellar") mechanism and protein-based enantioselection mechanism.

5. CHIRAL LIGAND-EXCHANGE MECHANISM

The utilization of enantioselective metal complexes represents one of the oldest approaches to the solution of chiral resolution. Studies of chiral complexes of Co^{3+} and Cr^{3+} with ethylenediamine, oxalate, *o*-phenanthroline, dipyriddy, *trans*-cyclohexane-1,2-diamine and amino acids as ligands were performed using high-performance paper electrophoresis [39-46]. Their behaviour in chiral support electrolytes consisting of antimonyl tartrate, arsenyl tartrate and tartrate enantiomers for separations of cations and acetates of quinine, cinchonine and brucine for separations of anions was described. Fig. 3 shows the effect of the "chiral composition" of the background electrolyte on the separation of racemic $\text{Co}(\text{en})_3^{3+}$ complexes (en = ethylenediamine).

It was found that optically active cations form outer-sphere complexes with optically active anions, mobility differences depending on their optical form. In addition, the anion-enantioselector must have certain suitable geometrical properties. If these conditions are not fulfilled when outer-sphere complexing takes place, no separation is obtained.

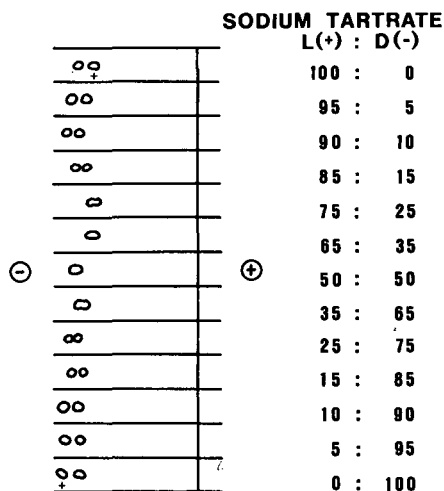


Fig. 3. High-voltage paper electropherograms of racemic $\text{Co}(\text{en})_3^{3+}$ on Whatman No. 1 paper at 2500 V for 35 min at 6°C. Electrolytes contained mixtures of sodium L-(+)- and D-(-)-tartrate. From ref. 46.

The papers used in the chiral separations mentioned are built up from cellulose fibres consisting of poly- β -1,4-glucopyranose chains; hence the paper could not only be a stabilizing but also provide a chiral environment for the paper electrophoretic separation of enantiomers.

This type of investigation may help to extend the number of chiral complexes which are of potential use as enantioselective pseudo-phases.

The experiments with enantioselective metal complexes were transferred to capillary zone electrophoresis. Diastereomeric ternary complex formation is theoretically applicable to the resolution of enantiomeric molecules with two correctly spaced polar groups which can simultaneously act as ligands for the central metal ion. Therefore, especially α -amino acids, with both amino and carboxy groups, are very suitable for both formation of the enantioselective phase and utilization as solutes.

The chiral pseudo-phase may be obtained simply by adding complex-forming components to the support (background) electrolyte without the need for its immobilization on the surface of any chiral stationary phase.

Zare and co-workers [47–49] suggested a chiral separation based on electrokinetic separations through the combined action of electrophoretic and electroosmotic motions in an open-tubular capillary. They applied this technique to the resolution of dansylated amino acid mixtures using different diastereomeric interactions between the D- and L-amino acids and transition metal–chiral ligand complexes (the Cu^{2+} –L-histidine and/or Cu^{2+} –aspartame complex) present in the separation buffer. The Cu^{2+} –aspartame complex significantly improves the electrokinetic resolution in comparison with the Cu^{2+} –L-histidine complex. In the presence of aspartame (dipeptide L-aspartyl-L-phenylalanine methyl ester), chelation of the metal ions probably occurs through the formation of a six-membered ring formed by the Cu^{2+} , the α -amino and the α -carboxyl groups of the aspartyl residue of the aspartame molecule. Such a six-membered ring is less stable than the five-membered ring involving the α -amino and α -carboxyl group of an amino acid. Thus, when an amino acid is added to an electrolyte solution containing the Cu^{2+} (aspartame)₂ complex, it can replace one aspartame ligand, leading to the formation of a ternary complex. This formation is

essential for the resolution of the enantiomeric forms of amino acids. Specific hydrophobic interactions between the aspartame phenylalanine residue and the amino acid side-chain can take place, leading to slightly different stability constants for each enantiomeric form of the amino acids. The dansyl group of the amino acid derivatives can also take part to an unknown extent in these interactions. The migration order is the same for all of the amino acids studied: the D-isomer appears first.

The formation of a double layer on the capillary inner wall is crucial for the separation of amino acids and for run-to-run and day-to-day reproducibility. This results in an increased operation time because of having to clean the capillary or preparing a new one.

The typical electropherogram in Fig. 4 shows the chiral separation of a mixture of four pairs of dansylated racemic amino acids (DNS-AAAs). The neutral amino acids, *i.e.*, those having an aliphatic or an aromatic side-chain, have almost the same migration times. This means that, although they could be

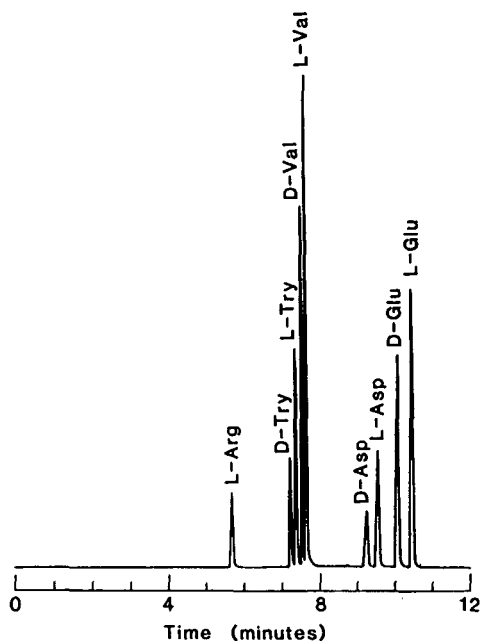


Fig. 4. CZE chiral separation of a mixture of four pairs of DNS-DL-amino acids. DNS-L-Arg = internal standard. Buffer, 2.5 mM $\text{CuSO}_4 \cdot 5\text{H}_2\text{O}$ + 5 mM aspartame + 10 mM ammonium acetate (pH 7.4); capillary, 75 μm I.D. \times 100 cm (75 cm to the detection zone); applied voltage, 30 kV; current, 33 μA . From ref. 48.

resolved when run separately, they are not readily separated in a mixture. In order to increase the differentiation of these neutral amino acids, a micellar electrolyte solution of sodium tetradecyl sulphate was employed. Micelles add another dimension to the separation, in that each amino acid will partition itself to a different extent between the aqueous and the micellar phase.

6. CHIRAL MICELLAR MECHANISM

Optical isomers have been separated successfully by EKC using several types of micellar systems. They can be classified as (a) mixed micelles, consisting of a non-chiral detergent (*e.g.*, sodium dodecyl sulphate) and a chiral detergent and/or ligand-exchange complexing agents, and (b) “pure” chiral micelles, built up of optically pure chiral surfactants.

Cohen *et al.* [50] used a mixed chiral metal chelate micelle system for the enantioseparation of DNS-AAAs. The chiral chelate detergent, didecyl-L-alanine, in the presence of sodium dodecyl sulphate (SDS) forms the mixed micelles in aqueous solution. The reagent is incorporated into the micelle in such a way that the hydrophilic chiral centres of L-alanine are on the surface, whereas the hydrophobic tail is in the interior. The use of mixtures of detergents to form micelles may allow manipulation of the micelle surface, which could prove useful in controlling the distance between ligand-exchange chiral centres [51].

Preliminary results on the enantiomeric resolution of six racemic phenylthiohydantoin amino acids (tryptophan, norleucine, norvaline, valine, α -aminobutyric acid and alanine) (PTH-AAAs) by micellar electrokinetic chromatography using mixed micelles of a non-ionic surfactant (digitonin) with anionic SDS were published by Otsuka and Terabe [52]. Under acidic conditions (pH 3.0), PTH-AAAs were separated from each other and optically resolved. The use of an anionic chiral surfactant, sodium N-dodecanoyl-L-valine, was also examined under neutral conditions. In this instance, the same enantiomers as above except PTH-DL-Ala were resolved in a shorter time.

The five [53] or six [54] PTH-DL-AAAs were separated from each other and each pair of enantiomers was optically resolved in a basic (pH 9.0) buffer system containing a mixture of sodium N-dodecanoyl-

L-valinate and SDS, urea and methanol. It was found that the addition of SDS to N-dodecanoyl-L-valinate–urea–methanol solutions caused a change in selectivity and provided a good enantiomeric resolution. The addition of urea to the buffer was effective in improving the peak shapes and resolution. The same micellar electrolyte mixture was used for the enantioseparation of benzoin and warfarin racemates.

The effects of methanol and urea on the optical resolution of PTH-DL-amino acids by EKC with sodium N-dodecanoyl-L-valinate in phosphate buffer of pH 7.0 were studied [55].

The development of a rapid, sensitive and precise method for the separation of PTH-AAAs is of great importance for the determination of peptide sequences by the Edman degradation method [56,57].

Dobashi *et al.* [58,59] used chiral micellar systems consisting of surfactants functionalized with L-amino acid residues, sodium N-dodecanoyl-L-amino acidates, for the separation of enantiomers of N-acylated amino acid esters by electrokinetic chromatography. The influence of the steric bulkiness of amino acid side-chains in the chiral surfactants and the effect of the derivatization of the amino acids to be resolved on the extent of the enantiomer resolution were studied.

N-Dodecanoyl-L-valine and -L-alanine were tested as chiral surfactants. The chiral micelles of the former made possible the most effective enantio-resolution. The separation was influenced by forming mixed micellar systems (comicellar systems) consisting of a chiral surfactant and a non-chiral surfactant, SDS. Resolution of the enantiomeric mixtures was improved by adding methanol to the mixed micellar solution. The main effect of an organic modifier may be to change the micellar size (changing the aggregation number of the surfactant) in addition to the electroosmotic flow.

It was found the D-enantiomer of the racemic amino acid separated eluted faster than the corresponding L-enantiomer in all cases, indicating that the chiral micelle binds to the L-enantiomer having the same configuration as its chiral component to a greater extent than to the D-enantiomer.

The 3,5-dinitrobenzoyl derivatives of racemic amino acid tested were the most effectively resolved in all the solutes examined (Ala, Val, Leu and Phe) in comparison with 4-nitrobenzoyl and/or benzoyl

derivatives. Esterification of N-acylated AAs was the next crucial requirement for an enantiomer resolution.

Terabe *et al.* [60] extended the application of electrokinetic chromatography for the separation of racemic DNS-AAAs by using chiral micelles consisting of one type of common biological surfactant among various chiral surfactants, namely bile acid salts. Sodium salts of taurocholic, tauroolithocholic, deoxycholic, cholic, dehydrocholic and taurodeoxycholic acids added to phosphate buffer solutions were tested. The most successful separation of enantiomers was achieved especially with the last-mentioned bile acid salt under acidic conditions.

The chiral selectors above mentioned consist of a relatively flat-shaped steroid portion, in which the A ring is *cis* with respect to the B ring, and a side-chain having a carboxyl group, which may be conjugated, *e.g.*, by taurine or glycine. All the hydroxyl groups bound to the steroid portion are oriented in the same direction nearly perpendicular to the steroidal frame, and consequently the bile salts possess a hydrophobic and a hydrophilic face. They are generally considered to form small or primary micelles which are composed of up to ten monomers by the hydrophobic interaction between the non-

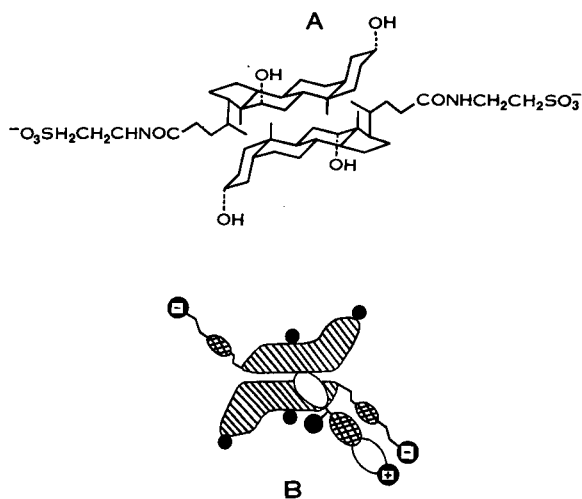


Fig. 5. (A) Structural formulae of taurodeoxycholate and (B) a possible spatial arrangement of configuration of DNS-L-Ala interacting with a bimolecular aggregate of taurodeoxycholate. Black parts indicate OH, COO⁻, SO₃⁻ and NH₂ groups, cross-hatched parts NH and sulphonamide groups and the other parts (open and hatched) hydrophobic moieties. From ref. 60.

polar face of the monomers [61]. A possible structure of a bimolecular aggregate of sodium taurodeoxycholate is shown in Fig. 5. In acidic media the dimethylamino group on the DNS group of an amino acid may be partly protonated and therefore the positively charged amino group will interact strongly with the negatively charged sulphonyl group of the taurine moiety on the side-chain through electrostatic attraction. The amino acid residue, if it is hydrophobic, will also be combined concurrently with the non-polar part of the bile salt micelle by the hydrophobic interaction as shown in Fig. 5.

As a continuation of the above-mentioned study, the effects of bile salt species or structures and of the pH and composition of the buffer solution on the separation of optical isomers of diltiazem, trimetoprim, carboline derivatives A and B, 1-naphthylethylamine and 1,1'-bi(2-naphthol) [63] and related compounds [64] were investigated.

Approaches to optimizing the bile salt-based CZE separation of substituted binaphthyl enantiomers [1,1'-bi(2-naphthol), 1,1'-binaphthalene-2,2'-diyl hydrogenphosphate, 1,1'-binaphthalene-2,2'-dicarboxylic acid and 9,9'-bi(10-phenanthrol)] were published [65]. A possible mechanism for chiral recognition based on the model of bile salt micelles possessing a helical structure, with the hydrophilic region facing the interior of the micelle, was outlined [66]. The effect of methanol added to the buffer micellar solution on the enantiomer resolution was tested.

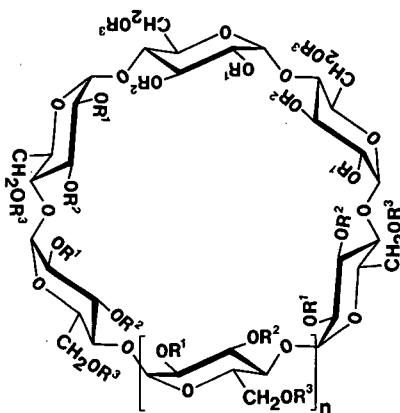


Fig. 6. Structure of cyclodextrins. For non-derivatized CDs, R¹-R³ = hydrogen atoms. For explanation of *n*, see text.

7. CHIRAL INCLUSION MECHANISM

The next type of chiral selectors are the cyclodextrins (CD). These are cyclic, non-reducing oligosaccharides built up of D-(+)-glucopyranose units (Fig. 6). The α -CD consist of six units ($n = 1$), β -CD comprises seven units ($n = 2$) and γ -CD has a ring constituted of eight glucose units ($n = 3$). The CD structure is unique in that it resembles a truncated cone with both "ends" open. The top of the torus corresponds to the more open side, which is rimmed with secondary hydroxyl groups, and the smaller opening of the cone is rimmed with the more polar primary hydroxyl groups. The interior of the CD cavity is relatively hydrophobic. The surface is relatively hydrophilic, and CDs are therefore soluble in water. The solubility of CDs in both water and organic solvents (mainly β -CD) is substantially increased by derivatization, *e.g.*, methylation of CDs. For more physical chemical data and properties useful in EMM, see refs. 18 and 67.

A remarkable property of CDs and their derivatives is the ability to include selectively in their cavity or to interact stereospecifically with a wide variety of organic and inorganic molecules or ions. The relative stability of CD complexes is governed by such factors as hydrogen bonding, hydrophobic interactions, solvation effects and especially the space-filling ability of the interacting molecule.

The most interesting from the separation point of view is the use of CDs as chiral discriminators (or enantioselectors), which permit the chiral resolution of a wide variety of optical isomers. The first successful attempts to separate optical isomers by means of the application of cyclodextrin enantioselectors in EMM were made in capillary isotachopheresis (ITP). Using β -CD and heptakis(2,6-di-O-methyl)- β -CD (DM- β -CD) as additives to the leading electrolyte (LE) in ITP, the complete chiral resolution of pseudoephedrine alkaloid enantiomers was achieved [68]. Comparative measurements with β -CD and its dimethyl and trimethyl derivatives demonstrated that the changes in size and hydrophobicity of the cavity collar, caused by methylation, substantially alter the efficiency of chiral resolution of pseudoephedrine, norpseudoephedrine (N Ψ E), O-acetylpseudoephedrine and *p*-hydroxynorpseudoephedrine (HN Ψ E) enantiomers. Optimization of the ITP conditions confirmed the signif-

icant influence of the CD concentration and pH value on the separation efficiency. The optimum concentration of CDs for practical use is about 10 mM. An example of the successful separation of N Ψ E and HN Ψ E enantiomers is shown in Fig. 7.

The next example of a successful chiral separation in CD-modified ITP is the complete resolution of chiral phenothiazines: thioridazine, promethazine and cyamepromazine [69]. The first compound was separated with γ -CD and the other two racemates were resolved by means of β -CD added to the LE. In this study it was shown that some additional parameters, such as the type of counter ion used, play a crucial role in the quality of the chiral resolution and must be involved in the optimization procedure.

β -CD and DM- β -CD proved to be effective enantioselective leading electrolyte additives suitable for the resolution of the drug ketotifen and its polar synthesis intermediate enantiomers [70]. There was no reference in the literature to the existence of ketotifen enantiomers and hence it may be presumed that capillary ITP using CD selectors permitted the discovery of their existence. Addition of β -CD to the LE at concentrations higher than 0.5 mM makes it possible to distinguish clearly the pairs of enantiomers.

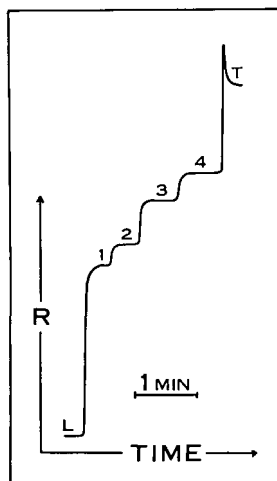


Fig. 7. ITP separation of norpseudoephedrine (1 and 2) and *p*-hydroxynorpseudoephedrine (3 and 4) enantiomers. 1 and 3 = (-)-isomers; 2 and 4 = (+)-isomers; R = response of conductivity detector; L and T = LE and TE zones, respectively. LE = 5 mM sodium acetate containing 0.2% hydroxyethylcellulose adjusted with acetic acid to pH 5.48 + 10 mM DM- β -CD; TE = 10 mM β -Ala. Capillary, 370 \times 0.5 mm I.D.; current, 150 μ A (9 min), 50 μ A for detection.

The ITP enantioseparations presented above were performed in an ITP device equipped with a one-column separation compartment. An instrument with coupled columns offers the possibility of performing a one-run, two-step chiral separation in two columns filled with LE modified by different types of chiral selectors. This type of separation is called two-dimensional chiral separation [71]. As chiral selectors two types of cyclodextrins, DM- β -CD and γ -CD, were used. The model compounds were racemates of pseudoephedrine and norpseudoephedrine, which were resolved into optical isomers by DM- β -CD selector and racemates of thioridazine and hydrothiadene were resolved by γ -CD. Practical examples of the two-dimensional chiral separation of a mixture of racemates are illustrated in Fig. 8. This method proved to be useful for the investigation of complicated mixtures of racemates. The main advantages are a short separation time compared with two runs in a one-column system filled gradual-

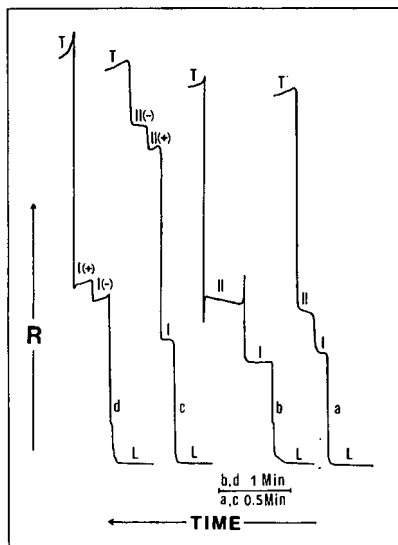


Fig. 8. Two-dimensional ITP separation of the optical isomers of pseudoephedrine (I) and thioridazine (II), (a and b) without CD, (c) with 5 mM γ -CD and (d) with 10 mM DM- β -CD in the LE with the two-column system; (a and c) in the first capillary and (b and d) in the second capillary. LE = 10 mM sodium acetate + 0.08% hydroxyethylcellulose adjusted with acetic acid to pH 5.47; TE = 10 mM β -Ala. R = Response of conductivity detector; L and T = LE and TE zones, respectively. First column: 170 \times 0.8 mm I.D.; current, 200 μ A (800 s), 100 μ A for detection. Second column: 170 \times 0.3 mm I.D.; current, 50 μ A. The strong complexation with DM- β -CD and the retardation of compound II led to their disappearance in the zone of the TE. From ref. 71.

ly with an enantioselector, a lower consumption of the samples and chiral selectors and the possibility of using two interfering selectors in one two-step separation.

On the basis of experimental experience, a simple mathematical model of 1:1 cyclodextrin-solute complex formation was proposed which is applicable to chiral ITP separations, performed using CD enantioselectors. A possible role of two limiting CD-solute interactions, introduced as effective and non-effective complex formation, on the quality of ITP (chiral) resolution has been studied [72].

The effect of competitive counter ion inclusion complex formation on the separation efficiency in LE modified with CDs was published [73]. The racemates of pseudoephedrine and *p*-hydroxynorpseudoephedrine were used as model samples for monitoring the effectiveness of the separation process with changing counter ions. On the basis of the analysis of complex-forming equilibria established in the sample mixed zone, it was concluded that an increased stability of the counter ion inclusion complex results in a decreased efficiency of the separation process. This model was verified experimentally on the set of aliphatic and aromatic acids used as counter ions in LE.

The next area of EMMs in which the CDs were used with success is capillary zone electrophoresis (CZE) and its modifications. Guttman *et al.* [74] incorporated cyclodextrins into polyacrylamide gel capillary columns and obtained excellent chiral

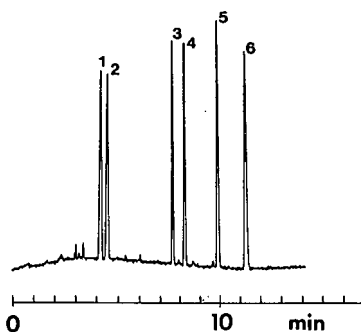


Fig. 9. Separation of DNS-amino acids enantiomers by gel-filled capillary electrophoresis. (1) L- and (2) D-Glu, (3) L- and (4) D-Ser, (5) L- and (6) D-Leu. Capillary, 150 \times 0.075 mm I.D.; E = 1000 V/cm; gel, T = 5%, C = 3.3%, 0.1 M Tris + 0.2 M boric acid (pH 8.3), 7 M urea. The buffer and gel contained 10% (v/v) methanol and 75 mM β -CD. From ref. 74.

separations of racemates of DNS-AAAs (Leu, Ser, Val, Glu, Asp, Met, Norleu, Norval, γ -amino-*n*-butyric acid, Phe and Trp were tested). Various parameters, such as concentration of CDs, addition of methanol to the buffer and temperature were examined in terms of their influence on retention and selectivity. The best results were achieved using β -CD. An example of the high-efficiency separation of some DNS-DL-AAAs under optimum conditions is given in Fig. 9.

A retention model of the above-mentioned chiral separation has been developed which emphasizes that the mobility of the free species and the complex must differ significantly from one another in order to utilize the complexation equilibria for enantioselectivity optimization.

Capillary zone electrophoresis with CD-modified background electrolyte was used for the separation of ephedrine, norephedrine, epinephrine, norepinephrine and isoproterenol enantiomers by Fanali [75]. Swartz [76] tested the effects of different pH values of buffer systems and the type of cyclodextrin used in the resolution of ephedrine enantiomers. The separation of enantiomers of structurally related compounds, including norephedrine, pseudoephedrine and phenylpropanolamine, performed under similar conditions was mentioned. Unlike the capillary isotachophoretic method [68] mentioned above, separations of ephedrine alkaloid-like structural type enantiomers by using a low pH (2.4) electrolyte with addition of DM- β -CD were achieved.

The CZE enantioseparation of tryptophan racemate was achieved with α -CD as a chiral selector in the background electrolyte of low pH. The effect of counter ions at pH 2.5 was investigated [77]. A CD-modified buffer solution was successfully used for the CZE resolution of terbutaline enantiomers [78].

As a continuation of experiments in paper electrophoresis [39–46] (mentioned in Section 5), Fanali *et al.* [79] published a CZE method for the separation of enantiomers and/or diastereomers of Co^{3+} complexes. The ligands were ethylenediamine, *o*-phenanthroline, glycine, methionine, proline and phenylalanine. Based on experience with paper electrophoresis, L-(+)-tartrate was selected as the complexing counter ion of the electrolyte. The effective electrophoretic mobilities of all complexes studied were too close to each other, however. Hence, in

order to improve the selectivity of separation, β -CD was used as an electrolyte additive.

Our ITP and CZE experiments with CDs and their alkyl derivatives confirmed the great significance of the size of the cyclodextrin ring, chemical modification of hydroxyl groups of the cavity collar and/or the pH and ionic strength of the buffer system used for chiral separations. In some instances both the enantioselectivity and efficiency of separation can be influenced by changing the electroosmosis by using anticonvective additives [80] or coating the inner capillary walls. Fig. 10 shows a comparison of separations of the chiral solutes ketotifen (K), its synthesis intermediate (i) and the N-oxide of ketotifen (O) under four different circumstances, and also a means for the possible improvement of enantioseparation. Whether the addition of methylhydroxyethylcellulose (MHEC) (b) improves the separation owing to suppression of electroosmosis only or a combination of this effect with some specific interaction between the cyclodextrin and MHEC remain unclear. The major problems with this approach are the high viscosity of the electrolyte, precipitation and frequent plugging of the separation capillaries. The use of a longer capillary (c) without MHEC addition again improves the resolution, but only at the expense of a longer analysis time and increased peak asymmetry

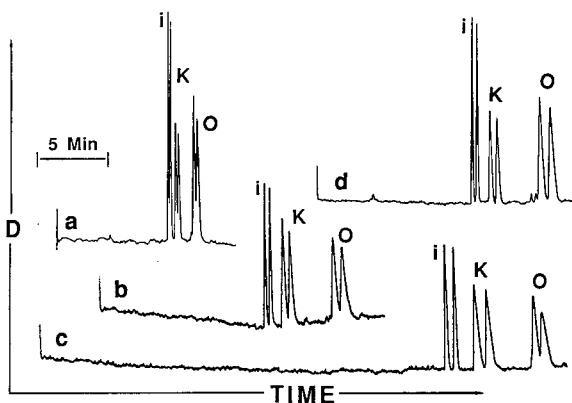


Fig. 10. CZE chiral separation of ketotifen (K), its synthesis intermediate (i) and N-oxide (O). Capillary: 50 μm I.D. \times (a, b and d) 60 cm (40 cm to the detector) or (c) 100 cm (80 cm to the detector); (a–c) uncoated and (d) coated by the method described in ref. 94. Buffer: (a, c and d) 40 mM β -alanine + citric acid to pH 3.33 + 15 mM γ -CD and (b) the same + 0.1% MHEC. $E = 20$ kV. $D =$ Response of UV detector at 254 nm.

due to a prolonged interaction of the solutes with the untreated surface and increased diffusion of their zones. The results obtained with a surface-coated capillary (d) are clearly superior [81]. Further changes in the resolution of enantiomer separations result from adding organic solvents to the buffer system containing cyclodextrin enantioselectors. An example is at least the partial enantioresolution of propranolol enantiomers. An improvement in resolution was achieved with increasing concentrations of methanol (up to 30%) in electrolyte containing β -CD enantioselector and urea [78].

Electrokinetic chromatography based on inclusion complex formation with CD derivatives also seems to be a useful tool for the chiral separation of DNS-AA enantiomers (DL-Phe, -Norval, -Met, -Ser, -Thr, -Glu) [82]. Two β -CD derivatives were used as the enantioselecting carriers: 2-O-carboxymethyl- β -CD and mono-(6- β -aminoethylamino-6-deoxy)- β -CD in acidic phosphate buffer (pH 3.0) containing 0.1% of hydroxypropylcellulose.

Chiral separations performed under cyclodextrin-modified micellar electrokinetic chromatographic conditions were published by Terabe and co-workers [83–85]. By means of this method the separation of dansylated amino acid enantiomers was achieved. If underivatized cyclodextrins are added to the micellar solution, they do not interact with the micelle because of their electroneutrality and the hydrophilicity of the surface. Hence, CDs migrate with the same velocity as the bulk solution (= electroosmotic flow). Consequently, when a solute tends to interact with CD through the formation of an inclusion complex, the migration time for that solute becomes less than that obtained in MEKC without CD. The enantiomers of DNS-Thr, -Norval, -Norleu, -Phe, -Val, -Leu, -Met, -Glu and γ -aminobutyric acid were separated by γ -CD in SDS solution in the buffer [83]. The D-enantiomers were included more strongly by CD than the L-enantiomers, and migrated faster than the corresponding L-enantiomers. The use of β -CD instead of γ -CD resulted in a partial resolution of some of the enantiomers. However, the addition of either β - or γ -CD alone to the buffer solution (*i.e.*, without SDS) did not result in chiral separation.

The chiral separation of naphthalene-2,3-dicarboxaldehyde (NDA)-labelled amino acid enantiomers by cyclodextrin-modified micellar electroki-

netic chromatography with very sensitive (detection limits in the attomole range) laser-induced fluorescence detection was reported [86]. Amino acids (Thr, Ser, Tyr, Leu, Ile, Phe, Val and Arg) form 1-cyano-2-substituted (by appropriate amino acid) benz[*f*]-isoindoles (CBI) by reaction with NDA in the presence of CN^- ions. Generally, γ -CD MEKC is more effective than β -CD MEKC in terms of the enantiomeric selectivity for CBI-DL-amino acids in borate buffer of pH 9.0.

α -, β -, Dimethyl- β -, trimethyl- β - and γ -cyclodextrins were used for studying the chiral recognition of 2,2'-dihydroxy-1,1'-binaphthyl, 2,2,2-trifluoro-1-(9-anthryl)ethanol, pentobarbital and thiopental enantiomers [84] and 1,1'-binaphthyl-2,2'-diyl hydrogenphosphate [85]. Chiral recognition was achieved by using four cyclodextrins (α -CD was not included). The cyclodextrin-modified micellar solutions were prepared by dissolving the appropriate CD and SDS in a phosphate-borate buffer with the addition of urea. A schematic illustration of the probable solute interaction in the SDS buffer solution containing the cyclodextrin is shown in Fig. 11.

The addition of methanol to the buffer system mentioned above was effective for the separation of enantiomers of lipophilic compounds in reducing peak tailing. However, chiral recognition of the enantiomers was reduced, probably owing to the inclusion of methanol. To enhance chiral recognition, the effect of the addition of sodium D-camphor-10-sulphonate and menthoxyacetic acid to the SDS solution containing the CD was investigated. The improvements in enantioselectivity may be ascribed to the simultaneous or competitive inclusion of these chiral additives and/or co-inclusion of solute in the γ -CD cavity.

The EKC with buffer electrolyte consisting of a mixed carrier system of SDS, tetrabutylammonium hydrogensulphate and β -CD was used for enhancing the selectivity of the separation of antihistamine drugs [87]. In this study the pair of chlorpheniramine enantiomers included in the mixture of nine antihistamines were separated. A major advantage of such a separation system is its high selectivity achieved in a short analysis time.

The feasibility of chiral separation under isoelectric focusing (IF) conditions was published by Righetti *et al.* [88]. The separation of enantiomeric forms of DNS-AAs by IF in an immobilized pH

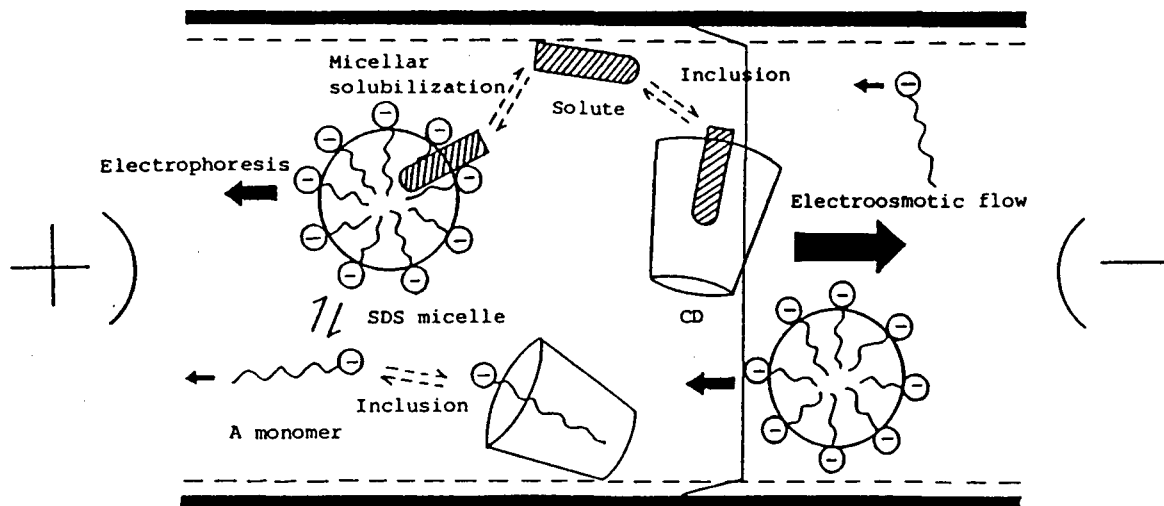


Fig. 11. Schematic illustration of the probable solute interaction in the SDS buffer solution containing the cyclodextrin. From ref. 85.

gradient (IF-IPG) was carried out in the pH 3.0–4.0 IPG interval in the presence of urea, methanol and β -CD as the chiral inclusion discriminator. As the complexes of DNS-AAAs with CD are stable in the electric field for at least 15 h, this separation mechanism could probably be exploited for purifying large amounts of pure D- and L-form racemates in multi-component electrolyses with isoelectric Immobiline membranes, as described by Righetti *et al.* [89].

8. PROTEIN-BASED ENANTIOSELECTION MECHANISM

Electrophoretic enantioselective separations can be obtained when enantiomers form complexes or stereospecific agglomerates with different stabilities with the chiral selector represented by a suitable protein. The exact mechanism of the chiral binding is usually unknown. However, some empirical conclusions on structural requirements for chiral binding have been presented for some similar separations in liquid chromatography [90,91].

Cellulase, or cellobiohydrolase I, produced by the fungus *Trichoderma reesei*, dissolved in phosphate buffer with addition of isopropanol was successfully used for the CZE chiral separation of pindolol, propranolol, metoprolol and labetolol enantiomers [92].

Bovine serum albumin incorporated in gel was

used for the capillary gel electrophoresis of optical isomers of tryptophan [93]. The problem in this instance, however, results from the reproducibility of the preparation of gel-filled capillaries.

9. CONCLUSIONS

The use of enantioselectors (chiral discriminators or pseudo-phases) is the only means of direct separation of optical isomers in electromigration methods in general. Their utilization allows the introduction of other important factors which may contribute to the improvement of both analytical and preparative separations of mirror-image isomeric molecules. As was shown, there is no sharp boundary between the application or utilization of individual enantioselectors. In some instances separations were achieved by a combination of two or more enantioselection mechanisms.

What progress may be expected in the future? Although it is impossible to predict all of the possible avenues that this research might take, future developments in several areas are likely. New possibilities exist for the use of newly synthesized chiral selectors, *e.g.*, chiral crown ethers and chiral micellar systems, in EMM. Another possible approach is to use multi-dimensional separation procedures, which can greatly increase the selectivity and decrease the time necessary for separation. The

demand for detectors that provide information on the chirality of the solute being separated will increase. However, these detection techniques may have limited sensitivity. Hence it may be necessary to use the laser-based detection method. Although analytical separations are becoming more common, the demand for analogous preparative-scale separations is growing.

Finally, the expansion of these techniques to as yet unexpected areas is certain. The forces that govern chiral analyte–enantioselector interactions are the same as those governing all molecular chiral recognition systems, including drug–receptor and enzyme–substrate interactions. Hence this type of electrophoretic separation system could be advantageous for modelling and studying such biological interactions.

10. ADDENDUM

Three new approaches to chiral separations by EMM appeared after the submission of this paper. The increasing interest in chiral separations by capillary electromigration methods was clearly seen at the *4th International Symposium on High-Performance Capillary Electrophoresis, Amsterdam, February 9–13th, 1992*.

The use of chiral crown ethers, predicted some years ago [18] and repeatedly in conclusions in this review, was realized by using an 18-crown-6-tetra-carboxylic acid enantiomer in an excellent contribution by Kuhn *et al.* [95]. D,L-Dopa, -phenylalanine, -tryptophan, -tyrosine and qinagolide enantiomers were separated by using the chiral selector mentioned above under CZE conditions. The synergistic effect of α -CD and the chiral crown ether was also demonstrated with the example of the separation of tryptophan enantiomers.

The antibiotic vancomycin was used as a chiral selector added to the CZE buffer for the separation of dipeptide isomers [96].

Enantiomer separation by means of a cyclodextrin selector chemically bonded to the inner capillary surface has been reported [97]. The model racemic compounds separated were 1,1'-binaphthyl-2,2'-diylhydrogenphosphate, 1-phenylethanol and ibuprofen.

Detailed descriptions of the methods for chiral separation presented at the above-mentioned sym-

posium in Amsterdam will be published in Vol. 000 of the *Journal of Chromatography*.

REFERENCES

- 1 A. J. P. Martin and F. M. Everaerts, *Proc. R. Soc. London, Ser. A*, 316 (1970) 393.
- 2 F. M. Everaerts, J. L. Beckers and Th. P. E. M. Verheggen, *Isotachophoresis*, Elsevier, Amsterdam, 1976.
- 3 S. Hjertén, *Chromatogr. Rev.*, 9 (1967) 122.
- 4 F. Mikkers, F. Everaerts and Th. P. E. M. Verheggen, *J. Chromatogr.*, 169 (1979) 11.
- 5 J. W. Jorgenson and K. D. Lukacs, *Anal. Chem.*, 53 (1981) 1298.
- 6 J. W. Jorgenson and K. D. Lukacs, *Clin. Chem.*, 27 (1981) 1551.
- 7 J. W. Jorgenson and K. D. Lukacs, *J. Chromatogr.*, 218 (1981) 209.
- 8 J. W. Jorgenson and K. D. Lukacs, *Science*, 222 (1983) 266.
- 9 R. A. Wallingford and A. G. Ewing, *Adv. Chromatogr.*, 29 (1989) 1.
- 10 W. G. Kuhr, *Anal. Chem.*, 62 (1990) 403R.
- 11 B. Koppenhoefer and E. Bayer, *Chromatographia*, 19 (1984) 123.
- 12 R. W. Souter, *Chromatographic Separation of Stereoisomers*, CRC Press, Boca Raton, FL, 1985.
- 13 D. W. Armstrong, *Anal. Chem.*, 59 (1987) 84A, and references cited therein.
- 14 C. Pettersson, *Trends Anal. Chem.*, 7 (1988) 209.
- 15 W. A. König, *The Practice of Enantiomer Separation by Capillary Gas Chromatography*, Hüthig, Heidelberg, 1989.
- 16 *The Separation of Chiral Molecules and Control of Optical Purity by TLC, GLC, HPLC*, Macherey–Nagel, Düren, 1989; and references cited therein.
- 17 W. H. Pirkle and T. C. Pochapsky, *Chem. Rev.*, 89 (1989) 347, and references cited therein.
- 18 J. Snopek, I. Jelinek and E. Smolková-Keulemansová, *J. Chromatogr.*, 452 (1988) 571.
- 19 L. D. Barron, *Mol. Phys.*, 43 (1981) 1395.
- 20 L. D. Barron, *Molecular Light Scattering and Optical Activity*, Cambridge University Press, Cambridge, 1982.
- 21 L. D. Barron, *Chem. Phys. Lett.*, 123 (1986) 423.
- 22 L. D. Barron, *J. Am. Chem. Soc.*, 108 (1986) 5539.
- 23 L. D. Barron, *Chem. Soc. Rev.*, 17 (1986) 189.
- 24 L. D. Barron, in P. G. Mezey (Editor), *New Developments in Molecular Chirality (Understanding Chemical Reactivity, Vol. 5)*, Kluwer, Dordrecht, 1991, p. 1.
- 25 P. Jungwirth, L. Skála and R. Zahradník, *Chem. Phys. Lett.*, 161 (1989) 502.
- 26 O. Costa de Beauregard, *Time, the Physical Magnitude*, Reidel, Dordrecht, 1987.
- 27 C. E. Dalglish, *J. Chem. Soc.*, (1952) 3940.
- 28 F. M. Everaerts, F. E. P. Mikkers, Th. P. E. M. Verheggen and J. Vacík, in E. Heftmann (Editor), *Chromatography: Fundamentals and Applications of Chromatographic and Electrophoretic Methods, Part A: Fundamentals and Techniques*, Elsevier, Amsterdam, 1983, Ch. 9.
- 29 A. W. Adamson, *Physical Chemistry of Surfaces*, Interscience, New York, 2nd ed., 1967, Ch. 4.

- 30 J. C. Giddings, *Sep. Sci.*, 4 (1969) 181.
- 31 S. Terabe, K. Otsuka, K. Ichikawa, A. Tsuchiya and T. Ando, *Anal. Chem.*, 56 (1984) 111.
- 32 S. Terabe, K. Otsuka and T. Ando, *Anal. Chem.*, 57 (1985) 834.
- 33 K. L. Mittal (Editor), *Micellization, Solubilization and Microemulsions*, Vol. 1, Plenum Press, New York, 1977.
- 34 P. Boček, M. Deml, P. Gebauer and V. Dolnik, *Analytical Isotachopheresis*, VCH, Weinheim, 1988.
- 35 F. Kohlrausch, *Ann. Phys. Chem., N.F.*, 62 (1897) 209.
- 36 E. Leopold, *Separation of Chiral Amino Acids and Peptides by Capillary Electrophoresis Using P/ACE System 2000*, Beckman, Palo Alto, CA, 1989.
- 37 A. D. Tran, T. Blanc and E. J. Leopold, *J. Chromatogr.*, 516 (1990) 241.
- 38 H. Nishi, T. Fukuyama and M. Matsuo, *J. Microcol. Sep.*, 2 (1990) 234.
- 39 H. Yoneda and T. Miura, *Bull. Chem. Soc. Jpn.*, 43 (1970) 574.
- 40 L. Ossicini and C. Celli, *J. Chromatogr.*, 115 (1975) 655.
- 41 V. Cardaci and L. Ossicini, *J. Chromatogr.*, 198 (1980) 76.
- 42 S. Fanali and L. Ossicini, *J. Chromatogr.*, 212 (1981) 374.
- 43 S. Fanali, V. Cardaci and L. Ossicini, *J. Chromatogr.*, 256 (1983) 131.
- 44 S. Fanali, L. Ossicini and T. Prosperi, *J. Chromatogr.*, 318 (1985) 440.
- 45 S. Fanali, P. Masia and L. Ossicini, *J. Chromatogr.*, 403 (1987) 388.
- 46 S. Fanali, M. Lederer, P. Masia and L. Ossicini, *J. Chromatogr.*, 440 (1988) 361.
- 47 E. Gassman, J. E. Kuo and R. N. Zare, *Science*, 230 (1985) 813.
- 48 P. Gozel, E. Gassman, H. Michelsen and R. N. Zare, *Anal. Chem.*, 59 (1987) 44.
- 49 P. Gozel and R. N. Zare, *ASTM Spec. Tech. Publ.*, 1988, No. 1009, p. 41; *C.A.*, 110 (1989) 169654s.
- 50 A. S. Cohen, A. Paulus and B. L. Karger, *Chromatographia*, 24 (1987) 15.
- 51 B. Feibush, M. J. Cohen and B. L. Karger, *J. Chromatogr.*, 282 (1983) 3.
- 52 K. Otsuka and S. Terabe, *J. Chromatogr.*, 515 (1990) 221.
- 53 K. Otsuka and S. Terabe, in K. Jinno and P. Sandra (Editors), *12th International Symposium on Capillary Chromatography, Kobe, Japan, September 11–14, 1990*, Industrial Publishing and Consulting, Tokyo, 1990, p. 646.
- 54 K. Otsuka, J. Kawahara, K. Tatekawa and S. Terabe, *J. Chromatogr.*, 559 (1991) 209.
- 55 K. Otsuka and S. Terabe, *Electrophoresis*, 11 (1990) 982.
- 56 J. B. C. Findlay and M. J. Geisow, *Protein Sequencing (a Practical Approach) (Practical Approach Series)*, IRL Press, Oxford, 1989.
- 57 G. Allen, *Sequencing of Proteins and Peptides (Laboratory Techniques in Biochemistry and Molecular Biology, Vol. 9)*, Elsevier, Amsterdam, 2nd ed., 1989.
- 58 A. Dobashi, T. Ono, S. Hara and J. Yamaguchi, *J. Chromatogr.*, 480 (1989) 413.
- 59 A. Dobashi, T. Ono, S. Hara and J. Yamaguchi, *Anal. Chem.*, 61 (1989) 1984.
- 60 S. Terabe, M. Shibata and Y. Miyashita, *J. Chromatogr.*, 480 (1989) 403.
- 61 D. Attwood and A. T. Florence, *Surfactant Systems*, Chapman and Hall, London, 1983, pp. 185–188.
- 62 H. Nishi, T. Fukuyama, M. Matsuo and S. Terabe, *Anal. Chim. Acta*, 236 (1990) 281.
- 63 H. Nishi, T. Fukuyama, M. Matsuo and S. Terabe, *J. Microcol. Sep.*, 1 (1989) 234.
- 64 H. Nishi, T. Fukuyama, M. Matsuo and S. Terabe, *J. Chromatogr.*, 515 (1990) 233.
- 65 R. O. Cole, M. J. Sepaniak and W. L. Hinze, *J. High Resolut. Chromatogr.*, 13 (1990) 579.
- 66 N. V. Pavel, E. Giglio, G. Eposito and A. Zanabi, *J. Phys. Chem.*, 91 (1987) 356.
- 67 J. Snopek and E. Smolková-Keulemansová, *Cyclodextrins in Electromigration Methods (New Trends in Cyclodextrins and Derivatives)*, Edition de Santé, Paris, 1991, Ch. 14, p. 483.
- 68 J. Snopek, I. Jelínek and E. Smolková-Keulemansová, *J. Chromatogr.*, 438 (1988) 211.
- 69 I. Jelínek, J. Dohnal, J. Snopek and E. Smolková-Keulemansová, *J. Chromatogr.*, 464 (1989) 139.
- 70 I. Jelínek, J. Snopek and E. Smolková-Keulemansová, *J. Chromatogr.*, 439 (1988) 386.
- 71 J. Snopek, I. Jelínek and E. Smolková-Keulemansová, *J. Chromatogr.*, 472 (1989) 308.
- 72 I. Jelínek, J. Snopek, J. Dian and E. Smolková-Keulemansová, *J. Chromatogr.*, 470 (1989) 113.
- 73 I. Jelínek, J. Snopek and E. Smolková-Keulemansová, *J. Chromatogr.*, 557 (1991) 215.
- 74 A. Guttman, A. Paulus, A. S. Cohen, N. Grinberg and B. L. Karger, *J. Chromatogr.*, 448 (1988) 41.
- 75 S. Fanali, *J. Chromatogr.*, 474 (1989) 441.
- 76 M. E. Swartz, *J. Liq. Chromatogr.*, 14 (1991) 923.
- 77 S. Fanali and P. Boček, *Electrophoresis*, 11 (1990) 757.
- 78 S. Fanali, *J. Chromatogr.*, 545 (1991) 437.
- 79 S. Fanali, L. Ossicini, F. Foret and P. Boček, *J. Microcol. Sep.*, 1 (1989) 190.
- 80 J. Snopek, H. Soini, M. Novotny, E. Smolková-Keulemansová and I. Jelínek, *J. Chromatogr.*, 559 (1991) 215.
- 81 J. Snopek and M. Novotny, to be published.
- 82 S. Terabe, *Trends Anal. Chem.*, 8 (1989) 129.
- 83 Y. Miyashita and S. Terabe, *Separation of Dansyl DL-Amino Acids by Micellar Electrokinetic Capillary Chromatography With and Without Cyclodextrins Using P/ACE System 2000*, Application Data, DS-767, Beckman, Palo Alto, CA, 1990.
- 84 H. Nishi, N. Fujimura, H. Yamaguchi, T. Fukuyama, M. Matsuo and S. Terabe, in K. Jinno and P. Sandra (Editors), *12th International Symposium on Capillary Chromatography, Kobe, Japan, September 11–14, 1990*, Industrial Publishing and Consulting, Tokyo, 1990, p. 640.
- 85 H. Nishi, T. Fukuyama and S. Terabe, *J. Chromatogr.*, 553 (1991) 503.
- 86 T. Ueda, F. Kitamura, R. Mitchell, T. Metcalf, T. Kuwana and A. Nakamoto, *Anal. Chem.*, 63 (1991) 2979.
- 87 C. P. Ong, C. L. Ng, H. K. Lee and S. F. Y. Li, *J. Chromatogr.*, 588 (1991) 335.
- 88 P. G. Righetti, C. Ettori, P. Chafey and J. P. Wahrmann, *Electrophoresis*, 11 (1990) 1.
- 89 P. G. Righetti, E. Wenisch and M. Faupel, *J. Chromatogr.*, 475 (1989) 293.
- 90 J. Hermansson and G. Schill, in P. R. Brown and R. A.

- Hartwich (Editors), *High-Performance Liquid Chromatography*, Wiley, New York, 1989, p. 337.
- 91 R. K. Gilpin, S. E. Ehtesham and R. B. Gregory, *Anal. Chem.*, 63 (1991) 2825, and references cited therein.
- 92 L. Valtcheva, J. Mohammad, G. Pettersson and S. Hjertén, paper presented at the *Euchem Conference on Capillary Electro-separations, December 9–11th, 1991, Storlien, Sweden*.
- 93 S. Bernbaum, paper presented at the *Euchem Conference on Capillary Electro-separations, December 9–11th, 1991, Storlien, Sweden*.
- 94 S. Hjertén, *J. Chromatogr.*, 347 (1985) 191.
- 95 R. Kuhn, T. Bereuter, F. Stoecklin, C. Morin and F. Erni, presented at the *4th International Symposium on High-Performance Capillary Electrophoresis, Amsterdam, February 9–13th, 1992*.
- 96 J. L. Carpenter, D. M. Goodall, P. Camilleri and G. N. Okafo, presented at the *4th International Symposium on High-Performance Capillary Electrophoresis, Amsterdam, February 9–13th, 1992*.
- 97 S. Mayer and V. Schurig, presented at the *4th International Symposium on High-Performance Capillary Electrophoresis, Amsterdam, February 9–13th, 1992*.

Shock layer thickness in the case of wide bands of single components and binary mixtures in non-linear liquid chromatography

Zidu Ma and Georges Guiochon

Department of Chemistry, University of Tennessee, Knoxville, TN 37996-1501, and Division of Analytical Chemistry, Oak Ridge National Laboratory, Oak Ridge, TN 37831-6120 (USA)

(First received January 28th, 1992; revised manuscript received May 21st, 1992)

ABSTRACT

The ideal model predicts the formation of a concentration shock on one side of an elution band, depending on the curvature of the isotherm. However, when a real column is used, a true concentration shock cannot form and a very steep boundary occurs instead, which is called a shock layer. It propagates at the same velocity as the ideal shock. The thickness of the shock layer has been defined and calculated by Rhee and co-workers in the case when the injection profile is a rectangular band wide enough for the elution profile to contain a constant state, *i.e.*, a plateau at the injection composition. This result is used to investigate the properties of binary frontal analysis in chromatography. Experimental results are in good agreement with the theory.

INTRODUCTION

When large-size samples are injected into a chromatographic column and the equilibrium isotherms of the sample components are not linear, the elution band profile is highly unsymmetrical. The theory of ideal, non-linear chromatography (assuming an infinite column efficiency) predicts a very different behavior for the two sides of the band. One side is diffuse. A self-sharpening effect, leading eventually to the formation of a concentration discontinuity or shock, takes place on the other side of the elution band [1–8]. This result is explained by considering the profile of a band moving along an ideal column as a concentration wave [4–7,9].

The ideal model predicts that under isothermal, isocratic conditions, each concentration moves at a constant velocity [1–4,7–10]. The velocity associated with a concentration depends on the slope of the

equilibrium isotherm for this concentration, and increases with decreasing slope of the isotherm. Hence, for a convex upward isotherm, the concentration velocity increases with increasing concentration. However, high concentrations cannot pass low ones. When this phenomenon tends to occur, the band acquires a front concentration discontinuity instead [4,7,8,11]. Conversely, if the isotherm is convex downward, a discontinuity appears on the band rear. In the wave theory, these discontinuities are called shocks or shock waves [1,4–8].

Actually, chromatography can never be carried under the ideal model conditions. Although the efficiency of modern columns is high, it is never infinite as postulated by the ideal model, but remains finite. The separation process is not described by the ideal model but by the non-ideal, equilibrium-dispersive model [1–4,8,12–15]. This model predicts an erosion or smoothing of the discontinuity, resulting in a steady-state layer in which the concentration varies very steeply. This thin layer is called a shock layer [1,5–8,12–15]. It is centered on the shock

Correspondence to: Dr. G. Guiochon, Department of Chemistry, University of Tennessee, Knoxville, TN 37996-1501, USA.

predicted by the ideal model and travels at the same velocity [12–14].

The formation of shock layers results from the competitive influence of two phenomena, one of thermodynamic and the other of kinetic origin. The phenomenon has been studied in detail by Rhee and co-workers [12–15] from a theoretical viewpoint. On the one hand, as just explained, different concentrations propagate at different velocities because of the non-linear behavior of the isotherm. Because there can be only one concentration value at a given time in a given point of the column, concentrations tend to pile up either at the front (convex upward isotherm) or the rear (convex downward isotherm) of the band. The corresponding part of the profile becomes steeper and steeper and a discontinuity would form, but for the finite column efficiency. On the other hand, the concentration gradient at a discontinuity would be infinite, which creates (Fick's law) an infinite flux of axial diffusion; the rate of mass transfers in the column is finite and this does not permit the propagation of a concentration discontinuity, *i.e.*, of an instantaneous change in concentration.

Thus, at the band boundary resulting from the competition between the sharpening thermodynamic process and the dispersing kinetic process, a dynamic equilibrium or steady state is reached and a shock layer is formed. Because the phenomenon is related to the mass transfer kinetics, we can expect a relationship between the shock layer thickness and the column efficiency. The shape of the other band boundary is determined by the combination of the non-sharpening (or spreading) thermodynamic process and the dispersing kinetic process, both of which disperse the boundary. In the case of a single component, the above phenomena result simply in one boundary being self-sharpening and very steep, while the other is non-sharpening and tails. With two components, the general trend can still be observed, but with more complications [2–4, 7–9, 15, 16].

Shock layers play an important role in the practice of non-linear chromatography and especially in frontal analysis, in displacement chromatography and in overloaded elution. One of the many applications of a shock layer theory would be the prediction of the minimum column efficiency necessary for a correct measurement of competitive isotherms by

frontal analysis. The observation of an intermediate plateau in the breakthrough curve of the binary mixture is necessary for the calculation of the amount of each solute adsorbed on the stationary phase, using an integral mass balance [17]. The formation of this intermediate plateau is not instantaneous with a column of finite efficiency [9, 16–18]. If the time needed for the formation of the intermediate plateau is longer than the retention time of the lesser retained component, this plateau does not appear and the results of the isotherm measurement are erroneous. An interpolation method can be used [17, 18], but some minimum efficiency is needed to ensure the necessary accuracy.

Other applications of a shock layer theory are in displacement and overloaded elution preparative chromatography. The yield of the separation run of a mixture in fractions of certain components having a given degree of purity is determined by the width of the intermediate zone between the two purified fractions, hence by the shock layer thickness for each component. Being able to predict the shock layer thickness would permit a rapid estimate of these yields.

In this paper, we discuss the mathematical concepts of shock and shock layer, show how these concepts can be used for practical applications and give a numerical study of the formation and stabilization of a shock layer. Finally, we discuss the dependence of the shock layer thickness and of the time needed for its formation on the height of the concentration jump and the column efficiency.

THEORY

A general model for the behavior of a multi-component mixture in a chromatographic column is obtained by combining the mass balance equation for each component of the system and the kinetic equations relating the rate of variation of the concentration of each component in the stationary phase to the concentrations of all the components in both phases. The mass balance is written as

$$\frac{\partial c_i}{\partial t} + F \cdot \frac{\partial q_i}{\partial t} + u_0 \cdot \frac{\partial c_i}{\partial x} = D_{a,i} \cdot \frac{\partial^2 c_i}{\partial x^2} \quad (1)$$

where c_i and q_i are the concentrations of component i in the mobile and the stationary phase, respectively, $F = (1 - \epsilon)/\epsilon$ is the phase ratio, u_0 is the linear

velocity of the mobile phase and $D_{a,i}$ is the apparent dispersion coefficient. We shall assume here that the column efficiency exceeds 100 theoretical plates, so that the solution of the problem is identical with the solution of the equilibrium-dispersive model [4,8]. In this latter model, the concentration in the stationary phase is given by the equilibrium isotherm [$q_i = q_i(c_1, c_2, \dots, c_k)$ for a k -component mixture] and the influence of the finite column efficiency, due to the axial dispersion and the finite rate of the kinetics of mass transfers, is accounted for by using a proper apparent dispersion coefficient in the right-hand side of eqn. 1. We see later in the discussion the extent of the validity of the equilibrium-dispersive model and its limitations.

The integration of the system of partial differential equations such as eqns. 1 written for each component of the mixture requires initial and boundary conditions. Typical conditions are

$$c_i(t, x = 0) = \phi_i(t) \quad (2)$$

$$c_i(t = 0, x) = 0 \quad (3)$$

$$i = 1, 2$$

where $\phi_i(\cdot)$ is the boundary condition of the problem or concentration profile of each component at the column inlet. In elution, it is a pulse called the injection profile and often represented by an impulse (Dirac problem). In frontal analysis, it is a concentration jump (Riemann problem). When a rectangular band of concentrations C_i^0 and width t_p is injected, and t_p is large enough that the elution profile contains a constant state, *i.e.*, a plateau at C_i^0 , the solution is practically equivalent to that of two successive Riemann problems corresponding to concentration jumps of the same magnitude and opposite signs.

In the particular case of this study, q_i is related to the mobile phase concentration of the two solutes, c_1 and c_2 , through the competitive Langmuir isotherm:

$$q_i = \frac{a_i c_i}{1 + \sum_{j=1}^2 b_j c_j} \quad a_i = q_{s,i} b_i \quad (4a)$$

or

$$Q_i = \frac{C_i}{1 + \sum_{j=1}^2 C_j} \quad i = 1, 2 \quad (4b)$$

where $C_i = b_i c_i$ and $Q_i = q_i / q_{s,i}$. For the sake of clarity in the forthcoming equations, we denote by C_i and Q_i the dimensionless concentrations of the i th component in the mobile and the stationary phases, respectively. Eqns. 4 are thermodynamically consistent only if $q_{s1} = q_{s2}$ (case of certain enantiomeric separations [19]). Otherwise, the Levan-Vermeulen competitive isotherm [20] must be used and only numerical solutions are possible.

The concentration profile through the shock layer can be calculated analytically in the case of a breakthrough curve and a Langmuir (single component [12–14]) or a competitive Langmuir (binary mixture [15]) isotherm. The demonstration is briefly summarized in the next section for convenience.

Shock layer profile in the case of a single component

The study of the experimental conditions under which a breakthrough curve adopts a constant pattern behavior (*i.e.*, propagates unchanged) and of how long a time or distance of travel is required for it to approach this steady state goes back to the 1940s and the work of Thomas [21]. This work, and the results of other early studies, were summarized by Vermeulen [22]. Cooney and Lightfoot [23] established the constant pattern conditions and Thomas and Lombardi [24] gave experimental proofs of the validity of this work. Finally, Rhee and co-workers [12–15] derived an equation relating the shock layer thickness to the experimental parameters, provided that the kinetics of mass transfer are rapid and can be accounted for by a constant dispersion coefficient, D_a , which lumps axial dispersion and finite mass transfer kinetics. Although this is an approximation, it is consistent with the agreement previously reported between experimental band profiles and the prediction of the equilibrium-dispersive model in most cases of practical interest in preparative chromatography [19].

Let $\eta = x/U_s - t$, where U_s is the velocity of the shock [4]:

$$U_s = \frac{u_0}{1 + k'_0 \Delta Q / \Delta C} \quad (5)$$

where ΔQ and ΔC are the amplitudes of the concentration shock in the stationary and mobile phases, respectively, and $k'_0 = Fa$ is the column capacity factor (or retention factor). In practice, we shall consider either profiles along the column ($t =$

constant) or profiles at the column exit ($x = L$). We assume that the shock velocity is constant, *i.e.*, that we have reached a dynamic steady state. Then, the profile of the shock layer does not depend on time any longer, it depends only on η . For a single component, when the kinetics of mass transfer are infinitely fast, but apparent dispersion remains finite, eqn. 1 becomes

$$\frac{D_a}{u_0 U_s^2} \cdot \frac{d^2 C}{d\eta^2} - \frac{1}{U_s} \cdot \frac{dC}{d\eta} + \frac{1}{u_0} \left(1 + k'_0 \cdot \frac{dQ}{dC} \right) \frac{dC}{d\eta} = 0 \quad (6)$$

It is known that in the case of a convex-upward isotherm, a front shock layer appears on the breakthrough curve and stabilizes [4,7]. When η tends towards $-\infty$ or $+\infty$, C tends towards C_0 or 0, respectively, and in both cases the differential $dC/d\eta$ tends towards 0. Eqn. 6 can be integrated and we obtain [15]

$$\Delta\eta = D_a \cdot \frac{(1 + K)^2}{u_0^2 K} \cdot \left(\frac{C_0 + 1}{C_0} \cdot \ln \left| \frac{C_r - C_0}{C_1 - C_0} \right| - \frac{1}{C_0} \cdot \ln \left| \frac{C_r}{C_1} \right| \right) \quad (7)$$

where $\Delta\eta$ is the time between the moments when the component concentrations are C_1 and C_r at the column outlet, respectively, C_0 is the dimensionless mobile phase concentration at the injection, D_a is the apparent axial dispersion coefficient accounting for the deviations from the ideal equilibrium theory and

$$K = k'_0 / (1 + C_0) \quad (8a)$$

is the amount adsorbed by the stationary phase at equilibrium between the two phases. The isotherm is given by eqn. 4b, for a single component. As a first approximation, we could assume that

$$D_a = H u_0 / 2 \quad (8b)$$

where H is the column height equivalent to a theoretical plate. It would probably be more exact to use another equation, derived previously in an investigation of the kinetic models of chromatography (ref. 25, eqn. 19), and which gives a different weight to the axial dispersion and the mass transfer resistance terms than the conventional HETP equation of linear chromatography. However, this question deserves a more thorough investigation, currently undergone in connection with an experimental study.

Obviously, eqn. 7 gives the concentration profile across the shock layer. This profile is symmetrical, which is due to the assumption of a constant dispersion coefficient. Experiments show the validity of this conclusion in most practical cases, as long as the column efficiency is not very low. In theory, eqn. 7 only applies to the wave in an infinitely long column. We can record the profile as it moves past

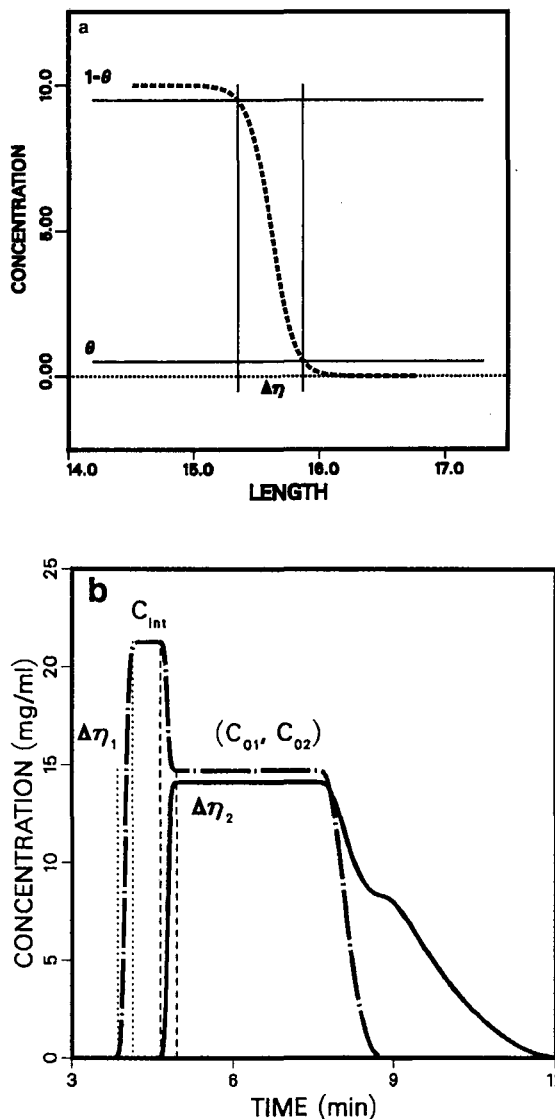


Fig. 1. Schematic diagrams of the shock layer profile and definition of the symbols introduced. (a) Single-component case; (b) two-component case. Length in cm.

certain positions along this column and follow the trend towards an asymptotic profile.

The thickness of the shock layer as given by eqn. 7 depends on the choice of the concentrations C_1 and C_r . It is convenient to define and use the following parameter:

$$\theta = \frac{C_1^* - C_1}{C_1^* - C_r^*} = \frac{C_r - C_r^*}{C_1^* - C_r^*} \quad (9)$$

Fig. 1 shows a schematic diagram of the shock layer profile and of the symbols just defined. In the case of the injection of a concentration plateau, C_0 , into an empty column, $C_1^* = C_0$ and $C_r^* = 0$, so $C_1 = (1 - \theta)C_0$. As expected for an actual column, it takes an infinite time to achieve the total concentration variation, from C_1^* to C_r^* , *i.e.*, for $\theta = 0$, the thickness of the shock layer is infinite. On the other hand, for $C_1 = C_r = C_m$, $\theta = 1/2$ and the thickness is 0. For small but finite values of θ , the thickness of the shock layer is finite and is given by

$$\Delta\eta(\theta) = \frac{H(1+K)^2}{2u_0K} \cdot \frac{2+C_0}{C_0} \cdot \ln\left|\frac{1-\theta}{\theta}\right| \approx \frac{H(1+K)^2}{2u_0K} \cdot \frac{2+C_0}{C_0} |\ln\theta| \quad (10)$$

Finally, we note that to derive the thickness of the shock layer along the column or in time units, we need to project the thickness $\Delta\eta$, calculated along the η axis, on the corresponding, length or time, coordinate axis.

Shock layer profile in the case of two components

In the case of two components, the apparent dispersion (molecular and eddy diffusion) and the resistance to mass transfer between the two phases both contribute to the thickness of the shock layer [15]. Rhee and Amundson [15] have shown that if the column efficiency is finite because either the kinetics of mass transfer are infinitely fast and the axial dispersion is finite, or the axial dispersion is negligible but the rate of the mass transfer kinetics is finite, the profile of the shock layer can be integrated in closed form. However, when both the axial dispersion and the mass transfer kinetic contributions to the column efficiency are significant, which is most often the case in chromatography, there is no closed-form solution. A numerical solution only can be derived.

In the case of a wide rectangular injection band or a step input, we have a simple wave solution for the breakthrough front [4,5,8,15,16]. When the mass transfer kinetics are infinitely fast and the equilibrium isotherm is convex upwards, concentration shocks take place in the front boundary of the profiles [4,15]. The following relationship results from the simple wave solution of the system of eqns. 1 for two components, $i = 1, 2$:

$$c_1 = \xi c_2 + A \quad (11)$$

where ξ satisfies the following equation [4–6,8,16]:

$$\xi^2 f_{21} + \xi(f_{22} - f_{11}) - f_{12} = 0 \quad (12a)$$

where

$$\xi = \frac{dc_1}{dc_2}, f_{ij} = \frac{\partial q_i}{\partial c_j} \text{ with } i, j = 1, 2 \quad (12b)$$

Eqn. 12a is a general relationship which holds for any kind of isotherm function (Appendix I); ξ is known whenever the isotherm function is available.

In the case of the Langmuir isotherm (eqns. 4), however, ξ and A in eqn. 11 are constant for a given experiment, *i.e.*, they depend only on the concentrations C_1^0, C_2^0 of the wide rectangular injection pulse. Then, eqn. 11 becomes

$$c_1 = \xi c_2 + \frac{a_1 - a_2}{a_2 b_1 + a_1 b_2 / \xi} \quad (13)$$

Using eqn. 8, we can rewrite the isotherm of the second component (eqn. 4, $i = 2$) as follows:

$$q_2 = A_2 c_2 / (1 + B_2 c_2) \quad (14)$$

with

$$A_2 = a_2 / (1 + b_1 A) \quad (14a)$$

and

$$B_2 = (b_1 \xi + b_2) / (1 + b_1 A) \quad (14b)$$

with

$$A = \frac{a_1 - a_2}{a_2 b_1 + a_1 b_2 / \xi} = \frac{1 - \alpha}{\alpha b_1 + b_2 / \xi} \quad (14c)$$

Thus, in the case of a simple wave solution (frontal analysis or wide rectangular injection), the competitive isotherm of the two solutes, when these isotherms are accounted for by the competitive Langmuir model, can be decoupled in the interactive

region [4–6,8,16]. Because separation takes place between the two components, as shown in Fig. 2, the profile of the shock layer at the front of the less retained component band is given by the same mass balance equation as in the single-component case with the single-component isotherm (eqn. 4), while the shock layer at the front of the more retained component band is given by the same form of the mass balance equation, but using the decoupled isotherm function (eqn. 14a):

$$\frac{D_a}{u_0 U_{s,2}^2} \cdot \frac{d^2 C_2}{d\eta^2} - \frac{1}{U_{s,2}} \cdot \frac{dC_2}{d\eta} + \frac{1}{u_0} \left(1 + K_0 \cdot \frac{dQ_2}{dC_2} \right) \frac{dC_2}{d\eta} = 0 \quad (15)$$

where

$$U_{s,2} = \frac{u_0}{1 + K_0 \Delta Q_2 / \Delta C_2} \quad (16)$$

and $K_0 = FA_2$. Note that, in order to apply this concerted disturbance approach, we have to assume that the two dispersion coefficients, $D_{a,1}$ and $D_{a,2}$, are identical.

The shock layer thickness of the first component band is given by the same equation as used in the case of a single component (*i.e.*, eqn. 10), with a single-component isotherm function, provided, however, that the concentration of the intermediate plateau, $C_{1,m}$, be used instead of $C_{1,0}$. The shock layer thickness at the boundary between the two components is obtained also with eqn. 10, but using the isotherm parameters given above in eqns. 14 [15]. For concentration profiles along the column ($t = \text{constant}$), the less retained component profile drops from the intermediate concentration to zero with increasing abscissa, whereas for the more retained component it drops from $C_{2,0}$ to zero. Eqn. 6 can be used in the two-component case to calculate the thickness of the shock layers. The parameters of the single-component isotherm are used for the less retained component and the decoupled isotherm parameters for the more retained component.

The concentration profile of the rear shock layer of the first component band given in reduced units (*i.e.*, θ) is the same as the concentration profile of the front shock layer of the second component band, except that the change in concentration is negative for the first component and positive for the second.

Formation of the intermediate plateau in the frontal analysis of binary mixtures

When a step of a binary mixture is introduced into a column, the front of the first-component band moves faster than the front of a band of the same first component, pure, at the same concentration. This is the displacement effect. As a consequence, the concentration of the first component in the first part of the breakthrough front, where it is pure, exceeds the boundary concentration, $C_{1,0}$ (Fig. 2). Ideally, with an infinitely efficient column, the concentration plateau is reached immediately at injection. With a real column, the formation of this intermediate plateau is not instantaneous. It takes a certain time before a steady state is achieved for the front of the breakthrough curve. We can calculate this time if we know the dependence of the thickness of the shock layer on the experimental parameters, and especially on the column efficiency and the height of the concentration plateau injected into the column. Beyond that time, the shock layer profile remains identical and the plateau expands because the front shock layer propagates faster than the intermediate one. Hence, there is a minimum column efficiency below which the accurate determination of competitive isotherm by frontal analysis is not possible. The shock layer theory permits its determination.

At the front boundary of the breakthrough profile, the fluxes of both solutes caused by convection are

$$J_1 = c_{1,0} U_1 \quad (17a)$$

$$J_2 = c_{2,0} U_2 \quad (17b)$$

where the two shock velocities, U_1 and U_2 are

$$U_1 = \frac{u_0}{1 + F \Delta q_1 / \Delta c_1} \quad (18a)$$

$$U_2 = \frac{u_0}{1 + F \Delta q_2 / \Delta c_2} \quad (18b)$$

where Δc_i and Δq_i are the concentration jumps in the mobile phase and the stationary phase, respectively. The difference between the flux given by eqns. 17a and 17b gives the amount, n_1 , of the less retained compound which is separated from the mixture and elutes pure, between the two shocks, after a certain

time Δt , has elapsed. It is

$$n_1 = \int_0^{\Delta t} (J_1 - J_2) dt = (c_{1,0}U_1 - c_{2,0}U_2)\Delta t \quad (19)$$

With a real column, the intermediate plateau does not appear instantaneously. As shown in Fig. 2, the amplitude of the first-component shock layer grows progressively, so a peak appears in front of the injection plateau. When the height of this peak becomes equal to the concentration of the intermediate plateau, the amount of the less retained compound which is between the two shock layers is

$$n_1 = \frac{1}{2} \Delta c_{\text{int}} (\Delta \eta_1 + \Delta \eta_2) \quad (20)$$

Combining eqns. 17 and 18 gives the following relationship:

$$\Delta t = \frac{1}{2} \frac{\Delta c_{\text{int}} (\Delta \eta_1 + \Delta \eta_2)}{c_{1,0}U_1 - c_{2,0}U_2} \quad (21)$$

where Δc_{int} is the difference between the first-component concentrations on the intermediate, enriched plateau and just before the injection; $c_{1,0}$ and $c_{2,0}$ are the concentrations of the two components after the injection. $\Delta \eta_1$ and $\Delta \eta_2$ are the thicknesses of the two shock layers in length units. Eqn. 21 is a useful approximation. A more exact relationship can be obtained (Appendix II).

Numerical calculations

For numerical calculations, a finite difference scheme was used [26,27]. The continuous plane z, t , in which the concentrations c_i are defined, is replaced by a grid $j\Delta z, \eta\Delta t$, where Δz and Δt are the space and time increments chosen for the integration and j and n are integers. The partial differential eqns. 1 are replaced by the finite difference equations

$$\frac{c_{i,j}^{n+1} - c_{i,j}^n}{\Delta t} + F \cdot \frac{q_{i,j}^{n+1} - q_{i,j}^n}{\Delta t} + u_0 \cdot \frac{c_{i,j}^n - c_{i,j-1}^n}{\Delta x} = 0 \quad (22)$$

This equation defines a computation scheme which is implicit with respect to the unknown concentration [28]. By setting the time increment, Δt , to a small enough value, the numerical dispersion introduced in the calculations can be made relatively independent of the concentration because the simulated

HETP is related to the time and space increment, in the case of single component, by the following equation [26]:

$$H = \Delta x - \frac{u_0 \Delta t}{1 + Fdq/dc} \quad (23)$$

Then, the space increment can be set equal to H . The program is written in Fortran and run on the VAX8800 cluster of the UTCC.

The thickness of the shock layers of the profiles obtained by numerical calculations can be obtained either directly from the breakthrough curve, using eqn. 9 and interpolating linearly between the calculated points of the numerical solution, or by differentiating the front of the concentration profiles of the two solutes (Fig. 3), computing the second-order moment of these differential profiles which are nearly Gaussian and taking a value equal to four times the standard deviation corresponding to this variance.

For the numerical calculations discussed in this work, we have chosen a column length of 25 cm and a phase ratio $F = 0.35$. The hold-up time, t_0 , is 3.00 min and the width of the rectangular injection plug is 4.50 min. In many instances the elution profile of the band tail, which is not relevant to this work, is not reported. Unless the influence of the column efficiency is studied, $H = 0.0125$ cm. Unless the influence of the height of the pulse is studied, $C_0 = 10$ mg/mL for both solutes. The isotherm parameters are $a_1 = 1.97$, $a_2 = 3.70$, $b_1 = 0.0396$ and $b_2 = 0.0411$. The relative retention of the two components under analytical conditions is 1.87. The ratio of the integration increments, $\delta t/\delta x$, was set equal to 0.2, unless the influence of that ratio was being studied (the Courant number is $u_z \delta t/\delta x$).

RESULTS AND DISCUSSION

We present successively the results of the numerical calculations explained in the previous section and a series of experimental results collected in frontal analysis, using equipment, products and procedures described previously [16,29] or separately [18]. The separation studied is that of 2-phenylethanol and 3-phenylpropanol on a 25×0.45 cm I.D. column packed with $10\text{-}\mu\text{m}$ particles of Vydac (Separations Group, Hesperia, CA, USA) C_{18} chemically bonded silica, with water-methanol

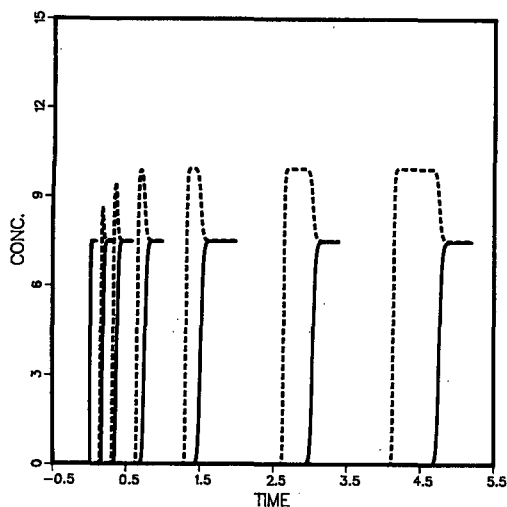


Fig. 2. Elution profiles at different column lengths. From left to right, 1 = 0.1 cm, 2 = 1 cm, 3 = 2 cm, 4 = 4 cm, 5 = 8 cm, 6 = 16 cm, 7 = 25 cm. The parameters used in the calculation are the same as in Table I. Solid line, more retained compound; dashed line, less retained compound. Column: $L = 25$ cm; $H = 0.0125$ cm; $F = 0.35$; hold-up time, $t_0 = 3.00$ min. Isotherm parameters: $a_1 = 1.97$; $a_2 = 3.70$; $b_1 = 0.0792$; $b_2 = 0.0822$. Sample concentration: $C_0 = 7.5$ mg/ml for both solutes. Time in min; concentrations in mg/ml.

(50:50) as the mobile phase (1 ml/min). The column efficiency was 2500 theoretical plates for a very small injection of 3-phenylpropanol. Nearly rectangular plugs 4.5 min wide were injected.

Results of calculations

Fig. 2 shows the profiles of the breakthrough curves for the components of a binary mixture, at the exit of columns of increasing lengths. One can see

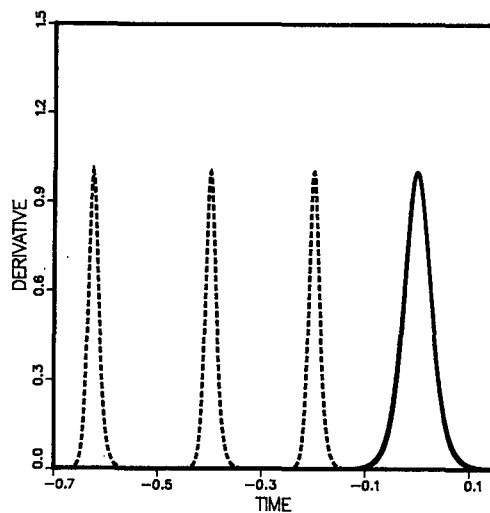


Fig. 3. Differentials of the fronts of last three sets of bands in Fig. 2. Solid line, more retained compound; dashed line, less retained compound. The origin of the time coordinate is at the front of the more retained compound, so differentials of the bands of the more retained compound are superimposed whereas those of the less retained compound are shifted. Units as in Fig. 2.

the rapid stabilization of the two shock layers, a peak rising at the top of the first-component breakthrough curve and the gradual formation of the enriched plateau of the lesser retained component accompanying the separation of the fronts of the two solutes. Differentials of the shock layer profiles are shown in Fig. 3 for the last three breakthrough curves in Fig. 2. These three differentials nearly coincide in the case of the second component. Since

TABLE I
RETENTION TIME AND THICKNESS OF SHOCK LAYERS

$t_{R,1}$ and $t_{R,2}$ are the retention times of the lesser and the more retained components, respectively. The velocities of the ideal concentration shocks are $U_{s,1} = 5.7350$ and $U_{s,2} = 4.8544$ cm/s. L is the column length. The parameters used for the calculations are the same as those used for Fig. 4.

L (cm)	$t_{R,1}$ (min)	$t_{R,2}$ (min)	$\Delta\eta_1$ (min)	$\Delta\eta_2$ (min)	U_{s1} (cm/s)	U_{s2} (cm/s)
2	0.3439	0.4064	0.0515	0.0886	5.816	4.921
4	0.6917	0.8185	0.0601	0.1104	5.783	4.887
8	1.3890	1.6428	0.0628	0.1267	5.760	4.870
12	2.7839	3.2921	0.0632	0.1345	5.747	4.860
25	4.3547	5.1490	0.0651	0.1364	5.741	4.855

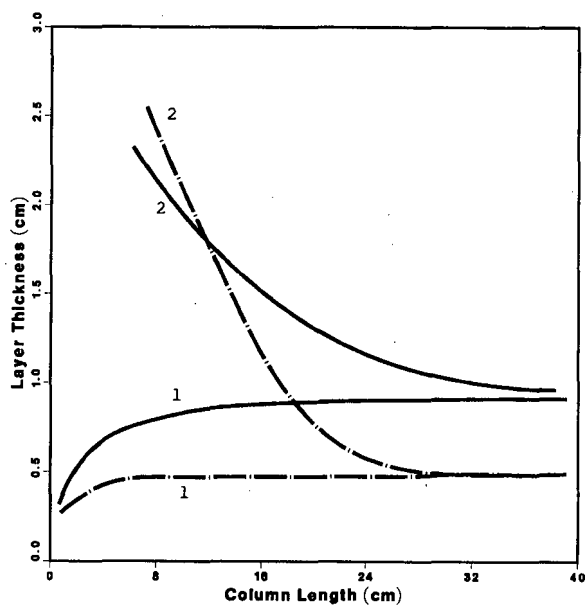


Fig. 4. Plot of the shock layer thickness versus the migration distance. Solid line, second front; dot-dashed line, first-component front. Lines 1, rectangular plug injection; lines 2, non-rectangular injection profile. Column: $L = 25$ cm; $H = 0.0125$ cm; $F = 0.35$; $t_0 = 3.00$ min. Isotherm parameters: $a_1 = 1.97$; $a_2 = 3.70$; $b_1 = 0.0396$; $b_2 = 0.0411$. Injection time: $t_p = 4.50$ min. Sample composition: $C_0 = 10$ mg/ml for both solutes.

the time origin is set at the center of the second shock layer, the distance between the two profiles increases with increasing column length and the differentials of the three profiles of the first-component breakthrough curves are almost identical but shifted. The values of the shock layer thicknesses are reported in Table I.

The injection profile is rectangular, *i.e.*, the front of the injection profile is a true shock and the initial thickness of the shock layer is zero. Because of the axial dispersion, the shocks of the two components separate, acquire round edges, a finite thickness which increases with increasing migration distance while the enriched plateau forms and reaches a stable height, defined by the isotherm function as shown in eqn. 8, and equal to A [16]. The shock layer profiles of both solutes tend rapidly towards a stable, steady-state shape, as shown in Fig. 3. The shock layer thickness tends towards a limit which is different for the two compounds (Fig. 4 and Table I). This behavior is profoundly different from what is observed in linear chromatography. In this last

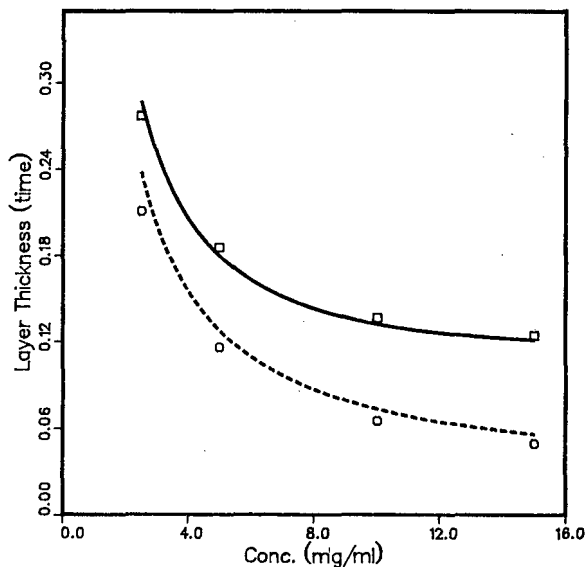


Fig. 5. Comparison of the shock layer thicknesses predicted by eqn. 10 (lines) and derived by numerical calculations (symbols) with different column loading concentrations. The thickness is in minutes. Solid line, more retained compound; dashed line, less retained compound. Calculation parameters as in Fig. 4.

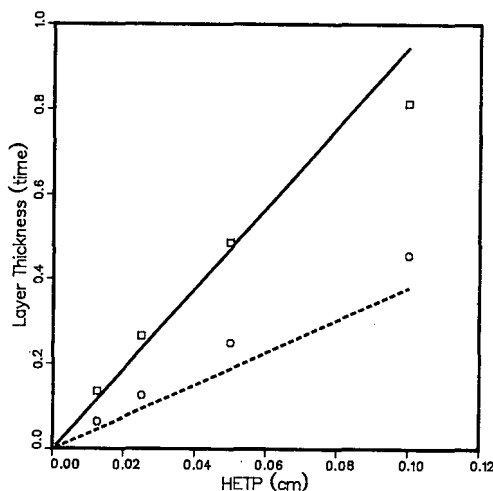


Fig. 6. Comparison of the shock layer thicknesses predicted by eqn. 10 (lines) and derived by numerical calculations (symbols) with columns having different efficiencies. The thickness is in minutes. Solid line, more retained compound; dashed line, less retained compound. Calculation parameters as in Fig. 4.

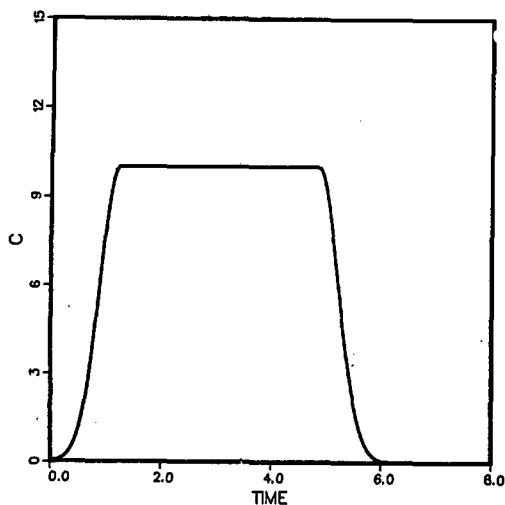


Fig. 7. Injection profile for the calculation of the diffused fronts. The other calculation parameters are the same as in Fig. 4. The injection concentration is 10 mg/ml for both solutes. Units as in Fig. 2.

case, the width of the front boundary of a profile is proportional to the square root of the column length and broadens constantly with increasing migration distance. In non-linear chromatography, in contrast, the thickness of the shock layer stabilizes rapidly when the enriched concentration plateau has been formed.

In Figs. 5 and 6 we compare the prediction of eqn. 10 for the thicknesses of the two shock layers and the results of the numerical calculations for the dependence of the thickness of the shock layer on either the height of the input concentration step (Fig. 5) or the column HETP (Fig. 6). The agreement is excellent. The minor discrepancies observed are due to numerical errors or result from the constraints of the numerical calculation of solutions of the chromatographic equations in the case of a binary mixture. These constraints have been discussed previously [26,27]. This problem is beyond the scope of the present study.

The calculations reported above were carried out using a rectangular injection profile. In order to assess the effect of a diffuse front of the injected step on the formation of the shock layers and on their profiles, the same calculations were performed using the injection profile shown in Fig. 7. Fig. 8a shows the front of the elution profiles inside the column at increasing times and, for the sake of comparison,

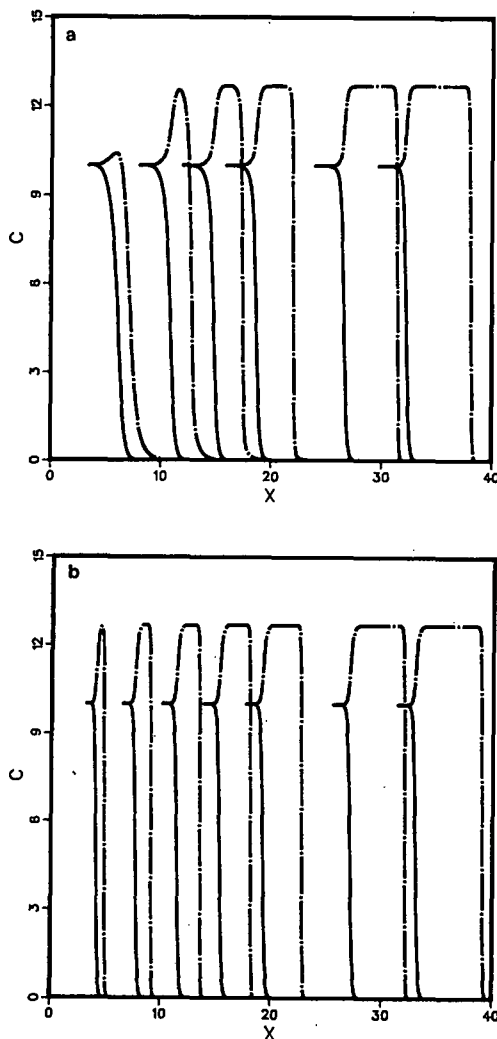


Fig. 8. Concentration profiles inside the column at different times (min). (a) From left to right, 1 = 2.042, 2 = 3.021, 3 = 3.833, 4 = 4.637, 5 = 6.282, 6 = 7.443. (b) From left to right, 1 = 0.842, 2 = 1.578, 3 = 2.352, 4 = 3.149, 5 = 3.956, 6 = 5.583, 7 = 6.801. Calculation parameters as in Fig. 4. The injection concentration is 10 mg/ml for both solutes. X in cm, C in mg/ml.

Fig. 8b shows the front of the elution profiles obtained for a truly rectangular plug injection. In the latter instance, the enriched plateau is more rapidly reached, after only *ca.* 8 cm, whereas in the former the enriched plateau forms more slowly, after *ca.* 16 cm. However, the shock layer profiles and their thicknesses reach the same limit value in both instances, as shown in Fig. 4, which compares the

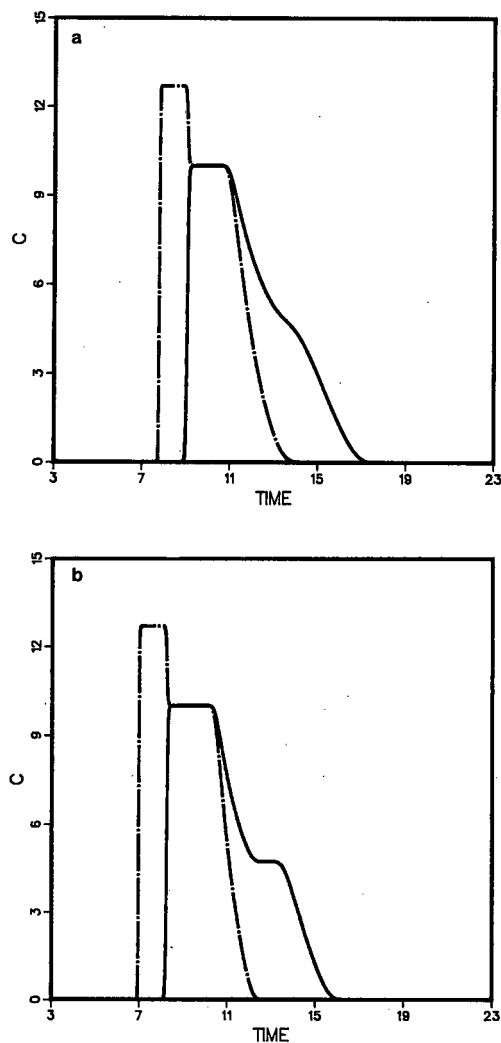


Fig. 9. Complete elution profile of a wide band at the outlet of a 40-cm long column. Solid line, more retained solute; dot-dashed line, less retained solute. Calculation parameters as in Fig. 4. The injection concentration is 10 mg/ml for both solutes. (a) Injection profile as in Fig. 7; (b) the injection profile is a rectangular plug. Units as in Fig. 2.

variation of the shock layer thickness with increasing column length for the two injection profiles. In Fig. 9a and 9b we compare the elution profiles corresponding to the two injection profiles, at the end of a 40-cm long column. Because of the strong selfsharpening effect due to the non-linear behavior of the isotherm, the breakthrough front of a binary mixture band at the outlet of a long enough column is the same in the case of a rectangular plug injection

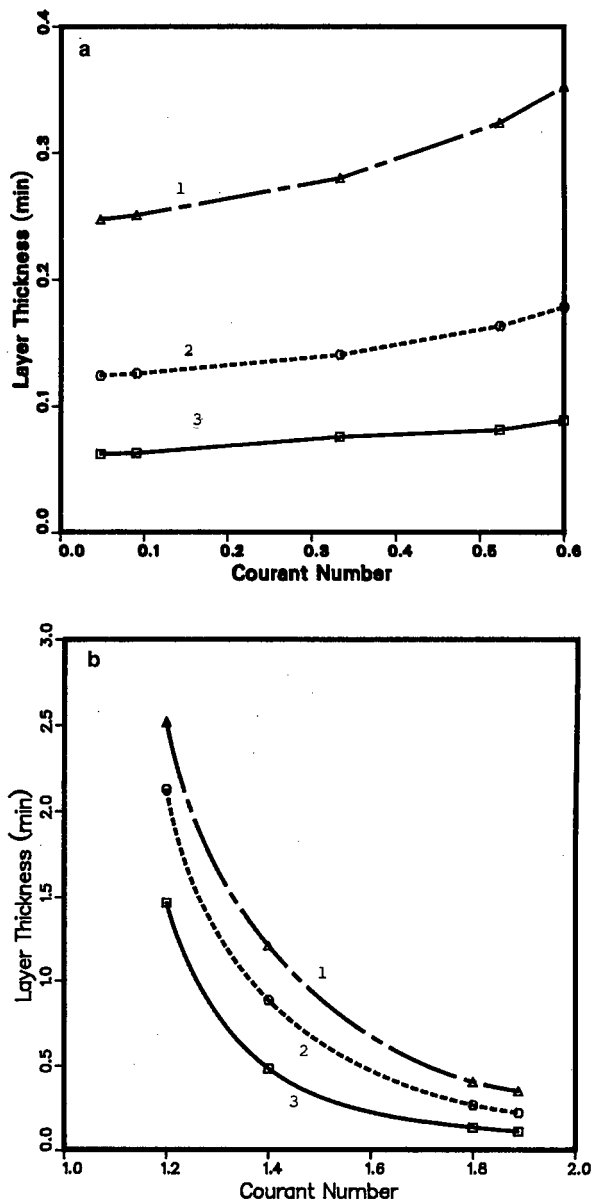


Fig. 10. Plot of the shock layer thickness versus the Courant number, $u_z \delta t / \delta x$, where δt and δx are integration increments. Line 1, $H = 0.05$ cm; line 2, $H = 0.025$ cm; line 3, $H = 0.0125$ cm. The other calculation parameters are as in Fig. 4. The injection concentration is 10 mg/ml for both solutes. (a) Calculations made using the Craig (space-like propagation) algorithm described in this work (eqn. 22); (b) calculations made using an alternate algorithm (time-like propagation, ref. 30).

or when the input step has a diffuse instead of a vertical front. The only difference between the elution profiles is in the diffuse, rear parts [16].

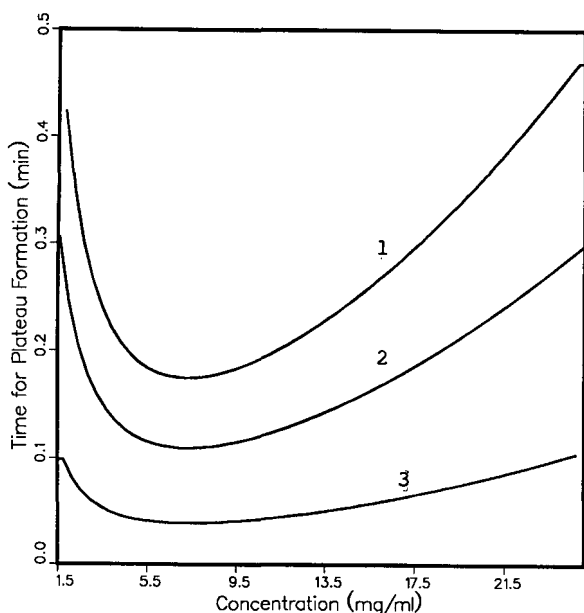


Fig. 11. Plot of the time (min) needed for the formation of the intermediate plateau. Results predicted by eqn. 21. The calculation was done using the same parameters as for Fig. 4. Curve 1, $\theta = 0.002$; curve 2, $\theta = 0.02$; curve 3, $\theta = 0.2$.

Next, we studied the dependence of the shock layer thickness on the parameters used in the numerical calculation. We show in Fig. 10a the variation of the shock layer with the Courant number, $u_z \delta t / \delta x$, where δt and δx are the integration increments, $u_z = u_0 / (1 + k'_0)$, u_0 is the mobile phase velocity and k'_0 is the retention factor under linear conditions [30]. Although the shock layer thickness is not constant, which is due to numerical approximations, the dependence is weak and can be neglected as a first approximation. The results presented here have been obtained with a ratio $\delta t / \delta x = 0.2$. For the sake of comparison, we show in Fig. 10b the same result for another calculation scheme [31], which has the great advantage over that used here of requiring approximately ten times less CPU time because the competitive Langmuir isotherm does not have to be inverted [27]. Unfortunately, that scheme exhibits a considerable dependence of the shock layer thickness on $u_z \delta t / \delta x$, and we had to use values of this ratio of the order of 2. Then, very similar results are obtained with both methods. Further calculations have shown that the thickness of the shock layer calculated by the method of

orthogonal collocation on finite elements is equal to the one predicted by eqn. 10 and does not depend on the values of δt and δx in the range of values where convergence is achieved [32].

Finally, we compare in Fig. 11 the plots of the time needed for the formation of the enriched plateau versus the intensity of the concentration jump in the input step, as derived from eqn. 21. Different values of θ were used. In the numerical calculations, we assume that the enriched plateau is formed when the theoretical value of its concentration is reached at two successive nodes of the grid (for two successive values, k and $k + 1$, of j , see eqn. 22), *i.e.*, if the plateau in a concentration profile along the column is more than $2H$ wide. We note in Fig. 11 that the formation time of the plateau is shorter when large values of θ are used, although the shape of the plot remains unchanged.

The existence of an optimum step height for which the plateau formation time is a minimum is one of the most important features of eqn. 21. Other calculation results (not shown) indicate that, when the HETP is low and a diffuse injection front is used, the minimum is shifted towards higher concentration jumps. When frontal analysis is used for isotherm determination, the height of the successive step should be kept neither too low nor too high to ensure the formation of the enriched plateau at the column outlet and achieve accurate results [18].

Experimental results

Fig. 12a and b compare the dependence of the shock layer thickness on the concentration jump, as calculated from eqn. 10, using the same isotherm parameters as used in Fig. 5 (solid line), and as measured experimentally (symbols). The experimental data in Fig. 12a derived from the detector response (Fig. 13a), by calculating the response differential (Fig. 13b) and determining the width of the peak obtained at half-height. We see that the derivative peaks in Fig. 13b are unsymmetrical. A detailed study of the cause of the asymmetry of the derivative peaks has been made by Rhee and Amundson [15]. In this study we were interested only in the width of the shock layer, not its shape.

The experimental results obtained are in general agreement with the prediction of the shock layer theory and confirm its validity. The shock layer thickness was calculated from eqn. 10, using a value

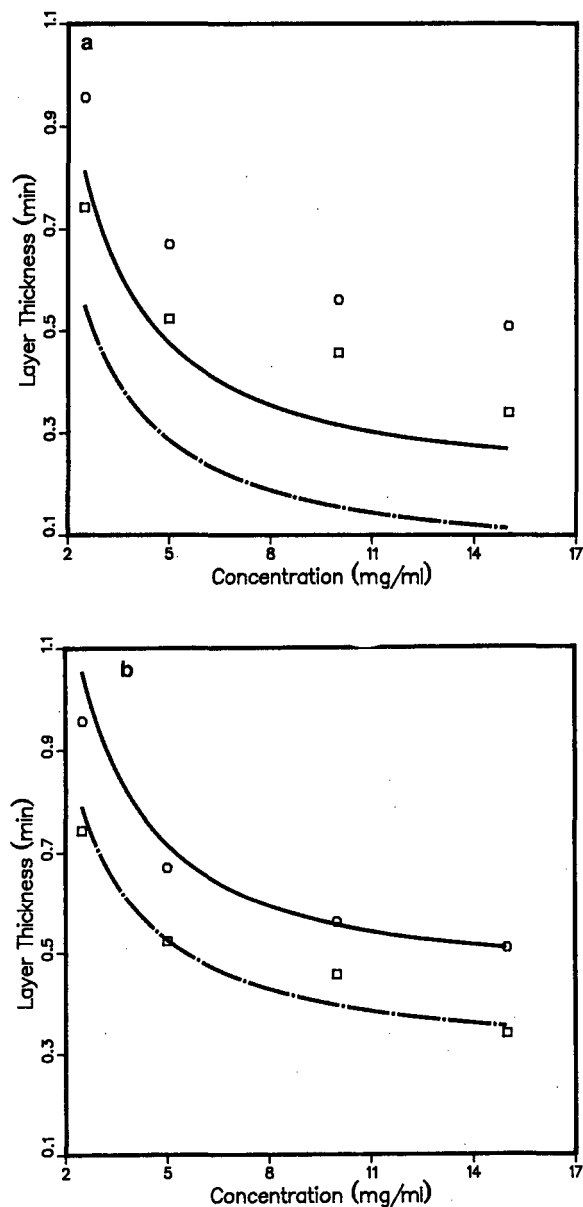


Fig. 12. Comparison between the variations of the shock layer thickness with the concentration jump as predicted by eqn. 10 (lines) and as measured experimentally (symbols). (a) Results. Solid line, more retained compound; dot-dashed line, less retained compound. (b) Same as (a), but theoretical curve shifted upward by 0.25 mm.

of $\theta = 0.02$ and a column HETP of 0.01 cm. The experimental and calculated results follow the same trend. However, for a given step concentration,

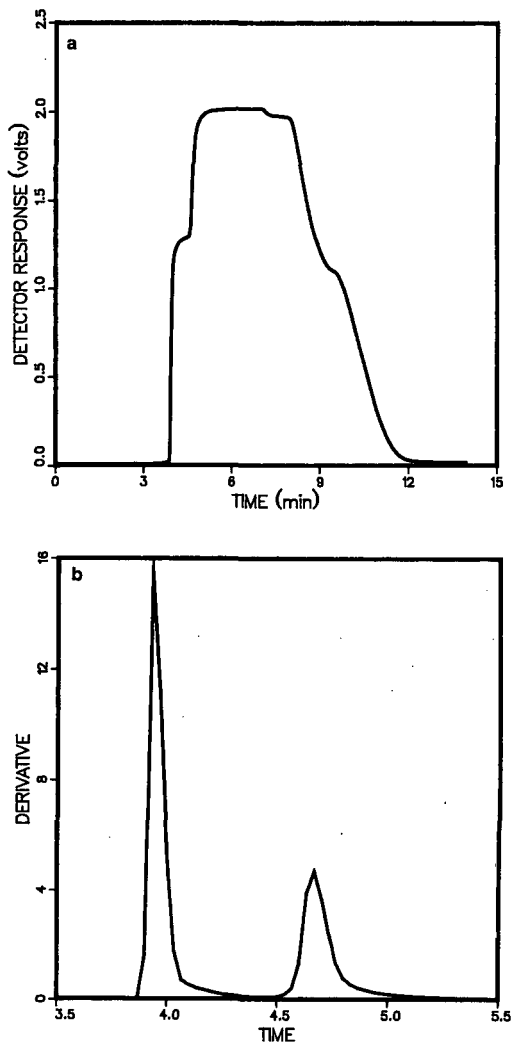


Fig. 13. (a) Elution profile of a wide injection band of a binary mixture and (b) its differential. Time in min.

there is a nearly constant difference of 0.25 mm between the measured and predicted thickness. A vertical shift of the theoretical curve by 0.25 mm would bring it into coincidence with the data points. The predicted shock layer is 10-50 s, so a significant detector contribution is improbable, but there might be several reasons for observing a shock layer thickness greater than predicted. For example, the theoretical curve would fit exactly the experimental data points with $H = 0.0275$ cm. The column HETP measured at infinite dilution is different for the two components. An average value is used when apply-

ing eqn. 10 to calculate the second-component shock layer thickness, which is incorrect [15]. More important, the actual system used does not follow the competitive Langmuir behavior, but deviates significantly from it [16,33], which may have an effect on the shock layer thickness. Further investigations are needed to clarify this question.

CONCLUSIONS

Experimental results and those of calculations based on the semi-ideal model confirm the validity of the shock layer theory derived by Rhee and Amundson [12–15]. Shock layers do travel at nearly the same velocity as predicted by the ideal model for the concentration shock itself. The thickness of the shock layer, once it has fully developed, *i.e.*, when a dynamic steady state has been established, depends only on the isotherm, on the height of the concentration jump injected and on the HETP of the column, as shown by eqn. 10. On the other hand, it is independent of the column length.

The development of a shock layer, at the difference of a concentration shock in the ideal model, is not instantaneous. The formation of the enriched plateau of the lesser retained compound is not instantaneous. The time it takes to appear depends on the height of the concentration jump and on the column HETP.

As we have shown, the shock layer theory permits the calculation of the minimum column efficiency necessary to perform an accurate determination of competitive isotherms by frontal analysis. Preliminary experimental results demonstrate the usefulness of the approach. The agreement between the theoretical prediction (eqn. 10) and the experimental data is still not exactly quantitative, however, because of some experimental problems (definition of the HETP in high-concentration chromatography, deviation of the competitive isotherm from Langmuir behavior), problems which have been identified but not yet solved. Further investigations of these problems are in progress. The application of this theoretical study to the determination of the relationship between recovery yield and column efficiency and to the optimization of the experimental conditions in displacement chromatography has also been examined [18].

ACKNOWLEDGEMENTS

We acknowledge Sadroddin Golshan-Shirazi (University of Tennessee) for fruitful discussions. This work was supported in part by grant CHE-89-01382 from the National Science Foundation and by the cooperative agreement between the University of Tennessee and the Oak Ridge National Laboratory. We acknowledge support of our computational effort by the University of Tennessee Computing Center.

APPENDIX I

The total differentials of the two stationary phase concentrations are

$$\frac{Dq_1}{Dc_1} = \frac{\partial q_1}{\partial c_1} + \frac{\partial q_1}{\partial c_2} \cdot \frac{Dc_1}{Dc_2} = \frac{\partial q_1}{\partial c_1} + \frac{\partial q_1}{\partial c_2} \cdot \frac{1}{\xi} \quad (\text{I-1a})$$

$$\frac{Dq_2}{Dc_2} = \frac{\partial q_2}{\partial c_1} \cdot \frac{Dc_1}{Dc_2} + \frac{\partial q_2}{\partial c_2} = \frac{\partial q_2}{\partial c_1} \xi + \frac{\partial q_2}{\partial c_2} \quad (\text{I-1b})$$

and the mass balance equations of the ideal model (eqns. 1 with $D_a = 0$) become

$$\left(1 + F \cdot \frac{Dq_1}{Dc_1}\right) \frac{\partial C_1}{\partial t} + u_0 \cdot \frac{\partial C_1}{\partial x} = 0 \quad (\text{I-2a})$$

$$\left(1 + F \cdot \frac{Dq_2}{Dc_2}\right) \frac{\partial C_2}{\partial t} + u_0 \cdot \frac{\partial C_2}{\partial x} = 0 \quad (\text{I-2b})$$

The directional derivatives for the two components are

$$U_{s,1} = \frac{\frac{\partial c_1}{\partial t}}{\frac{\partial c_1}{\partial x}} = \frac{u_0}{1 + F \cdot \frac{Dq_1}{Dc_1}} \quad (\text{I-3a})$$

$$U_{s,2} = \frac{\frac{\partial c_2}{\partial t}}{\frac{\partial c_2}{\partial x}} = \frac{u_0}{1 + F \cdot \frac{Dq_2}{Dc_2}} \quad (\text{I-3a})$$

These directional derivatives are the characteristic directions, and they give the velocities associated with the corresponding concentrations. The characteristic lines give the propagation trajectories of the different concentrations in the x, t space. Because of the coherence condition [4,16], the directional

derivatives are equal. Then:

$$\frac{Dq_1}{Dc_1} = \frac{Dq_2}{Dc_2} \quad (\text{I-4a})$$

$$\frac{\partial q_1}{\partial c_1} + \frac{\partial q_1}{\partial c_2} \cdot \frac{1}{\xi} = \frac{\partial q_2}{\partial c_1} \cdot \xi + \frac{\partial q_2}{\partial c_2} \quad (\text{I-4b})$$

Rearrangement of eqn. 4b gives eqn. 12a. This equation can be used to find the composition of the mixed zones during the progressive separation of two bands and the profiles of the shock layers.

APPENDIX II

The amount n_1 of the less retained component which elutes pure between the two shocks is given by

$$n_1 = S_1 + S_2 \quad (\text{II-1})$$

where S_1 and S_2 are the integrals of the concentrations C_1 and C_2 along the two shock layers,

$$S_i = \int_{\eta_1}^{\eta_2} C_1 d\eta \quad (\text{II-2})$$

Eliminating n_1 between eqns. 19 and II-1 gives

$$\Delta t = \frac{S_1 + S_2}{c_{1,0}U_1 - c_{2,0}U_2} \quad (\text{II-3})$$

The calculation of S_i is done from the differential of the shock layer thickness [18],

$$d\eta = \frac{H(1+K)^2}{2u_0K} \left(\frac{C_0+1}{C_0} \cdot \frac{1}{C-C_0} - \frac{1}{CC_0} \right) dC \quad (\text{II-4})$$

with $K = k_0/(1 + C_0)$ (eqn. 8a). Thus:

$$\begin{aligned} S_i &= \frac{H(1+K)^2}{2u_0K} \int_{c_1}^{c_r} \left(1 + \frac{1+C_0}{C-C_0} \right) dC \\ &= \frac{H(1+K)^2}{2u_0K} \left[(2\theta-1)C_0 + (1+C_0) \ln \left| \frac{1-\theta}{\theta} \right| \right] \end{aligned} \quad (\text{II-5})$$

The first-component isotherm is used to calculate S_1 and the decoupled isotherm (eqn. 14) to calculate S_2 . Putting these results into eqn. II-3 gives the width of the plateau, Δt .

REFERENCES

- H.-K. Rhee and N. R. Amundson, *Philos. Trans. R. Soc. London, Ser. A*, 267 (1970) 419.
- E. Glueckauf, *Discuss. Faraday Soc.*, 7 (1949) 12.
- G. Guiochon and L. Jacob, *Chromatogr. Rev.*, 14 (1971) 77.
- R. Aris and N. R. Amundson, *Mathematical Methods in Chemical Engineering*, Prentice-Hall, Englewood Cliffs, NJ, 1973.
- G. B. Whitham, *Linear and Nonlinear Waves*, Wiley, New York, 1974.
- A. Jeffrey, *Quasilinear Hyperbolic Systems and Waves*, Pitman, London, 1976.
- B. C. Lin, S. Golshan-Shirazi, Z. Ma and G. Guiochon, *Anal. Chem.*, 60 (1988) 2647.
- B. C. Lin, Z. Ma, S. Golshan-Shirazi and G. Guiochon, *J. Chromatogr.*, 500 (1990) 185.
- Z. Ma and G. Guiochon, *Anal. Chem.*, 62 (1990) 2330.
- J. N. Wilson, *J. Am. Chem. Soc.*, 62 (1940) 1583.
- D. DeVault, *J. Am. Chem. Soc.*, 65 (1943) 532.
- H.-K. Rhee, B. F. Bodin and N. R. Amundson, *Chem. Eng. Sci.*, 26 (1971) 1571.
- H.-K. Rhee and N. R. Amundson, *Chem. Eng. Sci.*, 27 (1972) 199.
- H.-K. Rhee and N. R. Amundson, *Chem. Eng. Sci.*, 28 (1973) 55.
- H.-K. Rhee and N. R. Amundson, *Chem. Eng. Sci.*, 29 (1974) 2049.
- Z. Ma, A. M. Katti and G. Guiochon, *J. Phys. Chem.*, 94 (1990) 6911.
- J. M. Jacobson, J. H. Frenz and Cs. Horvath, *Ind. Eng. Chem. Res.*, 26 (1987) 43.
- Z. Ma and G. Guiochon, *J. Chromatogr.*, 603 (1992) 13.
- S. Jacobson, S. Golshan-Shirazi and G. Guiochon, *AIChE J.*, 37 (1991) 836.
- M. D. Levan and T. Vermeulen, *J. Phys. Chem.*, 85 (1981) 3247.
- C. Thomas, *J. Am. Chem. Soc.*, 66 (1944) 1664.
- T. Vermeulen, in R. H. Perry, C. H. Chilton and S. D. Kirkpatrick (Editors), *Chemical Engineers' Handbook*, Academic Press, New York, 4th ed., 1963.
- D. O. Cooney and E. N. Lightfoot, *Trans. Ind. Eng. Chem. Fundam.*, 4 (1965) 233.
- W. J. Thomas and J. L. Lombardi, *Inst. Chem. Eng.*, 49 (1971) 240.
- S. Golshan-Shirazi and G. Guiochon, *J. Chromatogr.*, 603 (1992) 1.
- M. Czok and G. Guiochon, *Anal. Chem.*, 62 (1990) 189.
- M. Czok and G. Guiochon, *Comput. Chem. Eng.*, 14 (1990) 1435.
- S. Golshan-Shirazi and G. Guiochon, in F. Dondi and G. Guiochon (Editors), *NATO ASI on Theoretical Advances in Chromatography and Related Separation Methods, Ferrara, Italy, August 1991*, Kluwer, Delft, in press.
- A. M. Katti and G. Guiochon, *Am. Lab. (Fairfield, Conn.)*, 21, No. 10 (1989) 17.
- G. Guiochon, S. Golshan-Shirazi and A. Jaulmes, *Anal. Chem.*, 60 (1988) 1856.
- Z. Ma and G. Guiochon, *Comput. Chem. Eng.*, 15 (1991) 415.
- Z. Ma and G. Guiochon, in preparation.
- A. M. Katti, M. Czok and G. Guiochon, *J. Chromatogr.*, 556 (1991) 205.

Optimization of the experimental conditions and the column design parameters in displacement chromatography

Attila Felinger^{*} and Georges Guiochon

Department of Chemistry, University of Tennessee, Knoxville, TN 37996-1501, and Division of Analytical Chemistry, Oak Ridge National Laboratory, Oak Ridge, TN 37831-6120 (USA)

(First received December 31st, 1991; revised manuscript received May 14th, 1992)

ABSTRACT

Optimization of the experimental conditions (sample size, reduced mobile phase velocity and displacer concentration) and the column design parameters (column length and average particle size) was performed for the maximum production rate of either component of a binary mixture. The displacement chromatograms were calculated by means of the equilibrium-dispersive model of chromatography, assuming competitive Langmuir isotherms. Binary mixtures of separation factor 1.2, 1.5 and 1.8 and relative concentrations 3:1 and 1:3 were studied. For the systems studied, no optimum displacer concentration was found, the maximum production rates being achieved at the highest displacer concentration allowed by its solubility. The optimum column characteristics depend strongly on the separation factor and on the mixture composition. The maximum production rates were achieved at a much lower value of the retention factor than usually chosen in displacement chromatography. The optimum value of the retention factor of the less retained component was found to be between 1.2 and 2.0, depending slightly on the mixture composition and more strongly on the separation factor.

INTRODUCTION

Displacement chromatography was introduced by Tiselius [1] in 1942. Its theory in the case of Langmuir isotherms was developed soon afterwards by Glückauf [2], later by Helfferich and Klein [3] and subsequently by Rhee and Amundson [4], all these workers using the ideal model of chromatography, *i.e.*, assuming infinite column efficiency. After a period of intensive use during the Manhattan project [5], the method fell into oblivion as a separation technique for 30 years, until it was reintroduced by Horváth *et al.* [6].

There is currently strong interest in displacement chromatography [7–9] because it can deliver purified fractions which are much more concentrated than overloaded elution [1–10], although it is more difficult to use. The question of which one of these two modes of chromatography permits the highest production rate remains controversial because they have never been optimized simultaneously for the same separation problem. In a recent study, Katti *et al.* [11] compared on a theoretical basis the performance of displacement and overloaded elution chromatography, using the same column. The maximum production rates of the two modes were similar. Overloaded elution gives a better recovery yield, whereas the concentration of the fraction collected was one to two orders of magnitude higher in the displacement mode.

In this work, we applied to displacement chromatography the multi-parameter optimization method

Correspondence to: Professor G. Guiochon, Department of Chemistry, University of Tennessee, Knoxville, TN 37996-1501, USA.

^{*} On leave from the Department of Analytical Chemistry, University of Veszprém, H-8201 Veszprém, Hungary.

previously developed and applied to the study of the optimization of the experimental conditions in overloaded elution chromatography [12]. This method uses the numerical solution of the equilibrium-dispersive model of chromatography developed by Guiochon and co-workers [13–15]. Previously, Katti and Guiochon [16] have calculated band profiles in displacement chromatography by means of the same model and solution and discussed some of their properties.

In displacement chromatography, first the sample is introduced into the column equilibrated with the carrier. Then a solution of the displacer, a compound which is more strongly adsorbed on the stationary phase than any sample component, is pumped continuously into the column. The steep front of the displacer moves at a constant velocity, proportional to the carrier velocity and to the column capacity for the displacer at the concentration used. Being the most strongly retained component, the displacer pushes all the sample components in front of its band.

When a steady state is achieved, all the component bands travel at the same velocity, forming the isotachic train [2–4,6]. These bands are nearly rectangular and, unless the amount of a component is very small, the maximum concentration of the band does not depend on the size injected, but on the displacer concentration and on the adsorption isotherms of the component and the displacer.

THEORY

The band profiles of the two components of the binary mixture and that of the displacer were calculated using the method first developed by Rouchon *et al.* [13] and employed by Katti and Guiochon [16] for the calculation of the band profiles in displacement chromatography. This approach is based on the numerical solution of the equilibrium-dispersive model of chromatography. The mass balance equation and an isotherm model are written for each component of the sample and for the displacer. No mass balance is needed for the inert carrier [17]. The individual band profiles are obtained as numerical solutions of this system of equations, calculated using a finite difference method [18].

When the band profiles have been calculated, an

integration routine allows the determination of the cutting times at a given purity for the fractions of either component. The amount produced, the recovery yield and the production rate are then calculated.

Column properties

The following assumptions were made for the characteristics of the chromatographic system in the calculations. The total column porosity was $\varepsilon = 0.8$, the viscosity of the mobile phase was $\eta = 1$ cP and the molecular diffusivity of each compound in the mobile phase was $D_m = 1 \cdot 10^{-5}$ cm²/s. The column inner diameter was 4.6 mm. A maximum inlet pressure of 125 atm was allowed. The sample was injected as a rectangular plug, with a volume $V_p = 0.5$ ml. The values given for the loading factor (L_f) refer to the total loading of both components, and were calculated as

$$L_f = \frac{V_p}{(1 - \varepsilon) s L} \left(\frac{C_1^0}{q_{1,s}} + \frac{C_2^0}{q_{2,s}} \right) \quad (1)$$

where C_1^0 and C_2^0 are the concentrations of the first and the second component in the injected sample, respectively, $q_{1,s}$ and $q_{2,s}$ are the column saturation capacities of the two components, respectively, s is the column cross-sectional area and L is the column length.

The column efficiency was calculated using the Knox plate-height equation [19]:

$$h = \frac{2}{v} + v^{1/3} + \frac{v}{10} \quad (2)$$

where $h = H/d_p$ is the reduced plate height, H is the actual height equivalent to a theoretical plate, $v = ud_p/D_m$ is the reduced mobile phase velocity and u is the actual mobile phase velocity.

In the first part of the calculations, we optimized the operating parameters for an arbitrary column, with a length $L = 25$ cm, packed with particles of average diameter $d_p = 20$ μ m. In this instance, only the reduced mobile phase velocity, the sample loading factor and the displacer concentration were optimized. In the second part of the calculations, the column length and the average particle diameter were also optimized. Throughout this work a maximum displacer solubility of 300 mg/ml was assumed.

The required purity of the collected fractions was 99%, allowing 1% of the second component as an

impurity in the collected fraction of the first component, and 0.5% of the first component and 0.5% of the displacer as impurities in the collected fraction of the second component.

The same general properties (column porosity, mobile phase viscosity, molecular diffusivity, maximum inlet pressure, column saturation capacities, column cross-sectional area, coefficients of the plate-height equation and required purity) were assumed in our previous work, investigating the optimum conditions for maximum production rate in the overloaded elution mode [12].

Equilibrium isotherms

We assumed that the isotherms of the two components of the sample and of the displacer are given by the competitive Langmuir isotherm model [20]:

$$q_i = \frac{a_i C_i}{1 + b_1 C_1 + b_2 C_2 + b_3 C_3} \quad i = 1, 2, 3 \quad (3)$$

where q_i and C_i are the concentrations of component

i at equilibrium in the stationary and the mobile phase, respectively, and a_i and b_i are numerical coefficients. As the Langmuir model is valid only if the column saturation capacities are identical for all components [21], the numerical parameters were chosen accordingly, with $a_1 = k'_1/0.25$, $a_2 = \alpha a_1$, $a_3 = \alpha a_2$, $b_1 = k'_1/325$ ml/mg, $b_2 = \alpha b_1$ and $b_3 = \alpha b_2$, where k'_1 is the retention factor of the first component at infinite dilution and α is the separation factor between subsequently eluted components. The separation factor for the less retained and the more retained components of the sample is assumed to be equal to the separation factor of the more retained sample component and the displacer. With these parameters, the saturation capacity of all compounds is 1300 mg/ml.

Definitions

The production rate was defined as the amount of the purified component produced per unit cross-sectional area and per unit time, in $\text{mg}/\text{cm}^2 \cdot \text{s}$. The

TABLE I
OPTIMUM OPERATING CONDITIONS FOR A GIVEN COLUMN^a

α	Compound			Production rate ($\text{mg}/\text{cm}^2 \cdot \text{s}$)	Yield (%)	v	L_r (%)	C_d (mg/ml)
	C_1/C_2	No.	k'_1					
1.2	3:1	1	2.7	1.430	35.9	113	10.0	103
1.2	3:1	2	2.5	0.085	29.7	42	6.7	41
1.2	1:3	1	3.1	0.196	43.1	57	8.8	57
1.2	1:3	2	3.6	0.709	43.9	75	7.8	75
1.5	3:1	1	1.8	14.38	53.8	353	20.9	187
1.5	3:1	2	1.9	1.63	44.6	232	12.5	40
1.5	1:3	1	2.0	2.14	48.5	335	11.6	91
1.5	1:3	2	1.9	8.20	63.5	230	16.4	112
1.5	3:1	1	1.9	14.36	60.0	303	20.7	188
1.5	3:1	2	1.9	1.47	60.0	158	14.0	73
1.5	1:3	1	2.0	1.99	60.0	255	12.2	99
1.5	3:1	1	2.3	8.69	90.0	153	16.2	154
1.5	3:1	2	2.0	0.98	90.0	153	8.2	28
1.5	1:3	1	2.2	1.53	90.0	155	9.9	80
1.5	1:3	2	2.0	5.51	90.0	178	14.7	178
1.8	3:1	1	1.4	35.60	63.0	371	34.5	276
1.8	3:1	2	1.6	4.49	60.9	266	21.0	81
1.8	1:3	1	1.6	5.48	62.5	293	23.3	171
1.8	1:3	2	1.4	19.22	65.1	242	24.1	176

^a $L = 25$ cm; $d_p = 20$ μm .

cycle time, *i.e.*, the time between two consecutive injections, was defined as the breakthrough time of the displacer front. No provision is made for the regeneration of the column.

Calculation procedures

The modified simplex algorithm extended by Dose [22] to handle boundary problems was used in this work. The convergence of the simplex was checked by the standard deviation of the coordinates of the simplex vertices. The convergence was achieved when the standard deviation for all the parameters to be optimized decreased below 0.1%. The optimum separation conditions were calculated successively for the less and the more retained components. Binary mixtures of relative concentrations 1:3 and 3:1 were studied at three values of the separation factor ($\alpha = 1.2, 1.5$ and 1.8).

RESULTS AND DISCUSSION

Optimization of the experimental conditions for a given column

In the first part of this work the column design parameters (column length and particle size) were not changed, only the experimental conditions (sample loading factor, reduced velocity of the mobile phase and concentration of the displacer) were optimized simultaneously, for a given column. The optimum values of the parameters, the production rate and the corresponding value of the recovery yield are given in Table I.

Influence of the retention factor. As the separations that use displacement chromatography are usually carried out at high values of the retention factor, the optimization procedure was re-run several times, using decreasing values of the retention factor, starting with $k'_1 = 6$. This procedure was repeated with different combinations of the relative mixture composition and the separation factor. In Fig. 1, the production rates of both components are plotted against k'_1 for a separation factor of $\alpha = 1.8$. The optimum value of the retention factor, k'_1 , was always found to be between 1.4 and 1.6 for either mixture composition studied, irrespective of the component for which the production rate is optimized. The production rates at the optimum retention factor are 48–67% higher than at $k'_1 = 6$, which is a significant increase. However, when the reten-

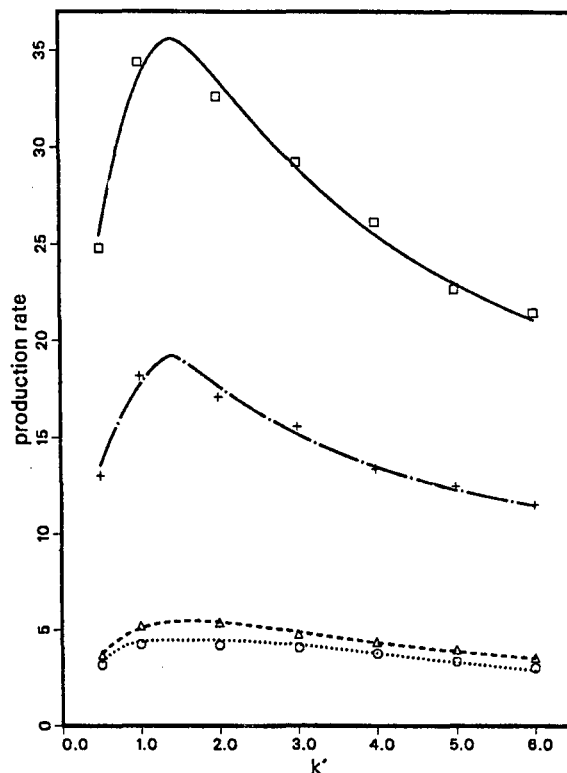


Fig. 1. Plot of the maximum production rates of either component versus the retention factor of the less retained component, $\alpha = 1.8$. (□) First and (○) second component of a 3:1 mixture; (△) first and (+) second component of a 1:3 mixture.

tion factor is decreased below the optimum value, the production rate drops rapidly.

The same trend is observed at all values of the separation factor. For example, in Fig. 2a and b the maximum production rates corresponding to different yield constraints and mixture compositions are plotted versus k'_1 at $\alpha = 1.5$. The optimum value of k'_1 is now close to 2.0, and the gain in production rate on decreasing k'_1 from 6 to the optimum retention factor is less important than it was at $\alpha = 1.8$, but it is still 28–38%. At $\alpha = 1.2$ (Fig. 3), the optimum value of k'_1 is still higher, 2.4–3.6, and the gain in production rate associated with the decrease in k'_1 from 6 to the optimum value is only 16–25%.

Influence of a constraint on the recovery yield. Without any constraints, the recovery yield corresponding to the maximum production rate at $\alpha = 1.5$ was between 45 and 64% (Table I), depending on

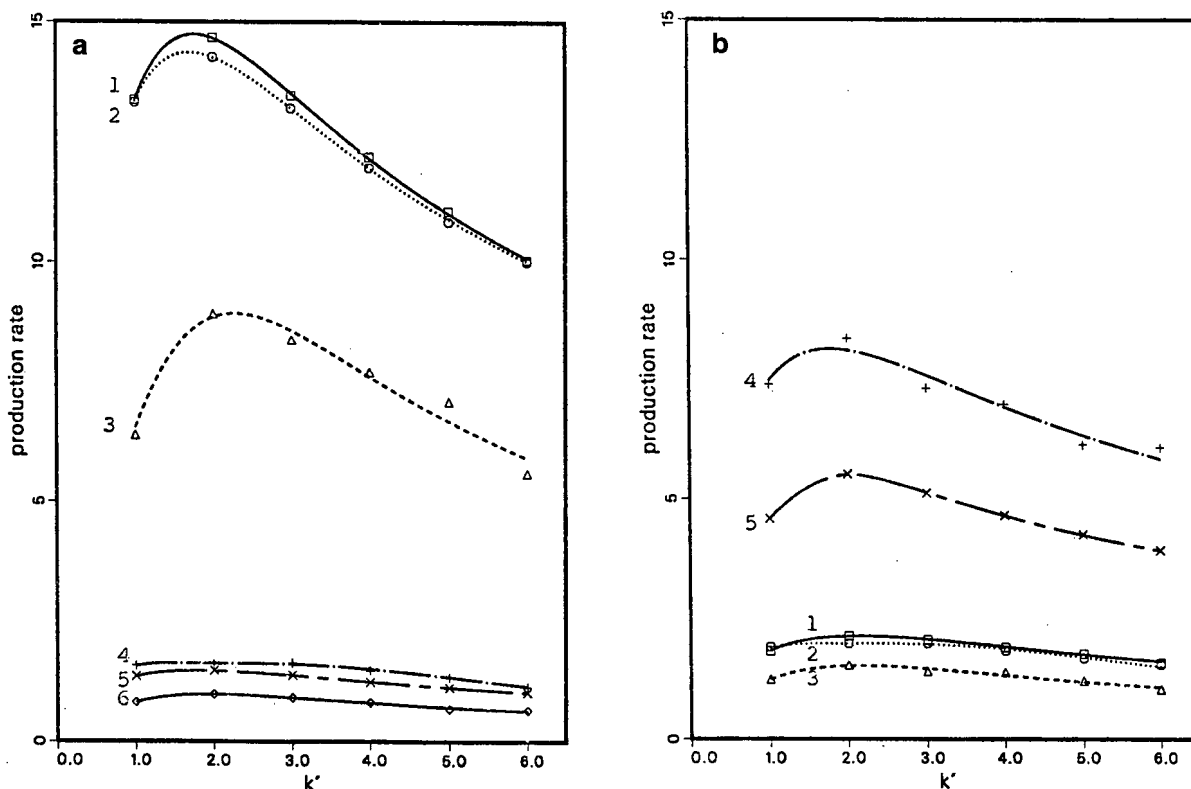


Fig. 2. Plot of the maximum production rates of either component *versus* the retention factor of the less retained component and influence of a recovery yield constraint, $\alpha = 1.5$. (a) Feed composition 3:1. 1 = First component without yield constraint; 2 = first component, 60% recovery yield; 3 = first component, 90% recovery yield; 4 = second component without yield constraint; 5 = second component, 60% recovery yield; 6 = second component, 90% recovery yield. (b) Feed composition 1:3. 1 = First component without yield constraint; 2 = first component, 60% recovery yield; 3 = first component, 90% recovery yield; 4 = second component without yield constraint; 5 = second component, 90% recovery yield.

the mixture composition and on whether the production rate of the first or the second component was optimized. The effect of a recovery yield constraint on the production rate was studied, setting minimum yield requirements of 60% and 90%.

The recovery yield achieved when no constraints are applied does not change significantly with the retention factor as long as this factor is higher than its optimum value, but decreases rapidly with decreasing retention factor if the separation is carried out at k' values smaller than the optimum. The effect of a recovery yield constraint on the production rate is shown in Fig. 2a and b ($\alpha = 1.5$). Since in this instance the recovery yield without constraint is only slightly less than 60% (or, even in one instance, is higher), there is no real change in the production rate

when setting the constraint to 60%. When a minimum recovery yield of 90% is required, however, the production rate drops by about 30–40% compared with the global optimum. The optimum value of k'_1 is slightly higher when a recovery yield constraint is applied.

Influence of the separation factor. The optimization was carried out for three values of the separation factor, 1.2, 1.5 and 1.8 (Table I). As noted above, the optimum value of the retention factor increases with decreasing separation factor.

The production rate increases enormously when the separation factor is increased from 1.2 to 1.5. In three cases, a 10–11-fold increase was observed, while the gain is 17-fold for the purification of the second component of a 3:1 mixture. These gains are

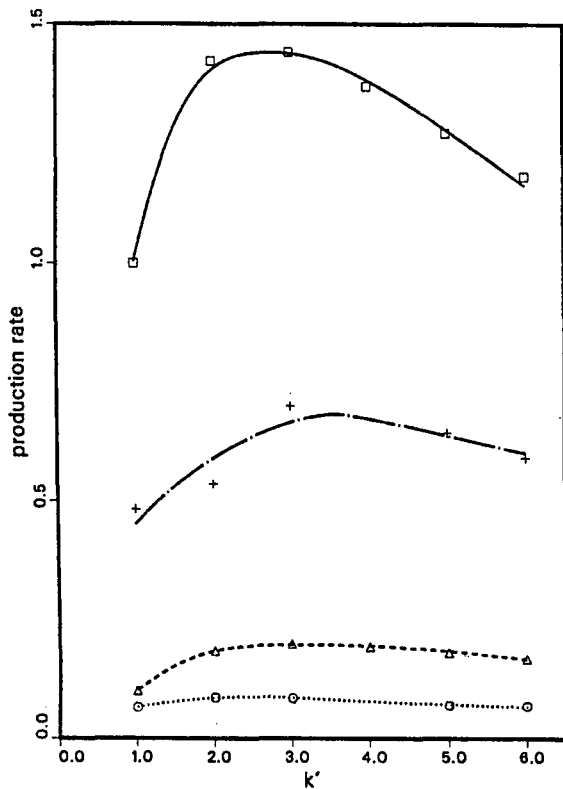


Fig. 3. Same as Fig. 1, except $\alpha = 1.2$.

achieved by large increases in both the optimum reduced velocity and optimum sample size. In the purification of the second component of a 3:1 mixture, a minor component is eluted between a main component and the displacer. For this separation at $\alpha = 1.2$ a very low reduced velocity ($v = 42$) is required to obtain the second component of the sample at a desired degree of purity, and the recovery yield is only 30%. At $\alpha = 1.5$, the optimum velocity is six times higher, the optimum sample size is doubled and the recovery yield is increased by 50% (relative).

The increase in production rate resulting from an increase in the separation factor from 1.5 to 1.8 is less significant, the improvement being by a factor of only *ca.* 2.3-2.75. These values are consistent with a production rate approximately proportional to $(1 - \alpha)^3$. The optimum experimental conditions are summarized in Table I.

Simultaneous optimization of the column design parameters and the operating conditions

The simultaneous optimization of the experimental conditions and the column design parameters leads to a five-dimensional maximum search. However, by utilizing the effects of the displacer concentration and the column length, as will be shown below, the problem can be reduced to a three-dimensional optimization. The optimum values of the parameters are given in Table II.

TABLE II

OPTIMUM VALUES OF THE PARAMETERS OF OPERATING CONDITIONS AND COLUMN DESIGN

α	Compound			Production rate (mg/cm ² · s)	Yield (%)	v	L_r (%)	d_p (μ m)	d_p^2/L (μ m ² /cm)	N
	C_1/C_2	No.	k'_1							
1.2	3:1	1	2.0	4.57	58.4	64	14.00	13.7	3.75	3 509
1.2	3:1	2	1.8	0.648	59.8	14	12.69	8.1	1.32	15 774
1.2	1:3	1	1.5	1.011	36.0	27	23.81	10.2	2.08	8 578
1.2	1:3	2	1.9	3.15	67.1	30	11.33	10.7	2.29	7 610
1.5	3:1	1	1.8	21.59	71.7	207	27.50	20.2	8.19	934
1.5	3:1	2	1.7	4.07	67.0	57	30.00	13.2	3.48	3 997
1.5	1:3	1	1.4	5.18	64.6	106	29.49	16.2	5.24	2 007
1.5	1:3	2	1.6	15.22	71.0	112	23.64	16.5	5.44	1 896
1.8	3:1	1	1.5	40.80	74.0	320	38.80	23.5	11.00	544
1.8	3:1	2	1.4	9.01	66.9	111	43.90	16.4	5.35	1 993
1.8	1:3	1	1.2	9.28	75.1	167	36.20	18.8	7.09	1 197
1.8	1:3	2	1.3	28.14	74.5	183	30.52	19.5	7.63	1 064

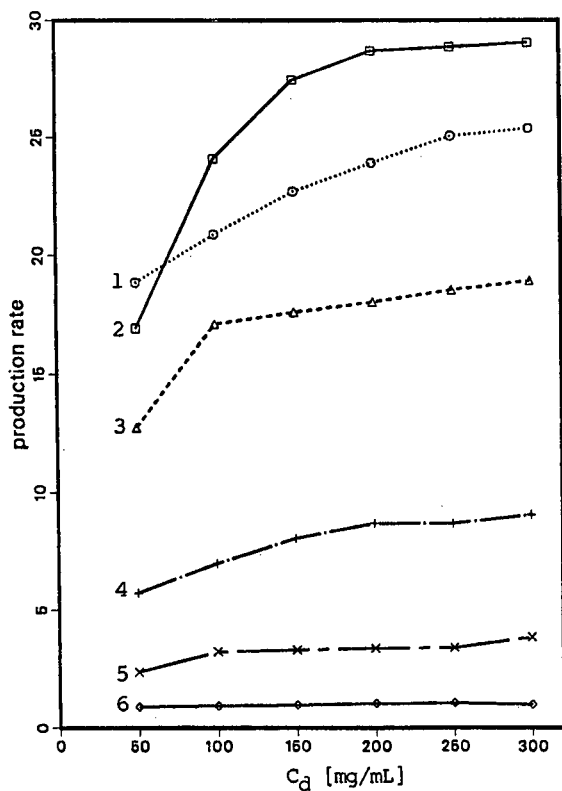


Fig. 4. Effect of the displacer concentration on the production rate of either component. 1 = Second component of a 1:3 mixture, $\alpha = 1.8$, $k'_1 = 1$; 2 = first component of a 3:1 mixture, $\alpha = 1.8$, $k'_1 = 6$; 3 = second component of a 1:3 mixture, $\alpha = 1.8$, $k'_1 = 6$; 4 = first component of a 1:3 mixture, $\alpha = 1.8$, $k'_1 = 1$; 5 = first component of a 3:1 mixture, $\alpha = 1.2$, $k'_1 = 6$; 6 = first component of a 1:3 mixture, $\alpha = 1.2$, $k'_1 = 1$.

Influence of the displacer concentration. To understand the effect of the displacer concentration on the production rate, we fixed the value of this parameter and optimized the others. However, we found that the higher the displacer concentration, the higher is the production rate. As the displacer concentration range was limited by a supposed solubility at 300 mg/ml, the production rate maximum was found at this concentration. The optimum values of the column design parameters, of course, change with varying displacer concentration, but the resulting recovery yield was independent of the displacer concentration. In Fig. 4 the effect of the displacer concentration on the production rate is shown for a few selected but typical sets of values of the retention

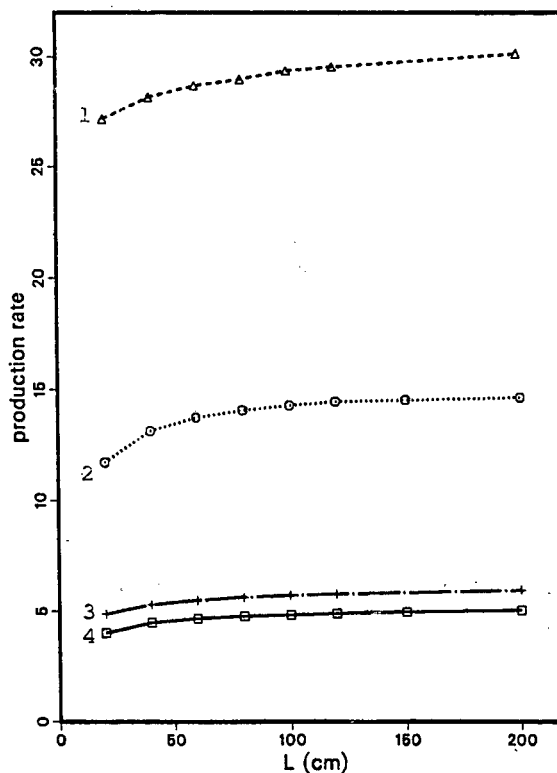


Fig. 5. Effect of the column length on the production rate. 1 = First component of a 3:1 mixture, $\alpha = 1.8$, $k'_1 = 6$; 2 = second component of a 1:3 mixture, $\alpha = 1.5$, $k'_1 = 2$; 3 = first component of a 1:3 mixture, $\alpha = 1.8$, $k'_1 = 6$; 4 = first component of a 3:1 mixture, $\alpha = 1.2$, $k'_1 = 2$.

factor, the separation factor and the mixture composition.

Consequently, in all subsequent calculations, a constant displacer concentration (300 mg/ml) was applied.

Influence of column length. The next calculations were carried out to optimize the average particle diameter, the sample size and the reduced velocity for a given column length. Different columns having lengths between 10 and 200 cm were considered, but no optimum value was found, as the longer the column the higher was the production rate of either component. The optimum average particle size increases with increasing column length, keeping the ratio d_p^2/L unchanged. It was found that, at the same time as the production rate, the recovery yield increases slightly with increasing column length. In

Fig. 5, some examples of the variation of the production rate with the column length are given.

As no optimum column length was found, we chose for further calculations a column of constant length (50 cm), and only the other column design parameter, *i.e.*, the average particle diameter, was optimized. This length is in agreement with the current practice. We see in Fig. 5 that the production rate gain associated with the use of a longer column is only marginal. With this restriction, of course, we shall not find the global optimum conditions for separation. However, the aim of this work was to draw qualitative information regarding the best practical conditions under which preparative separations should be conducted.

Optimum column design parameters. The analysis of the solution of the ideal model of chromatography demonstrates that neither the column length nor the average particle size has optimum values, but

that there is an optimum value for the ratio d_p^2/L at which the maximum production rate will be achieved [23]. This result was essentially confirmed by numerical optimization of the overloaded elution mode based on the equilibrium-dispersive model of chromatography [12]. In the latter instance, only a very flat maximum was found when optimizing both the column length and the particle size.

The same phenomenon was observed for the displacement mode in this work. As reported above, when the experimental conditions are optimized for a particular column length, as shown in Fig. 5, the optimum particle size depends on the column length, and the ratio d_p^2/L remains virtually constant. The optimum values of the d_p^2/L ratios obtained for the same conditions as discussed in Fig. 5 are plotted *versus* the column length in Fig. 6. We see that the optimum value of the ratio changes very slowly with the column length. For this reason, we shall use also

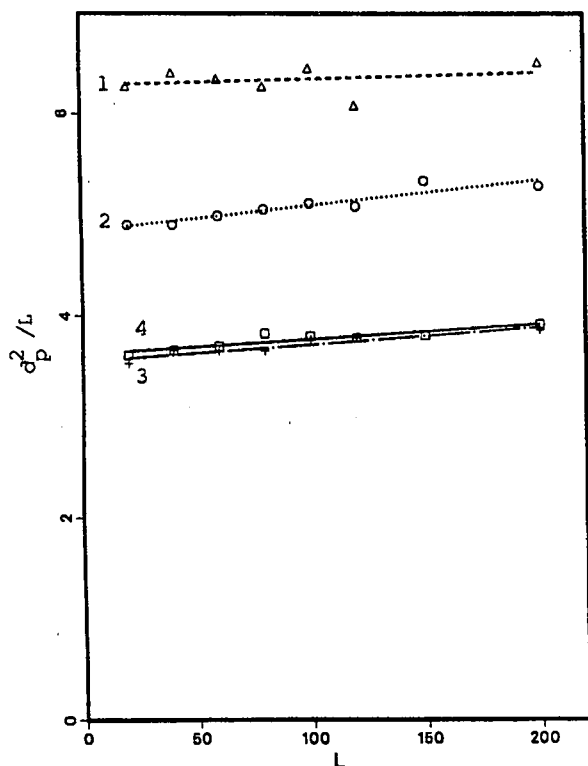


Fig. 6. Optimum value of d_p^2/L versus the column length. The lines correspond to the same conditions as in Fig. 5.

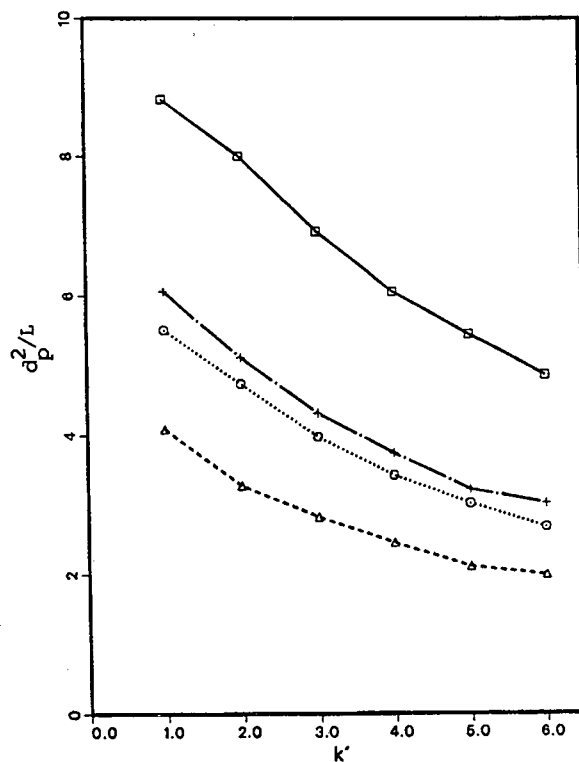


Fig. 7. Optimum value of d_p^2/L versus the retention factor of the less retained component; $\alpha = 1.5$. (\square) First and (Δ) second component of a 3:1 mixture; (\circ) first and ($+$) second component of a 1:3 mixture.

in the displacement mode the ratio d_p^2/L for characterizing the column dimensions.

The optimum ratio d_p^2/L decreases rapidly with increasing retention factor, k'_1 . In Fig. 7, the optimum value of d_p^2/L is plotted against k'_1 for some selected cases.

For the column used in the first part of this work ($L = 25$ cm, $d_p = 20$ μm), $d_p^2/L = 16$. For all the mixture compositions and the separation factors studied in this work, the optimum value of d_p^2/L is much smaller than 16. The closer the separation factor is to unity, the smaller is the optimum particle size for a column of given length (see Table II), because a higher column efficiency is required to separate the components of a mixture when the separation factor approaches 1.0.

Small particles are needed to purify the more retained component of a 3:1 mixture, *i.e.*, when a component at a relatively low concentration is

eluted between the less retained component and the displacer. In this instance, the purity of the collected fraction is strongly influenced by the separation from the bands on both sides of the band of interest. For this reason, the production rate of the second component in a 3:1 mixture with $\alpha = 1.2$ increases about 7.6 times on switching from the standard column (Table I) to the optimum column (Table II).

In contrast, the easiest task is the purification of the less retained component from the same 3:1 mixture. In this instance the presence of both the second component of the sample and the displacer band tends to concentrate the first component band. The improvement of the production rate observed on replacing the standard column (Table I) by the optimum column (Table II) is 3.2-fold at $\alpha = 1.2$.

The difficulty with the other two cases studied, the purification of either the less or the more retained components from a 1:3 mixture, is intermediate

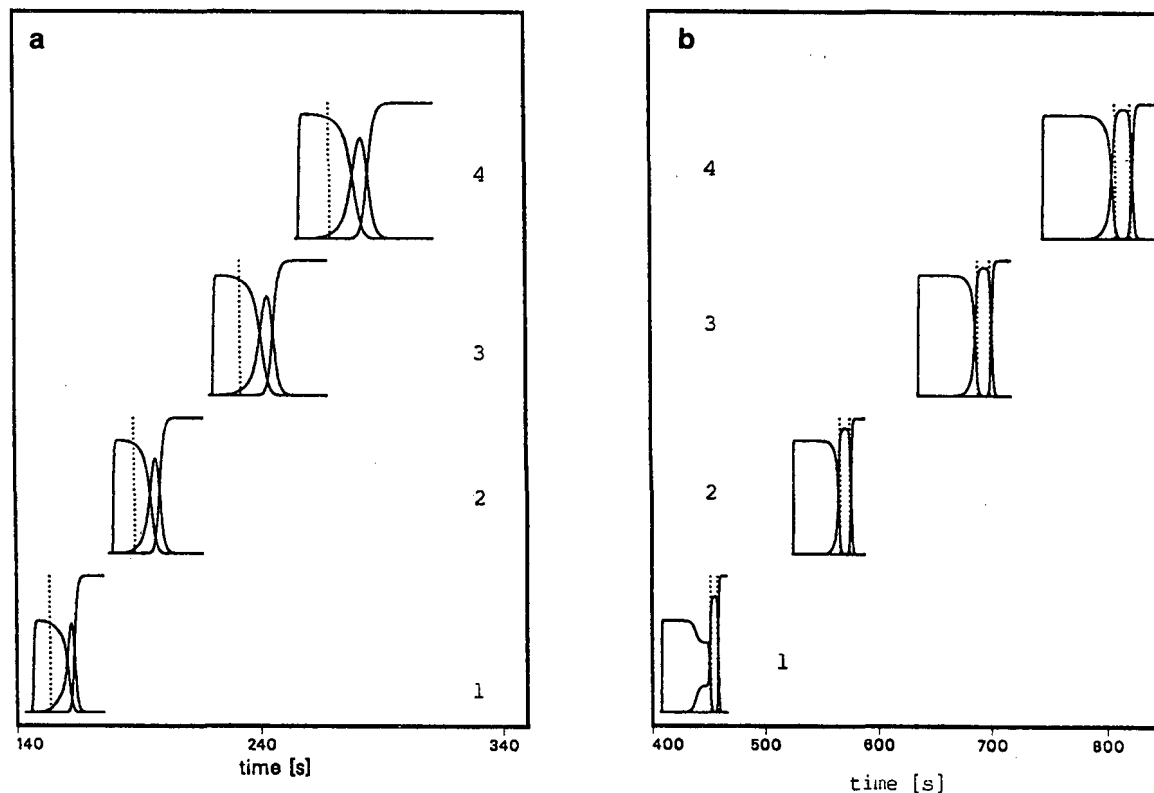


Fig. 8. Optimum chromatograms corresponding to the maximum production rate of (a) the less retained and (b) the more retained component in a mixture of relative concentration 3:1; the separation factor is $\alpha = 1.2$. Values of the retention factor: (1) $k'_1 = 1.0$; (2) $k'_1 = 2.0$; (3) $k'_1 = 3.0$; (4) $k'_1 = 4.0$. The vertical dotted lines indicate the cut points for fraction collection.

between the two situations described above. Nearly identical column characteristics are required (Table II).

Influence of mixture composition. As we have seen in the previous discussions, the relative concentration of the components of the mixture and whether the production rate of the less or the more retained component is optimized have a strong influence on the optimum column design.

In Fig. 8, two series of calculated chromatograms are plotted, corresponding to the maximum production rate of the less (Fig. 8a) and the more (Fig. 8b) retained components of a 3:1 binary mixture, with $\alpha = 1.2$, and for different values of the retention factor. In Fig. 8a, the band of the less retained component has a very steep front, and high concentration fractions can be collected. However, in this instance the column efficiency is poor, the second

component band is broad and no pure second component at all can be recovered.

When the production of the second component is optimized (Fig. 8b), a much smaller reduced velocity (Table II) allows a much higher resolution between the second component band and those of the first component and the displacer, permitting the collection of 99% pure fractions of the second component, but the cut times on the two sides of the band are very close to one another.

Optimum value of the retention factor. At low values of the separation factor, the optimum retention factor at which the maximum production rate is reached is lower when using the optimum column (Table II) than with the standard column (Table I). For example, at $\alpha = 1.2$, the optimum retention factor, k'_1 is between 1.5 and 2.0 when all the column design parameters are optimized (Fig. 9), compared with the optimum value of k'_1 between 2.5 and 3.6 that was obtained for the column studied in Table I

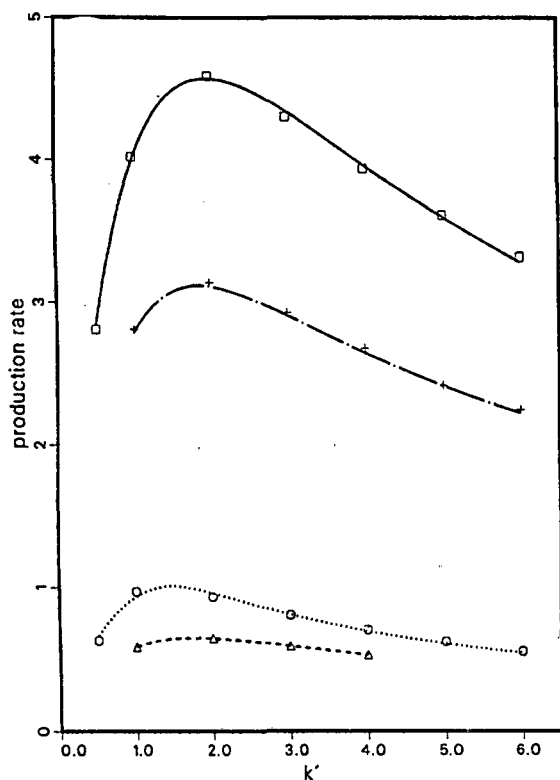


Fig. 9. Plots of the maximum production rate of either component versus the retention factor of the less retained component; $\alpha = 1.2$. (\square) First and (Δ) second component of a 3:1 mixture; (\circ) first and ($+$) second component of a 1:3 mixture.

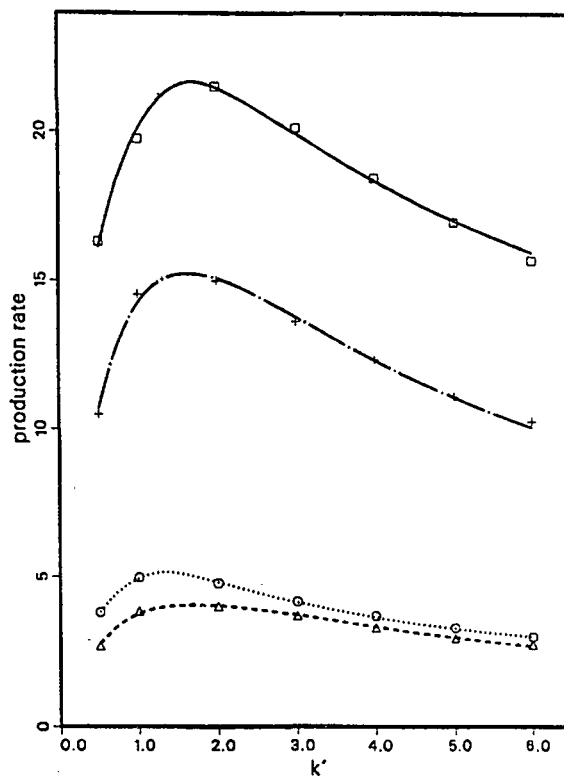


Fig. 10. Same as Fig. 9, except $\alpha = 1.5$.

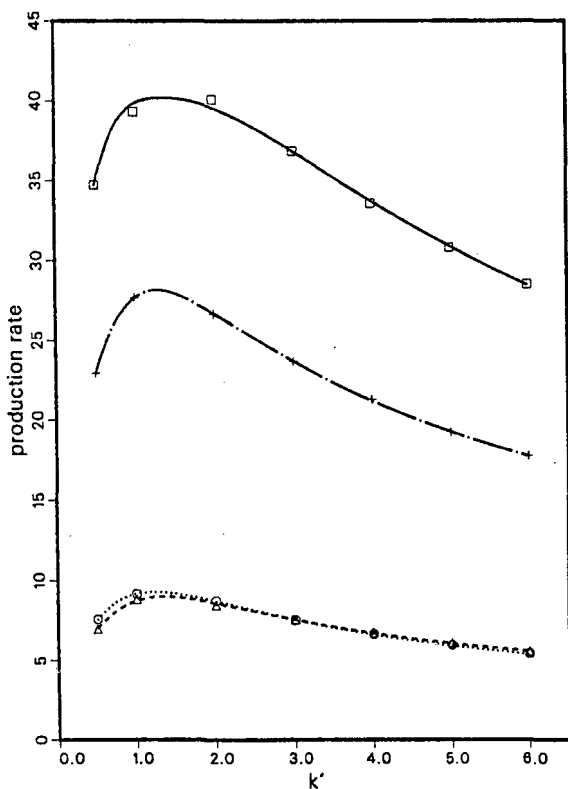


Fig. 11. Same as Fig. 9, except $\alpha = 1.8$.

and Figs. 1-4. At higher values of the separation factor, the value of the optimum retention factor is nearly independent of whether or not the column design parameters are optimized (Figs. 10 and 11). The optimum conditions are summarized in Table II.

The optimum sample size increases with increasing retention factor (as can be seen in Fig. 8a and b), but so does the cycle time, and it is the ratio of the sample size to the cycle time, multiplied by the recovery yield, which determines the production rate.

Optimum mobile phase velocity. When we optimized both the column characteristics and the experimental conditions for the separation, the optimum reduced velocity of the mobile phase was always determined by the maximum allowed inlet pressure. This confirmed previous theoretical results [23] that the maximum production rate for a given

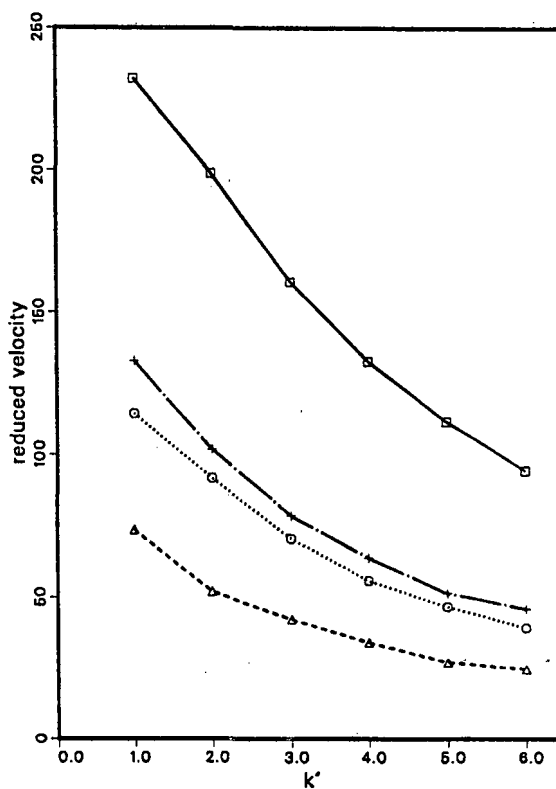


Fig. 12. Plot of the optimum mobile phase reduced velocity versus the retention factor of the first component for an optimum designed column. Same conditions as in Fig. 7.

separation increases with increasing maximum allowed inlet pressure.

In contrast, in the first part of this work, when we optimized the operating conditions for a particular column, the maximum inlet pressure was never reached. Interestingly, as is seen in Fig. 12, the optimum reduced velocity decreases with increasing retention factor. The behavior of both the reduced velocity and the ratio d_p^2/L is just the opposite of what was found when optimizing the production rate in the overloaded elution mode [11].

As a consequence of this behavior, the column efficiency required to perform the separation at the optimum retention factor, is smaller than the efficiency needed when the separation is carried out at a retention factor higher than the optimum value. The dependence of the required efficiency on the retention factor and the influence of the mixture composition are illustrated in Fig. 13.

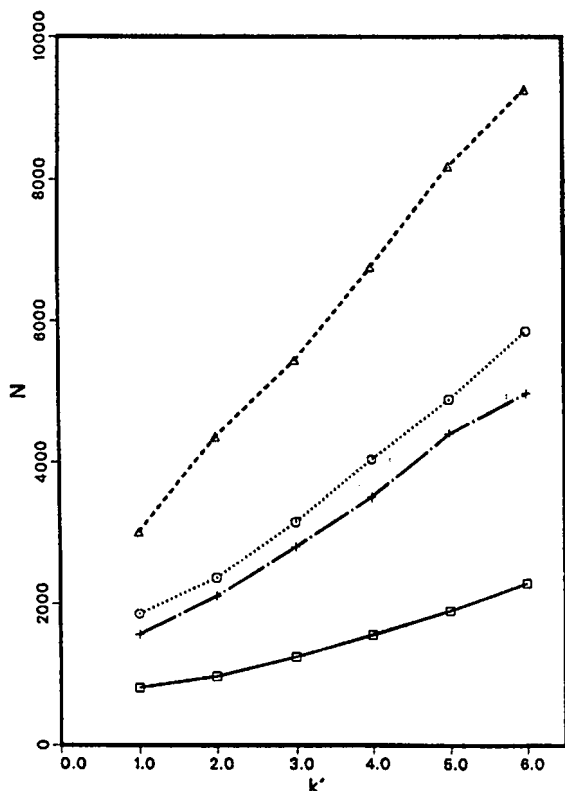


Fig. 13. Plot of the column efficiency required to perform the separation. Same conditions as in Fig. 7.

CONCLUSIONS

A few general rules can be derived from the results of this work, in spite of the fact that numerical solutions are always specific to a set of particular experimental conditions.

First, there always exists an optimum value for the retention factor. This optimum value is relatively low, much lower than the retention factors currently used in practice. It depends slightly on the mixture composition and on the component for which the production rate is to be maximized. The dependence of the optimum value of k' on the separation factor is more significant. The optimum retention factor is higher if the column design parameters are not optimum. The optimum sample size, and hence the throughput, increase with increasing retention factor, but the optimum conditions at higher k'_1 demand a more efficient column and the cycle time also increases.

Second, in the instances studied, no optimum displacer concentration was found. The more concentrated the displacer, the higher is the production rate. Third, no optimum column length was detected. The production rate of either component increases with increasing column length. However, there is always an optimum value for the ratio d_p^2/L . As long as this ratio is kept constant, the production rate does not change significantly.

Finally, the maximum production rate can be several times higher when the column having the optimum characteristics is chosen compared with a standard column operated under optimum conditions. This incentive to optimize the column design is most important when optimizing the production rate of the more retained component from a feed where its concentration is lower than that of the less retained component.

In all instances, the optimum conditions were found to be such that the isotachic train is not yet formed, but nearly so. Probably because the characteristics of our standard column were relatively closer to those of the optimum column, the chromatograms were also closer to the isotachic train than in our previous study, as in this case the fractions of both components could be collected at very high concentrations.

ACKNOWLEDGEMENTS

This work was supported in part by grant CHE-8901382 from the National Science Foundation and by the cooperative agreement between the University of Tennessee and the Oak Ridge National Laboratory. We acknowledge support of our computational effort by the University of Tennessee Computing Center.

REFERENCES

1. A. Tiselius, *Ark. Kemi Mineral. Geol.*, 16a (1943) 1.
2. E. Glückauf, *Proc. R. Soc. London*, 186A (1946) 35.
3. F. Helfferich and G. Klein, *Multicomponent Chromatography—A Theory of Interference*, Marcel Dekker, New York, 1970.
4. H.-K. Rhee and N. R. Amundson, *AIChE J.*, 28 (1982) 423.
5. F. H. Spedding, E. I. Fulmer, T. A. Butler and J. E. Powell, *J. Am. Chem. Soc.*, 72 (1950) 2349.
6. Cs. Horváth, A. Nahum and J. H. Frenz, *J. Chromatogr.*, 218 (1981) 365.

- 7 J. Frenz and Cs. Horváth, in Cs. Horváth (Editor), *High-Performance Liquid Chromatography —Advances and Perspectives*, Vol. 5, Academic Press, New York, 1988, p. 211.
- 8 Gy. Vigh, G. Quintero and Gy. Farkas, *J. Chromatogr.*, 484 (1989) 237.
- 9 G. Subramanian and S. M. Cramer, *J. Chromatogr.*, 484 (1989) 225.
- 10 G. Guiochon and A. M. Katti, *Chromatographia*, 24 (1987) 165.
- 11 A. M. Katti, E. V. Dose and G. Guiochon, *J. Chromatogr.*, 540 (1991) 1.
- 12 A. Felinger and G. Guiochon, *J. Chromatogr.*, 591 (1992) 31.
- 13 P. Rouchon, M. Schonauer, P. Valentin and G. Guiochon, *Sep. Sci. Technol.*, 22 (1987) 1793.
- 14 G. Guiochon, S. Golshan-Shirazi and A. Jaulmes, *Anal. Chem.*, 60 (1988) 1856.
- 15 G. Guiochon and S. Ghodbane, *J. Phys. Chem.*, 92 (1988) 3682.
- 16 A. M. Katti and G. Guiochon, *J. Chromatogr.*, 449 (1988) 25.
- 17 E. sz. Kováts, in F. Bruner (Editor), *The Science of Chromatography*, Elsevier, Amsterdam, 1985, p. 205.
- 18 M. Czok and G. Guiochon, *Comput. Chem. Eng.*, 14 (1989) 1435.
- 19 J. H. Knox, *J. Chromatogr. Sci.*, 15 (1977) 352.
- 20 G. M. Schwab, *Ergebnisse der Exakten Naturwissenschaften*, Vol. 7, Springer, Berlin, 1928, p. 276.
- 21 M. D. Levan and T. Vermeulen, *J. Phys. Chem.*, 85 (1981) 3247.
- 22 E. V. Dose, *Anal. Chem.*, 59 (1987) 2420.
- 23 S. Golshan-Shirazi and G. Guiochon, *Anal. Chem.*, 61 (1989) 1368 and 2464.

Application of non-porous silica ultramicrospheres to high-performance liquid chromatographic column packings

Futaba Honda

PHD Inc., 3-23-18-803, Tomioka-cho, Hakodate-shi, Hokkaido 041 (Japan)

Hiroataka Honda and Masumi Koishi

Faculty of Industrial Science and Technology, Science University of Tokyo, 102-1, Tomino, Oshamanbe-cho, Yamakoshi-gun, Hokkaido 049-35 (Japan)

(First received January 31st, 1992; revised manuscript received April 29th, 1992)

ABSTRACT

Silica-composite particles were made from silica ultramicrospheres and polyethylene microspheres by a dry impact blending method for application as high-performance liquid chromatographic column packings. A column packed with silica-composite particles has a double packing structure, which consists of the spatial configuration of silica-composite particles in the column and a dense arrangement of silica on the polyethylene microsphere surfaces. This structure enables silica ultramicrospheres to be utilized as the stationary phase while simultaneously maintaining the flow of the mobile phase. Proteins with MW from 6500 to 669 000 were separated satisfactorily on a column packed with *n*-octadecyldimethylchlorosilane-coated silica-composite particles.

INTRODUCTION

In the separation of polypeptides and proteins by reversed-phase high-performance liquid chromatography (HPLC), many studies have been reported on the relationship between column configurations and column performance [1–8]. The column configuration includes the length and bore, the average particle diameter, the pore diameter of the packings, the accessible surface area and the type of ligand and the column performance includes resolution, retention time, peak capacity and theoretical plate number. In these reports, however, there were considerable differences between experimental results and

the theories on the basis of analyses of small molecules. These differences are believed to be due to the following effects. First, the diffusion coefficient of proteins with large molecules is decreased as the protein diameters approach the pore diameter in the column packing [4,9,10]. Second, solutes are bound to silanol groups on column packings [3,4, 11]. Third, equilibrium rates between different forms (native vs. denatured) are slow [4,12,13]. These effects contribute significantly to the increase in band width and the spread of band shape, and lead to still lower values of *N*. Therefore, recent studies of retention behaviour have involved mainly small peptides [14–18]. In protein analysis, wide-pore silica packings were applied in order to promote the free diffusion of solutes in the internal and external region of the pores [3,7]. Wide-pore silica packings, however, must have increased particle diameters, when the pore diameters required are large [19], and

Correspondence to: Futaba Honda, Faculty of Industrial Science and Technology, Science University of Tokyo, 102-1, Tomino, Oshamanbe-cho, Yamakoshi-gun, Hokkaido 049-35, Japan (present address).

an increase in particle diameter leads to a decrease in N . Hence the increase in pore diameter is a limiting factor. In addition, wide-pore silica packings have a lower packing stability [20].

In view of the above, the application of non-porous, very small particles has been proposed as an alternative to totally porous silica particles [21–27]. Non-porous particles were designed for the employment of the external surfaces of the particles instead of the internal surface of pores. Short columns packed with non-porous particles should permit the rapid separation of large molecules such as proteins, and the recovery of proteins is increased [27]. However, the disadvantages of non-porous silica packings are that the column length is restricted because high pressure is required for an adequate mobile phase flow and it is difficult to pack a column densely and homogeneously [28]. Guiochon and Martin [29] indicated that it would be almost impossible to use a high-efficiency column packed with less than 1- μm diameter particles. This suggests that the decrease in the particle diameter reaches a limit if particles are to be packed into columns directly.

On the other hand, Hersey [30] reported that fine particles could be made to adhere to the surface of coarse particles by a binary powder mixture. Koishi and co-workers [31–33] developed a binary mixture as composite particles by using a dry impact blending method. This procedure has been employed for the improvement of powder properties and in mixing homogeneously a small amount of material such as drugs and pigments with a large amount of excipient, etc. [34,35]. It was confirmed experimentally that small particles were fixed on large particles when the ratio of the diameter of the large particle to that of the small particle was larger than 10:1. Fig. 1 shows a schematic diagram of the processes. The small particles fixed on large particles were stable in spite of being dispersed and stirred in liquid phases.

This paper described the application of these composite particles to HPLC column packings utilizing the orderly and the close-packed arrangement of small particles. As small particles, we employed non-porous silica ultramicrospheres, which have rarely been utilized for column packings. We investigated whether the orderly arrangement formed by silica ultramicrospheres can be utilized

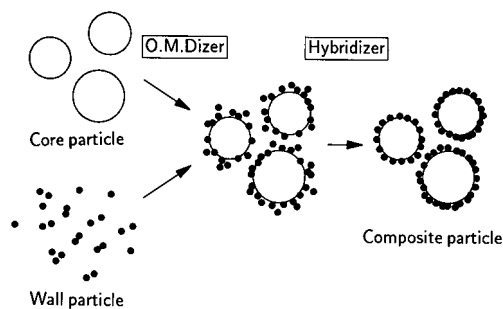


Fig. 1. Schematic diagram of wall particles adhering to core particles in a dry blending and a dry impact blending.

effectively as a stationary phase and whether the orderly arrangement is suitable especially for the separation of proteins, taking advantage of the non-porous and ultramicrosphere aspects. First, these silica-composite particles were examined with respect to some basic properties as column packings, and then low- and high-molecular-weight proteins were studied to examine the ineffective separation in columns packed with composite particles.

EXPERIMENTAL

Chemicals and reagents

The composite particles were low-density spherical polyethylene (PE) beads (average diameters 5 and 10 μm , density 0.92 g/cm^3) and high-density PE (average diameter 20 μm , density 0.958 g/cm^3) as core particles, supplied by Sumitomo Seika (Osaka, Japan). Monodisperse silica ultramicrospheres (average diameter 0.3, 0.6 and 0.9 μm , density 2.01 g/cm^3 , specific surface area 6.0 m^2/g) as wall particles were supplied by Mitsubishi Kasei (Tokyo, Japan). *n*-Hexane, isopropanol, acetonitrile, trifluoroacetic acid (TFA), toluene and nitrobenzene of analytical-reagent grade were purchased from Wako (Osaka, Japan). All proteins were purchased from Sigma (St. Louis, MO, USA). These proteins were aprotinin from bovine lung, cytochrome *c* from horse heart, bovine serum albumin, fibrinogen from bovine plasma, apoferritin from horse spleen and bovine thyroglobulin.

Shimpack CLC-SIL (150 mm \times 4.6 mm I.D., average particle diameter 5 μm , pore diameter 10 nm, specific surface area 300 m^2/g) (Shimadzu, Kyoto, Japan) and Vydac 214TP54 (250 mm \times 4.6 mm I.D., average particle diameter 5 μm , pore

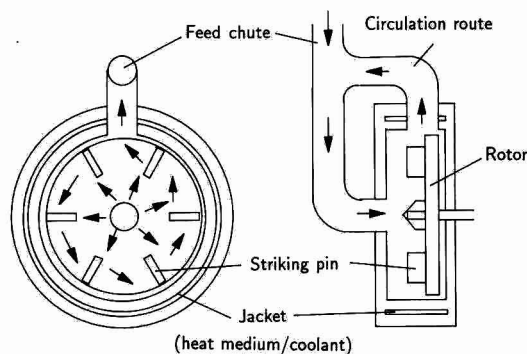


Fig. 2. Schematic diagram of hybridizer. Arrows indicate the direction of movement of powder particles.

diameter 30 nm, specific surface area 90 m²/g) (Separations Group, Hesperia, CA, USA) were used as totally porous silica packed columns.

Dry impact blending method

For the preparation of silica–composite particles, an O. M. Dizer and a Hybridizer (type NHS-0; Nara Machinery, Tokyo, Japan) were used. Schematic diagrams of the machine for producing mechanical impact are shown in Fig. 2. The machine is surrounded by a jacket through which heat medium or coolant is circulated.

PE and silica powders were blended (1400 rpm, 10 min) by the O.M. Dizer at room temperature. The total amount was fixed at 15 g. The mixing ratios are shown in Table I. These mixing ratios were calculated on the assumption that silica ultramicrospheres were closest arranged on these PE particle surfaces [36]. After preparing the interactive mixture, the mixtures were treated by the dry impact

blending method using the Hybridizer, with a rotational speed of 16 000 rpm and treatment time of 10 min at room temperature.

This hybridization process can be summarized as follows: the powder particles placed in the Hybridizer are mixed in a high-speed air stream caused by the rotation of the rotor at 16 000 rpm, and are hit repeatedly by the striking pins on the rotor. As a result of these mechanical actions, the smaller particles become fixed to the surface of the larger particles. Further details of this method were described in previous papers [31,32].

Observation of the particle surface by scanning electron microscopy (SEM)

Each of the silica–composite particles was coated with gold by an ion sputtering apparatus (JFC-1100; JEOL, Tokyo, Japan) and observed by SEM (JSM-T220; JEOL).

Measurement of specific surface area

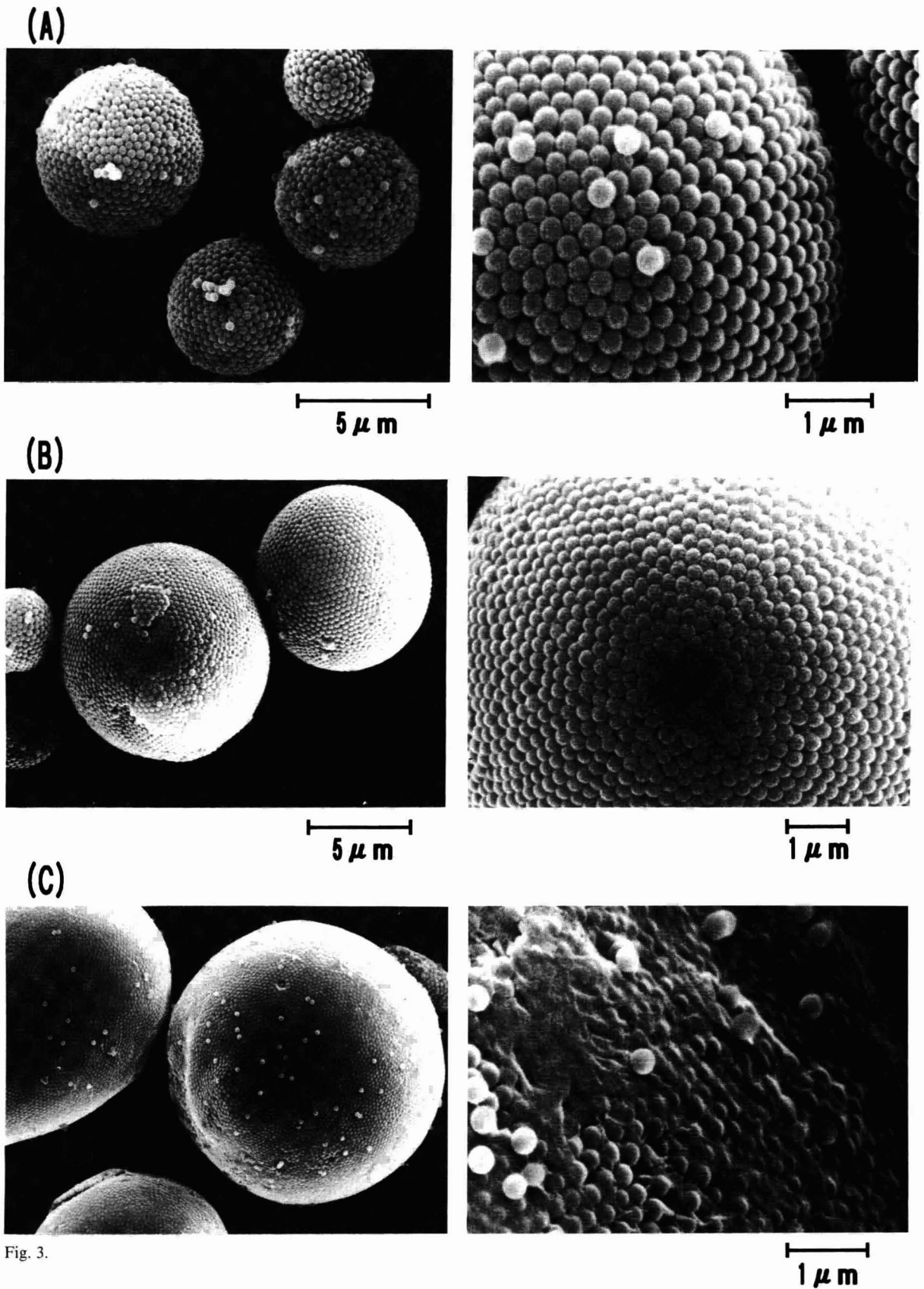
The specific surface areas of the silica–composite particles were determined by the BET method (Autosorb 6; Quantachrome, Syosset, NY, USA).

Chromatographic procedures

All chromatographic tests were performed on an LC-6A gradient system with a Rheodyne 7125 injection valve, connected to an SPD-6A UV spectrophotometric detector and to a Chromatopac C-R6A (Shimadzu). The silica–composite particles were packed into a stainless-steel column (250 mm × 4 mm I.D.) by tapping and equilibrated with *n*-hexane containing 0.5% of isopropanol at a flow-rate of 0.2 ml/min. Sample solution (1 μl)

TABLE I
COMPOSITION OF SILICA–COMPOSITE PARTICLES

Composite particle	Polyethylene particle size (μm)	Silica	
		Particle size (μm)	Mixing ratio (wt. %)
03/5	5	0.3	35
0.3/10	10	0.3	20
0.3/20	20	0.3	11
0.6/10	10	0.6	35
0.9/10	10	0.9	46



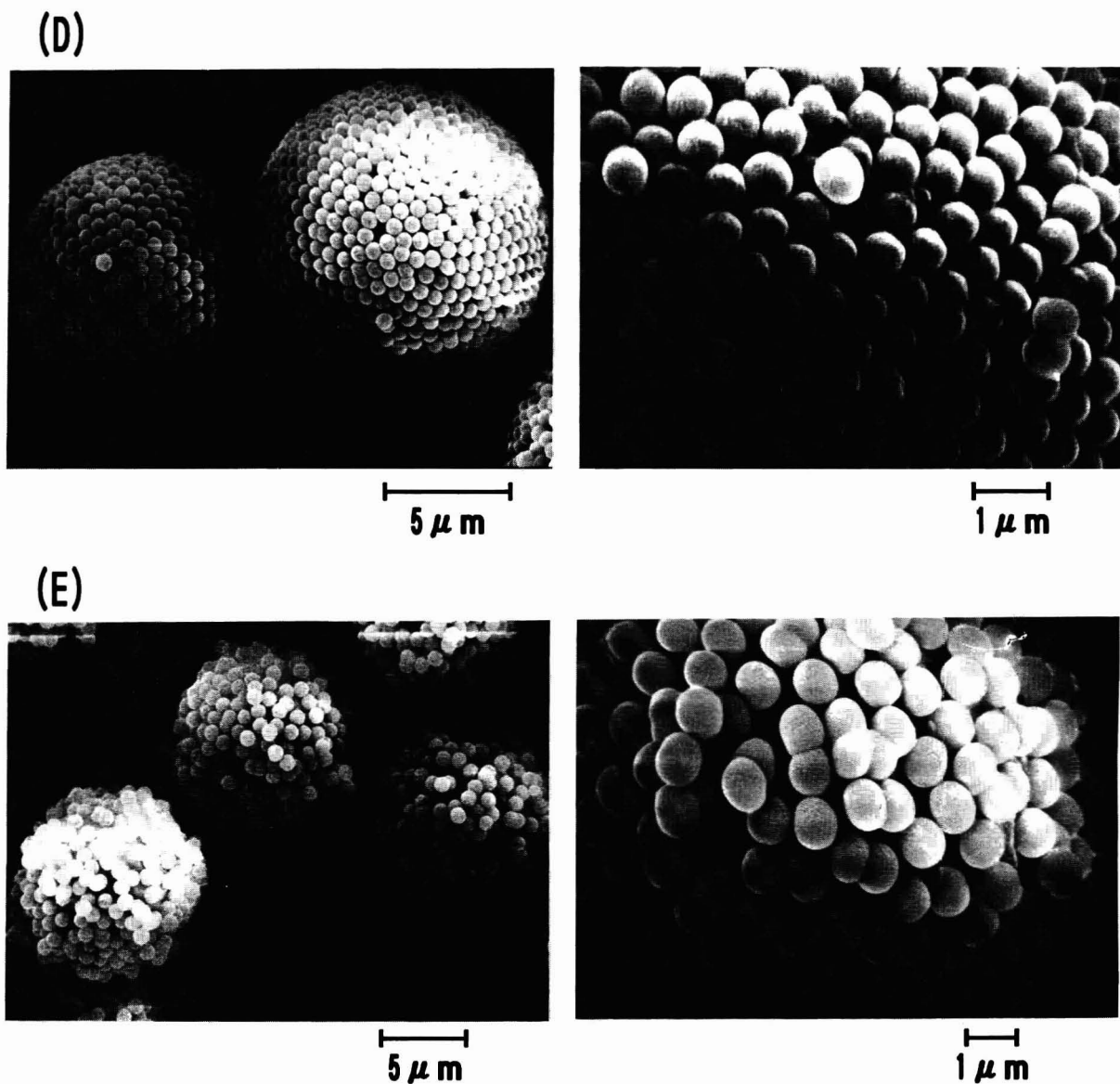


Fig. 3. Typical SEM photographs of silica-composite particles: (A) 0.3/5; (B) 0.3/10; (C) 0.3/20; (D) 0.6/10; (E) 0.9/10 combinations.

containing toluene (2000 ppm) and nitrobenzene (16 ppm) was applied to the column, and elution was followed using the UV detector set at 220 nm. The experiments using CLC-SIL were performed in a similar manner.

Separation of proteins

Silica 0.6 μm in diameter was converted into its *n*-octadecyl-bonded derivative with *n*-octadecyl-

dimethylchlorosilane according to the procedure of Kinkel and Unger [37] and then end-capping was carried out with trimethylchlorosilane (Shinetsu Chemical Industry, Tokyo, Japan) once. The ODS-coated silica ultramicrospheres and 10- μm PE were prepared as composite particles as described under *Dry impact blending method*. The 0.6-ODS/10 composite particles, which consist of ODS-coated 0.6- μm silica ultramicrospheres and 10- μm PE,

were slurry-packed into a stainless-steel column (50 mm × 4 mm I.D.) with 50% acetonitrile at a pressure of 50 kg/cm².

Standard proteins were separated with a linear gradient of acetonitrile in 0.1% TFA and detected 220 nm. The Vydac 214TP54 column (250 mm × 4.6 mm I.D.) was employed for the separation of the proteins in a similar manner. The recovery of proteins from both columns was determined by rationing the peak areas found for the injected proteins with and without the column. For controls, the column was replaced with an empty stainless-steel tube (0.8 mm I.D.) which was cut to a suitable length corresponding to the void volume of the columns.

RESULTS AND DISCUSSION

Observations of silica–composite particles

SEM photographs of silica–composite particles are shown in Fig. 3. On each particle except the combination of 0.9- μ m silica and 10- μ m PE (0.9/10), it was observed that the silica ultramicrospheres were arranged and fixed densely on the surface of the PE particles. In the dry impact blending method, it was empirically confirmed that this fixing and arrangement of small particles were achieved when the size of the large particles was more than ten times that of the small particles. With the 0.9/10 combination, it is considered that an orderly arrangement would not be achieved because the size ratio is near to the critical value.

Further examination of the surface of the silica–composite particles indicated that an orderly arrangement of silica particles approximated to the closest packing structure of spheres on a plane. In the 0.3/20 combination, which consists of high-density PE particles, the silica particles are deeply embedded in the surface of the PE particles and a large part of the silica surface is lost, although in the 0.3/5, 0.3/10 and 0.6/10 combinations, consisting of low-density PE particles, the silica particles are superficially fixed.

Such differences are attributed to the mechanisms of the fixing of the small particles by the dry impact blending method. The mechanisms assume that the local area of large-particle surfaces are deformed and melted by pressure and friction forces because of collisions between the large and small particles or between particles and the striking pins. Consequent-

ly, small particles are embedded and fixed on the surface of large particles.

The embedded depth was evaluated by measuring hole diameters on large particles. The holes arose as a result of small particles being deliberately torn off. The ratio of hole depth to the small particle diameter in the 0.3/5, 0.3/10, 0.6/10 and 0.9/10 combinations were 0.23, 0.10, 0.18 and 0.21, respectively. However, with the 0.3/20 combination, silica particles would not be torn off because they are too deeply embedded. As a result, it is suggested that the depth ratio is influenced by the ratio of particle diameters rather than the PE and silica particle diameters.

The physical properties and diameters of the core particles affect the depth ratio, as compared with the 0.3/10 to 0.3/20 combinations. The difference in embedding mechanisms between 5- and 10- μ m PE and 20- μ m PE is assumed to be follows. With 5- and 10- μ m PE particles, the deformation and the melting in the local area of the core particle surface (PE) occur proportionally, and silica particles are fixed at an adequate depth. In contrast, with 20- μ m PE particles of high density, the energy generated by collision with silica particles and the striking pins is large because of the large mass, and the PE particle is relatively hard. These effects result in most of the energy being used to melt the local surface area rather than for deformation and the wall particle is thus embedded more deeply. As 20- μ m PE particles of low density were not available, we could not compare the embedded depth ratio directly. However, as 0.6- and 0.9- μ m silica particles were used to make composite particles with 20- μ m PE of high density, the composite particle surfaces showed evidence of melting and large depth ratios were obtained. From these results, the large embedded depth ratio such as that obtained with the 0.3/20 combination is attributed not to the size ratio of PE particles to silica particles, but to the PE particles themselves.

In summary, to achieve an orderly and dense arrangement with well proportioned embedding it is necessary to deform and melt in the local area of the PE particle surfaces proportionally. Accordingly, it is confirmed that the sizes of the large and the small particles, the size ratio of the large to the small particle and the physical properties of materials affect the configuration of silica–composite particles.

TABLE II
THEORETICAL SPECIFIC SURFACE AREA (S) OF SILICA ON COMPOSITE PARTICLES AND THE TOTALLY POROUS SILICA PARTICLE

Composite particle	S	
	m ² /g	m ² /ml
0.3/5	2.58	1.20
0.3/10	1.79	0.792
0.3/20	0.510 ^a	0.256
0.6/10	1.38	0.610
0.9/10	1.16	0.547
CLC-SIL ^b	300	150

^a The embedded depth ratio was assumed to be 0.5 (not measured).

^b Totally porous silica packing of diameter 5 μm .

Specific surface area

The theoretical values of the specific surface area of silica in the silica–composite particles were calculated as described below.

When silica ultramicrospheres with a radius r are arranged and fixed on a PE particle surface with a radius R in closest order, the number of silica ultramicrospheres (A) on the PE particle is given by

$$A \approx \frac{4\pi[R + r(1 - 2k)]^2}{\pi r^2} \cdot \frac{\pi}{\sqrt{12}} \quad (1)$$

where k is the embedded depth ratio and $\pi/\sqrt{12}$ is the coating ratio of the PE surface area due to the silica monoparticle layer. Therefore, the silica specific surface area (S) of composite particles of unit weight is given by

$$S = \frac{4\pi r^2(1 - k)A}{\frac{4}{3}\pi R^3 \rho_p + \frac{4}{3}\pi r^3 \rho_s A} = \frac{3r^2(1 - k)A}{R^3 \rho_p + r^3 \rho_s A} \quad (2)$$

where ρ_p and ρ_s are density of PE and silica, respectively. Calculated S values are given in Table II.

Using the BET method, the S values were 0.31–2.32 m²/g for all silica–composite particles. These experimental results support the calculated values in Table II. The order of these experimental data, however, were near to the experimental error range of the BET method, because silica–composite particles have lower S values than totally porous silica.

Therefore, the calculated values were used in subsequent considerations.

Resolution and theoretical plate numbers

Silica–composite particles were packed into columns by the tapping method. The tapping densities of the 0.3/5, 0.3/10, 0.3/20, 0.6/10 and 0.9/10 silica–composite particles were 0.48, 0.47, 0.51, 0.46 and 0.48 g/cm³, respectively. The packing porosities were 63.1, 58.6, 52.9, 64.5 and 66.5%, respectively. These large porosities suggest the presence of a void volume caused by physical particle aggregates in the columns, because the theoretical porosities of the closet and the loosest packing structure models of spheres are 25.95 and 47.64%, respectively. However, columns packed with the 0.3/10, 0.3/20 and 0.6/10 combinations had constant column pressures and did not show a decrease in the bed volume at a flow-rate of 1.0 ml/min. These results indicate that the packing structures formed are considered to be in stable states. In contrast, columns packed with the 0.3/5 and 0.9/10 combinations showed a sudden increase in column pressure and a decrease in bed volume at a flow-rate 0.5 ml/min. Therefore, the packing structures were considered to be in an unstable state. Further, although the slurry packing method was applied to pack the 0.3/5 and 0.9/10 combinations, the columns could not be employed in the analysis because of high pressure. The cause of such high pressure is attributed to blocking of the path of the mobile phase. With the 0.3/5 combination, small particles, which were included in PE particles because the PE particles were not well classified precisely, may clog the path. The 0.9/10 combination has an irregular form, as shown in Fig. 3E, hence the particles may form aggregates in the column.

Consequently, the tapping method was employed for packing particles and the flow-rate was fixed at 0.2 ml/min in order to apply analysis under the same conditions for all silica–composite particles.

Silica–composite particles were packed into columns and their properties were investigated in adsorption chromatography. The resolution and theoretical plate number (N) calculated from the chromatograms of toluene and nitrobenzene are shown in Table III.

In comparison with the 0.3/5, 0.3/10 and 0.3/20, combinations, the resolution and N increase with a

TABLE III
THEORETICAL PLATE NUMBER AND RESOLUTION OF
A COLUMN PACKED WITH SILICA-COMPOSITE PAR-
TICLES

Composite particle	Theoretical plates per meter (N) ^a	Resolution
0.3/5	4080	1.26
0.3/10	2428	1.09
0.3/20	1356	—
0.6/10	6640	1.69
0.9/10	2716	0.884
CLC-SIL ^b	38600	6.25

^a Calculated from peak of nitrobenzene.

^b Totally porous silica packing of diameter 5 μm .

decrease in PE particle diameter. The specific surface area of silica particles increases with a decrease in the diameter of PE particles (see Table II). Therefore, the decrease in the PE particle diameter provides high resolution and N because of the large specific surface area.

The separation of two peaks was scarcely achieved with the 0.3/20 combination, owing to the loss of the silica surface area, as apparently shown in Fig. 3C.

When 10- μm PE was used as core particles, the 0.6/10 combination provided the highest resolution and N . Although there is not much differences in the S values between the 0.3/10, 0.6/10 and 0.9/10 combination, N for 0.6/10 is more than double that for 0.3/10 and 0.9/10. These results indicate that the performance represented by resolution and N is not determined only by S and the diameters of the silica-composite particles that form the packing structures in the columns. The performance is also affected by the size of the silica ultramicrospheres. With the 0.3/10 and 0.6/10 combinations, on the assumption that the spatial configuration of 0.3/10 in the column is nearly equal to that of 0.6/10, it is suggested that diffusion of solutes and mobile phases at the surface and the interstices of silica ultramicrospheres influences the column performance. With the 0.0/10 combination, it is explained by the disorder arrangement of silica particles on the PE particles in Fig. 3E as follows: the actual amount of silica particles fixed on PE particles is smaller than the calculated value, hence the value of the silica

surface area is smaller than the theoretical value. Also, the randomness of the arrangement may cause an irregular flow of the mobile phase. Consequently, this leads the broadening of the peak and a decrease in resolution.

The resolution and N of CLC-SIL, which is a commercial column packed with totally porous silica of 5 μm diameter, are shown in Table III. The N values of CLC-SIL are 6-28 times higher than those of columns packed with silica-composite particles, so that a high performance of ultramicrospheres was not displayed with silica-composite particles. From the results, the specific surface area per unit column length is much less than that of totally porous silica (see Table II). Second, diffusion of mobile phases and solutes occurs at the large interstices of silica-composite particles, and this effect is further enhanced because of the loose packing structure of the silica-composite particles which is attributable to the slightly broader size distribution.

Consequently, silica-composite particles are not regarded as having the packing structures of ultramicrosphere silica, but regarded as composites which have much better configurations.

In conclusions, silica-composite particles, which

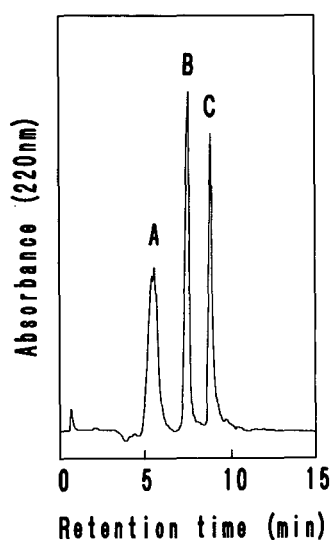


Fig. 4. Gradient elution of proteins on the column packed with silica-composite particles (0.6-ODS/10). Conditions: column, 50 mm \times 4 mm I.D.; gradient, 5 to 70% acetonitrile in 0.1% TFA in 15 min; flow-rate, 0.5 ml/min; detection, UV at 220 nm. Peaks: A = aprotinin; B = cytochrome c; C = BSA.

TABLE IV
RECOVERY OF PROTEINS FROM COLUMNS PACKED
WITH COMPOSITE PARTICLES

Protein	Recovery (%)	Protein	Recovery (%)
Aprotinin	100.1	Fibrinogen	96.7
Cytochrome <i>c</i>	99.4	Apoferitin	92.8
BSA	102.3	Thyroglobulin	70.1

consist of 0.6- μm silica ultramicrosphere arranged on the surface of 10- μm PE, showed the highest *N*, and the silica ultramicrospheres were arranged orderly and densely on PE. Therefore, it is confirmed that the 0.6/10 combination is the most appropriate for HPLC column packings.

Separations of proteins

As the 0.6/10 combination was ascertained to be the best composite particle for packings, ODS-treated silica-composite particles (0.6-ODS/10) were prepared using 0.6- μm silica ultramicrospheres with previously introduced ODS groups and 10- μm

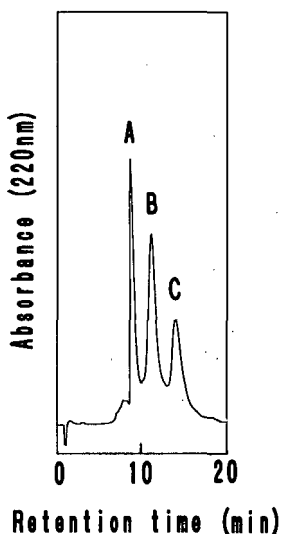


Fig. 5. Gradient elution of high-molecular-weight proteins on the column packed with silica-composite particles (0.6-ODS/10). Conditions: Column, 50 mm \times 4 mm I.D.; gradient, 30 to 70% acetonitrile in 0.1% TFA in 15 min; flow-rate, 0.3 ml/min; detection, UV at 220 nm. Peaks: A = fibrinogen; B = apoferitin; C = thyroglobulin.

PE. 0.6-ODS/10 was packed into a column, and aprotinin, cytochrome *c* and BSA were separated (see Fig. 4). Three separated peaks were obtained within 10 min with an elution volume of 5 ml, and these three proteins demonstrated excellent recoveries, as shown in Table IV. From these results, it is clear that separations in a short time and with high recovery, which are features of non-porous silica packings, can be achieved by using silica-composite particles consisting of silica ultramicrospheres.

In another experiment, the separation of three high-molecular-weight proteins, fibrinogen (340 000) apoferritin (443 000) and thyroglobulin (669 000) was attempted. As shown in Fig. 5, these proteins could be separated as sharp and symmetrical peaks within 20 min and the recoveries were also satisfactory (see Table IV).

The Vydac 214TP54 column was also employed to separate these three high-molecular-weight proteins (see Fig. 6). The column was packed with wide-pore silica of average pore diameter 30 nm. However, apoferritin and thyroglobulin could not be separated. This result indicates that specific hindrance factors, which limit the permeability of the solute in the pores [2], were unavoidable with such high-

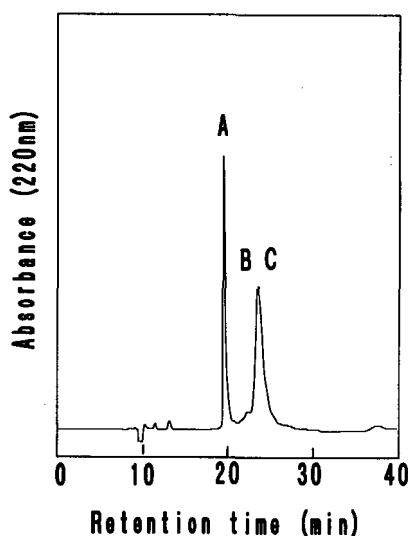


Fig. 6. Gradient elution of high-molecular-weight proteins on Vydac 214TP54. Conditions: column, 250 mm \times 4.6 mm I.D.; gradient, 30 to 70% acetonitrile in 0.1% TFA in 20 min; flow-rate, 0.3 ml/min; detection, UV at 220 nm. Peaks: A = fibrinogen; B = apoferitin; C = thyroglobulin.

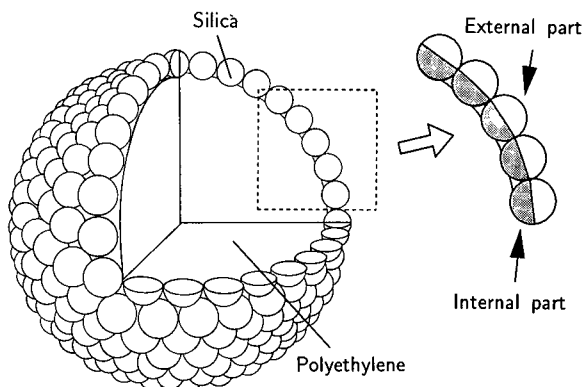


Fig. 7. Schematic diagram of a silica-composite particle and the internal and external parts of the silica surface.

molecular-weight proteins using a porous silica packing.

When porous packings are used for the separation of solutes, it is reported that the pore diameter must be ten times greater than the solute diameter for complete access of all solute molecules to the internal surface area of the pores [2]. We applied this theory for porous packings to silica-composite particles which have a fine structure on the surface.

The diameters of the three high-molecular-weight proteins that were separated in this study are estimated to be 10–15 nm [29]. Fig. 7 shows the silica surface of a composite particle where the stationary phase is divided roughly into two parts. One is the external part, which means the outer surface of silica on composite particles. The other is the internal part of composite particles, which means the surface of silica facing the PE particles. With the 0.6/10 combination, the cusp-shaped pore formed between close-packed silica ultramicrospheres approximates a triangle of 300 nm side, and the area of the pores is equivalent to a circle of diameter 136 nm. Approximately 2000 cusp-shaped pores are formed on each composite particle surface. The structure consisting of the interstices can also be regarded as an accurate pellicular porous structure which is formed on the 10- μm PE particles. This assumption suggests that the column packed with the 0.6/10 combination could be employed for the separation of solutes with molecular diameters up to 30 nm without specific hindrance factors.

These three kinds of proteins are able to access the external and the internal parts of the stationary phase, and similarly low-molecular-weight solutes are able to access both parts.

The arrangement of silica ultramicrospheres on the surface of 10- μm PE particles is valuable for improving the stationary phase utilization. It was found that 0.6-ODS/10 was able to separate proteins of MW up to 669 000.

Use of composite particles for HPLC packings

There are three aspects of using composite particles for HPLC packings. The first aspect is the arrangement of ultramicrospheres which are fixed orderly and densely, the second is a pellicular particle which has uniform pores and the third is a complex particle which consists of some kinds of materials.

In this study, a dense packing structure consisting of ultramicrospheres was utilized to form the rapid and homogeneous interaction system between the solute and the stationary phase and the mobile phase. It was found that the diameter of silica ultramicrosphere itself affects the N values. The structure of the composite particles led to the successful separation of proteins with a wide molecular weight range. For example, with the 0.6/10 combination, although the apparent particle diameter is 10 μm , the surface area of the composite particle is equal to that of a 3- μm non-porous silica microsphere per unit volume.

If silica-composite particles are regarded as pellicular particles, it should be noted that these particles were not prepared by the conventional method in which the pore diameters are regulated by controlling the conditions of synthesis, but by a novel method in which the pores are formed by arranging silica ultramicrospheres. It is possible to make any form of pores if the combination of core materials and wall materials are suitable for preparing composite particles. A homogeneous surface can be obtained easily by the employment of previously coated particles.

Finally, if silica-composite particles are regarded as complexes consisting of several particles, it suggests the possibility of preparing particles which have different properties. In this study, non-porous silica ultramicrospheres were utilized for HPLC column packings by being arranged on the surface of

large particles. Some materials which have never been considered as column packings, e.g., a needle-like, a plate-like or a fibre-like substance, may be proposed as column packings in a similar manner as described above. Also, several kinds of particles may be blended to prepare multi-functional particles.

It is suggested that silica-composite particles which possess unique properties due to the structure not only can be utilized for the separation of high-molecular-weight proteins but also represent a new concept for preparing column packings.

CONCLUSIONS

The double packing structure, which consists of the spatial configuration of silica-composite particles in the column and the dense arrangement of silica ultramicrospheres on the PE particle surface, enable silica ultramicrospheres to be utilized as stationary phases in HPLC while simultaneously maintaining the flow of the mobile phase. The diameters of the silica ultramicrospheres affected N ; of the six kinds of composite particles examined the 0.6/10 combination gave the highest N . Silica-composite particles are non-porous and have a large surface area, which are the conditions required for column packings for protein analysis, and achieved the separations of proteins with a wide range of molecular weights.

ACKNOWLEDGEMENT

The authors are grateful to Mr. Eiji Hattori, Mitsubishi Kasei, for measuring specific surface areas by the BET method.

REFERENCES

- 1 J. D. Pearson, N. T. Lin and F. E. Regnier, *Anal. Biochem.*, 124 (1982) 217.
- 2 M. T. W. Hearn and B. Grego, *J. Chromatogr.*, 282 (1983) 541.
- 3 H. Engelhardt and H. Muller, *Chromatographia*, 19 (1984) 77.
- 4 M. T. W. Hearn and B. Grego, *J. Chromatogr.*, 296 (1984) 61.
- 5 M. A. Stadalius, H. S. Gold and L. R. Snyder, *J. Chromatogr.*, 327 (1985) 27.
- 6 M. A. Stadalius, M. A. Quarry and L. R. Snyder, *J. Chromatogr.*, 327 (1985) 93.
- 7 F. V. Warren and B. A. Bidlingmeyer, *J. Liq. Chromatogr.*, 8 (1985) 619.
- 8 Y. S. Kim, B. W. Sands and J. L. Bass, *J. Liq. Chromatogr.*, 10 (1987) 839.
- 9 C. N. Satterfield, C. K. Colton and W. H. Pitcher, *AIChE J.*, 19 (1973) 62826.
- 10 R. R. Walters, *J. Chromatogr.*, 249 (1982) 19.
- 11 J. Koehler, D. B. Chase, R. D. Farlee, A. J. Vega and J. J. Kirkland, *J. Chromatogr.*, 352 (1986) 275.
- 12 K. A. Cohen, K. Schnellenberg, K. Benedek, B. L. Karger, B. Grego and M. T. W. Hearn, *Anal. Biochem.*, 140 (1984) 223.
- 13 S. A. Cohen, K. P. Benedek, S. Dong, Y. Tapui and B. L. Karger, *Anal. Chem.*, 56 (1984) 217.
- 14 M. A. Stadalius, B. F. D. Ghrist and L. R. Snyder, *J. Chromatogr.*, 387 (1987) 21.
- 15 M. T. W. Hearn, M. I. A. Aguilar, C. T. Mant and R. S. Hodges, *J. Chromatogr.*, 438 (1988) 197.
- 16 A. W. Purcell, M. I. Aguilar and M. T. W. Hearn, *J. Chromatogr.*, 476 (1989) 113.
- 17 K. D. Lork, K. K. Unger, H. Brueckner and M. T. W. Hearn, *J. Chromatogr.*, 476 (1989) 135.
- 18 M. C. J. Wilce, M. I. Aguilar and M. T. W. Hearn, *J. Chromatogr.*, 536 (1991) 165.
- 19 J. C. Giddings, *Adv. Chromatogr.*, 20 (1982) 217.
- 20 K. K. Unger, J. N. Kinkel, B. Anspach and H. Giesche, *J. Chromatogr.*, 296 (1984) 3.
- 21 K. K. Unger, W. Messer and K. F. Krebs, *J. Chromatogr.*, 149 (1978) 1.
- 22 C. Dewaele and M. Verzele, *J. Chromatogr.*, 282 (1983) 341.
- 23 K. K. Unger, G. Jilge, R. Janzen, H. Giesche and J. N. Kinkel, *Chromatographia*, 22 (1986) 379.
- 24 K. K. Unger, G. Jilge, J. N. Kinkel and M. T. W. Hearn, *J. Chromatogr.*, 359 (1986) 61.
- 25 G. Jilge, R. Janzen, H. Giesche, K. K. Unger, J. N. Kinkel and M. T. W. Hearn, *J. Chromatogr.*, 397 (1987) 71.
- 26 R. Janzen, K. K. Unger, H. Giesche, J. N. Kinkel and M. T. W. Hearn, *J. Chromatogr.*, 397 (1987) 81.
- 27 Y. Kato, S. Nakatani, T. Kitamura, Y. Yamasaki and T. Hashimoto, *J. Chromatogr.*, 502 (1990) 416.
- 28 H. Giesche, K. K. Unger, U. Esser, B. Eray, U. Truedinger and J. N. Kinkel, *J. Chromatogr.*, 465 (1989) 39.
- 29 G. Guiochon and M. Martin, *J. Chromatogr.*, 326 (1985) 3.
- 30 J. A. Hersey, *Powder Technol.*, 11 (1975) 41.
- 31 M. Koishi, H. Honda, T. Ishizaka, T. Matsuno, T. Katano and K. Ono, *Chimicaoggi*, July–August (1987) 43.
- 32 H. Honda, K. Ono, T. Ishizaka, T. Matsuno, T. Katano and M. Koishi, *J. Soc. Powder Technol. Jpn.*, 24 (1987) 593.
- 33 M. Koishi, in K. Iinoya, K. Gotoh and K. Higashitani (Editors), *Powder Technology Handbook*, Marcel Dekker, New York, 1991, p. 453.
- 34 T. Ishizaka, H. Honda, Y. Kikuchi, K. Ono, T. Katano and M. Koishi, *J. Pharm. Pharmacol.*, 41 (1989) 361.
- 35 T. Tanaka, Y. Kikuchi and K. Ono, *Zairyo Gijyuu*, 8 (1990) 274.
- 36 H. Honda and M. Koishi, *Studies in Liberal Arts and Sciences*, Science University of Tokyo, Tokyo, 24 (1992) 183.
- 37 J. N. Kinkel and K. K. Unger, *J. Chromatogr.*, 316 (1984) 193.

Short fibrous supports for preparative chromatographic separations of biomolecules

Jy-Kung King and Neville G. Pinto

Department of Chemical Engineering, University of Cincinnati, Cincinnati, OH 45221-0171 (USA)

(First received February 20th, 1991; revised manuscript received June 1st, 1992)

ABSTRACT

The characteristics of short, fibrous supports for chromatographic separations of biomolecules have been studied. A non-porous, silica-based fiber with an anion-exchange functionality was developed, and the performance of this support for protein separations was determined. It was established that the short-fiber column exhibits a low pressure drop, allowing separations to be performed at elevated flow-rates. The dynamic adsorption capacity of the column for three proteins, myoglobin, ovalbumin and bovine serum albumin, have been determined as a function of solution pH and salt concentration. It has been shown that the column can be used to separate mixtures of these proteins at elevated flow-rates.

INTRODUCTION

The significant growth in the market for bioproducts has led to the need to adapt chromatography to the process scale [1]. The criteria for evaluating the performance of a process-scale purification have been shown to be product purity, throughput, and cost [2]. For this reason, systems developed for analytical separations are not always suitable for process-scale separations. In recognition of this, substantial efforts are now being devoted to the development of systems that involve new operating procedures [3] and novel equipment configurations [4–9].

The use of chromatographic supports with a fibrous geometry is one novel approach to developing chromatographic systems for scaled-up separations. Two types of fiber columns have recently been developed. In one type, fibers, either solid or hollow, are packed into a column such that the longest dimension of the fibers is aligned with the

direction of flow of the mobile phase [10–13]. The second type uses relatively short fibers, and these are packed with random orientations [14]. The short-fiber column and columns packed with aligned hollow fibers have been shown to exhibit very low pressure drops [11,14], making them potentially suitable for high-throughput separations.

Though both types of columns have potential applications in high-throughput separations, the randomly packed short-fiber columns are of immediate interest, since the procedures for packing and operating these columns are essentially the same as those used for conventional columns packed with spherical supports. Thus, the developmental task involves only the synthesis of appropriate supports, and not the development of packing and operating procedures that is required for systems that are radically different.

At the present time, only one type of short-fiber support [14], a silica-based affinity support, has been developed. In this paper, the synthesis of a short-fiber anion-exchange support is described; an ion-exchange support was developed because a great number of downstream processing protocols use an ion-exchange step. The characteristics of this

Correspondence to: Dr. N. G. Pinto, Department of Chemical Engineering, University of Cincinnati, Cincinnati, OH 45221-0171, USA.

support for protein separations have been evaluated.

EXPERIMENTAL

Materials

Bulk Q-106 quartz fiber was a gift from Manville Sales (Toledo, OH, USA). This non-porous fiber consists of 98.5% (w/w) silica (SiO₂) and has a nominal fiber diameter of 0.7 μm. PAE-300, a porous silica-based chromatographic packing, was purchased from Amicon (Danvers, MA, USA).

Reagents

3-Glycidoxypropyltrimethoxysilane (Z-6040) was a gift from Dow Corning (Midland, MI, USA). Polyethyleneimine (PEI-6, molecular mass 600) was purchased from Polysciences (Warrington, PA, USA). Solvents (acetone, methanol, etc.) and reagents (sulfuric acid, nitric acid, etc.) were purchased from Fisher Scientific (Cincinnati, OH, USA).

Proteins

The proteins, bovine serum albumin (BSA), ovalbumin (OVA) and myoglobin (MYO) from horse heart, were purchased from Sigma (St. Louis, MO, USA).

Instrumentation

A SP8800 ternary HPLC pump system (Spectra-Physics, San Jose, CA, USA) was used for the chromatographic evaluations. Absorbance was monitored with a Model 2550 UV detector (Varian, Walnut Creek, CA, USA).

Preparation of fiber substrate

Bulk quartz fiber Q-106 was cut in water with a homogenizer (Biospec Products, Bartlesville, OK, USA). The nominal length of the cut fiber, characterized with an optical microscope, is 115 μm. The fiber was cleaned by washing with acetone and deionized water. It was then hydroxylated, to increase the number of reactive silanol groups on the surface. This was achieved by refluxing in a 50:50 (v/v) mixture of concentrated sulfuric acid and nitric acid for 8 h [15,16]. Subsequently, the fiber was thoroughly washed with deionized water and dried in a vacuum oven at 110°C for 2 h.

Surface modification of hydroxylated fiber

A 2-g amount of the hydroxylated fiber was refluxed in 10% (v/v) Z-6040 solution in dry toluene (dried over sodium metal) for 24 h [14,15,17,18]. After filtering off the silane solution, the fiber was dried in a vacuum oven at 110°C for 8 h. It was then washed with 60 ml acetone and dried in a vacuum oven at room temperature for 8 h. At the end of this step, the Z-6040 is covalently attached to the fiber through the silanol group.

Immobilization of polyethyleneimine on the fiber

The Z-6040 bonded fiber was treated with a solution of 20% (w/v) PEI-6 in methanol for 12 h [17,19,20]. After filtering off the PEI-6 solution, the fiber was dried in a vacuum oven at 80°C for 12 h. Subsequently, it was washed with 60 ml methanol and 60 ml acetone, and dried in vacuum at room temperature for 8 h. This process immobilizes the PEI-6 on the fiber by covalent attachment to the Z-6040. The procedure used here to attach the PEI-6 to the silica fiber is similar to that developed by Regnier and co-workers [17,19-24] for spherical silica supports, indicating that already developed activation methods can be adapted to making silica supports with a fibrous geometry.

Column packing

A packing procedure involving sedimentation followed by pressurization was used to pack the anion-exchange fiber into a standard high-performance liquid chromatography (HPLC) (150 mm × 4.6 mm I.D.). The column was vertically oriented, and the fiber suspended in methanol was poured into the top end. A weak vacuum was applied to the bottom to remove the solvent. The column was then attached to a HPLC pump and a pressure drop of 2400 p.s.i. was applied for about 10 min. This compressed the packing in the column. The entire process was repeated a number of times until the column was full and tightly packed.

In order to allow a comparison of pressure drop characteristics with conventional columns, PAE-300 (10 μm), a commercial, porous, silica support, was packed in a column of the same dimensions. In this case, conventional slurry packing at a pressure of 6000 p.s.i. was used. A Haskel air-driven liquid pump purchased from Alltech (Deerfield, IL, USA) was utilized for this purpose.

Measurement of column pressure drop

The column pressure drop was determined by subtracting the system pressure drop in the absence of the column from that when the column was part of the flow circuit. These measurements were made for both the Q-106 fiber column and the PAE-300 column. A 0.05 mg/ml BSA in 0.01 M Tris-HCl (pH 8.0) solution was used in all cases. The pressure drop behavior was studied for flow-rates between 1 and 10 ml/min.

Measurement of dynamic capacity

The dynamic capacity of the fiber column was determined with frontal chromatography. The capacity was determined for three proteins, BSA, OVA and MYO, at pH 6.0 and 8.0, and at two salt concentrations. The buffers used were 0.01 M histidine at pH 6.0 and 0.01 M Tris at pH 8.0, and NaCl was used as the salt.

The frontal experiments involved washing the column with 0.5 M NaCl and equilibrating it with the required carrier solution. The column was then disconnected, and the upstream tubing was filled with the protein solution. The column was reconnected, and the frontal injection was initiated. Column response was monitored with the UV detector at 280 nm. All the experiments were performed at room temperature.

Chromatographic evaluation

Chromatographic evaluations of the column were made in the gradient elution mode. A sample size of 10 μ l was used in all cases. The gradient elutions involved a 20-min linear gradient of NaCl from 0.0 to 0.5 M. Three buffers, Tris (pH 8.0), imidazole (pH 7.0) and histidine (pH 6.0), were used. The column response was monitored at 280 nm.

RESULTS AND DISCUSSION

Column pressure drop

The experimentally obtained pressure drop characteristics of the fiber column and reference PAE-300 column are shown in Fig. 1. It is immediately evident that the fiber column exhibits a substantially lower pressure drop, with pressure drops of no more than about 20% of those in the PAE-300 column at the same flow rate.

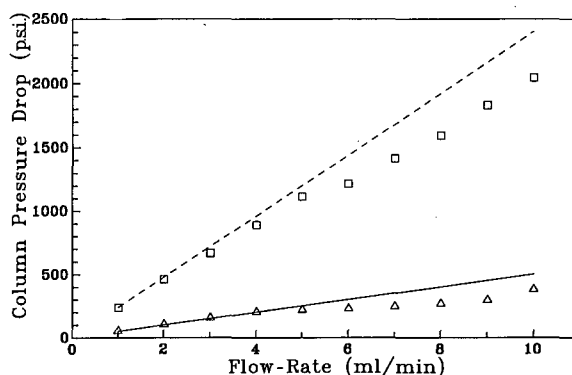


Fig. 1. Column pressure drop as a function of flow-rate for the fiber column (Δ) and PAE-300 column (\square). Column length, 15 cm; ---- and —, theoretical predictions [25].

Due to equipment limitations on the maximum volumetric throughput, the pressure drop experiments could not be extended to flow-rates above 10 ml/min. However, an attempt was made to theoretically estimate the pressure drop at higher volumetric flow rates. A correlation developed by Leva [25] for packed beds was used for this purpose:

$$\Delta P = \frac{2f_m G^2 L (1 - \epsilon)^{3-n}}{d g_c \rho \Phi_s^{3-n} \epsilon^3} \quad (1)$$

The predictions of this correlation for the two columns studied experimentally are shown in Fig. 1; the bed porosities, 0.4 for the PAE-300 column and 0.92 for the fiber column, were calculated independently from unretained component data. It is seen that Leva's correlation predicts the pressure drop reasonably well; the slight over prediction at higher flow-rates is suspected to be due to pump characteristics at 6 ml/min and higher, rather than a failure of the equation. Thus, for the purposes of a rough theoretical estimate at flow-rates beyond the experimental range the correlation should be adequate. Shown in Table I are the predictions at higher flow rates. These data show that it will be possible to operate the 15-cm fiber column at 40–50 ml/min while maintaining acceptable pressure drops. This implies linear velocities of 240–300 cm/min at pressure drops of about 140 p.s.i./cm.

Dynamic adsorption capacity

Frontal chromatography was used to evaluate the dynamic adsorption capacity of the fiber col-

TABLE I
PREDICTIONS OF PRESSURE DROP AT HIGHER FLOW-RATES

Flow-rate (ml/min)	Linear velocity (cm/min)	Column	ΔP (p.s.i.)	$\Delta P/L$ (p.s.i./cm)
20	120	Q-106	1037	69
		PAE-300	4717	315
30	181	Q-106	1459	97
		PAE-300	7308	487
40	241	Q-106	2021	135
		PAE-300	9666	644
50	301	Q-106	2600	173
		PAE-300	12 144	810

umn. Three proteins, BSA, OVA and MYO, were used. The adsorption isotherms constructed from the breakthrough curves for each of these proteins and for a number of mobile phase conditions are shown in Figs. 2-5. These capacities are calculated on the basis of the breakthrough of 50% of the feed concentration. Figs. 2 and 3 show the effect of pH on capacity. For both cases, the adsorption isotherm is roughly Langmuirian in shape. At pH 8.0 the fiber has a capacity of about 1.2 mg/g for BSA, 0.6 mg/g for OVA, and virtually no capacity for MYO. At the lower pH of 6.0, the capacity for BSA drops to about 0.8 mg/g, while for OVA it increase slightly to about 0.7 mg/g. Once again there is virtually no capacity for MYO. The observed effects of pH can be qualitatively explained on the basis of the pI values of the proteins (Table II) and the weakly

basic nature of the ion-exchange fiber. The low pI values of BSA and OVA, 4.9 and 4.7, respectively, ensure that these proteins have a high charge density at pH 8.0. When the pH is lowered to 6.0, the ion-exchange capacity of the weakly basic support is increased, but the charge density of both proteins is lowered. In the case of BSA these oppositely acting effects lead to a net decrease in capacity, while OVA shows a slight increase. For MYO, a pI of 7.3 should give, as observed, no capacity at pH 6.0. At pH 8.0, the protein will have a low charge density, but the ion-exchange capacity of the support is lowered, once again giving virtually no adsorption. Though the adsorption behavior can be explained qualitatively on the basis of charge density, other factors such as charge asymmetry, hydrophobic interactions, conformational changes, and hydrogen

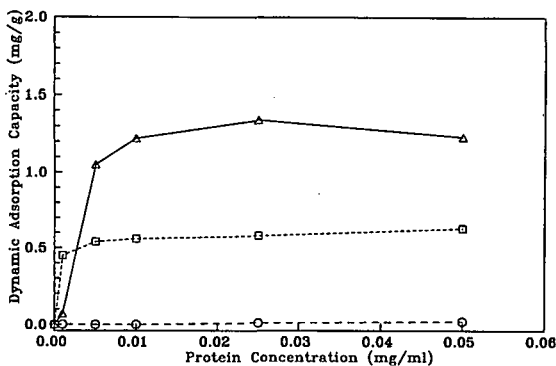


Fig. 2. Adsorption isotherms of BSA (Δ), OVA (\square) and MYO (\circ) at pH 8.0.

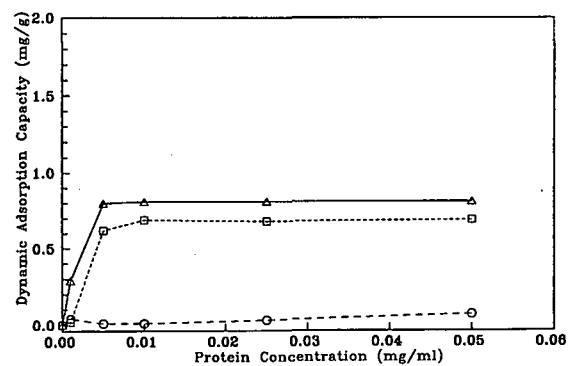


Fig. 3. Adsorption isotherms of BSA (Δ), OVA (\square) and MYO (\circ) at pH 6.0.

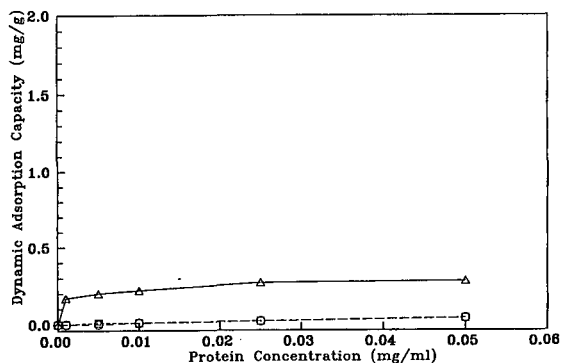


Fig. 4. Adsorption isotherms of BSA (Δ), OVA (\square) and MYO (\circ) at pH 8.0 with 0.05 M NaCl.

bonding can also be expected to influence the adsorption capacity [24,26,27].

The effects of salt concentration on adsorption are shown in Figs. 4 and 5. Two salt concentrations were used: 0.05 M NaCl (Fig. 4) and 0.1 M NaCl (Fig. 5). Once again, the adsorption isotherms are roughly Langmuirian. However, it is clear that the presence of salt leads to a rapid decrease in protein capacity, with virtually no capacity remaining at 0.1 M NaCl.

An important factor for columns operating at elevated flow rates is the sensitivity of the column capacity to the mobile phase velocity. Shown in Fig. 6 is the typical dependence of column capacity on flow-rate. These data were obtained with frontal experiments with BSA at pH 8.0. Once again, 50% of the feed concentration was used to determine ca-

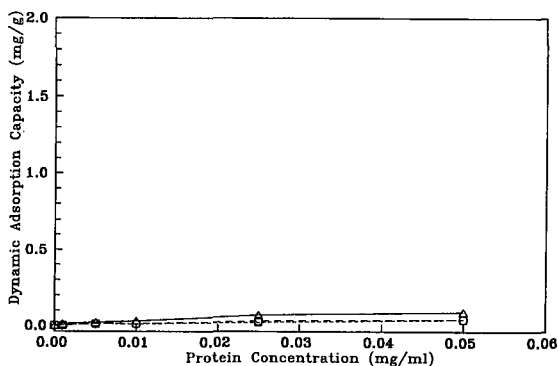


Fig. 5. Adsorption isotherms of BSA (Δ), OVA (\square) and MYO (\circ) at pH 8.0 with 0.10 M NaCl.

TABLE II
CHARACTERISTICS OF PROTEINS

Protein	Isoelectric point	Molecular mass
BSA	4.9	69 000
OVA	4.7	44 000
MYO	7.3 (major) 6.9 (minor)	17 500

capacity. It can be seen that the dynamic capacity is maintained at higher flow-rates. The reason for this is that the fiber is non-porous, restricting the mass transfer resistance to the liquid phase. In this case, since the fluid velocities are in the laminar flow region, the liquid mass transfer coefficient is essentially independent of flow-rate. Thus, the shape of the concentration fronts is not affected significantly by mass transfer, leading to a dynamic capacity that is essentially independent of flow-rate.

Gradient elution chromatography

The separation of BSA, OVA and MYO was attempted on the fiber column using gradient elution. A mixture of 5 mg/ml BSA, 5 mg/ml OVA and 0.5 mg/ml MYO was used for all the separations. Shown in Fig. 7 are typical chromatograms obtained at 1 ml/min for carrier solutions at pH 6.0, 7.0 and 8.0. While the MYO is separated cleanly from the other two proteins, since it is essentially unretained, the separation of BSA from OVA is strongly dependent on the solution pH. A good sep-

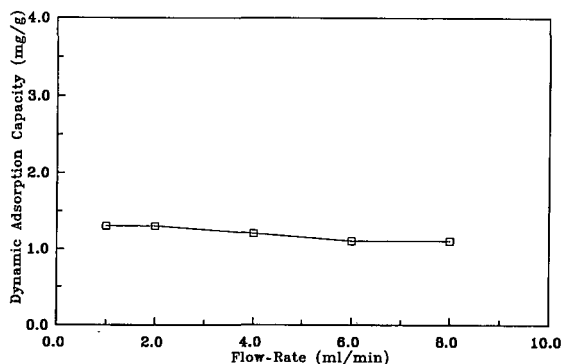


Fig. 6. Dynamic adsorption capacity of fiber column for BSA as a function of flow-rate.

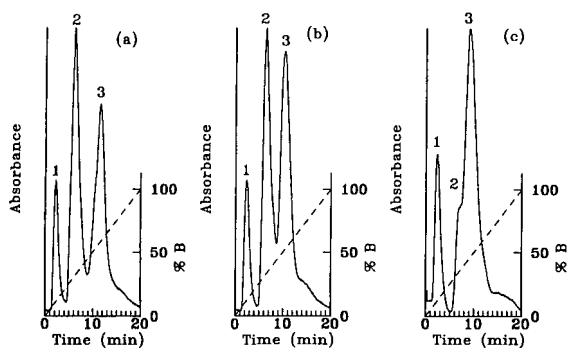


Fig. 7. Gradient elution separation of BSA, OVA and MYO as a function of pH. Flow-rate, 1 ml/min. Gradient, 20 min, linear, 0.0 to 0.5 M NaCl. (a) pH 8; (b) pH 7; (c) pH 6.

aration is obtained at pH 8.0, a poor separation at pH 6.0, and a separation intermediate between these at pH 7.0. With regard to the resolution between OVA and BSA, a decrease is observed with decreasing pH. This can be explained on the basis of the pH dependence of the retention times. Retention times for BSA and OVA, with each obtained separately using the same gradient protocol as was used for the mixtures, changed in opposite directions with an increase in pH; an increase in the retention time for BSA and a decrease for OVA were observed. This behavior is consistent with the frontal capacity data, and, as was stated earlier, is related to the charge density of the proteins and the ion-exchange capacity of the support.

A significant characteristic of the fiber column is the low pressure drop it exhibits at high flow-rates.

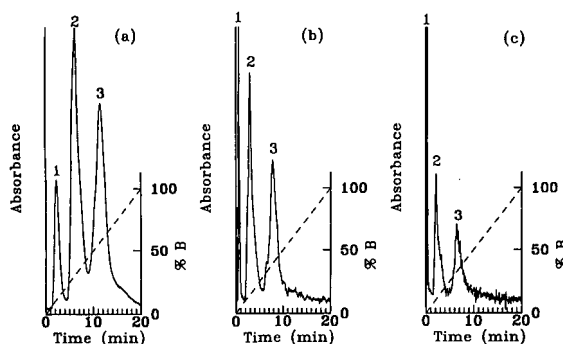


Fig. 8. Gradient elution separation of BSA, OVA and MYO as a function of flow-rate. pH, 8.0. Gradient, 20 min, linear, 0.0 to 0.5 M NaCl. (a) 1 ml/min; (b) 4 ml/min; (c) 8 ml/min.

Thus, it is important to determine if elution separations can be achieved at higher flow-rates. Fig. 8 shows the effect of flow-rate on the separation of MYO, OVA and BSA at pH 8.0. Three chromatograms at 1, 4 and 8 ml/min are shown. Identical 20-min salt gradients were used for all three cases. It should be noted that the noisy signal obtained at the highest flow-rate is due to slight flow fluctuations produced by the pump, which is operating close to its upper limit; these fluctuations are independent of the column. From Fig. 8 it is clear that the proteins can be separated on the fiber column at higher flow rates. In fact the resolution between the OVA and BSA peaks actually improves with increasing flow-rate. However, this improved resolution at higher flow-rates is due to the salt gradient applied, rather than any particular characteristic of the column. If the salt gradients are compared on the basis of volume of eluent rather than time, it is immediately evident that the steepest gradient was applied at the lowest flow-rate. Thus, with increasing flow-rate the retention time difference between OVA and BSA increases. This results in improved resolution between peaks. The smaller gradient at higher flow-rates also results in lowered peak concentrations as is clearly evident in Fig. 8.

Implications of experimental results

The attainment of high flow-rates in chromatographic columns does not by itself guarantee high column throughputs. Equilibrium and kinetic characteristics are essential factors that must also be considered. The non-porous fiber support used in this work shows good pressure-drop characteristics, but has a low adsorption capacity. Thus, the throughput attainable is very limited, even at high fluid velocities. An obvious way of enhancing capacity, without losing the favorable pressure drop characteristics, is to use a porous fiber in place of the non-porous support. Based on the surface area reported for equivalent porous carbon fibers, it is expected that the available surface area in the porous silica fiber will be approximately two orders of magnitude greater than the non-porous fiber. This will give the fiber a capacity comparable to that of conventional, porous, spherical supports.

Porous supports provide the high capacities required for preparative separations, but their kinetic characteristics are generally inferior to non-porous

supports, due to the additional mass transfer resistance in the stationary phase. Thus, poor chromatographic resolution can result, especially in the separation of large biomolecules. In order to overcome this problem, small-diameter spherical supports ($\leq 20 \mu\text{m}$) are used. However, since small diameters lead to high pressure drops, $2 \mu\text{m}$ is generally recognized [28] as the lower limit for the particle diameter; at smaller diameters, excessive pressure drops lead to detrimental effects associated with localized viscous heating, even at low linear velocities. The pressure drop behavior observed with the fiber column indicates that with a short-fiber support the lower limit on the diameter can be reduced to the sub-micron range. In fact, a sub-micron diameter of $0.7 \mu\text{m}$ was used in this study. The implication is that with a porous, sub-micron fiber good intra-particle mass transfer characteristics will be obtained in combination with low pressure drops and high capacities. These are highly desirable characteristics for preparative separations.

One disadvantage of fiber columns is that flow dispersion can be expected to be significantly higher than in comparable columns packed with spherical supports, and, depending on characteristics of the separation and on operating conditions, this effect may partially or completely counter the advantage gained with respect to intra-particle mass transfer. Consequently, the low pressure drop and intra-particle mass transfer characteristics of fiber columns will not necessarily translate into higher throughputs than sphere packed columns. A complete comparison requires the optimization of both systems with respect to throughput, in order to compare the maximum throughput attainable in each.

CONCLUSIONS

The potential of using chromatographic packings with a short, fibrous geometry for preparative separations of proteins has been investigated. Specifically, a non-porous, anion-exchange silica fiber was synthesized. It has been established that short-fiber supports give very porous beds, and, consequently, high linear velocities can be achieved at acceptable column pressure drops; it is estimated that linear velocities of 240–300 cm/min can be attained at pressure drops of about 140 p.s.i./cm. Also, because of the non-porous nature of the support, the dy-

namic column capacity is maintained at high flow-rates, indicating good mass transfer characteristics. A sample protein separation was performed on the column using gradient elution. It has been shown that the peaks can be resolved even at elevated flow-rates. One disadvantage of the non-porous support was found to be its low capacity. However, it is anticipated that replacing the sub-micron non-porous fiber with an equivalent sub-micron porous fiber will result in an adequate enhancement in capacity, while retaining good mass transfer characteristics.

SYMBOLS

d	diameter of particle
f_m	friction factor
g_c	gravitational constant
G	mass flow-rate
L	column length
n	state of flow factor
ΔP	pressure drop of column

Greek symbols

ε	bed porosity
ρ	fluid density
Φ_s	shape factor

ACKNOWLEDGEMENTS

This work was supported by Grant No. CTS-8909742 from the National Science Foundation, and by The Center for Excellence in Membrane Technology at The University of Cincinnati. This support is gratefully acknowledged.

REFERENCES

- 1 P. Knight, *Bio/Technology*, 7 (1989) 243.
- 2 C. Becker, *Aust. J. BioTechnol.*, 2 (1988) 34.
- 3 Cs. Horváth, in F. Bruner (Editor), *The Science of Chromatography*, (*Journal of Chromatography Library*, Vol. 32), Elsevier, Amsterdam, 1985, p. 179.
- 4 Y. D. Clonis, *Bio/Technology*, 5 (1987) 1290.
- 5 J.-C. Jandon and P. Hedman, *Adv. Biochem. Eng.*, 25 (1982) 43.
- 6 J. J. Piotrowski and M. H. Scholla, *BioChromatography*, 3 (1988) 161.
- 7 V. Saxena and M. Dunn, *Bio/Technology*, 8 (1989) 250.
- 8 N. B. Afeyan, S. P. Fulton, N. F. Gordon, I. Mazsaroff, L. Várady and F. E. Regnier, *Bio/Technology*, 8 (1990) 203.

- 9 W. M. Skea, in P. R. Brown and R. A. Hartwick (Editors), *High Performance Liquid Chromatography*, New York, 1989, p. 479.
- 10 R. D. Hegedus, *J. Chromatogr. Sci.*, 26 (1988) 425.
- 11 H. Ding, M.-C. Yang, D. Schisla and E. L. Cussler, *AIChE J.*, 35 (1989) 814.
- 12 M. Czok and G. Guiochon, *J. Chromatogr.*, 506 (1990) 303.
- 13 A. C. R. Tsuei and V. C. Yang, *Polym. Prepr.*, 31 (1990) 238.
- 14 P. Wikström and P. Larsson, *J. Chromatogr.*, 388 (1987) 123.
- 15 M. C. Hennion, C. Picard and M. Caude, *J. Chromatogr.*, 166 (1978) 21.
- 16 D. G. Kingston and B. B. Gerhart, *J. Chromatogr.*, 116 (1976) 182.
- 17 F. E. Regnier and S. P. Gupta, *US Pat.*, 44 560 704 (1985).
- 18 J.-C. Janson and L. Rydén, *Protein Purification, Principles, High Resolution Methods, and Applications*, VCH, New York, 1989.
- 19 G. Vanecek and F. E. Regnier, *Anal. Biochem.*, 121 (1982) 156.
- 20 A. J. Albert and F. E. Regnier, *J. Chromatogr.*, 185 (1979) 375.
- 21 G. Vanecek and F. E. Regnier, *Anal. Biochem.*, 109 (1980) 156.
- 22 W. Kopaciewicz and F. E. Regnier, *J. Chromatogr.*, 358 (1986) 119.
- 23 M. A. Pound, W. Kopaciewicz and F. E. Regnier, *J. Chromatogr.*, 362 (1986) 187.
- 24 W. Kopaciewicz, M. A. Rounds and F. E. Regnier, *J. Chromatogr.*, 318 (1985) 157.
- 25 M. Leva, *Chem. Eng.*, 56 (1949) 115.
- 26 W. Kopaciewicz, S. Fulton and S. Y. Lee, *J. Chromatogr.*, 409 (1987) 111.
- 27 L. A. Haff, L. G. Fagerstam and A. R. Barry, *J. Chromatogr.*, 266 (1983) 409.
- 28 K. K. Unger, W. Messer and K. F. Krebs, *J. Chromatogr.*, 149 (1978) 1.

Mechanism of retention of benzodiazepines in affinity, reversed-phase and adsorption high-performance liquid chromatography in view of quantitative structure-retention relationships

Roman Kaliszan[☆], Anna Kaliszan and Terence A. G. Noctor

Pharmacokinetics Division, Department of Oncology, McGill University, 3655 Drummond, Montreal, PQ H3G 1Y6 (Canada)

William P. Purcell

Department of Medicinal Chemistry, College of Pharmacy, University of Tennessee, 26 South Dunlap Street, Memphis, TN 38163 (USA)

Irving W. Wainer

Pharmacokinetics Division, Department of Oncology, McGill University, 3655 Drummond, Montreal, PQ H3G 1Y6 (Canada)

(First received March 27th, 1992; revised manuscript received June 2nd, 1992)

ABSTRACT

Quantitative structure-retention relationships (QSRRs) were compared for a set of 1,4-benzodiazepine (BDZ) test solutes analyzed by high-performance liquid affinity chromatography (HPLAC), reversed-phase (RP) and adsorption (normal-phase, NP) high-performance liquid chromatography (HPLC). The HPLAC data reflected the enantioselective retention on a human serum albumin-based chiral stationary phase (HSA-CSP); RP-HPLC data were determined on a specially deactivated hydrocarbon-bonded silica material; NP-HPLC was performed on a graphitized carbon stationary phase. Molecular descriptors reflecting additive-constitutive properties of the solutes as well as their geometry and electron charge distribution were generated using molecular modelling software. The QSRR equations derived for each chromatographic mode involved different sets of molecular descriptors. Analysis of the physical meaning of the individual descriptors allowed for interpretation of separation mechanisms at molecular (submolecular) level and rationalization of the observed separation patterns. For HPLAC the contributions by hydrophobic, steric and electrostatic factors were quantified and accounted for the differential retention of enantiomers. Retention in RP-HPLC was demonstrated to be a net effect of both non-specific (dispersive) and directional (electrostatic) intermolecular interactions between solute and molecules of both stationary and mobile phases. QSRR equations derived for NP-HPLC proved the predominance of specific dipolar and charge-transfer attractive interactions. The QSRR-based models obtained appear a reliable and convincing proof for involvement of distinctive mechanisms in different HPLC systems.

INTRODUCTION

One of the most extensively studied manifestations of linear free-energy relationships are the quantitative structure-chromatographic retention relationships (QSRRs). These are statistically derived relationships between the structure of a solute

Correspondence to: Professor Irving W. Wainer, Pharmacokinetics Division, Department of Oncology, McGill University, 3655 Drummond, Suite 701, Montreal, PQ H3G 1Y6 Canada.

[☆] On leave from Department of Biopharmaceutics and Pharmacodynamics, Medical Academy, Gen. J. Hallera 107, 80-416 Gdansk, Poland.

and its chromatographic retention. Using the tools of QSRRs, the chromatographic column becomes a “free-energy transducer”, translating differences in chemical potentials of solutes, arising from differences in structure, to chromatographic retention. One of the ultimate goals of QSRR studies, *i.e.*, accurate prediction of retention parameters prior to an experiment, appears rather remote, except for particular solutes and separation systems [1]. Like in other structure–property relationships, this limitation is due to the shortage of relevant, unequivocally defined and quantitatively precise structural descriptors.

However, this is not the case when QSRRs are used to gain insight into the molecular mechanism of chromatographic retention. Using this approach, it is possible to identify the dominant factors which define the interactions of solute molecules with chemical entities forming the chromatographic system. This can be achieved if statistically significant QSRRs are derived and if these equations approximate the experimental retention data for a representative set of model solutes. Although QSRRs are extrathermodynamic in nature and, as such, lack the formal rigor of thermodynamics, there is no doubt that mechanistic conclusions based on QSRRs are much more reliable than those based on qualitative comparisons of structure and retention of a limited number of preselected solutes.

QSRRs have been employed to analyze the mechanism of reversed-phase high-performance liquid chromatographic (RP-HPLC) separations of simple aromatic test solutes on octadecylsilica [2,3] and polybutadiene-coated alumina [4] stationary phase materials. Retention in adsorption HPLC on metallic stationary phases has also been analyzed in terms of QSRRs [5,6]. Recently, we succeeded in deriving quantitative structure–enantioselective retention relationships (QSERs) for a series of 1,4-benzodiazepines subjected to enantioselective high-performance liquid affinity chromatography (HPLAC) on a human serum albumin-based chiral stationary phase (HSA-CSP) [7].

For each of the above HPLC modes (affinity, reversed-phase, adsorption) the QSRR derived revealed different predominant properties of solutes which determined retention. However, different sets of test solutes employed in individual studies [2–7] preclude direct comparison of respective QSRRs

and, thus of the mechanisms of retention. With that in mind predesigned, comparative QSRR studies were undertaken and are reported here.

EXPERIMENTAL

Materials

The series of 1,4-benzodiazepine test solutes comprised 9 achiral compounds, 4 single enantiomers and 16 individual isomers of 8 racemates. The solutes alprazolam, 4-hydroxy-alprazolam and triazolam were kindly supplied by Upjohn Labs. (Kalamazoo, MI, USA). The compounds Ro 23-0983/001, Ro 11-3128/002, Ro 14-8935/000, Ro 11-5073/000, Ro 23-1117/000 and Ro 23-3880/000 were generously provided by Hoffman-La Roche (Nutley, NJ, USA). Racemic oxazepam hemisuccinate, and its individual enantiomers, were gifts from Dr. Carlo Bertucci (Pisa, Italy). The remaining benzodiazepines as well as deuteromethanol ($C^2H_5O^2H$) and deuterium oxide (2H_2O) were purchased from Sigma (St. Louis, MO, USA).

Apparatus

The chromatographic system consisted of a Spectroflow 400 pump; 480 injector module equipped with 20- μ l loop; 783 programmable absorbance detector (all from ABI Analytical, Ramsey, NJ, USA). A DataJet integrator (Spectra-Physics, San Jose, CA, USA) or a Shimadzu (Kyoto, Japan) C-R6A integrator were used. In the case of affinity chromatography the column was thermostated using a CH-30 temperature regulating jacket (FIA-tron Laboratory Systems, Oconomowoc, WI, USA).

The experiments were carried out using a flow-rate of 1 ml min⁻¹.

Chromatographic conditions

Affinity mode [7]. The column (15 cm \times 4.6 mm I.D.), packed with HSA-CSP was prepared according to Domenici *et al.* [8] by Shandon Scientific (Runcorn, UK).

Chromatography was carried out isocratically using the mobile phase based on sodium dihydrogenphosphate–disodium hydrogenphosphate (100 mM, pH 6.90), modified with 5% (v/v) propan-1-ol. Column temperature was maintained at 28 \pm 0.1°C. Capacity factors (k') were calculated taking the signal of water as the dead time marker.

Reversed-phase mode. A Suplex pKb-100 column (15 cm × 4.6 mm I.D.) was purchased from Supelco (Bellefonte, PA, U.S.A.).

Chromatography was carried out polycratically using eluents of following proportions (v/v) of methanol to buffer: 80:20, 70:30, 60:40, 50:50, 40:60, 30:70 and 20:80. The buffer of pH 7.00 was prepared by adding 0.1 M NaOH to a solution of 0.02 M CH₃COOH, 0.02 M H₃PO₄ and 0.02 M H₃BO₃.

Capacity factors were calculated assuming constant dead volume of the column. Corresponding numerical data were obtained by measuring signals of deuteromethanol (C²H₃O²H) or deuterium oxide (²H₂O) chromatographed with neat methanol (CH₃OH) or water (H₂O) eluents, respectively [9].

Logarithms of capacity factors (log *k'*) for individual solutes were plotted against the volume fraction of methanol in the eluent. Excellent linearity of the relationships in the whole eluent composition range studied (correlation coefficient *r* > 0.995) allowed for extrapolation of log *k'* to 0% methanol (100% buffer). Only the retention parameters normalized to pure buffer (log *k'_w*) were subjected to further analysis.

Adsorption mode. The Knox graphitized carbon [10] column Shandon Hypercarb S (10 cm × 4.6 mm I.D.) was obtained from Shandon Scientific.

Measurable retention data for all solutes, excepting oxazepam hemisuccinate, were obtained employing hexane–propan-1-ol (97:3, v/v) mobile phase. Column dead volume was obtained injecting C²H₃O²H when neat CH₃OH was the eluent. With the value obtained one solute of 21 appeared excluded (*k'* < 0). The value of log *k'* of oxazepam hemisuccinate, corresponding to the hexane–propan-1-ol (97:3, v/v) eluent, was estimated by extrapolation to this composition of the mobile phase using the log *k'* data determined at hexane–propan-1-ol proportions 40:60, 50:50 and 55:45 (v/v).

Determination of structural descriptors

Structural analysis was carried out by means of a molecular modeling program InsightII (Biosym Technologies, San Diego, CA, USA) executed on an IBM (Austin, TX, USA) RISC System 6000 computer. Molecular geometry was optimized and the distribution of electron charge within the molecule was calculated by appropriate molecular orbit-

al package (MOPAC) procedures [11,12] within InsightII. Angles and distances of interest were displayed and measured conveniently due to InsightII molecular graphics facilities.

The InsightII-generated structural descriptors which were considered included total energy, orbital energies, electron excess charges on individual atoms, dipole moments, planar and torsion angles formed by common sets of atoms and distances between selected structural moieties in a molecule. The structural descriptors which were eventually employed in QSRR equations included: submolecular polarity parameter (*P_{SM}*), molecular width (*W*), electron excess charge on carbon atom C(3) of 1,4-diazepine system [*C*(3)], angle formed by atoms C(2)–C(3)–N(4) of diazepine ring (*β_{CCN}*), energy of the lowest unoccupied molecular orbital (*E_{LUMO}*) and total dipole moment (*μ*). To determine *P_{SM}*, at first the difference in electron excess charge between the hydrogen atom at position C(3) and the most negatively charged atom in other substituent at C(3) was calculated. Next, that charge difference was multiplied by the distance (in Å) between these two atoms [7]. The width, *W*, was measured from the extremity of the phenyl substituent.

In addition to the descriptors generated by molecular modeling, meaningful in QSRRs appeared fragmental hydrophobic constants of substituents at position 7 (*f_Y*) and 2' (*f_X*) according to Taylor [13], their sum (*f_{X+Y}*) and molecular refractivity of a whole molecule (*M_R*) calculated after Vogel [14]. Theoretical values of logarithms of octan-1-ol–water partition coefficient for whole molecules (CLOGP) were calculated by the ProLog program (CompuDrug Chemistry, Budapest, Hungary).

Deriving of QSRR equations

Logarithms of capacity factors and structural descriptors were mutually related by means of multi-parameter regression analysis using the CSS package (StatSoft, Tulsa, OK, USA) run on a personal computer. The equations were derived by a stepwise regression analysis and next, refined by a standard regression method taking into consideration significance of individual descriptors, intercorrelations among them, number of data points and variable data range and distribution. The relationships derived were tested according to the requirements of a meaningful correlation analysis [15].

RESULTS AND DISCUSSION

Structures of 1,4-benzodiazepine (BDZ) test solutes are given in Fig. 1. Respective chromatographic data are collected in Table I and structural parameters are listed in Tables II and III.

HPLAC

The QSRR equations 1 and 2 were previously derived [7] which described retention of the first ($\log k'_1$) and the second ($\log k'_2$) eluting enantiomers in HPLAC on HSA-CSP. For achiral solutes it was assumed that $k'_1 = k'_2$ and the actual capacity factor confirmed both QSRR equations for individual enantiomers.

In eqns. 1 and 2 the values in parentheses are standard deviations of regression coefficients, R is the correlation coefficient, F is the f -test value, t is the t -test value and p is the significance level of individual variables and of the whole equation; n is the number of data points used to derive regression. Of 21 BDZs studied we had 17 second-eluting enantiomers available. In the case of eqn. 2 the number of data points (n) is 16 because (*S*)-temazepam was excluded from regression as an outlier.

Eqns. 1 and 2 suggest high stereospecificity of BDZ–HSA retentive interactions. BDZ solutes are assumed to interact with two main types of ste-

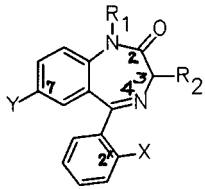
reospecific binding sites: one nonenantioselective and another at which there is significant binding by only one enantiomer. Both binding sites were postulated [16] to be composed of a hydrophobic anchoring pocket (positive input by f_Y), a size restrictive region (negative input by W) and a cationic area repulsive towards positively charged carbon C(3) of diazepine system [negative input by $C(3)$]. In the case of the enantioselective binding site an extended cationic area is assumed to attract negatively charged atoms in the substituent at C(3) (positive input by polarity parameter, P_{SM}) providing that the actual configuration of a chiral molecule allows for close contact of interacting moieties. Hydrophobicity of other parts of BDZ seems to be of little importance for retention on HSA-CSP. Some positive input is provided by hydrophobicity of substituents at position 2' of the phenyl system, but this is at the lowest limits of statistical significance. An even less informative term including β_{CCN} completely loses significance in eqn. 2.

One of the referees indicated that the number of descriptors incorporated in eqns. 1 and 2 is relatively high compared to the number of observations and thus, there was a possibility of chance correlations. The statistically significant equations with reduced number of variables are given in eqns. 1', 1'', 2' and 2''.

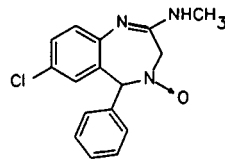
$$\begin{aligned} \log k'_1 = & -1.7497 + 0.3895 (\pm 0.0751) f_Y - 1.8392 (\pm 0.5020) C(3) - 0.1609 (\pm 0.0485) W + \\ & t = 5.19, p \leq 10^{-4} \quad t = -3.66, p \leq 2 \cdot 10^{-3} \quad t = -3.31, p \leq 5 \cdot 10^{-3} \\ & + 0.0354 (\pm 0.0150) \beta_{CCN} + 0.1736 (\pm 0.0939) f_X \\ & t = 2.36, p \leq 3 \cdot 10^{-2} \quad t = 1.85, p \leq 8 \cdot 10^{-2} \\ n = & 21, R = 0.8814, F = 10.5, p < 2 \cdot 10^{-4} \end{aligned} \quad (1)$$

$$\begin{aligned} \log k'_2 = & 1.9922 + 0.8926 (\pm 0.1147) P_{SM} + 0.4830 (\pm 0.0751) f_Y - 4.1482 (\pm 0.7367) C(3) - \\ & t = 7.78, p \leq 2 \cdot 10^{-5} \quad t = 6.43, p \leq 8 \cdot 10^{-5} \quad t = 5.63, p \leq 2 \cdot 10^{-4} \\ & 0.1197 (\pm 0.0544) W + 0.1324 (\pm 0.0814) f_X \\ & t = -2.20, p \leq 5 \cdot 10^{-2} \quad t = 1.63, p \leq 0.13 \\ n = & 16, R = 0.9702, F = 32.0, p < 8 \cdot 10^{-6} \end{aligned} \quad (2)$$

$$\begin{aligned} \log k'_1 = & -0.8218 + 0.3518 (\pm 0.0775) f_Y - 1.8866 (\pm 0.5379) C(3) - 0.1737 (\pm 0.0516) W + \\ & t = 4.54, p \leq 3.4 \cdot 10^{-4} \quad t = -3.51, p \leq 2.9 \cdot 10^{-3} \quad t = -3.77, p \leq 3.9 \cdot 10^{-3} \\ & + 0.0292 (\pm 0.0157) \beta_{CCN} \\ & t = 1.86, p \leq 8.1 \cdot 10^{-2} \\ n = & 21, R = 0.8521, F = 10.6, p < 2.1 \cdot 10^{-4} \end{aligned} \quad (1')$$

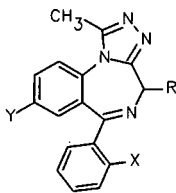


Compounds 2-15

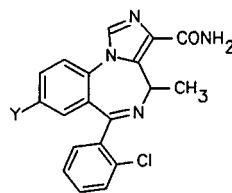


Chlordiazepoxide

Compound	R ₁	R ₂	X	Y	
1	Chlordiazepoxide	See above	-	-	
2	(R,S)-Oxazepam H.	H	OCO(CH ₂) ₂ COO ⁻	H	Cl
3	Nitrazepam	H	H	H	NO ₂
4	Flunitrazepam	CH ₃	H	F	NO ₂
5	Clonazepam	H	H	Cl	NO ₂
6	Delorazepam	H	H	Cl	Cl
7	Desmethyldiazepam	H	H	H	Cl
8	Diazepam	CH ₃	H	H	Cl
9	(R,S)-Lormetazepam	CH ₃	OH	Cl	Cl
10	(R,S)-Lorazepam	H	OH	Cl	Cl
11	(R,S)-Oxazepam	H	OH	H	Cl
12	(R,S)-Temazepam	CH ₃	OH	H	Cl
13	(S)-Ro 14-8935/000	CH ₃	CH ₃	Cl	NH ₂
14	(S)-Ro 23-0983/001	H	CH ₃	Cl	F
15	(R,S)-Ro 11-3128/002	H	CH ₃	Cl	NO ₂



Compounds 16-19



Compounds 20 and 21

Compound	R	X	Y	
16	(R,S)-Alprazolam, 4-OH	OH	H	Cl
17	Alprazolam	H	H	Cl
18	Triazolam	H	Cl	Cl
19	(S)-Ro 11-5073/000	H	F	Cl
20	(S)-Ro 23-1117/000	-	-	F
21	(R,S)-Ro 23-3880/000	-	-	Cl

Fig. 1. Structures of 1,4-benzodiazepine test solutes.

TABLE I

HPLC retention parameters of a series of benzodiazepine solutes determined in affinity (HPLAC), reversed-phase (RP-HPLC) and normal-phase (NP-HPLC) modes.

No. ^a	HPLAC [7] log k'_1 ^b	HPLAC [7] log k'_2 ^c	RP-HPLC log k'_w ^d	NP-HPLC log k'_{H-P} ^e
1	0.8645	0.8645	2.9746	-0.5574
2	0.8512	1.8938	3.1550	1.5413 ^f
3	0.6243	0.6243	2.6155	0.2791
4	0.4857	0.4857	2.7687	-0.0025
5	0.7679	0.7679	2.8696	0.4229
6	1.0614	1.0614	3.2752	-0.1663
7	1.0969	1.0969	3.2002	-0.4310
8	1.1216	1.1216	3.1588	-0.5452
9	0.7672	0.9745	3.1870	0.2142
10	0.8068	0.9360	3.0201	0.3082
11	0.6561	1.0261	2.8348	0.2764
12	0.5224	1.1793	2.8987	-0.0923
13	0.3892	—	2.4293	-0.7411
14	0.6628	—	3.1670	— ^g
15	0.7193	0.7193	2.9853	-0.1546
16	0.2648	0.4533	2.5959	0.5812
17	0.4200	0.4200	2.8580	0.0934
18	0.6243	0.6243	3.0971	0.4081
19	0.3838	—	3.0360	-0.2611
20	0.7404	—	3.1836	0.2447
21	1.0523	1.1156	3.4041	0.3374

^a Solute are numbered as in Fig. 1.

^b First-eluting enantiomer.

^c Second-eluting enantiomer.

^d Extrapolated data corresponding to pure buffer.

^e Determined at mobile phase composition hexane–propan-1-ol (97:3, v/v).

^f Extrapolated from data determined at higher concentrations of propan-1-ol.

^g Excluded solute; $k' = -0.0077$.

$$\log k'_1 = 2.6402 + 0.2998 (\pm 0.0774) f_Y - 1.5929 (\pm 0.5504) C(3) - 0.1996 (\pm 0.0531) W$$

$$t = 3.87, p \leq 1.2 \cdot 10^{-3} \quad t = -2.89, p \leq 1.0 \cdot 10^{-2} \quad t = -3.76, p \leq 1.6 \cdot 10^{-3}$$

$$n = 21, R = 0.8165, F = 11.3, p < 2.5 \cdot 10^{-4} \quad (1'')$$

$$\log k'_2 = 2.2061 + 0.8458 (\pm 0.1191) P_{SM} + 0.4756 (\pm 0.0804) f_Y - 3.95 (\pm 0.7792) C(3)$$

$$- 0.1371 (\pm 0.0572) W$$

$$t = 7.10, p \leq 2.0 \cdot 10^{-5} \quad t = 5.91, p \leq 1.0 \cdot 10^{-4} \quad t = -5.07, p \leq 3.6 \cdot 10^{-4}$$

$$t = -2.40, p \leq 3.5 \cdot 10^{-2}$$

$$n = 16, R = 0.9622, F = 34.28, p < 4.0 \cdot 10^{-6} \quad (2'')$$

$$\log k'_2 = 1.0664 + 1.0116 (\pm 0.1146) P_{SM} + 0.4562 (\pm 0.0946) f_Y - 5.0103 (\pm 0.7586) C(3)$$

$$t = 8.83, p \leq 1.0 \cdot 10^{-5} \quad t = 4.82, p \leq 4.2 \cdot 10^{-4} \quad t = -6.60, p \leq 3.0 \cdot 10^{-5}$$

$$n = 16, R = 0.9418, F = 31.4, p < 6.0 \cdot 10^{-6} \quad (2'')$$

TABLE II

MOLECULAR DESCRIPTORS DERIVED FROM THE GEOMETRY OPTIMIZED STRUCTURES OF BENZODIAZEPINE SOLUTES

No. ^a	P_{SM}^b	$C(3)^c$	W^d	β_{CCN}^e	E_{LUMO}^f	μ^{2g}
1	0.0849	0.1035	9.30	108.01	-0.6967	8.8506
2	1.8635	0.2785	8.74	115.80	-0.9463	3.0976
3	0.0703	0.0960	8.54	112.61	-1.6124	3.1826
4	0.0609	0.0882	9.63	112.22	-1.3241	1.5475
5	0.0680	0.0966	8.67	112.25	-1.6027	0.9722
6	0.0635	0.0977	8.69	112.39	-0.8502	9.8596
7	0.0634	0.0979	8.59	112.45	-0.8534	6.7912
8	0.0578	0.0933	9.56	112.83	-0.8337	6.9907
9	0.6120	0.2388	9.76	112.66	-0.9072	13.1624
10	0.5953	0.2425	8.71	111.39	-0.9306	15.3664
11	0.7049	0.2451	8.60	109.46	-0.9260	10.7387
12	0.6113	0.2353	9.49	112.52	-0.8921	11.1156
13	0.0675	0.0549	10.02	114.06	-0.5324	29.2140
14	0.0600	0.0624	8.64	109.62	-0.8338	7.6286
15	0.0633	0.0651	8.70	109.48	-1.2830	0.9274
16	0.5862	0.3169	10.50	108.56	-1.3073	33.4662
17	0.0784	0.1722	10.29	109.84	-1.2428	27.4995
18	0.0730	0.1725	10.26	109.85	-1.2691	30.0414
19	0.0484	0.1379	10.24	108.51	-1.2497	27.9947
20	0.0320	0.1309	9.20	107.84	-1.1838	32.1489
21	0.0441	0.1184	9.22	107.45	-1.2276	33.8608

^a Solutes are numbered as in Fig. 1.^b Submolecular polarity parameter.^c Electron excess charge on carbon at position 3.^d Molecular width in Å.^e Angle between atoms 2, 3 and 4.^f Energy of the lowest unoccupied molecular orbital (eV).^g Square of total dipole moment (D²).

It seemed interesting to compare QSRRs derived for the same set of BDZs in the case of HPLAC with the QSRRs for RP-HPLC. RP-HPLC is widely used to determine hydrophobicity of solutes. The most recommended [17] chromatographic measure of hydrophobicity is $\log k'_w$. This is the logarithm of capacity factor obtained by extrapolation of the linear part of the relationships between $\log k'$ and volume percent of organic modifier in binary aqueous eluent to the pure water eluent. The $\log k'_w$ data for BDZs are collected in Table I.

The standard reference parameter of hydrophobicity is logarithm of octan-1-ol–water partition coefficient, $\log P$. Since $\log P$ is tedious to determine experimentally, computational methods for its evaluation have been developed [18]. Theoretical values of logarithms of octan-1-ol–water partition coefficient for the solutes used in this study, CLOGP,

were calculated by the ProLog program and are presented in Table III. We were able to calculate apparently realistic $\log P$ values only for the first 15 structures in Fig. 1. Nonetheless, correlation between chromatographic measure of hydrophobicity, $\log k'_w$, and the calculated hydrophobicity parameter was rather poor ($R = 0.7500$).

When undertaking QSRR studies on data derived by affinity HPLC (the starting hypothesis was that the first eluting enantiomer was retained solely due to non-stereo- and non-enantiospecific, hydrophobic interactions with HSA-CSP. We found that neither chromatographic hydrophobicity parameter, $\log k'_w$, nor the calculated one, CLOGP, accounted for the first enantiomer retention ($\log k'_1$). Correlation between $\log k'_1$ and CLOGP was $R = 0.5976$ and that with $\log k'_w$ was $R = 0.7410$. In all subsequent QSRRs the $\log k'_w$ performed better

than CLOGP in contradiction to occasional suggestions [19,20] that the calculated hydrophobicity parameters can be more reliable than those derived by HPLC.

Eqns. 1 and 2, describing retention on HSA-CSP, comprise hydrophobicity terms. Attempts to replace these submolecular hydrophobicity parameters by $\log k'_w$, a measure of the hydrophobicity of the whole molecule, yielded QSRR eqns. 3 and 4.

Eqns. 3 and 4 are highly significant statistically but their predictive value, as expressed by the correlation coefficient, is lower than that of the corresponding eqns. 1 and 2. Nevertheless, eqns. 3 and 4 which comprise a molecular width term, W , provide additional proof for the steric requirements of retentive interactions between BDZs and HSA-CSP.

The predictive value of QSRR regarding the second eluting enantiomer increases if, in addition to terms present in eqn. 4, the parameter f_X is intro-

duced as in eqn. 5. The negative sign at the coefficient at f_X in eqn. 5 suggests that in this specific instance the parameter f_X reflects steric hindrance rather than solute's hydrophobicity.

The predictive potency of eqns. 3 and 4 is illustrated in Figs. 2 and 3, respectively. Intercorrelations among individual variables in eqns. 3–5 are highest for pairs $\log k'_1$ vs. $\log k'_w$ ($R = 0.7410$), $\log k'_2$ vs. P_{SM} ($R = 0.6623$) and $\log k'_2$ vs. $\log k'_w$ ($R = 0.6344$); for other pairs of variables $R < 0.5$.

Reversed-phase HPLC

Retention in RP-HPLC, as quantified by $\log k'_w$, is assumed to be due to hydrophobic intermolecular interactions [21]. From the QSRR point of view it seems interesting which structural features provide greatest input to what is called "hydrophobicity". The "best" regression equation describing $\log k'_w$ is shown in eqn. 6.

$$\log k'_1 = 0.2821 + 0.6246 (\pm 0.1334) \log k'_w - 0.1547 (\pm 0.0487) W \quad (3)$$

$t = 4.68, p \leq 1.9 \cdot 10^{-4} \quad t = -3.17, p \leq 5.3 \cdot 10^{-3}$

$$n = 21, R = 0.8431, F = 22.1, p < 4 \cdot 10^{-5}$$

$$\log k'_2 = -0.2740 + 0.8685 (\pm 0.1366) \log k'_w + 0.4534 (\pm 0.0652) P_{SM} - 0.1721 (\pm 0.0465) W \quad (4)$$

$t = 6.36, p \leq 4 \cdot 10^{-4} \quad t = 6.96, p \leq 2 \cdot 10^{-4} \quad t = 3.70, p \leq 3 \cdot 10^{-3}$

$$n = 16, R = 0.9548, F = 41.3, p < 10^{-6}$$

$$\log k'_2 = -0.6120 + 1.0528 (\pm 0.1057) \log k'_w + 0.4079 (\pm 0.0464) P_{SM} - 0.1798 (\pm 0.0320) W$$

$t = 9.96, p \leq 10^{-5} \quad t = 8.80, p \leq 10^{-5} \quad t = -5.62, p \leq 1.6 \cdot 10^{-4}$

$$- 0.2638 (\pm 0.0695) f_X \quad (5)$$

$t = -3.79, p \leq 3 \cdot 10^{-3}$

$$n = 16, R = 0.9807, F = 69.2, p < 10^{-6}$$

$$\log k'_w = 1.6541 + 0.5081 (\pm 0.0422) f_Y + 0.3084 (\pm 0.0588) f_X - 1.6641 (\pm 0.2940) C(3)$$

$t = 12.04, p \leq 10^{-5} \quad t = 5.25, p \leq 10^{-4} \quad t = -5.66, p \leq 5 \cdot 10^{-5}$

$$- 0.0103 (\pm 0.0022) \mu^2 + 0.0155 (\pm 0.0034) M_R \quad (6)$$

$t = -4.88, p \leq 2.4 \cdot 10^{-4} \quad t = 4.51, p \leq 4.1 \cdot 10^{-4}$

$$n = 21, R = 0.9582, F = 33.7, p < 10^{-6}$$

TABLE III

MOLECULAR DESCRIPTORS OF BENZODIAZEPINE SOLUTES CALCULATED FROM ADDITIVE-CONSTITUTIVE STRUCTURAL CONSTANTS

No. ^a	f_Y^b	f_X^c	M_R^d	CLOGP ^e
1	0.88	0.17	80.132	3.029
2	0.88	0.17	95.240	3.103
3	-0.11	0.17	74.994	2.048
4	-0.11	0.31	79.596	2.136
5	-0.11	0.88	79.828	2.788
6	0.88	0.88	78.338	3.788
7	0.88	0.17	73.504	3.048
8	0.88	0.17	78.342	2.919
9	0.88	0.88	84.620	2.853
10	0.88	0.88	79.782	2.982
11	0.88	0.17	74.948	2.242
12	0.88	0.17	79.786	2.113
13	-1.06	0.88	92.834	2.402
14	0.31	0.88	77.916	3.784
15	-0.11	0.88	84.476	3.307
16	0.88	0.17	87.272	—
17	0.88	0.17	85.828	—
18	0.88	0.88	90.662	—
19	0.88	0.31	91.916	—
20	0.31	0.88	95.288	—
21	0.88	0.88	100.358	—

^a Solutes are numbered as in Fig. 1.

^b Hydrophobic constant of substituent at position 7.

^c Hydrophobic constant of substituent at position 2'.

^d Molecular refractivity according to Vogel [14].

^e Logarithm of octan-1-ol-water partition coefficient calculated theoretically.

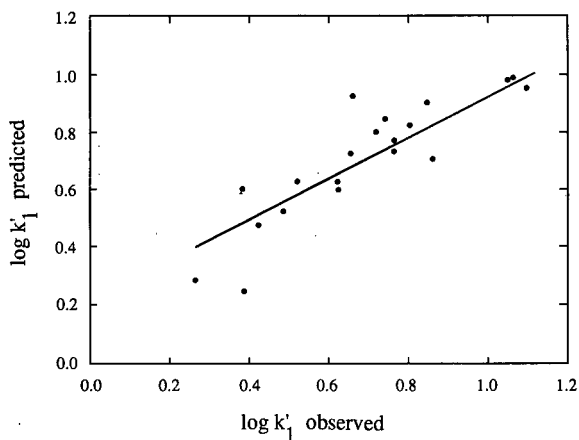


Fig. 2. Relationship between the retention parameters for the first-eluting enantiomer of 1,4-benzodiazepines ($\log k'_1$) determined experimentally by HPLAC on HSA-CSP and calculated from $\log k'_w$ and W using eqn. 3.

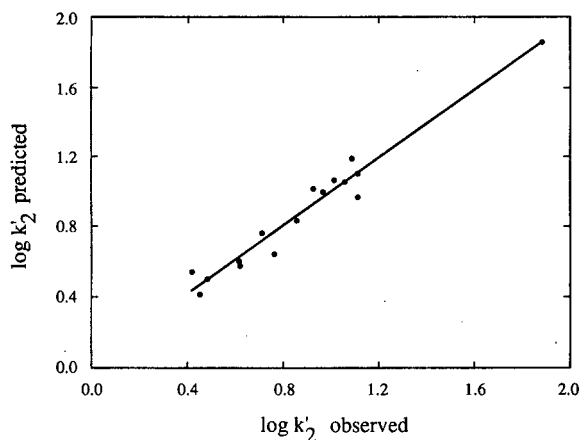


Fig. 3. Relationship between the retention parameters for the second-eluting enantiomer of 1,4-benzodiazepines ($\log k'_2$) determined experimentally by HPLAC on HSA-CSP and calculated from $\log k'_w$ and descriptors using eqn. 5.

Intercorrelations among individual variables are low: the highest being $R = 0.6862$ for μ^2 vs. M_R and $R = 0.5850$ for $\log k'_w$ vs. f_Y . The predictive quality of eqn. 6 is illustrated in Fig. 4.

The variables f_Y and f_X in eqn. 6 are highly significant and the regression coefficients at these variables also differ significantly. This observation would suggest the different inputs to the reversed-

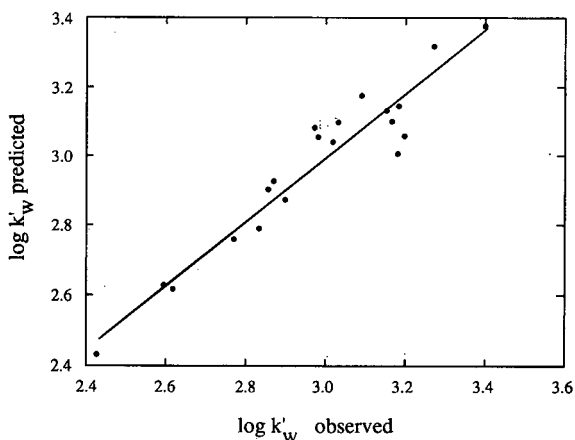


Fig. 4. Relationship between the retention parameters of 1,4-benzodiazepines corresponding to pure buffer eluent ($\log k'_w$) determined experimentally by RP-HPLC on a hydrocarbon-bonded deactivated silica stationary phase and calculated from descriptors using eqn. 6.

phase retention of BDZs due to hydrophobicities of individual molecular regions. Additivity rules for fragmental hydrophobicity parameters usually require the application of some specific correction factors [13,18]. At first approximation, however, the variables f_Y and f_X can be replaced by their arithmetic sum, f_{X+Y} . The resulting eqn. 6' is of high statistical quality.

Eqn. 6 shows that a molecular bulkiness related structural descriptor, M_R , provides positive input to hydrophobic retention, whereas the molecular polarity related descriptors, $C(3)$ and μ^2 , account for the retention decreasing effects in RP-HPLC. This can be rationalized as follows:

(1) M_R reflects the ability of a solute to participate in dispersive (London type) intermolecular interactions. These nonspecific, molecular-size-dependent interactions are obviously stronger between a BDZ solute molecule and a bulky hydrocarbonaceous moiety of Suplex pKb-100 stationary phase than between the same solute molecule and small molecules forming a mobile phase. Thus, the larger M_R the stronger retention.

(2) The reverse holds true when considering parameters reflecting the ability of a solute to take part in more structurally specific, size-independent intermolecular interactions (so called polar interac-

tions), like dipole–dipole, dipole–induced dipole, charge transfer and hydrogen bonding interactions. Such interactions, involving solute and polar molecules of eluent (water, methanol), will increase with the magnitude of polarity descriptors $C(3)$ and μ^2 , being at the same time negligible in the case of the system involving the solute molecule and the hydrocarbon moiety of the stationary phase.

Eqn. 6 strongly resembles the QSRR equations describing retention on regular octadecylsilica [3] and polybutadiene-coated alumina [4] reversed-phase materials. In the later equations the net positive input to retention due to dispersive intermolecular interactions was quantified by such molecular-size-dependent descriptors as total energy, molecular-graph-derived indices, molecular refractivity or just molecular mass. The net negative input to retention was evaluated by means of a total dipole, a localized dipole or by a parameter reflecting maximum electron excess charge differences within the molecule.

If in QSRR analysis of the RP-HPLC retention data the submolecular polarity parameter, P_{SM} , is considered instead of the square of total dipole moment, μ^2 , eqn. 7 results.

Replacing the variables f_X and f_Y in eqn. 7 by their sum, f_{X+Y} , results in eqn. 7':

$$\begin{aligned} \log k'_w = & 1.8226 + 0.4442 (\pm 0.0456) f_{X+Y} - 1.1866 (\pm 0.3122) C(3) - 0.0096 (\pm 0.0026) \mu^2 + \\ & t = 9.73, p \leq 1.0 \cdot 10^{-5} \quad t = -3.80, p \leq 1.6 \cdot 10^{-3} \quad t = -3.59, p \leq 2.5 \cdot 10^{-3} \\ & + 0.0120 (\pm 0.0040) M_R \quad (6') \\ & t = 2.97, p \leq 9.0 \cdot 10^{-3} \\ n = & 21, R = 0.9302, F = 25.68, p < 1.0 \cdot 10^{-6} \end{aligned}$$

$$\begin{aligned} \log k'_w = & 2.8824 + 0.5129 (\pm 0.0460) f_Y + 0.3728 (\pm 0.0597) f_X - 3.0641 (\pm 0.4570) C(3) + \\ & t = 11.16, p \leq 10^{-5} \quad t = -6.70, p \leq 10^{-5} \quad t = -6.70, p \leq 10^{-5} \\ & + 0.3164 (\pm 0.0719) P_{SM} \quad (7) \\ & t = 4.40, p \leq 4.5 \cdot 10^{-4} \\ n = & 21, R = 0.9478, F = 35.4, p < 10^{-6} \end{aligned}$$

$$\begin{aligned} \log k'_w = & 2.8105 + 0.4658 (\pm 0.0440) f_{X+Y} - 2.7234 (\pm 0.4684) C(3) + 0.3097 (\pm 0.0787) P_{SM} \\ & t = 10.59, p \leq 1.0 \cdot 10^{-5} \quad t = -5.81, p \leq 2.0 \cdot 10^{-5} \quad t = 3.93, p \leq 1.0 \cdot 10^{-3} \\ n = & 21, R = 0.9329, F = 38.0, p < 1.0 \cdot 10^{-6} \quad (7') \end{aligned}$$

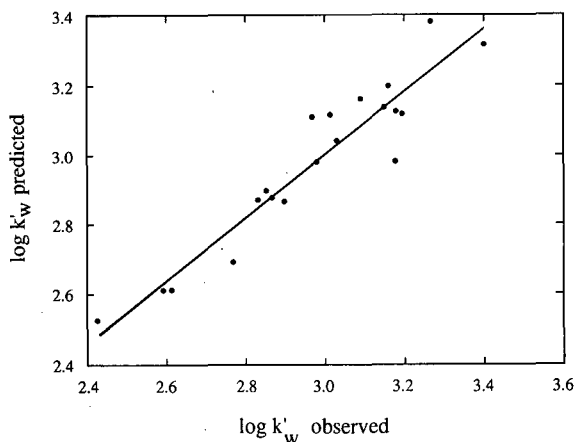


Fig. 5. Relationship between the retention parameters of 1,4-benzodiazepines corresponding to pure buffer eluent ($\log k'_w$) determined experimentally by RP-HPLC on a hydrocarbon-bonded deactivated silica stationary phase and calculated from descriptors using eqn. 7.

The statistical quality of eqn. 7 is similar to that of eqn. 6 as is its predictive value (Fig. 5). The highest intercorrelations among the variables of eqns. 7 and 7' are between $C(3)$ and P_{SM} ($R = 0.7651$) and between $\log k'_w$ and f_{X+Y} ($R = 0.7781$). The parameter P_{SM} seems to be able to replace μ^2 and M_R in eqn. 6. This can, however, be fortuitous and discussion of P_{SM} as a net hybrid measure of dipolar and dispersive properties appears premature.

Adsorption HPLC

The QSRR equation derived for $\log k'_{H-P}$ data (eqn. 8) has a different form from the relationships so far discussed. The relationship between the experimental and calculated $\log k'_{H-P}$ is given in Fig. 6. There is an intercorrelation of $R = 0.7187$ between $\log k'_{H-P}$ and P_{SM} . Other intercorrelations are $R < 0.5$. Similarity between eqn. 8 and eqns. 2 and 4, describing retention of second eluting enantiomer in HPLAC, is limited to the presence of submolecular polarity term, P_{SM} . Evidently, some kind of dipole–dipole and/or dipole–induced dipole interac-

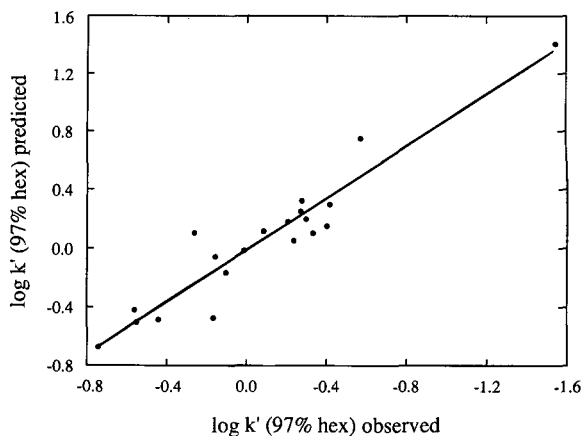


Fig. 6. Relationship between the retention parameters of 1,4-benzodiazepines [$\log k' (97\% \text{ hex})$] determined experimentally by NP-HPLC on a graphitized carbon stationary phase with hexane–propan-1-ol (97:3, v/v) eluent and calculated from descriptors using eqn. 8.

tions is operating at site II of HSA-CSP and in NP-HPLC on graphitized carbon. In the latter case there are no steric restrictions for effective interactions. Instead, the variables E_{LUMO} and (to a lesser extent) μ^2 account for retention. Equations comprising a measure of localized dipole similar to P_{SM} and the E_{LUMO} parameter as independent variables were previously derived to describe retention of a series of monofunctional benzene derivatives on metallic stationary phases [5,6]. The dominant retention mechanism postulated was an electron pair donor–electron pair acceptor interaction. This mechanism appears to operate also in the case of BDZs chromatographed on porous graphitic carbon under normal-phase conditions.

CONCLUSIONS

The results of this study demonstrate differences in mechanism of retention in affinity, reversed-phase and adsorption HPLC modes. At the same time, the conclusions which can be drawn from the

$$\log k'_{H-P} = -1.5582 + 1.0250 (\pm 0.0999) P_{SM} - 1.1220 (\pm 0.1564) E_{LUMO} + 0.0078 (\pm 0.0036) \mu^2 \quad (8)$$

$$t = 10.26, p \leq 10^{-5} \quad t = -7.17, p \leq 10^{-5} \quad t = 2.19, p \leq 0.05$$

$$n = 20, R = 0.9428, F = 42.6, p < 10^{-6}$$

QSRRs are consistent with the commonly recognized qualitative models. The QSRRs identify retention affecting structural factors and provide quantitative estimation of their importance. Thus, a question arises whether QSRR analysis should not replace the speculations that a given property or functional group rather increases and another tends to decrease retention. Certainly, detection of informative and quantifiable structural descriptors still requires experience (and chemical intuition) but accessibility of modern molecular modelling facilities simplifies the task. QSRR analysis could be an important component in introduction of new separation modes and/or stationary phase materials.

QSRR analysis is especially challenging for highly stereospecific separations. We found a single report by Wolf *et al.* [22] on calculating the capacity factor of one of the enantiomers of a series of racemates chromatographed on cellulose triacetate. The authors used a negative electrostatic potential around the chiral centre of the solute, E_{00} , and the probability, Ω , of assuming a flat conformation by the molecule as variables in a regression equation. The enantiomer distinguishing structural parameter P_{SM} in our eqns. 2 and 4 is similar in nature to E_{00} , however, P_{SM} is simpler and more readily determinable. At the same time the retention on HSA-CSP appears to be a more complex process than that on cellulose triacetate. Eqns. 1 and 2 compensate for this complexity and were of help in establishing the topography of benzodiazepine binding sites on HSA [16,23].

QSRR regression equations are readily interpretable in mechanistic physical terms. There is another multivariable statistical approach to QSRR which is based on factorial methods of data analysis. The approach consists in condensing most of the information dispersed over a multitude of various molecular descriptors into a few abstract principal factors or components. It usually appears difficult to assign a definite physical meaning to individual principal components and the approach is rather aimed at prediction of retention data, *e.g.*, enantioselectivity [24]. Another approach attempts to associate substituents with contributions to the observed enantioselectivity [25].

Retention in RP-HPLC was found to be a net effect of non-specific, dispersive, bulkiness-dependent interactions and directional electrostatic inter-

actions involving solute molecules and molecules of both mobile and stationary phases. Former interactions are stronger for a solute–stationary phase system than for a solute–mobile phase system. The reverse is true with polar interactions. QSRRs derived here support generally observed mechanism of RP-HPLC on hydrocarbonaceous stationary phase materials [2–4]. The material used here, Suplex pKb-100, is characterized by an extremely high level of deactivation. Suppression of silanophilic interactions has been confirmed by our observation of excellent linearity of dependence of $\log k'$ on organic modifier concentration in mobile phase at a wide eluent composition range. This property would facilitate determinations of reliable and reproducible chromatographic measures of the hydrophobicity of solutes.

A separate question is whether the chromatographic hydrophobicity scale parallels the reference $\log P$ scale determined by slow equilibration methods. This is probably not the case since the correlation between the normalized chromatographic hydrophobicity parameter, $\log k'_w$, and the calculated $\log P$ (CLOGP) is low. Besides, hydrophobicity is a property which depends as much on the nature of the solutes considered as on the properties of the environment in which it is measured. Chromatographic and octan-1-ol–water experimental hydrophobicity parameters may differ more or less but this does not imply lower reliability of the HPLC approach. Chromatographic measurement of hydrophobicity is certainly more reliable than an *a priori* calculated $\log P$.

The mechanism of retention in NP-HPLC on graphitized carbon revealed by eqn. 8 is as expected for adsorption chromatography. Retention is not affected significantly by molecular size of solutes. Non-specific, dispersive interactions are dominated by the more chemically specific directional electrostatic and charge transfer interactions. There are no geometric restrictions regarding the fitting of a solute to any definite binding (adsorption) site as it is the case with HPLAC.

As demonstrated here QSRR analysis provides rationale for different separation patterns observed in individual HPLC systems. Meaningful QSRRs can be of help in understanding fundamental processes at the basis of chromatographic separations and in a rationally guided search for optimum

separating systems. With further progress in molecular modelling and chemometrics also the analytical prediction of retention data will no longer be restricted to closely congeneric sets of solutes.

REFERENCES

- 1 R. Kaliszan, *Quantitative Structure–Chromatographic Retention Relationships*, Wiley, New York, 1987.
- 2 R. Kaliszan, K. Osmialowski, S.A. Tomellini, S.-H. Hsu, S.D. Fazio and R.A. Hartwick, *Chromatographia*, 20 (1985) 705.
- 3 R. Kaliszan, K. Osmialowski, S.A. Tomellini, S.-H. Hsu, S.D. Fazio and R.A. Hartwick, *J. Chromatogr.*, 352 (1986) 141.
- 4 R. Kaliszan and K. Osmialowski, *J. Chromatogr.*, 506 (1990) 3.
- 5 B. J. Bassler, R. Kaliszan and R. A. Hartwick, *J. Chromatogr.*, 461 (1989) 139.
- 6 R. Kaliszan, K. Osmialowski, B. J. Bassler and R. A. Hartwick, *J. Chromatogr.*, 499 (1990) 333.
- 7 R. Kaliszan, T. A. G. Noctor and I. W. Wainer, *Chromatographia*, in press.
- 8 E. Domenici, C. Bertucci, P. Salvadori, G. Felix, I. Cahagne, S. Motellier and I. W. Wainer, *Chromatographia*, 29 (1990) 170.
- 9 J. H. Knox and R. Kaliszan, *J. Chromatogr.*, 349 (1985) 211.
- 10 J. H. Knox, B. Kaur and G. R. Millward, *J. Chromatogr.*, 352 (1986) 3.
- 11 M. J. S. Dewar and W. Thiel, *J. Am. Chem. Soc.*, 99 (1977) 4899.
- 12 M. J. S. Dewar and H. S. Rzepa, *J. Comp. Chem.*, 4 (1983) 158.
- 13 P. J. Taylor, in C. Hansch, P.G. Sammes and J.B. Taylor (Editors), *Comprehensive Medicinal Chemistry*, Vol. 4, Pergamon, Oxford, 1990, pp. 241–294.
- 14 A. I. Vogel, *Textbook of Practical Organic Chemistry*, Chaucer, London, 1977, p. 1034.
- 15 M. Charton, S. Clementi, S. Ehrenson, O. Exner, J. Shorter and S. Wold, *Quant. Struct.–Act. Relat.*, 4 (1985) 29.
- 16 R. Kaliszan, T. A. G. Noctor and I. W. Wainer, *Mol. Pharmacol.*, in press.
- 17 T. Braumann, *J. Chromatogr.*, 373 (1986) 191.
- 18 C. Hansch and A. Leo, *Substituent Constants for Correlation Analysis in Chemistry and Biology*, Wiley, New York, 1979.
- 19 C. V. Eadsforth, *Pestic. Sci.*, 17 (1986) 311.
- 20 A. J. Leo, *J. Pharm. Sci.*, 76 (1987) 166.
- 21 Cs. Horváth, W. Melander and I. Molnár, *J. Chromatogr.*, 125 (1976) 129.
- 22 R. M. Wolf, E. Francotte and D. Lohmann, *J. Chem. Soc., Perkin Trans. II*, (1988) 893.
- 23 T. A. G. Noctor, C. D. Pham, R. Kaliszan and I. W. Wainer, *Mol. Pharmacol.*, in press.
- 24 U. Norinder and J. Hermansson, *Chirality*, 3 (1991) 422.
- 25 A. Berthod, S.-C. Chang and D. W. Armstrong, *Anal. Chem.*, 64 (1992) 395.

Gel chromatographic evaluation of the binding constant for the interaction of thiamin diphosphate with magnesium ion

Christine K. Booth, Peter F. Nixon and Donald J. Winzor

Department of Biochemistry, University of Queensland, Brisbane, Queensland 4072 (Australia)

(First received March 11th, 1992; revised manuscript received May 27th, 1992)

ABSTRACT

A simple gel chromatographic procedure is devised for characterizing the interactions of nucleotides and other coenzymes with metal ions. Its application is illustrated by determining the binding constant for the interaction of thiamin diphosphate with Mg^{2+} ion by frontal gel chromatography on Sephadex G-10. An association constant of $3200 (\pm 400) M^{-1}$ is obtained for the interaction in 0.1 M Tris-HCl buffer (pH 7.6) supplemented with poly(ethylene glycol) (50 mg/ml) and mercaptoethanol (25 mM).

INTRODUCTION

Because all enzymes that are dependent upon thiamin diphosphate also require a divalent cation for activity, it is generally considered that the active cofactor is the complex of coenzyme with metal ion. In experimental studies Mg^{2+} is most frequently included with thiamin diphosphate to generate active holoenzyme; and yet, surprisingly, the binding constant for this interaction does not seem to have been reported. Some information is available on the interaction of thiamin diphosphate with manganous ion, a metal ion substitution that has allowed resort to electron paramagnetic resonance for establishing the 1:1 stoichiometry and association constant of $5000 M^{-1}$ for the Mn^{2+} -coenzyme interaction [1]. Associated proton magnetic resonance studies revealed the existence of that complex as a folded structure with the pyrophosphate looped back over the thiazole ring [1].

From the physiological viewpoint it is clearly im-

portant to characterize the interaction of thiamin diphosphate with Mg^{2+} ion rather than with some other metal ion that happens to be convenient for study by a particular method. In that regard a subsequent ^{31}P nuclear magnetic resonance study [2] has confirmed the 1:1 stoichiometry of the Mg^{2+} -coenzyme interaction, and has also signified the likelihood that this complex is folded in similar fashion to its manganous counterpart. However, no attempt was made to evaluate the equilibrium constant. Gel chromatography is a general procedure that has the capacity to provide this quantification; and has, indeed, been recommended for the study of metal-nucleotide interactions [3]. As noted previously [4], that recommendation was premature in the sense that no allowance was made for the consequences of the above-mentioned change in shape/size of the coenzyme that accompanies complex formation in many metal-nucleotide interactions—a phenomenon that should give rise to a difference in gel chromatographic migration rates for thiamin diphosphate in free and complexed states.

Determination of association constants for acceptor-ligand interactions by gel chromatography is relatively simple in instances where the acceptor is

Correspondence to: Dr. D. J. Winzor, Department of Biochemistry, University of Queensland, Brisbane, Qld. 4072, Australia.

macromolecular and hence where acceptor and acceptor–ligand complex comigrate [5–7]. However, the situation in which both reactants are small molecules introduces complexity into the analysis because of the different velocities, or elution volumes, exhibited by the acceptor and acceptor–ligand species [4,8]. Although procedures have been devised to cover these circumstances [4,6,8–10], the sophistication of those analyses may well deter the biochemist whose prime interest is the magnitude of the equilibrium constant rather than the physicochemical elegance of the procedure by which it is obtained. In response to a situation requiring the assignment of a magnitude to the binding constant for the interaction of magnesium ion with thiamin diphosphate, a simple gel chromatographic procedure has been devised to obtain the first direct estimate of the equilibrium constant for this physiologically important metal–nucleotide interaction.

EXPERIMENTAL^a

Reactant solutions

Separate stock solutions of thiamin diphosphate (Sigma) and reagent-grade MgCl_2 in buffer medium [0.1 M Tris–HCl (pH 7.6) supplemented with poly(ethylene glycol) 600 (50 mg/ml) and β -mercaptoethanol (25 mM)] were prepared on a weight/volume basis. Mixtures comprising a fixed total concentration (100 μM) of thiamin diphosphate ($[\bar{A}]_0$) and a range (0–0.1 M) of magnesium ion concentrations ($[\bar{S}]_0$) were then prepared from these stock solutions. Because only small volumes of stock magnesium ion solution were required for the preparation of these mixtures, atomic absorption spectroscopy was used to establish the precise magnitudes of $[\bar{S}]_0$. The incorporation of the poly(ethylene glycol) and mercaptoethanol into the buffer medium was a legacy of conditions required for apotransketolase stability in the enzyme kinetic studies that precipitated the need for evaluation of the Mg^{2+} –coenzyme binding constant.

^a Symbols: $[\bar{A}]_0$ = total concentration of acceptor (thiamin diphosphate) in applied mixture; $[\bar{S}]_0$ = corresponding total concentration of ligand (Mg^{2+} ion); $[A]_0$ = concentration of uncomplexed acceptor in applied mixture; \bar{V}_A , \bar{V}_S = constituent elution volumes of acceptor and ligand components, respectively; V_A , V_S , V_C = elution volumes of acceptor, ligand and acceptor–ligand complex.

Gel chromatographic procedure

Mixtures (100 ml) of thiamin diphosphate and Mg^{2+} ion were subjected to frontal gel chromatography [11–15] at room temperature (20–22°C) on a column (20 × 2.5 cm) of Sephadex G-10 that had been preequilibrated with the appropriate Mg^{2+} -supplemented buffer medium. The column effluent, maintained at a nominal flow-rate of 2 ml/min by means of a peristaltic pump, was monitored continuously at 280 nm, a wavelength that allowed measurement of the total concentration ($[\bar{A}]$) of thiamin diphosphate constituent (irrespective of its presence as free coenzyme or as Mg^{2+} –coenzyme complex). During application of each mixture, the precise flow-rate was determined by collecting the column effluent in a previously tared vessel over an accurately defined time interval.

The constituent elution volume (\bar{V}_A) of the thiamin diphosphate component of each mixture was obtained as the median bisector [6,12] of the advancing elution profile via the expression

$$\bar{V}_A = \{\Sigma([\bar{A}]_0 - [\bar{A}])\Delta V\}/[\bar{A}]_0 \quad (1)$$

where $[\bar{A}]$ denotes the constituent (total) concentration of acceptor (thiamin diphosphate) in a volume increment ΔV at effluent volume V in an experiment with applied concentration $[\bar{A}]_0$ of coenzyme component. Since the advancing elution profile sufficed for determination of \bar{V}_A , the trailing profile generated by application of buffer medium was not subjected to analysis.

Method of analysis

The above frontal gel chromatographic procedure establishes the magnitude of the constituent elution volume, \bar{V}_A , of thiamin diphosphate in each applied mixture with respective total concentrations $[\bar{A}]_0$ and $[\bar{S}]_0$ of coenzyme and ligand (magnesium ion). In the absence of ligand ($[\bar{S}]_0 = 0$) the measured parameter defines V_A , the elution volume of thiamin diphosphate, whereas a similar experiment conducted with a very high concentration of Mg^{2+} (sufficient to saturate the single binding site [1,2] on the coenzyme) defines V_C , the elution volume of the Mg^{2+} –coenzyme complex. For intermediate concentrations of magnesium ion the elution volume defined by eqn. 1 is related to V_A and V_C by

$$\bar{V}_A = \{V_A[A]_0 + V_C([\bar{A}]_0 - [A]_0)\}/[\bar{A}]_0 \quad (2)$$

which allows the concentration of free thiamin diphosphate, $[A]_0$, in the applied mixture to be evaluated from the expression

$$[A]_0 = [\bar{A}]_0(\bar{V}_A - V_C)/(V_A - V_C) \quad (3)$$

The association equilibrium constant, K , for the acceptor–ligand interaction is then obtained from its definition as

$$K = [AS]_0/[A]_0[S]_0 \quad (4a)$$

$$= ([\bar{A}]_0 - [A]_0)/\{[A]_0([\bar{S}]_0 - [\bar{A}]_0 + [A]_0)\} \quad (4b)$$

A value of K is therefore obtained by evaluating \bar{V}_A for each mixture with defined composition ($[\bar{A}]_0$, $[\bar{S}]_0$).

RESULTS

Fig. 1 presents advancing elution profiles for thiamin diphosphate ($100 \mu M$) in the absence of metal ion, and also for the coenzyme component in mixtures containing $0.245 M$ and $0.1 M$ magnesium ion. The first point to note is the skewed nature of the elution profile in each case. Asymmetry of the profile for thiamin diphosphate in the absence of Mg^{2+} was certainly an unexpected finding, because symmetrical boundaries are normally observed for single solutes. Secondly, although this skewness led to location of the median bisector of the boundary at $0.66[\bar{A}]_0$ rather than the $0.50[\bar{A}]_0$ for a symmetrical boundary, the elution profiles obtained in exper-

iments with mixtures of coenzyme and Mg^{2+} ion exhibited similar asymmetry (Fig. 1). Any contribution to the skewness resulting from heterogeneity of the thiamin diphosphate is therefore exhibiting a similar bias on \bar{V}_A in all experiments. Thirdly, the elution volume corresponding to the median bisector (\bar{V}_A) increases with increasing concentration of metal ion, a finding consistent with the existence of the Mg^{2+} –coenzyme complex as a more folded, compact structure than the free coenzyme [1,2].

Fig. 2 summarizes the inverse dependence of the constituent elution volume of thiamin diphosphate, \bar{V}_A , upon total Mg^{2+} concentration, $[\bar{S}]_0$. It is apparent that the elution volume of 58.3 ml obtained from the experiment with $0.1 M$ Mg^{2+} ion on the present Sephadex G-10 column (Fig. 1) suffices to define the elution volume of Mg^{2+} –coenzyme complex (V_C), which is the limiting value of \bar{V}_A as $[\bar{S}]_0 \rightarrow \infty$. Experiments conducted in the absence of metal ion established the elution volume of thiamin diphosphate (V_A) as 52.4 ml . These values of V_A and V_C were therefore used in conjunction with eqn. 3 and the measured elution volumes (\bar{V}_A) for other reaction mixtures to obtain the concentration of free thiamin diphosphate, $[A]_0$, in each applied mixture. Results of those calculations, and also of the consequent evaluation of K via eqn. 4b, are summarized in Table 1. The interaction between thiamin diphosphate and Mg^{2+} under the present conditions is thus described by an association constant of $3200 (\pm 400) M^{-1}$. This value is of the same order of magnitude as, but smaller than, the binding con-

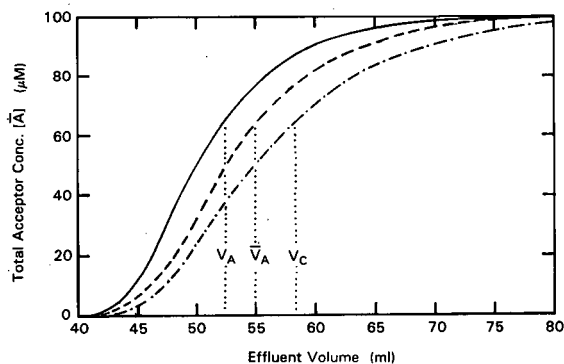


Fig. 1. Advancing elution profiles obtained in frontal gel chromatography of thiamin diphosphate ($100 \mu M$) on a column ($20 \times 2.5 \text{ cm}$) of Sephadex G-10 in the absence of metal ion (—) and in the presence of $0.245 M$ (---) and $0.1 M$ $MgCl_2$ (- · -).

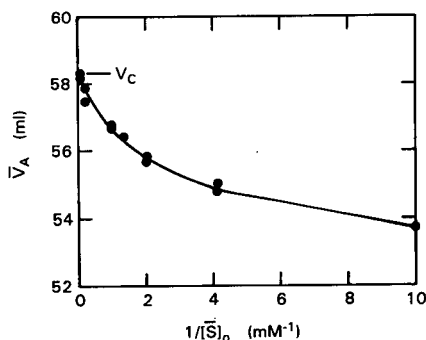


Fig. 2. Evaluation of the elution volume for Mg^{2+} –coenzyme complex (V_C) as the limiting value of the constituent elution volume (\bar{V}_A) of thiamin diphosphate in the limit of infinite magnesium ion concentration.

TABLE I
GEL CHROMATOGRAPHIC EVALUATION OF THE
BINDING CONSTANT FOR THE INTERACTION OF
MAGNESIUM ION WITH THIAMIN DIPHOSPHATE

Conditions: 0.1 M Tris-HCl (pH 7.6) supplemented with poly (ethylene glycol) (50 mg/ml) and mercaptoethanol (25 mM).

$[\bar{S}]_0$ (mM)	\bar{V}_A (ml) ^a	$[A]_0$ (μ M) ^b	K (M^{-1}) ^c
0	52.4	—	—
100	58.3	—	—
0.098	53.7	78.0	3700
0.245	55.0	55.9	3900
0.245	54.8	59.3	3400
0.490	55.6	45.8	2700
0.490	55.8	42.4	3100
0.735	56.4	32.2	3200
0.980	56.6	28.8	2700
0.980	56.7	27.1	3000

^a Elution volume in frontal chromatography of mixtures of thiamin diphosphate (100 μ M) and the indicated Mg^{2+} concentrations on a column (20 \times 2.5 cm) of Sephadex G-10.

^b Equilibrium concentration of thiamin diphosphate calculated from eqn. 3.

^c Equilibrium constant calculated from eqn. 4b.

stant of 5000 (\pm 200) reported [1] for the interaction of manganous ion with thiamin diphosphate.

DISCUSSION

Resort to frontal chromatography to define the dependence of the constituent elution volume (\bar{V}_A) of the acceptor (thiamin diphosphate) as a function of mixture composition has yielded a relatively direct and simple gel chromatographic procedure for evaluating the binding constant describing the interaction of magnesium ion with thiamin diphosphate. In that regard the zonal gel chromatographic procedure [5] that has been recommended by Colman [3] could also have been used. However, as noted previously [4], the non-identity of V_A and V_C introduces the requirement that the apparent steady-state values, K_{ss}^{app} , so obtained be extrapolated to zero acceptor concentration (infinite dilution) to obtain the true steady-state parameter, K_{ss}^{∞} , which must then be converted to the thermodynamic association constant, K , via the expression

$$K = K_{ss}^{\infty}(V_s - V_A)/(V_s - V_C) \quad (5)$$

Rigorous evaluation of K by the Hummel–Dreyer technique [3,5] thus requires not only extrapolation of data to infinite dilution but also a magnitude for the elution volume of ligand (V_s) in addition to those of V_A and V_C .

Having established that the present frontal gel chromatographic procedure for evaluating K is much more readily applied than its zonal counterpart [3–5], we conclude by showing that it also surpasses existing frontal chromatographic procedures for simplicity of application. One such procedure for evaluation of the association constant is based on the expression [8–10]

$$[A]_0 = \{[\bar{A}]_0(\bar{V}_A - V_s) - [\bar{S}]_0(\bar{V}_s - V_s)\} / (V_A - V_s) \quad (6)$$

which involves \bar{V}_s , the constituent elution volume of ligand, and thus requires delineation of separate elution profiles for ligand and acceptor components. It does, however, have the advantage of being applicable in instances where direct measurement of V_C is impractical. Another frontal gel chromatographic technique employs the relationship [6,16]

$$[A]_0 = \{[\bar{A}]_0(\bar{V}_A - V_s) - ([\bar{S}]_0 - [S]^\beta)(\bar{V}_s - V_s)\} / (V_A - V_s) \quad (7)$$

and hence relies on an ability to resolve accurately the trailing elution profile into a reaction boundary (across which all acceptor species are eluted) and a second boundary corresponding to elution of a pure ligand (Mg^{2+} ion) phase β with concentration $[S]^\beta$.

From the foregoing discussion of existing methods, the present procedure based solely on dependence of the constituent elution volume of acceptor (\bar{V}_A) upon mixture composition is clearly the simplest gel chromatographic method available for the determination of binding constants for acceptor–ligand interactions when $V_C \neq V_A$. It is, however, only applicable to interactions for which the concentration of ligand can be varied over a sufficiently wide range for V_C to be determined either directly (Fig. 1) or by extrapolation of \bar{V}_A to infinite ligand concentration (Fig. 2). Whereas the frontal methods discussed in the preceding paragraph were developed in the context of protein–protein interactions, for which evaluation of V_C by such means is precluded, the requirement that V_C be determined

experimentally could be met for the Mg^{2+} –thiamin diphosphate system. Furthermore, this requirement is unlikely to be a limiting factor in the quantitative study of other metal–nucleotide interactions.

In summary, the difficulties inherent in the evaluation of ligand-binding constants by gel chromatography when both reactants are small have been resolved satisfactorily in the sense that measurement of the constituent elution volume of acceptor as a function of mixture composition is likely to provide a straightforward and rigorous method of evaluating K . On the basis of its application to frontal gel chromatographic results for mixtures of thiamin diphosphate and magnesium ion on Sephadex G-10, the dissociation constant for the interaction of metal ion with coenzyme is 0.31 mM under the conditions examined [0.1 M Tris–HCl (pH 7.6) supplemented with poly(ethylene glycol) and mercaptoethanol]. In view of the physiological importance of the interaction between thiamin diphosphate and Mg^{2+} , it seems extraordinary that this is the first occasion on which the binding has been quantified. Finally, this very simple gel chromatographic method of evaluating equilibrium constants for metal–nucleotide interactions only requires delineation of the elution profile for the nucleotide component, and therefore has potential for quantifying the binding of any nucleotide to the metal ion of physiological relevance rather than one for which there happens to be a more convenient assay.

ACKNOWLEDGEMENTS

The financial support of this investigation by the Australian Research Council (D.J.W.) and the Australian National Health and Medical Research Council (P.F.N.) is gratefully acknowledged.

REFERENCES

- 1 H. J. Grande, R. L. Houghton and C. Veeger, *Eur. J. Biochem.*, 37 (1973) 563.
- 2 A.-M. Chauvet-Monges, M. Hadida, A. Crevat and E. J. Vincent, *Arch. Biochem. Biophys.*, 207 (1981) 311.
- 3 R. F. Colman, *Anal. Biochem.*, 46 (1972) 358.
- 4 J. R. Cann, A. G. Appu Rao and D. J. Winzor, *Arch. Biochem. Biophys.*, 270 (1989) 173.
- 5 J. P. Hummel and W. J. Dreyer, *Biochim. Biophys. Acta*, 63 (1962) 530.
- 6 L. W. Nichol and D. J. Winzor, *J. Phys. Chem.*, 68 (1964) 2455.
- 7 L. W. Nichol, W. J. H. Jackson and G. D. Smith, *Arch. Biochem. Biophys.*, 144 (1971) 438.
- 8 J. R. Cann and D. J. Winzor, *Arch. Biochem. Biophys.*, 256 (1987) 78.
- 9 G. A. Gilbert and G. L. Kellett, *J. Biol. Chem.*, 246 (1971) 6079.
- 10 L. W. Nichol, G. D. Smith and D. J. Winzor, *J. Phys. Chem.*, 77 (1973) 2912.
- 11 D. J. Winzor and H. A. Scheraga, *Biochemistry*, 2 (1963) 1263.
- 12 D. J. Winzor and L. W. Nichol, *Biochim. Biophys. Acta*, 104 (1965) 1.
- 13 G. K. Ackers, *Adv. Protein Chem.*, 24 (1970) 343.
- 14 H. E. Swaisgood and I. M. Chaiken, in I. M. Chaiken (Editor), *Analytical Affinity Chromatography*, CRC Press, Boca Raton, FL, 1987, p. 65.
- 15 D. J. Winzor and J. de Jersey, *J. Chromatogr.*, 492 (1989) 377.
- 16 L. W. Nichol, A. G. Ogston and D. J. Winzor, *Arch. Biochem. Biophys.*, 121 (1967) 517.

Progress in the design of selectors for buckminsterfullerene

Christopher J. Welch and William H. Pirkle

School of Chemical Sciences, University of Illinois, Urbana, IL 61801 (USA)

(First received March 4th, 1992; revised manuscript received June 16th, 1992)

ABSTRACT

The chromatographic retentions of buckminsterfullerene (C_{60}), the related C_{70} carbon cluster, and several polycyclic aromatic hydrocarbons are evaluated using ten high-performance liquid chromatography stationary phases, including several stationary phases designed specifically for recognition of the fullerenes. All of the stationary phases examined provide some degree of retention and selectivity in the separation of C_{60} and C_{70} . A novel tripodal π -acidic stationary phase designed for simultaneous multipoint interaction with buckminsterfullerene provides the greatest retention and the greatest separation factor for the C_{60} - C_{70} mixture.

INTRODUCTION

Improved methods for the preparative synthesis [1–3] of the spherical carbon cluster, buckminsterfullerene (C_{60}), and related “fullerenes” have precipitated an explosion of interest in the investigation of these molecules and their derivative (for a recent review, see ref. 4). Current methods for the preparation of buckminsterfullerene yield a complex mixture consisting primarily of C_{60} and C_{70} . None of the methods for the chromatographic purification of buckminsterfullerene which have been reported to date allow for convenient purification of gram quantities of material [1–8]. We recently reported that an unusual effect of temperature on the chromatographic behavior of C_{60} and C_{70} on a π -acidic 3,5-(dinitrobenzoyl)phenylglycine-derived stationary phase can be exploited for improved preparative resolution of these compounds [7]. Nevertheless, only about 100 mg of the crude C_{60} - C_{70} mixture can be resolved per run on a 4 ft. \times 2 in. I.D. preparative column containing this stationary phase, a column which can normally separate 20 g

per run of a soluble mixture having a similar separation factor.

The difficulty in the preparative chromatographic purification of buckminsterfullerene lies in its relative insolubility. Several hundred ml of benzene or toluene (“good” solvents for the crude fullerene mixture) would be required for injection of 1 g of this material. Furthermore, use of benzene or toluene as a mobile phase with a column containing the aforementioned π -acidic stationary phase results in virtually no retention of the analytes. Use of hexane as a mobile phase gives suitable retention, however, several *liters* of hexane would be required to dissolve 1 g of the fullerene mixture. In the previously cited study, we settled upon a method using hexane as a mobile phase with injection of the fullerene mixture in benzene.

An efficient and convenient method for large scale purification of buckminsterfullerene may be beyond the scope of liquid chromatography, even though the development of improved solvent systems and improved stationary phases can be expected. Nevertheless, investigation of the ever growing family of fullerenes and fullerene derivatives, many of which exist as closely related geometrical isomers, will require improved analytical tools. In this

Correspondence to: Dr. C. J. Welch, 8210 Austin Avenue, Morton Grove, IL 60053, USA (present address).

study, the chromatographic behavior of C_{60} , C_{70} , and eight polycyclic aromatic hydrocarbons (PAHs, Fig. 1) was investigated using the ten high-performance liquid chromatography (HPLC) stationary phases illustrated in Fig. 2.

The chromatographic separation of π -electron-rich polycyclic aromatic hydrocarbons on π -electron deficient stationary phases has been known for quite some time [9,10]. Thus, the report by Hawkins *et al.* [5] of the ability of the π -acidic stationary phase **I** to separate C_{60} and C_{70} was not without precedent. The chirality of phase **I** is irrelevant to the separation of achiral analytes such as C_{60} and C_{70} . In these laboratories, chiral stationary phases such as phase **I** are often used to separate non-enantiomeric analytes such as diastereomers, positional isomers, etc.

Commercially available columns containing phase **I** and the closely related phase **II** were used in this study. In addition, commercially available columns containing π -basic phases **III** and **IV** were ex-

amined to assess the ability of π -basic stationary phases to afford retention for the fullerenes. The π -acidic stationary phase **V–X** were prepared for this study.

Phase **V**, an achiral glycine analog of phases **I** and **II**, was prepared as illustrated in Fig. 3. Acylation of glycine, **11**, with 3,5-dinitrobenzoyl chloride affords acid **12**. Coupling with 4-aminobutyldimethylmethoxysilane affords silane **13** which was immobilized upon silica gel to give phase **V**.

Phase **VI**, which contains an isolated 3,5-dinitrobenzamide system, was prepared as illustrated in Fig. 4. Acylation of 4-aminobutyldimethylmethoxysilane, **14**, with 3,5-dinitrobenzoyl chloride provides silane **15** which was bonded to silica gel to afford phase **VI**.

Phase **VII**, which contains the 2,4-dinitroaniline system, was prepared as illustrated in Fig. 5. Reaction of allyl amine, **16**, with 2,4-dinitrofluorobenzene provides olefin **17** which was hydrosilylated to afford silane **18**. Immobilization of silane **18** on sil-

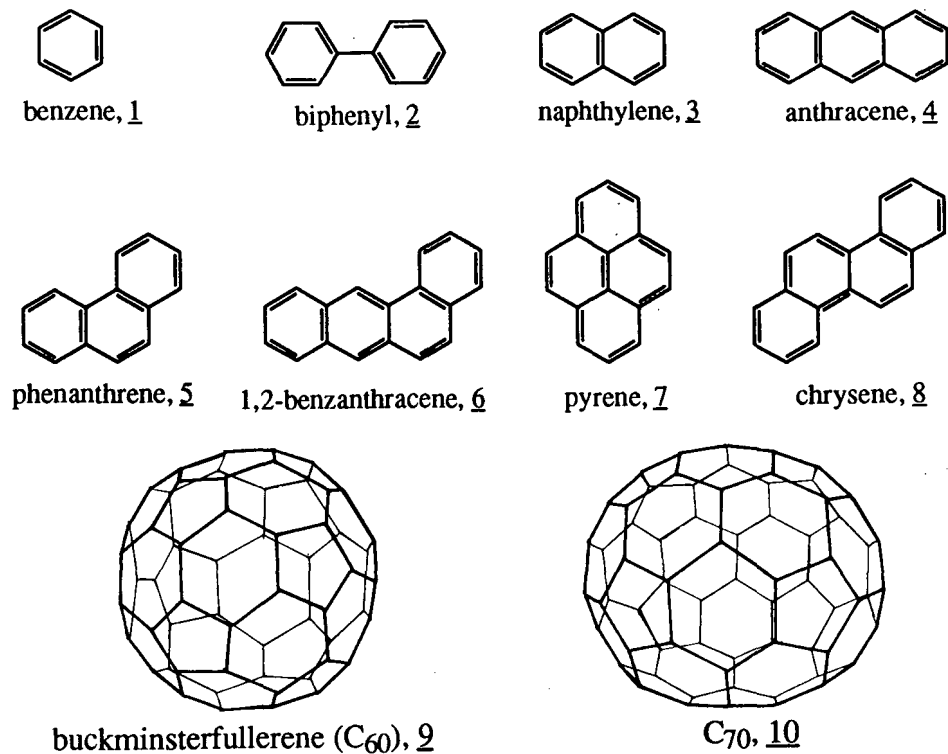


Fig. 1. Polycyclic aromatic hydrocarbons and fullerenes used in the study.

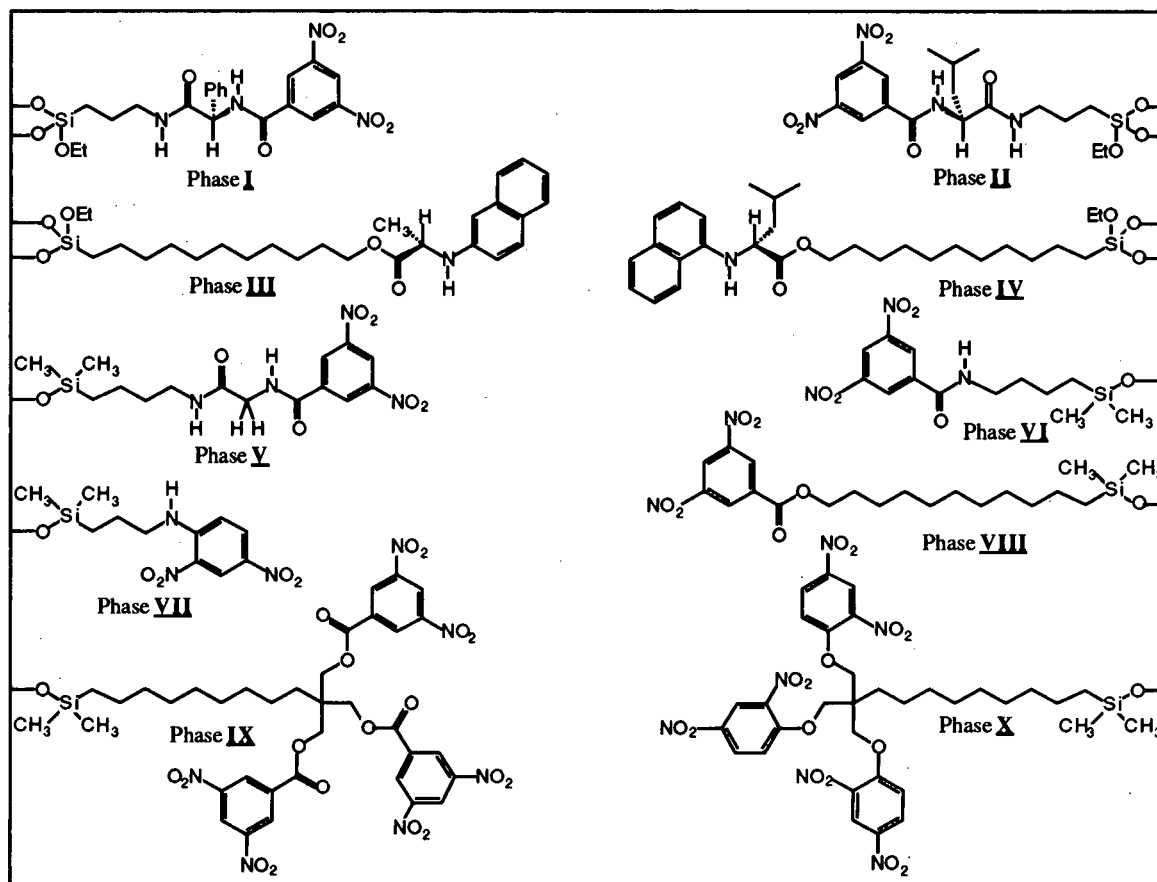


Fig. 2. Stationary phases used in the study. Et = Ethyl; Ph = phenyl.

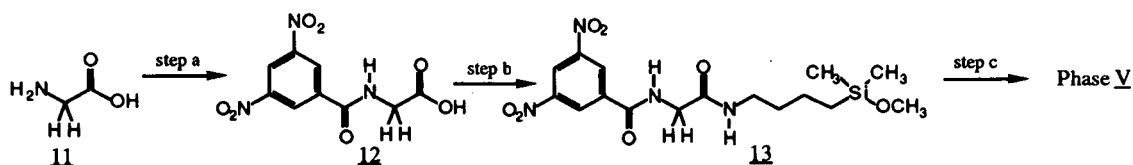


Fig. 3. Synthetic route for preparation of phase V. Step a: 3,5-dinitrobenzoyl chloride–triethylamine, tetrahydrofuran. Step b: 1-ethoxycarbonyl-2-ethoxy-1,2-dihydroquinoline (EEDQ)–aminobutyltrimethylmethoxysilane, tetrahydrofuran. Step c: 5 $\mu\text{m}/100 \text{ \AA}$ silica gel, 130°C, 1 Torr, 18 h.

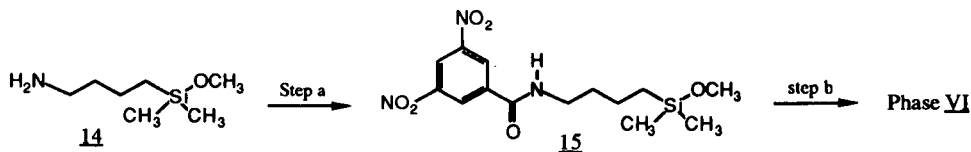


Fig. 4. Synthetic route for preparation of phase VI. Step a: 3,5-dinitrobenzoyl chloride–triethylamine, dichloromethane. Step b: 5 $\mu\text{m}/100 \text{ \AA}$ silica gel, 130°C, 1 Torr, 18 h.

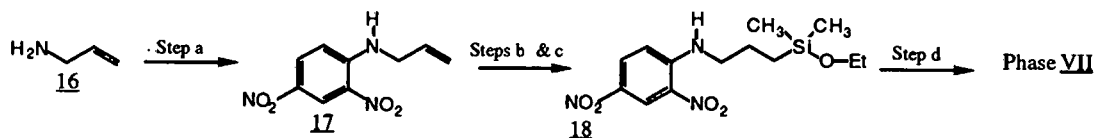


Fig. 5. Synthetic route for preparation of phase VII. Step a: 2,4-dinitrofluorobenzene–triethylamine, dichloromethane. Step b: dimethylchlorosilane, chloroplatinic acid (catalyst), dichloromethane. Step c: ethanol, triethylamine, diethyl ether. Step d: 5 $\mu\text{m}/100 \text{ \AA}$ silica gel, 130°C, 1 Torr, 18 h.

ica gel affords phase VI. Cox *et al.* [6] reported the use of a “dinitroaniline stationary phase” for the separation of the C₆₀–C₇₀ mixture. Although the structure of this stationary phase was not reported, it is probably similar, if not identical, to phase VII.

Phase VIII, which contains a 3,5-dinitrobenzoate ester, was prepared as illustrated in Fig. 6. Acylation of ω -undecenylenyl alcohol, 19, with 3,5-dinitrobenzoyl chloride provides ester 20 which was hydrosilylated to provide silane 21. Bonding of silane 21 to silica gel affords phase VIII.

Selector preorganization is known to have a dramatic effect upon the binding guest molecules [11]. We reasoned that functionalization of triols such as 23, readily prepared using a variation of the pentaerythritol synthesis [12,13], could afford selectors containing a concave disposition of π -acidic aromatic rings complementary to the convex surface of C₆₀. Using this approach, phases IX (Fig. 7) and X (Fig. 8) were prepared. While the selectors in these stationary phases admittedly possess some degree of conformational “floppiness” and are thus not ideally preorganized, examination of Corey–Paul-

ing–Koltun (CPK) space-filling molecular models indicates that they should be capable of some degree of simultaneous multipoint interaction with the fullerene analytes.

The tripodal 3,5-dinitrobenzoate ester phase, IX, was prepared as illustrated in Fig. 7. Reaction of ω -undecenylenyl aldehyde, 22, with formaldehyde under basic conditions provides triol 23, which was acylated with 3,5-dinitrobenzoyl chloride to afford triester 24. Hydrosilylation of 24, followed by immobilization on silica gel, affords phase IX.

The tripodal 2,4-dinitrophenyl ether phase, X, was prepared as illustrated in Fig. 8. Reaction of triol 23 with 2,4-dinitrofluorobenzene provides triether 26 which was hydrosilylated to afford silane 27. Bonding of silane 27 to silica gel affords phase X.

MATERIALS AND METHODS

Apparatus

Chromatographic analysis was performed using

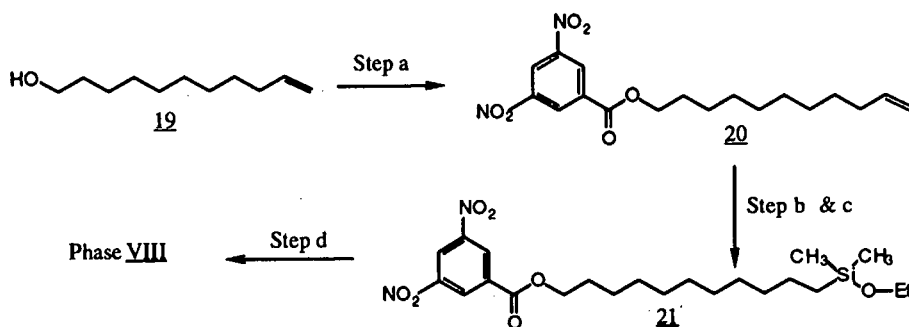


Fig. 6. Synthetic route for preparation of phase VIII. Step a: 3,5-dinitrobenzoyl chloride–triethylamine, tetrahydrofuran. Step b: dimethylchlorosilane, chloroplatinic acid (catalyst), dichloromethane. Step c: ethanol, triethylamine, diethyl ether. Step d: 5 $\mu\text{m}/100 \text{ \AA}$ silica gel, 120°C, 1 Torr, 24 h.

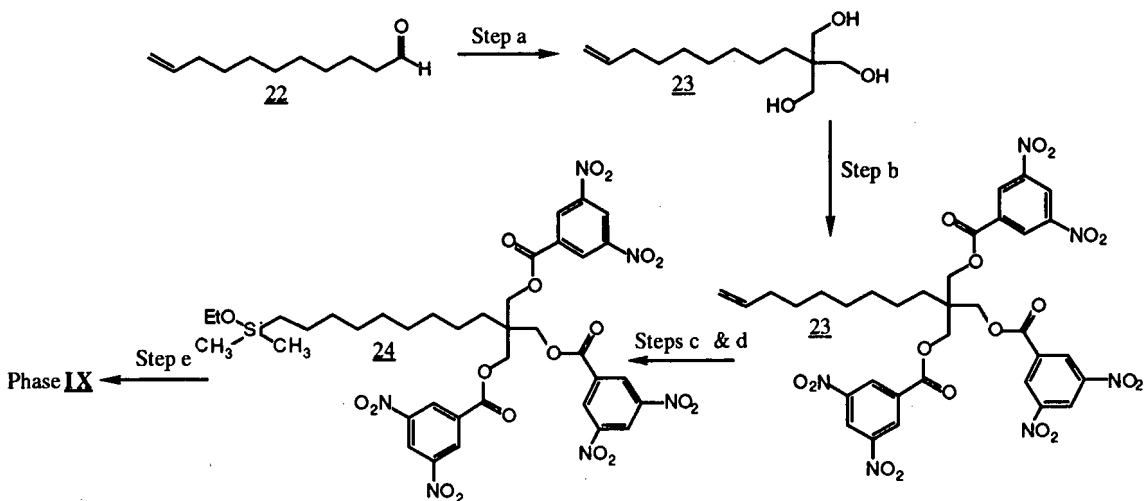


Fig. 7. Synthetic route for preparation of phase IX. Step a: formaldehyde–KOH, ethanol–water. Step b: 3,5-dinitrobenzoyl chloride–triethylamine, dichloromethane. Step c: dimethylchlorosilane, chloroplatinic acid (catalyst), dichloromethane. Step d: ethanol, triethylamine, diethyl ether. Step e: 5 $\mu\text{m}/100 \text{ \AA}$ silica gel, 120°C, 1 Torr, 24 h.

a Beckman-Altex 100-A pump, a Rheodyne Model 7125 injector with a 20- μl sample loop, a Linear UVIS 200 variable-wavelength absorbance monitor set at 254 nm, and a Hewlett-Packard HP 3394-A integrating recorder. All ^1H NMR spectra were recorded on a Varian XL 200 FT NMR spectrometer. ^1H NMR chemical shifts are reported in ppm (δ) relative to tetramethylsilane.

Materials

Rexchrom 5 $\mu\text{m}/100 \text{ \AA}$ silica gel and columns

containing phases I–IV were obtained from Regis, Morton Grove, IL, USA. Phases V–X were prepared as outlined in the *Synthesis* section below. Dimethylchlorosilane and 4-aminobutyldimethylmethoxysilane were obtained from Petrarch Systems, Bristol, PA, USA. PAHs (analytes 1–8) were available from previous studies. A crude mixture containing C_{60} and C_{70} was obtained within the department from Drs. John Shapley and Scott Kofod.

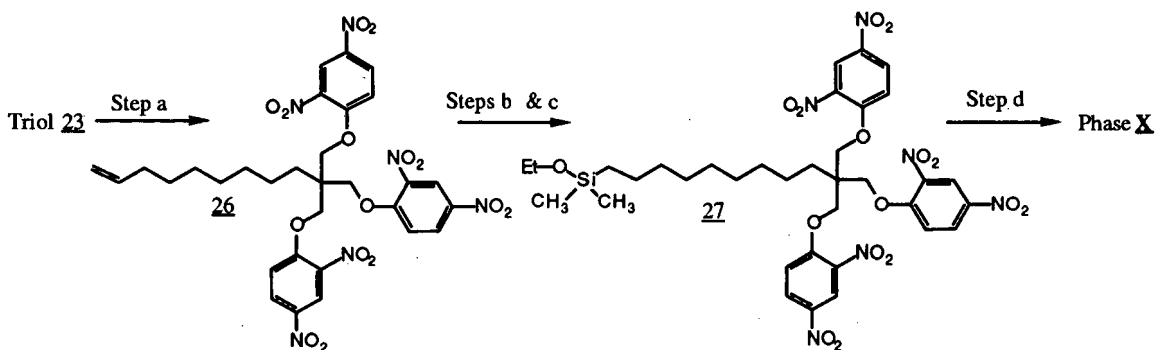


Fig. 8. Synthetic route for preparation of phase X. Step a: 2,4-dinitrofluorobenzene–triethylamine, dichloromethane. Step b: dimethylchlorosilane, chloroplatinic acid (catalyst), dichloromethane. Step c: ethanol, triethylamine, diethyl ether. Step d: 5 $\mu\text{m}/100 \text{ \AA}$ silica gel, 120°C, 1 Torr, 24 h.

Methods

All chromatographic experiments were carried out at a nominal flow rate of 2.00 ml/min. Column void time was determined by injection of tri-*tert.*-butylbenzene [14].

Synthesis

Preparation of phase V

The synthetic route for the preparation of phase V is illustrated in Fig. 3.

Preparation of 3,5-(dinitrobenzamido)glycine, 12. Glycine (**11**, 5.0 g) was suspended in 100 ml of dry tetrahydrofuran and cooled in an ice bath. 3,5-Dinitrobenzoyl chloride (16.9 g) and propylene oxide (7.0 ml) were added and the mixture was stirred under a nitrogen atmosphere and gradually allowed to warm to room temperature. After 10 h, the crude reaction mixture was evaporated to afford a brown oil. Addition of 100 ml of dichloromethane resulted in crystallization after several min. Filtration, followed by several washes with dichloromethane and drying under high vacuum, gave 13.9 g **12** (78% yield) as a pale yellow powder. $^1\text{H NMR}$ ($[\text{D}_6]\text{DMSO}$) δ : 12.8 (s, 1H), 9.6 (t, 1H), 9.1 (s, 2H), 9.0 (s, 1H), 4.0 (d, 2H).

Preparation of organosilane 13. To a cooled (ice bath) solution of 1.0 g of acid **12** in tetrahydrofuran was added 0.92 g 1-ethoxycarbonyl-2-ethoxycarbonyl-2-ethoxy-1,2-dihydroquinoline (EEDQ). This mixture was stirred 45 min. under a nitrogen atmosphere, 0.50 g of 4-aminobutyldimethylmethoxysilane was added, and the reaction mixture was allowed to gradually warm to room temperature. After 10 h, the crude reaction mixture was evaporated and purified by flash chromatography on silica to give 0.65 g (42% yield) of **13** as a slightly pink foam.

Preparation of phase V. Silica gel (5.0 g, Rexchrom, 5 $\mu\text{m}/100 \text{ \AA}$) was placed in a round-bottom flask fitted with a Dean–Star trap, condenser, and boiling stick. About 30 ml of benzene were added and the mixture was heated to reflux for several hours. Dimethylformamide (1 ml) was then added to the benzene slurry and the sample was evaporated to near dryness on a rotary evaporator. A dichloromethane solution of silane **13** (0.65 g) was then added and the resulting slurry was sonicated for several minutes before being evaporated to near

dryness. The sample was again slurried in dichloromethane, sonicated, and evaporated to near dryness, this sequence being repeated several times to insure complete coverage of the silica gel. The nearly dry silica gel–silane mixture was then heated on an oil bath under reduced pressure (130°C, 1 Torr, 18 h). The silica gel was then slurried in ethanol, filtered through a fine sintered glass funnel, and washed repeatedly with ethanol and then methanol. Evaporation and analysis of the ethanol washes can be done at this point to monitor degradation of the silane during the course of the bonding reaction. The washed silica gel was then slurried in methanol and packed into a 25 cm \times 4.6 mm I.D. stainless-steel HPLC column using an air-driven Haskell pump operating at about 9000 p.s.i. Stationary phase recovered from the column packer was dried thoroughly under high vacuum and submitted for elemental analysis (C 3.39%) which indicates a loading of $1.9 \cdot 10^{-4}$ mol of selector per gram of stationary phase. Residual silanols on the chromatographic support were then “endcapped” by passing a solution of 1 ml of hexamethyldisilazane dissolved in 50 ml of dichloromethane through the dichloromethane-equilibrated column at a flow rate of 1 ml/min [15]. The column was then sequentially eluted with dichloromethane, methanol and 20% 2-propanol in hexane.

Preparation of phase VI

The synthetic route for the preparation of phase VI is illustrated in Fig. 4.

Preparation of organosilane 15. Triethylamine (0.69 g) and 4-aminobutyldimethylmethoxysilane (1.00 g) were dissolved in 20 ml dichloromethane and cooled in an ice bath. 3,5-Dinitrobenzoyl chloride (1.43 g) dissolved in 10 ml of dichloromethane was then added dropwise over several minutes with stirring under a nitrogen atmosphere. The reaction mixture was allowed to warm to room temperature and stirred for an additional h. The crude reaction mixture was evaporated to dryness and purified by flash chromatography (silica gel, 5% acetonitrile in dichloromethane) to afford **15** as a clear oil (840 mg, 69.4% yield). $^1\text{H NMR}$ (C_2HCl_3) δ : 9.15 (s, 1H), 9.0 (s, 1H), 6.8 (bs, 1H), 3.55 (m, 2H), 4.3 (s, 3H), 1.75 (m, 2H), 1.5 (m, 2H), 0.65 (t, 2H), 0.15 (s, 6H).

Preparation of phase VI. The bonding of silane **15**

to silica and the subsequent packing of the resulting stationary phase into an HPLC column followed the procedure reported for the preparation of phase V except that a Kügelrohr distillation apparatus was used in the bonding reaction (130°C, 1 Torr, 18 h). Stationary phase recovered from the column packer was submitted for elemental analysis (C 4.69%) indicated a loading of $3.0 \cdot 10^{-4}$ mol of selector per gram of stationary phase.

Preparation of phase VII

The synthetic route for the preparation of phase VII is illustrated in Fig. 5.

Preparation of olefin 17. To a cooled, stirred solution of allylamine (**16**, 0.46 g) and triethylamine (0.90 g) in dichloromethane was added 2,4-dinitrofluorobenzene (1.5 g). After warming to room temperature, the reaction mixture was stirred for 3 h, then evaporated to dryness and purified by flash chromatography (silica, dichloromethane) to afford olefin **17** as a crystalline solid (1.09 g, 61% yield). $^1\text{H NMR}$ (C_2HCl_3) δ : 9.25 (d, 1H), 8.8 (bs, 1H), 8.3 (dd, 1H), 7.0 (d, 1H), 6.0 (m, 1H), 5.8 (dd, 2H), 4.1 (t, 2H).

Preparation of Organosilane 18. Olefin **17** (1.09 g) was dissolved in 10 ml of dichloromethane and 10 ml of dimethylchlorosilane. Chloroplatinic acid (10 mg) dissolved in a minimum amount of 2-propanol was then added and the mixture was heated at reflux. Progress of the reaction was monitored by disappearance of starting material in quenched reaction aliquots (the quenching solution was composed of 5 ml of absolute ethanol, 5 ml of triethylamine, and 5 ml of diethyl ether). The assay procedure consists of removing several drops of reaction mixture, evaporating to dryness under high vacuum to remove excess dimethylchlorosilane, and addition of several drops of quenching solution. The mixture was then heated for several min on an oil bath, diluted with dichloromethane, and examined by thin-layer chromatography (TLC). After about 3 h, TLC analysis of quenched reaction aliquots indicated complete consumption of starting material. The crude reaction mixture was evaporated to dryness, with several additions and evaporations of dichloromethane to insure complete evaporation of residual dimethylchlorosilane, then quenched by addition of the quenching solution with stirring for 30 min. The quenched solution was filtered to remove pre-

cipitated triethylamine hydrochloride, then evaporated and purified by flash chromatography on silica using 2% ethanol in dichloromethane to afford 0.80 g **18** (50% yield). $^1\text{H NMR}$ (C_2HCl_3) δ : 9.2 (s, 1H), 8.6 (bs, 1H), 8.3 (d, 1H), 7.0 (d, 1H), 3.6 (m, 2H), 3.4 (m, 2H), 1.8 (m, 2H), 1.2 (t, 3H), 0.7 (t, 2H), 0.1 (s, 6H).

Preparation of phase VII. Silane **18** was bonded to silica and the resulting stationary phase was packed into an HPLC column as described for phase V, except that a Kügelrohr distillation apparatus was used in the bonding reaction (115°C, 1 Torr, 24 h). Packing material recovered from the column packer was submitted for elemental analysis, the result (C, 3.28%) indicates a loading of $2.5 \cdot 10^{-4}$ mol of selector per gram of stationary phase.

Preparation of phase VIII

The synthetic route for the preparation of phase VIII is illustrated in Fig. 6.

Preparation of olefin 20. To a cooled solution of ω -undecenyl alcohol (**19**, 1.0 g) and triethylamine (0.65 g) in 10 ml of dry tetrahydrofuran were added 3,5-dinitrobenzoyl chloride (1.36 g) with stirring. The reaction mixture was allowed to warm to room temperature and stirred for an additional h. The heterogeneous solution was diluted with diethyl ether and extracted three times with a 1.0 M HCl solution. The organic layer was washed with water, then brine, then dried over anhydrous magnesium sulfate. Filtration and evaporation yielded **20** (2.00 g, 93% yield) as a pale yellow solid. $^1\text{H NMR}$ (C_2HCl_3) δ : 9.25 (d, 1H), 9.2 (d, 2H), 5.8 (m, 1H), 4.95 (m, 2H), 4.4 (t, 2H), 2.05 (m, 2H), 1.85 (m, 2H), 0.9 (m, 12H).

Preparation of organosilane 21. Olefin **20** was converted into ethoxysilane **21** using the hydrosilylation procedure reported for preparation of organosilane **18**. Crude **21** was purified by flash chromatography on silica using dichloromethane to afford 1.04 g **21** (80.6% yield) as a yellow oil. $^1\text{H NMR}$ (C_2HCl_3) δ : 9.25 (d, 1H), 9.15 (d, 2H), 4.45 (t, 2H), 3.65 (q, 2H), 1.85 (m, 2H), 1.3 (m, 16H), 0.6 (t, 2H), 0.1 (s, 6H).

Preparation of phase VIII. Silane **21** was bonded to silica and the resulting stationary phase was packed into an HPLC column as described for phase V (120°C, 1 Torr, 24 h). Stationary phase recovered from the column packer was submitted for

elemental analysis, the result (C, 3.94%) indicates a loading of $1.6 \cdot 10^{-4}$ mol of selector per gram of stationary phase.

Preparation of phase IX

The synthetic route for the preparation of phase IX is illustrated in Fig. 7.

Preparation of triol 23. Undecylenic aldehyde (**22**, 50 g) and 200 g of 40% formaldehyde solution were dissolved in 500 ml of ethanol–water (1:1). Potassium hydroxide (16.30 g) dissolved in 150 ml of ethanol–water (1:1) was then added dropwise to the cold (0°C) stirred solution. The reaction was allowed to warm to room temperature, stirred for 4 h then heated to 60°C and stirred for an additional 2 h at which time TLC indicated complete consumption of starting material and formation of a new product. The crude reaction mixture was concentrated under vacuum to remove ethanol and then extracted several times with diethyl ether. The combined ether extracts were washed several times with water, washed with brine, dried over anhydrous magnesium sulfate, filtered and evaporated to dryness. Flash chromatography on silica gel using 10% methanol in dichloromethane gave triol **23** (28.2 g, 41.4% yield) as a white solid. $^1\text{H NMR}$ (C^2HCl_3) δ : 5.85 (m, 1H), 5.0 (m, 2H), 3.75 (d, 6H), 2.75 (t, 3H), 2.05 (m, 2H), 1.3 (m, 12H).

Preparation of triester 24. Triol **23** (1.0 g) and triethylamine (1.5 g) were dissolved in 50 ml of dry tetrahydrofuran and cooled in an ice bath. 3,5-Dinitrobenzoyl chloride (3.0 g) was then added and the solution was allowed to gradually warm to room temperature, then stirred overnight under a nitrogen atmosphere. Precipitated triethylammonium chloride was removed by filtration and the filtrate was washed several times with a 1 M HCl solution dried over anhydrous magnesium sulfate, filtered, and evaporated to dryness. Ether trituration of the resulting oil give triester **24** (1.64 g, 47% yield) as a white solid. $^1\text{H NMR}$ (C^2Cl_3 , [$^2\text{H}_6$]dimethyl sulfoxide) δ : 9.2 (d, 3H), 9.1 (d, 6H), 5.75 (m, 1H), 4.9 (m, 2H), 4.65 (s, 6H), 2.0 (m, 2H), 1.8 (m, 2H), 1.4 (m, 10H).

Preparation of silane 25. Triester **24** (1.60 g) was converted into ethoxysilane **25** using the hydrosilylation procedure reported for preparation of organosilane **18**. Crude **25** was purified by flash chromatography (silica, 5% acetonitrile in dichloromethane)

ane) to afford **25** (1.03 g, 57.2% yield) as a yellowish solid. $^1\text{H NMR}$ (C^2HCl_3) δ : 9.25 (d, 3H), 9.15 (d, 6H), 4.6 (s, 6H), 3.6 (q, 2H), 1.8 (m, 2H), 1.6 (m, 2H), 1.3 (m, 12H), 0.5 (t, 2H), 0.05 (s, 6H).

Preparation of phase IX. Silane **25** was bonded to silica and the resulting stationary phase was packed into an HPLC column as described for the preparation of phase V (120°C, 1 Torr, 24 h). Stationary phase recovered from the column packer was submitted for elemental analysis, the result (C, 6.30%) indicates a loading of $1.5 \cdot 10^{-4}$ mol of selector per gram of stationary phase.

Preparation of phase X

The synthetic route for the preparation of phase X is illustrated in Fig. 8.

Preparation of triether 26. Triol **23** (1.0 g) and triethylamine (2.2 g) were dissolved in 50 ml of dichloromethane and cooled in an ice bath. 2,4-Dinitrofluorobenzene (2.7 g) was then added. After 30 min, the ice bath was removed and the reaction mixture was allowed to stir overnight at room temperature under a nitrogen atmosphere. The crude reaction mixture was evaporated and purified by flash chromatography on silica gel using dichloromethane to give **26** (1.39 g, 44% yield) as a pale yellow foam. $^1\text{H NMR}$ (C^2HCl_3) δ : 8.8 (d, 3H), 8.5 (dd, 3H), 7.35 (d, 3H), 5.8 (m, 1H), 4.95 (m, 2H), 4.5 (s, 6H), 2.05 (m, 2H), 1.85 (m, 2H), 1.4 (m, 12H).

Preparation of silane 27. Triether **26** (1.39 g) was converted into ethoxysilane **27** using the hydrosilylation procedure reported for preparation of organosilane **18**. Crude **27** was purified by flash chromatography on silica using 5% acetonitrile in dichloromethane as eluent to afford 1.0 g **27** (63% yield) $^1\text{H NMR}$ (C^2HCl_3) δ : 8.8 (d, 3H), 8.5 (dd, 3H), 7.35 (d, 3H), 4.45 (s, 6H), 3.65 (q, 2H), 1.85 (m, 2H), 1.25 (m, 14H), 1.2 (t, 3H), 0.55 (t, 2H), 0.1 (s, 6H).

Preparation of phase X. Silane **27** was bonded to silica, and the resulting stationary phase was packed into an HPLC column as described for the preparation of phase V (130°C, 1 Torr, 24 h). Stationary phase recovered from the column packer was submitted for elemental analysis, the result (C, 6.29%) indicates a loading of $1.6 \cdot 10^{-4}$ mol of selector per gram of stationary phase.

RESULTS AND DISCUSSION

Evaluation of phases I–X

All of the stationary phases evaluated in the study provided some degree of retention and separation for the C₆₀–C₇₀ mixture. Table I shows chromatographic data relevant to the separation of analytes 1–10 on phases I–X. Phase X affords the largest capacity factor (*k'*) for buckminsterfullerene, 9, and is the only phase to offer increased retention of this analyte relative to phase I. Phases III–X all afford improved separation factors (α') relative to phase I for separation of the C₆₀–C₇₀ mixture. Interestingly, even the π -basic phases III, and IV, are quite effective in retaining and separating the fullerenes although these phases provide only marginal retention of the polycyclic aromatic hydrocarbons (analytes 1–8).

The phenylglycine-derived phase, I, consistently affords greater retention than does the leucine-derived phase, II. In the plot of the the relative capacity factors observed with the two columns (Fig. 9), it can be seen that all of the data points fall approximately on a line having a slope of about 0.37. A linear plot indicates that each analyte in the series is being retained by essentially the same mechanistic process on each column, although the processes may differ between columns. When comparing two

identical columns, a slope of unity would be expected. Two columns containing the same selector with different loadings (*i.e.* surface coverage) would be expected to give a straight line, the slope of which is indicative of the relative loadings of the two phases. When comparing two nonidentical columns, differences in selector structure and differences in loading will both contribute to the observed slope.

The loadings of phases I and II are approximately the same, thus the differences in retention observed with the two phases must reflect differences in the selectors. We recently suggested that π -acidic stationary phases such as phase I (which contains a π -basic phenyl substituent at the stereogenic center) may be capable of undergoing simultaneous face to edge and face to face π - π interactions with π -basic analytes [16]. If this is indeed the explanation for the increased retention of the PAH analytes on phase I relative to phase II, then the fullerenes, which have no "edges", must derive a similar benefit from the presence of the phenyl group in phase I, since the data points for analytes 9 and 10 fall upon the line described by the PAH analytes.

Stationary phases III and IV provide substantial retention for the fullerene analytes but only moderate retention of the PAH analytes. Phases III and IV were included in the study to assess the ability of π -basic stationary phases to provide retention of the

TABLE I
CAPACITY FACTORS FOR ANALYTES 1–10 ON STATIONARY PHASES I–X

Conditions: mobile phase = 5% dichloromethane in hexane, flow-rate = 2.00 ml/min, ambient temperature. Void time determined using 1,3,5-tri-*tert.*-butylbenzene [14]. α = separation factor for C₆₀ and C₇₀.

Analyte	Stationary phase									
	I	II	III	IV	V	VI	VII	VIII	IX	X
1	0.18	0.15	0.11	0.12	0.12	0.13	0.10	0.10	0.14	0.17
2	0.53	0.35	0.19	0.17	0.33	0.34	0.22	0.19	0.38	0.44
3	0.77	0.46	0.19	0.19	0.40	0.44	0.26	0.27	0.58	0.58
4	2.19	1.06	0.34	0.30	1.12	1.24	0.70	0.70	1.74	1.28
5	2.57	1.19	0.34	0.31	1.22	1.35	0.72	0.81	2.06	1.41
6	5.55	2.27	0.57	0.47	3.00	3.31	1.97	1.88	5.61	3.30
7	5.96	2.27	0.43	0.39	2.53	2.73	1.49	2.11	5.84	2.68
8	6.30	2.43	0.60	0.50	3.23	3.46	2.09	2.13	6.45	3.57
9	2.99	1.19	1.98	2.62	1.01	2.26	2.45	0.50	1.61	6.59
10	4.65	1.90	4.16	5.31	1.80	4.76	7.10	0.80	3.28	20.77
α	1.60	1.56	2.10	2.03	1.78	2.11	2.89	1.60	2.03	3.15

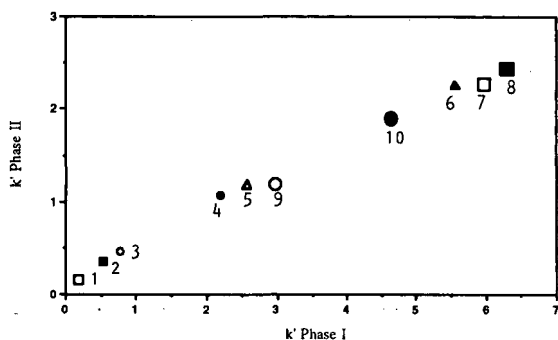


Fig. 9. Relative capacity factors for analytes 1-10 (as indicated) on phases I and II.

fullerenes. In the plot of the the relative capacity factors observed with the two columns (Fig. 10), it can be seen that the data points for fullerene analytes 9 and 10 fall far from the line defined by the PAH analyte data points (slope = 0.07). This indicates that adsorption of the fullerenes occurs by a different mechanism than adsorption of the PAH analytes on phases III and IV. This unexpected finding suggests that the fullerene analytes may be polarized during adsorption so as to respond as either π -bases or π -acids. Alternatively, the aniline hydrogens of phases III and IV may hydrogen bond to the π -clouds of the fullerene analytes. Hydrogen bonds to π -clouds of aromatic systems are well preceded [17] and the convex surface of the fullerenes may render these analytes better able to undergo this interaction than the planar PAH molecules.

The glycine-derived phase V offers little advan-

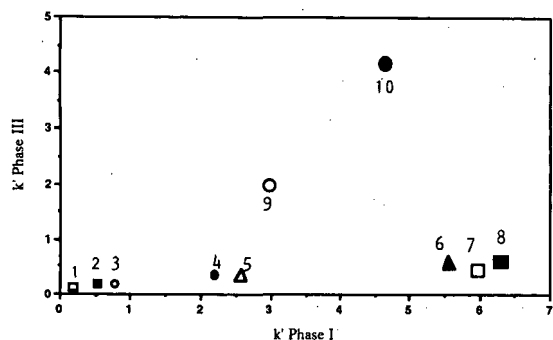


Fig. 10. Relative capacity factors for analytes 1-10 (as indicated) on phases I and III.

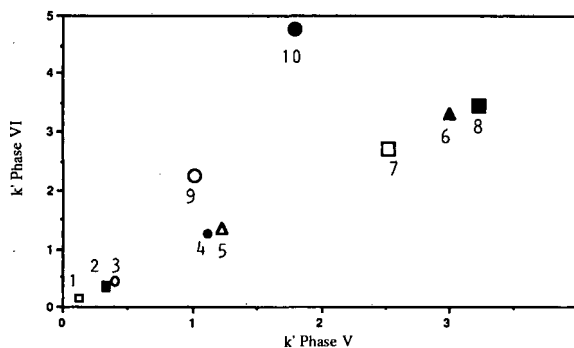


Fig. 11. Relative capacity factors for analytes 1-10 (as indicated) on phases V and VI.

tage over the related π -acidic amino acid-derived phases, I and II. Capacity factors on phase V are similar those provided by phase II and smaller than those provided by phase I, again suggesting the involvement of the phenyl ring of phase I in interaction with the analytes.

The isolated dinitrobenzamide system of phase VI retains the PAH analytes to about the same extent as do phases II and V but to a lesser extent than the phenylglycine-derived phase I. Fig. 11 shows the relative retentions of analytes 1-10 on phases V and VI. The data points for the PAH analytes 1-8 fall on a line having a slope of 1.08, the fullerene analytes lying off of this line owing to their selective adsorption by phase VI. Whatever the nature of this selective adsorption, it can be readily seen that the second amide group of the amino acid-derived π -acidic phases, II and V, makes little contribution to the retention of the fullerenes. Possibly, intramolecular hydrogen bonding between the 3,5-dinitrobenzamide hydrogen and the C-terminal carbonyl oxygen may interfere with the ability of phases II and V to hydrogen bond to the fullerenes.

The dinitroaniline-containing phase, VII, does not retain the PAH analytes as well as the dinitrobenzamide-containing phase, VI, but retains the fullerene analytes rather more strongly than does phase VI. Fig. 12 illustrates the relative capacity factors of analytes 1-10 on these two stationary phases. The data points for the PAH analytes fall on a line of slope 0.58 with the data points for the fullerene analytes lying considerably off of this line. The selective retention of the fullerene analytes (especially C_{70}) on phase VII relative to phase VI may

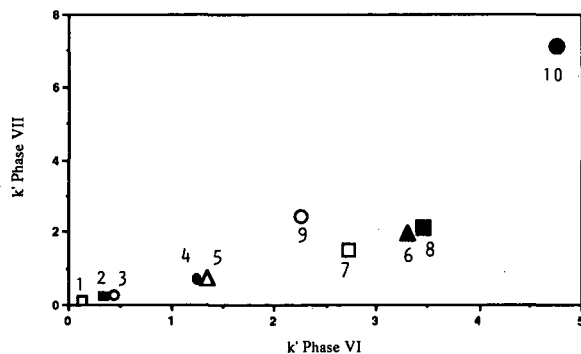


Fig. 12. Relative capacity factors for analytes 1-10 (as indicated) on phases VI and VII.

be attributable to a difference in the hydrogen bonding ability of the aniline and amide hydrogens which may be oriented differently with respect to the π -acidic aromatic ring. The 3,5-dinitrobenzamide and 2,4-dinitroaniline moieties differ in π -acidity but this might not be expected to differentially affect the PAH and fullerene retentions.

As shown in Fig. 13, the dinitrobenzoate ester phase, VIII, shows reduced retention for the PAH analytes relative to the dinitrobenzamide phase, VI, the best line through these data points having a slope of 0.63. The data points for the fullerene analytes fall significantly below the line described by the PAH analyte data points, reflecting the poor retention of the fullerenes on the ester phase (which contains no hydrogen bond donors) relative to the amide phase (which does contain such a donor). This result may again indicate the importance of

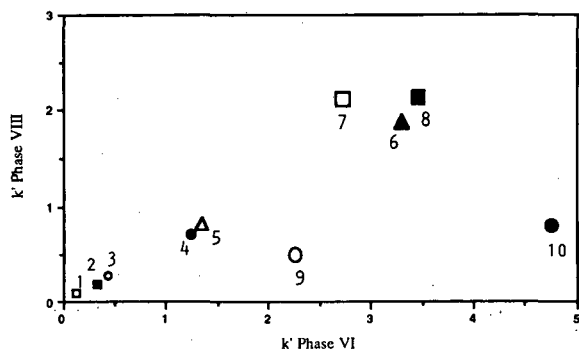


Fig. 13. Relative capacity factors for analytes 1-10 (as indicated) on phases VI and VIII.

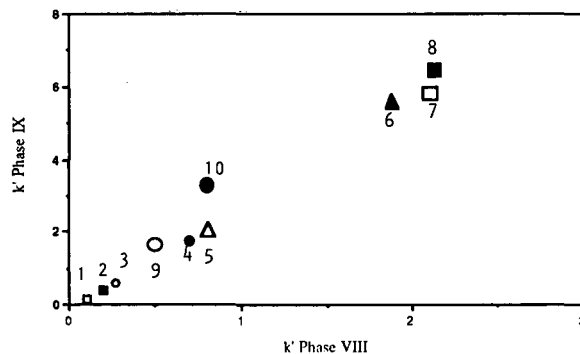


Fig. 14. Relative capacity factors for analytes 1-10 (as indicated) on phases VIII and IX.

hydrogen bonding interactions in the retention of the fullerene analytes.

The tripodal ester phase, IX, is similar to phase VIII, except that it may be capable of simultaneous multipoint interaction with the fullerene and PAH analytes. Interestingly, phase IX is the only one of the stationary phases examined which shows retentions for the PAH analytes which are comparable to those provided by phase I. Phases VIII and IX have similar loadings (about $1.5 \cdot 10^{-4}$ mol/g). However, since phase IX contains three π -acidic dinitrobenzoyl groups on every strand of selector, the "effective" loading of phase IX is roughly three times that of phase VIII. Fig. 14 depicts the relative capacity factors of analytes 1-10 on these two stationary phases. The best line through the data points for the PAH analytes has a slope of 3.03, which would seem to indicate that each of the π -acidic rings of the tripodal phase IX are acting independently in retention of the PAH analytes. The data points for the fullerene analytes fall only slightly above the line defined by the PAH analytes, suggesting that simultaneous multipoint interaction of phase IX with the fullerene analytes is not a predominant retention mode.

Tripodal phase X afford excellent retention and separation for all of the analytes, showing the greatest retention for the fullerenes and the best separation factor for the C_{60} - C_{70} mixture. The relative capacity factors for analytes 1-10 on the two tripodal phases IX and X are illustrated in Fig. 15. The reason why phase X provides the degree of increased retention for the fullerenes relative to the

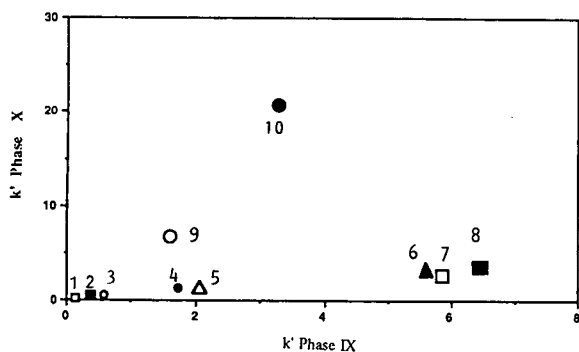


Fig. 15. Relative capacity factors for analytes 1–10 (as indicated) on phases IX and X.

tripodal ester phase IX is currently not well understood. A dinitrophenyl ether stationary phase analogous to phase VIII would be helpful in determining the contribution of the 2,4-dinitrophenyl group itself to this behavior. The π -acidic groups in phase X are positioned one atom closer to the branching point than those of phase IX, and this might conceivably impart some degree of conformational rigidity or a more favorable geometry for simultaneous multipoint interaction than in the case of phase IX.

Development of improved selectors

Although phase X provides superior retention and separation for the fullerene analytes, the current study suggests several possibilities for further improvements. The apparent ability of π -basic selector to afford significant retention for these compounds should be further investigated to determine whether it is π - π interaction or hydrogen bonding which retains the fullerenes on phases III and IV. The apparent importance of hydrogen bonding in fullerene retention and the complete absence of hydrogen bond donors in phase X (the best phase developed to date) suggests that phases such as the triamine-derived analogues of phases IX and X may prove even more useful for fullerene separation. In addition to having both π -acidic and hydrogen bonding groups, such phases may also adopt conformations in which intramolecular hydrogen bonding stabilizes the concave disposition of aromatic groups, thus providing a more preorganized selector for the fullerenes.

We recently described the use of the “immobi-

lized guest method” in the development of improved selectors for enantioselective recognition of the non-steroidal anti-inflammatory drug, naproxen [18]. In this approach the “guest” is immobilized on silica gel to afford a stationary phase which is used to evaluate candidate “hosts”. Such an approach offers the advantage of requiring only very small amounts of prospective selectors for analysis, in contrast to developing a new stationary phase for every selector to be evaluated. We initially reasoned that such an approach would be impossible for the fullerenes since they possess no functionality through which they can be conveniently immobilized. However, recent advances in the functionalization of buckminsterfullerene [19,20] suggest that this approach may, at some point, be feasible.

CONCLUSIONS

All of the stationary phases examined in the study provide some degree of retention and separation for the fullerenes, C_{60} and C_{70} . The π -acidic tripodal phase, X, designed for simultaneous multipoint interaction with the fullerenes, provides the highest degree of retention and the highest separation factor for C_{60} and C_{70} . This stationary phase may prove useful for preparative scale chromatographic purification of buckminsterfullerene as well as for chromatographic analysis and purification of the ever growing family of fullerenes and fullerene derivatives.

In one sense, this study raises a many questions as it answers. For example, it suggests that fullerene selectors affording greater retention and selectivity than does phase X may be developed. Selectors with dramatically increased retention and/or selectivity might allow for purification of multigram quantities of buckminsterfullerene, perhaps through batch adsorption techniques or other non-traditional purification methods. In broader terms, polypodal selectors may prove useful in a host of other molecular recognition and nanotechnological applications.

ACKNOWLEDGEMENTS

This work was funded in part by a Department of Education Advanced Opportunities in Chemistry Graduate Fellowship and by a grant from the National Science Foundation.

REFERENCES

- 1 W. Krättschmer, L. D. Lamb, K. Fostiropoulos and D. R. Huffman, *Nature (London)*, 347 (1990), 354.
- 2 R. Taylor, J. P. Hare, A. K. Abdul-Sada and H. W. Kroto, *J. Chem. Soc., Chem. Commun.*, (1990) 1423.
- 3 J. B. Howard, J. T. McKinnon and E. Johnson, *Nature (London)*, 352 (1991) 139.
- 4 H. W. Kroto, A. W. Allaf and S. P. Balm, *Chem. Rev.*, 91 (1991) 1213.
- 5 J. M. Hawkins, T. A. Lewis, S. D. Loren, A. Meyer, J. R. Heath, Y. Shibato and R. J. Saykally, *J. Org. Chem.*, 55 (1990) 1039.
- 6 D. M. Cox, S. Behak, M. Disko, S. M. Gorun, M. Greney, C. S. Hsu, E. B. Kollin, J. Millar, J. Robbins, W. Robbins, R. O. Sherwood and P. Tindall, *J. Am. Chem. Soc.*, 113 (1991) 2940.
- 7 W. H. Pirkle and C. J. Welch, *J. Org. Chem.*, 56 (1991) 6973.
- 8 R. D. Johnson, D. S. Meijer and D. S. Bethune, *J. Am. Chem. Soc.*, 112 (1990) 8983.
- 9 C. H. Lochmüller, in D. E. Leyden and W. Collins (Editors), *Silylated Surfaces*, Gordon and Breach, New York, 1980, p. 231.
- 10 L. Nondek, *J. Chromatogr.*, 373 (1986) 61.
- 11 D. J. Cram, *Angew. Chem., Int. Ed. Engl.*, 25 (1986) 1039.
- 12 G. Newkome, Z. Yao, G. Baker and V. Gupta, *J. Org. Chem.*, 50 (1985) 2003.
- 13 B. Weibull and M. Matell, *Acta Chem. Scand.*, 16 (1962) 1062.
- 14 W. H. Pirkle and C. J. Welch, *J. Liq. Chromatogr.*, 14 (1991) 1.
- 15 W. H. Pirkle and R. S. Readnour, *Chromatographia*, 31 (1991) 129.
- 16 W. H. Pirkle, C. J. Welch and M. H. Hyun, *J. Chromatogr.*, 607 (1992) 126.
- 17 J. L. Atwood, F. Hamada, K. D. Robinson, G. W. Orr and R. L. Vincent, *Nature (London)*, 349 (1991) 683.
- 18 W. H. Pirkle, C. J. Welch and B. Lamm, *J. Org. Chem.*, 57 (1992) 3854.
- 19 P. J. Krusic, E. Wasserman, P. N. Keizer, J. R. Morton and K. F. Preston, *Science (Washington, D.C.)*, 254 (1991) 1183.
- 20 T. Suzuki, Q. Li, K. C. Khemani, F. Wudl and O. Almarsson, *Science (Washington, D.C.)*, 254 (1991) 1186.

9-Fluoreneacetyl-tagged, solid-phase reagent for derivatization in direct plasma injection

F.-X. Zhou and I. S. Krull

Department of Chemistry and The Barnett Institute (341 MU), Northeastern University, 360 Huntington Avenue, Boston, MA 02115 (USA)

B. Feibush

Supelco, Inc., Supelco Park, Bellefonte, PA 16823-0048 (USA)

(First received January 22nd, 1992; revised manuscript received May 13th, 1992)

ABSTRACT

We describe here a resin-based derivatization reagent, containing a 9-fluoreneacetyl tag on a controlled-pore substrate, for direct injection analysis of amphetamine in plasma. On-line, pre-column derivatization was performed by direction injection of diluted plasma sample into an sodium dodecyl sulfate-containing mobile phase. Amphetamine was trapped in the hydrophobic derivatization column and derivatized at elevated temperature by the activated solid-phase reagent. The derivatized 9-fluoreneacetyl amphetamine was separated by reversed-phase high-performance liquid chromatography with a step gradient and determined by fluorescence detection. The synthesis scheme, characterization, and optimization of the derivatization conditions for the solid-phase reagent are described. The method was evaluated by reproducibility tests and single blind spiking analysis. This solid-phase reagent combined with a surfactant containing mobile phase provided a sensitive and simple procedure for on-line derivatization in direct injection analysis of biological fluids.

INTRODUCTION

Liquid chromatography is a principal method for analysis of drugs in biological fluids [1]. Plasma, serum, urine, etc., are complex mixtures that contain a multitude of components. When analyzing for drugs, some special problems arise due to the nature of the samples. The presence of large amounts of protein in serum or plasma, the strong affinity between these proteins and drugs, the low levels and poor UV absorbance for some drugs and/or the small amount of sample available, all put high demands on effective sample preparation and chromatographic separation. Sample pre-treatment is

the most laborious step and the main source affecting accuracy of the analytical procedures, especially for such biological samples. The extensive pre-treatment removal of the protein content is necessary for drug analysis in biological fluids, otherwise these proteins would denature and accumulate on the surface of conventional octadecylsilica reversed-phase packings, causing column clogging after only a few sample injections.

The sample treatment process includes extraction of the drugs or protein precipitation by an organic solvent, evaporation of the organic solvent, dissolution of the extracted drugs in mobile phase, etc. As analytes can co-precipitate with the proteins and only be partially extracted from the supernatant, inaccuracy and reduced detectability can be expected. Recently, high-performance liquid chromatography (HPLC) column packings with a hydrophilic

Correspondence to: Dr. I. S. Krull, Department of Chemistry and The Barnett Institute (341 MU), Northeastern University, 360 Huntington Avenue, Boston, MA, 02115, USA.

outer zone and a hydrophobic inner zone were developed for direct analysis of drugs in biological fluids [1–3]. Protein precipitation is avoided by restricting the access of the larger proteins to the hydrophilic zone only.

Another way to directly analyze drugs is by using surfactants in the mobile phase [4–6]. Under reversed-phase conditions, the surfactants solubilize the denatured proteins and modify the reversed-phase column creating an external hydrophilic surface. The surfactant also helps to displace the drug from the serum proteins and increases retention by the stationary phase. Various types of surfactants can be used as mobile phase modifiers, including anionic, cationic, or non-ionic compounds. For example, the surfactant sodium dodecyl sulfate (SDS) has been used successfully, below its critical micelle concentration (CMC), for direct drug analysis under reversed-phase conditions without protein precipitation [5]. However, poor detectability and low concentrations of many analytes still prevent these direct injection methods from becoming a good tool.

By derivatization with an appropriate chromophore, separation and more importantly detection of analytes at low concentration can be drastically improved with the most commonly used detection techniques (UV, fluorescence, electrochemical detection) in HPLC [7]. Compared to derivatization in solution, solid-phase derivatization reagents have the following advantages: (i) they give more selective derivatization with fewer side products; (ii) they are non-volatile and thus have greater stability in air and during storage; and (iii) excess reaction reagents are not present with the soluble products [8]. In solid-phase derivatization, the detection-sensitive tags are immobilized on solid supports. Analytes must diffuse into the pores of the solid-phase reagent in order to react with the bonded, reactive tags. By restricting the pore size of the rigid resin, the large protein molecules are excluded from the pores. This has two effects. First, proteins cannot precipitate on the hydrophobic internal surface. Consequently, they do not block the access of analyte to the active tag. Second, the nucleophilic residues on the proteins will not deplete the solid-phase reagent of its activity. The proteins contact only the external part of the solid-phase reagent particles. Protein will stay completely in the external solution

as long as the conditions causing protein denaturation and precipitation are avoided [9]. After solid-phase derivatization, low-molecular-mass analytes modified with the chromophore can be detected with high sensitivity. Detailed chemical procedures for synthesizing similar solid-phase reagents have been published [10–15].

This paper describes the preparation of a covalently bound, fluorescence (FL)-sensitive tag, 9-fluoreneacetyl (FA), on a pore size-controlled, rigid polystyrene-divinylbenzene resin (Figs. 1 and 2). Gradient elution, using SDS surfactant in the mobile phase, was applied for direct injection of plasma samples containing amphetamine. The FL-sensitive tag was covalently bonded to the resin through a nitrobenzophenol ester linkage. Derivatization conditions were tested in the on-line, pre-column mode using amphetamine. Controlled pore size of the polymeric reagent restricted the access of high-molecular-mass serum components into the pores, where the chromophore was immobilized. This restriction prevented blocking of the reagent inside the pores by protein precipitation. Low detection limits were achieved for diluted plasma without extraction. Reproducibility and accuracy of the analysis were shown by repeated injections and single blind spiked sample tests.

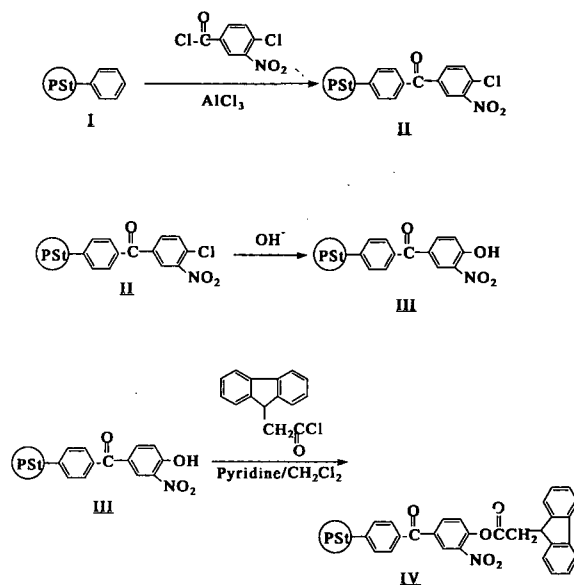


Fig. 1. Synthesis of 9-fluoreneacetyl-tagged solid-phase reagent.

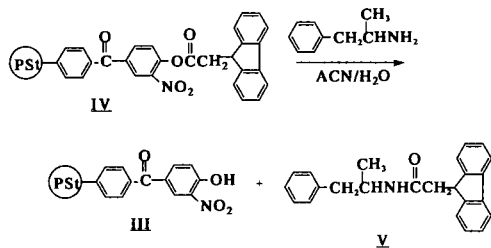


Fig. 2. Derivatization of amphetamine by FA-tagged solid-phase reagent.

EXPERIMENTAL

Reagents

9-Fluoreneacetic acid (99%), triethylamine (TEA, 98%), SDS and dichloromethane (99%) were obtained from Aldrich (Milwaukee, WI, USA). IMPAQ RG 1020 Si silica was obtained from the PQ Co. (Valley Forge, PA, USA). Omnisolv brand acetonitrile (ACN) was donated by EM Science (Gibbstown, NJ, USA). HPLC mobile phases were prepared based on volume ratio, and used after filtration through a 0.45- μm HVHP type solvent filter (Millipore, Bedford, MA, USA), and degassed under vacuum with stirring. Amphetamine sulfate was obtained from Research Biochemicals (Natick, MA, USA). Lyophilized human plasma was obtained from Sigma (St. Louis, MO, USA), reconstituted in deionized water and diluted 5-fold with 0.05 M NaOH before spiking. The pH of this plasma solution was 11.

Apparatus

The HPLC system consisted of a Waters 6000A solvent-delivery pump (Waters Chromatography Division, Millipore, Milford, MA, USA), two Rheodyne Model 7125 injection valves (Rainin, Woburn, MA, USA), a Waters 420 FL detector (excitation wavelength 254 nm, emission wavelength 313 nm), a LiChrospher C₁₈ reversed-phase column (5 μm , 250 \times 4 mm I.D., EM Science), a Supelcosil LC-ABZ column 150 \times 4.6 mm I.D. (Supelco, Bellefonte, PA, USA). Data were recorded on a Linear strip-chart recorder (Linear Instruments, Reno, NV, USA), a Hewlett-Packard 3380A integrator (Hewlett-Packard, Avondale, PA, USA) or a Dynamax data system (Rainin). The UV and FL spectra

were measured on an LDC Spectronic 1201 UV spectrophotometer (Milton Roy/LDC Division, Riviera Beach, FL, USA) and a Perkin-Elmer 650-105 fluorescence spectrophotometer (Perkin-Elmer, Norwalk, CT, USA), respectively.

Procedures

Synthesis

Preparation of controlled pore size polystyrene-divinylbenzene. The porous rigid resin was prepared by a templated polymerization technique of a 24:6:70 (v/v/v) mixture of divinylbenzene-ethylstyrene-styrene using trimethylsilyl-modified silica (IMPAQ RG 1020 Si, having 102 Å average pore size, 1.08 ml/g pore volume, 366 m²/g surface area and 16–20 μm irregular particle shape) [16].

Synthesis of nitrobenzophenol intermediate. The porous rigid resin was extracted with dioxane for 8 h in a Soxhlet apparatus to remove impurities and unreacted monomers. Modification of the cross-linked polystyrene followed literature procedures, to produce nitrobenzophenol intermediate **III** (Fig. 1) [17].

Synthesis of 9-fluoreneacetyl acid chloride. To 4.0 g of 9-fluoreneacetic acid (17.7 mmol), 3.9 ml of oxalyl chloride (44.6 mmol), 30 ml of benzene (dried with anhydrous sodium sulfate) and 3 drops of triethylamine were added. The mixture was heated at 55°C for 1 h. Excess oxalyl chloride was removed by rotary evaporation. The product was dissolved in 35 ml of dichloromethane, to yield a solution of 0.12 g/ml 9-fluoreneacetyl chloride, based on total conversion of 9-fluoreneacetic acid [18].

Preparation of nitrobenzophenol 9-fluoreneacetate **IV** (Fig. 1). A 1.3-g amount of intermediate **III**, 4.2 ml of 9-fluoreneacetyl chloride solution (2.0 mmol), and 0.3 ml of triethylamine (2.0 mmol) in 20 ml of dichloromethane was stirred at room temperature for 1 h. The solid reagent **IV** (Fig. 1) was filtered and washed with 2 \times 30 ml acetonitrile.

Synthesis and characterization of 9-fluoreneacetyl-tagged amphetamine standard derivative **V** (Fig. 2). A solution of 0.032 g amphetamine sulfate (0.17 mmol), 0.4 ml of TEA (1.7 mmol) and 0.18 g of 9-fluoreneacetyl chloride (0.8 mmol) in 20 ml of dichloromethane was stirred at room temperature for 2 h. The reaction mixture was evaporated to dryness under vacuum. The solid was dissolved in 40

ml of ethyl acetate and extracted with 3×50 ml of 0.5 M aqueous HCl, followed by 3×50 ml of 0.5 M aqueous NaOH. Preparative-scale reversed-phase HPLC with ACN–water (60:40, v/v) mobile phase, using a Waters Novapak 100×25 mm I.D. C₁₈ column, a Waters WISP 712 auto-injection system and a ISCO FOXY 2150-001 fraction collector (ISCO, Lincoln, NE, USA) was used for further purification. The melting point of derivative V was 163.0–163.5°C. Mass spectrometry with chemical ionization was used to identify the product. Major fragments (m/z) were 342.3 ($M + 1^+$), 250.2, 178.1, 165.1 and 91.0. Elemental analysis results were: C% = 84.61 (84.45), H% = 6.89 (6.74) and N% = 4.08 (4.10). Numbers in parentheses represent the calculated values for C₂₄H₂₃NO. UV maximum was determined at 260 nm with E (molar absorptivity) = $2.0 \cdot 10^4 \text{ cm}^{-1} \text{ M}^{-1}$. Maximum excitation and emission wavelengths were 308 and 320 nm, respectively, in the FL spectrum. For fluorescence detection in HPLC, 254 nm instead of 308 nm was used as the excitation wavelength to avoid interference from the scattering of incident light.

Characterization of the tagged resin

Hydrolysis. A sample of 20 mg of solid reagent IV was vigorously agitated in 4.0 ml of 0.5 M aqueous NaOH–ACN (2:1, v/v) solution and heated at 70°C for 20 min. The released 9-fluoreneacetic acid was diluted to 80 ml after filtration and quantified by HPLC–FL. The recovery percentage of standard 9-fluoreneacetic acid was $99.95 \pm 0.05\%$ (mean \pm standard deviation, $n = 3$) under hydrolysis conditions. A calibration plot of standard 9-fluoreneacetic acid was used for concentration determinations by HPLC, using 0.03% trifluoroacetic acid in ACN–water (50:50, v/v) mobile phase.

Elemental analysis of intermediates II and III (Fig. 1). Polymeric reagent intermediates II and III were dried to constant weight. Approximately 20 mg of each product were sent for elemental analysis (Galbraith Laboratories, Knoxville, TN, USA). The results were: intermediate II: C% = 85.71, H% = 7.03, N% = 1.29 and Cl% = 3.47; intermediate III: C% = 85.99, H% = 6.67, N% = 1.27 and Cl% = 0.19. Loading capacity, in mmol/g, was calculated based on: (1) decrease in chloride content from the intermediate II to III, and (2) nitrogen content in the intermediates II and III, respectively.

On-line, pre-column derivatization. A stainless-steel reaction column (35 \times 2 mm I.D.) capped with a porous 2- μm frit was packed with solid-phase reagent IV in an ACN slurry by applying vacuum to one end. The surface was flattened by removing excess reagent particles from the column after packing, then a 2- μm frit was placed at this end of the reaction column. The packed reaction column was installed on-line in the HPLC system, between the injection valve and the analytical column (Fig. 3). A defined amount of sample was injected at room temperature. After 10 s, the second valve was rotated to trap the sample within the derivatization column. Then the derivatization column was heated in a thermostated water bath (30–85°C) for a set time. The switching valve was rotated again to wash out the reaction product and the derivatization column was cooled to room temperature. Mobile phase was continuously passed through the derivatization column, at room temperature, during the chromatographic separation. Injection and derivatization of amphetamine spiked plasma were performed in 1 mM SDS in ACN–water (10:90) mobile phase. The 9-FA derivative was eluted from the derivatization column by step gradient elution, from 1 mM SDS in ACN–water (10:90) to 1 mM SDS in ACN–water (55:45), for the analytical separation. Low ACN concentrations in the initial mobile phase wash avoided the precipitation of proteins and the gradient elution procedure decreased the total analysis time. Complete elution of derivatives from derivatization column has been demonstrated by using authentic 9-fluoreneacetyl amphetamine under the same gradient conditions.

RESULTS AND DISCUSSION

The purpose of this work was to develop a fluorescent reagent, covalently attached to a resin, to derivatize nucleophilic analytes during direct injection of biological fluids. Solid-phase reagents show selective derivatization of small molecules, with high yields. Controlled pore size reagent-resin and the use of SDS-containing mobile phases allow selective modification of small analytes in the presence of large amounts of protein. Here, a polystyrene–divinylbenzene resin modified with an activated FA tag was synthesized and evaluated by on-line

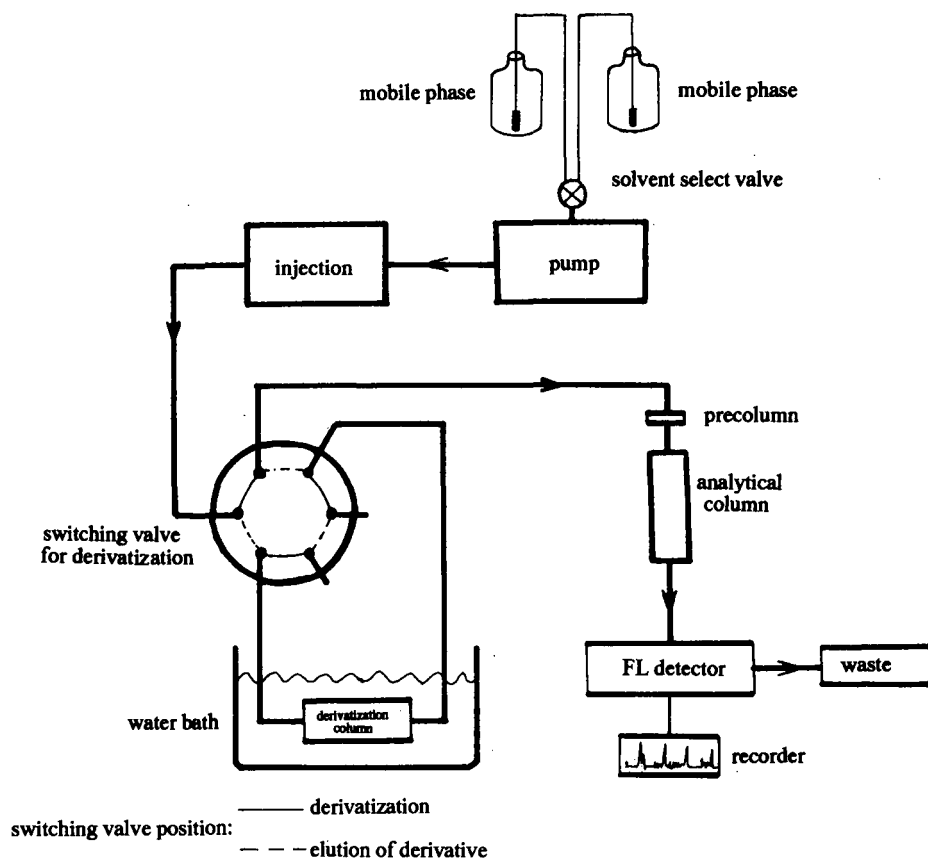


Fig. 3. Block diagram for on-line pre-column solid-phase derivatization.

derivatization of amphetamine (Figs. 1 and 2). The phenol content of the intermediate **III** was determined to be 0.92 mmol/g, based on elemental analysis results (see Experimental). Actual available loading of the FA tag on the solid-phase reagent was 0.83 ± 0.03 mmol/g (mean \pm standard deviation, $n = 3$), as determined by hydrolysis of the FA tag.

Temperature and time optimization for derivatization

To obtain an efficient derivatization of amine samples, the solvent, temperature and other conditions should be optimized. Acetonitrile was found to be a good solvent for amine derivatizations [11]. A short derivatization time, combined with low derivatization temperatures, should be used to obtain a reasonably short analysis time, less decomposition of the solid-phase reagent, and higher selec-

tivity. This combination also provides longer reagent life, lower detection limits, and fewer interferences during the chromatographic separation.

The effect of temperature was studied by using on-line, pre-column derivatization of amphetamine in ACN–water (65:35, v/v). Fig. 4 describes the conversion yield at different temperatures. At 60°C an optimum value was obtained, as shown by the turning point of the curve in Fig. 4. The time optimization curve at 60°C is shown in Fig. 5. There is no apparent increase in derivatization yield after 10 min. Based on these results, 60°C for 10 min was selected as the optimum combination for on-line derivatization of amphetamine in ACN–water (65:35, v/v) mobile phase. Under these conditions, a 70% derivatization yield was obtained for amphetamine on this resin-based reagent.

For direct injection of biological samples, espe-

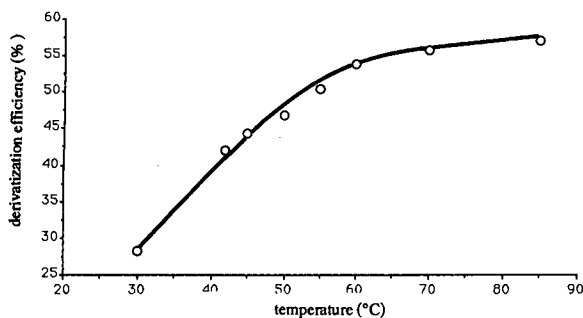


Fig. 4. Temperature optimization of on-line pre-column derivatization. Conditions: mobile phase: ACN–water (65:35, v/v); flow-rate: 1.5 ml/min; injection volume: 20 μ l; sample: 10 μ g/ml amphetamine in ACN–water (65:35, v/v) (pH 10); separation column: LiChrospher 250 \times 4 mm I.D. ODS; FL detection: excitation wavelength: 254 nm, emission wavelength: 313 nm; derivatization column: 35 \times 2 mm I.D.; derivatization time: 2 min.

cially plasma samples, onto a conventional C_{18} column, SDS containing mobile phase was used to avoid protein precipitation [5]. In this study, a 1 mM SDS in ACN–water (10:90, v/v) mobile phase was used for solid-phase derivatization of amphetamine spiked plasma. SDS in the mobile phase accelerated hydrolysis of the bonded reagent, particularly at elevated temperatures, resulting in more 9-fluoreneacetic acid in the front peak of the chromatogram. A lower derivatization yield (25%) was obtained in 1 mM SDS containing ACN–water (10:90, v/v) than in ACN–water (60:40, v/v) without SDS (70% yield), under the same derivatization conditions. To get a higher yield and reproducible derivatization in a practical derivatization time, 75°C was selected as the amphetamine derivatization temperature for the SDS containing mobile

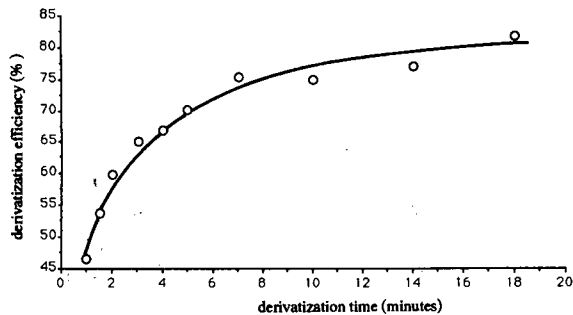


Fig. 5. Time optimization for on-line derivatization. Conditions as in Fig. 4, except derivatization at 60°C.

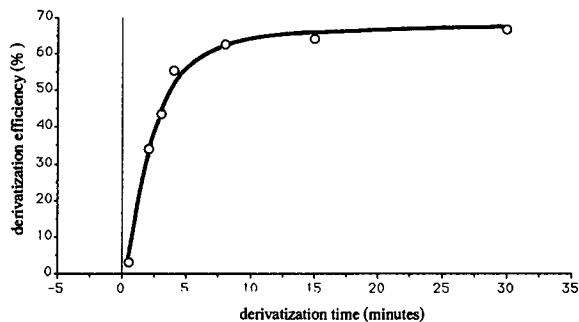


Fig. 6. Optimization of derivatization time under 1 mM SDS in ACN–water (10:90, v/v) mobile phase at 75°C. Sample: 20 μ l of 10 μ g/ml amphetamine-spiked plasma.

phase. At this temperature, the derivatization time dependency was determined for the on-line derivatization of 10 ppm amphetamine spiked plasma, as shown in Fig. 6. A reaction time of 8 min was selected as the optimum time for derivatization under these conditions.

Calibration plot for amphetamine derivatization

The calibration curve for on-line derivatization of amphetamine sample [prepared in ACN–water (65:35, v/v), pH 10] was obtained with ACN–water (65:35, v/v) mobile phase (without SDS). The relationship was linear for a 0.03–30 ppm concentration range, as shown by eqn. 1:

$$y = 22.5x \pm 0.4, r^2 = 0.997 \quad (1)$$

where x is the concentration of standard free amphetamine in μ g/ml and y is the peak area ($\times 10^{-6}$, arbitrary units from Hewlett-Packard integrator) of the amphetamine–FA derivative from the solid-phase derivatization. Standard deviations of the slope and intercept are 0.7 and 0.4, respectively. Non-linear relationship between peak area and amphetamine concentration was observed for concentrations higher than 100 μ g/ml.

The calibration curve for the on-line derivatization of amphetamine in plasma was determined from standard addition analysis of amphetamine-spiked plasma. The plasma sample was derivatized on-line in ACN–water (10:90, v/v) with 1 mM SDS at 75°C for 8 min. The relationship was linear for a 2–40 ppm concentration range, as shown by eqn. 2:

$$y = 3.58x \pm 0.5, r^2 = 0.999 \quad (2)$$

where x is the ppm concentration of amphetamine in plasma and y is peak area ($\times 10^{-6}$, arbitrary units from Dynamax data system) of amphetamine-FA derivative from solid-phase derivatization. Standard deviations of the slope and intercept are 0.06 and 0.5, respectively.

Regeneration of reagent

A given amount of the bonded FA reagent in the reaction column is used up for each sample. The tagged reagent is quickly depleted by a high concentration of amines or by derivatization at elevated temperatures, which accelerates hydrolysis. Since compound **III** is the resulting product, reactivity can be regenerated by tagging with more 9-fluorenylacetyl chloride. To demonstrate this possibility, 100 mg of the polymeric reagent was depleted off-line by derivatizing 5 samples of 1 ml 0.1% butylamine in ACN. The exhausted reagent was washed with 3×50 ml 0.5 M aqueous HCl-ACN (2:1, v/v), followed by 3×50 ml ACN-water (1:1, v/v) and

finally dried in vacuum. The depleted reagent was regenerated off-line as described for the preparation of compound **IV**. The recovered activity was demonstrated by the percent derivatization of amphetamine. The derivatization yield was $69.2 \pm 3.6\%$ ($x \pm$ S.D., $n = 3$) with the fresh reagent, $5.1 \pm 0.7\%$ with the exhausted reagent, and $66.2 \pm 4.6\%$ with the regenerated reagent, respectively. Derivatization yield tests were performed on-line with $20 \mu\text{l}$ of $10 \mu\text{g/ml}$ amphetamine in ACN-water (65:35, v/v) mobile phase, at 60°C for 10 min, and expressed as $x \pm$ S.D. ($n = 3$). Here a fresh reagent means that the solid-phase reagent was prepared and used the same day.

Shelf life determination

Freshly prepared reagents are always needed for solution derivatizations to ensure high yields, fewer side products and reproducible results. Solid-phase reagents, on the other hand, can be stored for prolonged time periods without affecting their activity.

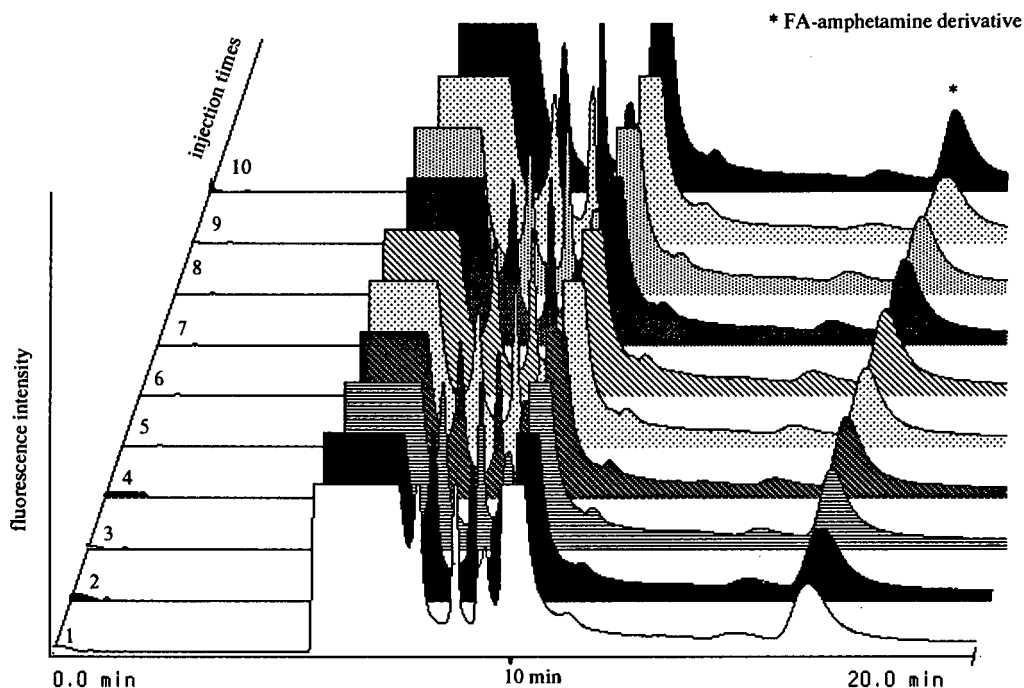


Fig. 7. Chromatograms for repeated on-line derivatizations of $10 \mu\text{g/ml}$ amphetamine-spiked plasma. Chromatographic conditions: mobile phase: step gradient from 1 mM SDS in ACN-water (10:90, v/v) to 1 mM SDS in ACN-water after derivatization; flow-rate: 1.5 ml/min ; injection volume: $20 \mu\text{l}$; separation column: Supelcosil LC-ABZ, $150 \text{ mm} \times 4.6 \text{ mm}$ I.D.; derivatization column: $35 \times 2 \text{ mm}$ I.D.; derivatization temperature: 75°C ; derivatization time: 8.0 min.

Activity of a freshly prepared resin tagged reagent was compared to its activity after 3 months storage in a capped glass bottle at room temperature without any special protection. Derivatization yield of a 10 $\mu\text{g}/\text{ml}$ standard amphetamine solution, was $69.2 \pm 3.6\%$ ($x \pm \text{S.D.}$, $n = 3$) for freshly prepared reagent and $67.5 \pm 2.9\%$ for the stored reagent. These results show good storage stability of the solid-phase reagent for at least 3 months under laboratory conditions.

Reproducibility of on-line solid phase reagent derivatization of amphetamine spiked plasma

Forty 20- μl aliquots of 10 $\mu\text{g}/\text{ml}$ amphetamine-spiked plasma were injected with an on-line, stop-

flow, pre-column derivatization. For these 40 injections, the relative standard deviation for the derivative peak heights was 5.87%. Fig. 7 shows chromatograms of some of these runs with on-line, pre-column derivatization.

Minimum detectable amount of amphetamine in ACN–water and in plasma

The minimum detectable amount of amphetamine solutions in ACN–water and in plasma, 0.4 ng (33 ng/ml, 20- μl injection) and 4.0 ng (200 ng/ml, 20 μl injection), respectively, was attained by normalizing the signal-to-noise ratio to 3:1 with on-line solid-phase derivatizations in ACN–water and SDS–ACN–water mobile phases, respectively. Figs.

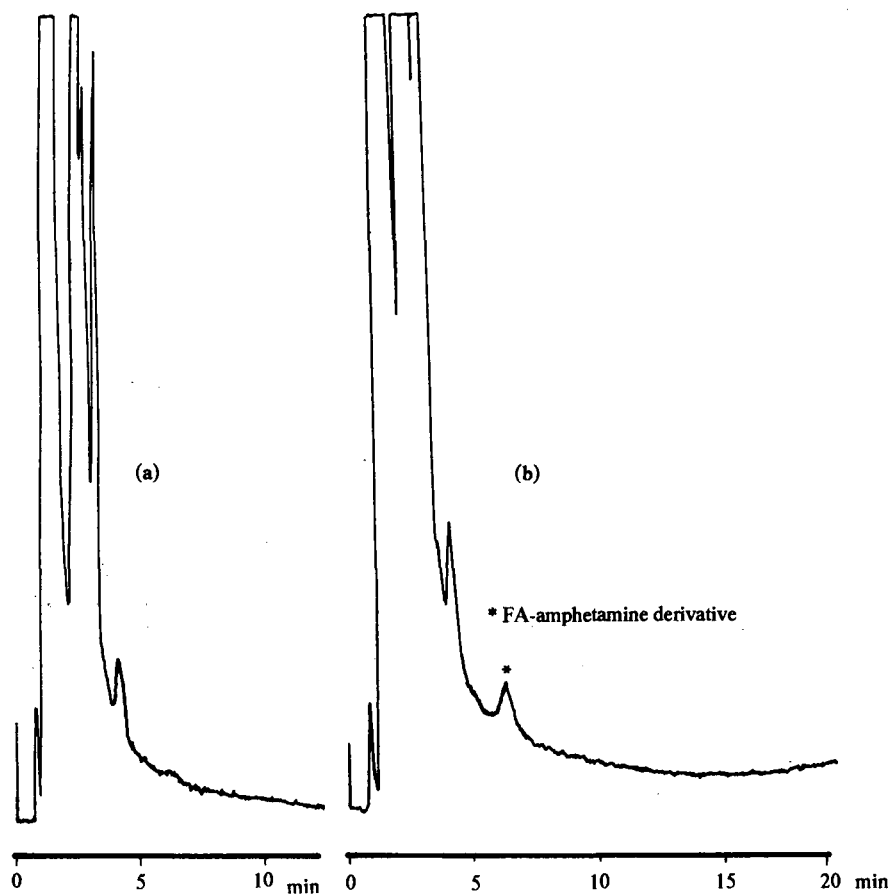


Fig. 8. Chromatogram for on-line derivatization of amphetamine in water. (a) Blank test with 20 μl ACN–water (65:35, v/v) (pH 10), (b) 20 μl of 33 ng/ml amphetamine in ACN–Water (65:35, v/v) (pH 10). Conditions as in Fig. 4, except derivatization at 60°C for 10 min.

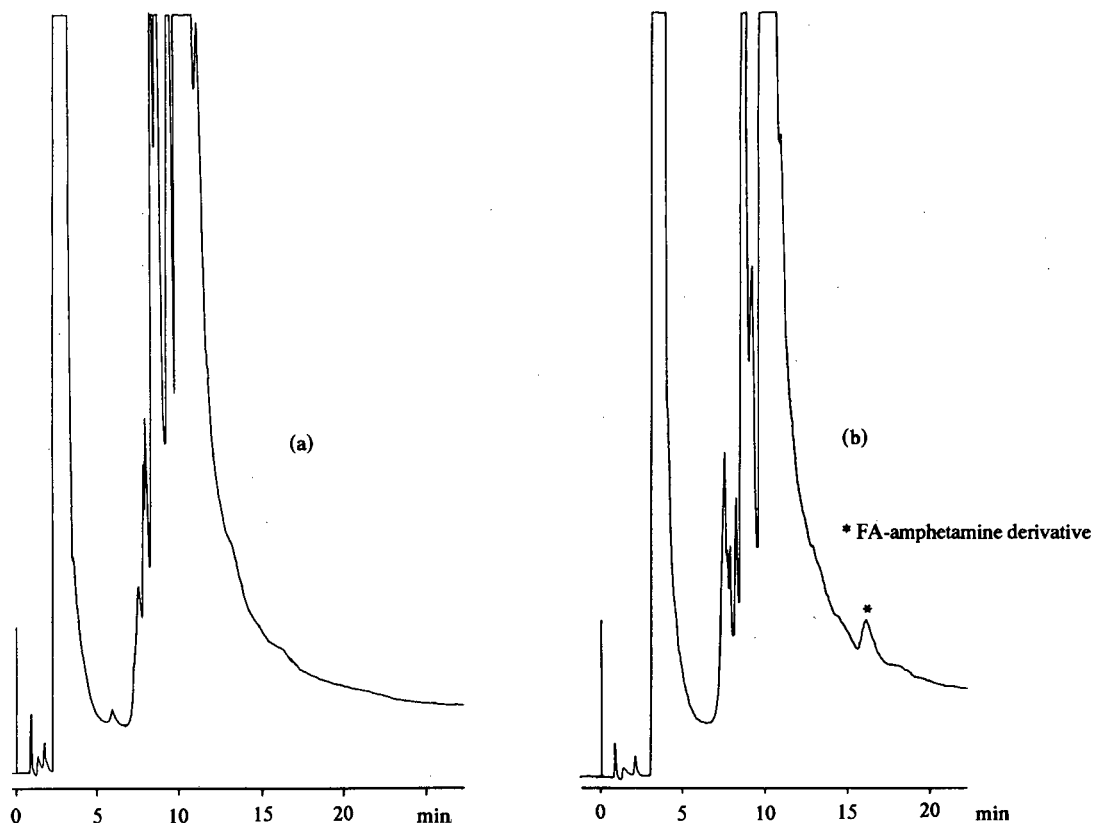


Fig. 9. Chromatogram for on-line derivatization of amphetamine in plasma. (a) Blank test with 20 μ l of diluted plasma, (b) 20 μ l of 0.2 μ g/ml amphetamine-spiked plasma. Conditions as in Fig. 7.

TABLE I
DETERMINATION OF AMPHETAMINE SPIKED INTO HUMAN PLASMA

Derivatization conditions: 75°C, 8.0 min at 1 mM SDS in ACN–water (10:90, v/v); mobile phase: step gradient from 1 mM SDS in ACN–water (10:90, v/v), to 1 mM SDS in ACN–water (55:45, v/v) after derivatization; flow-rate: 1.5 ml/min; column: Supelcosil LC-ABZ 150 mm \times 4 mm I.D., 5 μ m; FL detection: excitation wavelength 254 nm, emission wavelength 313 nm.

Sample	Spiked (μ g/ml)	Found (S.D.) (μ g/ml) ^a	R.S.D. (%) ^b	RE (%) ^c
No. 1	2.25	2.36 \pm 0.21	8.89	4.89
No. 2	5.87	6.29 \pm 0.37	5.88	7.16
No. 3	11.52	11.80 \pm 0.79	6.69	2.43

^a Mean \pm standard deviation ($n = 3$).

^b Relative standard deviation = $s/x \cdot 100$.

^c Relative error = (value found – true value)/true value $\cdot 100$.

8 and 9, respectively, are the chromatograms of these low-concentration amphetamine derivatizations.

Single blind spiked amphetamine detection

To validate the use of this on-line derivatization system, three spiked plasma samples were analyzed by the standard addition method. The spiked plasma (diluted before spiking, see Experimental) was injected into a solid-phase reactor and derivatized in 1 mM SDS in ACN–water (10:90, v/v) at 75°C. The results are shown in Table I. The detected amphetamine concentrations were in agreement with the spiked levels.

CONCLUSIONS

We have demonstrated the synthesis and evaluation of a resin-based derivatization reagent contain-

ing 9-fluoreneacetyl tag. This reagent was used for on-line derivatization of amphetamine by the direct injection analysis of plasma. Under optimized conditions, approximately 70% derivatized amphetamine was obtained. This approach is compatible with reversed-phase HPLC separations for direct drug analysis in plasma or in other biological fluids. The overall approach was simple, accurate and reproducible. This method is fully compatible with all commercially available HPLC equipment, and in combination with an automatic sample pre-treatment system, it should have a wide range of applications [19].

ACKNOWLEDGEMENTS

We gratefully acknowledge support by Supelco, Inc., (Bellefonte, PA, USA). The Dynamax system used in this work was donated by Rainin Instrument, Inc. We thank D. J. Magiera, M. E. Szulc and J. R. Mazzeo for helpful discussions and Dr. Kuo-Tsai Lai for the synthesis of the porous rigid resin used in this study.

This is contribution number 526 from the Barnett Institute of Chemical Analysis and Materials Science at Northeastern University.

REFERENCES

- 1 I. H. Hagestam and T. C. Pinkerton, *Anal. Chem.*, 57 (1985) 1757.
- 2 D. J. Gisch, B. Hunter and B. Feibush, *J. Chromatogr.*, 433 (1988) 264.
- 3 J. Haginaka and J. Wakai, *Anal. Chem.*, 62 (1990) 997.
- 4 F. J. Deluccia, M. Arunyanart and L. J. Cline Love, *Anal. Chem.*, 57 (1985) 1564.
- 5 R. A. Grohs, F. V. Warren, Jr. and B. A. Bidlingmeyer, *Anal. Chem.*, 63 (1991) 384.
- 6 F. Palmisano, A. Guerrieri, P. Zambonin and T. R. I. Cataldi, *Anal. Chem.*, 61 (1989) 946.
- 7 H. Lingeman and W. J. M. Underberg, in H. Lingeman and W. J. M. Underberg (Editors), *Detection-Oriented Derivatization Techniques in Liquid Chromatography*, Marcel Dekker, New York, 1990, Ch. 1.
- 8 S. T. Colgan and I. S. Krull, in I. S. Krull (Editor), *Reaction Detection in Liquid Chromatography*, Marcel Dekker, New York, 1986, Ch. 5.
- 9 H. Yoshida, I. Morita, T. Masujima, and H. Imai, *Chem. Pharm. Bull.*, 30 (1982) 3327.
- 10 I. S. Krull, S. T. Colgan and C. M. Selavka, in P. R. Brown and R. A. Hartwick (Editors), *High Performance Liquid Chromatography*, Wiley-Interscience, New York, 1989, Ch. 10.
- 11 C.-X. Gao, T.-Y. Chou and I. S. Krull, *Anal. Chem.*, 61 (1989) 1538.
- 12 C.-X. Gao and I. S. Krull, *J. Pharm. Biomed. Anal.*, 7 (1989) 1183.
- 13 K. Jedrezejczak and V. S. Gajnd, *Analyst (London)*, 115 (1990) 1359.
- 14 J. M. Rosenfeld, G. M. Brown, C. H. Walker and C. Sprung, *J. Chromatogr.*, 325 (1985) 309.
- 15 A. J. Bourque and I. S. Krull, *J. Chromatogr.*, 537 (1991) 123.
- 16 B. Feibush and N.-H. Li, *US Pat.*, 4 933 372 (1990).
- 17 B. J. Cohen, H. Karoly-Hafeli and A. J. Patchornik, *J. Org. Chem.*, 49 (1984) 924.
- 18 H.-M. Zhang, *M.S. Thesis*, Northeastern University, Boston, MA, 1990.
- 19 A. J. Bourque, I. S. Krull and B. Feibush, *Biomed. Chromatogr.*, (1992) in press.

Liquid chromatography–electrochemistry procedure for the determination of chlorophenolic compounds in pulp mill effluents and receiving waters

E. C. V. Butler and G. Dal Pont

CSIRO Division of Oceanography, Marine Laboratories, GPO Box 1538, Hobart, Tasmania 7001 (Australia)

(Received April 13th, 1992)

ABSTRACT

An isocratic, reversed-phase liquid chromatography procedure is described for the separation and determination of chlorophenolic compounds, including several priority pollutant chlorophenols. The separation was experimentally optimised, and selective and sensitive detection was obtained by dual electrode amperometry. The most suitable combination was a silica-based column with phenyl functional groups, and a mobile phase of acetonitrile–acetate buffer (40:60, pH 5). Dual glassy-carbon electrodes were used in a parallel configuration in a thin-layer flow cell, with differential current measurement (+0.90 V relative to +0.60 V).

A solid-phase extraction scheme using a polymeric sorbent (Chromosorb 102) was devised for the extraction and preconcentration of selected chlorophenols, chloroguaiacols, and a chlorosyringol from aqueous samples. Use of tribromophenol as an internal standard was also investigated. The total procedure—preconcentration and chromatography—was applied to the analysis of effluents discharged by a paper mill, and a pulp mill.

INTRODUCTION

The industrial discharge of chlorinated organic compounds into natural waters, and the environment in general, has caused concern now for several decades [1,2]. It should be noted that not all of these organochlorines are necessarily harmful [3]; indeed such compounds are also produced by natural processes [4]. Therefore, it is essential to develop sensitive analytical methods capable of detecting individual organochlorines in order to characterise toxicity or other harmful effects.

The pulp and paper industry, through the chlorine bleaching of pulp, are major producers of organochlorines. Some of the compounds derived from the chlorination of the organic components of wood are both toxic and persistent [5–7]. One such

group of compounds are the chlorophenolics, which are derived from the action of chlorine, and its hydrolysed derivatives, on the phenolic units that arise from the breakdown of lignin in the pulping process. World-wide, there is a growing requirement to monitor organochlorines, including chlorophenolics, in receiving waters as well as effluents [8,9]. The US Environmental Protection Agency (USEPA) lists eleven phenols as priority pollutants—among these are the chlorinated compounds 2-chlorophenol, 2,4-dichlorophenol, 4-chloro-3-methylphenol, 2,4,6-trichlorophenol and pentachlorophenol [10]. In Australia, recent commonwealth guide-lines for bleached kraft pulp mills [11,12] state that total levels of chlorophenolics must be measured in effluent, water, sediments and biota, with the additional qualification that individual chlorinated phenols found to be important may be included in revised monitoring schedules.

Analysis of aqueous samples for phenolics has traditionally involved methods that provide a mea-

Correspondence to: Dr. E. C. V. Butler, CSIRO Division of Oceanography, Marine Laboratories, GPO Box 1538, Hobart, Tasmania 7001, Australia.

sure of the total phenol concentration (phenol index). Spectrophotometric procedures with 4-aminoantipyrine [13] are examples of such procedures. More recently analytical methods have been evolved that can determine individual phenolic compounds. The gas chromatography procedure of Voss *et al.* [14], with its preliminary formation and extraction of the acetate derivatives, is a commonly used procedure for the determination of chlorinated phenolic compounds in pulp mill effluents. High-performance liquid chromatography (HPLC) is an alternative and complementary procedure for the measurement of chlorophenolics. Early work with this technique used spectrophotometric [15,16] and fluorimetric detectors [17,18], in most instances derivatisation steps were necessary. The combination of HPLC with electrochemical detection (ED) has proved to be well-suited for determining phenolic compounds, because the sensitivity and selectivity of the detector permit the use of a simple isocratic mobile phase [19–22] with minimal pretreatment and without the requirement of derivative formation.

In this paper we present the results of an optimisation of an LC–ED procedure to determine chlorophenolics (especially those with multiple chlorine substitution) in both pulp and paper mill effluents and natural receiving waters. Also considered are means of pretreatment and preconcentration of chlorophenolics from natural waters. Chromatograms are presented for total effluents from representative pulp and paper mills as an application of the recommended procedure.

EXPERIMENTAL

Instrumentation

The components of the LC–ED system were a Waters M45C pump, 0.2 μm in-line filter, a Rheodyne 7125 injector (with 200- μl loop and position-sensing switch), and an EG&G Princeton Applied Research Model 400 electrochemical detector. To reduce pulsation at the detector, a Waters high-pressure noise filter was installed between the pump and injector. The analytical column was a Waters Nova-Pak Phenyl cartridge (8NVP4, 100 mm \times 8 mm) mounted in a Waters RCM-100 Compression Module. A Brownlee PRP-1 guard cartridge (PRP-GU, 30 mm \times 4.6 mm), in a Brownlee 30 mm

MPLC cartridge holder, protected the main reversed-phase column. All tubing in the LC–ED system was conventional 316 grade stainless steel. Chromatograms were displayed on a Yew Type 3056 dual-pen recorder; the detector output was also fed, via an analog-to-digital interface, to an IBM-style personal computer for processing with integration and data analysis software (DAPA Scientific).

The thin-layer flow cell used in the electrochemical detector was that supplied by the manufacturer, as were the reference (Ag/AgCl) and auxiliary electrodes. However, we used a BAS MF-1000 dual glassy carbon electrode (3-mm diameter disks) as the working electrode. The channel in the flow-cell gasket was enlarged to a width of 7.5 mm to accommodate the electrodes mounted in the parallel configuration.

We used a syringe apparatus similar to that described by Renberg and Lindström[23] for preconcentration of phenolic compounds from aqueous samples. Solid-phase sorbents, not supplied in cartridges, were dry-packed into empty polyethylene cartridges (Dionex OnGuard) that contained filter inserts.

Reagents

All reagents salts were of analytical grade or better. We used 2,4,6-tribromophenol as supplied (99% pure; Aldrich). Standards for the chlorinated phenolics (Chem Service or Helix Biotech.) were dissolved in acetonitrile, with working standard solutions typically at a concentration of 10 $\mu\text{g}/\text{ml}$. Aqueous standards for preconcentration studies were prepared by diluting saturated aqueous (stock) solutions of the individual phenolic compounds with high purity water. The concentration of each aqueous stock solution (10–40 $\mu\text{g}/\text{ml}$) was determined by comparison with the detector response for standards dissolved in eluent. Whereupon working solutions of the aqueous standards (typically 2 $\mu\text{g}/\text{ml}$) were prepared by dilution of the stock solutions, and were refrigerated in borosilicate-glass, screw-cap vials with PTFE cap-liners. Acetonitrile in the eluents was of liquid chromatography grade. High-purity water was prepared by distillation, and then by passing the distillate through a three-cartridge Milli-Q water purification system (Millipore). All eluents were filtered under vacuum

through an 0.45- μm Millipore HV Durapore membrane in an all-glass apparatus, and just prior to use a litre of eluent was degassed by ultra-sonicating under vacuum.

The recommended eluent was prepared in the following manner. 10 ml of a stock acetic acid–sodium acetate buffer solution (2.0 M sodium acetate adjusted to pH 4.15 with glacial acetic acid) was passed through a cartridge packed with XAD-4 resin (75–125 μm). The first 3 ml were discarded; the next 6 ml were added to pure water, and the volume made up to 600 ml. To this solution, acetonitrile was added to bring the final volume to 1 l (pH is 5.0).

Procedures

Eluents were pumped through the LC–ED system at 1.5 ml/min. Apart from dilute standard solutions prepared in the eluent that were injected directly onto the column, samples were pre-treated as described below before chromatographic analysis. In general, we attempted to ensure that the bulk composition of the injected analyte solutions was as similar as possible to the eluent. Chromatography was performed at $20 \pm 2^\circ\text{C}$.

Preliminary surface treatment of the electrodes required only polishing with alumina paste (0.05 μm), and then washing with pure water. The electrochemical detector was operated in the dual potentiostat mode, with the lower potential (E_1) at +0.60 V vs. Ag/AgCl, and the upper (E_2) at +0.90 V vs. Ag/AgCl. Current sensitivity was set between 2 and 20 nA, and the filter time constant was 2 s.

Pretreatment of samples involved acidification to pH 2.8 with sulphuric acid. With pulp and paper mill effluents it was advantageous to centrifuge the sample (1500 g for 15 min) to deposit the flocculate of fine particles resulting from the initial acid treatment. The samples were cleaned up and preconcentrated by extraction onto solid-phase sorbents. Sorbents were activated by passing acetonitrile (5 ml) through the cartridge, and then washing with pure water (10 ml). The sample volume of 5 to 500 ml was injected through the sorbent cartridge by gas-tight glass syringe; flow-rates were between 1 and 2 ml/min. For volumes greater than 10 ml, we used an apparatus similar to Renberg and Lindström [23] for refilling the syringe, and collected the effluent in a measuring cylinder to monitor throughput. After

loading the sample, the sorbent was rinsed with 5 ml of pure water, and dried by passing through 250 ml of air. The chlorophenolics were then eluted with 2.0 ml of acetonitrile. Before chromatography, the eluate from the sorbent was made up to 5.0 ml with 0.02 M acetate buffer (pH 4.15).

Effluent samples were collected by immersing a sample bottle in the mill's effluent discharge channel, and filling to the bottle's lip to avoid any air space above the liquid. The sample (and storage) bottle were either glass or high-density polyethylene with screw caps. These containers were typically pre-cleaned with methanol, and rinsed with pure water. To preserve effluent samples they were simply refrigerated at 4°C , or refrigerated after addition of anhydrous copper sulphate (3.25 g per 4 l). The copper salt serves as a bio-toxin to prevent biological transformation of effluent constituents [21], and it could also remove interference from sulphide in the LC–ED procedure.

RESULTS AND DISCUSSION

Initial experiments

Chromatography of the chlorophenol compounds and their derivatives may be effected by using their general phenolic character, and the subtle differences in chemical properties that result from changes in substituents. Another characteristic that is relevant to the chromatography of these compounds is the increase in acidity that is linked with increasing degree of chlorination (*cf.* phenol, $pK_a = 10.1$; pentachlorophenol, $pK_a = 4.9$) [24]. The former aspects of chlorophenolics favour the use of reversed-phase chromatography, whereas the varying acidity of these compounds suggest that ion-exclusion chromatography might be possible (by analogy with the separation of other weak organic acids).

We confirmed the work of Jupille *et al.* [19] [using a Brownlee Polypore-H column (250 mm \times 4.6 mm), and phosphoric acid–acetonitrile eluents] that ion exclusion chromatography with amperometric detection could separate chlorinated phenolic compounds dissolved in the eluent. The order of elution was not in the order expected if the separation of the chlorophenolics was by an ion exclusion mechanism, but rather it was akin to a low-efficiency reversed-phase process. To test the procedure with a real sample matrix, pulp mill effluent samples were

spiked with chlorophenolics, pretreated as above, and then injected directly onto the column. The result in each case was a total loss of chromatographic resolution; the chlorophenolics could not be detected. We suspected that the many other weak organic acids (such as resin acids and fatty acids) present in the effluents interfered strongly in the chromatography step. Therefore, a more practicable option was to improve the reversed-phase chromatographic method for chlorophenolics determination, and tailor it for analysis of pulp mill effluents and receiving waters.

In applying published LC–ED methods based on reversed-phase chromatography [20–22], the approach appeared quite feasible, but we identified a number of drawbacks for our intended application. These were: (i) a large background current at the detector, (ii) excessive baseline noise, (iii) lengthy retention of pentachlorophenol, and (iv) inadequate resolution of early eluting chlorophenolics when effluent samples were analysed. It was anticipated that the first problem may contribute to the second.

Optimisation

We adopted an experimental approach to improve the performance of the reversed-phase LC–ED procedure for chlorophenolics determination. The presence of contaminants in reagents used for preparing the mobile phase was checked, sequentially, by solid-phase extraction of 100-ml volumes onto XAD-4 resin. The procedure was essentially that described above for the purification of eluents, with adsorbed contaminants being stripped from the resin with 1.5 ml of acetonitrile. Phenol, itself, proved to be a ubiquitous trace impurity in all reagents. Clean-up of the mobile phase reagents by solid-phase extraction proved to be effective in both decreasing the magnitude of the background current at the detector, and suppressing baseline noise.

The composition of the eluent reported in published papers on LC–ED of chlorophenolics [20–22] seemed unnecessarily complex and of high ionic strength. Modern electrochemical detectors perform well with minimal supporting electrolyte. Therefore, we dispensed with the often used sodium perchlorate. A mixed pH buffer of acetic acid and citrate, was replaced with a simple sodium acetate–acetic acid buffer solution. The citrate may have been added previously to combat the formation of

iron(III)–phenolate complexes. In analyses of natural waters and pulping effluents, iron(III) concentrations are unlikely to reach levels that would cause interference.

A Nova-Pak C₁₈ column was used in initial experiments, but this was later replaced with the same type of column, but with phenyl functional groups. The phenyl packing proved to separate the early eluting chlorophenolics with at least equal efficiency to the C₁₈ packing, but for the same eluent, retention times of the polychlorinated compounds were much shorter. The factor that has a strong impact on retention of the later eluting, polychlorinated phenols — 2,4,6-trichlorophenol and pentachlorophenol — is the pH of the eluent (Fig. 1). The low pK_a values of these chlorophenols (6.5 and 4.9, respectively [24]) mean that, with the increased ionisation of their hydroxyl groups under more alkaline conditions, retention time declines sharply for pentachlorophenol and begins to fall for 2,4,6-trichlorophenol for pH > 6. Shoup and Mayer [20] made a similar observation, but here we have used these properties to enhance the performance of the analytical column so that separation of the full range of chlorophenolics is effected in under 25 min (Fig. 2).

To augment chromatographic resolution when complex samples are analysed, LC–ED procedures benefit from the selectivity of the electrochemical

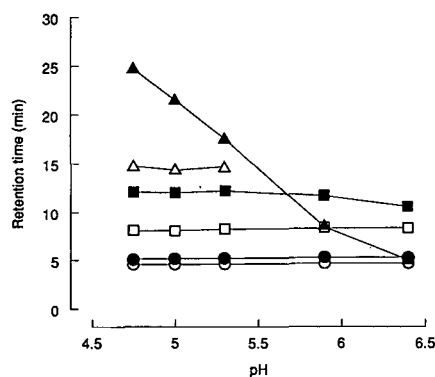


Fig. 1. Relationship of retention time of phenolic compounds with pH, under the chromatographic conditions described in the text. ○ = *m*-Cresol; ● = 2-chlorophenol; □ = 2,4-dichlorophenol; ■ = 2,4,6-trichlorophenol; △ = 3,4,5-trichloroguaiacol; ▲ = pentachlorophenol. Conditions: acetonitrile–sodium acetate buffer (40:60), flow-rate 1.5 ml/min.

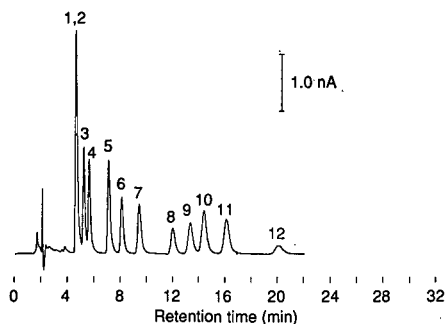


Fig. 2. Separation of standard suite of chlorophenolic compounds and *m*-cresol under the recommended chromatographic conditions described in the text. Peaks: 1 = *m*-cresol; 2 = 6-chlorovanillin; 3 = 2-chlorophenol; 4 = 4-chlorophenol; 5 = 4-chloro-3-methylphenol; 6 = 2,4-dichlorophenol; 7 = 4,6-dichloroguaiacol; 8 = 2,4,6-trichlorophenol; 9 = 4,5,6-trichloroguaiacol; 10 = 3,4,5-trichloroguaiacol; 11 = trichlorosyringol; 12 = pentachlorophenol.

detector. When a two-electrode flow cell is used the opportunities for specific detection are even greater [25]: with the electrode in a *series* configuration, analytes can be oxidised or reduced at the upstream electrode before detection at the second working electrode; in *parallel* configuration, the difference current can be monitored between the two working electrodes, set at different potentials (E_1 , E_2). We chose the latter approach to discriminate against some of the more easily oxidised compounds (*i.e.* oxidised at potentials $< E_1$) in pulp mill effluents and natural waters that might co-elute with chlorophenolic compounds.

Hydrodynamic voltammograms are depicted in Fig. 3 for the oxidation of some of the chlorophenolic compounds at a glassy carbon electrode (*vs.* Ag/AgCl). There is anodic response from most chlorophenolics for potentials greater than 600 mV, with limiting currents at about 900 mV. These results are consistent with hydrodynamic voltammograms presented by Galceran and Santos [26]; their investigations were performed at neutral pH, which causes a general shift to slightly lower potentials. Therefore, using the eluent and pH recommended above, we should be able to accentuate the anodic detection of chlorophenolic compounds by monitoring the difference in output current (Δi) for dual parallel electrodes with $E_1 = 600$ mV and $E_2 = 900$ mV. The effectiveness of this approach is addressed in the applications discussed below.

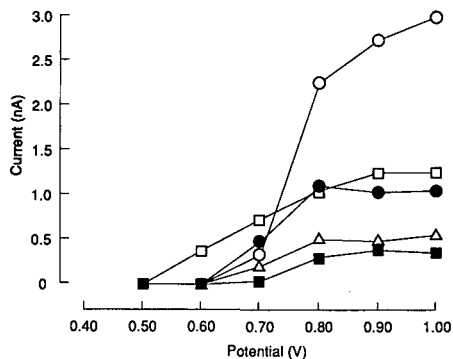


Fig. 3. Hydrodynamic voltammograms for the oxidation of chlorophenolic compounds 2,4-dichlorophenol (○), 2,4,6-trichlorophenol (●), 4,5,6-trichloroguaiacol (□) and pentachlorophenol (■), and tribromophenol (△) in eluent at a glassy carbon electrode (*vs.* Ag/AgCl).

Performance characteristics

A standard suite of 11 chlorophenolics and one alkylphenol were used for testing the optimised LC-ED procedure. This included the five chlorophenols in the USEPA designation of priority pollutant phenols, and five chlorophenolic compounds known to occur in pulp mill effluents [5,6]—6-chlorovanillin, 4,6-dichloroguaiacol, 3,4,5-trichloroguaiacol, 4,5,6-trichloroguaiacol and trichlorosyringol. 4-Chlorophenol and *m*-cresol were also added to the mixed standard solutions; the former to test the chromatographic separation of positional isomers, and the latter provided an example of a non-chlorinated simple phenol. Fig. 2 shows the separation of the standard compounds when injected in a solution identical to the eluent.

Precision was assessed by repeatedly injecting samples of the mixed standard solution, with each component at a concentration of 40 $\mu\text{g/l}$. For 50- μl injections, the relative standard deviation ($n = 10$) for the 12 standard phenolic compounds was 1–3%. Limits of detection ($3 \times$ baseline noise) for the same compounds using 50- μl injections ranged from 0.4 $\mu\text{g/l}$ (or 4 nM, for *m*-cresol) to 6 $\mu\text{g/l}$ (or 23 nM, for pentachlorophenol). In general, the limit of detection decreased for the chlorophenolics with longer retention times. Much lower limits of detection are possible with preconcentration, as discussed below.

The response index, r , defined in the power function:

$$y = Ac^r$$

(where y is detector output, c is solute concentration and A is a constant) is a measure of detector linearity [27]. For a truly linear detector $r = 1$, but the practical bounds for response linearity given by Scott [27] are 0.98–1.02. Linear regression analysis of peak area data in the concentration range 10–100 $\mu\text{g/l}$ for all phenolic compounds in the mixed standard, generally produced results $0.98 < r < 1.02$. For low signal-to-noise ratios (*i.e.* at concentrations $< 10 \mu\text{g/l}$), artefacts arising from the peak integration can produce slight curvature; very occasionally this may extend to higher concentrations.

Calibration

Peaks in the chromatogram were identified from their co-elution with standard chlorophenolics added to the sample matrix. Further corroboration may be obtained from peak current ratios for individual peaks at different detector potentials, that are compared with ratios for likely standard compounds. This approach has been recommended by Shoup and Mayer [20]; it is a useful adjunct to the co-elution technique, but was not used in this study. Definitive characterisation of chlorophenolics may require collection of eluate fractions for subsequent gas chromatography–mass spectrometry, or possibly the use of a parallel LC–mass spectrometry procedure.

To quantify the concentrations of chlorophenolics in samples, the method of standard additions is appropriate, but laborious. An alternative procedure is to use an internal standard. If an analytical method involves a preconcentration step, an internal standard not only permits estimation of the analytes, but it also can obviate the need to continually monitor extraction recoveries. 2,4,6-Tribromophenol (TBP) has already been used as an internal standard in gas chromatography procedures, and it is suitable for our LC–ED system because it elutes in a vacant region of the chromatogram (retention time, $t_r \approx 17.8$ min with pH 5.0 eluent). Investigation of TBP as an internal standard is discussed in the following section on preconcentration.

Preconcentration

For analysis of natural samples, it is often necessary to both separate and preconcentrate the analytes. Chlorophenolics can be extracted from the sample matrix using either organic solvents or solid-phase sorbents. Extraction of acidified aqueous samples with one of the solvents, methylene chloride, diethyl ether or hexane, and then back-extraction into dilute alkali was unsuitable in each case because of incomplete recovery of the chlorophenolics. There was also the disadvantage that the solution for injection onto the chromatography column was quite unlike the eluent. We attempted to overcome this problem by re-acidifying the back extract, and passing it through a reversed-phase sorbent. However, this too was unsuccessful because traces of the original organic solvent remaining in the back-extract led to incomplete sorption of the chlorophenolics. Another problem with liquid–liquid extraction of complex natural samples, such as effluents, is the formation of emulsions among other factors that can cause incomplete phase separation. Therefore, no further investigations were made of liquid–liquid extraction as a means of preconcentration.

A range of solid-phase sorbents were tested as listed in Table I. Those marked with an asterisk in the table proved to be the most suitable in initial experiments. Recoveries of chlorophenolics (added to pure water) for these three sorbents—Sep-Pak C₁₈, Amberlite XAD-4 and Chromosorb 102—ranged between 70–90%, depending upon the individual compound, and the total concentration of adsorbed compounds. Other solid phases returned lower recoveries of the analytes.

After more detailed investigations, the Sep-Pak C₁₈ phase was set aside because it bled contaminants that eluted late in the LC–ED chromatogram (see Fig. 4). The loading of weakly acidic samples (pH ≈ 3) seemed to generate these artefacts, particularly from fresh or little used Sep-Pak sorbents. At this pH there was also the added problem of the hydrolysis of the silica support. Of the polymeric phases, Chromosorb 102 was the more suitable. It did not have to be ground and sieved to produce the appropriate particle size; it was less prone to swelling and shrinking with changes in solution pH and ionic strength; and it contained fewer contaminants than Amberlite XAD-4. Otherwise, both polymeric

TABLE I

SOLID-PHASE SORBENTS TESTED FOR PRECONCENTRATION OF CHLOROPHENOLIC COMPOUNDS

For meaning of asterisks, see text.

Solid-phase sorbents	Particle size (μm)
*Sep-Pak C ₁₈ (Waters Associates)	55–105
Sep-Pak Accell QMA (Waters Associates)	37–55
*Amberlite XAD-4 (Rohm and Haas)	75–125
BN-X4 (Benson)	50
Chromosorb 101 (Johns-Manville)	45–75
*Chromosorb 102 (Johns-Manville)	45–75
Bond-Elut -PH, -C ₈ , -C ₁₈ , -CN, -CBA and -NH ₂ (Analytichem)	40

sorbents behaved similarly; they were more efficient extractants than Sep-Pak C₁₈ for phenol and early eluting phenolics, but at the same time tended to adsorb a wider spectrum of organic compounds (as also noted recently by Hennion [28]). We found that salt (NaCl) addition was unnecessary for the efficient adsorption of the chlorophenolics used in this study.

A thorough evaluation of recoveries for a selection of chlorophenolic compounds was made using the recommended preconcentration procedure with Chromosorb 102 as sorbent. The compounds chosen for the study generally covered the range of polarities for multiple chlorine substitution. Detector response, *after* preconcentration, for an individual analyte dissolved in pure water was compared with the response for the same level of analyte spiked in a

paper mill effluent. All results were related to the detector response for direct injection of standard solutions of the chlorophenolics made up in the aqueous acetonitrile eluent. The investigation was run over a range of concentrations to permit regression analysis. In parallel experiments, the spike was added to (i) the effluent sample before loading onto the Chromosorb 102 cartridge, and (ii) the acetonitrile eluate resulting from extraction of the effluent sample. Hence, it should be possible to discern the efficiency of adsorption/desorption of chlorophenolics on Chromosorb 102 in contrast to the interference from co-extracted organic compounds at the detector's working electrode. To assess TBP as an internal standard, it was added initially to all sample and standard solutions.

Calculated recoveries for selected chlorophenolics and TBP preconcentrated on Chromosorb 102 are presented in Table II. When the standard spike was added to the effluent extract after the preconcentration step, there appeared to be some diminution of peak currents for all compounds, apart from pentachlorophenol. Since the decrease in detector response varied for each chlorophenolic, interference in the LC-ED chromatography from other extracted compounds is more likely than depressed working electrode performance. For additions of the chlorophenolics to the paper mill effluent prior to the preconcentration, recoveries ranged from 84 to 100%. Recoveries increased with increasing degree of chlorine substitution and more non-polar character. This trend is more obvious when recoveries are calculated on the basis of peak areas obtained from preconcentration of aqueous standards on Chromosorb 102 (figures in parentheses in Table

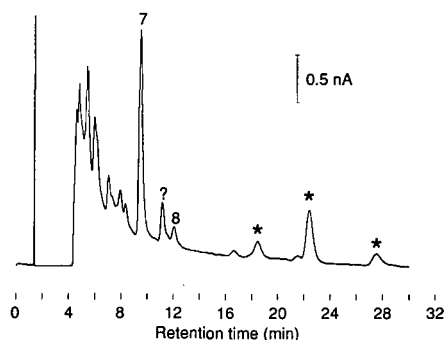


Fig. 4. LC-ED chromatogram of a total effluent from Paper mill A using the recommended chromatographic procedure after extraction on a Sep-Pak C₁₈ cartridge. Peaks as in Fig. 2; the peaks marked with an asterisk are artefacts introduced by the Sep-Pak C₁₈ sorbent, and the one with a question mark is unidentified.

TABLE II

RECOVERIES OF CHLOROPHENOLIC COMPOUNDS AND TRIBROMOPHENOL AFTER PRECONCENTRATION ON CHROMOSORB 102 SORBENT

DCP = 2,4-dichlorophenol; DCG = 4,6-dichloroguaiacol; TCP = 2,4,6-trichlorophenol; TCG = 4,5,6-trichloroguaiacol; PCP = pentachlorophenol; TBP = 2,4,6-tribromophenol. Recoveries are related to standard solutions for each compound that were made up in eluent and injected directly onto the analytical column, apart from figures in parentheses that are related to standards that were put through the preconcentration procedure.

Experiment	Recovery (%)					
	DCP	DCG	TCP	TCG	PCP	TBP
Standards	109.4	96.7	101.0	95.2	102.9	102.2
Effluent (post-) ^a	97.2 (88.9)	86.6 (89.6)	92.1 (91.2)	92.3 (97.0)	101.6 (98.8)	92.2 (90.2)
Effluent (pre-) ^b	91.9 (84.0)	84.2 (87.0)	86.3 (85.5)	84.4 (86.6)	101.0 (98.8)	87.0 (85.2)

^a Spike added to effluent extract after preconcentration.

^b Spike added to effluent sample before preconcentration.

II). Some sources of random error are removed from these latter data, because additions of standards were made from the one spiking solution for all preconcentration trials.

In a second trial of the preconcentration technique with a total effluent from the paper mill collected at later date, the same chlorophenolics were added, but with trichlorosyringol in place of 4,6-dichloroguaiacol. Recoveries were quantitative in this instance, apart from 2,4-dichlorophenol which was marginally diminished at 96%. The discrepancy between these two recovery trials can be attributed to differences in the sorbent loading caused by variability in (i) effluent composition (from changes in feedstock, and variation of pulping and bleaching chemistry), and possibly (ii) slight changes in sample pre-treatment. The original mill effluent had a pH of 6; while effluent used in the subsequent trial had a pH of 9.5, and it also had a high clay particulate loading that necessitated filtration (0.5 μm , Whatman GF/F) in place of centrifugation. The former effluent was diluted 6% with pure water in pretreatment procedures whereas the latter was diluted by 16%. In monitoring effluents for chlorophenolic compounds it is recommended that extraction recoveries are monitored regularly.

Very similar recoveries were recorded for TBP as for the chlorophenolics. Hence, on the basis that TBP does not interfere in the chromatographic separation of the chlorophenolics, and that it behaves very similarly in the preconcentration procedure, it

can function as an internal standard. The other important proviso is that the compound chosen as an internal standard cannot be present in samples to be analysed. TBP is not a natural compound, and it has not been observed in pulp mill effluents (although in one instance with mill effluent samples we have observed an unknown compound that overlapped with TBP). Even for a compound like pentachlorophenol which is often extracted with different efficiency than TBP, it is still possible to calibrate via the internal standard method provided that the analyte: internal standard ratio is calculated from data derived from the preconcentration procedure, rather than from comparison of detector response for standards that are injected directly onto the LC-ED column. For accurate assessment of recovery or use of an internal standard it should also be emphasised that complete dissolution of chlorophenolic compounds should be ensured in aqueous standards; many of these compounds have very low solubilities in water, and tend to remain as a surface film.

Application

Effluent samples were obtained from a paper mill processing softwood and hardwood pulps (hereafter referred to as Paper mill A), and a pulp mill that uses mostly hardwoods as feedstock (hereafter referred to as Pulp mill B). The chlorophenolics proved to be quite stable under the storage conditions described above, and we noticed no difference

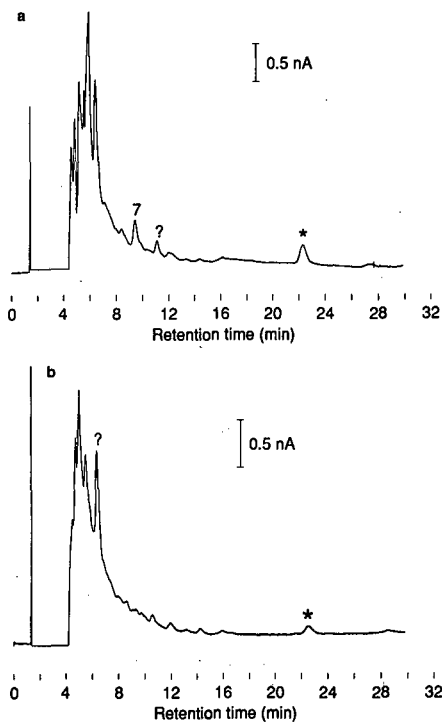


Fig. 5. LC-ED chromatograms of total effluent samples collected from Pulp mill B on two separate occasions (a and b), with different AOX levels: (a) 17 mg/l, (b) 11 mg/l. The analyses were performed on extracts from Sep-Pak C_{18} cartridges. Peaks as in for Fig. 4.

between samples treated and not treated with the copper sulphate.

Chromatograms for the total effluents from the mills are shown in Figs. 4 and 5. Chlorophenolics identified in the effluent from Paper mill A were 4,6-dichloroguaiacol and 2,4,6-trichlorophenol; their concentrations were estimated by standard additions technique to be $213 \pm 20 \mu\text{g/l}$ and $9.9 \pm 0.5 \mu\text{g/l}$, respectively. Confirmation of peak identity in collected fractions from the HPLC column was made by gas chromatography–mass spectrometry [29], after derivatising chlorophenolics in the mill effluent by using essentially the method of Voss *et al.* [14]. Effluents from Pulp mill B contained lesser amounts of the polychlorinated phenolics. Only the 4,6-dichloroguaiacol was tentatively identified. Pulp mill B provided data from “adsorbable organohalogen” (AOX) measurements for the two effluent samples analysed here (Fig. 5). As expected,

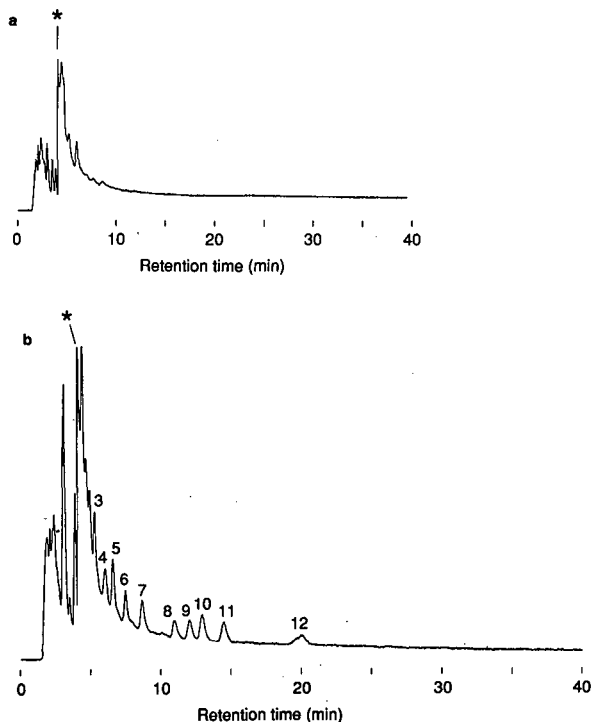


Fig. 6. LC-ED chromatograms of Fig. 5b effluent sample after spiking with the standard mixture of chlorophenolic compounds (chlorophenols: $7 \mu\text{g/l}$, other chlorophenolics: $10 \mu\text{g/l}$). Peaks as in Fig. 2; the asterisk indicates a change in current sensitivity from 100 to 10 nA f.s. (a) Single-electrode amperometry: current trace recorded at an applied potential of + 600 mV vs. Ag/AgCl (E_1). (b) Dual-electrode amperometry: differential current trace (Δi), for $E_1 = + 600 \text{ mV vs. Ag/AgCl}$, $E_2 = + 900 \text{ mV vs. Ag/AgCl}$.

concentrations (by inspection) of polychlorinated phenolics diminish with a decrease in AOX level of the effluent.

The efficacy of using dual-electrode detection, and monitoring the differential current is demonstrated in Fig. 6. We added the standard suite of chlorophenolic standards to the effluent sample shown in Fig. 5b. The current trace recorded at an applied potential of + 600 mV (E_1) shows no response to the chlorophenolics (Fig. 6a). However, the differential current trace (Δi , for $E_1 = 600 \text{ mV}$, $E_2 = 900 \text{ mV}$) shows peaks for all the chlorophenolics apart from 6-chlorovanillin which is masked by other clearly eluting compounds in the mill effluent (Fig. 6b). We found that there was no need to frequently re-polish the electrodes, as there was no

obvious deterioration in electrode performance over several days with the repeated injection of extracted effluent samples.

In a preliminary experiment, we attempted to remove some of the maze of early eluting peaks that can interfere with the determination of the monochlorophenolic compounds. Ultra-filtration was the method of choice. A sample of Paper mill A effluent was filtered through a GF/F filter (Whatman), and then a 15-ml aliquot was ultra-filtered using a centrifugation process (Millipore Ultrafree-20 filter unit; 10 000 NMWL polysulfone membrane). The ultra-filtration using the procedure as recommended by the manufacturer should yield a filtrate with 10 000 molecular mass cut-off. Comparative analysis of this filtrate with a sample that was subjected to primary filtration alone, with the GF/F filter, indicated that <3% of the chlorophenolics were recovered. Either the chlorophenolic compounds adsorbed to the membrane, or more likely they were mostly associated with > 10 000 molecular mass organic material in a hydrophobic interaction. Further investigations are required to find pretreatment procedures that will more selectively extract the early eluting chlorophenolics from samples of pulp mill effluents.

Although we did not analyse a natural receiving water sample, the capabilities of the analytical procedure were tested by successively diluting Paper mill A effluent with 1% NaCl solution. These diluted samples were preconcentrated by solid-phase extraction using the recommended procedure to give a final concentration equivalent to that in the original effluent. The recovery was gauged by comparing the concentration determined in the concentrate with that of the undiluted effluent. Within the precision of the analytical procedure, recovery was complete for at least a 50-fold dilution of the effluent. A lack of interference from natural organic compounds in individual receiving waters would need to be verified for legitimate application of the preconcentration procedure.

The LC-ED method for determining chlorophenolics as described here, is not intended to supplant existing analytical procedures that definitively identify chlorophenolic compounds in aqueous samples, such as that of Voss *et al.* [14] when coupled with mass spectrometry. It is a complementary technique that with its simpler pretreatment steps is well suit-

ed to routine monitoring once an effluent or receiving water has been well characterised. As demonstrated by Rennie [30] with an earlier HPLC method for phenols, it could also be automated easily.

ACKNOWLEDGEMENTS

We are grateful to Teresa O'Leary, Michele Herpich, Des Richardson, and Martin Neilson for their assistance in bringing this work to fruition. We also thank John Volkman and Des Richardson for commenting on an earlier version of this paper.

NOTE ADDED IN PROOF

A very recently published paper (Tolosa *et al.*, *Mar. Pollut. Bull.*, 22 (1991) 603–607) reports on the occurrence of 2,4,6-tribromophenol in estuarine sediment extracts. Therefore, TBP might be disqualified as an internal standard for the analysis of some environmental samples by our LC-ED procedure. Some of the isomers of tetrachlorophenol could be suitable substitutes.

REFERENCES

- 1 S. Jensen, *New Sci.*, 32 (1966) 612.
- 2 J. Paasivirta, *Wat. Sci. Tech.*, 20 (1988) 119–129.
- 3 J. E. Portmann, in G. Kullenberg (Editor), *The Role of the Oceans as a Waste Disposal Option*, D. Reidel, Dordrecht, 1986, pp. 427–440.
- 4 D. J. Faulkner, in O. Hutzinger (Editor), *The Natural Environment and the Biochemical Cycles — The Handbook of Environmental Chemistry*, Vol. 1A, Springer, Berlin, 1980, pp. 229–254.
- 5 K. P. Kringstad and K. Lindstrom, *Environ. Sci. Technol.*, 18 (1984) 236A–248A.
- 6 C. Leuenberger, W. Giger, R. Coney, J. W. Graydon and E. Molnar-Kubica, *Water Res.*, 19 (1985) 885–894.
- 7 D. J. McLeay, B. McKague and C. C. Walden, *Aquatic Toxicity of Pulp and Paper Mill Effluent: a Review; Report EPS 4/PF/1*, Environment Canada, Ottawa, 1987, p. 191.
- 8 A. Södergren, *Biological Effects of Bleached Pulp Mill Effluents; SNV Report 3558*, Bratts Tryckeri, Jönköping, 1989, p. 139.
- 9 D. Halliburton and A. Chung, in *Proc. Int. Conf. on Bleached Kraft Pulp Mills — Technical and Environmental Issues*, Melbourne, Australia, February 4–7, 1991, National Pulp Mills Research Program, Canberra, 1991, pp. 397–408.
- 10 L. H. Keith and W. A. Telliard, *Environ. Sci. Technol.*, 13 (1979) 416–423.
- 11 C. B. Fandry, R. E. Johannes and P. J. Nelson, *Pulp Mills: Modern Technology and Environmental Protection; Report to Senator the Hon. John Button, Minister for Industry, Technology and Commerce*. CSIRO, Canberra, 1989, p. 68.

- 12 *Environmental Guidelines for New Bleached Eucalypt Kraft Pulp Mills*, Commonwealth of Australia, Canberra, 1989.
- 13 W. Fresenius, K. E. Quentin and W. Schneider (Editors), *Water Analysis – a Practical Guide to Physico-Chemical, Chemical and Microbiological Water Examination and Quality Assurance*, Springer, Berlin, 1988, pp. 536–540.
- 14 R. H. Voss, J. T. Wearing and A. Wong, in L. H. Keith (Editor), *Advances in the Identification and Analysis of Chlorinated Phenolics in Pulp Mill Effluents*, Ann Arbor Sc. Publ., Ann Arbor, MI, 1981, pp. 1059–1095.
- 15 K. Kuwata, M. Uebori and Y. Yamazaki, *Anal. Chem.*, 52 (1980) 857–860.
- 16 H. C. Smit, T. T. Lub and W. J. Vloon, *Anal. Chim. Acta*, 122 (1980) 267–277.
- 17 A. W. Wolkoff and R. H. Larose, *J. Chromatogr.*, 99 (1974) 731–743.
- 18 J. F. Lawrence, *J. Chromatogr. Sci.*, 17 (1979) 147–151.
- 19 T. Jupille, M. Gray, B. Black and M. Gould, *Am. Lab.*, 13 (1981) 80–86.
- 20 R. E. Shoup and G. S. Mayer, *Anal. Chem.*, 54 (1982) 1164–1169.
- 21 T. J. Cardwell, I. C. Hamilton, M. J. McCormick and R. K. Symons, *Int. J. Environ. Anal. Chem.*, 24 (1986) 23–35.
- 22 G. E. Batley, *J. Chromatogr.*, 389 (1987) 409–416.
- 23 L. Renberg and K. Lindström, *J. Chromatogr.*, 214 (1981) 327–334.
- 24 L. Song, M. Paleologou and W. C. Purdy, *J. Chromatogr. Sci.*, 29 (1991) 66–69.
- 25 D. A. Roston, R. E. Shoup and P. T. Kissinger, *Anal. Chem.*, 54 (1982) 1417A–1434A.
- 26 M. T. Galceran and F. J. Santos, *Water Supply (Barcelona)*, 7 (1989) 69–75.
- 27 R. P. W. Scott, *Liquid Chromatography Detectors*, Elsevier, Amsterdam, 2nd ed., 1986, p. 12.
- 28 M. C. Hennion, *Trends Anal. Chem.*, 10 (1991) 317–323.
- 29 T. O’Leary and J. K. Volkman, unpublished results.
- 30 P. J. Rennie, *Roy. Chem. Soc., Anal. Proc.*, 24 (1987) 295–297.

High-performance liquid chromatography of oligosaccharide alditols and glycopeptides on a graphitized carbon column

Michael Davies, Kevin D. Smith, Anne-Marie Harbin and Elizabeth F. Hounsell

Glycoconjugates Section, Clinical Research Centre, Watford Road, Harrow, Middlesex HA1 3UJ (UK)

(First received April 15th, 1992; revised manuscript received June 12th, 1992)

ABSTRACT

The chromatographic behaviour of oligosaccharide alditols and glycopeptides containing neutral and acetamido sugars and sialic acid has been investigated on a HyperCarb porous graphitised carbon column. The alditols were substantially retained and could be eluted in 0–25% acetonitrile–0.05% trifluoroacetic acid in 0.05% aqueous trifluoroacetic acid between 3–30 min for mono- to hexasaccharides. Elution patterns were based on both size, charge and linkage such that isomeric compounds could be separated from each other.

INTRODUCTION

The diversity of closely related carbohydrate structures found in nature provides a unique challenge for the chromatographer. Purification of isomeric oligosaccharides is essential for assigning specific functions and antigenicity [1] and improved methods for high-resolution separation are constantly being sought. A porous graphitised carbon (PGC) stationary phase [2,3] (Shandon Hypercarb) has therefore been investigated as a possible additional column material providing an alternative separation potential to reversed-phase (RP), normal-phase (NP) and anion exchange packings. In order to separate series of related oligosaccharide sequences a combination of RP (normally octadecylsilyl) and NP (amine-bonded) high-performance liquid chromatography (HPLC) has usually been adopted [4,5]. More recently high-pH anion-exchange chromatography has been introduced for

isomer separation [5,6]. In the latter methodology neutral reduced oligosaccharides are in general not retained sufficiently for adequate separation and reproducible chromatography and therefore we have been particularly interested in studying the PGC phase for chromatography of isomeric alditols. Koizumi *et al.* [7] have recently published HPLC on PGC columns of monosaccharides and malto-oligosaccharides which show good separation of the α and β anomers. It is therefore more appropriate to use this phase for alditol or glycopeptide separation without the additional complication of anomerisation.

EXPERIMENTAL

Materials

The oligosaccharides studied are shown in Table I together with the abbreviations used. GlcNAc, CB, CT, SAL, fetuin and trypsin were obtained from Sigma Poole, UK. ^1H NMR studies showed that SAL (sialyllactose or N-acetylneuramin-lactose) from bovine colostrum (Sigma batch No. A3001) consisted of approximately 75% of the

Correspondence to: Dr. E. F. Hounsell, Glycoconjugates Section, Clinical Research Centre, Watford Road, Harrow, Middlesex HA1 3UJ, UK.

TABLE I

STRUCTURES OF THE OLIGOSACCHARIDES STUDIED AS THEIR ALDITOLS

GalNAc = N-Acetylgalactosamine; GlcNAc = N-acetylglucosamine; Gal = galactose; Glc = glucose; Fuc = fucose; NeuAc = N-acetylneuraminic acid.

	D-GalNAc
	D-GlcNAc
CB	β -D-GlcNAc-(1→4)-D-GlcNAc (chitobiose)
CT	β -D-GlcNAc-(1→4)- β -D-GlcNAc-(1→4)-D-GlcNAc (chitotriose)
(G3GN)	β -D-Gal-(1→3)-D-GlcNAc
(G4GN)	β -D-Gal-(1→4)-D-GlcNAc
(G6GN)	β -D-Gal-(1→6)-D-GlcNAc
03	β -D-Gal-(1→4)- β -D-GlcNAc-(1→6)-D-GalNAc
04	β -D-Gal-(1→3)- β -D-GlcNAc-(1→3)-D-GalNAc β -D-Gal-(1→4)- β -D-GlcNAc-(1→3)-D-GalNAc β -D-Gal-(1→4)- β -D-GlcNAc-(1
NI	β -D-Gal-(1 <div style="margin-left: 100px;"> \swarrow 6) -D-GalNAc 3) \nearrow β-D-Gal-(1 </div>
K5(3)	β -D-Gal-(1→4)- β -D-GlcNAc-(1 <div style="margin-left: 100px;"> \swarrow 6) -D-GalNAc 3) \nearrow </div>
LNT	β -D-Gal-(1→3)- β -D-GlcNAc-(1→3)- β -D-Gal(1→4)-D-Glc
LNNT	β -D-Gal-(1→4)- β -D-GlcNAc-(1→3)- β -D-Gal(1→4)-D-Glc
LNFIH	β -D-Gal-(1→4)- β -D-GlcNAc-(1→3)- β -D-Gal(1→4)-D-Glc
	\uparrow 3 \uparrow 1 α -L-Fuc α -L-Fuc \uparrow 1 \downarrow 4
LNFIH	β -D-Gal-(1→3)- β -D-GlcNAc-(1→3)- β -D-Gal-(1→4)-D-Glc
LNFI	α -L-Fuc-(1→2)- β -D-Gal-(1→3)- β -D-GlcNAc-(1→3)- β -D-Gal-(1→4)-D-Glc
SA3L	α -D-NeuAc-(2→3)- β -D-Gal-(1→4)-D-Glc
SA6L	α -D-NeuAc-(2→6)- β -D-Gal-(1→4)-D-Glc
	α -D-NeuAc \downarrow 2 \downarrow 6
DSLNT	α -D-NeuAc-(2→3)- β -D-Gal-(1→3)- β -D-GlcNAc-(1→3)- β -D-Gal-(1→4)-D-Glc

(2→3) isomer (SA3L) and also contained 10% of the (2→6) isomer (SA6L) and 15% of a third unidentified sialylated component, whereas SAL from human milk (Sigma batch No. A2423) was predominantly the (2→6) isomer. The disaccharides G3GN, G4GN and G6GN were obtained by chemical synthesis and kindly supplied by Dr. A. Veyrières (Université Pierre et Marie Curie, Paris, France). The oligosaccharides designated 03, 04, N1 and K5(3) purified from meconium glycoproteins as previously described [8,9] were obtained as their alditols after alkaline-borohydride release of oligosaccharides. The oligosaccharides LNT, LNNT, LNFIII, LNFII, LNFI and DSLNT were from Research Sugars, Long Crendon, Aylesbury, UK. The oligosaccharides obtained from commercial sources and by chemical synthesis were reduced using 20 mM sodium borohydride in 0.05 M NaOH at 4°C for 18 h, excess borohydride was then destroyed by addition of acetic acid and the sample desalted using Dowex 50-X8 acetate form (3 × 1 cm column) eluted with water.

Apparatus and columns

HPLC analysis was performed using a Gilson system (Anachem, Luton, UK) consisting of two 302 pumps, a 116 UV monitor, 802 manometric module, 802B mixing chamber, Gilson 715 Systems Manager and a Rheodyne 7125 injector. The column was Shandon Hypercarb (Shandon Scientific, Runcorn, UK) 100 × 4.6 mm with an ODS (Hypersil) guard column.

HPLC of oligosaccharide alditols

The flow-rate was 0.75 ml/min using an eluent of acetonitrile–water–0.05% trifluoroacetic acid (TFA) and UV detection at 206 nm. The gradient for neutral oligosaccharide alditols was as follows for eluent A (0.05% aqueous TFA) and B (acetonitrile–0.05% TFA): 0–5 min, 0% B; 5–20 min, 0–15% B; 20–30 min, 15% B; 30–40 min, 15–0% B. For sialylated oligosaccharide alditols the gradient was: 0–5 min, 0% B; 5–40 min, 0–40% B; 40–50 min, 40–0% B.

Glycopeptide mapping

Fetuin was digested with chymotrypsin-free N tosyl-L-phenylalanine-chloromethylketone (TPCK)-treated trypsin (Sigma) as described previously [10]

and chromatographed on the PGC column using detection at 210 nm, a flow-rate of 1 ml/min and solvent system as follows for eluent A (0.1% aqueous TFA) and B (acetonitrile/0.1% TFA): 2% B to 82% B in 80 min. Peaks were monitored for hexose using a modification [10] of the method of Dubois *et al.* [11] and the amino acid sequence of peptides in selected peaks were determined using a Model 473A protein sequencer (Applied Biosystems, Warrington, UK) in the pulsed liquid mode. The sample was applied to a polybrene treated filter disc which had been subjected to three pre-wash cycles in 30 μl 0.1% aqueous TFA. Sequencing was carried out for 6–7 cycles of the instrument.

RESULTS

Table II shows the retention times for HPLC of alditols of the oligosaccharides shown in Table I. Monosaccharide acetamido sugar alditols (D-GlcNAc-ol and D-GalNAc-ol) were eluted early

TABLE II

THE RETENTION TIMES OF THE ALDITOLS (-ol) STUDIED USING THE GRADIENT DESCRIBED IN EXPERIMENTAL. RETENTION TIMES (t_R) ARE GIVEN FOR THE ALDITOLS RUN SEPARATELY AND AS A MIXTURE OF THE GROUPS INDICATED BY THE BRACKETS (t_R MIX)

	t_R	t_R mix
GalNAcol	3.64	3–4
GlcNAcol	3.94	3–4
CB-ol	16.97	16.73
CT-ol	18.18	18.15
G3GN-ol	12.75	12.72
G4GN-ol	13.40	13.41
G6GN-ol	15.82	15.75
LNT-ol	20.51	20.42
LNNT-ol	20.98	20.87
LNFII-ol	17.73	17.71
LNFIII-ol	17.65	
LNFI-ol	19.74	
03-ol	18.06	
04-ol	16.90 and 17.25	
N1-ol	18.06	
K5(3)-ol	20.78 (single peak)	
SA3L-ol	22.03	22.03
SA6L-ol	18.50	18.62
DSLNT-ol	27.46	27.56

and could not be separated from each other on the gradient used. There was a good separation of the mono-, di- and trisaccharide alditols of D-GlcNAc (D-GlcNAc-ol, CB-ol and CT-ol) showing a general increased elution time with increased size. The same resolution was achieved when 2 mg of material were loaded and a preparative recovery of >90% was achieved. The presence of a hexose residue as in G3GN-ol, G4GN-ol and G6GN-ol reduced the elution time as compared to CB-ol and the presence of a fucose residue reduced the retention time further, as shown for example by a comparison of the retention times of the linear tetrasaccharide alditols (LNT-ol and LNNT-ol) and their fucosylated analogues (LNF III-ol, LNFII-ol and LNFI-ol).

Within isomeric groups of neutral oligosaccharides the presence of a (1→6) linkage increased the retention time as shown for the disaccharide alditols G3GN-ol, G4GN-ol and G6GN-ol and the trisaccharide alditols 04-ol and 03-ol. More importantly, oligosaccharides having a (1→3) linkage

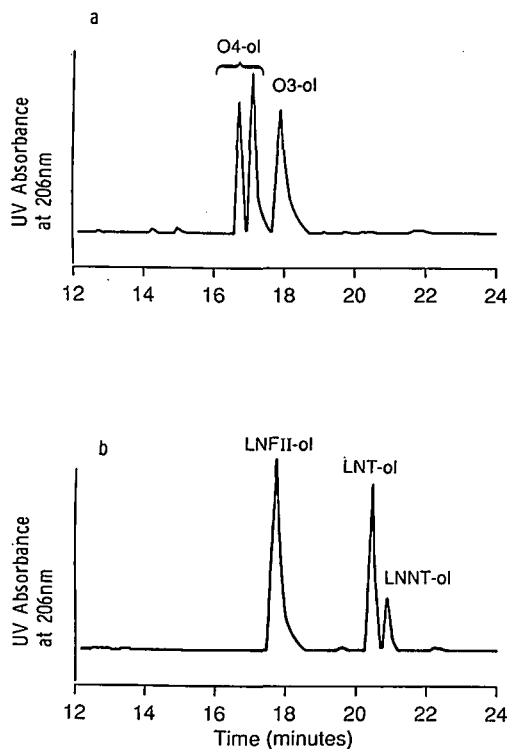


Fig. 1. HPLC on Hypercarb PGC using an acetonitrile-water-0.05% TFA gradient of (a) 1 μ g and 3 μ g, respectively, of 04-ol (two isomers) and 03-ol, and (b) 10, 5 and 2 μ g, respectively, of LNFII-ol, LNT-ol and LNNT-ol.

eluted before those having a (1→4) linkage as shown by separation of the two isomers in 04-ol from each other and LNT-ol from LNNT-ol (Fig. 1). However, separation could not be achieved of LNFII-ol and LNFIII-ol which vary in the C-3 and C-4 linkage of D-Gal and L-Fuc to D-GlcNAc, nor of the two isomers present in K5(3)-ol.

The sialic acid-containing oligosaccharide alditols were amongst the longest retained of the alditols tested, but still gave symmetrical peaks with baseline separation, eluting within less than 1 min (Fig. 2). Here the (2→3)-linked trisaccharide alditol was retained longer than the (2→6) which differed from that shown for the neutral oligosaccharide alditols. This represents a facile separation and iden-

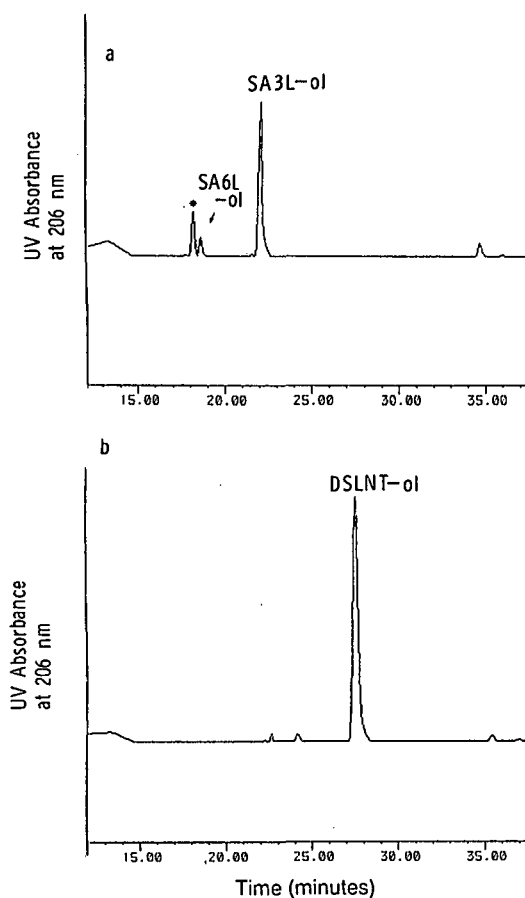


Fig. 2. HPLC on Hypercarb PGC using an acetonitrile-water-0.05% TFA gradient of the alditols obtained from (a) 10 μ g of the preparation of SA3L from Sigma, containing 10% SA6L and 15% unknown (*), and (b) DSLNT-ol.

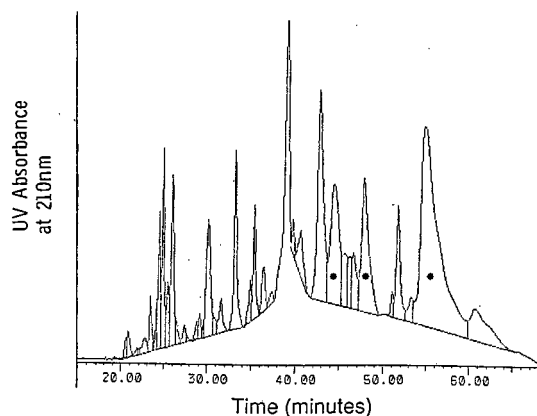


Fig. 3. HPLC on Hypercarb PGC using an acetonitrile–water–0.1% TFA gradient of 200 pmol of a tryptic digest of fetuin; * = peaks containing major glycopeptides.

tification of these oligosaccharides from each other and from an as yet unidentified sialylated component. The chromatographic behaviour of sialylated oligosaccharide sequences has also been studied by analysis of glycopeptides in a trypsin digest of fetuin which has three N-linked and three O-linked sialylated oligosaccharide chains [10]. The conditions chosen for PGC chromatography were the same as those previously used for RP-HPLC on an ODS column [10]. Glycopeptides were identified by hexose assay (Fig. 3) and characterised further by peptide sequence analysis (Table III). The results summarised in Table III show the relative hydrophobicity of the peptides and the diagnostic amino acids detected. The hexose-positive peak eluting at 44–45 min contained the glycopeptide AA 127–168

TABLE III

CHARACTERISATION BY PEPTIDE SEQUENCING OF THE HEXOSE POSITIVE PEAKS IN THE PGC PROFILE OF TRYPSIN DIGESTED FETUIN (GLYCOSYLATION SITES ARE IDENTIFIED BY ASTERISKS)

Elution time (min)		Sequence identification (detected amino acids in bold) ^b	Hydrophilicity/ hydrophobicity index ^c
PGC	ODS ^a		
44	ND ^d	VWPR	–357
44	42	LCPDCPLLAPLND [*] SR ^e	–170
		VVHAVEVALATFNAESNGSYLQLVEISR	–94
48	50	EPACDDPDTEQAALAAVDYINK	175
		 LCPGR ^e IRYFK	–402
55	54	R-PTGEVYDIEIDTLETTCHVLDPTPLANCSVR [*] ^e	–77
		QQTQHAVEGDCDIHVLK	232
55	62	AQFVPLPVSVSVEFAVAATDCIAK	–130
		 EVVDPTK-CNLLAEK	29

^a Data taken from Smith *et al.* [10].

^b | = disulphide bond.

^c Calculated for individual non-glycosylated peptides by dividing the sum of the free energy of transfer from solution to surface (ΔF) values for each amino acid [23] by the total number of amino acids present [24]. The most hydrophobic peptides have the lowest negative value.

^d ND = Not detected.

^e – = Previously identified [10] non-digested tryptic cleavage site due to close proximity of a glycosylation site or disulphide bond.

having two N-glycosylation sites due to inhibition of hydrolysis of the tryptic cleavage site at arginine 141 by the oligosaccharide chain at asparagine 138. The hydrophobic tetrapeptide VWPR was also detected in this peak. The peak eluting at 48–49 min contained the peptides AA 11–32 and AA 331–335 which are disulphide bonded together. Hexose detection is due to the additional presence of the large glycopeptide AA 228–288 having three O-linked chains, for which peptide sequence data are not obtained [10]. The peak eluting at 55–58 min contained the glycopeptide AA 54–113 having one N-linked chain and two non-digested tryptic cleavage sites. This peak also included a disulphide-linked peptide pair AA 169–103 and AA 194–207 with an undigested tryptic cleavage site adjacent to one of the cystines involved in the disulphide bond.

DISCUSSION

The separation of oligosaccharide alditol isomers differing only by a (1→3) or (1→4) linkage confirms PGC chromatography as a useful adjunct to RP and NP HPLC. The oligosaccharide isomers in 04 for example were not separated in our earlier study [8] although separation was achieved by Lamblin *et al.* [12] who introduced an anion-exchange chromatography step on Durrum AX4 resin (a forerunner of Dionex pellicular anion-exchange resin now being used so successfully in high-pH anion-exchange chromatography to give separation of isomers of non-reduced oligosaccharides [6,13]). In addition, the good baseline and reproducible chromatography together with the high loading that can be achieved without loss of resolution add further to its efficiency. The chromatographic behaviour of alditols on RP (ODS), NP (amine-bonded) and PGC HPLC is different in each case as shown from the following relative t_R data for 03-ol, 04-ol and N1-ol, respectively, RP 1.0/1.2/0.8; NP 1.0/0.9/1.2; PGC 1.0/0.9-0.95/1.0 *i.e.* in RP oligosaccharides having a (1→6) linkage are eluted first and separation is not achieved of the (1→4) and (1→3) isomers [4], whereas in NP the order is reversed [4]. The elution pattern of PGC is similar to NP in that 03-ol and N1-ol elute after the isomers in 04-ol but differs by the fact the separation of the (1→6) containing tri- and tetrasaccharide is not achieved, whereas separation of (1→3) and (1→4) trisaccharide alditols

is. A combination of the three phases is probably therefore still required for more complete separation of oligosaccharides of different linkages and sizes. Unfortunately PGC HPLC failed to separate the fucosylated pentasaccharide isomers LNFII-ol and LNFIII-ol which have been successfully resolved only in unreduced form by high-pH anion-exchange [6,13], recycling cation-exchange [14] or RP [4] chromatography.

The separation of non-reduced oligosaccharides varying in their linkage of sialic acid has previously been achieved by HPLC on an amine-bonded NP column using phosphate buffer [5] and more recently by high-pH anion-exchange chromatography [6]. Sialylated oligosaccharide alditols have also been separated by high-pH anion-exchange chromatography [15,16]. The disadvantage of these methods is that they require a high salt concentration which is not as readily removed compared to TFA, thus inhibiting further analysis and making the PGC separation by far the preferred chromatography. For sialylated glycopeptides, similar retention times were found by PGC to HPLC on ODS [10] using the same solvent elution conditions (Table III).

The chromatographic behaviour described herein for oligosaccharide alditols, peptides and glycopeptides and by Koizumi *et al.* [7] for reducing mono- and disaccharides adds to the debate on the mechanism of separation achieved by PGC [17–22]. Compared to the study of Koizumi *et al.* on neutral oligosaccharides we have used 0.05%–0.1% TFA in the eluent in order to widen the scope of the technique to sialylated oligosaccharides and glycopeptides as used by the previous authors [21,22] studying PGC chromatography of other classes of compounds. These authors found the retention of anionic compounds to be dominated by electronic interaction between the solute and delocalised electron clouds on the graphitised carbon whilst cationic compounds were mainly retained by reversed-phase interaction with the hydrophobic carbon surface. Our results agree with a dual chromatographic mechanism based on long retention of glycopeptides having a low negative hydrophilicity/hydrophobicity index (Table III) and others having acidic amino acids and/or sialic acids ionised at pH 2.0 of the eluent. The unique physicochemical properties of PGC provide us with an additional column packing for separation of oligosaccharide alditols, glyco-

peptides and peptides at high sensitivity and preparative efficiency.

ACKNOWLEDGEMENT

The authors are grateful to Paul Purkiss and the Haemostasis Research Group for carrying out the peptide sequencing and to Elaine White for typing the manuscript.

REFERENCES

- 1 E. F. Hounsell, *Chem. Soc. Rev.*, 16 (1987) 161–185.
- 2 M. J. Gilbert, J. H. Knox and B. Kaur, *Chromatographia*, 16 (1982) 138–146.
- 3 J. H. Knox, B. Kaur and G. R. Millward, *J. Chromatogr.*, 352 (1986) 3–25.
- 4 E. F. Hounsell, N. J. Jones and M. S. Stoll, *Biochem. Soc. Trans.*, 13 (1985) 1061–1064.
- 5 E. F. Hounsell, in C. K. Lim (Editor), *HPLC of Small Molecules*, IRL Press, Oxford, 1st ed., 1986, pp. 49–68.
- 6 R. Townsend, M. Hardy and Y.-C. Lee, *Methods Enzymol.*, 179 (1989) 65–76.
- 7 K. Koizumi, Y. Okada and M. Fukuda, *Carbohydr. Res.*, 215 (1991) 67–80.
- 8 E. F. Hounsell, A. M. Lawson, J. Feeney, H. C. Gooi, N. J. Pickering, M. S. Stoll, S. C. Lui and T. Feizi, *Eur. J. Biochem.*, 148 (1985) 367–377.
- 9 E. F. Hounsell, A. M. Lawson, M. S. Stoll, D. P. Kane, G. C. Cashmore, R. A. Carruthers, J. Feeney and T. Feizi, *Eur. J. Biochem.*, 186 (1989) 597–610.
- 10 K. D. Smith, A.-M. Harbin, R. A. Carruthers, A. M. Lawson and E. F. Hounsell, *Biomed. Chromatogr.*, 4 (1990) 261–266.
- 11 M. Dubois, K. A. Gilles, J. K. Hamilton, P. A. Rebers and F. Smith, *Anal. Chem.*, 28 (1956) 350–356.
- 12 G. Lamblin, M. Lhermitte, A. D. Boersma, P. Roussel and V. N. Reinhold, *J. Biol. Chem.*, 255 (1980) 4595–4598.
- 13 G. P. Reddy and C. A. Bush, *Anal. Chem.*, 198 (1991) 278–284.
- 14 A. S. R. Donald and J. Feeney, *Carbohydr. Res.*, 178 (1988) 79–91.
- 15 S. Honda, S. Suzuki, S. Zaiki and K. Kakehi, *J. Chromatogr.*, 523 (1990) 189–200.
- 16 K. O. Lloyd and A. Savage, *Glycoconjugate J.*, 8 (1991) 493–498.
- 17 A. F. Fell, T. A. G. Noctor, J. E. Mama and B. J. Clark, *J. Chromatogr.*, 434 (1988) 377–384.
- 18 B. J. Bassler, R. Kaliszan and R. A. Hartwick, *J. Chromatogr.*, 461 (1989) 139–147.
- 19 R. Kaliszan, K. Osmialowski, B. J. Bassler and R. A. Hartwick, *J. Chromatogr.*, 499 (1990) 333–344.
- 20 N. Tanaka, T. Tanigawa, K. Kimata, K. Hosoya and T. Arai, *J. Chromatogr.*, 549 (1991) 29–41.
- 21 C. K. Lim, *Biomed. Chromatogr.*, 3 (1989) 92–93.
- 22 G. Gu and C. K. Lim, *J. Chromatogr.*, 515 (1990) 183–192.
- 23 H. B. Bull and K. Breese, *Arch. Biochem. Biophys.*, 161 (1974) 665–670.
- 24 S. Naylor, G. Moneti and S. Guyan, *Biomed. Environ. Mass Spectrom.*, 17 (1988) 393–397.

Silver ion high-performance liquid chromatography of derivatives of isomeric fatty acids

Boryana Nikolova-Damyanova[☆]

Hannah Research Institute, Ayr KA6 5HL (UK)

B. G. Herslof

Karlshamns LipidTeknik AB, P.O. Box 15200, Stockholm S104 65 (Sweden)

W. W. Christie

Hannah Research Institute, Ayr KA6 5HL (UK)

(First received January 17th, 1992; revised manuscript received April 21st, 1992)

ABSTRACT

Silver ion high-performance liquid chromatography was used to study the retention characteristics of series of monoenoic, dienoic and polyunsaturated esters. Two columns with stationary phases consisting of bonded phenylsulphonic moieties in the silver ion form were used, with a mobile phase consisting of dichloromethane–dichloroethane (1:1) with various proportions of acetonitrile at fixed temperatures. Accurate capacity factors relative to octadecene as an internal standard were obtained. Each column had distinctive characteristics, and methyl ester derivatives were less well resolved than phenacyl derivatives. For example, baseline resolution of three naturally occurring isomers (6-, 9- and 11-18:1) was possible. The distance of the double bond from the carboxyl group was much more important than the nature of the terminal moiety in its effect on retention values. Fixed temperatures were necessary for reproducible retention times, but lowering the temperature improved the resolution merely by extending the time of chromatography. The results are discussed in terms of a hypothetical mechanism involving simultaneous interaction between one silver ion and either two double bonds, or one double bond and one other electron-rich moiety such as the ester group.

INTRODUCTION

Since its introduction in 1962, silver ion or argentation chromatography has been one of the more important tools available to lipid analysts for the separation of molecular species of lipids[1,2]. The topic has been the subject of many reviews[3–5], most recently by Nikolova-Damyanova [6]. Perhaps surprisingly for such a well established tech-

nique, the mechanism of the interaction between unsaturated centres and silver ions in chromatographic systems is poorly understood. In most of the published work, the technique has been used in conjunction with thin-layer chromatography (TLC) with silver nitrate being incorporated into a silica gel G layer by various means. R_F values of different components are then highly variable, being dependent on such factors as the proportion of silver nitrate in the layer, its degree of hydration, atmospheric humidity and temperature and the nature of the mobile phase. These are not easily controlled.

Recently, a stable silver ion column for high-performance liquid chromatography (HPLC) has been

Correspondence to: Dr. W. W. Christie, Hannah Research Institute, Ayr KA6 5HL, UK.

Present address: Institute of Organic Chemistry, Centre of Phytochemistry, Sofia 1113, Bulgaria.

developed in which the silver ions are linked via ionic bonds to phenylsulphonic acid moieties which are in turn bound to a silica matrix [7]. This column has been used extensively for the separation of fatty acid derivatives [8–11] and triacylglycerols [12–16]. In particular, excellent separations of positional and configurational isomers of derivatives of unsaturated fatty acids were achieved [10].

With this column, it is possible to control many of the chromatographic parameters, especially mobile phase composition, flow-rate and column temperature, with a high degree of accuracy. The chromatographic behaviour of derivatives of isomeric fatty acids were investigated in this study in order to obtain a better understanding of the quantitative nature of the interactions between the double bonds in lipids and silver ions.

EXPERIMENTAL

Materials and reagents

Most of the isomeric *cis*-octadecenoic acids [17], the isomeric methylene-interrupted *cis,cis*-octadecadienoic acids [18] and the non-methylene-interrupted *cis,cis*-octadecadienoic acids [19] had been prepared earlier by total synthesis. 9,10-Octadecadienoic acid was a gift from Dr. M. S. F. Lie Ken Jie, University of Hong Kong. All other fatty acids and reagents were purchased from Sigma (Poole, UK). All solvents were analytical reagent or HPLC grade and were supplied by FSA Scientific Apparatus (Loughborough, UK).

High-performance liquid chromatography

The HPLC equipment and the silver ion column were as described previously [7]. In brief, a Spectra-Physics (St. Albans, UK) Model 8700 solvent-delivery system was used; together with an Applied Chromatography Systems (Macclesfield, UK) Model 710/14 mass detector. A column (250 mm × 4.6 mm I.D.) of Nucleosil 5SA (HPLC Technology, Macclesfield, UK) was flushed with 1% aqueous ammonium nitrate solution at a flow-rate of 0.5 ml/min for 1 h, then with distilled water at 1 ml/min for 1 h. Silver nitrate (0.2 g) in water (1 ml) was injected on to the column via the Rheodyne valve in 50- μ l aliquots at 1-min intervals, and 20 min after the last injection the column was washed with methanol for 1 h, then with 1,2-dichloroethane–dichloromethane

(1:1, v/v) for a further 1 h. A commercial silver ion column prepared in a similar way (ChromSpher Lipids; Chrompack International, Middelburg, Netherlands) was donated by the manufacturer. The column was fitted into a water jacket (Alltech UK, Carnforth, UK) through which ethylene glycol was pumped from a Chrompack Model RTE-110B temperature control unit, so that the temperature could be maintained at predetermined levels. In general, 1,2-dichloroethane–dichloromethane (1:1, v/v) admixed with various proportions of acetonitrile at a flow-rate of 1.5 ml/min was the mobile phase.

Derivatization

Esterified fatty acids were hydrolysed with 1 M potassium hydroxide in 90% ethanol at room temperature overnight. After acidification and extraction, the free fatty acids were converted into the phenacyl derivatives as described by Wood and Lee [20]. Prior to HPLC analysis, phenacyl esters were purified by elution from a Bond Elut NH₂ column (Analytichem International, Cambridge, UK) with hexane–diethyl ether (9:1, v/v). Alternatively, a Bond Elut ODS column was used, with impurities being eluted with acetonitrile–water (1:1, v/v) before the pure phenacyl esters were recovered by elution with acetone. The methyl ester derivatives of the fatty acids were prepared by acid-catalysed esterification [5].

RESULTS

In preliminary work to optimize the system, ester derivatives of the *cis*-6-, *cis*-9- and *cis*-11-octadecenoates were used, as these are the most important naturally occurring isomers. In earlier work [7–16], chlorinated solvents in general were found to give the best results in terms of resolution and peak symmetry, and no improvement upon 1,2-dichloroethane–dichloromethane (1:1, v/v) was observed with chloroform or carbon tetrachloride. Only acetonitrile as a polar modifier gave consistently good results. For the monoene standards, a mobile phase of 1,2-dichloroethane–dichloromethane–acetonitrile (50:50:0.025, v/v/v) was selected as the standard as it gave good resolution of the standards in 10–20 min. When the flow-rate was reduced from 1.5 ml/min, a small improvement in resolution was

obtained but with some decrease in peak symmetry. In general, the Nucleosil 5SA and the ChromSpher Lipids columns gave similar results, except for strange temperature effects with the latter (see below), with slightly stronger complexation to the Nucleosil 5SA column.

The dead volume of the column was measured by using octadecane as an unretained molecule. The capacity factor (k') was used as a measure of the retention characteristics in some experiments, but in others detailed below more reproducible results were obtained by using the ratio (k'') of the capacity factor of the analyte to that of octadec-1-ene. This was selected as an unsaturated internal standard, because it is a simple hydrocarbon where the main interaction with the support would be via silver ion complexation.

The nature of the ester moiety had an effect on the capacity factors and on resolution. Methyl esters are widely used in the analysis of fatty acids, so it was important to determine their retention characteristics. Phenacyl, naphthacyl and anthrylmethyl derivatives, which are commonly used as UV-absorbing derivatives in reversed-phase HPLC separations of fatty acids [21] and also give good separation in silver ion HPLC [10], were also prepared and tended to give similar results. On the other hand, 2,4-dinitrophenylmethyl esters, *i.e.* with powerful electron-withdrawing substituents, gave poorly shaped peaks and the standards were not separated. Phenacyl esters were selected as an example of the second type of derivative for further study. The separation of the phenacyl esters of the standard monenes at 20°C on the Nucleosil 5SA column with 1,2-dichloroethane–dichloromethane–acetonitrile (50:50:0.025, v/v/v) is illustrated in Fig. 1. Each isomer was resolved to the baseline, with the 11-18:1 isomer eluting first and 6-18:1 last. The only separations by silver ion TLC that are at all comparable were achieved under extreme conditions, *i.e.* with 30% silver nitrate in the sorbent layer and at –25°C [22] or with 10% silver nitrate at –20°C [23]. The first of these has not proved easy to reproduce (Nikolova-Damyanova, unpublished observation).

It is well established that stronger complexation between silver ions and unsaturated lipids occurs as the temperature is lowered, and it has been suggested that improved resolution is thereby obtained

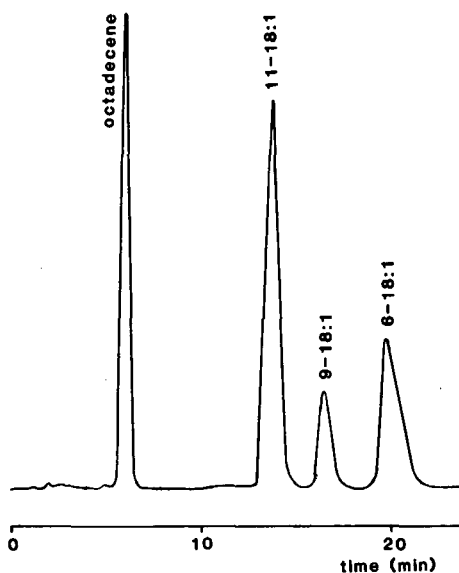


Fig. 1. Separation of the phenacyl esters of *cis*-11-, *cis*-9- and *cis*-6-octadecenoic acids and octadec-1-ene (internal standard) (0.1 mg of each) by silver ion HPLC on the silver-loaded Nucleosil 5SA column at 20°C with 1,2-dichloroethane–dichloromethane–acetonitrile (50:50:0.025, v/v/v) at a flow-rate of 1.5 ml/min as mobile phase and with evaporative light-scattering detection.

[2,3]. However, there does not appear to be any systematic data to support this contention. The changes in the capacity factors (k') for methyl and phenacyl oleate at temperatures from 0 to 35°C on the Nucleosil 5SA column are shown in Fig. 2; a three-fold difference was found between the two extremes. On the other hand, the k'' values remained constant over this temperature range. The ChromSpher Lipids column appeared to operate satisfactorily only at temperatures of 20°C or below; at higher temperatures, the analytes were strongly retained and gave badly shaped peaks. It is possible that some phase change in the organic moiety of the stationary phase occurs at this temperature, but it is not clear how this could affect silver ion complexation. The resolution of the phenacyl esters of 6-18:1 and 9-18:1 fatty acids decreased from 2.2 to 1.35 as the temperature was increased from 0 to 35°C. On the other hand, similar effects were seen on increasing the flow-rate or the concentration of acetonitrile in the mobile phase. When the latter was adjusted to give comparable retention times at different temperatures, little or no

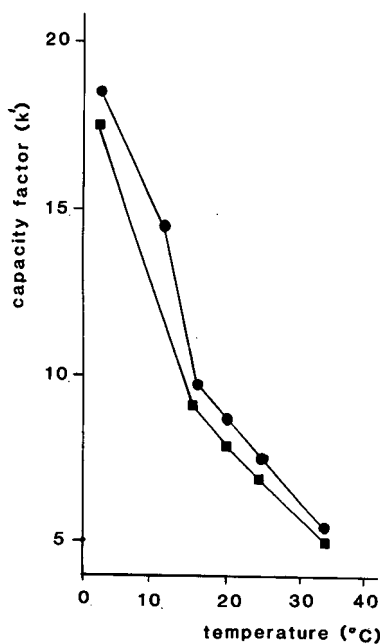


Fig. 2. Variation of the capacity factor ratios (k''), i.e. $k'(\text{analyte})/k'(\text{octadecene})$, for the (■) methyl and (●) phenacyl esters of oleic acid with respect to temperature. Chromatographic conditions as in Fig. 1.

effect of temperature on resolution was apparent.

The k'' values of the methyl and phenacyl esters of a series of *cis*-octadecenoates (3- to 17-18:1) on the silver-loaded Nucleosil column and of the methyl esters on the ChromSpher Lipids column are illustrated in Fig. 3. Values were obtained in triplicate and standard deviations were generally of the order of 0.1. Note that the chromatographic conditions for the two columns were not identical. As these were considered to be the optimum for each, the results are only comparable in a qualitative sense. With this proviso, the methyl ester data for the two columns are broadly similar. When the double bond is close to the carboxyl group, the retention time was lower, reaching a maximum for 5- and 6-18:1, falling for 7-18:1 and rising to almost a plateau for the 8- to 14-isomers; a further small maximum was evident for the 15-isomer. If the $1/k''$ values were plotted against double bond position, the results would be comparable to R_F values from silver ion TLC, but the data would not resemble the smooth "sinusoidal curve" seen with the latter technique [22,24]. The Nucleosil column tended to give

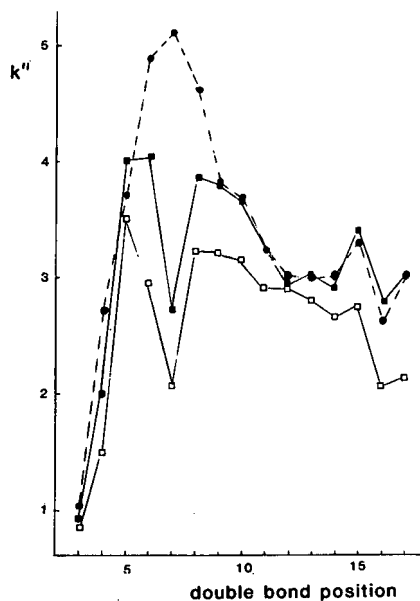


Fig. 3. The k'' values for silver ion HPLC of the methyl (■) and (●) phenacyl esters of the series of *cis*-octadecenoates at 10°C on the Nucleosil column with the mobile phase as Fig. 1, and for the methyl esters on the ChromSpher Lipids column (□) at 15°C with 1,2-dichloroethane–dichloromethane–acetonitrile (50:50:0.01, v/v/v) as mobile phase.

rather better separations of the natural isomers. A difference of 0.2 in the k'' values was sufficient for baseline separation. In contrast, there tended to be much greater differences between the chromatographic behaviour of isomers when they were in the form of the phenacyl esters, especially when the double bonds were relatively close to the carboxyl group. There was a maximum in this instance at the 7-18:1 derivative. It was evident that phenacyl (as opposed to methyl) esters would give better resolution of isomers in which the double bond was in positions 3 to 11, although beyond that point the k'' values were similar. The maxima and minima for the 15- and 16-isomers, respectively, were real and reproducible.

Both the proximal and terminal part of a monoenoic molecule have some potential to influence the interaction between silver ions and the double bond, and to determine which of these was more important methyl ester derivatives of 9-18:1, 11-18:1 and 11-20:1 fatty acids were chromatographed, with the results illustrated in Fig. 4. The 11-18:1 ($k'' = 3.20$) and 11-20:1 ($k'' = 2.90$) fatty acids,

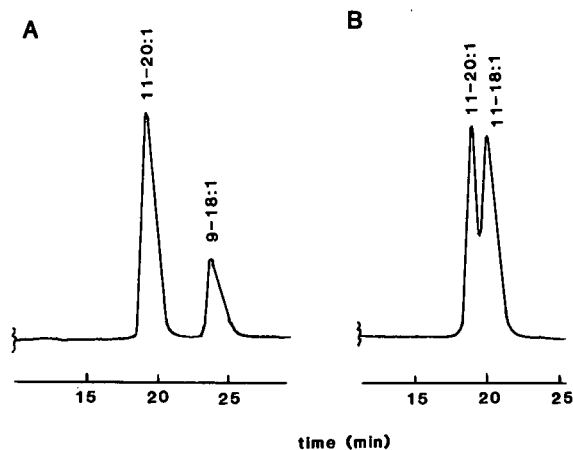


Fig. 4. Separation (partial chromatograms) of methyl esters of fatty acids by silver ion HPLC. Chromatographic conditions as in Fig. 1. (A) 11-20:1 and 9-18:1; (B) 11-20:1 and 11-18:1.

which have the same proximal structure, emerged as two peaks but were only partially separated. On the other hand, 11-20:1 and 9-18:1 ($k'' = 3.75$), which share the same terminal moiety, were fully resolved. Similarly, 9-16:1 ($k'' = 3.86$) was only partially separated from 9-18:1 (not illustrated), but 9-16:1 and 11-18:1 with the same terminal moiety were well resolved. Both parts of the molecule have some influence on resolution, but the major effect is that of distance from the carboxyl group. However, it was not possible to assign partial k'' values to each part of the molecule to predict the retention characteristics of other isomers, presumably because the overall hydrophobicity of the molecule is also relevant.

As expected, *trans*-isomers were less strongly retained than the corresponding *cis* compounds, as can be seen from the k'' values listed in Table I. Phenacyl esters were retained appreciably more than methyl esters, and the order of elution of the corresponding *trans*- and *cis* isomers was not always the same. Isomeric *cis*-octadecenols interacted very strongly with the stationary phase, possibly with oxygen atoms of the sulphonic acid moiety [25] or with residual silanol groups, as well as with the silver ions. However, the isomers were still well separated from each other. The only acetylenic fatty acid derivative available (9a-18:1) was less strongly retained than oleate, as has been reported for silver ion TLC [26].

TABLE I

CAPACITY FACTOR RATIOS (k''), *i.e.* $k''(\text{ANALYTE})/k''(\text{OCTADECENE})$, FOR THE METHYL AND PHENACYL ESTERS OF STANDARD OCTADECENOATES DIFFERING IN THE POSITION AND CONFIGURATION OF THE DOUBLE BOND AND FOR ANALOGOUS LONG-CHAIN ALCOHOLS AND AN ACETYLENIC FATTY ACID

Fatty acid	k''		
	Methyl ester ^a	Phenacyl ester ^b	Alcohol ^b
<i>trans</i> -6-18:1	0.94	2.45	
<i>trans</i> -9-18:1	1.00	2.57	
<i>trans</i> -11-18:1	0.88	2.12	
<i>cis</i> -6-18:1	2.96	4.9	44.6
<i>cis</i> -9-18:1	3.20	3.8	37.6
<i>cis</i> -11-18:1	2.91	3.2	24.4
9-Octadecynoate		2.9	

^a ChromSpher Lipids column.

^b Nucleosil 5SA column, conditions as in Fig. 1.

Limited amounts of a number of isomeric methylene-interrupted *cis,cis*-octadecadienoic acids were also available and their retention characteristics were determined as the methyl and phenacyl esters (Fig. 5). In this instance, the mobile phase was 1,2-dichloroethane–dichloromethane–acetonitrile (50:50:0.35, v/v/v). Again, when the first double bond was close to the carboxyl group, the retention time was low, increasing to a maximum in the region around the 6,9- to 8,11-isomers before tending to fall, although not uniformly. It appeared that adjacent isomers were in general more easily resolved as the phenacyl esters. The k'' values of specific dienes tended to be much greater than the sum of the k'' values for the appropriate *cis*-monoenes. For example, the sum of k'' for the phenacyl esters of 6-18:1 and 9-18:1 was 7.1 (with the same mobile phase), whereas that for 6,9-18:2 was 12.8. The difference of 5.7 units may represent some increase in the interaction of silver ions with the bis-double bond system because of its spatial arrangement. Only with the isomer with double bonds closest to the carboxyl group was the difference slightly negative. Note that k'' values of specific components increased as the concentration of acetonitrile in the mobile phase was increased, and factors were introduced into the calculations to ensure that all the data referred to a common base value. Similarly,

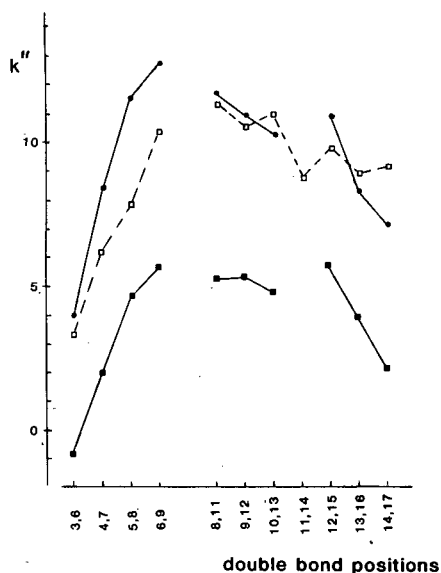


Fig. 5. The k'' values for silver ion HPLC of isomeric methylene-interrupted *cis,cis*-octadecenoates. □ = Methyl esters on the ChromSpher Lipids column with 1,2-dichloroethane–dichloromethane–acetonitrile (50:50:0.35, v/v/v) as mobile phase at 15°C; ● = phenacyl esters on the Nucleosil 5SA column under the same conditions; ■ = difference between the k' values for the dienes and those calculated by summation of the data for the appropriate monoenes.

small amounts of some non-methylene-interrupted octadecenoic acids were available, and k'' values were obtained and are listed in Table II. The allenic

TABLE II
CAPACITY FACTOR RATIOS (k''), *i.e.* $k'(\text{ANALYTE})/k'(\text{OCTADECENE})$, FOR THE METHYL AND PHENACYL ESTERS OF ISOMERIC OCTADECADIENOATES

Fatty acid	k''	
	Methyl ester ^a	Phenacyl ester ^b
9,10-18:2		0.7 ^c
9- <i>cis</i> ,11- <i>trans</i> -18:2		2.2 ^c
9- <i>cis</i> ,12- <i>cis</i> -18:2	10.3	10.9
6- <i>cis</i> ,10- <i>cis</i> -18:2	45.0	
8- <i>cis</i> ,12- <i>cis</i> -18:2	42.5	
6- <i>cis</i> ,11- <i>cis</i> -18:2	29.0	
7- <i>cis</i> ,12- <i>cis</i> -18:2	26.6	
5- <i>cis</i> ,12- <i>cis</i> -18:2	17.7	

^a ChromSpher Lipids column.

^b Nucleosil 5SA column, conditions as in Fig. 5.

^c Conditions as in Fig. 1.

compound, 9,10-18:2, was retained much less than oleate, presumably because of a very weak interaction between silver ions and the delocalized π -electrons of the double bonds, as had been reported earlier for silver ion TLC and methyl laballenate (5,6-18:2) [27]. For a similar reason, the conjugated diene (9-*cis*,11-*trans*-18:2) was only weakly retained, as for silver ion TLC [28]. In contrast, isomers with more than one methylene group between the double bonds were very strongly retained, those with two methylene groups between the double bonds being held most strongly of all, followed by those with three and then those with five.

It was not possible to find isocratic elution conditions to permit the separation of a wide variety of polyunsaturated fatty acid derivatives in a reasonable time. To obtain quantitative information on the degree of retention of such compounds, therefore, capacity factors for a range of fatty acids with 3–6 double bonds were determined relative to that of the corresponding linoleate derivative, which was in turn related to that of the oleate derivatives (taken as 1.0). The results are given in Table III. It appeared that the capacity factors of polyunsaturated esters on silver ion HPLC rose in an almost exponential manner with the number of double bonds, so that docosahexaenoate was retained up to 30 times as strongly as oleate. Phenacyl esters were

TABLE III
RATIO OF THE CAPACITY FACTORS (k') OF METHYL AND PHENACYL ESTERS OF SOME POLYUNSATURATED FATTY ACIDS (PUFA) TO THAT OF OLEATE

The Nucleosil 5SA column was used with a mobile phase of 1,2-dichloroethane–dichloromethane–acetonitrile in the proportions 50:50:1 (v/v/v) for the diene to tetraene and 50:50:1.5 (v/v/v) for the pentaene and hexaene at a flow-rate of 1.5 ml/min at 10°C.

Fatty acid	$k'_{\text{PUFA}}/k'_{18:1}$	
	Methyl ester	Phenacyl ester
9-18:1	1.0	1.0
9,12-18:2	2.9	3.5
6,9,12-18:3	7.1	9.4
9,12,15-18:3	7.9	9.9
5,8,11,14-20:4	10.3	14.2
5,8,11,14,17-20:5	16.7	19.7
4,7,10,13,16,19-22:6	21.5	30.1

again held consistently more strongly than methyl esters.

DISCUSSION

The mechanism of the interaction of silver ions with double bonds in chromatographic systems has never been fully elucidated. It is known that a single silver ion can interact with two double bonds simultaneously, since crystalline complexes with two moles of ethylene [29] and other olefins [30] have been isolated. In favourable circumstances, a silver atom may interact with two double bonds in the same molecule [31]. It would be expected that degree of retention would depend mainly on the strength of the interaction between the silver ions and the π -electrons of the double bonds. However, in silver ion TLC, interactions between parts of the molecule and silanol groups on the surface of the silica must also be considered. In the HPLC system described here, some interactions with residual silanol moieties are also possible, as is some form of bonding with the oxygen atoms of the sulphonic acid group or hydrophobic interactions with the propylphenyl moieties. Morris *et al.* [22] suggested that the greater mobility of the isomers with a double bond near the ester group in silver ion TLC was due to the partial withdrawal or delocalization of the π -electrons of the double bond caused by the inductive effect of the ester group. However, as such an effect decreases rapidly with increasing distance between the double bond and the ester group, it can explain the behaviour of the first members of the series only. Others [24] considered that a fatty acid methyl ester was held both by the double bond complex with the silver ion and by the interaction between the silanol groups and the ester group. Any isomer with a favourable conformation would be held more strongly.

On the other hand, results that were broadly comparable in a qualitative sense to those given by silver ion TLC were obtained with this HPLC system in which the presence of the propylphenylsulphonic acid moiety ensured that the distance between the silver ions and residual silanol groups was very different from that in a TLC system. The finding that one silver ion may interact with two unsaturated centres at the same time may point to an alternative explanation for the effect of double

bond position on retention characteristics. Thus, there may be some form of dual interaction with a silver ion and both the π -electrons of the double bond and those of the carbonyl moiety of methyl esters or the benzene ring of phenacyl esters. From 9-18:1 onwards, when the possibility of such a simultaneous interaction would seem to be less likely, there was no significant difference between methyl and phenacyl esters.

This suggestion does not imply that there is no effect of the oxygen atoms of the sulphonic acid group or of silanol moieties from the stationary phase on retention, merely that they are separate from the complexation effect. Thus, monoenoic alcohols were very strongly retained and positional isomers were completely resolved.

An interaction between one silver ion and two double bonds simultaneously may also explain the chromatographic behaviour of dienoic derivatives with silver ion HPLC. When the distance between the double bonds was optimum, *i.e.* with a 1,5-*cis,cis*-diene system as with 1,5-hexadiene [31], fatty acids were very strongly retained, and the effect diminished as the number of methylene groups between the double bonds changed. The k'' values remained higher than those of methylene-interrupted dienes, however, and the effect of double bond position was diminished. The theory of complexation between silver ions and *bis*-double bond systems could potentially be applied to polyenes. It would predict that a triene would be held twice as strongly as a diene, a tetraene three times as strongly, and so forth. Such a simple relationship was not found here, possibly because interactions with the ester moiety have to be taken into consideration and because the conformations of polyenes may permit some interactions between silver ions and double bonds that are remote from each other. With bulky molecules such as triacylglycerols, where an ester effect might be less important, one triene residue was retained by the same amount exactly as two dienes in the molecule [12].

This study has confirmed the value of silver ion HPLC for the separation of isomeric fatty acids, and it has shown that phenacyl esters have distinctive properties that facilitate separations. The ability of the system to give reproducible numerical values to describe retention characteristics has given some insight into the mechanism of the interaction

between silver ions and double bonds, and in particular has led us to suggest a mechanism involving a simultaneous interaction between one silver ion and either two double bonds, or one double bond and one other electron-rich moiety. Further work is planned to test this hypothesis.

ACKNOWLEDGEMENTS

This research was funded by the Scottish Office Agriculture and Fisheries Department and by the Karlshamns Scientific Board, Karlshamns, Sweden.

REFERENCES

- 1 L. J. Morris, *Chem. Ind. (London)*, (1962) 1238.
- 2 B. de Vries, *Chem. Ind. (London)*, (1962) 1049.
- 3 L. J. Morris, *J. Lipid Res.*, 7 (1966) 717.
- 4 L. J. Morris and B. Nichols, in A. Niederwieser (Editor), *Progress in Thin Layer Chromatography, Related Methods*, Ann Arbor–Humphrey Sci. Publ., Ann Arbor, MI, 1972, p. 74.
- 5 W. W. Christie, *Lipid Analysis*, Pergamon Press, Oxford, 2nd ed., 1982.
- 6 B. Nikolova-Damyanova, in W. W. Christie (Editor), *Advances in Lipid Methodology—One*, Oily Press, Ayr, 1992, pp. 181–237.
- 7 W. W. Christie, *J. High Resolut. Chromatogr. Chromatogr. Commun.*, 10 (1987) 148.
- 8 W. W. Christie, E. Y. Brechany and V. K. S. Shukla, *Lipids*, 24 (1989) 116.
- 9 W. W. Christie, E. Y. Brechany and K. Stefanov, *Chem. Phys. Lipids*, 46 (1988) 127.
- 10 W. W. Christie and G. H. M. Breckenridge, *J. Chromatogr.*, 469 (1989) 261.
- 11 K. Stefanov, M. Konaklieva, E. Y. Brechany and W. W. Christie, *Phytochemistry*, 27 (1988) 3495.
- 12 W. W. Christie, *J. Chromatogr.*, 454 (1988) 273.
- 13 W. W. Christie, *Fat Sci. Technol.*, 93 (1991) 65.
- 14 P. Laakso and W. W. Christie, *J. Am. Oil Chem. Soc.*, 68 (1991) 213.
- 15 P. Laakso, W. W. Christie and J. Pettersen, *Lipids*, 25 (1990) 284.
- 16 B. Nikolova-Damyanova, W. W. Christie and B. Herslof, *J. Am. Oil Chem. Soc.*, 67 (1990) 503.
- 17 A. Valicenti, F. J. Pusch and R. T. Holman, *Lipids*, 20 (1985) 234.
- 18 W. W. Christie and R. T. Holman, *Chem. Phys. Lipids*, 1 (1967) 407.
- 19 F. D. Gunstone and M. S. F. Lie Ken Jie, *Chem. Phys. Lipids*, 4 (1970) 1.
- 20 R. Wood and T. Lee, *J. Chromatogr.*, 254 (1983) 237.
- 21 W. W. Christie, *High-Performance Liquid Chromatography and Lipids*, Pergamon Press, Oxford, 1987.
- 22 L. J. Morris, D. M. Wharry and E. W. Hammond, *J. Chromatogr.*, 31 (1967) 69.
- 23 B. Breuer, T. Stuhlfauth and H. P. Fock, *J. Chromatogr. Sci.*, 25 (1987) 302.
- 24 F. D. Gunstone, I. A. Ismail and M. S. F. Lie Ken Jie, *Chem. Phys. Lipids*, 1 (1967) 376.
- 25 W. S. Powell, *Anal. Biochem.*, 115 (1981) 267.
- 26 L. J. Morris and M. O. Marshall, *Chem. Ind. (London)*, (1966) 460.
- 27 F. D. Gunstone and M. S. F. Lie Ken Jie, *Chem. Phys. Lipids*, 4 (1970) 131.
- 28 W. W. Christie, *Biochim. Biophys. Acta*, 316 (1973) (204).
- 29 P. H. Kasai, D. McLeod and T. Watanabe, *J. Am. Chem. Soc.*, 102 (1980) 179.
- 30 P. Ganis and J. D. Dunitz, *Helv. Chim. Acta*, 50 (1967) 2379.
- 31 *Gmelin's Handbuch der Anorganischen Chemie*, Vol. 61, Teil (Part) B5, Springer, Berlin, 1975 p. 26.

Rapid method for the determination of glutathione transferase isoenzymes in crude extracts

E. Martínez-Lara, P. Pascual, F. Toribio, J. López-Barea and J. A. Bárcena

Departamento de Bioquímica y Biología Molecular, Facultad de Veterinaria, Universidad de Córdoba, 14071-Córdoba (Spain)

(First received March 20th, 1992; revised manuscript received June 9th, 1992)

ABSTRACT

The analysis of glutathione transferase (GST) isoenzyme patterns is of interest in many fields as hepatic glutathione transferase activity is increased by exposure to a variety of xenobiotics and its isoenzymatic forms are induced differentially. A high-performance liquid chromatography method has been developed for the rapid determination of individual isoenzyme levels in crude extracts using an anion-exchange column connected to an on-line system to automatically detect GST activity with 1-chloro-2,4-dinitrobenzene as the substrate. When 50–200 μ l of a cytosolic fraction of fish liver containing up to 15 mg/ml of protein and less than 2 units of GST were injected, a high resolution and highly reproducible chromatogram was obtained. The activity profile determined automatically showed eight to twelve peaks (depending on the sample) that were quantified and could be classified into three groups. Starting from intact tissue, a complete isoenzyme pattern could be obtained in less than 3 h. The method has been applied to ecotoxicological studies with fish samples.

INTRODUCTION

corrected 17 June 93/AP

Glutathione transferases (GSTs) are a widespread family of isoenzymes implicated in the detoxification of electrophilic xenobiotics as well as in several endogenous functions. One isoform is membrane-bound [1] and another is nuclear [2]. Cytosolic GST isoenzymes are dimers of a number of subunits with molecular masses of about 25 000 and have been grouped into four classes with respect to physiological, structural and genetic similarities: α , μ , π and θ [3,4]. 1-Chloro-2,4-dinitrobenzene (CDNB) is used as a universal substrate for GST isoenzymes.

A wide variety of structurally unrelated compounds have been shown to increase hepatic GST activity in a number of organisms, mostly in laboratory animals (mice and rats). Differential induction of GST isoenzymes has been reported [5,6]. Induction of a particular isoform by a given compound

can be masked if only the overall GST activity of a crude extract is analysed, hence the whole isoenzyme pattern needs to be determined. To this end, several methods have been devised which include an initial affinity chromatography step on GSH-Sepharose or *S*-hexylglucirring (500 rpm). The levels of peroxyacids and hydrogen peroxide were expressed as the mean value of five repeated experiments.

Chromatographic apparatus and conditions

The chromatographic apparatus consisted of an LC-6A HPLC pump (Shimadzu, Japan) equipped with an additional external pulse damper (Shimadzu) and a Type 7125 injection valve (Rheodyne, Cotati, CA, USA). Solvents were degassed using a Type ERC-3110 degasser (Erma Optical Work, Japan). A LiChrosorb RP-18 (10 μ m do not bind or bind loosely lowering recovery yields [6,9,12].

This paper reports a single-step analytical method based on ion-exchange HPLC with automatic on-line detection of activity for the rapid determination of GST isoenzymes in crude biological samples, using CDNB as a non-specific substrate.

Correspondence to: Dr. J. A. Bárcena, Departamento de Bioquímica y Biología Molecular, Facultad de Veterinaria, Universidad de Córdoba, 14071 Córdoba, Spain.

MATERIALS AND METHODS

Chemicals

CDNB and salts for the mobile phases were from Merck; bovine serum albumin (BSA), reduced glutathione (GSH), dithiothreitol (DTT), hexylglutathione, phenylmethylsulphonyl fluoride (PMSF) and *S*-hexylglutathione-agarose were from Sigma. HPLC-grade water was obtained with a Milli-Q system (Millipore). All chemicals used were of analytical-reagent grade.

Buffers and reagents

Buffers were prepared at working temperatures (4°C and room temperature). The extraction buffer contained 10 mM Tris-HCl (pH 7.5), 1 mM EDTA, 5 mM GSH, 2 mM DTT and PMSF at a final concentration of 0.5 mg/g of tissue. The loading buffer (A in Fig. 1) contained 10 mM Tris-HCl (pH 8.0), 0.2 mM EDTA and 0.2 mM DTT; the salt buffer (B) was the same as the loading buffer supplemented with 0.5 M NaCl. To prepare 100 ml of reagent C the following solutions were mixed at room temperature in the order indicated: 30 ml of 13.3 mM CDNB in ethanol; 42 ml of water; 25 ml of 0.4 M sodium phosphate, pH 6.5; 1 ml of 0.1 M EDTA; 2 ml of 10 mg/ml BSA. The same procedure was followed to prepare 100 ml of reagent D except that CDNB was substituted for 30 ml of ethanol and 0.121 g of crystalline GSH was dissolved in the final

solution. Solutions C and D were sonicated. All solutions were filtered through a 0.45- μ m Millipore membrane and degassed.

Chromatographic arrangement

A schematic description of the HPLC set-up is presented in Fig. 1. P4 and D2 were a pump from a Series 2 liquid chromatograph and LC-55 B spectrophotometer, respectively, both from Perkin-Elmer. The rest of the equipment was from Beckman Instruments unless stated otherwise. P1, P2 and P3 were 110B pumps; D1 was a 263 UV variable-wavelength detector; the system was controlled by a 406 analog interface module; data collection and processing was carried out by an AT computer and System Gold software. The column was a DEAE-Spherogel TSK, 10 μ m particle size (7.5 \times 0.75 cm). Extracts were passed through a 0.45- μ m Millipore filter before injection into the column. A precolumn was used to avoid clogging and contamination of the analytical column.

Preparation of crude extracts and pure GST

Livers from the marine fish *Mugil* sp. were obtained immediately after capture and frozen in liquid nitrogen. They were ground in a mortar while immersed in the same coolant. The powder was kept at -80°C and, when needed, was suspended in extraction buffer (4 ml/g) and disrupted using an Ultra Turrax homogenizer. The resulting homogenate was centrifuged at 31 000 g for 30 min at 4°C in a J2-21 Beckman centrifuge. The supernatant was further cleared by ultracentrifugation at 105 000 g for 1 h at 4°C in a Beckman L8-80M apparatus. The first centrifugation step was occasionally omitted. In some experiments GST was further purified by affinity chromatography in a column (6 \times 0.5 cm) of hexylglutathione-agarose equilibrated in 50 mM phosphate buffer (pH 7.0), 1 mM EDTA and 2 mM DTT. The column was washed with 50 mM KCl in the same buffer and eluted with a pulse of 5 mM hexylglutathione in 50 mM Tris-HCl buffer (pH 9.6). The pooled fractions were concentrated by vacuum evaporation and dialysed against extraction buffer without PMSF.

Assays

GST activity was assayed at 37°C following the method of Habig and Jakoby [13] using 1 mM

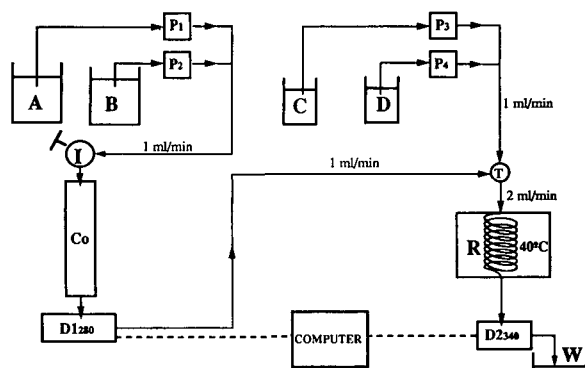


Fig. 1. Schematic diagram of the experimental set up. A = Loading buffer; B = elution buffer; C = CDNB solution; D = GSH solution; P1 and P2 = buffer pumps; P3 and P4 = reagent pumps; I = sample injector; Co = anion-exchange chromatographic column; D1₂₈₀ = protein detector set at 280 nm; D2₃₄₀ = activity detector set at 340 nm; T = T union; R = reactor coil in a water-bath at 40°C; W = waste.

CDNB and 1 mM GSH. When dilute enzyme preparations were assayed, 0.1 mg/ml BSA was included in the reaction mixture. The protein concentration was determined by the method of Lowry *et al.* [14] using BSA as the standard.

RESULTS AND DISCUSSION

System design and optimization of reaction conditions

Solutions C and D, containing CDNB and GSH, respectively (Fig. 1) were intended to have the same viscosity to allow for good mixing, thus giving a low-noise baseline. This is particularly important if only one reagent pump is available. Ethanol was needed to dissolve CDNB, but its concentration was compromised to allow good solubility of CDNB without reaching a limit above which phosphate might crystallize. The final composition of the assay mixture in the reactor was 15% (v/v) ethanol, 1 mM CDNB, 50 mM phosphate (pH 6.5), 0.5 mM EDTA, 0.1 mg/ml BSA and 1 mM GSH. With a 5 m long reactor the reaction time was 0.5 min. The effect of 15% ethanol on the enzymatic activity under the standard assay conditions was to decrease the activity by 11%, which was considered acceptable.

Initially, the response of the system was checked without the column. There was an excellent linearity between the amount of enzyme injected and the peak area. The peaks were symmetrical and their retention times, that is from the time the signal starts until the baseline value is reached again, were always between 1.6 and 1.9 min for sample volumes greater than 25 μ l. This was taken as an indication that mixing and flow through the coils were good.

The set-up of Fig. 1 without the column can be used as a spectrophotometric flow injection analysis (FIA) system. This application could be of value as it would allow the analysis of about 30 samples/h. Optimization would be completed by an automatic sample injector.

Chromatographic behaviour

Crude extracts from fish livers were run on the system equipped with a DEAE-Spherogel column equilibrated in loading buffer and eluted with a linear NaCl gradient (0–0.35 M) starting at 15 min and ending at 60 min. The separation was excellent and repetitive a judged either from the A_{280} profile for total protein or from the A_{340} profile for GST

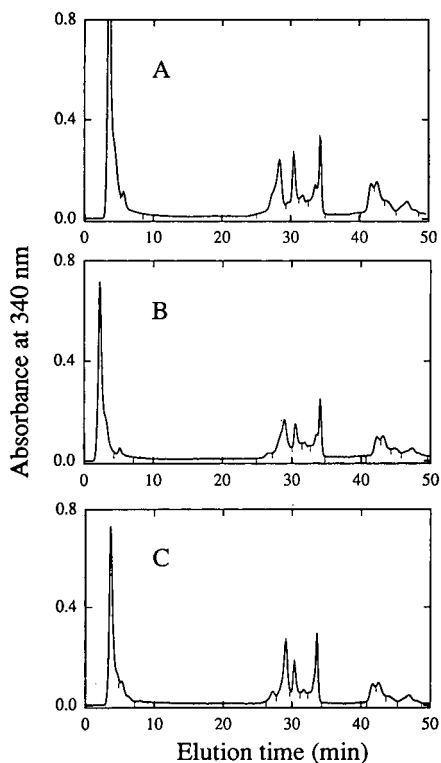


Fig. 2. GST activity profiles of an extract from fish liver. The sample was the soluble fraction from a pool of fish (*Mugil* sp.) livers with 16.0 U/ml GST. Volumes injected were 50 μ l of undiluted preparation in A and 100 μ l of a 1:3 dilution in B and C. The small downward vertical lines are integration marks indicating the beginning and end of each peak. See text for other details of the procedure.

activity. Variation of sample volume in the range 50–200 μ l, containing up to 15 mg/ml protein, did not affect separation, but too much activity in the sample saturated the detection system. Hence the GST activity of the extract was previously determined to define the amount of sample to be injected and this should not be higher than 2 units. If necessary, the sample was conveniently diluted in extraction buffer immediately before injection. Another way to circumvent the problem of saturating the detection set-up could be to shorten the length of the reactor or to lower its temperature, but we preferred to keep these factors unchanged to maintain the standard conditions of the whole arrangement. Alternatively, the length of the reactor could be increased to detect the isoenzyme pattern of samples with low GST activity towards CDNB (*e.g.*,

TABLE I
DETERMINATION OF INDIVIDUAL ISOENZYME CON-
TENTS

The data presented are averages of the three chromatograms shown in Fig. 2.

Peak No.	Retention time (mean \pm S.D.) (min)	Peak area ^a	
		Mean \pm S.D. (U/ μ l)	Relative standard deviation (%)
1	3.50 \pm 0.17	17.77 \pm 1.90	11
2	5.68 \pm 0.36	1.73 \pm 0.51	29
3 ^b	n.d.	n.d.	n.d.
4	28.8 \pm 0.32	6.64 \pm 0.60	9
5	30.4 \pm 0.09	3.40 \pm 0.32	9
6	31.7 \pm 0.09	1.38 \pm 0.13	9
7	34.0 \pm 0.30	5.47 \pm 0.04	1
8	41.9 \pm 0.29	1.87 \pm 0.03	2
9	42.7 \pm 0.32	2.80 \pm 0.11	4
10	44.2 \pm 0.44	0.97 \pm 0.07	7
11	47.0 \pm 0.22	1.71 \pm 0.08	5
Total		43.74 \pm 1.64	4

^a One arbitrary unit of peak area corresponds to 0.367 \pm 0.017 mUnits of GST activity. Peak area values have been divided by the volume of undiluted preparation injected, that is, 50 μ l for A and 33.3 μ l for B and C.

^b Peak No. 3 was not clearly separated in chromatogram A and for that reason was considered as part of peak 4 in all three chromatograms when calculating average peak areas. n.d. = Not determined.

<2 units/ml). However, this situation did not arise during this study.

Fig. 2 shows the activity profiles obtained when different volumes, 50 μ l in A and 100 μ l of a 1:3 dilution of the same sample in B and C, were injected. The repeatability of the method is demonstrated by the striking coincidence of the chromatograms. The results of integrating these chromatograms are summarized in Table I. Depending on the sample, between eight and twelve peaks were resolved and were numbered according to their order of elution from the column. Previously reported anion-exchange HPLC of GST from human placenta resolved just three peaks [15], whereas Fourman and Bend [16] separated five peaks of GST from the liver of skate on a preparative DEAE-cellulose column. Lee *et al.* [17] also separated five peaks on a DEAE-cellulose column from the anionic forms of rat liver.

The isoenzymes could be classified into three groups. Group I was composed of the isoforms that either passed through the column or were retarded but not adsorbed. Two isoenzymes were resolved in this instance. A prominent shoulder around 4.5 min was considered as part of the first peak, although many other samples gave three well separated peaks in this zone, whereas in conventional low-pressure DEAE-Sephacryl chromatography they co-elute [18,19]. Theoretically, these are the basic and neutral species comparable with those from other organisms. However, with ion-exchange chromatography apparently contradictory results can be obtained. For instance, Kispert *et al.* [20] found that "neutral" GST- μ from rat testes behaves as a true acidic form as it binds to a Mono-Q (anionic) column at pH 8.0 requiring 0.15 M NaCl for elution. Hence the order of elution from an ion-exchange chromatographic column cannot be used with confidence to classify the isoenzymes according to their acid-base or electrical properties. Other non-ionic interactions taking place between the exchanger matrix and the proteins have marked effects on their chromatographic behaviour.

Among the isoenzymes retained in the column, those interacting more weakly eluted before 35 min and were included in group II. Acidic isoenzymes that were more tightly bound to the column belonged to group III and were eluted with higher ionic strength (later than 35 min).

The data of Table I show how reproducible the method is, with the variability of peak elution times never exceeding 30 s, that is, less than 1% of the total elution time. The table also shows a very good proportionality between volume of sample injected and peak area (both total and individual). The highest deviations were found among isoenzymes of group I considered individually, although taken altogether their average total area per microlitre injected was 19.51 \pm 1.75, that is, a relative standard deviation of 9%.

When affinity purified GST preparations were run and protein profiles were matched with activity profiles, it was observed that isoenzymes of group II were those with the highest specific activity, whereas those eluting in group III had the lowest specific activity. Occasionally the column eluate was collected in fractions of 300 μ l to determine the activity manually. The chromatographic activity profile

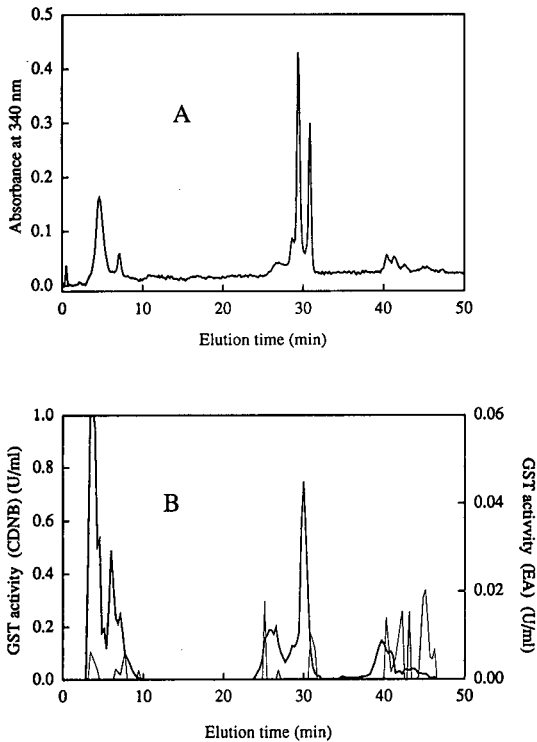


Fig. 3. Comparison of GST activity profiles obtained automatically and manually. The sample was a soluble fraction from fish (*Mugil* sp.) liver that had been purified by hexylglutathione affinity chromatography. The preparation had 66 U/ml GST. (A) 80 μ l of a five-fold diluted solution were injected and the activity was determined automatically. (B) 100 μ l of undiluted preparation were injected and the activity was determined manually in 300- μ l fractions; the elution time was obtained by extrapolation from the elution volume. Heavy line: activity with CDNB; light line: activity with ethacrynic acid. Other conditions as in Fig. 2.

obtained in this way basically coincided with that obtained automatically although, as expected, resolution of the peaks was lower (Fig. 3). When CDNB was replaced by ethacrynic acid in the manual assay of fractions, most of the activity was found in group III and particularly around 47 min (Fig. 3B). A similar result was obtained by Lee *et al.* [17].

Comments

It has been argued [12] that the determination of GST isoenzymes by methods based on activity measurements is not as reliable as that based on protein subunit determination. The method described herein, with the automatic on-line detection of activity, can be performed in less than 3 h from the

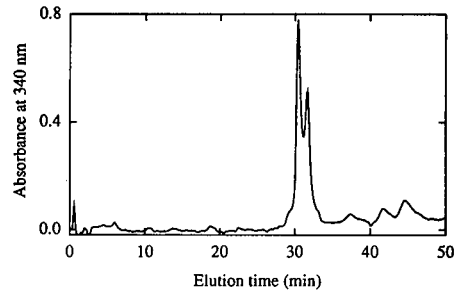


Fig. 4. GST activity profile of the fraction not bound to hexylglutathione-Agarose. A 100- μ l volume containing 630 mU of GST activity were injected into the column. The sample was the fraction of cytosolic extract from fish liver that passed unretained through a hexylglutathione-agarose column. Other conditions as in Fig. 2.

intact tissue to production of the chromatogram (centrifugation at 30 000 g during preparation of the soluble fraction can be bypassed). This rapid processing allows for the control of activity losses. It gives information on isoenzymes as they are *in vivo* and not of the subunit components artificially separated by the denaturing conditions of sodium dodecyl sulphate-polyacrylamide gel electrophoresis or reversed-phase HPLC. Moreover, when an affinity chromatography step is included before the determination of isoenzyme content, some of the isoenzymes may be lost in the fraction which is not bound to the affinity matrix [6,9,12]. Actually, in this work, unbound GST typically accounted for 10% of the total activity recovered after the affinity chromatography under conditions such that the capacity of the column was not exceeded. Fig. 4 shows the activity profile obtained when the unbound fraction was run on our HPLC-DEAE system. The chromatogram showed two main peaks at 30.4 and 31.6 min with small shoulders at 29 and 33 min and minor peaks at 37, 42 and 45 min, thus supporting the idea that the affinity chromatography step discriminates against some isoenzymes of group II and group III present in crude extracts.

Van Ommen *et al.* [21] have pointed out that GST determination using CDNB does not properly express sample variability due to the lack of specificity of this substrate, whereas other substrates give differences of several orders of magnitude between certain isoenzymes. We believe that it is most convenient to use a universal substrate that gives the maximum activity with all the isoforms, provided

that each isoenzyme has been characterized *ad hoc*. To set a “specificity calibration” is the aim of present investigations.

In preliminary experiments, the method has worked satisfactorily for the detection of differences in the levels of individual isoenzymes in hepatic extracts from fish captured in contaminated and non-contaminated waters [22].

ACKNOWLEDGEMENTS

This research was financed by grant SAL-89-1018 from the Spanish CICYT. Thanks are given to PEMARES for providing us with the fish.

REFERENCES

- 1 R. Morgenstern and J. W. de Pierre, *Eur. J. Biochem.*, 134 (1983) 591–597.
- 2 K. H. Tan, D. J. Meyer, N. Gillies and B. Ketterer, *Biochem. J.*, 254 (1988) 841–845.
- 3 B. Mannervik, *Adv. Enzymol. Relat. Areas Mol. Biol.*, 57 (1985) 357–417.
- 4 B. Mannervik, Y. C. Awasthi, P. G. Board, J. D. Hayes, C. Di Ilio, B. Ketterer, I. Listowski, R. Morgenstern, M. Muramatsu, W. R. Pearson, C. B. Pickett, K. Sato, M. Widersten and C. R. Wolf, *Biochem. J.*, 282 (1992) 305–306.
- 5 L. I. McLellan and J. D. Hayes, *Biochem. J.*, 263 (1989) 393–402.
- 6 W. R. Pearson, J. J. Windle, J. F. Morrow, A. M. Benson and P. Talalay, *J. Biol. Chem.*, 258 (1983) 2052–2062.
- 7 P. C. Simons and D. L. Van der Jagt, *Anal. Biochem.*, 82 (1977) 334–341.
- 8 D. L. Van der Jagt, L. A. Hunsaker, K. B. García and R. E. Royer, *J. Biol. Chem.*, 260 (1985) 11603–11610.
- 9 P. Ålin, U. H. Danielson and B. Mannervik, *FEBS Lett.*, 179 (1985) 267–270.
- 10 A. Aceto, C. Di Ilio, S. Angelucci, M. Felaco and G. Federici, *Biochem. Pharmacol.*, 38 (1989) 3653–3660.
- 11 L. I. McLellan and J. D. Hayes, *Biochem. J.*, 245 (1987) 399–406.
- 12 A.-K. Ostlund-Farrants, D. J. Meyer, B. Coles, C. Southan, A. Aitken, P. J. Johnson and B. Ketterer, *Biochem. J.*, 245 (1987) 423–428.
- 13 W. H. Habig and W. B. Jakoby, *Methods Enzymol.*, 77 (1981) 398–405.
- 14 O. H. Lowry, M. J. Rosebrough, A. L. Farr and R. J. Randall, *J. Biol. Chem.*, 193 (1951) 265–275.
- 15 L. L. Radulovic and A. P. Kulkarni, *Biochem. Biophys. Res. Commun.*, 128 (1985) 75–81.
- 16 G. L. Foureman and J. R. Bend, *Chem.-Biol. Interactions*, 49 (1984) 89–103.
- 17 E. Lee, S. Okuno and K. Kariya, *Comp. Biochem. Physiol.*, 86C (1987) 41–44.
- 18 E. Martínez-Lara, *Master's Thesis*, Veterinary Faculty, University of Córdoba, 1990.
- 19 P. Pascual, *Master's Thesis*, Veterinary Faculty, University of Córdoba, 1991.
- 20 A. Kispert, D. J. Meyer, E. Lalor, B. Coles and B. Ketterer, *Biochem. J.*, 260 (1989) 789–793.
- 21 B. Van Ommen, J. J. P. Bogaards, W. H. M. Peters, B. Blaauboer and P. J. Van Bladeren, *Biochem. J.*, 269 (1990) 609–613.
- 22 P. Pascual, E. Martínez-Lara, F. Toribio, J. López-Barea and J. A. Bárcena, *Biochem. Soc. Trans.*, 19 (1991) 302S.

Separation of dideoxyribonucleosides in trace amounts by automated liquid chromatography and capillary electrophoresis

Ram P. Singhal, Dianna Hughbanks and Jun Xian

Department of Chemistry, Wichita State University, Wichita, KS 67208 (USA)

(First received February 7th, 1992; revised manuscript received May 5th, 1992)

ABSTRACT

No satisfactory high-performance liquid chromatographic (HPLC) method is currently available for the separation of the major dideoxyribonucleosides (ddNs) and their derivatives. A method involving HPLC has been developed for the separation of five major ddNs [ddA, ddC, ddI, azT and 2',3'-dideoxy-2',3'-didehydrothymidine (d4T)]. Elution of the common and modified components of DNA was also examined under the selected separation conditions of HPLC. The elution characteristics of these compounds were studied using serum plasma samples spiked with ddN derivatives. In addition, capillary electrophoresis (CE) was investigated for the separation of ddNs and their derivatives. Picomolar amounts of the five major ddNs and the metabolic product of azT [5'-O-glucuronide-3'-azido-3'-deoxythymidine (Glo-azT)] were satisfactorily resolved in 10 min by using a modification of CE. The spectral properties of the ddNs were characterized under different pH conditions and compared with those of their parent deoxyribonucleosides (dNs) because these compounds are commonly measured in HPLC by their spectral properties. The spectra of ddC and ddT derivatives resemble very closely those of dC and dT, but those of ddA and ddI differ to some extent from their parent dNs. The HPLC method was extensively examined for satisfactory resolutions of these compounds. For example, an isocratic elution method, although simple, failed to resolve these compounds and ion-pair chromatography did not offer any advantage. Gradient elution involving buffered solutions and increasing amounts of an organic modifier yielded satisfactory results. Methanol appeared to be the organic modifier of choice. A reversed-phase matrix with smaller than octadecyl alkyl chains did not produce the necessary interactions. Uniform spherical beads of smaller diameter produced superior resolutions. The separation of these compounds on three commercially available columns is discussed. The separation of human plasma samples spiked with dideoxynucleoside derivatives by HPLC was accomplished in *ca.* 16 min. The presence of the dNs did not interfere in their separations.

INTRODUCTION

Simple, rapid, and accurate methods for the separation of dideoxyribonucleoside derivatives are needed to study the compounds directed towards suppressing human immunodeficiency virus (HIV). These methods are necessary to provide pharmacokinetics in patients with AIDS and related disorders. The distribution of 3'-azido-3'-deoxythymidine (azT) and its metabolic end product, 5'-O-glucuronide-3'-azido-3'-deoxythymidine (Glo-azT) in blood plasma and urine samples and different organs has been examined by numerous investigators using high-performance liquid chromatographic (HPLC) methods [1-13]. Pharmacokinetics of dideoxyribonucleoside derivatives [such as 2',3'-dideoxyadenosine (ddA), 2',3'-dideoxycytidine (ddC), 2',3'-dideoxyuridine (ddU) and 2',3'-dideoxyinosine (ddI)] have also been studied by using different HPLC methods [14-20]. Other techniques used for the study of these compounds include radioactive tracers [21], enzyme-linked time-released fluoroimmunoassay [22,23], and liquid chromatographic-thermospray mass spectrometric methods [24,38].

curonide-3'-azido-3'-deoxythymidine (Glo-azT) in blood plasma and urine samples and different organs has been examined by numerous investigators using high-performance liquid chromatographic (HPLC) methods [1-13]. Pharmacokinetics of dideoxyribonucleoside derivatives [such as 2',3'-dideoxyadenosine (ddA), 2',3'-dideoxycytidine (ddC), 2',3'-dideoxyuridine (ddU) and 2',3'-dideoxyinosine (ddI)] have also been studied by using different HPLC methods [14-20]. Other techniques used for the study of these compounds include radioactive tracers [21], enzyme-linked time-released fluoroimmunoassay [22,23], and liquid chromatographic-thermospray mass spectrometric methods [24,38].

Correspondence to: Professor R. P. Singhal, Department of Chemistry, Wichita State University, 1845 N. Fairmount, Wichita, KS 67208, USA.

In addition, 3'-azido-2',3'-dideoxy-5-methylcytidine [25] and 3'-azido-2',3'-dideoxythymidine [26] have also been separated by HPLC methods. A two-column HPLC method was recently employed for the separation of mono-, di- and triphosphates of azT [27].

The separation method of choice for the dideoxy-ribonucleosides (ddNs) appears to be HPLC and it has been used more extensively than other methods. Recently, Jang and Brown [28] described guidelines for predicting the resolutions of different ddNs and 3'-azido-3'-deoxy thymidine monophosphate (azTMP) in HPLC separations. In addition, they examined the effects of temperature, eluent pH and methanol. At present, no satisfactory HPLC method is available for the separation of major ddN derivatives. Here, we describe the development of an HPLC method for the separation of five drugs of major clinical significance [ddA, ddC, ddI, azT, and 2',3'-dideoxy-2',3'-didehydrothymidine (d4T)] and demonstrate the elution of the common and modified components of DNA under the selected separation conditions.

Electrokinetic chromatography is applied to both HPLC and capillary electrophoresis (CE). It is most effective for the separation of electrically neutral substances. Micellar electrokinetic capillary electrophoresis (MEKC) is most commonly used, and involves the electrophoretic migration of ionic micelles with a velocity different from that of the bulk solution [29–32]. In micellar EKC, the separation is based on differential partition of the solute between the micelles and the surrounding aqueous (polar) phase. Micelles display electrophoretic migration, often towards the sample electrode; the mobile polar solution (buffer) on the other hand, exhibits stronger movement towards the detector electrode because of electroosmosis. MEKC offers extremely high efficiency of separation in comparison with HPLC. In contrast, HPLC separation is based on the partition of the solute between the mobile polar phase and the stationary phase (non-polar in the reversed-phase mode). Not only does MEKC offers powerful separations of neutral substances, but it also enhances the selectivity of the ionic substances, in contrast to conventional CE. In this work, we examined the separation of the five representative ddNs and their derivatives by employing the MEKC principle. The separation of these com-

pounds by MEKC is compared with that obtained by HPLC.

EXPERIMENTAL

Analytical system and data-processing equipment

The chromatographic system utilized a manual injection valve (Rheodyne Model 7125), a programmable mobile phase gradient-elution pump (Perkin-Elmer Series LC 4), a reversed-phase liquid chromatographic (RP-LC) column and a diode-array detector (Pharmacia LKB Model 2140 rapid spectral detector). A microcomputer (Zenith Model Z-248, IBM-AT compatible) was used to operate the detection unit and also to collect and store the absorption spectra of the effluent every 1.0 s with the aid of Pharmacia LKB Wavescan-EG software. Analyses were carried out using the diode-array detector. Here the results are shown as topograms, and for clarity some chromatographic peaks are shown at only two wavelengths (260 and 280 nm). Details of this automated equipment have been published elsewhere [33,34].

Chromatographic columns

Silica-based RP-LC (octadecylsilane, C₁₈) columns from three manufacturers were employed: Econosphere C₁₈, 5- μ m beads (25 \times 0.46 cm I.D.), from Alltech (Deerfield, IL, USA), Supelcosil C₁₈, 5- μ m beads (25 \times 0.46 cm I.D.), from Supelco (Bellefonte, PA, USA), and Vydac C₁₈, 5- μ m beads (25 \times 0.46 cm I.D.) and Vydac C₁₈ (10- μ m beads) (25 cm \times 4.63 mm I.D.), from Separation Group (Hesperia, CA, USA). Each column was installed with a guard column.

Nucleoside samples

ddC, azT and Glo-azT were obtained from Sigma (St. Louis, MO, USA) and ddI, ddA and d4T were gifts from Dr. C. Sapino, Site Director, Bristol-Myers (Syracuse, NY, USA). Human plasma samples were obtained from normal donors (see below for sample preparation).

Preparation of dideoxyribonucleoside solutions

Concentrated stock solutions of ddNs were prepared in 1.0 ml of 20 mM succinate buffer (pH 5.5) in a 1.5-ml polyethylene micro centrifuge tube. To enhance the solubility of the purine derivatives and

that of d4T, 0.1 ml of methanol was added to the solution. Each solution was filtered through a 0.2- μ m filter tip–syringe assembly (Millipore, Bedford, MA, USA). Necessary dilutions were carried out with appropriate solutions (0.1 M HCl or 0.1 M NaOH or a buffer of pH 5.5 or 7.0) and the UV spectrum of each sample under different pH conditions was measured. The spectra were collected from 200 to 310 nm with a wavelength step of 0.5 nm. For spectral analyses, a Gilford Response spectrophotometer (Ciba Corning, Oberlin, OH, USA) was used and the data were downloaded using Responstar software (Gilford-Corning) to an IBM-compatible microcomputer and the results were analyzed using a spreadsheet software Excel version 3.0a (Microsoft, Redmond, WA, USA). For HPLC analyses, artificial mixtures of known concentrations of the five ddNs and also six dNs were prepared by mixing appropriate amounts of each compound.

Preparation of normal human plasma samples

A human blood sample (1 ml), drawn using a tuberculin syringe and transferred to a tube containing EDTA, was centrifuged at 1000 *g* at 10°C for 10 min. The supernatant (plasma) was transferred into Eppendorf tubes using a micropipette and diluted (1:10) using physiological saline solution.

Separation of dideoxyribonucleosides and spiked plasma samples

The dideoxyribonucleoside mixture was analysed by HPLC utilizing solvents of different polarities [methanol, tetrahydrofuran (THF) and acetonitrile], different buffer solutions containing an ion-pairing reagent [octanesulphonic acid (OSA)], and different RP-LC columns (see above). Analyses were carried out by using different solvent systems (see Table II in Results). The eluent which produced the best separations contained 20 mM sodium succinate–succinic acid and 1 mM sodium azide (pH 5.50) and various amounts of methanol. A 5–10 μ l-sample was applied by using a 25- μ l sample loop.

Capillary zone electrophoresis system

The CE equipment, designed in this laboratory [35], consisted of the following four basic components: (a) a polyimide-coated fused-silica capillary

tube (80 cm \times 75 μ m I.D. \times 280 μ m O.D.; 52 cm from sample-end electrode to the detector); (b) a specifically designed on-line Z-shaped flow cell with a light path of 3 mm (LC Packing, San Francisco, CA, USA); (c) a Spectroflow 757 variable-wavelength UV monitor (Kratos, Ramsey, NJ, USA), which was modified to accommodate the above-mentioned flow cell; and (d) a high-voltage power supply (0–30 kV) with features of programmable, reversible-polarity output (Bertan, Hicksville, NY, USA). The electric current was monitored by a digital multimeter (John Fluke, Everett, WA, USA). An elution pump (Waters Assoc., Milford, MA, USA) was used for washing the column and initiating the sample injection. The signals from the detector were fed to a strip-chart recorder for instant monitoring of the results. In addition, data were acquired with an IBM-compatible PC by using an analog-to-digital interface and retrieved with the help of software (Nelson Analytical, Cupertino, CA, USA).

Capillary zone electrophoresis operation

The capillary column was first washed by pumping a buffer through it and allowing the pressure to reach a constant value. The liquid flow was then disconnected and the capillary dipped into the sample contained in a miniature conical polyethylene tube. The positive liquid flow current generated by the pump and the gravitational force were enough to allow introduction of the sample into the fine capillary column. The sample flow was allowed for a specific time (between 5 and 20 s). This method of sample application was found to be very reproducible. For example, a 5-s injection introduced 3.0 nl of the sample into the capillary column. This value, having a standard deviation of 0.33 nl or 11%, was based on three different injections. The direction of the solution flow during the electrophoresis was selected by simply changing the polarity of the current.

RESULTS

Spectral properties of dideoxyribonucleosides

The absorption spectra of ddA, ddC, azT, d4T, and ddI under different pH conditions are shown in Fig. 1–5. The spectral properties of these compounds are compared with those of their parent

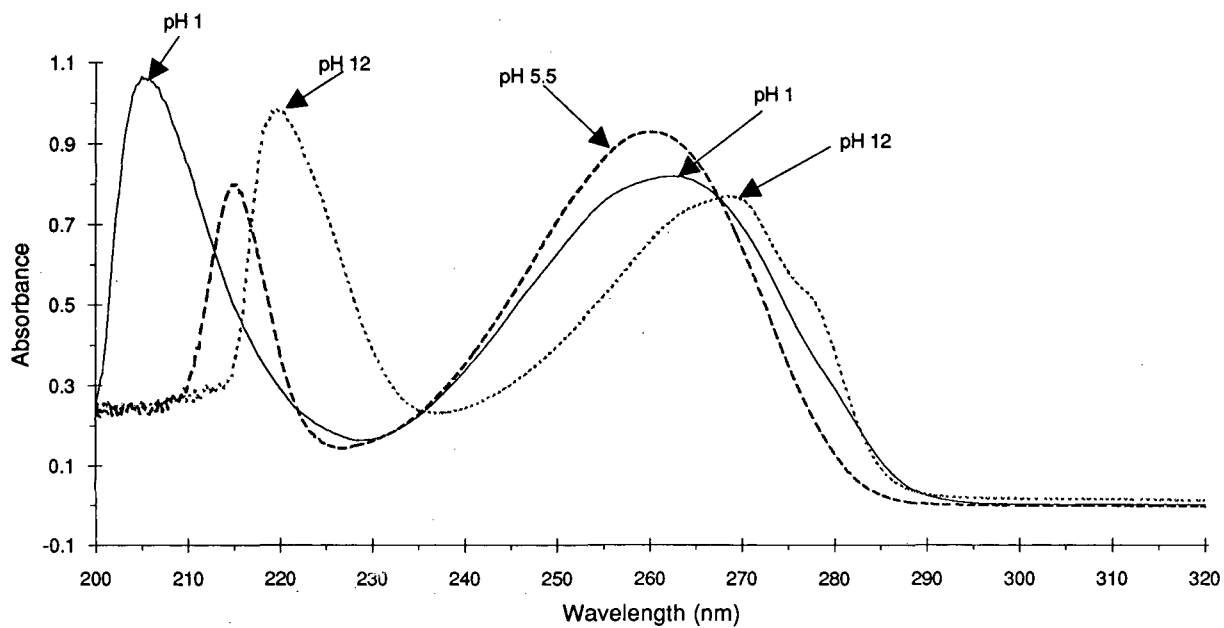


Fig. 1. Spectra of 2',3'-dideoxyadenosine (ddA) at different pH values.

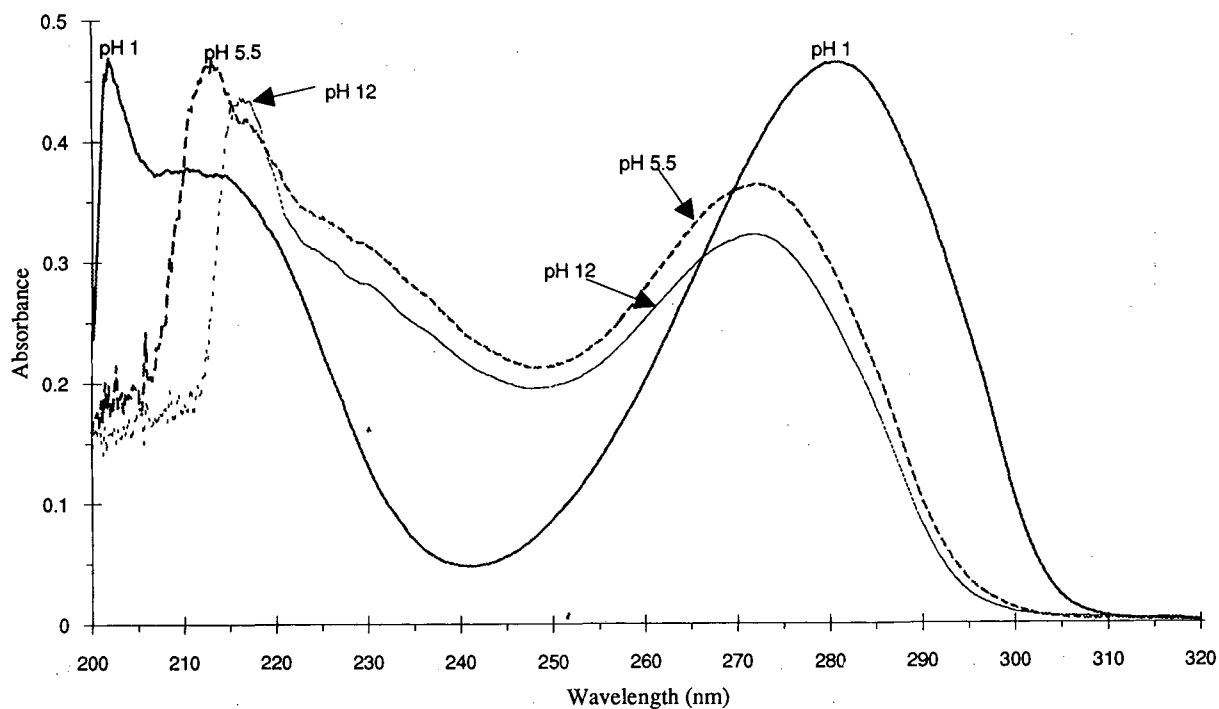


Fig. 2. Spectra of 2',3'-dideoxycytosine (ddC) at different pH values.

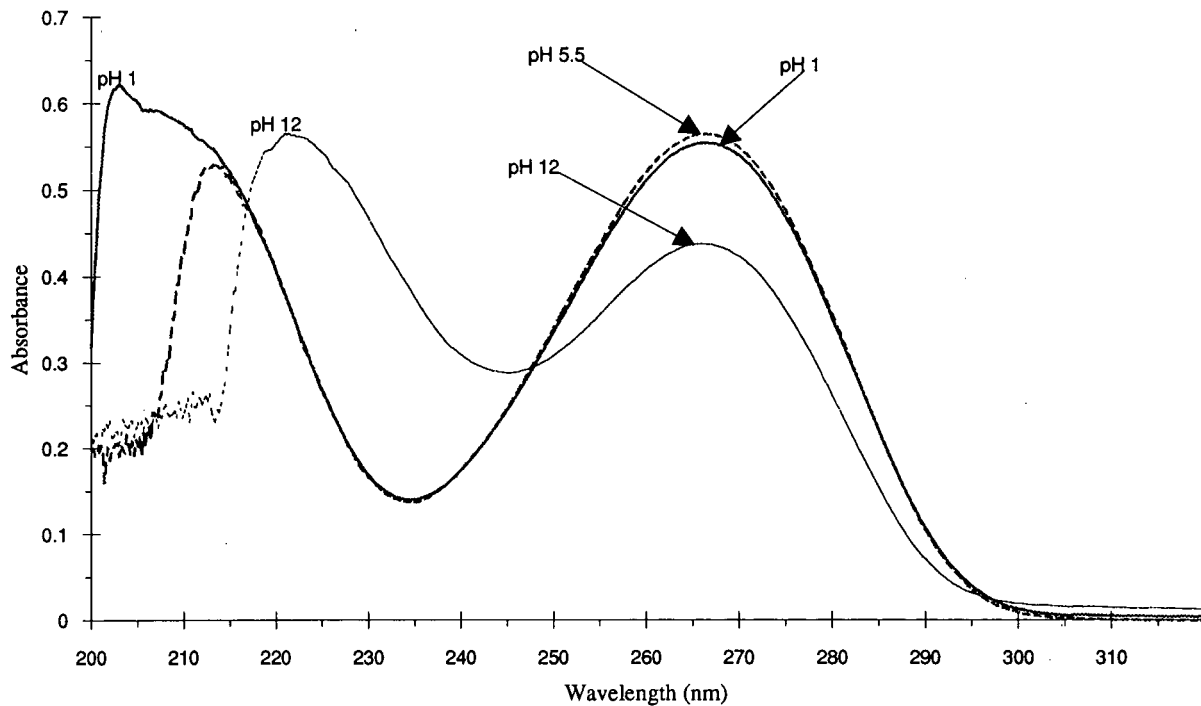


Fig. 3. Spectra of 3'-azido-3'-deoxythymidine (azT) at different pH values.

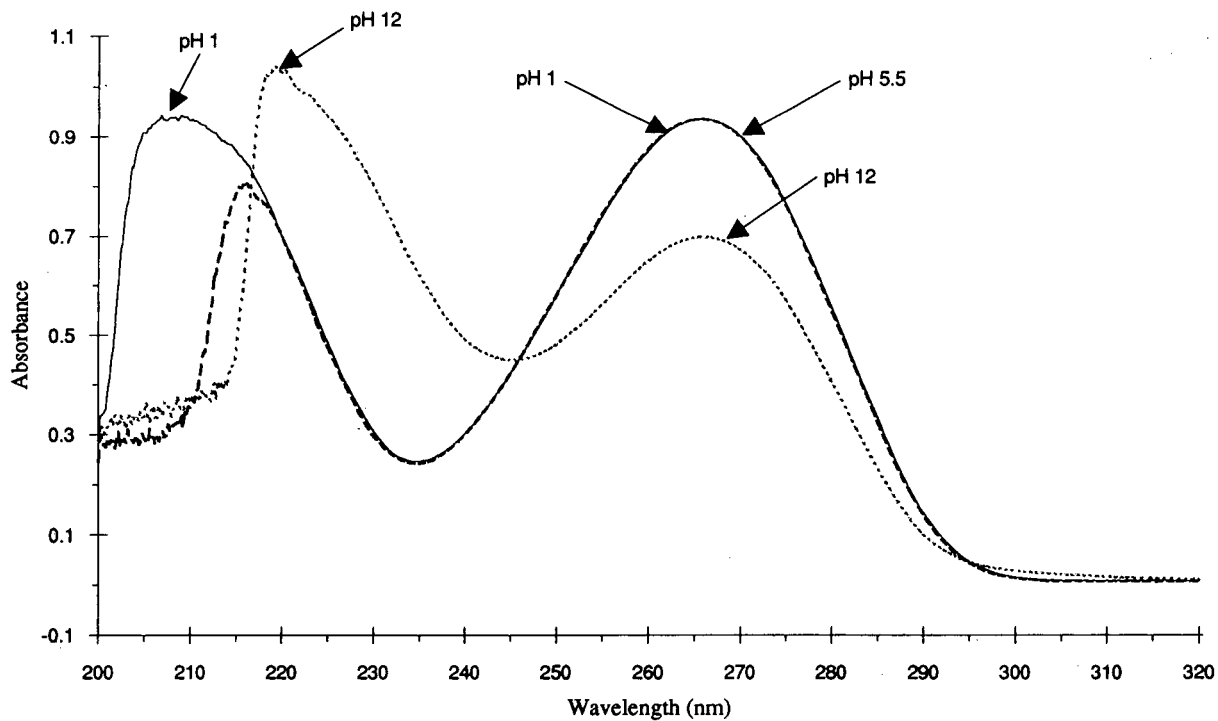


Fig. 4. Spectra of 2',3'-dideoxy-2',3'-dideoxythymidine (d4T) at different pH values.

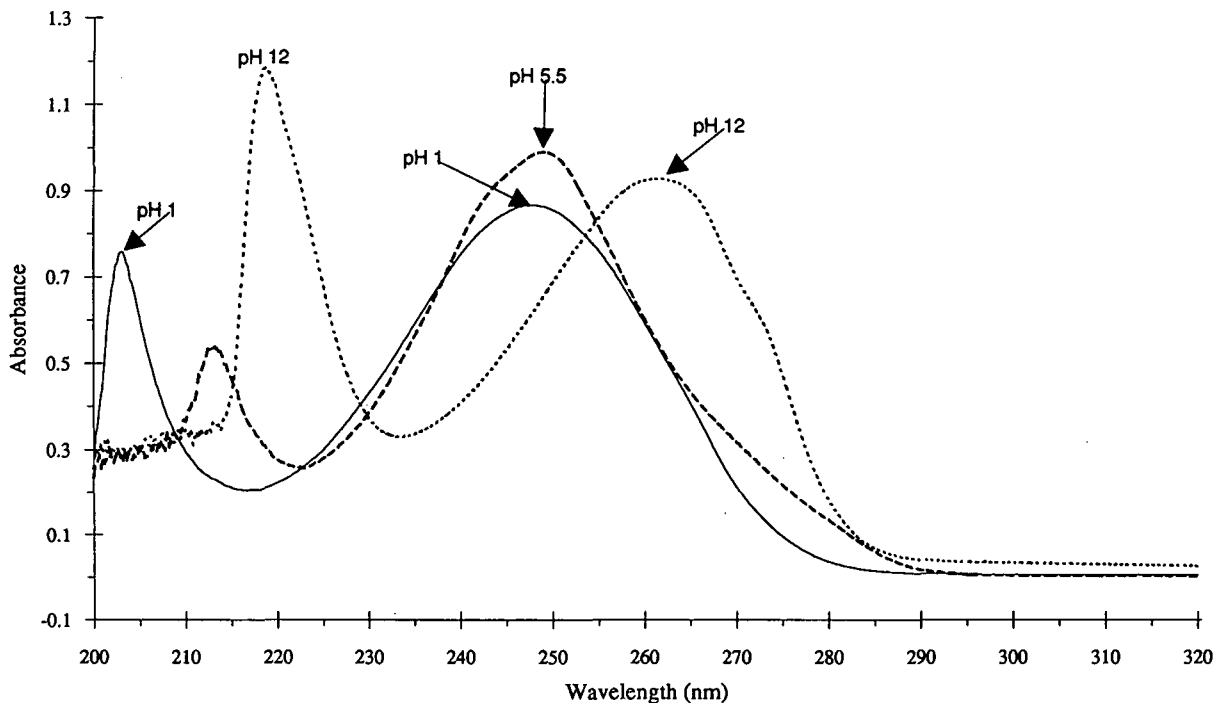


Fig. 5. Spectra of 2',3'-dideoxyinosine (ddI) at different pH values.

dNs in Table I. The ddA spectrum differs considerably from that of the parent compound, dA. Whereas the λ_{\max} of ddA is shifted to a higher wavelength at pH 1 and markedly at pH 12, the λ_{\max} at the neutral pH is changed to a lower wavelength (10 nm). The λ_{\min} values under acidic and neutral conditions do not change between the two adenosine compounds, but the values differ under basic conditions. Although the ddI spectra are very similar to those of dI under acidic and neutral conditions, the λ_{\max} of ddI shifts to a markedly higher wavelength under alkaline condition. The spectra of ddC resemble very closely those of dC and similarly the spectra of azT and d4T correspond to dT.

Development of HPLC methods

Effect of organic solvents in the mobile phase. The effect of three organic solvents having different polarities in the mobile phase was examined for the separation of a complex mixture of dNs and ddNs on a C_{18} column of 5- μm beads. Gradient programs used for different solvents are shown in Table II (see System A), and the results are shown in Fig. 6. Although the use of methanol required a longer analy-

sis time (18 min) as opposed to acetonitrile (15 min) and THF (13 min), the nucleosides were best resolved with methanol in the mobile phase. With THF, considerable baseline drift was observed and several components were poorly resolved. Methanol was selected as the organic modifier of the eluent for further studies. Deoxyribonucleosides and ddNs having more lipophilic character, such as azT and purine derivatives, required higher methanol contents for their elution from the column.

Effect of pH in the mobile phase. The difference in the dissociation constants of adenosine (3.8) and cytidine (4.3) derivatives could be exploited under acidic elution conditions. To induce strong positive charges on dN and ddN derivatives for ion-pair chromatographic separations, we used more acidic eluents (pH 2.5-3.0). However, in a separate study we observed that these compounds in HPLC are best resolved at pH 5.5. A decrease in pH causes loss in resolution between dC and 5-methyldeoxycytidine (m^5dC). An increase in pH at first failed to show any effect, but at $\text{pH} \geq 9$ the dissociation constants of inosine (8.8) and thymidine (9.8) derivatives exhibited an anionic character. However:

TABLE I
SPECTRAL PROPERTIES OF DEOXY- AND DIDEOXYRIBONUCLEOSIDES

Nucleoside	Acidic spectrum			Neutral spectrum			Basic spectrum					
	pH	Max. absorb. (nm)	ϵ_M ($\times 10^{-3}$) ($l \text{ mol}^{-1} \text{ cm}^{-1}$)	Min. absorb. (nm)	pH	Max. absorb. (nm)	ϵ_M ($\times 10^{-3}$) ($l \text{ mol}^{-1} \text{ cm}^{-1}$)	Min. absorb. (nm)	pH	Max. absorb. (nm)	ϵ_M ($\times 10^{-3}$) ($l \text{ mol}^{-1} \text{ cm}^{-1}$)	Min. absorb. (nm)
dA	1.0	257.4	14.5	228.6	5.5	269.6	15.2	226.2	12.0	261.2	14.9	232.8
ddA (Fig. 1)	1.0	262.0	nd ^a	229.0	5.5	260.0	nd	228.5	12.0	268.2	nd	237.0
dC	1.0	279.6	13.2	240.8	5.5	270.6	9.0	249.6	12.0	271.6	9.0	249.6
ddC (Fig. 2)	1.0	279.4	nd	241.5	5.5	272.0	nd	249.0	12.0	271.6	nd	249.5
dT	1.0	267.0	9.7	235.0	7.0	267.0	9.7	235.0	12.0	267.0	7.4	246.0
azT (Fig. 3)	1.0	266.6	nd	235.0	5.5	266.4	nd	235.0	12.0	266.4	nd	246.0
d4T (Fig. 4)	1.0	266.2	nd	235.0	5.5	265.5	nd	235.0	12.0	267.0	nd	246.0
dI	3.0	248.0	12.2	223.0	6.0	248.5	12.3	223.0	11.0	253.0	13.1	224.0
ddI (Fig. 5)	1.0	247.5	nd	217.2	5.5	249.2	nd	223.4	12.0	261.2	nd	234.0

^a nd, Not determined.

TABLE II
GRADIENT ELUTION SYSTEMS USED FOR HPLC SEPARATIONS

System	Stage	Time (min)	Flow-rate (ml/min)	Gradient mode	Elution solvent (%)						
					With methanol		With acetonitrile		With THF		
					Buffer ^a	Methanol	Buffer	Acetonitrile	Buffer	THF	
A	Equilibration Start	10	1.0	Step	95	5	97	3	98	2	
		3	1.0	Linear	80	20	86	14	90	10	
		5	1.0	Linear	70	30	79	21	83	17	
		4	1.0	Linear	40	60	51	49	64	36	
		4	1.0	Linear	5	95	7	93	33	67	
	Hold	3	1.0	Step	5	95	7	93	33	67	
		5	1.0	Linear	95	5	97	3	98	2	
						Buffer-OSA ^b		Methanol			
	B	Equilibration Start	10	1.0	Step	85	15				
			20	1.0	Linear	50	50				
Regeneration		1	1.0	Hold	50	50					
		3	1.0	Linear	5	95					
		5	1.0	Linear	95	5					
							Buffer-OSA ^b		Methanol		
C	Equilibration Start	10	1.2	Step	95	5					
		3	1.2	Linear	80	20					
		5	1.2	Linear	70	30					
		4	1.2	Linear	40	60					
		4	1.2	Linear	5	95					
	Regeneration	3	1.2	Step	5	95					
		5	1.2	Linear	95	5					
						Buffer ^c		Methanol			
	D	Equilibration Start	10	1.0	Step	95	5				
			3	1.0	Linear	80	20				
5			1.0	Linear	70	30					
4			1.0	Linear	40	60					
4			1.0	Linear	5	95					
Regeneration		3	1.0	Step	5	95					
		5	1.0	Linear	95	5					

^a 20 mM sodium succinate-succinic acid buffer with 1 mM sodium azide (pH 5.5).

^b 20 mM sodium citrate-citric acid buffer with 1 mM OSA, 0.2 mM EDTA, 1 mM sodium azide (pH 3.0).

^c 50 mM sodium phosphate-phosphoric acid buffer with 1 mM sodium azide (pH 2.5).

such a highly alkaline solution was unacceptable for the stability of the column. An eluent of pH 5.5 was selected for these studies.

Effect of column temperature. An increase in the column temperature enhanced the elution of purine derivatives more than those of the pyrimidines.

Similarly, the elution of ddN derivatives was enhanced more than those of their parent nucleosides (results not shown). An increase in column temperature significantly lowered the elution time, but not without a substantial decrease in the resolution of early-eluting peaks, such as dC, m⁵dC, dG, and

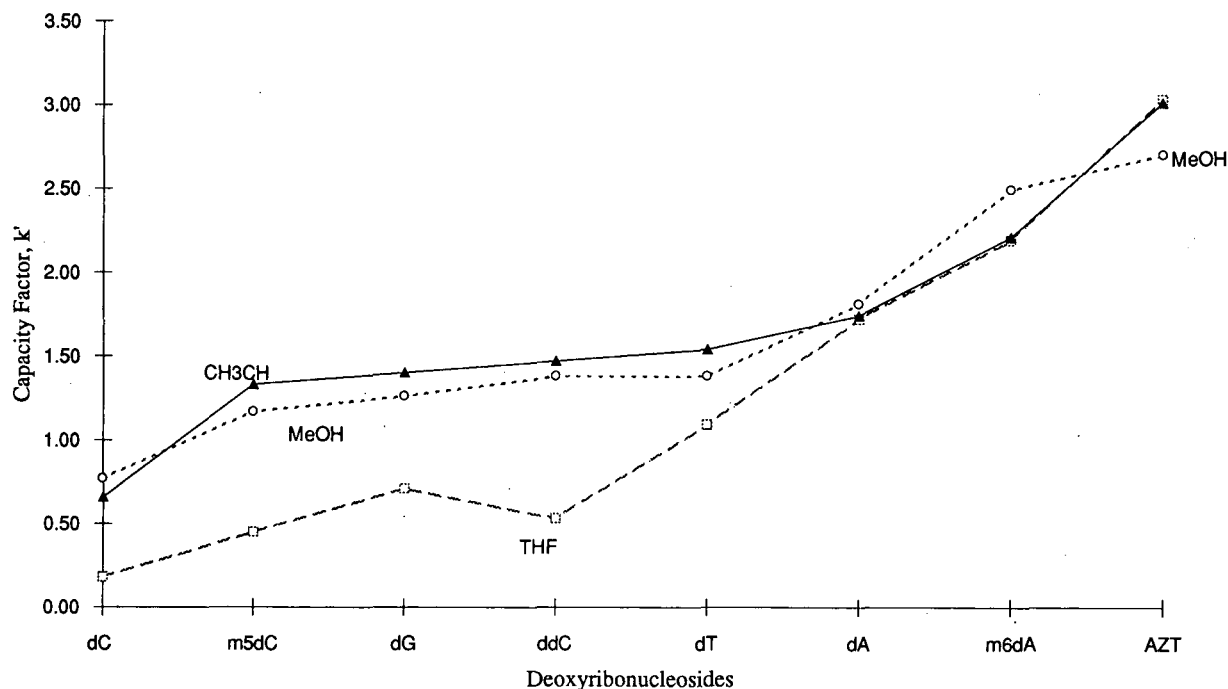


Fig. 6. Effect of organic modifiers [acetonitrile (CH₃CN), methanol (MeOH) and tetrahydrofuran (THF)] on the separation of nucleoside derivatives in HPLC.

ddC components of the mixture. For this reason and ease of operation, room temperature was used for subsequent work.

Separation by ion-pair chromatography. An ion-pairing agent, 1 mM OSA, was added to the elution buffer, 20 mM sodium citrate-citric acid (pH 3.0). Two isocratic elution methods were studied for the separation of a mixture of ddNs (ddA, ddC, ddI, d4T, and azT). A mixture of 95% buffer-OSA and 5% methanol failed to elute the nucleosides from the column. A 10% increase in the methanol content, *i.e.*, using 85% buffer-OSA and 15% methanol, eluted four of the five components of the mixture. The method was then modified to a gradient elution and two different gradient schemes were examined. The first gradient system (B in Table II) produced overlapping peaks of ddC and ddI, followed by a pure peak of d4T, and finally the last two components (ddA and azT) eluted as a mixed peak. The second gradient (C in Table II), although it yielded four sharp peaks in 17 min, it failed to resolve the fifth component (azT) and had a very

erratic baseline. To improve the resolution, a gradient (D in Table II) of lower pH (50 mM sodium phosphate buffer with 1 mM OSA, pH 2.5) and also an isocratic system (85% buffer-14% methanol) were tried. Again, only four of the five components could be resolved and the first two peaks were badly overlapped. From these results, the ion-pairing mode did not appear to offer any special advantage for the separation of these compounds. Several gradient systems involving no use of the ion-pairing agent were examined by systematically changing the methanol concentration. From these results, it was concluded that the separation of ddC from ddI cannot be achieved simply by altering the organic modifier in the gradient system.

Separation on different reversed-phase columns. Reversed-phase C₁₈ columns (25 cm × 0.45 cm I.D.) of 5- μ m and 10- μ m beads from different manufacturers were examined for the separation of a mixture of five nucleoside analogs (ddA, ddC, ddI, d4T, and azT) using gradient elution (System D in Table II). The results (capacity factors) are given in

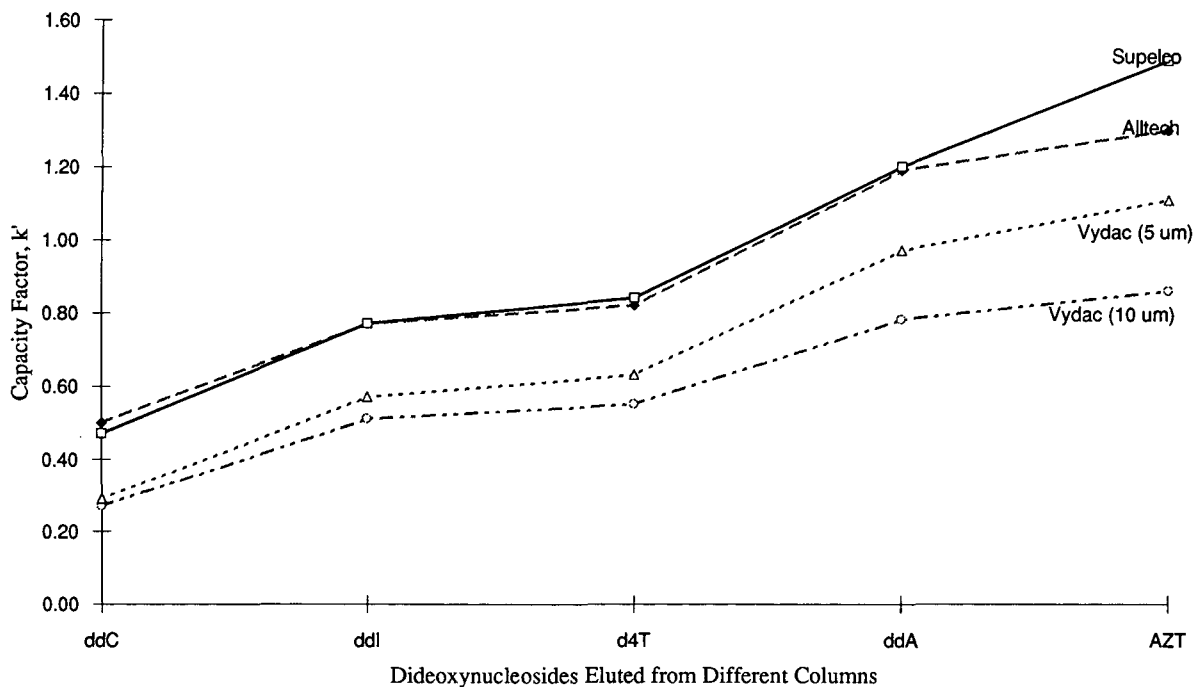


Fig. 7. Performance of different reversed-phase columns in the separation of dideoxyribonucleoside derivatives in HPLC.

Fig. 7. The two Vydac columns, with 5- and 10- μ m beads, gave poor resolutions in general and showed little separation between ddI and d4T components. The Supelco and Alltech columns produced larger k' values, but the former column resolved ddI more satisfactorily from d4T, and similarly ddA from azT. Whereas analysis with the Vydac columns required 18–20 min, separations were completed in less than 17 min with the other two columns. The Alltech column caused trailing of the peaks. The best and fastest separations were obtained with the use of Supelco columns.

Representative separations. A typical separation of a mixture of four common dNs and two minor components of DNAs (m^5dC and m^6dA) with the Supelco column and gradient elution System C (Table II, pH 5.5 buffer) is shown in Fig. 8. Under these conditions, the analysis is completed in 15.5 min and the baseline remains fairly stable. A DNA sample contains either m^5dC in prokaryotes or m^6dA in eukaryotes in addition to the common dNs. Thus, the analysis of a prokaryotic DNA sample is completed in less than 13 min. The analysis of the eu-

karyotic DNA sample can be reduced significantly by modifying elution System A, *i.e.*, by starting elution with 30% methanol and using a step gradient after 60% methanol in the system.

A typical separation of a mixture of five ddNs under conditions identical with those for dNs separation (see above) is shown in Fig. 9. A complex mixture of both six ddNs and six dNs was also separated under these conditions. Although all peaks were resolved satisfactorily for quantification, the separation among m^5dC , ddC and dG did not exceed a resolution factor of 1.0 [36]. No baseline drift at 260 nm was observed, but a small drift was noted in the eluent monitored at 280 nm.

A representative separation of a normal human plasma sample spiked with five ddNs is shown in Fig. 10. No interference is observed between several UV-absorbing plasma proteins and various ddNs, including dNs (results not shown). The plasma proteins are separated into three distinct peaks. Whereas the first two peaks eluted immediately after the void volume in a ratio of 1:1.4, the third peak, eluting in 4 min, varied in concentration from one plas-

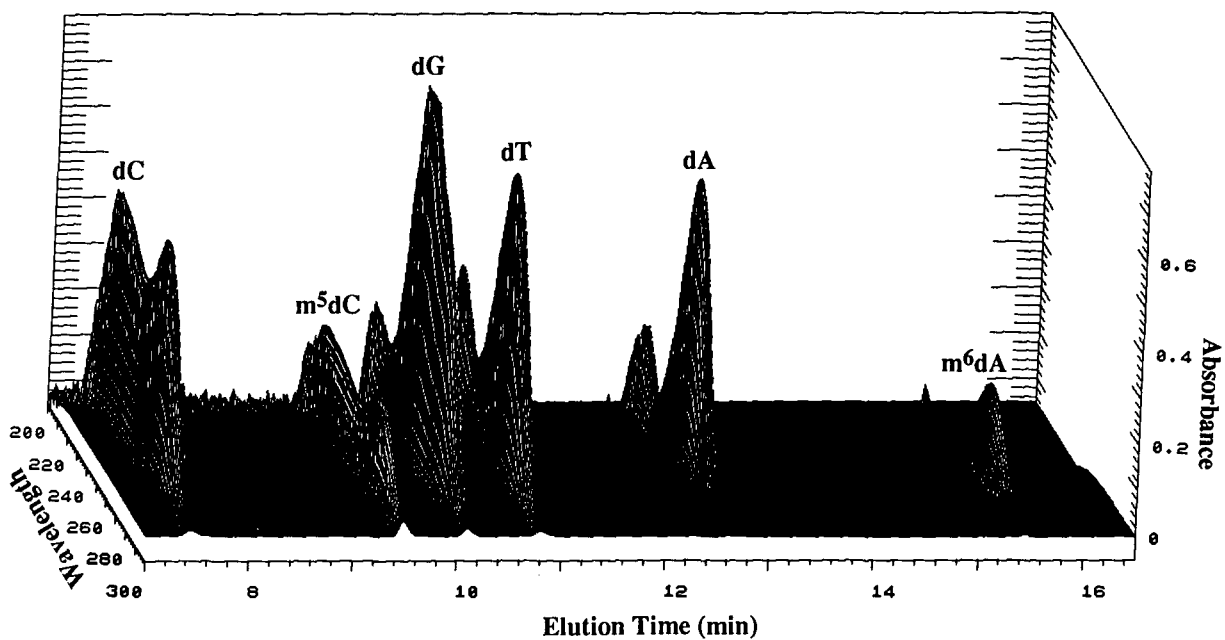


Fig. 8. HPLC: separation of a mixture of the common deoxyribonucleosides and two minor components of DNA (see Results for details).

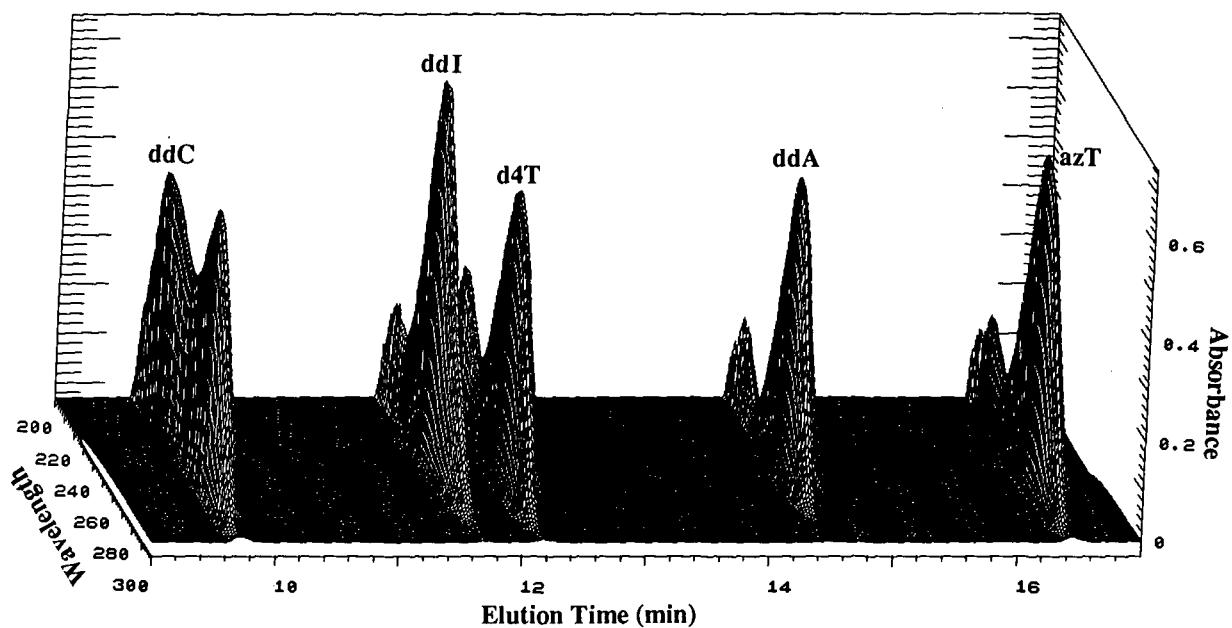


Fig. 9. HPLC: typical separation of a mixture of six dideoxynucleoside derivatives (see Results for details).

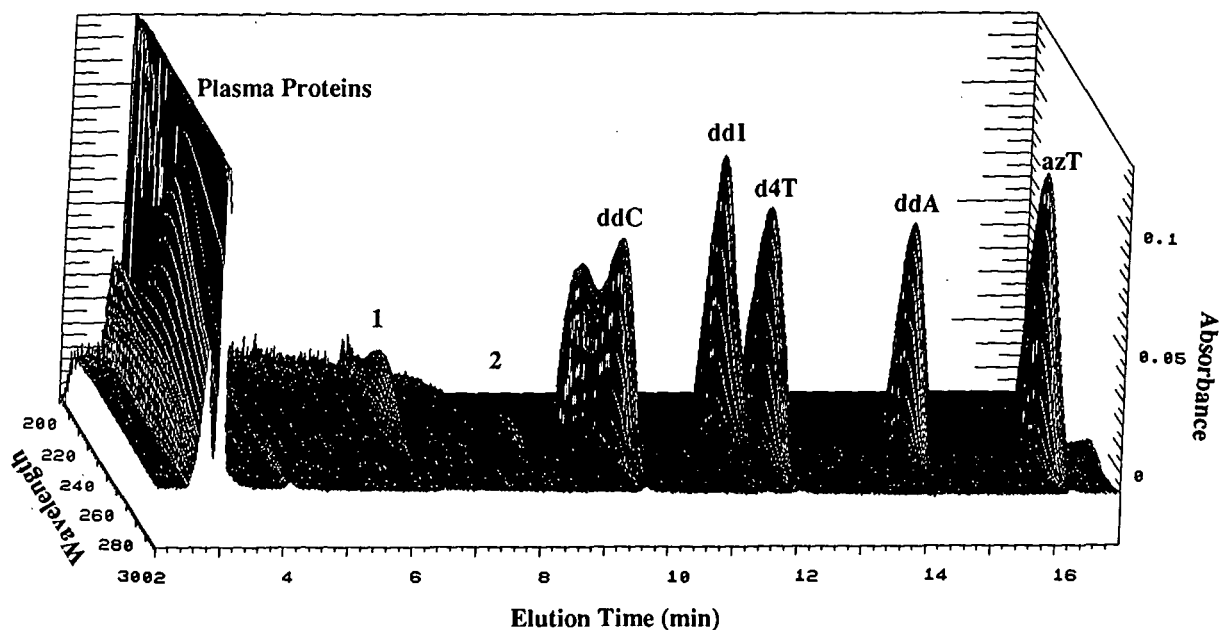


Fig. 10. HPLC: separation of a human blood plasma sample spiked with a mixture of six dideoxynucleoside derivatives (see Results for details).

ma donor to another, but never exceeded 10% of the other two peaks. Two contaminants (peak 1, 6.2 min, and peak 2, 8.2 min) elute between the plasma protein peaks and ddC; they are derived from ddNs and mostly from the ddI sample. The analysis is completed in 16 min. Numerous analyses of ddN mixtures have given identical results with no loss of resolution and repeated use of the same column, provided that appropriate safeguards are observed.

Development of a micellar electrokinetic capillary electrophoresis method

The separation of the ddNs and their derivatives could not be achieved by classical CE, *i.e.*, merely by electroosmosis, because these compounds hardly exhibit any charge difference. For this reason, MEKC was employed to resolve these compounds. To create micelles in the capillary columns, several surfactants in different buffers were examined. Cationic surfactants, such as tetrabutylammonium dihydrogenphosphate (TBAP) and dodecyltrimethylammonium bromide (DTAB) gave no separation of the ddN derivatives. This can be explained by the observation that the strong cationic group (N^+) of

these surfactants initially diminishes the electroosmotic force by furnishing counter charge to the capillary surface (silanol groups). A higher concentration of cationic surfactants caused a reversal of the electroosmotic (direction) flow and the sample solutes migrated towards the sample-end electrode. Peaks could be monitored only when the electrode polarity was altered, *i.e.*, sample-end electrode made cathode and the monitor-end electrode made anode. The ddN mixture eluted as the first peak of Glo-azT in the breakthrough (14 min) and thereafter all five ddNs derivatives co-eluted in 21 min. The reversal of the elution sequence and the decrease in resolution are caused by the charge reversal of the double layer at the capillary surface. However, satisfactory results were obtained by using an anionic surfactant, such as sodium dodecyl sulphate (SDS). A typical separation of a mixture of representative ddN derivatives is shown in Fig. 11 and Table III. The front peak eluting in 7.4 min was derived from contaminants, mostly present in the ddI sample. In contrast to HPLC, d4T and azT components elute much earlier in MEKC.

TABLE III
ANALYSIS OF A MIXTURE OF DIDEOXYNUCLEOSIDE DERIVATIVES BY MEKC

Peak No.	Dideoxynucleoside derivative	Retention time (min)	Absorbance at 260 nm	Amount (pmol)
1	Contaminant	7.4	0.14	0.73
2	d4T	7.7	0.19	0.89
3	ddC	7.9	0.16	0.84
4	ddI	8.4	0.10	0.52
5	azT	8.6	0.18	0.85
6	ddA	8.8	0.20	0.61
7	Glo-azT	9.9	0.18	0.80
Total		10	1.15	5.24

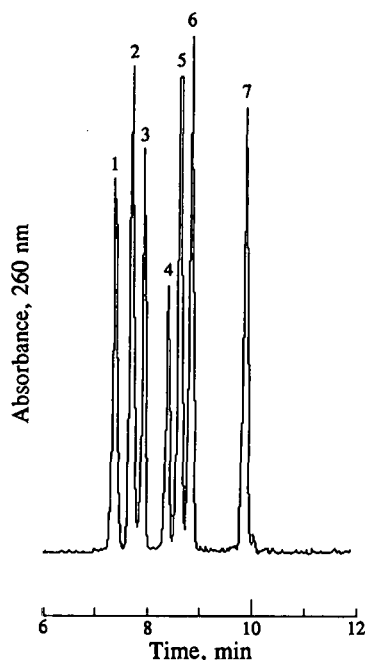


Fig. 11. An artificial mixture of five dideoxynucleosides and Glo-azT derivative was applied (5 s, 3.0 nl) to a fused-silica capillary column (52 cm \times 75 μ m I.D.) and electrophoresis was carried out in 50 mM phosphate buffer containing 40 mM SDS (pH 6.5). The separations were performed at 20 kV (116 μ A) at $21 \pm 0.5^\circ\text{C}$ and the liquid flow was monitored at 260 nm. The front peak was derived from impurities present in the synthetic ddi sample.

DISCUSSION

Development of HPLC methods for the separation of dideoxyribonucleosides

One or more of ddN derivatives have been separated using HPLC mostly with isocratic elutions [2,5-20] and rarely with a gradient elution system [3]. Almost all investigators have used a C_{18} reversed-phase column (25 \times 0.46 cm). Although mostly acetonitrile (in buffers of pH 6.8-7.0) has been used in an isocratic elution, DMF [6] and pH 2.7 [5] have also been employed. No systematic study has been carried out with regard to the use of isocratic *versus* gradient elution, the effect of different organic modifiers, ion-pair chromatography and the performance of reversed-phase columns from one manufacturer to the other.

A method for the separation of five selected ddN derivatives was studied here in detail. These compounds are either used currently (azT, ddi and ddC) or are under human trials (d4T and ddA) for treatment of HIV. The results of this study demonstrate the separation properties of these important nucleoside analogs in a systematic manner. Also included in this study were the separation of the common dNs because these compounds are expected to co-elute with their analogs because of similarities in their structures. The spectral properties of ddNs

were also compared with those of their parent derivatives because these compounds are detected in HPLC by UV absorption.

Spectral properties of dideoxyribonucleosides

The results indicate that the spectra of several ddNs (azT, d4T and ddC) resemble mostly those of their parent dNs because the dissociation constants do not appear to change with modifications in the sugar moiety of the nucleoside. However, ddA spectra are an exception to this rule and they differ from those of dA. While red shifts (towards lower energy) are noted at pH 1 and 12, a blue shift (towards higher energy) is observed at pH 5.5. Similarly, the ddI spectrum, as compared with the dA spectrum, exhibits a red shift under alkaline condition, but none under acidic conditions and very little at pH 5.5. Apparently the lack of an ionizable hydroxyl group in the 3'-position contributes to this difference in the spectrum of ddI (pK_a of 3'-OH = 12). However, spectral differences between ddA and dA cannot be explained on the basis of pK_a differences, since the dissociation constants of the two molecules are identical. Interestingly, the spectra of d4T and azT molecules resemble very closely those of dT, although the deoxyribose is extensively modified in the two structures.

Study of HPLC parameters

Isocratic elution offers simplicity of operation, but this method could not resolve components of the mixture. The effect of organic modifiers on the elution behavior of these compounds clearly indicates that methanol is the modifier of choice (see Table II and Fig. 6). A detailed study of the separation by ion-pair chromatography indicates that the ion-pairing agent (OSA), even under different elution conditions (solvent composition and pH), did not enhance the separation of these molecules. Hydrophobic interactions between the C₈-chain alkyl groups of the agent and the C₁₈ alkyl chains of the column present N⁺ surface charge for ion pairing with any counter ion (OH⁻) of the nucleosides. As pentose hydroxyls are not ionized unless in the vicinity of pH 12, only heterocyclic ring enols can contribute the counter charge. However, these enols are not ionized under the separation conditions employed. It is therefore not surprising to observe that the ion-pairing agent fails to improve resolution

of these compounds, which exhibit similar characteristics.

The bead size and the bead shape of the column matrix, as indicated in earlier studies [37], also appear to be important for these separations. The uniform spherical beads and those of the smaller diameter (5 vs. 10 μm) produced superior resolutions, e.g., less peak tailing and greater peak height-to-width ratio [36]. Reversed-phase columns with alkyl chains smaller than octadecyl, such as C₄ and C₈, did not offer hydrophobic interactions necessary for these separations (results not shown). The study of the reversed-phase C₁₈ columns from three manufacturers reveals that they produce different separations under identical conditions. Each column was described to have a column matrix of similar dimensions and properties. The difference in separation displayed by the different columns can therefore be explained only on the basis of actual uniformity of the beads and capping of the residual silanol groups.

HPLC method of choice

The selected separation method not only demonstrates the resolution of the five ddN derivatives but also those of the six common dNs. The method in addition allows the separation of these compounds even in the presence of blood plasma proteins. Although the metabolic end products of the ddN derivatives (i.e., ddN phosphates) were not included owing to their unavailability, these compounds are expected to behave differently and elute far away from the parent drug. For example, Glo-azT elutes last and away from azT when a mixture of ddNs and this compound is applied to the column (results not shown). The presence of polyols (glucuronide) in the structure makes the molecule slightly more hydrophilic, but the addition of glucuronide to the drug molecule promotes its elution later than the parent compound, azT.

Development of a micellar electrokinetic capillary electrophoresis method

Amphiphilic surfactants, such as SDS, tend to form water-dispersed structurally ordered micelles, which are globules of numerous surfactants arranged with their hydrophilic charged groups on the surface and the hydrophobic tail in the interior of micelles. The micelles are formed when a critical

concentration of the surfactant is reached in the aqueous phase. The separation in MEKC depends on the partition of solutes between the micelles and the aqueous phase. In this study, classical CE did not affect the separation of dN or ddN derivatives. The use of cationic surfactants, such as TBAP and DTAB, propelled ddNs towards the sample-end electrode and resulted in no separations (see Results for details). When SDS was used as the anionic surfactant, MEKC resolved all seven components of the ddN mixture in *ca.* 3 min, although a breakthrough peak appeared in 7.4 min (Fig. 11). This compares very favorably with HPLC separations of 16.5 min (Fig. 10).

Factors responsible for the separation of solutes in MEKC include their partitioning between the hydrophobic interior of the micelles and the polar aqueous phase, electroosmotic flow of the aqueous phase and electrophoretic migration of the micelles. Of these three factors, electroosmotic flow is the prominent force in determining the direction of flow in MEKC. The bulky micelles migrate at a slower rate than the polar buffer medium. Solutes having greater hydrophobic properties interact more strongly with the micelles than with the buffer, hence they exhibit a slower movement than those solutes having greater hydrophilic properties.

REFERENCES

- 1 T. Tatragnone, E. Holeman, K. Opheim, T. Smith and A. Collier, *J. Acquired Immune Defic. Syndrome*, 3 (1990) 32–34.
- 2 B. Patel, C. Chu and F. Boudinot, *J. Pharm. Sci.*, 78 (1989) 530–534.
- 3 G. Morse, J. Olson, A. Portmore, C. Taylor, C. Plank and R. Reichman, *Antiviral Res.*, 11 (1989) 57–66.
- 4 E. Singles, J. Pioger, A. Taburet, J. Colin and J. Fillastre, *Clin. Pharmacol. Ther.*, 46 (1989) 190–197.
- 5 S. Good, D. Reynolds and P. De Miranda, *J. Chromatogr.*, 431 (1988) 123–133.
- 7 M. Nokta, J. P. Loh, S. M. Douidar, A. E. Ahmed and R. B. Pollard, *J. Interferon Res.*, 11 (1991) 159.
- 8 A. M. Taburet, S. Naveau, G. Zorza, J. N. Colin, J. F. Del-fraissy, J. C. Chaput and E. I. Singlas, *Clin. Pharmacol. Ther.*, 47 (1990) 731.
- 9 R. M. Ruprecht, A. H. Sharpe, R. Jaenisch and D. Tries, *J. Chromatogr.*, 528 (1990) 371.
- 10 P. de Miranda, T. C. Burnette and S. S. Good, *Drug Metab. Dispos.*, 18 (1990) 315.
- 11 M. Mazzei, A. Balbi, E. Scottofattori, C. Bruzzo, G. Palamone and A. Nicolini, *Farmaco, Ed. Prat.*, 45 (1990) 737.
- 12 E. M. Staffic, J. H. King, J. F. Inciardi, N. F. Flynn, E. Goldstein, T. S. Tonjes and L. Z. Benet, *J. Acquired Immune Defic. Syndrome*, 3 (1990) 691.
- 13 J. S. Janiszewski, D. E. Mulvana, S. Kaul, K. A. Dandeker and R. H. Barbhuiya, *J. Chromatogr.*, 577 (1992) 151–156.
- 14 S. El Dareer, K. Tillery, J. Kalin and D. Hill, *Invest. New Drugs*, 7 (1989) 139–146.
- 15 K. Doshi, J. Gallo, E. Boudnot, R. Schinazi and C. Chu, *Drug Metab. Dispos.*, 17 (1989) 590–594.
- 16 R. Kupferschmidt and R. Schmid, *Clin. Chem.*, 35 (1989) 1313–1317.
- 17 S. Ibrahim and F. Boudinot, *J. Pharm. Pharmacol.*, 41 (1989) 829–834.
- 18 R. Klecker, J. Collins, R. Yarchoan, R. Thomas, N. McAtee, S. Broader and C. Myers, *J. Clin. Pharmacol.*, 28 (1988) 837–842.
- 19 J. H. Beijnen, P. L. Meenhorst, H. Rosing, R. van Gijn, G. Los and W. J. M. Underberg, *J. Drug. Dev.*, 3 (1990) 127.
- 20 N. R. Hartman, R. Yarchoan, J. M. Pluda, R. V. Thomas, K. S. Marczyk, S. Broder and D. G. Johns, *Clin. Pharmacol. Ther.*, 47 (1990) 647.
- 21 L. K. Tay, E. A. Papp and J. Timoszky, *Biopharm. Drug Dispos.*, 12 (1991) 258.
- 22 S. Tadepalli and R. Quinn, *J. Acquired Immune Defic. Syndrome*, 3 (1990) 19–27.
- 23 S. M. Tadepalli, L. Puckett, S. Jeal, L. Kanics and R. P. Quinn, *Clin. Chem.*, 36 (1990) 897.
- 24 P. Blau, J. Hines and R. Voyksner, *J. Chromatogr.*, 420 (1987) 1–12.
- 25 F. D. Boudinot, S. S. Ibrahim, Y. Quin, K. Chu and R. F. Schinazi, *Antiviral Chem. Chemother.*, 1 (1990) 367.
- 26 J. R. Turcotte, P. E. Pivarnik, S. S. Shirali, H. K. Singh, R. K. Sehgal, D. MacBride, N. I. Jang and P. R. Brown, *J. Chromatogr.*, 499 (1990) 55.
- 27 T. Toyoshima, S. Kimura, S. Muramatsu, H. Takahagi and K. Shimada, *Anal. Biochem.*, 196 (1991) 302–307.
- 28 N.-I. Jang and P. R. Brown, *J. Chromatogr.*, 550 (1991) 507–517.
- 29 S. Terabe, K. Otsuka, K. Ichikawa, A. Tsuchiya and T. Ando, *Anal. Chem.*, 56 (1984) 111–113.
- 30 S. Terabe, K. Otsuka and T. Ando, *Anal. Chem.*, 57 (1985) 834–841.
- 31 S. Terabe, K. Otsuka and T. Ando, *Anal. Chem.*, 61 (1989) 251–260.
- 32 W. G. Kuhr, *Anal. Chem.*, 62 (1990) 403R–414R.
- 33 R. P. Singhal and J. P. Landes, *J. Chromatogr.*, 458 (1988) 117–128.
- 34 R. P. Singhal, P. Landes, N. P. Singhal, L. W. Brown, P. J. Anevski and J. A. Toce, *Biochromatogr.*, 4 (1989) 78–88.
- 35 A. K. Kansal, W. R. Parkhurst and R. P. Singhal, *J. Liq. Chromatogr.*, 14 (1991) 97–114.
- 36 R. P. Singhal and W. E. Cohn, *Anal. Biochem.*, 45 (1973) 585–599.
- 37 R. P. Singhal and W. E. Cohn, *Biochemistry*, 2 (1973) 1532–1537.
- 38 H. J. Jojoo, S. M. Bennett and D. M. Kornhauser, *J. Chromatogr.*, 577 (1992) 299–304.

Chiral high-performance liquid chromatographic separations of vinca alkaloid analogues on α_1 -acid glycoprotein and human serum albumin columns

Ilona Fitos, Júlia Visy and Miklós Simonyi

Central Research Institute for Chemistry, Hungarian Academy of Sciences, P.O. Box 17, H-1525 Budapest (Hungary)

Jörgen Hermansson

ChromTech AB, Box 512, S-145 63 Norsborg (Sweden)

(First received February 14th, 1992; revised manuscript received May 7th, 1992)

ABSTRACT

Separations of the stereoisomers of a series of tetracyclic and pentacyclic vinca alkaloid analogues having two or three chiral centres were performed on Chiral-AGP and Chiral-HSA high-performance liquid chromatographic columns. Phosphate buffers with pH 5–7 containing 5–35% acetonitrile or 2-propanol were used as mobile phases. The results were in accordance with previous binding data obtained with native AGP and on an HSA-Sepharose column. Whereas on Chiral-AGP the retention of the *trans* isomers having 1(*R*),12*b*(*S*)-indolo[2,3-*a*]quinolizidine or the corresponding 3(*S*),16(*R*)-eburnane absolute configurations was exceedingly high, on Chiral-HSA the *trans* isomers, independently of their absolute configurations, were more retained. Eburnane-type compounds could also be separated according to the configuration of the chiral centre at position 14. A comparison of the chromatographic properties of the vinca alkaloids on the Chiral-AGP and Chiral-HSA columns demonstrates that these compounds are bound with higher affinity to the AGP phase. The AGP column resolves a very broad range of vinca alkaloids compared with the HSA column. Higher stereoselectivity and a much better chromatographic performance were also obtained on the Chiral-AGP column.

INTRODUCTION

It is well known that enantiomers of drugs have different biological activities [1,2]. Stereoselective binding to serum proteins, such as to α_1 -acid glycoprotein (AGP) and human serum albumin (HSA), can affect both the pharmacodynamics and the pharmacokinetics of the drug. The number of binding sites involved in the drug binding to AGP has been widely discussed. It is obvious that the experimental design influences the results to a large extent. From indirect drug displacement studies of

basic drugs with isolated AGP, the results suggest that AGP contains one binding site [3–6]. However, studies performed with a direct method, such as Scatchard plots, indicate more than one and in most studies two classes of binding sites [7–10]. AGP immobilized on silica particles (the Chiral-AGP column) has also been used in binding studies of drugs of different character [11]. The results obtained using this technique demonstrate, in accordance with the results obtained with the native protein, using Scatchard plots, that basic, acidic and non-protolytic drugs are bound to one high-affinity site and there is at least one more site to which the drugs are bound with lower affinity. It has also been demonstrated in a large number of chromatographic studies, using immobilized AGP, that stereoselec-

Correspondence to: Dr. I. Fitos, Central Research Institute for Chemistry, Hungarian Academy of Sciences, P.O. Box 17, H-1525 Budapest, Hungary.

tive binding of drugs can be obtained for an extremely broad range of solutes [12–14].

HSA is assumed to have two main ligand binding sites, the endogenous bilirubin and the *L*-tryptophan sites [15,16], corresponding to the warfarin and benzodiazepine drug sites, respectively [17]. It has been demonstrated that enantiomers can be bound stereoselectively to native HSA [18]. When using a chromatographic column with immobilized proteins, even small differences in binding affinity (low α -values) of the enantiomers can give a resolution of the racemate, provided that a high enough separation efficiency is generated by the column. If the immobilized protein also maintains its original binding ability and the mobile phase components do not affect the chiral binding properties of the protein, chromatography of chiral compounds on serum protein bonded phases can conveniently provide relevant information on binding stereoselectivity. This has been demonstrated for HSA immobilized on Sepharose [19,20]. It was also demonstrated in one study for tryptophan and warfarin [21], and in another study for some benzodiazepines, leucovorin and warfarin using HSA immobilized on silica [22].

The serum protein binding of a series of tetracyclic and pentacyclic vinca alkaloid analogues possessing two or three chiral centres was reported in a recent paper [23]. Their binding to AGP, measured by displacement of marker ligands, demonstrated very high stereoselectivities. The affinities of certain *trans* isomers were 20–100 times higher than those of the *cis* or the enantiomeric *trans* isomers. One of the purposes of this study was to investigate whether AGP bound to silica (Chiral-AGP) maintains this unique interaction.

The binding of the vinca alkaloids to HSA has also been characterized using an HSA-Sepharose column [23] and the binding affinities were found to be highly dependent on the chemical structure of the solutes. Separation factors up to 4 were reported with higher elution volumes for the *trans* isomers, independently of their absolute configurations. This paper also reports the separation of the stereoisomers of some of the vinca alkaloids on a Chiral-HSA high-performance liquid chromatographic (HPLC) column and a comparison with the previously reported *in vitro* results.

EXPERIMENTAL

Chromatography

The HPLC experiments were carried out using a system composed of a Jasco Model 880-PU pump, a Rheodyne Model 7125 injector (20- μ l loop), a Jasco Model 875 UV-VIS detector set at 263 nm and a Hewlett-Packard integrator or JCL-6000 chromatographic software. The sample concentration was 0.02–0.04 mg/ml.

Chiral-AGP stationary phase. This was obtained from ChromTech (Norsborg, Sweden). Preliminary tests were performed on a guard column (10 \times 3 mm I.D.) and the final chromatograms were recorded on an analytical column (50 \times 4 mm I.D.). The mobile phase was 0.01 *M* phosphate buffer (pH 6.0, 6.5 and 7.0) containing 20–35% (v/v) of 2-propanol (IP) or acetonitrile (AN).

Chiral-HSA stationary phase. This was obtained from ChromTech. The chromatograms were recorded on a 100 \times 4 mm I.D. column. The mobile phase was 0.1 *M* phosphate buffer of pH 7.0 containing 10% (v/v) of IP or AN, pH 6.15 containing 10% of IP and pH 5.00 containing 5% and 10% of IP.

Chemicals

Compounds **1–9** were obtained from the Chemical Works of Gedeon Richter (Budapest, Hungary): **1a** = *cis*-(-)-alcohol; **1b** = *trans*-(-)-alcohol; **2a** = *cis*-(-)-ethyl (Et) ester; **2b** = *trans*-(-)-Et-ester; **3a** = *cis*-(-)-methyl (Me) ester; **3b** = *trans*-(-)-Me ester; **3c** = *trans*-(+)-Me ester (**3b** and **3c** are enantiomers); **4a** = *cis*-(+)-Et apovincaminic acid (Cavinton); **4b** = *trans*-(+)-Et apovincaminic acid; **5a** = *trans*-(-)-Me apovincaminic acid; **5b** = *trans*-(+)-Me apovincaminic acid (**5a** and **5b** are enantiomers); **6a** = *cis*-(-)-lactam; **6b** = *trans*-(-)-lactam; **7a** = *cis*-(-)-eburnamonine; **7b** = *trans*-(-)-eburnamonine; **8a** = 3(*R*), 16(*S*), 14(*S*)-E (E = 14,15-dihydro-14-hydroxymethyl-eburnamonine); **8b** = 3(*S*), 16(*R*), 14(*R*)-E (**8a** and **8b** are enantiomers); **8c** = 3(*S*), 16(*R*), 14(*S*)-E; **9a** = laevorotatory mixture of *trans*-vincamine and *trans*-epivincamine; **9b** = dextrorotatory mixture of *trans*-vincamine and *trans*-epivincamine (**9a** and **9b** are enantiomeric mixtures of epimers).

Chromatograms were recorded with the separate

stereoisomers and also with their mixtures. Only **9a** and **9b** were epimeric at position 14.

RESULTS AND DISCUSSION

Separation on Chiral-AGP: effects of pH and organic modifier

The chromatographic properties of the hydrophobic vinca alkaloids were investigated using mobile phases containing a phosphate buffer with pH between 6.0 and 7.0 and acetonitrile or 2-propanol at concentrations of 20–35% (v/v) as uncharged organic modifiers. It has been observed previously that the retention and enantioselectivity of acidic, basic and non-protolytic compounds can be affected to a large extent by both the pH of the mobile phase and the nature and the concentration of an uncharged modifier [24]. Previous binding studies with native AGP suggested high affinities for some of the vinca alkaloids [23], and therefore preliminary chromatographic screening was performed on an immobilized AGP guard column, which did reveal high retentions in accordance with the previous findings. Without using mobile phase modifiers (2-propanol or acetonitrile), certain stereoisomers could not be eluted within a reasonable time. Detailed chromatographic studies were performed on a short (50 × 4.0 mm I.D.) AGP column. The chromatographic data, *i.e.* capacity factors (k'_1 and k'_2) and separation factors (α), for the vinca alkaloids are summarized in Table I; Figs. 1–3 show representative chromatograms.

A decrease in the pH of the mobile phase from 7.0 to 6.0 results in a decrease in k' values, which is in accordance with previous findings for basic compounds [24]. This effect was much more pronounced for the most retained stereoisomers. However, it is interesting to note the chromatographic behaviour of the lactam compound (**6**). A decrease in the pH from 7.0 to 6.0 results in an increase in retention for the first-eluted enantiomer and a decrease or no change in retention for the last-eluted enantiomer. The first-eluted enantiomer behaves with respect to retention as an acidic compound normally does on the AGP column by decreasing the pH. The most retained enantiomer behaves as can be expected for a basic compound on decreasing the pH if AN is used as the modifier. If IP is used, however, the retention is almost unaffected by

a decrease in pH, a behaviour which is normally observed for neutral compounds [24]. Obviously, the chiral binding properties of the protein are affected differently by IP and AN. Such observations have been made previously [25].

The stereoselectivity increases with increase in pH and decrease in modifier concentration for all the compounds studied. At the same modifier concentration a higher stereoselectivity is obtained with AN than IP.

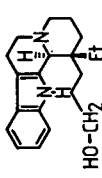
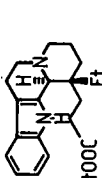
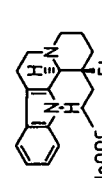
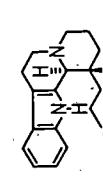
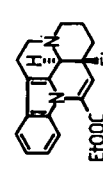
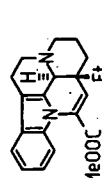

It has been observed that both 1-propanol and AN are adsorbed to a high extent on immobilized AGP, forming a multilayer on the protein surface, and 1-propanol is bound with the highest affinity [25]. Increasing the concentration of these modifiers in chromatographic experiments results in a decreased retention of the solutes owing to competition between the modifier and the solutes for binding to the immobilized protein molecules. As can be seen from Table I, the decrease in the retention of the most retained enantiomers is more pronounced. The more hydrophobic IP gives lower retention compared with the same concentration of AN.

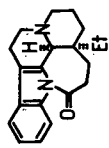
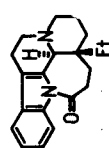
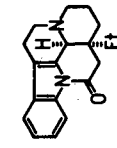
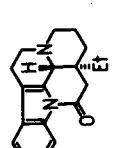
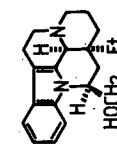
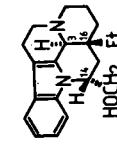
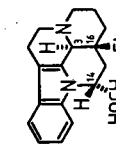
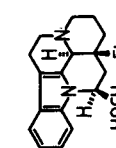
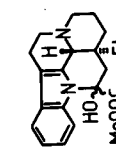

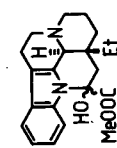

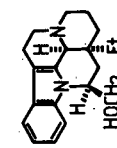
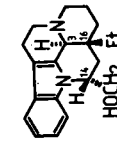
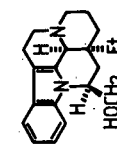
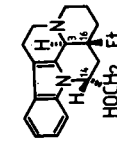
Considering the very high affinity for these types of compounds to AGP, optimum separations could be achieved at pH 6.0, with high concentrations [25–35% (v/v)] of either modifier. However, Herényi and Görög [26] utilized another approach for the resolution of some of the compounds that were investigated in this study, *i.e.*, the four stereoisomers of the hydrophobic ethyl apovincamate (**4**), on a 100 mm Chiral-AGP column. They applied gradient elution with increasing IP concentration in the mobile phase, from 18 to 35% (v/v), resulting in the elution order *cis*-(+), *trans*-(-), *cis*-(-), *trans*-(+).

Chemical structure and stereoselectivity

Similarly to the native protein, AGP immobilized on silica preferentially binds the compounds having 1(*R*), 12b(*S*)-indolo[2,3-*a*]quinolizidine (**1b**, **2b**, **3b**) or the analogous 3(*S*), 16(*R*)-eburnane (**4b**, **5b**, **6b**, **7b**, **8b**, **8c**, **9b**) absolute configurations. With compounds having the third chiral centre at position 14 (**8** and **9**), Chiral-AGP could also discriminate according to the absolute configuration of this centre (*cf.*, Figs. 2 and 3). Comparison between **8b** and **8c** suggests that the 14(*S*) absolute configuration is bound with the highest affinity, in agreement with data obtained when native AGP was used [23].

TABLE I
SEPARATION OF MIXTURES OF VINCA ALKALOID STEREOISOMERS ON CHIRAL-AGP COLUMN (50 × 4 mm I.D.)
Mobile phase, 0.01 M phosphate buffer with 2-propanol (IP) or acetonitrile (AN) modifier.

Samples	Chemical Structure	pH	Modifier		Elution order	k'_1	k'_2	α
			Compound	Concentration (%)				
1a and 1b		7.0	IP	25	a, b	2.81	10.12	3.61
			AN	25	a, b	2.73	23.08	8.46
2a and 2b		6.5	IP	25	a, b	2.65	6.03	2.28
			AN	25	a, b	2.87	13.65	4.76
3a and 3b		6.0	IP	25	a, b	2.46	4.08	1.66
			AN	25	a, b	2.29	5.59	2.45
4a and 4b		7.0	IP	25	a, b	2.84	36.38	12.81
			AN	25	a, b	2.77	21.07	7.61
5a and 5b		6.0	IP	25	a, b	2.56	11.60	4.54
			AN	30	a, b	1.86	6.20	3.34
6a and 6b		6.0	IP	35	a, b	0.87	4.14	3.61
			AN	35	a, b	2.42	11.57	4.77
7a and 7b		6.0	IP	25	a, b	1.75	6.09	3.49
			AN	35	a, b	0.76	3.44	4.55
8a and 8b		6.0	IP	25	c, b	2.81	11.57	4.11 ^a
			AN	30	c, b	1.88	6.06	3.23 ^a
9a and 9b		6.0	AN	35	c, b	0.78	3.56	4.56 ^a
			IP	30	a, b	1.33	7.72	5.80
10a and 10b		6.0	AN	30	a, b	1.81	23.07	12.75
			AN	35	a, b	0.77	8.54	11.04
11a and 11b		6.0	IP	30	a, b	1.97	7.30	3.70 ^a
			AN	35	a, b	0.78	8.91	11.42 ^a

		7.0	IP AN	25	a,b a,b	1.39 2.48	3.24 7.60	1.39 2.48	2.33 3.07
		6.5	IP AN	25	a,b a,b	1.73 4.00	3.41 7.36	1.73 4.00	1.97 1.84
		6.0	IP AN	25	a,b a,b	2.08 2.19	5.50 7.86	2.08 2.19	2.64 ^a 3.59 ^a
		6.0	IP AN	25	b,c b,c	5.50 7.86	11.03 15.88	5.50 7.86	2.00 2.02
		6.0	IP AN	20	nd ^b nd	2.04 2.75	2.92 4.05	2.04 2.75	1.43 1.47
		6.0	IP AN	20	nd nd	1.36 1.13	1.76 1.49	1.36 1.13	1.29 1.32
		6.0	IP AN	25	nd nd	5.22 12.93	14.19 31.27	5.22 12.93	2.72 2.42
		6.0	IP AN	25	nd nd	2.66 3.26	5.82 6.69	2.66 3.26	2.19 2.05

^a These values refer to enantioselectivity.

^b Not determined.

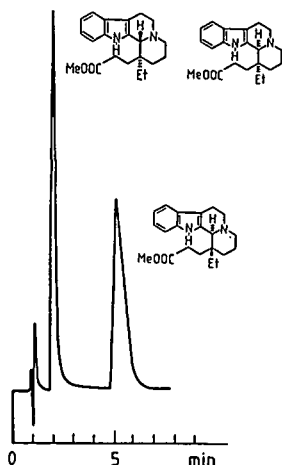


Fig. 1. Separation of the stereoisomers of 3 on a Chiral-AGP column (50×4 mm I.D.). Sample, mixture of 3a, 3b and 3c. Mobile phase, 35% (v/v) AN in 0.01 M phosphate buffer (pH 6.0); flow-rate, 0.5 ml/min. Et = Ethyl; Me = methyl.

Separations on Chiral-HSA

Previous studies of vinca alkaloid analogues on an HSA-Sepharose column showed [23] that the binding affinities varied within a broad range ($K = 10^3$ – 10^5 l/mol) and the *trans* isomers, regardless of the configurations of the two chiral centres, had two to four times higher affinities than the corresponding *cis* isomers. In extreme cases, such as for

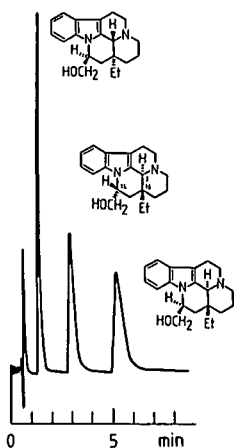


Fig. 2. Separation of the stereoisomers of 8 on a Chiral-AGP column (50×4 mm I.D.). Sample, mixture of 8a, 8b and 8c. Mobile phase, 30% (v/v) AN in 0.01 M phosphate buffer (pH 6.0); flow-rate, 0.9 ml/min.

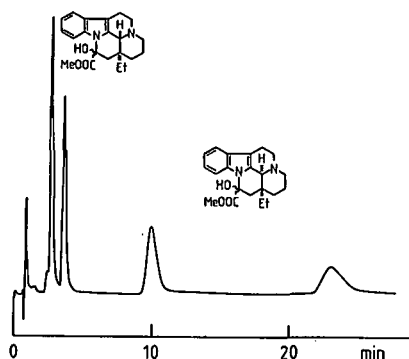


Fig. 3. Separation of the stereoisomers of 9 on a Chiral-AGP column (50×4 mm I.D.). Sample, mixture of 9a and 9b. Mobile phase, 20% (v/v) IP in 0.01 M phosphate buffer (pH 6.0); flow-rate, 0.5 ml/min.

the low-affinity alcohol (1) and the high affinity ethyl apovincamate (4), the elution volumes did not show significant differences. For structure 8 the *R* configuration of centre 14 was bound with the highest affinity.

Chromatographic data obtained on Chiral-HSA are summarized in Table II. The retention and stereoselectivity data obtained on the Chiral-HSA column were similar to those obtained on HSA-Sepharose gel. In general, the *trans* isomers are more retained than the *cis* species (see Fig. 4) and the configuration of the chiral centres in the *trans* isomer plays a minor role in determining the binding strength.

With the highly retained hydrophobic compounds 4 and 5 AN modifier produced the opposite elution order to IP. This is an interesting finding and this type of selectivity change has not been reported previously on HSA-bonded silica. As mentioned above, AN and 1-propanol are highly adsorbed on immobilized AGP [25], and it is also reasonable to assume adsorption of these modifiers on HSA. Thus, when adsorbed, the modifiers can compete with the enantiomers for binding to different hydrogen bonding groups in the binding sites. Accordingly, modifiers with different hydrogen bonding properties and different hydrophobicities affect the enantioselectivity in different ways. Another reasonable explanation for the modifier-induced changes in the enantioselectivity is that certain organic modifiers, present at high enough concentra-

TABLE II

SEPARATION OF MIXTURES OF VINCA ALKALOID ANALOGUES ON A CHIRAL-HSA COLUMN (100 × 4 mm I.D.)

Mobile phase, 0.1 M phosphate buffer (pH 7.0) with 10% of 2-propanol (IP) or acetonitrile (AN) modifier.

Sample	Modifier	Elution order	k'_1	k'_2	α
1a, 1b	IP	a,b	1.41	2.01	1.42
	AN	a,b	1.52	1.98	1.30
2a, 2b	IP	a,b	2.42	2.90	1.20
	AN	a,b	2.23	2.63	1.18
3a, 3b	IP	a,b	2.34	2.89	1.23
	AN	a,b	2.18	2.56	1.17
3a, 3c	IP	a,c	2.34	3.29	1.41
	AN	a,c	2.18	2.65	1.21
4a, 4b	IP	a,b	26.50	34.80	1.31
	AN	b,a	23.17	29.00	1.25
5a, 5b	IP	a,b	22.33	35.67	1.60 ^a
	AN	b,a	26.50	30.67	1.16 ^a
6a, 6b	IP	a,b	13.55	19.42	1.43
	AN	a,b	9.37	13.56	1.45
7a, 7b	IP	a,b	9.71	20.53	2.11
	AN	a,b	6.52	11.25	1.73
8a, 8b	IP	a,b	1.84	3.32	1.80 ^a
	AN	a,b	1.72	3.39	1.97 ^a
8c, 8b	IP	c,b	1.70	3.32	1.95
	AN	c,b	1.65	3.39	2.05
9a, 9b	IP	b,a	1.68	1.88	1.12
	AN	b,a	2.05	2.14	1.04

^a These values refer to enantioselectivity.

tion, induce small reversible changes of the secondary structure, transformation of parts of the peptide chain with β -conformation or an unordered structure into an α -helical form. The secondary structure of AGP in solution, with and without IP, has been studied by circular dichroism (CD) in an attempt to correlate modifier-induced changes in the enantioselectivity with changes in the secondary structure of the protein [25]. These studies were performed using AGP solutions containing 40% IP, but no clear indications of the formation of an α -helix was found. However, a reinvestigation of the old data together with new ones gave weak indications of the formation of an α -helix [27]. If the changes are small they can be difficult to detect by CD. However, it is reasonable to assume that even small local changes in the secondary structure, hardly detectable by CD, can induce large changes in the enantioselectivity, in line with the findings on the HSA column reported above for 4 and 5. So far, no CD studies of

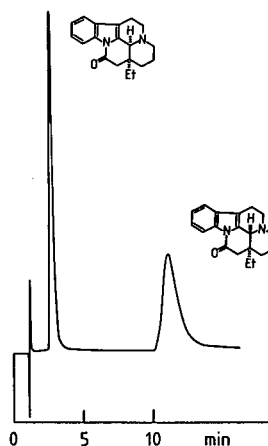


Fig. 4. Separation of a mixture of 7a and 7b on a Chiral-HSA column (100 × 4 mm I.D.). Mobile phase, 10% (v/v) IP in 0.1 M phosphate buffer (pH 5.0); flow-rate, 0.9 ml/min.

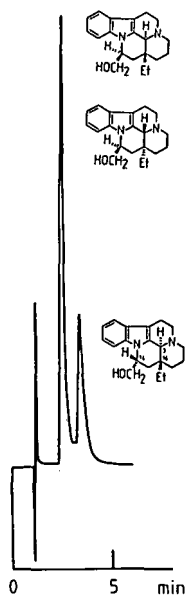


Fig. 5. Separation of the stereoisomers of **8** on a Chiral-HSA column (100×4 mm I.D.). Sample, mixture of **8a**, **8b** and **8c**. Mobile phase, 10% (v/v) IP in 0.1 M phosphate buffer (pH 6.15); flow-rate 0.9 ml/min.

HSA have been performed in the presence of AN and IP. On the HSA-Sepharose column both **4a** and **4b** and also **5a** and **5b** showed high affinities without a significant difference between the enantiomers. When the protein provided a high degree of stereoselectivity, the elution order was not influenced by mobile phase modifiers. In most instances the stereoselectivity was higher using IP as organic modifier. Higher capacity factors were also obtained for most compounds with IP. These findings are contrary to the findings on the AGP column. HSA, in contrast to AGP, prefers the *R* configuration at centre 14 in structure **8** (compare Figs. 5 and 2). Compounds **9a** and **9b** have low capacity factors and no separation could be detected according to centre 14.

The influence of the pH on the retention and the stereoselectivity was also studied for some of the compounds, **1a**, **1b**, **5a**, **5b**, **6a**, **6b**, **7a**, **7b**, **8a**, **8b** and **8c**, and the results are summarized in Table III. It can be noted that the separation factor for **7** was highly influenced by the pH in the range 5-7. The highest separation factor, 6.35, was obtained at pH

TABLE III

INFLUENCE OF pH ON THE CAPACITY FACTORS AND THE SEPARATION FACTORS OF VINCA ALKALOID STEREOISOMERS

Column, Chiral-HSA (100×4 mm I.D.); mobile phase, 0.1 M phosphate buffer with 2-propanol (IP) modifier.

Sample	pH 5.00, 5% IP		pH 5.00, 10% IP		pH 6.15, 10% IP		pH 7.00, 10% IP	
	k'	α	k'	α	k'	α	k'	α
1a	0.81		0.48	1.10	1.06	1.22	1.40	1.39
1b	0.81	1.00	0.53		1.29		1.94	
5a	3.55	1.93 ^a	2.06	1.72 ^a	12.55	1.91 ^a	21.18	1.71 ^a
5b	6.86		3.55		24.00		36.31	
6a	2.61	1.00	1.50	1.03	6.69	1.48	13.24	1.60
6b	2.61		1.55		9.92		21.18	
7a	2.01	7.37	1.32	6.35	5.35	3.32	8.71	2.30
7b	14.82		8.38		17.77		20.05	
8a	0.64	1.64 ^a	0.43	1.65 ^a	1.08	1.74 ^a	1.69	1.79 ^a
8b	1.05		0.71		1.88		3.03	
8c	0.65	1.62	0.43	1.58	1.08	1.73	1.59	1.91
8b	1.05		0.68		1.87		3.04	

^a These values refer to enantioselectivity.

5.0 where *trans*-7 also was least retained. The stereoselectivity of **1** and **6** increased on increasing the pH from 5 to 7. The retention of all the compounds increased at higher pH, as expected.

CONCLUSIONS

AGP and HSA immobilized on silica were used successfully for the separation of the stereoisomers of a series of vinca alkaloids. The native proteins, especially AGP, discriminate well between the stereoisomers of the vinca alkaloids. It has been demonstrated that the immobilized proteins follow the binding tendencies obtained by *in vitro* methods with the native proteins. Under certain chromatographic conditions the stereoselectivities, using immobilized proteins, can be significantly increased in comparison with the native proteins.

A comparison of the Chiral-AGP and Chiral-HSA columns concerning the retention of the vinca alkaloids demonstrated that these compounds are bound with higher affinity of the AGP phase. The Chiral-AGP column also gives higher stereoselectivity and better resolution owing to a much better chromatographic performance on the AGP phase.

ACKNOWLEDGEMENTS

This work was supported by project OTKA No. 1764. For the synthesis of the investigated compounds and for helpful discussions, the authors are indebted to L. Czibula (Chemical Works of Gedeon Richter) and also F. Sóti, M. Incze, Zs. Kardos-Balogh and I. Moldvai (Central Research Institute for Chemistry). Skilful technical assistance by Mrs. I. Kawka is greatly appreciated.

REFERENCES

- 1 M. Simonyi, *Med. Res. Rev.*, 3 (1984) 359.
- 2 P. N. Patil, J. B. LaPidus and A. Tye, *J. Pharm. Sci.*, 59 (1970) 1205.
- 3 D. L. Goolkasian, R. L. Slaughter, D. J. Edwards and D. Lalka, *Eur. J. Clin. Pharmacol.*, 25 (1983) 413.
- 4 J. Schley and B. Müller-Oerlinghausen, *J. Pharm. Pharmacol.*, 38 (1986) 102.
- 5 F. Brunner and W. E. Müller, *J. Pharm. Pharmacol.*, 39 (1987) 986.
- 6 I. Fitos, J. Visy, A. Magyar, J. Kajtár and M. Simonyi, *Biochem. Pharmacol.*, 38 (1989) 2259.
- 7 M. Brinkschulte and U. Breyer-Pfaff, *Naunyn-Schiedeborg's Arch. Pharmacol.*, 314 (1980) 61.
- 8 B. M. David, E. G. Whitford and K. F. Ilett, *Clin. Exp. Pharmacol. Physiol.*, 9 (1982) 478.
- 9 O. Teirlynck, F. M. Belpaire and F. Andreade, *Eur. J. Clin. Pharmacol.*, 21 (1982) 427.
- 10 R. K. Verbeeck, J. A. Cardinal, A. G. Hill and K. K. Midha, *Biochem. Pharmacol.*, 32 (1983) 2565.
- 11 M. Enquist and J. Hermansson, *J. Chromatogr.*, 519 (1990) 285.
- 12 J. Hermansson and G. Schill, in P. A. Brown and R. A. Hartwick (Editors), *High Performance Liquid Chromatography (Monographs on Analytical Chemistry Series)*, Wiley-Interscience, New York, 1988, pp. 337–374.
- 13 J. Hermansson, *Trends Anal. Chem.*, 8 (1989) 251.
- 14 *Chiral-AGP, Application Note No. 3*, ChromTech, Norsborg, 1991.
- 15 J. Jacobsen, *FEBS Lett.*, 5 (1969) 112.
- 16 R. J. McMenamy and J. L. Oncley, *J. Biol. Chem.*, 233 (1958) 1436.
- 17 I. Sjöholm, B. Ekman, A. Kober, I. Ljungstedt-Pählman, B. Seiving and T. Sjödin, *Mol. Pharmacol.*, 16 (1979) 767.
- 18 W. E. Müller and U. Wollert, *Mol. Pharmacol.*, 11 (1975) 52.
- 19 C. Lagercrantz, T. Larsson and H. Karlsson, *Anal. Biochem.*, 99 (1979) 352.
- 20 I. Fitos, Zs. Tegye, M. Simonyi, I. Sjöholm, T. Larsson and C. Lagercrantz, *Biochem. Pharmacol.*, 35 (1986) 263.
- 21 J. Hermansson, unpublished results.
- 22 E. Domenici, C. Bertucci, P. Salvadori, G. Félix, I. Cahagne, S. Motellier and I. W. Wainer, *Chromatographia*, 29 (1990) 170.
- 23 I. Fitos, J. Visy and M. Simonyi, *Biochem. Pharmacol.*, 41 (1991) 377.
- 24 J. Hermansson, *Trends Anal. Chem.*, 8 (1989) 251.
- 25 M. Enquist and J. Hermansson, *J. Chromatogr.*, 519 (1990) 271.
- 26 B. Herényi and S. Görög, *J. Chromatogr.*, 592 (1992) 297.
- 27 J. Hermansson, unpublished results.

Enhancement of detection sensitivity and cleanup selectivity for tobramycin through pre-column derivatization

Fran Lai and Terry Sheehan

Varian Chromatography Systems, 2700 Mitchell Drive, Walnut Creek, CA 94598 (USA)

(First received April 3rd, 1992; revised manuscript received June 9th, 1992)

ABSTRACT

Reversed-phase high-performance liquid chromatography, UV detection and reversed-phase solid-phase extraction (SPE) as analytical methods for pharmaceutical compounds face a challenge when the compound is rather polar and lack UV absorptivity. A good example is tobramycin. To overcome these problems, a method has been developed using pre-column derivatization of tobramycin with *o*-phthalaldehyde and automated with an autosampler with microrobotic routines.

The detection enhancement of the derivatives was achieved by using fluorescence detection which was forty times more sensitive than using UV detection.

Recovery studies of standards and spiked serum samples show that pre-SPE derivatization significantly enhances the recoveries (by at least a factor of 3) and the quality of cleanup over post-SPE derivatization.

INTRODUCTION

The combination of reversed-phase high-performance liquid chromatography (HPLC) and UV detection is among the most common methods of analysis for pharmaceutical compounds. This analytical methodology has practical limitations when the analyte (1) has low UV absorptivity, (2) absorbs only in the low UV or (3) is rather polar. Low UV absorptivity causes low detection sensitivity and unacceptable detection limits. Detection at the lower UV wavelengths is more prone to interferences and instability of the chromatographic baseline. High polarity decreases reversed-phase retention which increases the potential for coelution of polar matrix components from a sample such as serum or plasma. Furthermore, this loss of selectivity limits the quality of sample cleanup by reversed-phase solid-phase extraction (SPE).

Tobramycin, an aminoglycoside antibiotic, is a good example of a pharmaceutical that carries all three limitations. The ratio of amino and hydroxyl groups to the hydrocarbon backbone yields a relatively polar molecule. The lack of unsaturation limits UV absorbance detection to low UV wavelengths and poor UV absorptivity.

Post-column derivatization of tobramycin has been performed using *o*-phthalaldehyde (OPA) [1-2]. The pumps, tees and mixers required by post-column derivatization increase both the complexity and cost of the HPLC system. The post-column reaction enhances detection sensitivity and detection selectivity *versus* coeluting solutes that are not derivatized by OPA. It does not, however, alter the mechanism of the separation. Consequently, a polar analyte like tobramycin may not be adequately separated from matrix components. Longer run times (slower separations) may be required to minimize this limitation.

Pre-column derivatization of tobramycin has also been performed. 1-Fluoro-2,4-dinitrobenzene

Correspondence to: Dr. F. Lai, Varian Chromatography Systems, 2700 Mitchell Drive, Walnut Creek, CA 94598, USA.

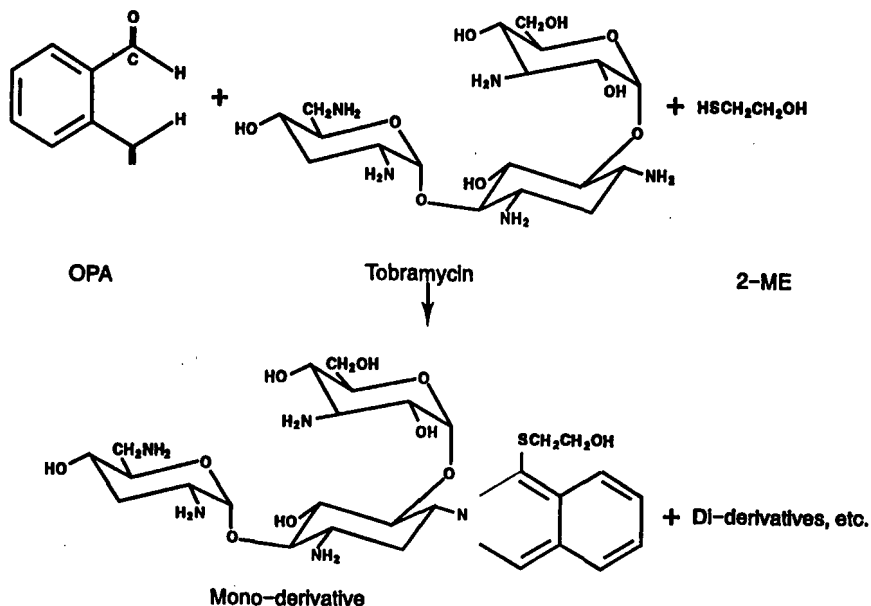


Fig. 1. Analysis of tobramycin using pre-column derivatization (OPA).

(FDNB) was used as the derivatization reagent [3,4]. The major drawback of this method is the toxicity of the reagent. The reaction is also slow and requires heating. OPA has been commonly applied to pre-column derivatization of primary amino acids [5-7]. Derivatization of aminoglycoside antibiotics in serum or plasma samples using OPA and extraction of the derivatives with ethyl acetate have been reported [8,9]. Essers [10] designed an automated HPLC method for the determination of aminoglycosides in serum using a column-switching technique for pre-column sample cleanup and derivatization.

In this study, the derivatization of tobramycin with OPA (Fig. 1) is automated using an LC autosampler from Varian that has an AutoMix microbotic feature. AutoMix permits all sample preparation steps, *i.e.*, reagent addition, mixing and extraction, to be carried out automatically [11].

Due to multiple amino sites on the structure, it is conceivable that more than one derivative may be obtained. The derivatization of individual amino groups should be affected by the reaction time, reaction medium and steric hindrance.

In *Part 1*, tobramycin is derivatized, separated and detected by fluorescence and by UV simultane-

ously. The results are compared. In *Part 2*, the effect (on recovery) of derivatization before and after SPE of serum samples is compared. When reversed-phase SPE is used in serum sample cleanup, the polarity of a compound like tobramycin should cause poor selectivity and low recovery in the cleanup. Derivatization is performed to render the analyte more non-polar, thus enhancing its retention on the reversed-phase SPE column relative to the non-derivatized polar constituents in a serum matrix. In *Part 3*, linearity and reproducibility for standards are determined. In *Part 4*, recoveries and reproducibility for spiked serum samples are studied in the clinical range.

EXPERIMENTAL

Instrumentation

The HPLC system, consisting of 9010 pump, 9095 AutoSampler, Fluorichrom II fluorescence detector, LC Star Workstation and MicroPak SP C₈ 15 cm × 4 mm column, was from Varian Chromatography Systems (Walnut Creek, CA, USA).

Materials

Tobramycin standard (Lot No. Y07147) was a

gift from Eli Lilly (Indianapolis, IN, USA). Potassium hydroxide, 45%, analyzed-reagent grade and potassium phosphate, monobasic, analyzed-reagent grade were from J. T. Baker (Phillipsburg, NJ, USA). Boric acid, analytical-Reagent grade was from Mallinckrodt (St. Louis, MO, USA). 2-Mercaptoethanol (2-ME) was from Pierce (Rockford, IL, USA). OPA was from Pickering Lab., (Mountain View, CA, USA). Acetic acid, glacial, acetonitrile, HPLC grade, acetone, HPLC grade, and methanol, HPLC grade were from Burdick & Jackson (Muskegon, MI, USA). 5-Sulfosalicylic acid was from Sigma (St. Louis, MO, USA). Blank serum (freeze dried) was from Utak Labs., (Saugus, CA, USA). Bond Elut C₁₈ cartridges were from Varian Sample Prep Products (Harbor City, CA, USA).

Methods

OPA reagent was prepared as in Bäck *et al.*'s report [8]: 1 g of boric acid is dissolved in 38 ml of deionized water and adjusted to pH 10.4 with potassium hydroxide (450 g/l). In another vessel, 200 mg of OPA are dissolved in 2 ml of methanol and 400 μ l of 2-mercaptoethanol are added. The two solutions are mixed and stored under nitrogen at +4°C.

Part 1: Derivatization of tobramycin standard and linearity study. Tobramycin stock standard (1.28 nM) was prepared by dissolving 30 mg in water. Working standards were prepared by dilution of the stock standard in water–acetonitrile (20:80) to 128, 96, 64, 32, 16 and 8 μ M. A blank without tobramycin was also included for comparison.

The 9095 AutoSampler was programmed to AutoMix 40 μ l of tobramycin standard (8–128 μ M)

and 40 μ l of OPA reagent, stand for the reaction time (0–30 min), and finally inject 25 μ l onto the HPLC System. Simultaneous detection with UV 254 nm and fluorescence (excitation 340 nm, emission 450 nm) was used for comparison.

HPLC conditions are shown in Table I.

Part 2: Comparison of recovery of tobramycin derivatized after solid phase extraction (method I) and before solid phase extraction (method II). Working standards (640 and 480 μ M) were prepared by dilution of stock standard with water.

Spiked serum samples were prepared by reconstituting serum with the working standards. A blank was prepared by reconstituting with water.

For method I, the 480 μ M standard and spiked serum samples were used. A 500- μ l aliquot of each was deproteinated^a with 500 μ l of 10% (w/v) sulfosalicylic acid, vortexed and centrifuged. For method II, the 640 μ M standard and spiked serum sample were used. A 100- μ l aliquot of each was diluted 5 times^b with water (final concentration: 128 μ M) and deproteinated as in method I.

The rest of the procedure is shown in Table II. Bond Elut C₁₈ cartridges were used for SPE.

HPLC conditions are shown in Table I.

Part 3: Linearity and reproducibility of standards using method II. Working standards (128, 96, 64, 32 and 12.8 μ M) were prepared by dilution of the stock standard. The working standards and a blank (water only) were processed with method II as in Part 2 (starting with deproteination step). Peak areas were plotted *versus* amounts on column.

Six aliquots of the 128 μ M standard were processed simultaneously for determination of reproducibility.

HPLC conditions are shown in Table I.

Part 4: Recoveries and reproducibility of spiked serum samples using method II. Working standards (640, 480, 320 and 160 μ M) were prepared by dilution of the stock standard with water. Spiked serum samples were prepared by reconstituting serum with the working standards. A blank was prepared by reconstituting with water.

All four spiked samples and blank were diluted 5 times with water. Final concentrations were 128, 96,

TABLE I
HPLC CONDITIONS

Column	MicroPak SP C ₈ 15 cm × 4 mm
Temperature	Ambient
Mobile phase	0.02 M phosphate buffer pH 6.5–acetonitrile (52:48) (can vary by 2%)
Flow-rate	2 ml/min
Detection	Fluorescence, excitation 340 nm, emission 450 nm.
UV	254 nm

^a Standards were treated similarly for control.

^b Following Bäck *et al.*'s finding, recoveries of derivatized serum samples improve with dilution [8].

TABLE II

DERIVATIZATION AND SOLID-PHASE EXTRACTION PROCEDURE FOR TOBRAMYCIN STANDARD/SAMPLES

Step	Method I (SPE-Derivatization)	Method II (Derivatization-SPE)
(1) Derivatization for method II		60 μ l supernatant was mixed with 240 μ l acetonitrile and derivatized with 300 μ l OPA reagent ^b
(2) Conditioning	1 ml acetonitrile 1 ml acetonitrile-buffer ^a	1 ml acetonitrile 1 ml acetonitrile-buffer ^a
(3) Load sample	100 μ l supernatant mixed with 100 μ l acetonitrile/buffer ^a Collect waste	600 μ l from step 1 and 300 μ l rinse mixed with 100 μ l acetonitrile-buffer ^a Collect waste
(4) Wash	200 μ l acetonitrile-buffer ^a Collect waste	500 μ l acetonitrile-buffer ^a Collect waste
(5) Elute in sample vial Add to sample vial	600 μ l acetonitrile 400 μ l 0.01 M phosphate buffer pH 11	440 μ l acetonitrile 40 μ l water
(6) Mix	Vortex sample vial	Vortex sample vial
(7)	Dilute waste from steps 3 and 4 with four volumes of water-acetonitrile (20:80) in separate sample vials	
(8) Derivatization for method I	Derivatize 40 μ l standard/samples from steps 6 and 7 on AutoSampler with 40 μ l OPA reagent	
(9) Inject	25 μ l from step 8	25 μ l from steps 3, 4 and 6 25 μ l from step 1 as calibration standard for both methods

^a Acetonitrile-0.02 M phosphate buffer pH 8 (10:90).

^b Derivatization is performed manually due to the SPE steps required before injection.

64, 32 and 0 μ M. The samples and blank were processed with method II as in *Part 2* (starting with the deproteination step). Relative recoveries were determined based on the 640 μ M standard.

Six aliquots of the 128 μ M spiked sample were processed simultaneously for determination of reproducibility.

HPLC conditions are shown in Table I.

RESULTS AND DISCUSSION

Part 1

It was found that the derivatization of tobramycin yields two peaks, as shown in Fig. 2. The first peak elutes at 4 min and the second at 10 min. It was noticed that the distribution of the two peaks varies with reaction time as well as the the amount

of organic in the reaction medium. The chromatogram in Fig. 2 represents 1 min reaction time and a

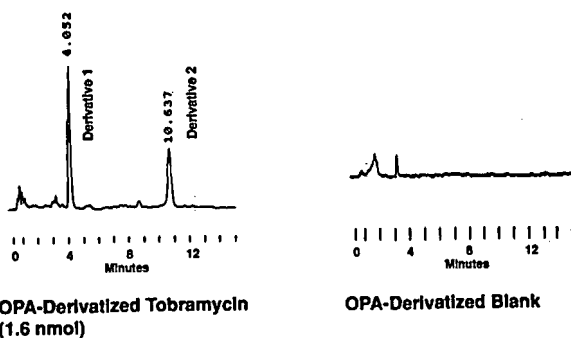


Fig. 2. OPA derivatization of tobramycin. Detection, fluorescence (excitation 340 nm; emission 450 nm).

TABLE III
FACTORS AFFECTING FINAL PRODUCT

Sample solvent	Reaction time (min)	Peak 2/Peak 1 ^a
Water	0	0.16
	1	0.17
	10	1.04
	20	2.90
	30	7.17
Acetonitrile-water	0	
	0:100	0.16
	60:40	0.68
	80:20	0.68

^a Peak 1 for derivative 1, peak 2 for derivative 2.

reaction medium containing 80% acetonitrile. There is no interference from the blank.

The effect of reaction time and reaction medium on the ratio of the area of peak 2/peak 1 is displayed in Table III. The ratio increases with increase in acetonitrile. Precipitation was observed after about 30 min in the low acetonitrile samples, but not at 60 or 80% acetonitrile. To ensure adequate acetonitrile in the sample solvent, 80% acetonitrile was used for the rest of the study. To allow adequate reaction time without making the analysis time too long, a reaction time of 30 min was used.

The difference between detection by UV (254 nm) and detection by fluorescence (excitation 340 nm, emission 450 nm) for OPA-derivatized tobramycin

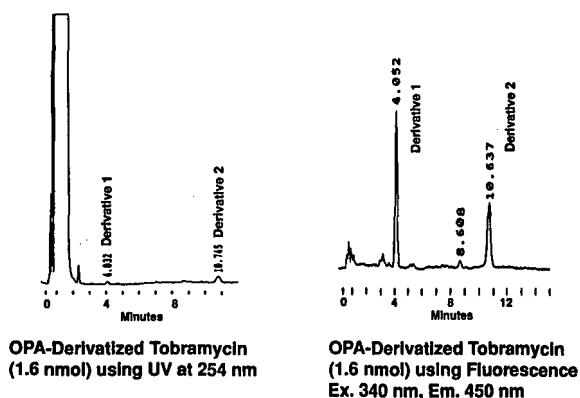


Fig. 3. Detection enhancement using fluorescence vs. UV.

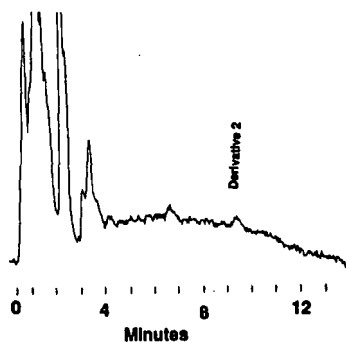


Fig. 4. Detection of OPA-derivatized tobramycin at 10 pmol on column using fluorescence (excitation 340 nm; emission 450 nm).

at 1.6 nmol (on column) is shown in Fig. 3. Fluorescence detection of derivatized tobramycin yields two sharp peaks with a sensitivity about 40 times that of UV detection. The detection limit was found to be 400 pmol (on column) for UV and 10 pmol for fluorescence (Fig. 4).

Peak areas and standard concentrations (peak 2) were linearly related from 0.1 to 1.2 nmol on column with a correlation coefficient of 0.998.

Part 2

The recoveries at each SPE step between methods I and II are shown in Table IV. In method I, where SPE was performed before derivatization, the standard lost 42.7 and 8.2% in the loading and washing steps, and the recovery was 33.7%. The spiked serum sample lost 35.4 and 3.9% in the loading and

TABLE IV
EFFECT OF DERIVATIZATION ON SAMPLE CLEANUP

	Method I, post-SPE derivatization		Method II, pre-SPE derivatization	
	Standard	Spiked serum	Standard	Spiked serum
Sample concentration (μ M)	480	480	640	640
Amount on column (pmoles)	300	300	200	200
Loss of sample (%) in				
Loading	42.7	35.4	0.0	0.0
Washing	8.2	3.9	0.0	0.0
Absolute recovery (%)	33.7	2.8	100.3	97.5

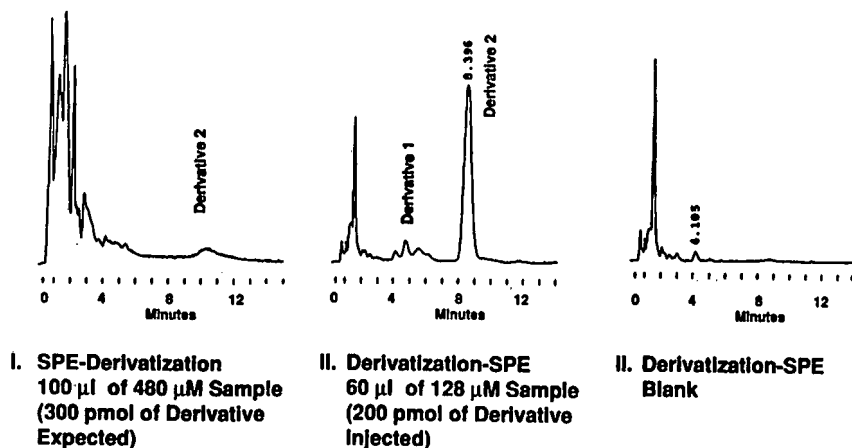


Fig. 5. Chromatograms of tobramycin-spiked serum: method I vs. method II. Detection, fluorescence (excitation 340 nm; emission 450 nm).

washing steps and the recovery was 2.8%. The difference between recoveries and loss in SPE is most likely due to protein binding and silanol effects on the SPE columns. On the other hand, using method II, where derivatization was performed before SPE, there was no loss in the loading and washing steps and the recoveries were 100.3% for the standard and 97.5% for the spiked sample.

The chromatograms of the eluates and a blank are shown in Fig. 5^a. The chromatogram from method II has much less matrix components than that from method I. There is also no interference from the blank.

The derivatization of tobramycin before SPE increased the hydrophobicity of the analyte (relative to the serum matrix) and enhanced its selectivity in the SPE, yielding cleaner chromatograms and higher recoveries than if the derivatization were performed after the SPE.

In method II, SPE was performed immediately after the derivatization. The time lapse between the derivatization and injection is about 15 min for the first sample to be injected. The following samples have a longer time lapse while sitting in the auto-sampler (15 min of run time for each preceding vial). The reproducibility data show that the differ-

ence in time lapse among the samples did not affect the area count. This is possibly due to a stabilization effect when the reaction medium is removed by the SPE (leaving only the pure derivatives).

Part 3

Peak areas and serum concentrations were linearly related, using method II (12.8 to 128 μ M corresponding to 20 to 200 pmol on column) with a correlation coefficient of 0.998.

The reproducibility of six standard runs (96 μ M) has a relative standard deviation of 1.1%.

Part 4

The recoveries of spiked samples in the concentration range of 160 to 640 μ M (32 to 128 μ M after dilution) are 92 to 106% with a relative standard deviation of 6.6%.

The reproducibility of 6 spiked samples 640 μ M (128 μ M after dilution) has an average recovery of 97% and a relative standard deviation of 3.6%.

An improvement that can be visualized for the application of method II is to have an on-line SPE processor to automate the SPE process in addition to the derivatization process and inject the SPE eluate onto the HPLC system.

CONCLUSIONS

The use of fluorescence detection of pre-column

^a Retention time of derivative 2 is shorter than in Part I due to an adjustment in mobile phase to 50% acetonitrile.

derivatized tobramycin has tremendously enhanced detection sensitivity compared to detection by UV. The derivatization is simple, occurs at room temperature, involves no highly toxic reagents and can be fully automated.

Derivatization preceding SPE decreases the polarity of the analyte (tobramycin), thus increasing the selectivity in reversed phase SPE. The results show very good recoveries, linearity, reproducibility and separation of the analyte from the matrix components.

ACKNOWLEDGEMENTS

The authors gratefully acknowledge the gift of tobramycin standard from Eli Lilly and the illustrations from Patti Morris and Alice Kaneshige.

REFERENCES

- 1 J. P. Anhalt and S. D. Brown, *Clin. Chem.*, 24 (1978) 1940–1947.
- 2 H. Fabre, M. Sekkat, M. D. Blanchin and B. Mandrou, *J. Pharm. Biomed. Anal.*, 7 (1989) 1711–1718.
- 3 D. M. Barends, J. S. Blauw, C. W. Mijnsbergen, C. J. L. R. Grovers and A. Hulshoff, *J. Chromatogr.*, 322 (1985) 321–331.
- 4 D. M. Barends, J. C. A. M. Brouwers and A. Hulshoff, *J. Pharm. Biomed. Anal.*, 5 (1987) 613–617.
- 5 S. Udenfried, S. Stein, P. Boehler, W. Dairman, W. Lein-gruber and M. Weigele, *Science (Washington, D.C.)*, 178 (1972) 871–872.
- 6 M. Roth, *Anal. Chem.*, 43 (1971) 880–882.
- 7 M. W. Dong, *LC · GC*, 5 (1987) 255–260.
- 8 S. E. Bäck, I. Nilsson-Ehle and P. Nilsson-Ehle, *Clin Chem.*, 25 (1979) 1222–1225.
- 9 J. D'Souza and R. I. Ogilvie, *J. Chromatogr.*, 232 (1982) 212–218.
- 10 L. Essers, *J. Chromatogr.*, 305 (1984) 345–352.
- 11 J. Bell, R. Simpson and A. Mayer, *Am. Lab.*, May (1987) 106–110.

Column liquid chromatography and microbiological assay compared for determination of cefadroxil preparations

Mei-Chich Hsu, Ya-Wen Chang and Yu-Tzer Lee

National Laboratories of Foods and Drugs, Department of Health, Executive Yuan, 161-2 Kuen Yang St., Nankang, Taipei 11513 (Taiwan)

(First received February 25th, 1992; revised manuscript received May 18th, 1992)

ABSTRACT

A reversed-phase column liquid chromatographic method was developed for the assay of cefadroxil in bulk drugs and pharmaceutical preparations. An equation was derived showing a linear relationship between peak-area ratios of cefadroxil to dimethylphthalate (internal standard) and the cefadroxil concentration over a range of 0.02–0.8 mg/ml ($r = 0.9999$). Standard addition recoveries were generally greater than 97.7%. The coefficients of variation in the within-day assay were between 0.36 and 0.65, and in the between-day assay was 0.71%. The column liquid chromatographic assay results were compared with those obtained from a microbiological assay, which indicated that the proposed method is a suitable substitute for the microbiological method for potency assays and stability studies of cefadroxil preparations.

INTRODUCTION

The present official assay method of the U.S. *Code of Federal Regulations* [1] describes two official methods for potency assay of cefadroxil: a microbiological method and hydroxylamine assay. The regulations state that the results obtained from the microbiological method shall be conclusive. The greatest disadvantage of the microbiological, and chemical methods in current use is their lack of specificity. This deficiency has prompted the search for an alternative method which is fast, simple and selective, e.g. column liquid chromatography (LC). Several LC methods for the determination of cefadroxil in biological fluids [2–4] and to separate cephalosporin compounds [5–8] have been reported.

In order to establish whether an LC method is acceptable, it is important to determine whether it is

robust enough for assaying samples kept under extreme conditions. Degradation in the sample should be equally reflected by microbiological and LC assays. This paper describes a comparison of a proposed LC method with a microbiological assay for the determination of cefadroxil in commercial formulations. Further, cefadroxil was kept at elevated temperatures as part of an accelerated degradation experiment and assayed by microbiological and LC methods.

EXPERIMENTAL

Apparatus

A Waters Model 600E consisting of two solvent pumps, a Model 484E UV detector and a Model 746 data module were employed during the study. Samples were introduced through a Model U6K injection valve (Waters Chromatography Division, Milford, MA, USA). The mobile phase was pumped through a reversed-phase column (μ Bondapak C₁₈, 30 cm \times 3.9 mm I.D., particle size 10 μ m; Waters P/N 27324) The mobile phase was aceto-

Correspondence to: Dr. Mei-Chich Hsu, National Laboratories of Foods and Drugs, Department of Health, Executive Yuan, 161-2 Kuen Yang St., Nankang, Taipei 11513, Taiwan.

nitrile-0.01 M phosphate buffer solution, pH 4.5 (60:40, v/v). The mobile phase was filtered (0.45- μ m Millipore filter) and degassed with an ultrasonic bath prior to use. Flow-rate was 1.0 ml/min. The detector was set at 254 nm. Chromatography was performed at room temperature. Injections of 10 μ l were made of all solutions to be analysed.

Reagents and materials

Acetonitrile, LC grade was supplied by J. T. Baker (Phillipsburg, NJ, USA). Potassium phosphate, monobasic, reagent grade, was supplied by Wako (Osaka, Japan). Dimethylphthalate, reagent grade, was supplied by E. Merck (Darmstadt, Germany). Cefadroxil was NLFD house standard (National Laboratories of Foods and Drugs, Taipei, Taiwan). Different lot numbers of cefadroxil bulk drugs were kindly donated by local manufacturers. Capsules and powders to make solutions of cefadroxil to be taken orally were obtained from com-

mercial sources. Double-deionized water was used for all solution preparations.

Standard solutions

Internal standard dimethylphthalate (3 g) was dissolved in 100 ml of acetonitrile-water (1:1). Exactly 0.5 ml of this internal standard solution were added to 5.0 ml of a 1 mg/ml cefadroxil standard solution and the volume was made up to 50.0 ml with 0.1 M phosphate buffer solution (pH 4.5).

Sample preparation

To accurately weighed samples of bulk drugs, homogeneous capsule contents or powders for oral solution formulations (equivalent to 50 mg of cefadroxil) were added 50 ml of 0.1 M (pH 4.5) phosphate buffer solution. Exactly 0.5 ml of internal standard solution was added to 5.0 ml of 1 mg/ml cefadroxil sample solution and the volume was made up to 50.0 ml with 0.1 M phosphate buffer solution (pH 4.5).

TABLE I

RECOVERY OF CEFADROXIL FROM VARIOUS COMMERCIAL COMPOSITES

Manufacturer	Added (mg)	Found (mg)	Average recovered (%)
Capsule (250 mg)			
A	1.0	0.99	99.5
B	1.0	0.99	
C	1.0	1.01	
Capsule (500 mg)			
B	1.2	1.19	99.8
D	1.2	1.21	
E	1.2	1.21	
F	1.2	1.21	
G	1.2	1.21	
H	1.2	1.20	
I	1.2	1.21	
J	1.2	1.19	
K-1	1.2	1.18	
K-2	1.2	1.18	
K-3	1.2	1.21	
K-4	1.2	1.21	
L	1.2	1.20	
M	1.2	1.17	
N	1.2	1.20	
Powders for oral solution (125 mg/5 ml)			
B	2.4	2.48	103.1
C	2.4	2.54	
I	2.4	2.48	
K	2.4	2.39	

Solution for linearity response

Ten solutions of cefadroxil, which ranged in concentration from 0.02 to 0.8 mg/ml, were prepared. Each solution was chromatographed six times.

Solutions for recovery studies

Different amounts of cefadroxil standard and appropriate amounts of internal standard solution were combined. Each solution was chromatographed in triplicate.

Microbiological assay procedure

Bacillus subtilis (Culture Collection and Research Center, Taiwan) was used in the microbiological assay. According to the cup plate method, standards and test drugs were diluted to 1.0 mg/ml (potency) with 0.1 M phosphate buffer solution (pH 4.5) and then diluted to 30.0 and 7.5 $\mu\text{g}/\text{ml}$ with 0.1 M phosphate buffer solution (pH 4.5) on the day of analysis. Five 9.0-cm-diameter Petri dishes were used for each sample. After incubation for 16–18 h, the zone diameter was measured by a zone analyser (Model ZA-F; Toyo, Tokyo, Japan).

RESULTS AND DISCUSSION

The linearity of the relationship between peak-area ratio (cefadroxil vs. internal standard) and cefadroxil concentration was verified by injection of ten solutions containing 0.2–8 μg of cefadroxil and 3 μg of dimethylphthalate. A straight line with a correlation coefficient of 0.9999 ($y = 11.3444x + 0.0010$) was obtained when the ratios of the area counts of the cefadroxil divided by the area counts of the internal standard were plotted against concentration of cefadroxil.

Reproducibilities for both within-day assays and between-day assays were evaluated. The coefficients of variation, on the basis of peak-area ratios for six replicate injections in the within-day assay, were between 0.36 and 0.65% at the cefadroxil amount of 1 μg . The coefficient of variation in the between-day assay ($n = 6$) was 0.71% at the same amount.

The results of standard addition recovery studies of cefadroxil from sample composites of commercial preparations and powders for oral solution are shown in Table I. The average recoveries were 99.5% for 250-mg capsules, 99.8% for 500-mg capsules and 103.1% for powders for oral solution.

These data indicate that the proposed LC method is relatively unaffected by the sample matrix.

Typical chromatograms of the cefadroxil commercial dosage forms are shown in Fig. 1. The retention time was about 2.4 min for cefadroxil and 4.7 min for the internal standard. Excipients from commercial formulations did not interfere.

When samples of capsule and powders for oral solution formulations were heat degraded, the resulting mixtures yielded chromatograms containing additional peaks, none of which interfered with the interpretation and measurement of the chromatographic peaks for cefadroxil and dimethylphthalate, as shown in Fig. 1. In addition, a decrease in peak

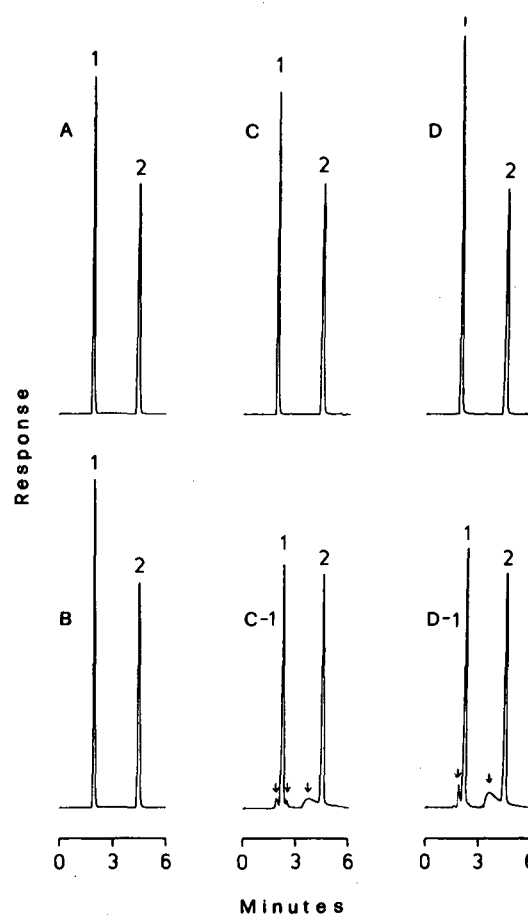


Fig. 1. Chromatograms of cefadroxil preparations: (A) house standard; (B) bulk drug substance; (C) capsule; (C-1) degraded capsule; (D) powder for oral solution; (D-1) degraded powder for oral solution. Peaks: 1 = cefadroxil; 2 = dimethylphthalate. Arrows indicate degradation compounds.

TABLE II
COMPARISON OF MICROBIOLOGICAL AND LC ASSAYS FOR CEFADROXIL

The potency was determined as micrograms per milligram for bulk drug and as a percentage of the declared amount for dosage forms. Values for the microbiological assay are averages of five determinations; values for LC are averages of three determinations.

Sample	Found in	
	Microbiological assay	LC
<i>Bulk drug</i>		
House standard	934.8	934.8
Brand C	909.9	915.3
Brand D	915.0	923.7
Brand E	918.6	923.7
Brand F	884.8	915.3
Brand G	896.1	915.3
Brand H	940.8	898.3
Brand I	918.4	915.3
Brand J	927.1	906.8
<i>Dosage form, declared</i>		
Brand A, 250 mg/capsule	105.1	104.4
Brand B		
250 mg/capsule	94.9	97.4
500 mg/capsule	94.0	95.6
125 mg/5 ml powders for oral solution	102.4	106.1
Brand C		
250 mg/capsule	105.9	107.8
125 mg/5ml powders for oral solution	110.3	113.9
Brand D, 500 mg/capsule	102.0	107.0
Brand E, 500 mg/capsule	102.7	104.4
Brand F, 500 mg/capsule	99.5	101.7
Brand G, 500 mg/capsule	103.9	102.6
Brand H, 500 mg/capsule	108.5	111.3
Brand I		
500 mg/capsule	103.3	100.9
125 mg/5ml powders for oral solution	107.4	104.4
250 mg/5ml powders for oral solution	105.2	103.5
Brand J, 500 mg/capsule	97.5	100.0
Brand K, 125 mg/5 ml powders for oral solution	108.2	119.2
Brand K-1, 500 mg/capsule	102.0	105.2
Brand K-2, 500 mg/capsule	97.3	99.1
Brand K-3, 500 mg/capsule	107.0	107.0
Brand K-4, 500 mg/capsule	101.3	99.1
Brand L, 500 mg/capsule	98.4	97.4
Brand M, 500 mg/capsule	95.0	103.5
Brand N, 500 mg/capsule	94.5	98.3

height (and/or peak area) with increase in temperature and time can be observed.

A number of samples of bulk drug substance and commercial preparations of fourteen brands were analysed for cefadroxil content by LC. These samples were also assayed by the microbiological meth-

od. The results are shown in Table II. A *t*-test was applied to the data: analysis showed no significant difference at the 99% confidence level for any of the preparations when assayed by the microbiological or LC methods.

A study was initiated to ascertain the suitability

TABLE III

COMPARISON OF PERCENTAGE POTENCY OF CEFADROXIL FORMULATION AS DETERMINED BY MICROBIOLOGICAL AND LC METHODS

Formulation	Percentage of declared concentration in	
	Microbiological assay	LC
Capsule (250 mg)	111.0	104.2
	91.6	93.0
	87.8	84.0
	63.2	69.0
Capsule (500 mg)	112.2	116.4
	104.3	104.3
	102.7	104.4
	101.6	100.7
	102.3	99.2
	100.5	96.8
	94.6	98.4
	90.1	91.2
	83.8	85.2
	69.0	75.6
	58.7	61.8
	36.8	40.4
Powders for oral solution (125 mg/5 ml)	32.8	37.6
	22.2	26.7
	15.7	20.6
	106.7	110.5
	101.2	101.3
	89.7	86.6

of the proposed method for stability studies. Samples were made to a concentration of 1 mg/ml and stored in temperature-controlled cabinets (ambient or 55–150°C). Samples were taken from the cabinets periodically for microbiological and LC assays. The assay values, expressed as a percentage of the level claim, are given in Table III. The 22 paired values in Table III have a correlation coefficient of 0.994. This value indicates that no significant difference was found in the assay values obtained by the two analytical methods for degraded or non-degraded samples.

This study demonstrates the applicability of the proposed LC method for the potency determination of cefadroxil in bulk drug, capsules and powders for oral solution formulations. The method can be successfully used for routine quality control and stabil-

ity assays and offers advantages in speed, simplicity and reliability.

ACKNOWLEDGEMENTS

This work was supported by the National Laboratories of Foods and Drugs, Department of Health, Executive Yuan, Taiwan. The authors thank Miss Hsiou-Chuan Chung for her assistance in the preparation of this manuscript.

REFERENCES

- 1 *Code of Federal Regulation*. Title 21, Part 440, US Government Printing Office, Washington, DC, 1988.
- 2 K. Lindgren, *J. Chromatogr.*, 413 (1987) 347.
- 3 J. A. McAteer, M. F. Hiltke, B. M. Silber and R. D. Faulkner, *Clin. Chem. (Winston-Salem, N.C.)*, 33 (1987) 1788.

- 4 M. C. Nahata and D. S. Jackson, *J. Liq. Chromatogr.*, 13 (1990) 1651.
- 5 I. Wouters, S. Hendrickx, E. Roets, J. Hoogmartens and H. Vanderhaeghe, *J. Chromatogr.*, 291 (1984) 59.
- 6 I. Wouters, S. Hendrickx, E. Roets, J. Hoogmartens and H. Vanderhaeghe. in S. Ahuja (Editor), *Chromatography and Separation Chemistry: Advances and Developments (ACS Symp. Ser., No. 297)* American Chemical Society, Washington, DC, 1986, p. 68.
- 7 S. Ting, *J. Assoc. Off. Anal. Chem.*, 71 (1988) 1123.
- 8 R. W. Slingsby and M. Rey, *J. Liq. Chromatogr.*, 13 (1990) 107.

Chiral separation of nipecotic acid amides

Z. Feng, R. Gollamudi and G. Han

Department of Medicinal Chemistry, University of Tennessee—Memphis, Memphis, TN 38163 (USA)

Y. Tang and D. W. Armstrong

Department of Chemistry, University of Missouri, Rolla, MO 65401 (USA)

(First received March 18th, 1992; revised manuscript received May 14th, 1992)

ABSTRACT

1-Decyl-3-(N,N-diethylcarbamoyl)piperidine (1) and α,α' -bis[3-(N-benzyl-N-methylcarbamoyl)piperidinol]-*p*-xylene (2) represent mono-N-substituted and bis-N-substituted carbamoylpiperidines, or nipecotic acid amides, respectively. Initially, several attempts were made to resolve these compounds using β -cyclodextrin, cellulose carbamate and Pirkle-type columns. However, the interactions of the stereoisomers of the two compounds with these stationary phases did not differ enough to permit satisfactory separations. Baseline resolution was achieved using an α_1 -acid glycoprotein (AGP) chiral column. The mobile phase was phosphate buffer (pH 7.0). Tetrabutylammonium (TBA) was used as the cationic modifier and ethanol as the uncharged modifier. Circular dichroism was used to identify the enantiomers. Compound 1 was resolved into positive and negative enantiomers and 2 into positive and negative enantiomers and a *meso* diastereomer. The influence of pH, buffer ionic strength, cationic and uncharged modifier concentrations on retention, chiral selectivity and resolution were evaluated. Based on the results, it is suggested that both ionic and hydrophobic interactions may be responsible for retention and resolution.

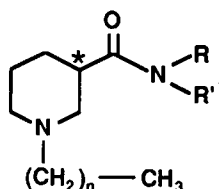
INTRODUCTION

Many drugs are marketed as racemates although one enantiomer may contribute to virtually all of the therapeutic activity [1]. In a few instances, the less active isomer happens to be the more toxic one [2]. Therefore, chiral resolutions of biologically active compounds assume considerable therapeutic importance.

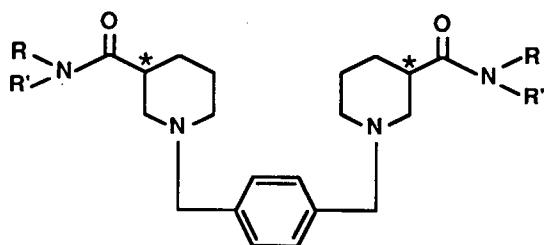
Our laboratory has been engaged in the synthesis of nipecotic acid amides (Fig. 1) of types I and II as potential antithrombotic agents. Although the precise mechanism of the antiplatelet action of these compounds has not yet been elucidated, it has been hypothesized that they interact with anionic phospholipids, *e.g.*, phosphatidylserine and phosphati-

dylinositol, of the platelet membrane [3,4] and of certain intracellular organelles [5,6]. As these phospholipid molecules contain many chiral centers, it is conceivable that stereoselective interactions occur with xenobiotics. Types I and II compounds have chiral centers at the 3-position of the piperidine ring and therefore could exhibit stereoselective interactions with anionic phospholipids. With a view to investigating such properties, we have attempted the resolution of these compounds. 1-Decyl-3-(N,N-diethylcarbamoyl)piperidine hydrobromide (1; type I, $n = 9$, R, R' = Et) and α,α' -bis[3-(N-benzyl-N-methylcarbamoyl)piperidinol]-*p*-xylene dihydrobromide (2; type II, R = Bz, R' = Me) were chosen for resolution as representatives of the two structural types. Compound 1 has been reported to inhibit ADP-induced human platelet aggregation *in vitro* (IC_{50} 174.3 μM) [7]. Compound 2 was potent in inhibiting platelet aggregation *in vitro* (IC_{50} 27.3 μM) [8] and in protecting mice from thromboembo-

Correspondence to: Dr. R. Gollamudi, Department of Medicinal Chemistry, University of Tennessee—Memphis, Memphis, TN 38163, USA.



Type I. 1-[3-(N,N-dialkylcarbamoyl)piperidino]-alkanes



Type II. α, α' -Bis[3-(N,N-dialkylcarbamoyl)piperidino]-*p*-xylenes

Fig. 1. Structures of nipecotic acid amides. The chiral center is indicated with an asterisk.

lic death upon challenge with collagen and epinephrine [9]. Compound **1** can exist as *R* and *S* enantiomorphs and **2**, which has two chiral centers, can exist as *R,R* and *S,S* enantiomers and *R,S* and *S,R* diastereomers. The *R,S* and *S,R* forms are superimposable and, therefore, achiral. Consequently, they are represented as the *meso* configuration. This paper describes the resolution of **1** and **2** on a chiral α_1 -acid glycoprotein (AGP) column.

EXPERIMENTAL

Materials

Tetrabutylammonium (TBA), hydrogensulfate, bromide, chloride and hydroxide were purchased from Sigma (St. Louis, MO, USA). Anhydrous Na_2HPO_4 (analytical-reagent grade) was obtained from Mallinckrodt (St. Louis, MO, USA) and NaH_2PO_2 (reagent grade) from MCB Manufacturing Chemists (Cincinnati, OH, USA). Platinum-(IV) oxide monohydrate was purchased from Aldrich (Milwaukee, WI, USA). High-performance

liquid chromatographic (HPLC) solvents including water were supplied by Burdick and Jackson (Muskegon, MI, USA). All solvents and buffers were filtered using nylon-66 (0.45- μm) filters (Rain-in Instruments, Woburn, MA, USA). The solvents were continuously degassed by purging with helium (ultrahigh purity; Liquid Air, Walnut Creek, CA, USA).

Instrumentation

The chromatographic system consisted of a Waters U6K injector, a Model 600E Powerline multi-solvent delivery system, a Model 484 tunable UV-VIS detector, a NEC PowerMate SX plus computer with an NEC P5200 printer/plotter and Baseline 810 Chromatography Workstation software. A chiral AGP (5- μm) analytical column (100 \times 4.0 mm I.D.) was purchased from Regis Chemical (Morton Grove, IL, USA). The following chiral HPLC columns (250 \times 4.6 mm I.D.) (5 μm) were used in the exploratory part of this investigation: (*R*)-naphthylalanine (covalent), (*S*)-naphthyleucine (covalent) (both from Regis Chemical), (*R*)-naphthylurea and (*R*)-(3,5-dinitrobenzoyl)phenylglycine (covalent) (both from J. T. Baker, Phillipsburg, NJ, USA) and (*S*)-naphthylethylcarbamate-derivatized β -cyclodextrin (Cyclobond I SN) (from Astec, Whippany, NJ, USA). Chiralcel AD and Chiralpak OD were both obtained from Chiral Technologies (Exton, PA, USA).

Synthesis

Compound **1** was synthesized as described [10]. Compound **2** was obtained by the catalytic reduction ($\text{PtO}_2\text{-H}_2$) of α, α' -bis[N-benzyl-N-methylcarbamoyl]pyridinium]-*p*-xylene dibromide, which was prepared by the condensation of α, α' -dibromo-*p*-xylene and N-benzyl-N-methylnicotinamide; the latter was obtained by reaction of nicotinoyl chloride with N-benzylmethylamine [8].

HPLC

In the exploratory phase of the chiral separations, the mobile phases consisted of various ratios of solvents at flow-rates ranging from 0.4 to 0.9 ml/min. The following are typical examples, where either very poor or no resolution occurred and **1** and **2** eluted as fused, or single peaks: with (*S*)-naphthyleucine column, *n*-hexane (with and without 0.0025

M triethylamine)-methanol, 2-propanol or 2-butanol, *n*-hexane (0.0025 *M* triethylamine)-2-butanol and chloroform, $k' = 1.5$ –14 when triethylamine was added to *n*-hexane and >60 when it was not added; with (*R*)-naphthylalanine column, *n*-hexane (0.0025 *M* triethylamine)-2-propanol-chloroform, $k' = 4$ –19; with Cyclobond I SN column, *n*-hexane-2-propanol, acetonitrile-triethylammonium acetate (pH 4.0 and 7.0), $k' = 4$ –14; and with Chiralcel AD column, 2-propanol-*n*-hexane, ethanol-*n*-hexane and methanol-*n*-hexane, $k' = 4$ –14.

Resolution of compounds 1 and 2 on a chiral α_1 -AGP column

A systematic study was carried out with a view to (i) establishing how separation is affected by altering experimental parameters such as pH, ionic strength and flow-rate, and (ii) obtaining an optimum separation of the isomers. The HPLC conditions and parameters were gradually changed and the resultant effects on the capacity factor (k'), selectivity (α) and resolution (R_s) were calculated using the following equations:

$$k' = (V_1 - V_0)/V_0$$

$$\alpha = (V_2 - V_0)/(V_1 - V_0)$$

$$R_s = (V_2 - V_1)/[1/2(W_1 + W_2)]$$

where V_1 and V_2 = retention volumes of the first- and second-eluted components, respectively, V_0 = void volume and W_1 and W_2 = widths of peaks A and B, respectively. Optimum conditions consisted of a mobile phase of 10% ethanol in 0.025 *M* phosphate buffer (PB) (pH 7.0) containing 0.025 *M* TBA · HSO₄. The flow-rate was 0.9 ml/min and the detector was set at 225 nm. Compounds 1 and 2 were dissolved in the mobile phase for injection into the column.

Circular dichroic spectra

A Jasco (Tokyo, Japan) J-600 spectropolarimeter was used to obtain circular dichroic (CD) spectra. The collected chromatographic fractions were extracted with diethyl ether (pH 9.0), the solvent was evaporated and the residues were dissolved in 2.2 ml of cyclohexane (HPLC grade, Aldrich). Dissolution was completed with the help of a vortex stirring device. A 1.0-cm path-length cylindrical quartz cell (Jasco) was used to hold the sample solution. The

conditions for CD data acquisition were as follows: band width = 2 nm; slit width = auto; time constant = 2.0 s; step resolution = 1 nm; scan speed = 50 nm/min; number of scans = 2; wavelength set from 180 to 500 nm. The raw data was further smoothed using a set data interval of 1.

RESULTS AND DISCUSSION

Compound 1 was resolved into two components, 1A and 1B (Fig. 2), and 2 was separated into three components, 2A, 2B and 2C (Fig. 3), achieving a baseline separation on the α_1 -AGP column with a mobile phase consisting of 10% ethanol in 0.025 *M* PB containing 0.025 *M* TBA · HSO₄ (pH 7.0) at a flow-rate of 0.9 ml/min. It is apparent from the CD spectra that 1A has a positive Cotton effect at 230 nm and that 1B is its optical antipode with a negative Cotton effect at the same wavelength (Fig. 4). Components 2A and 2C appear to be enantiomers, giving negative and positive Cotton effects respectively, at 235 nm (Fig. 5). Fraction 2B, which shows no Cotton effect, should be the *meso* isomer.

Several attempts were made to resolve these compounds on β -cyclodextrin, cellulose carbamate and Pirkle-type columns. The interactions of the two enantiomers of 1 and of the three isomers of 2 with the stationary phases of these columns did not differ sufficiently to afford satisfactory resolution. The α_1 -AGP column, derived from human plasma, has

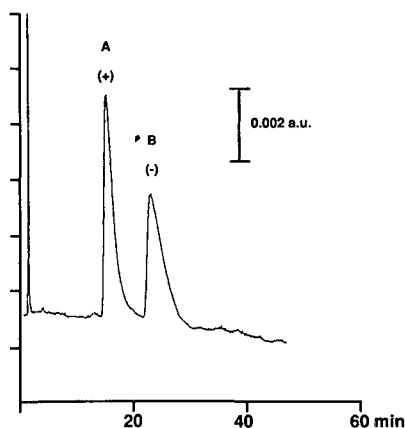


Fig. 2. Chromatogram showing resolution of 1 (2 μ g injected). A chiral AGP (5- μ m) analytical column (100 mm \times 4 mm I.D.) was used with a mobile phase consisting of 10% ethanol in 0.025 *M* PB (pH 7.0) containing of 0.025 *M* TBA · HSO₄. Flow-rate, 0.9 ml/min; temperature, ambient.

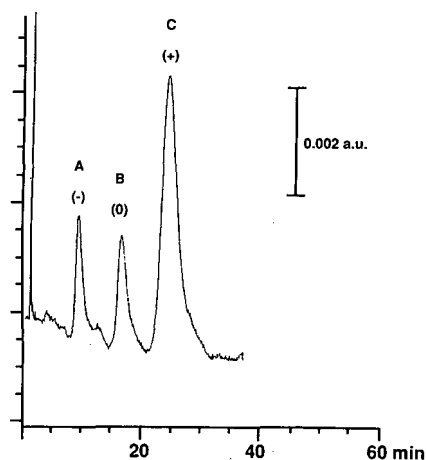


Fig. 3. Chromatographic resolution of **2**. Conditions as in Fig. 2.

been found to be useful for the separation of a number of basic pharmaceutical compounds, presumably because this acidic protein can interact with protonated bases by ion exchange [11]. It therefore appeared suitable for the resolution of nipecotic acid amides (3-carbamoylpiperidines). α_1 -AGP, with an isoelectric point at $\text{pH} \approx 2$, has a net negative charge at $\text{pH} 7.0$ [11]. The piperidine nitrogen of **1** and **2** is believed to be protonated at $\text{pH} 7.0$ and can be expected to be tightly bound to the stationary phase. Also, because of the presence of a C_{10} alkyl chain in **1** and the xylylene moiety in **2**, both ionic and hydrophobic interactions are possible. The cationic modifier TBA could compete with **1** and **2** for ionic bonding with anionic groups such as sialic acid residues present on the glycoprotein [11].

α_1 -AGP contains several chiral centers with different binding characteristics. It is therefore possible

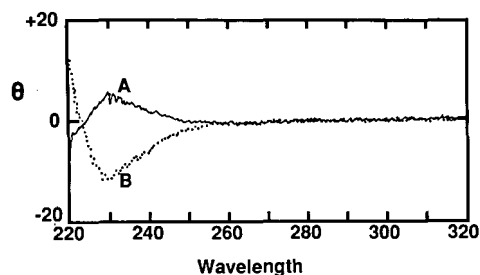


Fig. 4. CD spectrum of fractions A and B from **1**. Approximate concentrations: **1A** = 0.1 and **1B** = 0.5 mg/ml in cyclohexane. Wavelength in nm; θ in millidegrees.

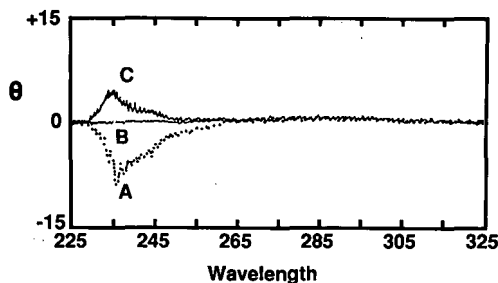


Fig. 5. CD spectrum of fractions A, B and C separated from **2**. Approximate concentrations: **2A** = 0.4, **2B** = 0.2 and **2C** = 0.5 mg/ml in cyclohexane. Wavelength in nm; θ in millidegrees.

to alter the retention time, selectivity and resolution by varying the mobile phase pH, molarity and organic and ionic modifiers, in order to arrive at an optimum separation.

Effect of pH

The influence of pH was more pronounced than the effects of organic and ionic modifiers. Retention and resolution increased with increasing pH, suggesting that an increase in the negative charge of the AGP molecule results in a greater ion-exchange binding of the positively charged sample molecules (Table I). Thus, for **1**, changing the pH from 6.0 to 7.0 increased α from 1.14 to 1.58 and increased R_s from 0.43 to 1.28, providing baseline separation of the two components. At pH 7.0, the three components of **2** showed baseline separation ($\alpha_1 = 1.87$, $\alpha_2 = 1.51$) but lower pH values resulted in incomplete resolution or no resolution at all. Because of the low efficiency of AGP columns, selectivity factors > 1.5 are believed to be required to achieve baseline separations [12].

It may be noted that with **1** and **2**, a cationic N^+ moiety (at pH 7.0 of the mobile phase) is separated from the chiral center by one carbon atom and also the hydrogen-bonding amide group is coupled directly to the chiral center, features deemed favorable for chiral resolution on an α_1 -AGP column [13].

Effect of uncharged modifier

Organic solvents influence resolution and selectivity by causing conformational changes in the protein molecules. The retention, selectivity and resolution of **1** decreased when the organic modifier was changed from ethanol to 2-propanol and from

TABLE I

EFFECT OF pH ON CAPACITY FACTOR (k'), SELECTIVITY (α) AND RESOLUTION (R_s)Mobile phase: 0.025 M phosphate buffer containing 10% ethanol and 0.025 M TBA · HSO₄. Flow-rate, 0.9 ml/min.

pH	1			2				
	k'^a	α	R_s	k'^b	α_1	α_2	R_{s1}^c	R_{s2}^d
6.0	10.82	1.14	0.43	One peak				
6.5	17.15	1.21	0.76	Two peaks				
7.0	19.91	1.58	1.28	21.65	1.87	1.51	1.29	0.88

^a Capacity factor of the second-eluted peak.^b Capacity factor of the third-eluted peak.^c Resolution of peaks A and B.^d Resolution of peaks B and C.

TABLE II

EFFECT OF ORGANIC MODIFIER ON CAPACITY FACTOR (k'), SELECTIVITY (α) AND RESOLUTION (R_s)Mobile phase: 0.025 M phosphate buffer (pH 7.0) containing 10% of organic modifier and 0.025 M TBA · HSO₄. Flow-rate, 0.9 ml/min.

Organic modifier	1			2				
	k'^a	α	R_s	k'^b	α_1	α_2	R_{s1}^c	R_{s2}^d
Ethanol	19.91	1.58	1.28	21.65	1.87	1.51	1.29	0.88
2-Propanol	10.94	1.40	0.76	12.49	1.46	1.32	0.93	0.62
Acetonitrile	9.31	1.18	0.69	10.49	1.35	1.62	0.84	1.33

^a Capacity factor of the second-eluted peak.^b Capacity factor of the third-eluted peak.^c Resolution of peaks A and B.^d Resolution of peaks B and C.

TABLE III

EFFECT OF MOBILE PHASE SOLVENT RATIO WHEN USING ETHANOL AS ORGANIC MODIFIER ON CAPACITY FACTOR (k'), SELECTIVITY (α) AND RESOLUTION (R_s)Mobile phase: 0.025 M phosphate buffer (pH 7.0) containing ethanol and 0.025 M TBA · HSO₄. Flow-rate, 0.9 ml/min. The values represent averages of three independent determinations.

Ethanol-buffer (v/v)	1			2				
	k'^a	α	R_s	k'^b	α_1	α_2	R_{s1}^c	R_{s2}^d
20:80	10.98	1.52	1.11	10.08	1.33	1.32	0.61	0.76
15:85	17.25	1.59	1.34	18.48	1.36	1.45	0.75	0.92
10:90	22.32	1.60	1.36	26.35	1.57	1.53	0.96	1.10
7:93	41.84	1.70	1.61	55.19	1.77	1.45	1.85	1.34
3:97	107.86	1.73	1.97	153.99	3.11	1.44	3.54	1.48

^a Capacity factor of the second-eluted peak.^b Capacity factor of the third-eluted peak.^c Resolution of peaks A and B.^d Resolution of peaks B and C.

TABLE IV

EFFECT OF BUFFER CONCENTRATION ON CAPACITY FACTOR (k'), SELECTIVITY (α) AND RESOLUTION (R_s)

Mobile phase: Phosphate buffer (pH 7.0) containing 10% ethanol and 0.025 M TBA · HSO₄. Flow-rate, 0.9 ml/min. The values represent averages of three independent determinations.

Buffer concentration (M)	1			2				
	k'^a	α	R_s	k'^b	α_1	α_2	R_{s1}^c	R_{s2}^d
0.01	24.52	1.40	1.21	29.04	1.46	1.61	0.84	1.28
0.015	24.19	1.49	1.28	28.56	1.57	1.56	0.88	1.14
0.025	22.32	1.60	1.36	26.35	1.57	1.53	0.96	1.10
0.035	18.00	1.60	1.37	25.32	1.69	1.43	1.00	0.81

^a Capacity factor of the second-eluted peak.

^b Capacity factor of the third-eluted peak.

^c Resolution of peaks A and B.

^d Resolution of peaks B and C.

2-propanol to acetonitrile (Table II). Similarly, the k' , α_1 and R_{s1} values of the first and second components of **2** decreased when the organic modifier was changed from ethanol to 2-propanol and then to acetonitrile. Consequently, ethanol was chosen as the organic modifier, although a better resolution of the second and third peaks of **2** was observed with acetonitrile than with ethanol as the modifier.

As would be expected, the retention times increased with decreasing ethanol concentration (Table III). The selectivity and resolution of both

compounds increased when the ethanol concentration was decreased from 20% to 3%. The separation factor (α_2) for peaks B and C of **2** increased with decreasing ethanol concentration from 20% to 10%. Further reduction to 3% resulted in a decrease in α_2 .

Effect of buffer and cationic modifier concentrations

The concentration of PB was increased stepwise from 0.01 to 0.035 M while maintaining the TBA · HSO₄ concentration at 0.025 M (Table IV). Increasing the buffer concentration resulted in a decrease in k' , suggesting an ion-exchange retention

TABLE V

EFFECT OF CATIONIC MODIFIER (TBA · HSO₄) ON CAPACITY FACTOR (k'), SELECTIVITY (α) AND RESOLUTION (R_s)

Mobile phase: 0.025 M phosphate buffer (pH 7.0) containing 10% ethanol and various concentrations of TBA · HSO₄. Flow-rate, 0.9 ml/min. The values represent averages of three independent determinations.

TBA · HSO ₄ concentration (M)	1			2				
	k'^a	α	R_s	k'^b	α_1	α_2	R_{s1}^c	R_{s2}^d
0.01	40.10	1.42	1.18	52.46	1.39	1.61	0.71	1.33
0.015	29.01	1.45	1.35	40.93	1.47	1.58	0.89	1.15
0.025	22.32	1.60	1.36	26.35	1.57	1.53	0.96	1.10
0.035	19.29	1.60	1.72	24.49	1.67	1.44	1.18	0.89

^a Capacity factor of the second-eluted peak.

^b Capacity factor of the third-eluted peak.

^c Resolution of peaks A and B.

^d Resolution of peaks B and C.

process. The selectivity and resolution increased with increasing buffer concentration. However, α_2 and R_{s2} decreased with increasing buffer concentration.

The relationship between selectivity and concentration of the charged modifier was also studied while the molarity of PB was maintained constant. Increasing the concentration of TBA from 0.01 to 0.035 M resulted in a decrease in the retention times and an increase in selectivity and resolution. However, the α_2 and R_{s2} values of **2** decreased with increasing TBA concentration (Table V). A change in the modifier concentration resulted in a change in selectivity, and as retention appears to be based on an ion-pairing mechanism, 3-carbamoylpiperidines can be presumed to bind to multiple chiral and achiral sites on the glycoprotein. If, on the other hand, the enantiomers were to be retained by a single type of binding site, then the stereoselectivity would not change with changes in the cationic modifier concentration [14].

The separation (α) and resolution (R_s) of the two enantiomers of **1**, and those of peaks A and B of **2**, followed the expected behavior. However, the α_2 and R_{s2} values of peaks B and C of **2** showed unexpected variability (Tables III–V). It is possible that stereochemical interactions between the latter two peaks and the chiral stationary phase are controlled by factors other than ion-exchange and hydrophobic interactions.

A flow-rate of 0.9 ml/min was chosen because of inefficient resolution at lower flow-rates. Ambient temperature was used for analysis. Higher or lower temperatures did not improve resolution.

The conditions that were chosen for further resolution of **1** and **2** consisted of a mobile phase of 10% ethanol in 0.025 M PB containing 0.025 M TBA · HSO₄ (pH 7.0) with a flow-rate of 0.9 ml/min. These conditions afforded baseline chiral resolution of **1** and **2**.

Column stability

Initially (1 week), the selectivity factor α for **1** was 1.60. After 4 weeks of use (200 injections), α was 1.47. During this period, the column was cleaned daily with water followed by 25% aqueous 2-propanol. It was also occasionally flushed with 0.01 M PB (pH 3.5) followed by 50% aqueous ethanol. The routine and diverse use of the column for 4 months and approximately 400 injections resulted in a

deterioration of its performance, and **2** was resolved into only two peaks ($\alpha = 1.46$) instead of three.

CONCLUSIONS

The resolution of mono- and bis-substituted nipe-cotic acid amides was not possible on many conventional chiral HPLC columns. Adequate separation was achieved on the α_1 -AGP column. Complete baseline chiral separation of **1** and **2** was achieved on this column with a mobile phase consisting of 10% ethanol in 0.025 M PB containing 0.025 M TBA · HSO₄ at pH 7.0. Compound **1** was separated into two enantiomers and **2** into two enantiomers and a diastereomer, as corroborated by their CD spectra. The effects of pH, ionic strength and ionic and uncharged modifiers were evaluated. Based on the results, an ion-pairing mechanism and hydrophobic interactions appear to be responsible for retention and resolution.

ACKNOWLEDGEMENT

This work was supported in part by a grant from the National Institutes of Health (HL 22236).

REFERENCES

- 1 M. Simonyi, J. Gal and B. Testa, *Trends Pharmacol. Sci.*, 10 (1989) 349.
- 2 Y. W. F. Lam, *Pharmacotherapy*, 8 (1988) 147.
- 3 R. P. Quintana, A. Lasslo, M. Dugdale and L. L. Goodin, *Thromb. Res.*, 22 (1981) 665.
- 4 E. O. Dillingham, A. Lasslo, R. Gollamudi, S. E. Bond and G. Carter-Burks, *Res. Commun. Chem. Pathol. Pharmacol.*, 58 (1990) 179.
- 5 A. Lasslo, *Res. Commun. Chem. Pathol. Pharmacol.*, 69 (1990) 133.
- 6 E. O. Dillingham, A. Lasslo, G. Carter-Burks, S. E. Bond and R. Gollamudi, *Biochim. Biophys. Acta*, 990 (1989) 128.
- 7 A. Lasslo, E. O. Dillingham, J. C. McCastlain, G. Carter-Burks, R. P. Quintana, R. W. Johnson and J. L. Naylor, *Med. Prog. Technol.*, 11 (1986) 109.
- 8 Z. Feng, R. Gollamudi, E. O. Dillingham, S. E. Bond, B. A. Lyman, W. P. Purcell, R. J. Hill and W. A. Korfmacher, *J. Med. Chem.*, 35 (1992) 2952.
- 9 W. H. Lawrence, R. H. Howell and R. Gollamudi, in preparation.
- 10 A. Lasslo and R. D. Waller, *J. Org. Chem.*, 22 (1957) 837.
- 11 J. Hermansson, *J. Chromatogr.*, 298 (1984) 67.
- 12 M. Lienne, M. Cauds, R. Rosseb and A. Tambrete, *J. Chromatogr.*, 448 (1988) 55.
- 13 J. Hermansson, K. Strom and R. Sandberg, *Chromatographia*, 24 (1987) 520.
- 14 G. Schill, I. W. Wainer and S. A. Barkan, *J. Liq. Chromatogr.*, 9 (1986) 641.

Normal-phase high-performance liquid chromatography with UV irradiation, morin complexation and fluorescence detection for the determination of organotin pesticides

Joan A. Stäb, Marcel J. M. Rozing, Bert van Hattum and Wim P. Cofino

Institute for Environmental Studies, Free University, De Boelelaan 1115, 1081 HV Amsterdam (Netherlands)

Udo A. Th. Brinkman

Department of Analytical Chemistry, Free University, De Boelelaan 1083, 1081 HV Amsterdam (Netherlands)

(First received March 20th, 1992; revised manuscript received June 1st, 1992)

ABSTRACT

A method has been developed for the determination of the organotin pesticides fentin, cyhexatin and fenbutatin oxide by high-performance liquid chromatography combined with UV photoconversion and post-column morin complexation followed by fluorescence detection. After optimization of the relevant parameters the feasibility of the method for analysing environmental samples was investigated. Detection limits are 1–2 ng in standard solutions, 0.02–0.03 µg/l in surface water and 0.2–0.3 µg/g in soil and sediment. The higher detection limits for soil and sediment samples are due to interfering compounds present in the matrix. The method allows trace level determinations in water samples. As an example, in a ditch adjacent to a potato field 16 days after a routine spraying with triphenyltin acetate, water concentrations of 0.03 µg/l could still be detected.

INTRODUCTION

Organotin compounds are used as poly(vinyl chloride) (PVC) stabilizers and as biocides in agriculture and antifouling paints. The annual worldwide production of organotins amounted to 40 000 tons in 1986 [1]. Since the disastrous effects of the use of organotins [mainly tributyltin salts (TBT)] in antifouling paints on the oyster culture in the bay of Arcachon (France), where oyster production fell by 70% in 2 years [2] and similar problems on the southern English coast [3], the environmental risk of organotin-based antifoulings became recognized. In many countries such as France, the UK, the

Netherlands and the USA, the use of organotin-based antifoulings is now restricted.

Another even larger deliberate input of organotin compounds into the environment occurs via their use as pesticides (Fig. 1) in agriculture. For example, in the Netherlands the annual use of fentin [triphenyltin acetate (TPT)] on potato crops was 300 tons of active compound in 1987[4]. This represents 8% of the total amount of fungicides used in agriculture in the Netherlands [5]; actually, compared with organotin-based antifoulings, three times more organotins were used in agriculture than in antifoulings in 1985 [1]. Fenbutatin oxide [hexakis-(2-methyl-2-phenylpropyl)distannoxane, FBTO] and cyclohexyltin compounds [cyhexatin; tricyclohexyltin hydroxide or azocyclotin; tricyclohexyltin-1,2,4-triazole (TCT)] were used in much more limited amounts, viz. 8 and 1 tons, respectively, in 1987.

Correspondence to: Dr. J. A. Stäb, Institute for Environmental Studies, Free University, De Boelelaan 1115, 1081 HV Amsterdam, Netherlands.

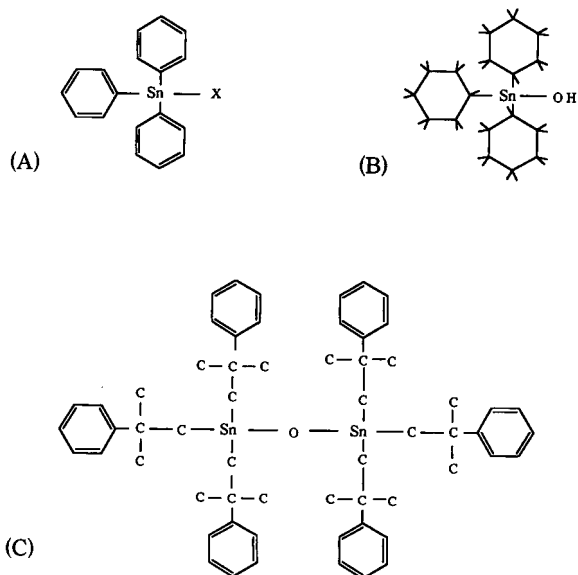


Fig. 1. Structural formulae of organotin pesticides. (A) Triphenyltin (TPT), for fentin, X = acetate. In the environment X is rapidly exchanged for a hydroxide ion. In the current study triphenyltin chloride (X = Cl) was used. (B) Tricyclohexyltin hydroxide, cyhexatin (TCT). (C) Fenbutatin oxide (FBTO). In the environment the dimeric form decomposes rapidly to the monomeric (hydroxide) form.

FBTO is mainly used on tomatoes and cucumbers and TCT is used on apples [4].

Sensitive techniques for the determination of organotin residues are essential in view of the environmental hazards. Several techniques exist for the determination of butyltin compounds. Gas chromatographic (GC) methods commonly rely on alkylation or hydride formation to obtain volatile derivatives. Several detection techniques can be applied: flame photometric [6,7], atomic absorption spectrometric (AAS)[8,9], mass spectrometric (MS) [10,11] and atomic emission detection [12].

High-performance liquid chromatography (HPLC) can handle more polar compounds than GC, therefore no derivatization prior to chromatography is needed. Unfortunately, common HPLC detectors do not offer the required sensitivity and selectivity. Some workers have used HPLC combined with specific detection techniques, such as graphite furnace AAS [13–16], hydride formation and quartz furnace AAS [17] or hydride formation–d.c. atomic emission spectrometry [18]. A drawback

of these techniques is that they require complicated interfacing of the HPLC effluent to the detector.

Another approach is to use post-column reaction detection where the organotin compounds are converted into products that are more easily detected by conventional HPLC detectors. Work has been done on oxine (8-hydroxyquinoline) and morin (3,5,7,2',4'-pentahydroxyflavone) complexation of organotin compounds. Oxine yields complexes that are usually determined with UV absorption detection [19,20]. Morin forms complexes that show strong fluorescence [21–25]. Langseth [21] used pre-/on-column complexation and Yu and Arakawa [22] used post-column morin complexation followed by fluorescence detection, but both only applied this technique to di- and monoorganotins. For triorganotin pesticides the formation of such complexes is not favourable, because the tin atom is shielded by bulky carbon chains. In this work, HPLC of triorganotins was combined with UV irradiation to cleave some of the carbon-tin bonds to obtain a product that can be complexed with morin.

A similar approach was used by Lakata *et al.* [19], who used oxine complexation and UV detection, reporting detection limits of 0.1–0.5 μg for several di- and triorganotins, except dibutyltin (DBT), which yielded a detection limit of 40 ng. As reported detection limits for morin complexes of diorganotins are much lower, with values in the range of 2 pg–1 ng [22,25], morin seems to be a better alternative than oxine, and was therefore used in the present study.

EXPERIMENTAL

Materials

Di-*n*-butyltin dichloride (DBT), diphenyltin dichloride (DPT) (96% purity), triphenyltin chloride (TPT) (95% purity) and morin (3,5,7,2',4'-pentahydroxyflavone) were obtained from Aldrich (Steinheim, Germany). Tri-*n*-butyltin acetate (TBT) was a gift from the Community Bureau for Reference (BCR) (Brussels, Belgium). Dicyclohexyltin dibromide (DCT) was purchased from Johnson Matthey Alfa (Karlsruhe, Germany). Cyhexatin (tricyclohexyltin hydroxide, TCT) (99% purity) was from Dr. Ehrenstorfer (Augsburg, Germany) and fenbutatin oxide (FBTO) (99.7% purity) was a gift from Atochem (Vlissingen, Netherlands). Ethanol

(HPLC grade), *n*-hexane (HPLC grade), tetrahydrofuran (THF) (HPLC grade), toluene (analytical-reagent grade), glacial acetic acid (analytical-reagent grade) and anhydrous sodium sulphate (Baker grade) were purchased from Baker (Deventer, Netherlands). Disposable cellulose nitrate filters (0.45 μm) for water filtration were supplied by Nalge (Rochester, NY, USA); 0.2- μm membrane filters (Rotrand) from Schleicher & Schüll (Dassel, Germany) were used to filter extracts before injection into the HPLC system.

Apparatus

The HPLC equipment consisted of a Kontron (Zürich, Switzerland) Model 410 single-piston pump or a Pharmacia (Uppsala, Sweden) LKB 2150 dual-piston pump, set at a flow-rate of 1 ml/min and equipped with a membrane pulse damper, a laboratory-made six-port injection valve with a 28- μl injection loop and a 15 cm \times 4.6 mm I.D. stainless-steel column packed with 3- μm cyanopropyl-bonded silica (Rosil Alltech, Zwijndrecht, Netherlands). The laboratory-made UV irradiation reactor contained a medium-pressure mercury lamp and was described by Scholten *et al.* [26]. The irradiation coil (length 76, 125 or 255 cm) and reaction coil (length 27 or 85 cm) were made of 0.5 mm I.D. \times 1.5 mm O.D. PTFE. A Valco (Houston, TX, USA) low-dead-volume T-piece was used as a mixing device. The reagent pump was a Labotron LDP-13 (Kontron) glass syringe pump delivering 0.15 ml/min of morin in ethanol (concentration 2.5–600 $\mu\text{g}/\text{ml}$). A Perkin-Elmer (Beaconsfield, UK) LS-4 fluorescence detector was used for detection.

The excitation wavelength was 430 nm and the emission wavelength 495 nm. Excitation and emission slits were set at a bandwidth of 15 and 20 nm, respectively. The set-up is shown in Fig. 2.

Extraction of water, sediment and soil

In order to study the selectivity of the method for organotin compounds in environmental matrices, field samples from different locations were taken for analysis. Straightforward extraction techniques were used. Sediment samples were taken from the Hertentocht canal in the Noordoostpolder at a location adjacent to apple orchards where TCT may be found and from an unpolluted location, Lake Maarsseveen, in the province of Utrecht. Soil samples were taken from the above mentioned apple orchard and from a potato field (Wiertocht), a location where TPT may be found, in the Oostelijk-Flevoland polder. The samples were taken in December 1990, at least 3 months after the spraying season. Surface water samples were taken in September 1991 just a few h and 16 days after field application of TPT from a ditch adjacent to a potato field near the village of Bant in the Noordoostpolder.

Surface water samples of 0.75 l were filtered through a 0.45- μm cellulose nitrate filter and spiked with 0.9 ml of toluene solution containing three organotin pesticides, TCT, FBTO and TPT, and were extracted twice with 40 ml of *n*-hexane by shaking for 5 min. The extracts were dried over anhydrous sodium sulphate and concentrated to *ca.* 2 ml in a Kuderna Danish concentrator prior to injection on to the HPLC column. Extracts were further reduced in volume to *ca.* 0.3 ml for trace-level determinations.

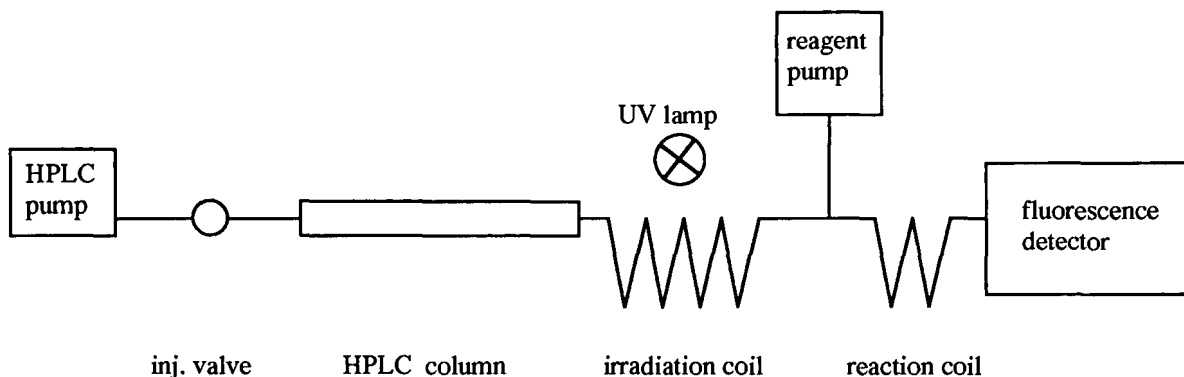


Fig. 2. Scheme of HPLC-reaction detection set-up.

Sediment and soil samples were wet-sieved through a 2-mm stainless-steel sieve and oven-dried at 105°C for 12 h. Amounts of 10 g of dry sediment or soil were spiked with 100 µl of toluene solution containing the organotin pesticides; adsorption was allowed to proceed for at least 4 h before extraction. Soxhlet extraction was carried out for 12 h using hexane–acetone (9:1) as extractant. The organic extracts were concentrated to *ca.* 4 ml in a Kuderna Danish concentrator, dried over anhydrous sodium sulphate and filtered through a membrane filter (0.2 µm) before injection. The injection volume was 28 µl in all experiments.

Non-spiked samples were used to study backgrounds and calculate attainable detection limits; spiked samples were used to calculate extraction efficiencies.

RESULTS AND DISCUSSION

Separation of the organotin compounds

Because of the high polarity of organotin halides, little or no retention can be achieved in reversed-phase HPLC [27]. Cyanopropyl-bonded silica columns have been used in several studies for the separation of organotin compounds in the normal-phase mode [21,22,27]. Because organotin compounds show strong interaction with residual silanol groups, different methods to mask this undesired phenomenon have been used. Periodic treatment of the column with iodine chloride as proposed by Praet *et al.* [27] proved to be unsatisfactory in our hands, giving irreproducible retention times and poor peak shapes. The addition of 0.5–5% of glacial acetic acid to the mobile phase gave good results. A mobile phase of *n*-hexane–THF–acetic acid (90:5:5) could be used for the separation of dialkyltin compounds but trialkyltin compounds showed only very little retention and eluted as one peak. The use of *n*-hexane–THF–acetic acid (96:2:2) gave good separation of the triorganotins except for TBT and TCT, which co-eluted. DBT and DPT can be separated in the same system. The use of a mobile phase of weaker elution strength, *n*-hexane–THF–acetic acid (98:1:1) or *n*-hexane–acetic acid (99.5:0.5), did not improve the separation of TBT and TCT.

Further work was done with *n*-hexane–THF–acetic acid (96:2:2) as mobile phase. Capacity factors of

TABLE I

CAPACITY FACTORS (k') AND DETECTION LIMITS OF SEVEN ORGANOTIN COMPOUNDS USING STANDARD SOLUTIONS

Organotin compound	k'	Detection limit (ng)
TCT	0.2	2
TBT	0.2	30
FBTO	0.6	1
TPT	1.5	1.5
DCT	1.4	0.5
DBT	2.8	0.6
DPT	5.6	0.6

seven investigated organotin compounds are given in Table I, and a chromatogram of a standard mixture containing five organotins is shown in Fig. 3. DPT and, to a lesser extent, TPT have broader peaks than would be expected on the basis of their retention times. Carrying out the separation at 45°C instead of at ambient temperature did not improve the peak shapes.

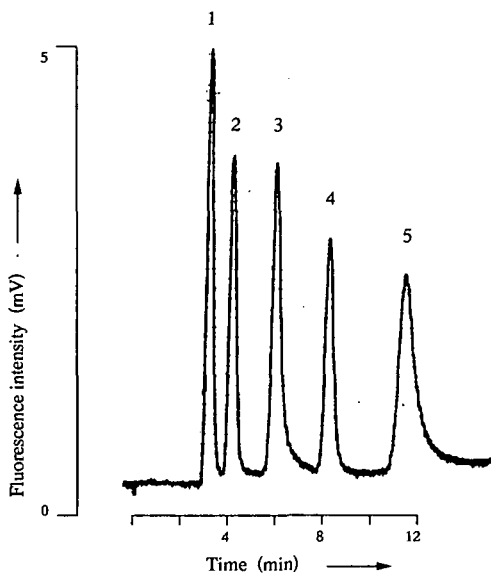


Fig. 3. HPLC of a standard mixture of organotin compounds. Column, 15 cm × 4.6 mm I.D. Rosil 3-µm cyanopropyl; mobile phase, *n*-hexane–THF–acetic acid (96:2:2); flow-rate, 1.0 ml/min; irradiation coil, 76 cm; reaction coil, 27 cm; reagent flow-rate, 0.15 ml/min of morin solution in ethanol (25 µg/ml). Peaks: 1 = TCT (0.8 µg); 2 = FBTO (0.7 µg); 3 = TPT (0.8 µg); 4 = DBT (0.8 µg); 5 = DPT (0.9 µg).

Optimization of the reaction detection system

Optimization of the reaction detection system was carried out for DBT, TBT, DPT and TPT. The HPLC eluent flow-rate was kept constant at 1 ml/min and the reagent pump flow-rate at 0.15 ml/min. Initial experiments were done by flow-injection analysis (FIA), to find near-optimum conditions. A 0.5 mm I.D. \times 1.5 mm O.D. PFTE capillary was used as the irradiation coil. PFTE with a thinner wall thickness (0.3 mm I.D. \times 0.8 mm O.D.), which has better UV transparency, was not satisfactory because it became brittle after a few h.

In the literature there is no consensus on the question of whether diorganotin [28] or monoorganotin [21] yield the highest fluorescence response with morin. Triorganotin and tin(IV) are reported to show relatively weak fluorescence. An optimum irradiation time is therefore expected to occur when the triorganotin are only partly degraded by UV light. The results presented in Fig. 4. show that TPT, TBT and DBT give the highest response when using the shorter 76 cm irradiation coil. With DPT there is some gain when using a coil length of 125 cm. The behaviour of DPT and DBT is not well understood. The response optimum for DPT at 125

cm seems to indicate that MPT forms a stronger fluorescent complex than the diorganotin, but the same effect is not found with DBT. The triorganotins behave as is expected: at a certain irradiation time, presumably corresponding to the photodegradation to a di- or monoorganotin, a response maximum is reached. When the compounds are exposed to UV light for a longer period of time, products are formed (mono-organotin or inorganic tin) that form less strong fluorescent complexes with morin. The 76-cm irradiation coil, which yields an irradiation time of 9 s, was used in subsequent studies.

For batch experiments optimum morin concentrations of 10–30 $\mu\text{g/ml}$ in *n*-hexane–ethanol (85:15) were reported by Arakawa *et al.* [28]. Using the set-up shown in Fig. 2, we used morin concentrations of 2.5–600 $\mu\text{g/ml}$ in ethanol as the reagent solution, which corresponded to morin concentrations of 0.32–78 $\mu\text{g/ml}$ in the eluent. Fig. 5 shows that the lowest concentration of morin gives the highest response for TPT and DPT. For the determination of butyltin compounds higher concentrations appear to be more favourable. With standard solutions, however, no compounds competing for morin are present, as will certainly be the case with real envi-

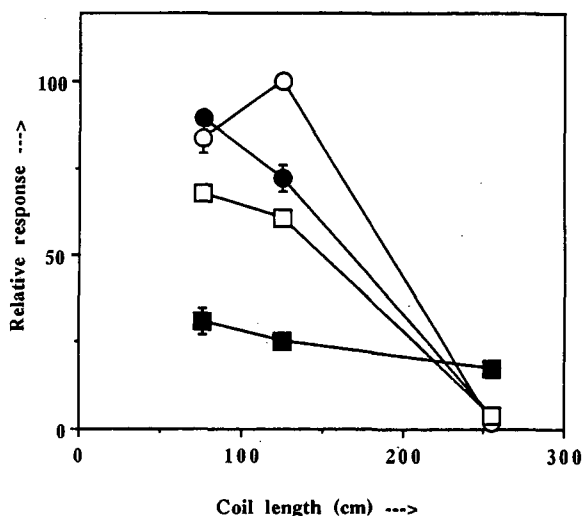


Fig. 4. Effect of irradiation coil length on fluorescence response of four organotin compounds in FIA. Organotin compounds: ● = TPT (1.7 μg); ○ = DPT (1.4 μg); ■ = TBT (3.0 μg); □ = DBT (1.3 μg). Mobile phase, *n*-hexane–THF (95:5); morin concentration after dilution with mobile phase, 0.33 $\mu\text{g/ml}$; reaction coil, 85 cm.

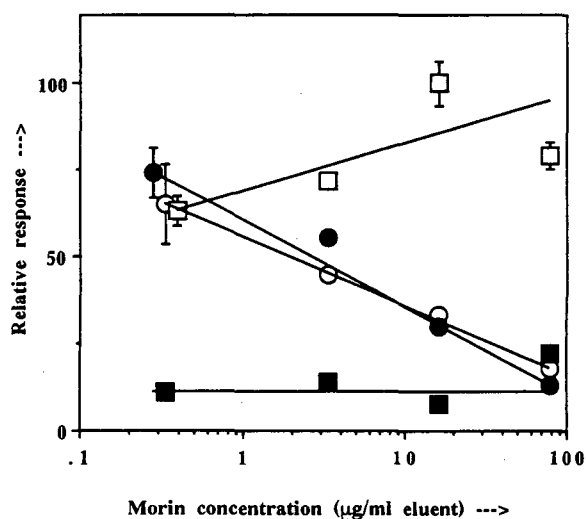


Fig. 5. Effect of morin concentration (after dilution with mobile phase) on fluorescence response of four organotin compounds. Column, 15 cm \times 4.6 mm I.D. Rosil 3- μm cyanopropyl; mobile phase, *n*-hexane–THF–acetic acid (96:2:2); irradiation coil, 76 cm; reaction coil, 85 cm. Organotin compounds: ● = TPT (1.7 μg); ○ = DPT (1.4 μg); ■ = TBT (3.0 μg); □ = DBT (1.3 μg).

ronmental samples. We therefore used a morin concentration of 25 $\mu\text{g}/\text{ml}$, corresponding to 3 $\mu\text{g}/\text{ml}$ in the mobile phase, for further investigations. In these experiments, the reaction coil length was 85 cm. Further work revealed that this length could be reduced to 27 cm (reaction time 2.8 s) without any decrease in response. The 27-cm reaction coil was used in further work.

Band broadening due to reaction detection was determined by comparing the variance (σ^2) observed for the preformed morin–DBT complex using the final set-up with the variance observed when injecting the complex on to the HPLC column directly connected with the fluorescence detector. High concentrations had to be injected because the complex turned out to be unstable on the cyanobonded column. The contribution of reaction detection to variance was calculated by means of the equation

$$\sigma_{\text{total}}^2 = \sigma_{\text{reaction detection}}^2 + \sigma_{\text{direct detection}}^2 (s^2) \quad (1)$$

Variances of the peaks were calculated using the method of Foley and Dorsey [29].

Band broadening due to reaction detection was found to be 7.1 ± 0.7 s. This is in line with the value of 5.5 s calculated for the irradiation plus reaction coil, neglecting the contribution of the T-piece, according to the equation [30]

$$\sigma_t = [(t_r d_i^2)/(96 D_m)]^{0.5} \quad (2)$$

where D_m is the molecular diffusion coefficient of the analyte in the eluent (for this calculation a value of 10^{-9} m^2/s was taken), t_r is the residence time in the irradiation plus reaction coil and d_i is the inner diameter of the coils. The contribution of the reaction detection system to band broadening is higher than the experimental value of 4.2 s reported by Lakata *et al.* [19]. For the present system dimensions, *ca.* 40% of the final peak width of TPT is caused by the reaction detection part. Although this result can be improved to a certain extent by using knitted coils, no attempt was made to do so, as even complete elimination of band broadening due to reaction detection will effect less than a two-fold increase in sensitivity.

Analytical data

Detection limits for seven organotin compounds were determined at a signal-to-noise ratio of 3:1 and

are given in Table I. The calibration plots were linear (within 10%) over two decades from the detection limit. The data are in line with the results found by Yu and Arakawa [22], who reported detection limits of 0.1–1 ng for dialkyltins in a similar system with postcolumn morin addition. In contrast, Langseth [25] reported much lower detection limits (2–6 pg) for dialkyltins in a system in which morin was added dissolved in the mobile phase. The difference between our work and that of Yu and Arakawa on the one hand and that of Langseth on the other cannot be explained completely. Factors influencing the results may be differences in the complex formation conditions, *i.e.* post-column *vs.* pre-/on-column, mobile phase composition and the quality of the detector used.

The repeatability of the method was found to be within 15% for all compounds and matrices investigated. Some drift in detector response was observed, which was due to contamination of the detector cell, flushing the detector with acetone and *n*-hexane restored the original response.

Determination of organotins in surface water

In monitoring programmes, water samples are usually filtered before analysis to eliminate differences due to varying loads of suspended matter. For a quick screening procedure, however, a method should preferably determine the total load of contaminant in the water. The present method was therefore tested with both filtered and non-filtered water samples. Recoveries at two spiking levels and detection limits were determined in triplicate and are given in Table II. Non-filtered water gives slightly lower recoveries than filter water at the same spiking level. It is known that triorganotins show strong sorption to particulate matter. Apparently the sorbed organotins are only partly extracted by *n*-hexane.

Experiments with surface water samples from different locations showed that the *n*-hexane extracts could be concentrated until the amount injected corresponded to *ca.* 60 ml of surface water, before background peaks became visible. Fig. 6A shows the chromatogram of a filtered water sample that was taken from a ditch (location Bant) a few h after the adjacent field had been sprayed with TPT. TPT was found at a level of 7 ± 3 $\mu\text{g}/\text{l}$ in non-filtered water and at 2.9 ± 0.3 $\mu\text{g}/\text{l}$ in filtered water. Water

TABLE II

RECOVERIES AND DETECTION LIMITS OF THREE ORGANOTIN COMPOUNDS IN SPIKED SURFACE WATER

Results are means \pm standard deviation for triplicate determinations.

Analyte	Non-filtered water		Filtered water				Detection limit ($\mu\text{g/l}$)
	Spike ($\mu\text{g/l}$)	Recovery (%)	Spike ($\mu\text{g/l}$)	Recovery (%)	Spike ($\mu\text{g/l}$)	Recovery (%)	
TCT	13	86 \pm 10	13	114 \pm 20	2.9	67 \pm 3	0.03
FBTO	6.7	70 \pm 10	6.7	97 \pm 15	1.5	61 \pm 3	0.02
TPT	8.2	72 \pm 23	8.2	101 \pm 32	1.0	80 \pm 10	0.02

samples were taken again 16 days after spraying; in the meantime no organotins had been applied. TPT could still be detected at a level of 0.02–0.04 $\mu\text{g/l}$ in filtered water (see Fig. 6B). In our laboratory another method based on pentylation followed by GC-MS is being developed. For confirmation the same sample was analysed by this technique and the concentration of TPT was found to be 0.015–0.02 $\mu\text{g/l}$. The main advantage of the HPLC method is that it is much faster and requires less sophisticated equipment.

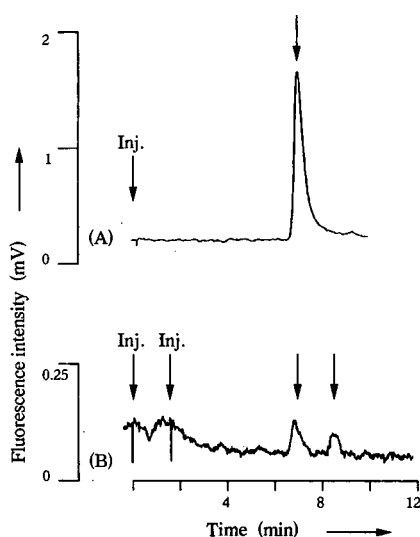


Fig. 6. (A) HPLC of filtered surface water (Bant) (amount injected corresponds to 8.0 ml of surface water) sampled a few h after the adjacent potato field had been sprayed with TPT (concentration found: $2.9 \pm 0.3 \mu\text{g/l}$). (B) HPLC of two injections of a sample taken at the same location 16 days later (amount injected corresponds to 66 ml of surface water) TPT (see arrows): 0.02–0.04 $\mu\text{g/l}$. Conditions as in Fig. 2.

Determination of organotins in sediments and soils

Preliminary studies were carried out to assess the potential of the present method for the determination of organotins in sediment and soil samples. Fig. 7 shows some typical examples. Fig. 7A shows a chromatogram of a Wiertocht soil. If the peak observed at the retention time of TPT (6.5 min) is indeed due to this compound, it represents a concentration level of about 0.4 $\mu\text{g/g}$ (however, also see below). Similar chromatograms were obtained for a Hertentocht soil sample (data not shown). Fig. 7B shows the chromatogram of a Hertentocht sediment. Obviously, in this instance the background is too high to allow any meaningful conclusion, especially because the organotins of interest elute in the same retention time range as do the major background peaks. Actually, the Hertentocht sediment with its high organic matter content can be considered as a worst-case example. The Maarsseveen sediment, which has a lower organic content, gave chromatograms that were similar to those of the soil samples. Further study revealed that the background peaks originate from fluorescent compounds present in the matrix and not from compounds that form fluorescent complexes with morin. This was verified by filling the reagent pump with pure ethanol instead of the morin solution. An injected sediment sample gave identical background peaks as with added morin.

Despite the unfavourable situation, recovery data (peak heights of spiked vs. non-spiked samples) and detection limits (signal-to-noise ratio 3:1) were collected to obtain an approximate idea of the potential of the method (Table III). Obviously, the recovery is satisfactory in all instances. Detection limits typically vary between about 0.2 and 3 $\mu\text{g/g}$.

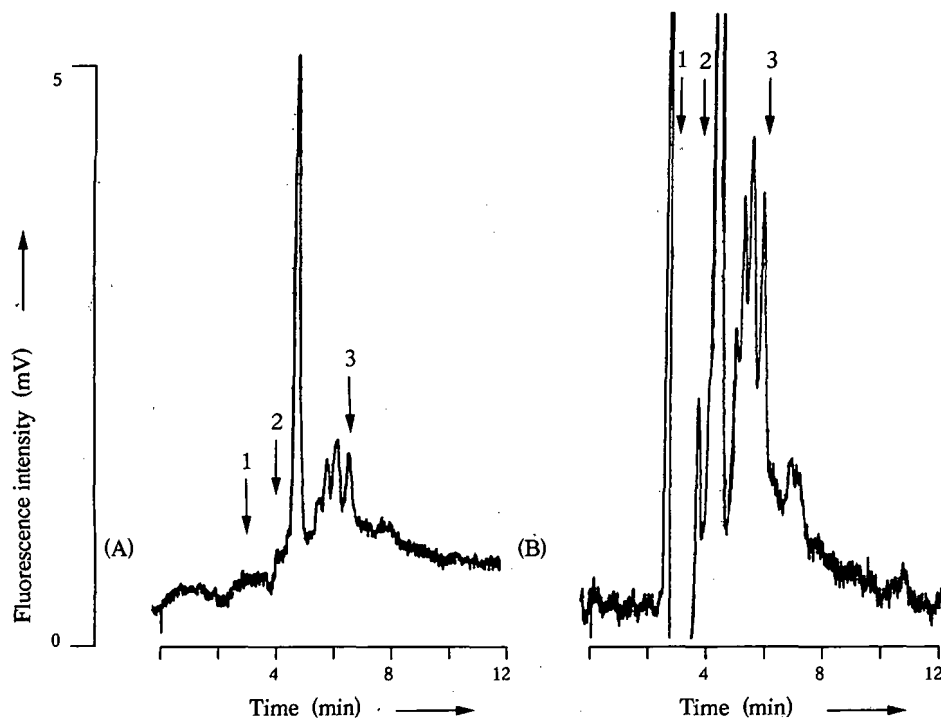


Fig. 7. (A) HPLC of a soil extract (Wiertocht) (amount injected corresponds to 55 mg soil). Retention times of the organotins are indicated: 1 = TCT; 2 = FBTO; 3 = TPT. (B) HPLC of sediment extract (Hertentocht) (amount injected corresponds to 60 mg of sediment). Conditions as in Fig. 2.

Reported sediment concentrations of TPT in a marina, originating from antifouling paints typically vary from 0.01 to 0.2 $\mu\text{g/g}$ [31]. Values of 0.2–4 $\mu\text{g/g}$ have been found in sediment adjacent to a potato field [32]. TCT concentrations after application in apple orchards were in the range 0.02–0.4 $\mu\text{g/g}$ in

sediments [33] and 0.07 $\mu\text{g/g}$ in soils [34]. On the basis of these few reported field study data, the detection limits for soils and sediments obtained with the proposed HPLC method are not really satisfactory and should be improved about ten fold, *i.e.*, the sample treatment requires further attention.

TABLE III

DETECTION LIMITS AND RECOVERIES OF TRIORGANOTIN COMPOUNDS IN SPIKED SEDIMENTS AND SOILS

Organotin compounds were added to the dried sediments and soils, soxhlet extracted and determined by HPLC. Results are for triplicate determinations.

Compound	Added ($\mu\text{g/g}$)	Sediments		Soils	
		Recovery (%)	Detection limit ^a ($\mu\text{g/g}$)	Recovery (%)	Detection limit ($\mu\text{g/g}$)
TCT	2.6	125–130	3	95–100	0.3
FBTO	0.8	100–135	2	91–93	0.2
TPT	1.2	65–105	3	44–59	1

^a Detection limits are calculated as worst-case example for Hertentocht sediment; detection limits for Maarsveen sediment are similar to those for soil samples.

CONCLUSIONS

Normal-phase HPLC on a cyano-bonded column coupled on-line with post-column photoconversion and morin complexation allows the determination of low nanogram amounts of triorganotin compounds. In this work, all three organotin pesticides currently in use in agriculture (TPT, FBTO and TCT) were determined in one HPLC run for the first time. Detection limits in surface water are ca. 0.02 µg/l and, apart from liquid–liquid extraction and evaporation, no clean-up is required. This makes the method a valuable tool for water analysis. As an example, TPT was determined in surface water adjacent to a potato field that had been sprayed with this pesticide.

Because of fluorescent background interferences, with sediments and soils the detection limits are distinctly higher, viz. in the low µg/g range. For real samples these limits are too high and further optimization of the (extraction) procedure is required. For surface water samples the present HPLC–reaction detection technique offers a simple and fast determination method.

ACKNOWLEDGEMENT

This work is part of a Ph.D. Thesis and is supported by a grant from the University Stimulation Fund of the Free University (USF Grant 89-27). The present research project was carried out within the context of the Rhine Basin Program (Waldbronn, Germany / Amsterdam, Netherlands). Mr. J. Meuleman (Creil, Netherlands) is thanked for his permission to take samples at his farm.

REFERENCES

- 1 *Organotin Compounds in the Netherlands*, Netherlands Central Bureau of Statistics, SDU, The Hague, 1987.
- 2 C. Alzieu, M. Heral and J.P. Dreno, *Equinoxe*, 24 (1989) 22.
- 3 M. J. Waldock and J. E. Thain, *Mar. Pollut. Bull.*, 14 (1983) 411.
- 4 A. G. Berends, *Bestrijdingsmiddelen en Oppervlaktewaterkwaliteit*, DBW/RIZA, Lelystad, 1988.
- 5 *Environmental Statistics of the Netherlands 1990*, Netherlands Central Bureau of Statistics, SDU, The Hague, 1990.
- 6 M. D. Müller, *Anal. Chem.*, 59 (1987) 617.
- 7 B. W. Wright, M. L. Lee and G. M. Booth, *J. High Resolut. Chromatogr. Chromatogr. Commun.*, 2 (1979) 189.
- 8 O. F. X. Donard, S. Rapsomanikis and J. H. Weber, *Anal. Chem.*, 58 (1986) 772.
- 9 W. M. R. Dirx, W. E. Van Mol, R. J. A. Van Cleuvenbergen and F. C. Adams, *Fresenius' Z. Anal. Chem.*, 335 (1989) 769.
- 10 B. Humphrey and D. Hope, in *Proceedings of Oceans '87 Conference, Halifax, Canada*, William MacNab & Son, Halifax, 1987, p. 1348.
- 11 M. D. Müller, *Fresenius' Z. Anal. Chem.*, 317 (1984) 32.
- 12 R. Lobinski, W. M. R. Dirx, M. Ceulemans and F. Adams, *Anal. Chem.*, (1992) 159.
- 13 K. L. Jewet and F. E. Brinckman, *J. Chromatogr. Sci.*, 19 (1981) 583.
- 14 F. E. Brinckman, W. R. Blair, K. L. Jewet and W. P. Iverson, *J. Chromatogr. Sci.*, 15 (1977) 493.
- 15 T. M. Vickrey, H. E. Howell, G. V. Harrison and G. J. Ramelow, *Anal. Chem.*, 52 (1980) 1743.
- 16 L. Ebdon and S. Hill, *Analyst (London)*, 110 (1985) 515.
- 17 D. Thorburn Burns, F. Glockling and M. Harriot, *Analyst (London)*, 106 (1981) 921.
- 18 I. S. Krull and K. W. Panaro, *Appl. Spectrosc.*, 39 (1985) 960.
- 19 W. G. Lakata, E. P. Lankmayr and K. Müller, *Fresenius' Z. Anal. Chem.*, 319 (1984) 563.
- 20 W. Langseth, *Inorg. Chim. Acta*, 87 (1984) 47.
- 21 W. Langseth, *J. Chromatogr.*, 315 (1984) 351.
- 22 T. Yu and Y. Arakawa, *J. Chromatogr.*, 258 (1983) 189.
- 23 W. R. Blair, E. J. Parks, G. J. Olson, F. E. Brinckman, M. C. Valerius-Price and J. M. Bellama, *J. Chromatogr.*, 410 (1987) 383.
- 24 L. Ebdon and J. I. Garcia Alonso, *Analyst (London)*, 112 (1987) 1551.
- 25 W. Langseth, *Talanta*, 31 (1984) 975.
- 26 A. H. M. T. Scholten, P. L. M. Welling, U. A. Th. Brinkman and R. W. Frei, *J. Chromatogr.*, 199 (1980) 239.
- 27 A. Praet, C. Dewaele, L. Verdonck and G. P. van der Kelen, *J. Chromatogr.*, 507 (1990) 427.
- 28 Y. Arakawa, O. Wada and M. Manabe, *Anal. Chem.*, 55 (1983) 1901.
- 29 J. P. Foley and J. G. Dorsey, *Anal. Chem.*, 55 (1983) 730.
- 30 U. A. Th. Brinkman, R. W. Frei and H. Lingeman, *J. Chromatogr.*, 492 (1989) 251.
- 31 K. Fent, J. Hunn and M. Sturm, *Naturwissenschaften*, 78 (1991) 219.
- 32 C. van Beersum, *Emissie en Emissieroutes van Bestrijdingsmiddelen in Oppervlaktewater*, DBW/RIZA Nota No. 90.004, DBW/RIZA Lelystad, 1990.
- 33 Zuiveringschap West-Overijssel, *Bestrijdingsmiddelengebruik en Oppervlaktewaterkwaliteit in een Fruitteeltgebied in de Noordoostpolder*, Zuiveringschap West-Overijssel, Zwolle, 1990.
- 34 M. D. Müller and H. P. Bosshardt, *Bull. Environ. Contam. Toxicol.*, 38 (1987) 627.

Determination of *Penicillium roqueforti* toxin by reversed-phase high-performance liquid chromatography[☆]

Karin Siemens and Jerzy Zawistowski

Agri-Food Biotechnology Laboratory, Manitoba Research Council–University of Manitoba, Food Science Department, Winnipeg, Manitoba R3T 2N2 (Canada)

(First received November 1st, 1991; revised manuscript received April 24th, 1992)

ABSTRACT

A method for the detection and quantification of *Penicillium roqueforti* toxin (PRT) using reversed-phase high-performance liquid chromatography has been established. The limit of quantitation of this method was 3 ng of PRT, while the limit of detection was 2 ng of toxin. The precision of the analysis based on numerous runs was good. Retention times for PRT were highly reproducible with an average coefficient of variation of about 1.6%. Analysis of PRT in liquid and solid samples showed no interference of the sample matrix. The accuracy of the method was 98.6%, with mean PRT recoveries of 96.8%, and 100.4% for the spiked culture medium and blue cheese extracts, respectively.

INTRODUCTION

Penicillium roqueforti toxin (PRT) is a toxic fungal metabolic first isolated from mouldy grains and corn silage [1] and then subsequently from cultures of *P. roqueforti* including some of those which are used in blue-veined cheese production [2,3]. PRT is lethal for rats and mice with LD₅₀ values of about 6–15 mg/kg by intraperitoneal administration [4]. In addition, PRT was found to be carcinogenic for rats [5,6] as well as mutagenic for *Salmonella typhimurium* [7].

A number of thin-layer chromatographic methods are available for the detection of PRT in a variety of media [8]. These methods are mainly used for identification and semi-quantitative determina-

tion of the PRT. More recently a normal-phase high-performance liquid chromatographic (HPLC) technique has been developed to measure the concentration of this toxin and other *P. roqueforti* metabolites in culture broths [9]. It has been used to follow the transformation of eremofortin C into PRT with a detection limit of 10 ng for the latter toxin [10–12]. In addition, reversed-phase HPLC analysis of PRT has also been briefly reported [13]. This technique, however, allows for detection of the toxin at a level of more than 50 ng. Although most of the above methods were successfully used for the detection of PRT in culture broths, determination of this toxin in cheese imposed problems due to its reactivity with proteins and amino acids as well as being influenced by the sample matrix [2,14].

In this paper we describe a method for the detection and determination of PRT using reversed-phase HPLC, which is more sensitive than chromatographic methods reported earlier. The feasibility to employ this method for the determination of PRT in culture broths and blue cheese was also investigated.

Correspondence to: Dr. J. Zawistowski, Agri-Food Biotechnology Laboratory, Manitoba Research Council–University of Manitoba, Food Science Department, Winnipeg, Manitoba R3T 2N2, Canada.

[☆] Contribution No. 211 of Food Science Department, University of Manitoba.

EXPERIMENTAL

Materials

Reference PRT was obtained from Sigma (St. Louis, MO, USA). High-performance thin-layer chromatography (HPTLC) silica gel 60 F-254 aluminium plates were purchased from BDH (Toronto, Canada). A PRT-producing strain of *P. roqueforti* (ATCC No. 10110) was obtained from the American Type Culture Collection (Rockville, MD, USA) while Danish blue cheese was purchased from a local supplier. All solvents were of HPLC grade.

Chromatography

The HPLC method was developed on a Waters ALC 204 liquid chromatograph. The system consisted of a Model 6000A solvent delivery system, a Model 440 absorbance detector equipped with a 254-nm filter and a U6K universal liquid chromatography injector.

Chromatographic analyses were carried out on a pre-packed LiChrosorb reversed-phase C₁₈ column (240 mm × 4.0 mm I.D.) of particle size 10 μm (E. Merck, Darmstadt, Germany). The signal from the detector was recorded by an SP4290 integrator (Spectra Physics) set at an attenuation of 8. A volume of 20 μl was injected for all samples. Mobile phases consisting of methanol–water in the ratios 70:30 (v/v) and 65:35 (v/v) were used for HPLC analysis. All runs were carried out at a flow-rate of 1.0 ml/min.

The presence of PRT in samples prior to reversed-phase HPLC analyses was assessed by analytical thin-layer chromatography (TLC) using chromatoplates of silica gel F-254 with methanol–chloroform (5:95, v/v) as the eluent [1].

Standard preparation

The reference PRT (Sigma) was further purified by normal-phase TLC. Toxin was dissolved in chloroform (0.5 μg/μl) and spotted on the TLC plate. The plate was developed using a mixture of methanol and chloroform in the ratio of 5:95 (v/v). The PRT spot, having an *R_F* value of 0.80, was located under short-wavelength UV light (254 nm) and clearly marked. The silica containing the PRT was carefully scraped from the plate, transferred to a vial and resuspended in 2.0 ml of methanol in order to extract the toxin. The resulting suspension was

filtered through Whatman No. 4 paper. The PRT was extracted from silica two more times with a total of 2.0 ml of methanol. The three filtrates were combined and evaporated to dryness at room temperature under a stream of nitrogen, yielding a crystalline PRT standard used in further studies. Purity of the PRT standard was first determined using a diode-array spectrophotometer (Hewlett-Packard). The PRT crystals dissolved in 1.0 ml of methanol exhibited a single peak at 248 nm corresponding to its absorption maximum described by other workers [3]. In addition, the ¹H NMR spectrum (300 MHz) of the purified toxin was measured in ²HCl₃ using a NMR spectrometer (Model AM 300, Bruker Spectrospin, Canada). The spectrum was identical to the PRT spectral data obtained by Wei *et al.* [14]. Finally, the effectiveness of the purification procedure was assessed by reversed-phase HPLC (Fig. 1). The chromatography yielded a single peak indicating a high purity of the PRT standard. The concentration of the toxin dissolved in methanol was measured spectrophotometrically at 248 nm ($\epsilon = 9000$) [3].

Standard curves were prepared by making a series of dilutions of PRT in methanol ranging in concentration from 0.15 to 30 ng/μl. Samples were ana-

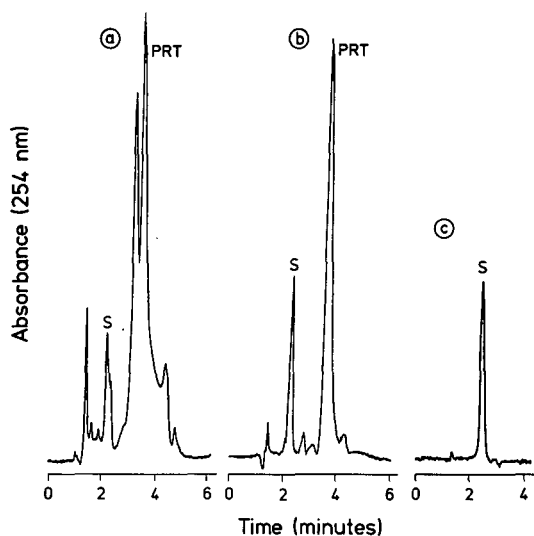


Fig. 1. Chromatograms of PRT standard: (a) 200 ng of an impure mixture containing PRT, (b) 60 ng of PRT after TLC purification and (c) 20 μl of methanol. Eluent, methanol–water (65:35, v/v); flow-rate, 1.0 ml/min. Peak S = methanol.

lyzed chromatographically as described above and the peak height and peak area were plotted against the corresponding concentration.

Sample preparation

To assess the suitability of reversed-phase HPLC for the determination of PRT in different samples, analysis of this toxin in culture broths (preparation 1) and cheese (preparation 2) was conducted.

Preparation 1. PRT was produced using the strain of *P. roqueforti* ATCC No. 10110, according to the procedure of Wei *et al.* [1]. The mould was grown for 14 days at room temperature in a culture medium containing yeast extract and sucrose (YES, Difco). Then, the mycelium was removed from the culture broth by paper filtration and the broth (100 ml) was extracted with chloroform to yield a crude sample containing PRT. The presence of PRT was confirmed by TLC as described earlier in this paper. Crude samples from two separate fermentation batches were evaporated to dryness, each dissolved in 1.0 ml of methanol, and used for HPLC analysis.

Preparation 2. Purified PRT standard (0.5 mg), dissolved in 1.0 ml of methanol, was added to 40 g of Danish blue cheese to give a final concentration of 12.5 mg/kg. The cheese was immediately homogenized in a Waring blender with 250 ml of methanol–water (55:45, v/v) and 150 ml of hexane for 5 min at high speed and then divided into two equal portions. Each portion was centrifuged at 1000 g at 4°C for 10 min. After removing the hexane layer, the methanol–water part was vacuum-filtered through Whatman No. 3 paper and the resultant

filtrate was extracted with two 60-ml volumes of chloroform. The two chloroform extracts from each portion were pooled and evaporated to dryness using a rotary evaporator. The dried extract was dissolved in 1.0 ml of methanol, 10 μ l were withdrawn, diluted 40-fold with methanol, and immediately analyzed by HPLC as described earlier. The remaining extract was stored at –5°C for 24 days and the PRT content was periodically analyzed by HPLC. Cheese used for this experiment was free of PRT as assessed by TLC. Part of cheese was extracted exactly as described above, and the extract was used as a control sample (see Fig. 4b).

Accuracy assessment

The accuracy of the HPLC method for PRT quantification was determined by an external standard method. Culture medium and blue cheese samples free of PRT were extracted with chloroform, evaporated to dryness, dissolved in methanol and spiked with PRT over the concentration range 1.0–8.3 ng/ μ l (20–166 ng per injection). Recoveries of PRT from extracts were assessed by HPLC using peak height measurements. A two-sample *t*-test was used to estimate the significance of the differences between known and measured values of PRT.

RESULTS AND DISCUSSION

The PRT retention times for two solvent systems containing methanol and water are shown in Table I. The average retention time for PRT using methanol–water in a 70:30 (v/v) ratio was 3.31 min based

TABLE I
REPRODUCIBILITY OF RETENTION TIME OF PRT AS ANALYSED BY REVERSED-PHASE HPLC

Trial No.	Solvent ^a ratio	<i>n</i> ^b	Retention time (min)			C.V. (%)
			Range	Mean	S.D.	
1	70:30	24	3.15–3.44	3.26	0.11	3.37
2	70:30	23	3.31–3.39	3.34	0.02	0.60
3	70:30	32	3.25–3.41	3.32	0.05	1.51
4	65:35	67	3.60–3.84	3.70	0.05	1.35
5	65:35	17	3.55–3.84	3.69	0.12	3.25
6	65:35	27	3.92–3.96	3.93	0.01	0.25
7	65:35	41	3.75–3.89	3.84	0.03	0.78

^a Methanol–water (v/v).

^b Number of injections.

TABLE II

REPRODUCIBILITY OF HPLC PEAK AREA AND PEAK HEIGHT FOR PRT USING 65:35 (v/v) METHANOL-WATER AS SOLVENT SYSTEM

PRT injected (ng)	n ^a	Peak area or height			C.V. (%)
		Range	Mean	S.D.	
Area					
55.0	20	125 952-218 709	163 445	21 628	13.2
28.0	12	60 017-92 814	72 088	9860	13.7
Height					
55.0	23	5525-6512	5899	388	6.58
28.0	6	3661-4023	3831	123	3.22

^a Number of injections.

on three separate trials over 4 days. Coefficients of variation (C.V.) ranged from 0.06 to 3.37%. Methanol-water in a 65:35 (v/v) ratio, as the eluting solvent resulted in an average retention time of 3.79 min for PRT, based on four trials over a 4-day period. C.V.s with this solvent ranged from 0.25 to 3.25%. The PRT retention times for both solvent systems were highly reproducible. However, the methanol-water in ratio 65:35 (v/v) allowed for longer retention of the toxin on the column and, hence, better resolution of the PRT peak from the initial solvent peak.

The precision and reproducibility of the peak height and the peak area were analyzed by injecting a volume (20 μ l) containing either 55 or 28 ng of the purified standard, over a 2-day period. The C.V.s

for the peak area measurements were 13.2 and 13.7%, respectively. Reproducibility of peak heights for the same injected amounts were better with C.V.s of 6.58 and 3.22%, respectively (Table II). Consequently, further determination of PRT by HPLC was based on the peak height measurements.

Total PRT recoveries and results of a Student *t*-test are shown in Table III. The accuracy of the method for PRT determination was 98.6%, with mean recoveries of 96.8%, and 100.4% for spiked culture medium and blue cheese extracts, respectively. No significant difference (at a 95% confidence level) was found between the means of the standard PRT and the recovered PRT from spiked culture medium or cheese samples over the concentration range tested. The only exception was the

TABLE III

ACCURACY OF REVERSED-PHASE HPLC TO DETECT PRT IN CULTURE MEDIUM AND BLUE CHEESE SAMPLES

Amount of standard PRT ^a (ng)	Culture medium samples			Blue cheese samples		
	Mean PRT recovered ^a (ng)	Student <i>t</i> -value ^b	Total recovery (%)	Mean PRT recovered ^a (ng)	Student <i>t</i> -value ^b	Total recovery (%)
166.0	158.4 \pm 3.96	2.24	95.4	151.6 \pm 5.60	3.84	91.3
125.0	111.7 \pm 7.83	3.14	89.4	126.6 \pm 18.5	0.15	101.3
84.0	81.1 \pm 6.35	0.78	96.5	84.0 \pm 9.70	0.00	100.0
62.0	64.7 \pm 1.83	2.02	104.4	60.1 \pm 15.0	0.22	96.9
50.0	45.5 \pm 0.66	3.24	91.0	50.0 \pm 7.00	0.00	100.0
20.0	20.8 \pm 0.65	1.50	104.0	22.6 \pm 0.79	4.39	113.0

^a Based on triplicate injections.^b Two-sample *t*-test made at a 95% confidence level where $t_{\alpha=0.05} = 4.30$.

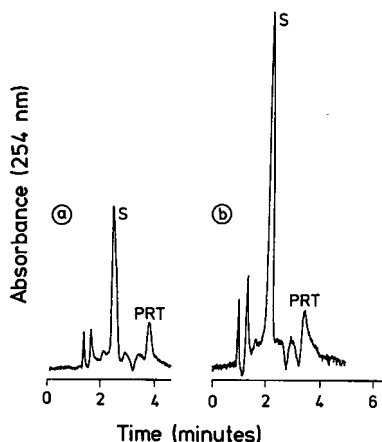


Fig. 2. Chromatograms of PRT standard: (a) 3.0 ng at attenuation 8 and (b) 2.0 ng at attenuation 4. Eluent, methanol–water (65:35, v/v); flow-rate, 1.0 ml/min. Peak S = methanol.

spiked cheese extract at the lowest concentration level of 20 ng PRT where the t -value was slightly higher (4.39) than the tabulated value (4.30).

The limit of detection of the method was determined with the integrator set at an attenuation of 8. The highest sensitivity setting of 1 resulted in a very noisy baseline that interfered with the interpretation of the chromatogram and, hence, a more appropriate setting of 8 was chosen. With the parameter at this setting, PRT could be measured at a concentration as low as 3 ng per run (Fig. 2a). Furthermore, at an attenuation setting of 4, an amount of 2 ng of toxin could be detected (Fig. 2b). This sensitivity was better than those reported earlier by other HPLC methods [9,13].

In order to carry out the quantitative analysis, it was necessary to study the linearity of the detector response (peak area and peak height) with respect to concentrations of PRT. The linearity was evaluated by injecting 20 μ l of increasing concentrations of the toxin standard, so that the injected amounts of PRT ranged from 3 to 600 ng. Regression analysis of the resulting calibration curves, obtained from three trials each ranging from 3 to 70 ng of PRT, indicated that the relationship between both peak height or peak area and the amount of PRT injected was linear over the tested concentration range, with correlation coefficients of 0.93 and 0.92, respectively. For the broader range of PRT concentration (3–600 ng) the correlation coefficient for

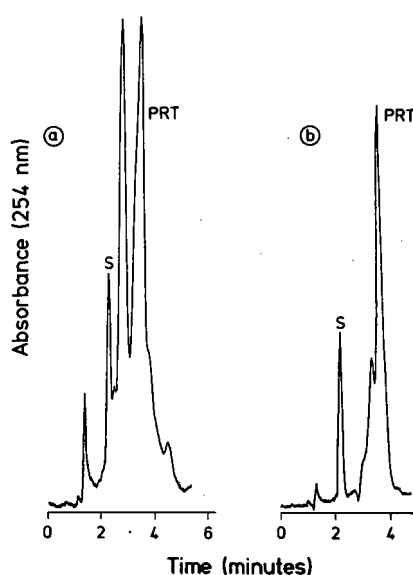


Fig. 3. Chromatograms of crude PRT extracts obtained from two separate fermentation batches of *P. roqueforti* in 100 ml of YES culture medium. Eluent, methanol–water (65:35, v/v); flow-rate, 1.0 ml/min. Peak S = methanol.

peak area and the amount of PRT injected was 0.97.

The selectivity of the developed reversed-phase HPLC method was assessed by the determination of PRT in samples each having a different matrix: *P. roqueforti* culture medium and blue-veined cheese. Fig. 3 shows chromatograms of crude PRT extracts obtained from two different fermentation batches. Both of these indicate the presence of the toxin produced by *P. roqueforti* during the fermentation process. Presence of the toxin was verified by spiking the extracts with standard PRT. Distinct PRT peaks in both chromatograms indicate that other extractable components do not interfere with the detection of the toxin. With the aid of the calibration curve (peak height versus concentration), a total PRT concentration of 0.6 and 2.3 mg/ml was detected in the first (Fig. 3a) and in the second (Fig. 3b) extract, respectively.

A typical chromatogram of PRT recovered from cheese is shown in Fig. 4a, while Fig. 4b shows a chromatogram of the extract obtained from cheese prior to the addition of the toxin. Also in this case, the PRT peak was distinct (Fig. 4a) and detection of

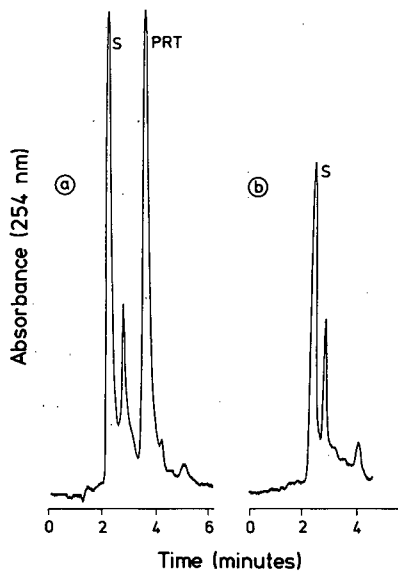


Fig. 4. Chromatograms of (a) crude PRT recovered from PRT-spiked blue-veined cheese (0.5 mg per 40 g) and (b) a control cheese extract. Eluent, methanol–water (65:35, v/v); flow-rate, 1.0 ml/min. Peak S = methanol.

the toxin was not influenced by other components present in the extract obtained from the cheese matrix (Fig. 4b). Numerous analyses of PRT in methanol extract of cheese stored at -5°C for 24 days resulted in an average retention time of 3.97 min, with C.V. of 2.5%. This indicates good reproducibility of this parameter. Although the retention time was slightly higher than that of the standard PRT (3.79 min), presence of the toxin was verified by spiking the sample with the standard.

The determination of PRT allowed for the assessment of the recovery of toxin added to cheese and subsequent stability analysis of the recovered PRT in methanol extract stored for 24 days (Table IV). Although the extraction procedure for cheese was designed to be simple and as rapid as possible, a mean recovery of only 43.6% PRT was obtained as determined with the aid of the peak height calibration curve. This is not unexpected since the instability of PRT in blue cheese and its low yield of recovery has been reported by other [15]. The toxin forms *P. roqueforti* imine with ammonia and reacts with neutral and basic amino acids present in cheese. It has been reported that the aldehyde group of the toxin is the moiety that reacts with the amino group

TABLE IV

STABILITY OF PRT IN METHANOL EXTRACT OF BLUE CHEESE AS DETERMINED BY REVERSED-PHASE HPLC

Based on triplicate runs and analysis performed using HPLC peak height.

Time after extraction (days)	Amount of PRT in extract ^a	
	$\mu\text{g}/\mu\text{l}$	%
0	0.218	43.6
1	0.217	43.4
4	0.219	43.8
5	0.194	38.8
11	0.135	27.0
17	0.125	25.0
20	0.122	24.4
24	0.119	23.8

^a PRT was added to cheese at 12.5 mg/kg and extracted as described under Experimental.

of the amino acids forming Schiff bases [15]. Moreover, PRT may react with the $\epsilon\text{-NH}_2$ group of lysine [16] and sulfhydryl group of cysteine [17].

Studies on the stability of PRT in methanol extract shows that the toxin was relatively stable over approximately 4 days. However, prolonged storage at -5°C for up to 24 days resulted in a 55% decrease in the amount of PRT present in the cheese extract (Table IV). Subsequent loss of PRT may be due to its reactivity with compounds such as tryptamine or other primary amines extracted from blue cheese that are present in concentrations of up to 2.3 mg/g [15,18]. This is supported by the fact that the standard PRT in pure methanol (0.01 $\mu\text{g}/\text{ml}$) was stable at -5°C for at least 1 month.

The developed reversed-phase HPLC method can be used for the determination of PRT produced by *P. roqueforti* in culture broth extracts. Moreover, because of its specificity and sensitivity, the HPLC method is suitable to detect the toxin in blue cheeses.

ACKNOWLEDGEMENTS

The authors are indebted to Dr. A. A. Frohlich for the valuable technical advice and helpful comments on the manuscript. Financial support for this study from the Natural Science and Engineering Research Council is gratefully acknowledged.

REFERENCES

- 1 R. D. Wei, P. E. Still, E. B. Smalley, H. K. Schnoes and F. M. Strong, *Appl. Environ. Microbiol.*, 25 (1973) 111.
- 2 M. Medina, P. Gaya and M. Nunez, *J. Food Prot.*, 48 (1985) 118.
- 3 L. Polonelli, F. Morace, F. Delle Monache and R. A. Samson, *Mycopathologia*, 66 (1978) 99.
- 4 P. M. Scott, in V. Betina (Editor), *Mycotoxins—Production, Isolation, Separation and Purification*, Elsevier, Amsterdam, 1984, Ch. 23, p. 469.
- 5 L. Polonelli, L. Lauriola and G. Morace, *Mycopathologia*, 78 (1982) 315.
- 6 J. Hradec and D. Vesely, *Carcinogenesis*, 10 (1989) 213.
- 7 D. E. F. Levin, E. Yamasaki and B. N. Ames, *Mutat. Res.*, 94 (1982) 315.
- 8 V. Betina, *J. Chromatogr.*, 334 (1985) 211.
- 9 S. Moreau, A. Masset and J. Biguet, *Appl. Environ. Microbiol.*, 37 (1979) 1059.
- 10 S. Moreau, A. Lablache-Combier and J. Biguet, *Appl. Environ. Microbiol.*, 39 (1980) 770.
- 11 S. C. Chang, Y. H. Wei, M. L. Liu and R. D. Wei, *Appl. Environ. Microbiol.*, 49 (1985) 1455.
- 12 S. Y. Li, S. C. Chang and R. D. Wei, *J. Chin. Biochem. Soc.*, 14 (1985) 52.
- 13 C. P. Gorst-Allman and P. S. Steyn, in V. Betina (Editor), *Mycotoxins—Production, Isolation, Separation and Purification*, Elsevier, Amsterdam, 1984, Ch. 6, p. 59.
- 14 R. D. Wei, H. K. Schnoes, P. A. Hart and F. M. Strong, *Tetrahedron*, 31 (1975) 109.
- 15 P. M. Scott and S. R. Kanhere, *J. Assoc. Off. Anal. Chem.*, 62 (1979) 141.
- 16 G. C. Shaw, Y. H. Wei and R. D. Wei, *J. Chin. Biochem. Soc.*, 13 (1984) 35.
- 17 Y. Nakamura, M. Ohta and Y. Ueno, *Chem. Pharmacol. Bull.*, 25 (1977) 3410.
- 18 S. L. Rice, R. R. Eitenmiller and P. E. Koehler, *J. Milk Food Technol.*, 39 (1976) 353.

Automated analyses of non-ionic surfactants in terms of hydrophobic and polyoxyethylated chain lengths

Tetsuo Okada

Faculty of Liberal Arts, Shizuoka University, Shizuoka 422 (Japan)

(First received March 10th, 1992; revised manuscript received May 13th, 1992)

ABSTRACT

A novel automated system for the analysis of polyoxyethylated (POE) non-ionic surfactants is proposed, which is capable of providing information on both hydrophobic and POE chain lengths. A polystyrene-divinylbenzene copolymer gel is effective for the hydrophobic chain analysis because the separation is not influenced by the distribution of POE chains. On the other hand, a K^+ -form cation-exchange resin is effective for elucidating the distribution of POE chains. An automated system was constructed by combining these two separation methods, and was applied to the analysis of the distributions of hydrophobic and POE chains in a commercial Brij 35.

INTRODUCTION

Polyoxyethylene (POE) chains play important roles in surface-active compounds, *e.g.*, POE chains are utilized to vary HLB (hydrophile-lipophile balance) values, wetting abilities, solubility in water, critical micelle concentration, Kraft points of ionic surfactants and cloud points of non-ionic surfactants [1]. According to statistics in the USA [2], the production of non-ionic surfactants comprised 24% of the total surfactant sector in 1989, and POE ethers represented more than 70% of the non-ionic surfactant production. The production and consumption of non-ionic surfactants appear to continue to increase because of the increasing variety of industries that require surfactants.

The analysis of POE surfactants has thus become increasingly important, and has been treated in a number of papers. Usually, non-ionic surfactants are polydisperse with regard to both the POE chain and the hydrophobic chain lengths [1]. It is obvious

that methods which are capable of providing information on both POE and hydrophobic moieties are necessary. Chromatography is therefore a suitable choice, and has been extensively employed for such analyses. Among gas [1], liquid [1,3–16] and supercritical fluid chromatographic methods [17,18], high-performance liquid chromatography (HPLC) is preferred mode because of the simple instrumentation and easy handling, even though the separation performance is not necessarily better than with the other methods.

Although reversed-phase or normal-phase chromatography has been usually utilized for the separation, and proved to be efficient in some instances [3–14], there remain some problems especially in the separation in terms of POE chain lengths; it is difficult to separate POE chains having many (*e.g.* > 30) oxyethylene (OE) units from each other; the separation conditions are different for each sample, and the resolution is poor when the compound has a long hydrophobic chain. Therefore, many repeated trial and error experiments are necessary until an acceptable separation is achieved.

In previous work, a novel method for the separation in terms of POE chain lengths was devel-

Correspondence to: Dr. T. Okada, Faculty of Liberal Arts, Shizuoka University, Shizuoka 422, Japan.

oped [15,16], wherein a cation-exchange resin was used in the alkali metal ion form. In this method, POE forms a complex with a counter cation in an ion-exchange resin, and is separated according to the complex formation ability; the longer the POE chain, the stronger is the complexation ability. Although hydrophobic chains also affect the retention, the effect is so marginal that the same separation conditions are applicable to different samples. If this method is efficiently combined with other methods capable of recognizing differences in the hydrophobic chain lengths, it will be useful in the analysis of non-ionic surfactants.

EXPERIMENTAL

The chromatographic system, illustrated in Fig. 1, was composed of Tosoh computer-controlled pumps CCPD (P1) and CCPM (P2), which were used for the separation in terms of hydrophobic chain lengths and POE chain lengths, respectively, an SPT-3-202U pump (Nippon Seimitsu Kagaku) in the concentration process, a CO-8000 column oven (Tosoh) and UV-8000 (Tosoh) and 875-UV (JASCO) UV detectors (D). A 150 mm × 4 mm

I.D. stainless-steel column packed with MCI gel CHP-5C (Mitsubishi Kasei) and a 50 mm × 4.6 mm I.D. TSK-gel IC-Cation-SW column were used as separation columns. The former column (C1), which contains styrene–divinylbenzene copolymer gel, was utilized for the separation according to the hydrophobic chain lengths, whereas the latter (C2), which contained a cation-exchange resin in the potassium form, was used in POE chain analyses. A PTFE concentration column (C3) (5 mm × 2 mm I.D.) was also packed with MCI gel CHP-5C.

Methanol of analytical-reagent grade was used after distillation. Acetonitrile of HPLC grade was purchased from Wako. POE(9) dodecyl ether [POE(9)D, where the number in parentheses denotes the average number of oxyethylene units] and POE(20) hexadecyl ether [POE(20)H] were gifts from Nikko Chemicals. POE(10) octadecyl ether [POE(10)O] and POE(20)O were purchased from Sigma. Other reagents were of analytical-reagent grade and used as received, unless stated otherwise.

According to the literature [6], terminal hydroxyl groups in POE were esterified by reaction with 3,5-dinitrobenzoyl (DNB) chloride in dry benzene. This derivatization facilitated the gradient separation and enhanced the detection sensitivity.

RESULTS AND DISCUSSION

Separation in terms of hydrophobic chains

The separation of non-ionic POE surfactants in terms of the hydrophobic chain length will be of primary importance. This procedure should not be affected by the distribution of POE chains. Although one might think that this separation could be performed under the usual reversed-phase conditions, it was not easy because reversed-phase stationary phases can usually differentiate POE chain lengths to some extent; peak broadening due to the distribution of POE chains was observed. Most published work has been focused on the distribution of POE chains, and very little attention has been paid to hydrophobic chain analysis [3,4].

Kudoh [3] reported that acetone–water was a suitable mobile phase for separations in terms of hydrophobic chains, and that POE chain lengths did not affect the retention times when acetone–water (9:1) was used as a mobile phase. Although systematic studies were not shown, the balance be-

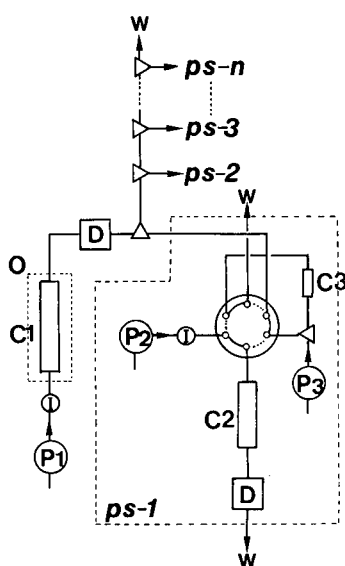


Fig. 1. Schematic diagram of the system for the analysis of POE surfactants. C1, C2 = Separation columns; C3 = concentration column; P1, P2, P3 = pumps; D = UV detector; I = injection valve; W = waste.

tween water and acetone concentrations seems to be important in eliminating the influence of the POE chain distribution. However, acetone is not in general a preferred solvent for UV detection.

Melander *et al.* [5] reported that the dependence of the retention on the number of OE units is reversed at a particular concentration of an organic solvent. They analysed this result with a two-state model; a POE chain exists as a zig-zag and a helix form in a mobile phase, and both the two have different retention abilities. Their results imply that a compound containing polydisperse POE chains can be eluted as a single peak regardless of the POE chain lengths, with a mobile phase of appropriate organic solvent content. However, as terminal groups and mobile phase compositions affect the equilibrium between the zig-zag and helix forms, their results are not directly applicable to the present case. Also, the best resolution is not necessarily obtained under the conditions, where all POE oligomers (or polymers) are simultaneously eluted.

In this study, C₈ and C₁₈-bonded silica gel and styrene–divinylbenzene copolymers were tested as stationary phases. DNB-POE was eluted at acceptable retention times when either C₈ or C₁₈-bonded phase was used with organic solvent (methanol, acetonitrile, tetrahydrofuran, etc.)–water (9:1) as mobile phases. However, in all instances, peak broadening according to the distribution of POE chains was observed. In contrast, MCI gel CHP-5C gave relatively narrow peaks and good separations when acetonitrile–methanol mixtures (1:5–1:4) were used as mobile phases. Table I gives the retention times of DNB-POE(10)O and DNB-POE(20)O as a

TABLE I

CHANGES IN THE RETENTION TIMES OF DNB-POE(10)O AND DNB-POE(20)O WITH TEMPERATURE

Retention times were measured on MCI gel CHP-5C with acetonitrile–methanol (1:4) mobile phase.

Temperature (°C)	Retention time (min)	
	POE(10)O	POE(20)O
14.0	40.5	37.0
23.0	25.6	25.0
33.6	16.8	16.0
43.8	11.3	11.2

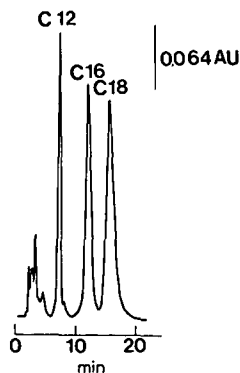


Fig. 2. Typical separation in terms of hydrophobic chain lengths. Column temperature, 43.8°C; mobile phase, acetonitrile–methanol (1:5); detection at 254 nm. Other conditions are given in the text.

function of temperature. The difference in the retention times becomes smaller with increase temperature, and is almost negligible at 43.8°C.

Fig. 2 shows the separation of DNB-POE adducts of dodecyl, hexadecyl and octadecyl alcohols under the condition mentioned above.

Separation in terms of POE chain lengths

Our previous work indicated that the separation according to POE chain lengths on a K⁺-form cation-exchange resin is sensitive to the temperature because the complexation process is exothermic [16,19]. Although then use of a thermostated system is essential, shifts of peak position due to changes in the column temperature were negligible for the experiments at room temperature (*ca.* 15°C).

As the retention of POE increased exponentially with increasing number of OE units, gradient elution should be considered. The retention of POE can be reduced by adding a solvent unfavourable for the resin phase complexation or by adding a salt to the methanolic mobile phase. Both water and acetone, for example, are solvents unfavourable for the resin phase complexation of POE, because the strong donor ability of water towards alkali metal ions and the low dielectric constant of acetone interfere with the complexation in the resin phase. However, the solubility of DNB-POE was lowered considerably in a solvent containing water, and acetone interfered with the UV detection of DNB-POE. In the latter instance, addition of a salt was therefore selected.

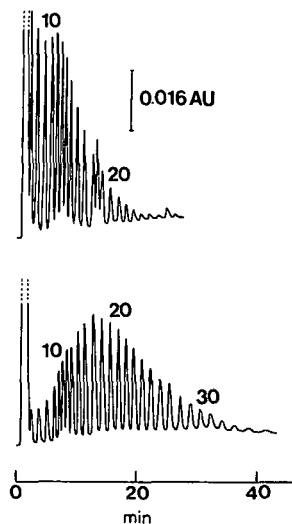


Fig. 3. Typical separation in terms of POE chain distribution of POE(10)O (top) and POE(20)O (bottom). Mobile phase, methanol (0–3 min) to 7.5 mM KCl in methanol (30 min). Other conditions are given in the text.

POE forms a complex with a cation added to the mobile phase, and the retention is reduced as a function of the concentration of the cation. It was confirmed in previous work [20] that POE complexes were not retained on the ion-exchange resin because of the lack of effective complexation sites and energetically unfavourable conformational changes of POE chains [19]. As the complexation ability in solution phases is enhanced with an increasing number of OE units, the retention of longer POE is more effectively reduced by adding a salt. Fig. 3 shows results of the analysis in terms of the distributions of POE chains in POE(10)O and POE(20)O. Peaks were identified by comparing the retention times with those of monodisperse compounds. More than 30 oligomers are separated within 1 h.

Preliminary study for constructing an automated system

To construct an automated system for the non-ionic surfactant analysis, the above two methods should be effectively combined. For such a purpose, column switching will be useful. However, as peaks obtained from the separation in terms of the hydrophobic chain length are not sharp enough because of the effect of the distribution of POE chains, column switching will cause marked peak broadening

TABLE II

RECOVERIES (%) OF DODECYL ALCOHOL ADDUCTS OF DNB-POE ON A CONCENTRATION COLUMN

The organic solvent and water flow through the concentration column for 10 min after loading a sample.

n^a	Flow-rate of water (ml/min)			
	1.63	2.28	3.42	5.7
7	51.0 ^b	63.7	97.4	97.4
8	50.1	66.4	97.4	95.4
9	50.3	66.9	102	95.9
10	51.9	66.8	99.5	96.0
11	50.6	66.1	94.4	98.0
12	50.1	65.6	93.7	93.7
13	51.3	65.4	94.1	92.7
14	51.9	65.1	94.4	102
15	54.7	51.6	97.1	96.4

^a Number of oxyethylene units.

^b The flow-rate of acetonitrile–methanol (1:4) was kept at 1 ml/min.

or poor detectability and thus low reliability in the POE analysis step. A use of a concentration column was therefore considered.

The same stationary phase as used in the first separation step was packed in a concentration column. Effluents from the first separation column were mixed with water and passed through the concentrator. Table II lists the recoveries of DNB-POE (9)D eluted from the first separation column with acetonitrile–methanol (1:4) as the mobile phase. Flow-rates of water mixed with the effluents from the first separation column were varied under a constant flow (1 ml/min) of the effluents. When the ratio of the flow rates reaches 3.42, the recovery becomes almost 100% regardless of POE chain lengths.

Automated system

The proposed automated system is illustrated in Fig. 1. Hydrophobic chain analyses are performed with pump P1 and separation column C1, and POE analyses with P2 and C2. Pump P3 delivers water to the concentration column, C3. Effluents from C1 flow down to the concentrator through a three-way valve. After the concentration is completed, the POE analysis starts by rotating the centre six-way valve. To desorb analytes completely from the con-

centrator, the injection of 100 μl of acetonitrile was necessary; this can be done through an injection valve (I). As can be seen in Fig. 3, typical POE analysis takes 1 h. If we use only one POE analysis system (denoted ps-1 in Fig. 1), this system should be repeatedly operated; it takes several hours until all analyses are completed. If we can prepare several POE analysis systems (ps-2, ps-3, ..., ps- n) such a time-consuming procedure can be avoided; that is, the peak eluted second from C1 is analysed with ps-2, that eluted third with ps-3, etc. Fig. 4 shows results of analysis of Brij 35, which is the trade-name of POE(23)D, according to the present concept. The instrumentation available in our laboratory was insufficient to construct several POE analysis systems. The analysis by ps-1 was therefore repeated until all analyses were completed; four chromatograms in which POE chains were separated according to the difference in the chain lengths were obtained with the same system. The chromatogram on the left-hand side shows the separation in terms

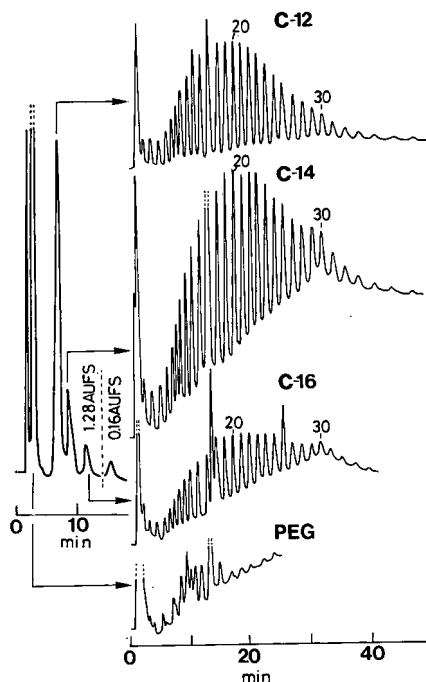


Fig. 4. Results of the analysis of Brij 35. Chromatographic conditions are given in the text and Figs. 2 and 3. Detection, 0.16 a.u.f.s. for DNB-POE(n)D and 0.04 a.u.f.s. for others in POE separation steps.

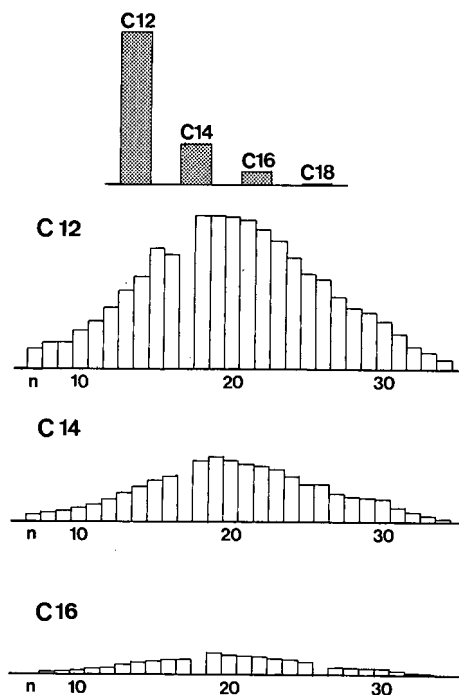


Fig. 5. Relative concentrations calculated from results in Fig. 4. The histogram at the top shows relative concentrations according to hydrophobic chains. The others are for POE chain lengths. The same absorption coefficient for all DNB-POE molecules was assumed.

of hydrophobic chain length; injection peaks and peaks corresponding to the elution of C₁₂, C₁₄, C₁₆, and C₁₈ appeared. Although the POE analysis could not be done for C₁₈ because of the extremely low concentration, POE distributions of C₁₂, C₁₄ and C₁₆ components are analysed as shown on the right-hand side of Fig. 4. Also, injection peaks involved the elution of di-DNB-PEG and mono-DNB-PEG, which show different retention abilities on the cation-exchange resin and thus result in the peak splittings in the chromatogram.

The absorption coefficients may vary for different DNB-POE molecules. In such a case, the peak areas do not reflect the concentrations of the DNB-POE oligomers. However, Desbene *et al.* [6] stated that the absorption coefficient is the same for all DNB-POE molecules. Fig. 5 shows the relative concentrations obtained for Brij 35 by assuming the same absorption coefficient for all DNB-POE molecules.

The average number of OE units contained in this surfactant was estimated to be 21.3.

In conclusion, non-ionic surfactants containing POE have been effectively analysed by the proposed method, which provides information both on the hydrophobic chain and the POE chain lengths. This POE analysis method has the weak point that compounds having less than six OE units cannot be separated. However, the uses of such surfactants are limited owing to their low solubility in water. If it is necessary to analyse such short POE chains, a reversed-phase stationary phase can be used instead of the present cation-exchange resin.

ACKNOWLEDGMENT

The author thanks Tosoh for generous gifts of separation columns.

REFERENCES

- 1 B. F. Greek, *Chem. Eng. News*, January 28 (1991) 25.
- 2 J. Cross, *Nonionic Surfactants*, Marcel Dekker, New York, 1987, and references cited therein.
- 3 M. Kudoh, *J. Chromatogr.*, 291 (1984) 327.
- 4 A. Otsuki and H. Shirai, *Anal. Chem.*, 51 (1979) 2329.
- 5 W. R. Melander, A. Nahum and Cs. Horváth, *J. Chromatogr.*, 185 (1979) 129.
- 6 P. L. Desbène, B. Desmazières, J. J. Basselier and A. D. Monvernay, *J. Chromatogr.*, 461 (1989) 305.
- 7 H. Shiraiishi, A. Otsuki and K. Fuwa, *Bull. Chem. Soc. Jpn.*, 55 (1982) 1410.
- 8 J. D. McClure, *J. Am. Oil Chem. Soc.*, 59 (1982) 364.
- 9 A. Aserin, N. Garti and M. Frenkel, *J. Liq. Chromatogr.*, 7 (1984) 1545.
- 10 G. R. Bear, *J. Chromatogr.*, 459 (1988) 91.
- 11 M. Kudoh, H. Ozawa, S. Fudano and K. Tsuji, *J. Chromatogr.*, 287 (1984) 337.
- 12 K. Noguchi, Y. Yanagihara, M. Kasai and B. Katayama, *J. Chromatogr.*, 461 (1989) 365.
- 13 M. Wiśniewski, J. Szymanowski and B. Atamańczuk, *J. Chromatogr.*, 462 (1989) 39.
- 14 P. Jandera, J. Urbánek, B. Prokeš and J. Churáček, *J. Chromatogr.*, 504 (1990) 297.
- 15 T. Okada, *Anal. Chem.*, 62 (1990) 327.
- 16 T. Okada, *Anal. Chem.*, 63 (1991) 1043.
- 17 T. L. Chester, *J. Chromatogr.*, 299 (1984) 424.
- 18 B. E. Richter, *J. High Resolut. Chromatogr. Chromatogr. Commun.*, 8 (1985) 297.
- 19 T. Okada, *J. Chem. Soc., Faraday Trans.*, 87 (1991) 3027.
- 20 T. Okada, *Macromolecules*, 23 (1990) 4216.

CHROM. 24 370

Erythrocyte partitioning in dextran–poly(ethylene glycol) aqueous phase systems

Events in phase and cell separation

Harry Walter

Laboratory of Chemical Biology—151, Veterans Affairs Medical Center, Long Beach, CA 90822-5201 (USA)

Frank D. Raymond

Department of Biochemistry and Chemistry, Royal Free Hospital School of Medicine, University of London, London NW3 2PF (UK)

Derek Fisher

Department of Biochemistry and Chemistry and Molecular Cell Pathology Laboratory, Royal Free Hospital School of Medicine, University of London, London NW3 2PF (UK)

(First received February 25th, 1992; revised manuscript received May 26th, 1992)

ABSTRACT

Early events in the partitioning process which involve characteristic kinetics of cell- and phase-specific interactions and phase separation have been described previously. This paper reports on red cell–phase droplet interactions pertaining at the time of usual phase sampling (*i.e.*, the time at which a clear bulk interface is first apparent) and beyond in cell partitioning and countercurrent distribution experiments. In non-charge-sensitive phase systems close to the critical point, cells can be free or attached to phase droplets. Cells that are free are virtually completely in the top phase, whereas different cell populations that show essentially complete binding to droplets can nevertheless have different partition ratios and be separated, thus reflecting the effects of the difference in the cells' avidity for the phase droplets during the early, elapsed events in partitioning. At higher polymer concentrations (*i.e.*, higher interfacial tensions), the cell populations, completely bound to phase droplets, partition completely to the interface, and consequently cannot be separated. When such systems are made charge-sensitive by the generation of a Donnan potential between the phases or made into affinity systems by the incorporation of PEG ligands (*e.g.*, PEG–palmitate), there is a decrease in the avidity of the cells for phase droplets. The resulting increase in the ratio of free to droplet-bound red cells in the top phase at the time of sampling correlates with an increase in the partition ratio, P , observed. The results show that a major difference (at the time of sampling) between non-charge-sensitive and charge-sensitive or affinity systems is that only in the former can cell populations be separated when they are almost completely bound to droplets. It was also found that although red cell–droplet interactions still pertain at the usual sampling times, there is a reduced involvement of kinetics at this late phase separation stage. This is operationally important as it provides leeway in selecting the sampling (settling) time.

INTRODUCTION

Partitioning in dextran–poly(ethylene glycol) aqueous phase systems is an established, sensitive method for the separation and fractionation of cell

Correspondence to: Dr. Harry Walter, Laboratory of Chemical Biology—151, Veterans Affairs Medical Center, Long Beach, CA 90822-5201, USA.

populations based on differences in their surface properties (for some recent reviews, see refs. 1–4). Unlike the partitioning of soluble materials, which occurs between the bulk phases and depends on the materials' relative solubility in them, the partitioning of cells generally take place between one of the bulk phases and the interface and is time dependent [1,2,5]. Early events in the partitioning process which involve characteristic kinetics of erythrocyte and phase-specific interactions and phase separation have been described previously [5–7]. In this paper we report on the red cell–phase droplet interactions pertaining at the time of usual phase sampling (see Experimental) and beyond in cell partitioning and countercurrent distribution experiments. We thereby (a) contribute further to an appreciation of the partitioning mechanism, (b) put into perspective the early events which, to a great extent, determine cell partition ratios but are usually unobserved in an operational sense, and the later events, which are observed without appreciation of basis, and (c) show the reduced involvement of kinetics in these later stages of partitioning.

EXPERIMENTAL

Reagents

Dextran T500 (lots 4094, 5556 and 11648) were obtained from Pharmacia LKB (Piscataway, NJ, USA). Poly(ethylene glycol) 8000 (PEG, Carbowax 8000) was from Union Carbide (Long Beach, CA, USA) and PEG 6000 was from BDH (Poole, UK). All salts used were of analytical-reagent grade. The ester of PEG 6000 and palmitic acid (PEG 6000–palmitate) was synthesized by the method of Shanbhag and Johansson [8]. Analysis established that 38% of the hydroxyl groups were esterified.

Preparation of two-polymer aqueous phase systems

Dextran–PEG aqueous two-phase systems having the compositions specified in the text were made up as previously described [1] and are designated by the nomenclature established there. In short, the first number in the description of phase systems denotes the percentage concentration of dextran (w/w). This is followed by a colon and a number giving the percentage concentration of PEG (w/w) (PEG 8000 unless indicated otherwise). The salt content follows as:

#1 being 0.11 *M* sodium phosphate buffer (pH 6.8);

#5 being 0.01 *M* sodium phosphate (pH 6.8) + 0.15 *M* NaCl.

Systems in which phosphate predominates have an electrostatic potential difference ($\Delta\psi$) between the phases (top phase positive) and are deemed charge-sensitive [1]. Phases in which NaCl is the main salt have virtually no potential between the phases and are non-charge-sensitive [1]. The interfacial tension between the phases increases with increasing polymer concentration [1,2].

Collection of blood and washing of erythrocytes

Volumes of 10 ml of blood from human donors and from dogs were obtained by venipuncture and collected in 3 ml of the anticoagulant acid–citrate–dextrose (ACD). A similar volume of blood was obtained, by heart puncture, from male Sprague–Dawley rats which weighed 275–400 g. Rabbit blood, usually 5 ml in 1.5–2 ml of ACD, was from the ear marginal vein. Sheep erythrocytes, in Alsevier's solution, were purchased from Mission Laboratories (Rosemead, CA, USA). Chicken blood was taken from the brachial vein by venipuncture and collected in Alsevier's solution. Aliquots of the erythrocyte populations were washed three times with at least ten times the cell volume of isotonic aqueous salt solution (saline) before being used in the experiments described below.

Partitioning of erythrocytes in aqueous two-phase systems

Erythrocyte partitioning was carried out as described previously [9]. Phase systems to be used, at 21–24°C, were mixed and 10 ml were poured into calibrated tubes (125 × 15 mm I.D.). The tubes were centrifuged to speed phase separation and the top and bottom phase volumes were adjusted to be equal. The top phase volumes were recorded. A 0.1-ml volume of washed, packed erythrocytes to be partitioned was added to each tube and the contents were well mixed. As phase separation (settling) times are, among other things, a function of phase column height [1,2,10] and increase markedly as one approaches the critical point (*i.e.*, the polymer concentrations below which no phase separation occurs), tubes were capped and permitted to settle

in a horizontal position when using low polymer concentrations (*i.e.*, 5:3.5) and in a vertical position when using higher polymer concentrations. Times for phase settling (indicated in the text and/or tables) were chosen such that the phase systems had just formed a sharp interface at the level of the initially determined interface. In a few experiments (see below) we also show, for comparative purposes, results at longer settling times. An aliquot of the top phase was withdrawn and the number of cells determined either by electronic counting (Celscope; Particle Data, Elmhurst, IL, USA) or by lysing and measuring the absorbance at 540 nm. The number of cells initially added to the partition tubes was similarly determined. The partition ratio, P , of cells is given as the number of cells in the top phase as a percentage of total cells added [1,2]. The partition ratio was found to be independent of the number of cells added to the partition tubes over the range tested (0.01–0.5 ml packed erythrocytes).

Microscopic examination of erythrocyte–phase droplet interactions

Between 0.015 and 0.035 ml of packed erythrocytes were added to partition tubes containing equal top and bottom phase volumes as described above. The tubes were mixed and permitted to settle. An aliquot of top (or bottom) phase was then removed with a Pasteur pipet and placed on a slide, covered with a cover-slip and immediately examined on a phase contrast microscope (American Optical, Buffalo, NY, USA). The percentage of cells attached to phase droplets was determined three times by counting a minimum of 100 cells each time during a period of not more than 2 min to prevent the slide from warming (due to the microscope lamp).

RESULTS

Non-charge-sensitive phases: attachment of cells to droplet surfaces

Microscopic examination of top and bottom phases of non-charge-sensitive dextran–PEG 8000 (or 6000) phase systems containing erythrocytes from rat, human, dog or rabbit reveals that the cells are bound on the PEG side of phase droplets (Fig. 1 shows an example for human blood cells). The percentage of these cells bound to phase droplets pres-



Fig. 1. Phase contrast light micrographs of human erythrocytes ($\times 585$) which attach to the outer surfaces of droplets of the dextran-rich bottom phase suspended in the top phase of a non-charge-sensitive phase system containing 5% (w/w) dextran T500, 4.75% (w/w) PEG 6000, 0.15 M NaCl and 0.01 M sodium phosphate buffer (pH 6.8). See text for discussion.

ent in the top phase (referred to as “dextran” droplets as they are composed of dextran-rich bottom phase) was determined at the same time as their partition ratios, P , were measured (Table I). In the phase system of lowest polymer concentration, 5:3.5 (lowest interfacial tension), the rat erythrocytes were completely in the top phase and were not bound to dextran droplets. Increasing the polymer concentrations (5:3.5 \rightarrow 5:3.7 \rightarrow 5:4 \rightarrow 7:4.4), thereby increasing the interfacial tension, led to increased binding to droplets and decreased P values. In the 5:3.5 phase system the partition ratios were in the order rat $>$ dog $>$ rabbit $>$ human as reported previously [9], indicating differences in the surface properties of these cells. However, the attachment

TABLE I

PARTITION RATIO, P , AND THE PERCENTAGE OF ERYTHROCYTES, FROM DIFFERENT SPECIES, BOUND TO BOTTOM PHASE DROPLETS IN THE TOP PHASE OF NON-CHARGE-SENSITIVE PHASE SYSTEMS

See text for discussion.

Species	Phase system ^a							
	5:3.5 #5 ^b		5:3.7 #5 ^c		5:4 #5 ^d		7:4.4 #5 ^e	
	P	% bound	P	% bound	P	% bound	P	% bound
Rat	102 ± 3(3)	1 ± 1(3)	37 ± 8(18)	62 ± 15(16)	16 ± 2(3)	92 ± 3(3)	3 ± 3(3)	93 ± 3(3)
Dog	89 ± 5(9)	83 ± 7(9)	—	—	—	—	—	—
Rabbit	71 ± 6(18)	81 ± 14(16)	—	—	—	—	—	—
Human	55 ± 5(3)	96 ± 1(3)	—	—	<5	97 ± 3(3)	—	—

^a Phase systems were composed of the indicated concentrations of dextran T500, poly(ethylene glycol) 8000 and 0.15 M NaCl + 0.01 M sodium phosphate buffer (pH 6.8). Data are presented ± S.D. with the number of experiments in parentheses.

^b Settling time: 7 min horizontal + 1 min vertical.

^c Settling time: 30 min vertical.

^d Settling time: 20 min vertical.

^e Settling time: 10 min vertical.

of cells to droplets was not as discriminatory as partitioning: erythrocytes of rat were unattached whereas those of dog, rabbit and human were predominantly attached (>80%), and rabbit and dog cells could not be distinguished by droplet binding. Further, cells could be virtually completely attached to droplets and still display different partitioning behavior, *e.g.*, the partition ratio of human erythrocytes decreased from 55 to <5% on increasing the polymer concentrations from 5:3.5 to 5:4, yet in both phases more than 95% of cells were attached to droplets.

Evidence that cells differ in their affinity for droplets was obtained by examining the sequence of detachment of the cells from phase droplets as the interfacial tension was reduced (Fig. 2): rat erythrocytes were virtually detached at all polymer concentrations, whereas the other species' cells, while attached in the 5:3.55 system, detached in the order dog > rabbit > human as the polymer concentrations were reduced.

Charge-sensitive phases: attachment of cells to droplet surfaces

Microscopic examination of the top and bottom phase of charge-sensitive phase systems of dextran

T500–PEG 8000 (or 6000) containing erythrocytes from rat, human, dog or rabbit revealed that the cells are bound on the PEG side of dextran droplets present in the top phase and on the PEG side of PEG droplets in the bottom phase. The percentage of these cells bound to dextran droplets present in the top phase was determined at the same time as their partition ratios, P , were measured (Table II). In the phase system of lowest polymer concentrations, 5:3.5, the rat erythrocytes have a high P value and were not bound to dextran droplets. Increasing the polymer concentrations (to 5:5 and to 7:4.4) led to increased binding to droplets and was accompanied by decreased cell partition ratios. A similar trend was also seen for human erythrocytes when increasing the polymer concentration from 5:3.5 to 5:4. In the 5:4 system the P values decreased (from 94 to 5%) in the order rat > dog > human > rabbit as reported previously [9] and were associated with an increase (from 0.3% to 97%) in the percentage of cells bound to dextran droplets. Unlike the behavior of these cells in non-charge-sensitive phase systems (Table I), high P values in charge-sensitive systems were associated with low percentages of cells bound to droplets.

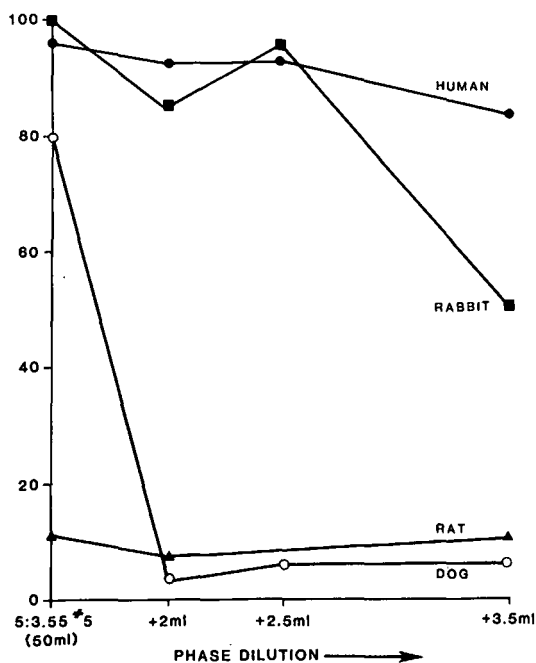


Fig. 2. Relative avidity of cells for bottom phase droplets suspended in the top phase as shown by the sequence of their detachment as the polymer concentrations of a non-charge-sensitive phase system [composed of 5% (w/w) dextran T500, 3.55% (w/w) PEG 8000, 0.15 M NaCl and 0.01 M sodium phosphate buffer (pH 6.8)] are reduced by titration with a solution containing 2% (w/w) PEG 8000, 0.15 M NaCl and 0.01 M sodium phosphate (pH 6.8). In the original system rat red blood cells are free, whereas dog, rabbit and human erythrocytes are bound. As the polymer concentrations are reduced, dog red blood cells become free first, followed by partial (50%) detachment of rabbit and (18%) human red cells. Human < rabbit < dog < rat is the sequence of these species' erythrocyte partition ratios in non-charge-sensitive phase systems [9]. See text for discussion.

Involvement of charge- or non-charge-related surface parameters in partitioning reflected by the extent of cell attachment to droplets

The P values of cells measured in charge-sensitive phase systems do not, in themselves, indicate the extent of involvement of charge- or non-charge-related parameters in effecting the observed partition ratio. The partition ratios and binding to droplets of dog and rabbit erythrocytes were examined in the non-charge-sensitive phase system 5:3.5 #5, the composition of which is close to the critical point, and its charge-sensitive counterpart, 5:3.5 #1 (Table III). While the P values of dog erythrocytes are

equally high in both phase systems, the cells are predominantly attached to droplets in the non-charge-sensitive system and virtually completely free in the charge-sensitive system. Hence the electrostatic potential difference between the phases in the latter system resulted in the detachment of the cells and the resulting P value can be ascribed to the dog cells' surface charge. By contrast, rabbit red cells (which have a very low surface charge [9]) showed no decrease in attachment to phase droplets on switching from 5:3.5 #5 to 5:3.5 #1. Rather, there was a slight increase in attachment which, most likely, is a consequence of the higher interfacial tension associated with phase systems containing phosphate [11]. Rabbit erythrocytes had similar P values in both phases. Thus, even in the charge-sensitive phase system the partitioning behavior of rabbit red blood cells reflects their non-charge-related surface properties.

Phases with a polymer ligand: attachment of cells to droplet surfaces

The percentage of chicken erythrocytes bound to dextran droplets present in the top phase was determined at the same time as their partition ratios, P , were measured in two non-charge-sensitive phase systems: 5:4.5 #5 and 5:5 #5 (Table IV). In each instance the P value was zero and all the cells were bound to the droplets. Incorporation of the hydrophobic affinity ligand, PEG-palmitate, into the phase systems caused an increase in P associated with a decrease in the percentage of cells bound to the droplets. Higher concentrations of PEG-palmitate were required in the phase system with higher polymer concentration (*i.e.*, with 5:5) to produce increases in the P value and free (unbound) cells similar to those obtained in the 5:4.5 system.

Relation of cell partition ratio (and percentages of cells bound to droplets) to sampling time

The effect of doubling the usual sampling time (defined earlier) on the P value of human erythrocytes and their attachment to dextran droplets in the top phase was examined in both non-charge-sensitive and charge-sensitive phase systems (Table V). There was little change observed in either the P value or the percentage of cells attached to droplets. In experiments (not shown) using erythrocytes from other species and a number of different phase sys-

TABLE II

PARTITION RATIO, P , AND THE PERCENTAGE OF ERYTHROCYTES, FROM DIFFERENT SPECIES, BOUND TO BOTTOM PHASE DROPLETS IN THE TOP PHASE OF CHARGE-SENSITIVE PHASE SYSTEMS.

See text for discussion.

Species	Phase system ^a							
	5:3.5 #1 ^b		5:4 #1 ^c		5:5 #1 ^c		7:4.4 #1 ^d	
	P	% bound	P	% bound	P	% bound	P	% bound
Rat	93 ± 2(3)	0	94 ± 2(3)	0.3 ± 1(3)	22 ± 3(3)	91 ± 6(3)	16 ± 1(3)	87 ± 9(3)
Dog	—	—	95 ± 6(6)	2 ± 3(6)	—	—	—	—
Human	87 ± 0(3)	1 ± 2(3)	52 ± 7(6)	53 ± 13(6)	—	—	—	—
Rabbit	—	—	5 ± 3(3)	97 ± 2(3)	—	—	—	—

^a Phase systems were composed of indicated concentrations of dextran T500, poly(ethylene glycol) 8000 and 0.11 M sodium phosphate buffer (pH 6.8). Data are presented ± S.D. with the number of experiments in parentheses. Note that the 5:3.5 #1 system reflects both charge-associated and non-charge-related surface properties of these cells, while 5:4 #1 reflects charge-associated properties of all species' erythrocytes except those from rat (where both charge-associated and non-charge-related properties are still reflected). At higher polymer concentrations charge-related properties determine the P value of all species' erythrocytes including those from rat. For a detailed discussion, see ref. 9.

^b Settling time: 7 min horizontal + 1 min vertical.

^c Settling time: 20 min vertical.

^d Settling time: 10 min vertical.

tems, small decreases in P value, usually less than 10% and never more than 20%, were observed. These data indicate that at the usual sampling times the kinetics of partitioning have become sufficiently

TABLE III

PERCENTAGE OF RABBIT AND DOG ERYTHROCYTES BOUND TO BOTTOM PHASE DROPLETS IN THE TOP PHASE AND THE CELLS' PARTITION RATIO, P , IN A NON-CHARGE-SENSITIVE (5:3.5 #5) AND A CHARGE-SENSITIVE (5:3.5 #1) PHASE SYSTEM

The latter system, also being close to the critical point (*i.e.*, having the same lower polymer concentrations as the non-charge-sensitive system), reflects in addition to charge also non-charge surface parameters. Phases were permitted to settle for 7 min horizontal + 1 min vertical. Data are presented ± S.D. with the number of experiments in parentheses. See text for details.

Species	Phase system			
	5:3.5 #5		5:3.5 #1	
	P	% bound	P	% bound
Rabbit	76 ± 15(3)	80 ± 7(9)	65 ± 11(3)	97 ± 3(9)
Dog	100 ± 0(2)	90 ± 8(6)	102 ± 2(2)	1 ± 1(6)

TABLE IV

PARTITION RATIO, P , AND THE PERCENTAGE OF CHICKEN ERYTHROCYTES BOUND TO BOTTOM PHASE DROPLETS IN THE TOP PHASE OF A NON-CHARGE-SENSITIVE PHASE SYSTEM CONTAINING DIFFERENT AMOUNTS OF PEG-PALMITATE

See text for discussion.

PEG-palmitate (μg)	Phase system ^a			
	5:4.5 #5		5:5 #5	
	P	% bound	P	% bound
0	0	100	0	100
2	32	78		
4	71	30		
6	95	30		
8	97	5		
20			59	89
40			92	11
60			83	3
80			91	3

^a Phase systems were composed of the indicated concentrations of dextran T500, poly(ethylene glycol) 6000, 0.15 M NaCl + 0.01 M sodium phosphate buffer (pH 6.8), and the indicated amounts of PEG 6000-palmitate. Partitions shown were carried out in 2-g phase systems (1 g of each phase) to which 0.01 ml of packed cells had been added. The P value was determined after 15 min of phase settling in the vertical position.

TABLE V

EFFECT OF DOUBLING THE "USUAL" SAMPLING TIME ON THE PERCENTAGE OF HUMAN ERYTHROCYTES BOUND TO BOTTOM PHASE DROPLETS IN THE TOP PHASE AND ON THE CELLS' PARTITION RATIO, *P*Data are presented \pm S.D. with the number of experiments in parentheses.

Settling time ^a	Phase system			
	5:3.5 #5		5:4 #1	
	<i>P</i>	% bound	<i>P</i>	% bound
7 min h + 1 min v	55 \pm 5(3)	96 \pm 1(3)	—	—
15 min h + 1 min v	58 \pm 10(3)	95 \pm 4(3)	—	—
20 min v	—	—	52 \pm 7(6)	53 \pm 13(6)
40 min v	—	—	49 \pm 8(18)	61 \pm 14(15)

^a h = Horizontal; v = vertical.

slow that the choice of this time is not overly critical.

DISCUSSION

Microscopic analysis of erythrocytes partitioned in (dextran T500–PEG) non-charge-sensitive phase systems has previously revealed that cells tend to adhere to the surfaces of the phase droplets and streams (microphases) that are formed as phase separation proceeds and are delivered to the developing bulk interface [5,7]. These early events are complex and depend on the strength of attachment determined by the surface properties of the cell being partitioned and on the phase system composition [12,13]. They generate the *P* value since their kinetics determine the proportion of cells delivered to the bulk interface, by the time that the partition ratio is measured, and the proportion present in the top phase (either as attached to phase droplets or as free cells). The partition ratio, *P*, can be seen actually to reflect the sum of free^a + droplet-bound cells in a bulk phase as a percentage of total cells added.

However, in most practical applications, such as the times employed in sampling a single partition tube to measure the *P* value or in the settling steps in countercurrent distribution, it is relatively late

stages in the cell partitioning process, when the phases have separated to form distinct bulk phases, that prevail. We have therefore, unlike in previous reports, concentrated on an examination of these later stages of the partitioning behavior of erythrocytes.

The partitioning of erythrocytes in dextran T500–PEG 8000 (or 6000) phase systems takes place between the top phase and the interface in both charge-sensitive and non-charge-sensitive systems. The cells adhere to the PEG side of the dextran droplets found in the top phase and also to the PEG side of the relatively few PEG droplets found in the bottom phase at the time of sampling. The bulk phase into which the cells partition is thus reflected by the side of the phase droplet to which they adhere.

Partitioning of cells in non-charge-sensitive phase systems is possible only when the polymer concentrations are adequately low (low interfacial tension) to permit cells to be found in one of the bulk phases (either free or on droplets) at the usual time of phase sampling. At higher polymer concentrations all cells are at the bulk phase interface and no partitioning takes place. Hence it is particularly intriguing that erythrocytes from different species, virtually totally bound to the surface of phase droplets (Table I), the physical properties of which are presumably identical with those of the bulk interface, can still have different *P* values and be separated ([9], Table I). In fact the non-charge-sensitive phase system appears to be the only kind of phase system

^a "Free" cells are those not bound to droplets of visible dimensions.

in which cells totally bound to droplets are separable at normal partition times (compare Tables I and II; also see ref. 14). Possible bases for these findings are suggested below.

The sequence of attachment/detachment of different species' red blood cells from phase droplets (Fig. 2) is a reflection of the cells' relative avidity for the interface. It indicates that whereas, in a given phase system (e.g., 5:3.5 #5, Table I), cells from different species may, essentially, have the same percentage of cells bound to droplets, these are not equally tightly held on the droplet surface. The sequence of detachment parallels the cells' relative P values (rat > dog > rabbit > human) in such a non-charge-sensitive phase system (see Table I).

The effect of the difference in relative avidity of erythrocytes from different species for phase droplets on the early stages of phase separation has been summarized [11,15] and presents the most likely sequence of occurrences which results in the separation of cells all of which are found to be phase droplet-bound at the usual time of sampling.

Whereas the cell- and phase-specific kinetic differences in cell binding to droplets and of cell-bound droplet delivery to the bulk interface are dramatic in the early stages of phase separation, the change in P value observed with a doubling of the usual sampling time is not large (Table V; see also ref. 16) and, hence, the time of sampling is not so critical in optimizing cell separations when made beyond the time that a sharp interface has appeared.

To determine appropriate polymer concentrations for partitioning cells in charge-sensitive phases, the lowest polymer concentrations at which cells are totally at the interface in a non-charge-sensitive phase system (e.g., one containing predominantly NaCl) are first established. Using the determined polymer concentrations one replaces the salt with one that produces an electrostatic potential difference between the phases (e.g., phosphate). Partitions carried out in charge-sensitive phases at or above such polymer concentrations are deemed to be charge-sensitive; below such polymer concentrations (i.e., in phases having lower interfacial tensions) partitioning can also reflect non-charge-associated surface properties [9,15,17].

Table II indicates that an inverse relationship exists between erythrocyte P values in charge-sensitive

phases and the percentage of cells bound to dextran phase droplets in the top phase. Cells totally bound to droplets in charge-sensitive phases would be exclusively at the bulk interface. This differs from the behavior of cells in non-charge-sensitive phases (Table I) in which, as already indicated, cells virtually completely bound to phase droplets can still have different P values. In charge-sensitive phases the partitioning of cells appears to take place because cells are "pulled" off the phase droplets in relation to their charge-associated properties (giving rise to the cell partition sequence shown in Table II). Just as with non-charge-sensitive phase systems, the effect of doubling the usual sampling time on the P value observed in charge-sensitive phases is not large (see Table V and Results) and hence some leeway exists in its choice.

The partition ratio of erythrocytes from different species in dextran T500-PEG phase systems increases with increasing amounts of PEG-palmitate ([9], Table IV). The higher cell P values result from a decrease in the number of phase droplet-bound cells. Cells in phases containing PEG-palmitate behave as if their interaction with phase droplets is weakened. Evidence for this has been provided by the wetting behavior of erythrocytes in dextran-PEG systems [11]. By binding to the cell surface (hydrophobically), PEG-palmitate increases the tendency for the PEG phase to wet the surface (contact angle measurements [11,15]) and, as it were, "pull" the cell free and into the PEG phase.

ACKNOWLEDGEMENTS

We thank Janet L. Anderson, Eugene J. Krob and John Morrison for expert technical assistance. The work in H. W.'s laboratory was supported by the Medical Research Service of the Department of Veterans Affairs and in D. F.'s laboratory by the Royal Free Hospital School of Medicine.

REFERENCES

- 1 H. Walter, D. E. Brooks and D. Fisher (Editors), *Partitioning in Aqueous Two-Phase Systems — Theory, Methods, Uses, and Applications to Biotechnology*, Academic Press, Orlando, FL, 1985.
- 2 P.-Å. Albertsson, *Partition of Cell Particles and Macromolecules*, Wiley-Interscience, New York, 3rd ed., 1986.
- 3 D. Fisher and I. A. Sutherland (Editors), *Separations Using*

- Aqueous Phase Systems —Applications in Cell Biology and Biotechnology*, Plenum Press, New York, 1989.
- 4 H. Walter, G. Johansson and D. E. Brooks, *Anal. Biochem.*, 197 (1991) 1.
 - 5 F. D. Raymond and D. Fisher, *Biochim. Biophys. Acta*, 596 (1980) 445.
 - 6 D. Fisher, *Biochem. J.*, 196 (1981) 1.
 - 7 F. D. Raymond and D. Fisher, in A. W. Prece and P. A. Light (Editors), *Cell Electrophoresis in Cancer and Other Clinical Research*, Elsevier North-Holland Biomedical Press, Amsterdam, 1981, pp. 65–68.
 - 8 V. P. Shanbhag and G. Johansson, *Biochem. Biophys. Res. Commun.*, 61 (1974) 1141.
 - 9 H. Walter, in H. Walter, D. E. Brooks and D. Fisher (Editors), *Partitioning in Aqueous Two-Phase Systems —Theory, Methods, Uses, and Applications to Biotechnology*, Academic Press, Orlando, FL, 1985, pp. 327–376.
 - 10 H. Walter and E. J. Krob, *Biochim. Biophys. Acta*, 966 (1988) 65.
 - 11 D. E. Brooks, K. A. Sharp and D. Fisher, in H. Walter, D. E. Brooks and D. Fisher (Editors), *Partitioning in Aqueous Two-Phase Systems —Theory, Methods, Uses, and Applications to Biotechnology*, Academic Press, Orlando, FL, 1985, pp. 11–84.
 - 12 F. D. Raymond, *Ph. D. Thesis*, University of London, London, 1981.
 - 13 F. D. Raymond and D. Fisher, in preparation.
 - 14 D. Fisher and H. Walter, *Biochim. Biophys. Acta*, 801 (1984) 106.
 - 15 B. N. Youens, W. D. Cooper, F. D. Raymond, P. S. Gascoine and D. Fisher, in D. Fisher and I. A. Sutherland (Editors), *Separations Using Aqueous Phase Systems —Applications in Cell Biology and Biotechnology*, Plenum Press, New York, 1989, pp. 271–280.
 - 16 H. Walter, E. J. Krob and L. Wollenberger, *J. Chromatogr.*, 542 (1991) 397.
 - 17 I. Shelton, P. S. Gascoine, D. M. Turner and D. Fisher, *Biochem. Soc. Trans.*, 13 (1985) 168.

Pair-wise interactions by gas chromatography

I. Interaction free enthalpies of solutes with non-associated primary alcohol groups[☆]

K. S. Reddy, J.-Cl. Dutoit^{☆☆} and E. sz. Kováts

Laboratoire de Chimie Technique, Ecole Polytechnique Fédérale de Lausanne, CH-1015 Lausanne (Switzerland)

(Received March 11th, 1992)

ABSTRACT

A method is presented for the determination of interaction free enthalpies between an interacting group, X, suspended in a paraffin solvent at ideal dilution and a volatile compound dissolved in the same solvent at ideal dilution. The measuring system consists of a family of non-volatile solvents suitable for use as liquid stationary phases in gas chromatography. Members of the family, P, are mono-X-functionalized derivatives of a parent branched paraffin, C₇₈H₁₅₈ (C78), with molecules having the same form and nearly the same size as those of the non-polar standard, C78. Consequently, the solvents P form nearly ideal, regular mixtures with the standard solvent. Gas chromatographic data of solutes on such mixtures allow the calculation of interaction parameters with the aid of equations given in this paper. The method was applied to the determination of interaction data of solutes with free, monomeric primary alcohol groups.

INTRODUCTION

In this paper, a method is proposed for the determination of the interaction free enthalpies between a solute, *j*, in a paraffin solvent at ideal dilution and an alone-standing interacting group, X, dissolved in the same paraffin solvent also at ideal dilution. The measuring system consists of a family of polar solvents, P, derivatives of a reference paraffin, A = C78 (C₇₈H₁₅₈), depicted in Fig. 1 [1]. The molecule of the solvent, P, has the same form and nearly the same size as that of the reference, A.

Therefore, members of this family should form regular A–P mixtures [2,3].

The determination of the molal Henry coefficient of a solute, *g_j*, in non-volatile solvents can easily be accomplished by gas chromatography. Using the A–P mixture as liquid stationary phase, the specific retention volume, *V_g*, can be measured at different temperatures, allowing the calculation of the molal Henry coefficient from the relationship

$$V_{g,j} = V_{N,j}/w_L = \mathcal{R}T/1000 g_j \quad (1)$$

where *V_{N,j}* is the net retention volume of the solute at temperature *T*(K), *w_L* is the mass of the liquid stationary phase, L, in the column and \mathcal{R} (cm³ atm mol⁻¹ K⁻¹) is the universal gas constant. In binary solvents the activity coefficient of a solute depends on the size difference between the solvent and solute and on differences in interaction free enthalpies between the solute and the two components of the solvent. In the simplest case, the standard chemical

Correspondence to: Professor E. sz. Kováts, Laboratoire de Chimie Technique, École Polytechnique Fédérale de Lausanne, CH-1015 Lausanne, Switzerland.

[☆] Partly taken from the Doctoral Thesis of J.-Cl. Dutoit.

^{☆☆} Present address: Laboratoire AC Spiez, CH-3700 Spiez, Switzerland.

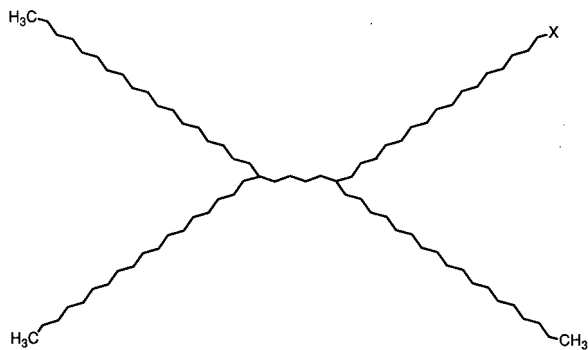


Fig. 1. Structure of the branched paraffin, C78, where X = CH₂CH₃, and its monofunctional derivative, POH (for primary alcohol), where X = CH₂OH, used as liquid stationary phases in this paper. Further monofunctional derivatives have also been prepared with X = CH₂CF₃, CH₂Cl, CH₂Br, CH₂CN, CH₂SH and OCH₃ [11].

potential difference, given by

$$\Delta\mu_j^{A/P} = RT \ln [g_j / (\text{atm kg mol}^{-1})] \quad (2)$$

is a linear combination of those measured in the pure components. In real A–P mixtures, slightly deviating from ideal behaviour, eqn. 3 holds:

$$\Delta\mu_j^{A/P} = \Delta\mu_j^A + \varphi_P \Delta\mu_j^P + \varphi_A \varphi_P m_j^{A/P} \quad (3)$$

where Δ and Δ designate a difference with reference states “ideal gas phase” and “ideal dilute solution in standard, A”, respectively. In our specific A–P mixtures the effect of the size of the solvent molecules, A and P, should be the same [4–10]. Therefore, the third term in eqn. 3 fully accounts for the slight curvature of the dependence of the chemical potential of the solute on composition due to non-ideality, as shown by the example of three solutes in Fig. 2. Supposing that the difference in the partial molar heat capacity of the solute in the two states, $\Delta C_{P,j}$ and $\Delta C_{P,j}$ is constant in the experimental temperature range (Kirchhoff's approximation), the temperature dependence of the three terms in eqn. 3 is given by the equations

$$\Delta\mu_j^A = \Delta H_j^A - T \Delta S_j^A + \Delta C_{P,j}^A \left[T - T^\dagger - T \ln \left(\frac{T}{T^\dagger} \right) \right] \quad (4)$$

$$\Delta\mu_j^P = \Delta H_j^P - T \Delta S_j^P + \Delta C_{P,j}^P \left[T - T^\dagger - T \ln \left(\frac{T}{T^\dagger} \right) \right] \quad (5)$$

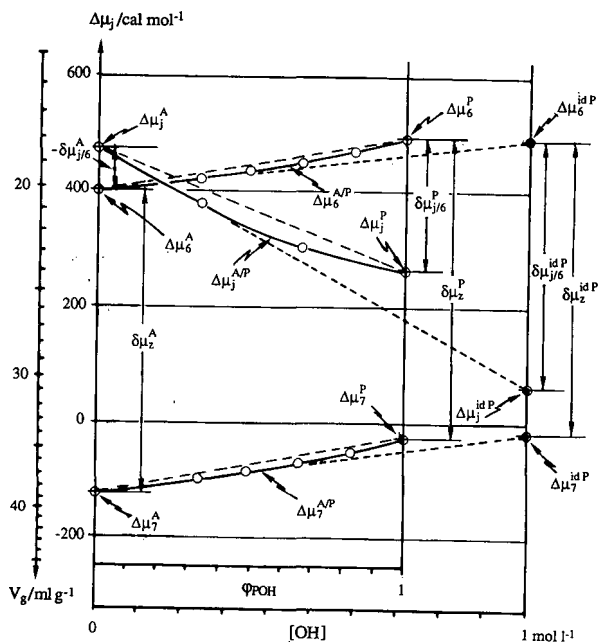


Fig. 2. Dependence of the standard chemical potential of a solute on composition in C78–POH mixtures illustrated on the example of 6 = hexane, 7 = heptane and j = propionitrile at 130°C. V_g is the specific retention volume, φ_{POH} is the volume fraction of POH and $[\text{OH}]$ is the molar concentration of primary alcohol groups in the liquid stationary phase. Open circles are experimental points. This figure helps in the understanding of equations and symbols explained in the text.

$$m_j^{A/P} = h_j - T s_j \quad (6)$$

where H_j and S_j are the partial molar enthalpy and entropy at the standard temperature $T^\dagger = 130 + 273.15$ K, respectively. The chemical potential contribution due to non-ideality, $m_j^{A/P}$, is supposed to be composed of an enthalpic, h_j , and an entropic, s_j , term, both of which are independent of temperature.

The eight constants in eqns. 3–6 can be determined by multiple linear regression if there are sufficient chemical potential differences measured at different temperatures (at least three) and A–P compositions (at least three). Knowledge of eqn. 3 allows one to calculate the standard chemical potential difference of the solute at zero concentration of the interacting group, X, in the liquid stationary phase. Use of eqn. 3 together with the relationship between the volume fraction, φ_P , of P, and the molar concentration of the interacting group, $[\text{X}]$, in the A–P mixture (monofunctional P, see Appendices B

and C) gives the necessary relationship as

$$\begin{aligned} \mathcal{A}'\mu_j^{\text{idP}} &\equiv \left(\frac{\partial \Delta\mu_j^{\text{A/P}}}{\partial [\text{X}]} \right)_{T, [\text{X}] = 0} = \\ &\left(\frac{\partial \Delta\mu_j^{\text{A/P}}}{\partial \varphi_{\text{P}}} \right)_{T, \varphi_{\text{P}} = 0} \left(\frac{\partial \varphi_{\text{P}}}{\partial [\text{X}]} \right)_T = (\mathcal{A}'\mu_j^{\text{P}} + m_j^{\text{A/P}})v_{\text{P}}/1000 \quad (7) \end{aligned}$$

The chemical potential difference of the solute at ideal dilution in an ideal polar stationary phase, idP, in which there is no interaction between the polar groups, X, (*i.e.*, at ideal dilution in the reference solvent, A) can now be given with the aid of the slope of the function $\Delta\mu_j^{\text{A/P}}$, at $[\text{X}] = 0$. Its value at any composition is given by

$$\mathcal{A}'\mu_j^{\text{idP}} = [\text{X}]\mathcal{A}'\mu_j^{\text{idP}} \quad (8)$$

Knowledge of the function $\mathcal{A}'\mu_j^{\text{idP}}$ at different temperatures permits the calculation of the corresponding partial molar enthalpy, entropy and mean partial molar heat capacity by fitting eqn. 9 to the experimental data.

$$\begin{aligned} \mathcal{A}'\mu_j^{\text{idP}} &= \mathcal{A}'H_j^{\text{idP}} - T\mathcal{A}'S_j^{\text{idP}} + \\ &\mathcal{A}'C_{\text{P},j}^{\text{idP}} \left[T - T^\dagger - T \ln \left(\frac{T}{T^\dagger} \right) \right] \quad (9) \end{aligned}$$

The meaning and use of eqns. 3–9 is illustrated in Fig. 2 on the example of three solutes, 6 = *n*-hexane, 7 = *n*-heptane and *j* = propionitrile in mixtures of the C78 branched paraffin and its derivative, POH, in which a methyl group is replaced with a primary hydroxyl (see Fig. 1).

In Fig. 2 are also shown the chemical potential differences between *j*-6 and 7-6 in a given liquid stationary phase (designated by δ) which are necessary for the calculation of the retention index. In fact, it can easily be shown (see Appendix D) that the retention index of a solute can also be interpreted as a measure of the chemical potential of the solute on the scale given by the chemical potentials of the *n*-alkanes. For a given liquid stationary phase, L (= A, P or an A–P mixture),

$$I = 100 \frac{\Delta\mu_j^{\text{L}} - \Delta\mu_z^{\text{L}}}{\Delta\mu_{z+1}^{\text{L}} - \Delta\mu_z^{\text{L}}} + 100z = 100 \frac{\delta\mu_{j/z}^{\text{L}}}{\delta\mu_z^{\text{L}}} + 100z \quad (10)$$

The difference between two *n*-alkanes, $\delta\mu_z$, is nearly independent of the carbon number if *z* is higher than 5. The temperature and composition dependence of this “methylene increment” due to the increase in

the chain length by a methylene group is given by $\delta\mu_z^{\text{A/P}} = \delta\mu_z^{\text{A}} + \varphi_{\text{P}}(\delta\mu_z^{\text{P}} - \delta\mu_z^{\text{A}}) + \varphi_{\text{A}}\varphi_{\text{P}}\delta m_z^{\text{A/P}}$ (11) where

$$\delta\mu_z^{\text{A}} = \delta H_z^{\text{A}} - T\delta S_z^{\text{A}} + \delta C_{\text{P},z}^{\text{A}} \left[T - T^\dagger - T \ln \left(\frac{T}{T^\dagger} \right) \right] \quad (12)$$

$$\delta\mu_z^{\text{P}} = \delta H_z^{\text{P}} - T\delta S_z^{\text{P}} + \delta C_{\text{P},z}^{\text{P}} \left[T - T^\dagger - T \ln \left(\frac{T}{T^\dagger} \right) \right] \quad (13)$$

$$\delta m_z^{\text{A/P}} = \delta h_z - T\delta s_z \quad (14)$$

Let us now put forward the question of the calculation of the retention index in the ideal polar stationary phase, I_j^{idP} (see Appendix E).

Let us suppose again that liquids A and P form a regular mixture and the coefficients in eqns. 11–14 have been determined experimentally. Further, the dependence of the retention index of a solute on temperature and composition is known. In fact, experimental retention indices measured at different temperatures and compositions can be described with sufficient precision by

$$I_j^{\text{A/P}} = I_j^{\text{A}} + \varphi_{\text{P}}\mathcal{A}I_j^{\text{P}} + \varphi_{\text{A}}\varphi_{\text{P}}\epsilon_j^{\text{A/P}} \quad (15)$$

with

$$I_j^{\text{A}} = I_{130,j}^{\text{A}} + A_{T,j}\Delta T + A_{TT,j}\Delta T^2 \quad (16)$$

$$\mathcal{A}I_j^{\text{P}} = \mathcal{A}I_{130,j}^{\text{P}} + \mathcal{A}A_{T,j}\Delta T + \mathcal{A}A_{TT,j}\Delta T^2 \quad (17)$$

$$\epsilon_j^{\text{A/P}} = A_{L,j} + A_{LT,j}\Delta T \quad (18)$$

where I_{130} is the retention index at the standard temperature $T^\dagger = 130 + 273.15$ K and $\Delta T = T - T^\dagger$. As a general rule, all coefficients *A* are small and in most instances the coefficients A_{TT} and $\mathcal{A}A_{TT}$ are not significant. Consequently, retention indices can be described by fewer coefficients than standard chemical potentials (six instead of eight). Therefore, certain thermodynamic functions of the solutes must closely correlate with those of the *n*-alkanes. Knowledge of the coefficients in eqns. 15–18 permits the calculation of the slope of the function $I_j^{\text{A/P}}([\text{X}])$ at $[\text{X}] = 0$ (see Appendix E)

$$\begin{aligned} \left(\frac{\partial I_j^{\text{A/P}}}{\partial [\text{X}]} \right)_{T, [\text{X}] = 0} &= \left(\frac{\partial I_j^{\text{A/P}}}{\partial \varphi_{\text{P}}} \right)_{T, \varphi_{\text{P}} = 0} \left(\frac{\partial \varphi_{\text{P}}}{\partial [\text{X}]} \right)_T = \\ &(\mathcal{A}'I_j^{\text{P}} + \epsilon_j^{\text{A/P}})v_{\text{P}}/1000 \quad (19) \end{aligned}$$

where $[X]$ is the molar concentration of the interacting group, X , in the monofunctional polar solvent, P , and v_P is its molar volume. Knowledge of the value of this slope permits the calculation of the retention index in the solvent, idP (see Appendix E), as

$$I_j^{\text{idP}} = I_j^{\text{A}} + \left(\frac{\partial I_j^{\text{A/P}}}{\partial [X]} \right)_{T, [X]=0} \frac{[X]}{1 + [X]\kappa} \quad (20)$$

where $\kappa = (\delta' \mu_z^{\text{idP}} - \delta' \mu_z^{\text{A}}) / \delta \mu_z^{\text{A}}$ is a small number. Let us insist that the retention index is not a linear function of the composition in mixed liquid stationary phases even if the mixture is ideal, but is given by an equation similar to eqn. 20. The index I_j^{idP} can now be calculated with a knowledge of the function κ and the retention index on the pure polar phase P (see Appendix E, case 2) or on the phase idP at $[X] = 1$.

In the following Experimental section first the determination of the thermodynamic functions of n -alkanes is described in mixtures where A is the branched alkane $C_{78}H_{158}$ (C78) and P is the primary alcohol $C_{77}H_{155}OH$ (POH) shown in Fig. 1. In a second part the retention indices of 156 solutes are given in the same solvents, which are then converted into thermodynamic data with a knowledge of those of the n -alkanes. Finally, thermodynamic data and retention indices are given in a hypothetical ideal primary alcohol, idPOH, having an alcohol concentration $[OH] = 1 \text{ mol l}^{-1}$.

EXPERIMENTAL

Materials

Solutes were research-grade compounds from Fluka (Buchs, Switzerland). Some of the properties of the stationary liquids, 19,24-dioctadecyltetracontane (C78) and 18,23-dioctadecylhentetracontan-1-ol (POH) (see Fig. 1), synthesized in our laboratory [1,11], are given in Table I together with the coefficients of eqn. 21 for the calculation of their density, ρ_L in the temperature range 80–200°C.

$$\ln \rho_L = \ln M_L - \ln v_L = \ln \rho^\dagger - \alpha^\dagger \Delta T - B \Delta T^2 \quad (21)$$

where ρ^\dagger and α^\dagger are the density and the isobaric coefficient of thermal expansion at the standard temperature $T^\dagger = 130 + 273.15 \text{ K}$ and $B = (1/2)(d\alpha/dT)$ [12]. The purity of the liquid stationary phases, C78 and POH, was higher than 99.5%. Fig. 3 shows that the ratio of the molar volume of the POH/C78 stationary phases is near unity and its variation with temperature is less than $\pm 0.2\%$. A batch of Chromosorb G HP from Supelco (Bellefonte, PA, USA) was sieved. The fraction with particle diameter 150–180 μm was dried overnight in air. An amount of 300 g of this material was placed in an ampoule together with 3.0 g of trimethyl(dimethylamino) silane in an argon atmosphere. The sealed ampoule was heated at 250°C whilst occasionally shaking. After 24 h, the silylated support was cooled, washed with diethyl ether and dried *in vacuo* at 120°C.

TABLE I

PROPERTIES OF THE LIQUID STATIONARY PHASES C78 AND POH

M = Molar mass; ρ^\dagger = density; v^\dagger = molar volume; α^\dagger = isobaric coefficient of thermal expansion at the standard temperature $T^\dagger = 130 + 273.15 \text{ K}$; $B = (1/2)(d\alpha/dT)$. σ is for the standard deviation around the regression in the temperature range 80–200°C. Data from refs. 11 and 12.

L	M.p.	M	ρ^\dagger	v^\dagger	$\alpha^\dagger \cdot 10^4$	$B \cdot 10^7$	σ	
Symbol	Formula	(°C)	(g mol ⁻¹)	(g cm ⁻³)	(cm ³ mol ⁻¹)	(K ⁻¹)	(K ⁻²)	
C78	C ₇₈ H ₁₅₈	69–75	1096.1	0.7714	1420.9	7.45	1.26	0.0004
POH	C ₇₇ H ₁₅₅ OH	70–74	1098.1	0.7820	1404.2	7.79	0.74	0.0002
A_{95}				± 0.00009	± 0.16	± 0.32	± 0.91	

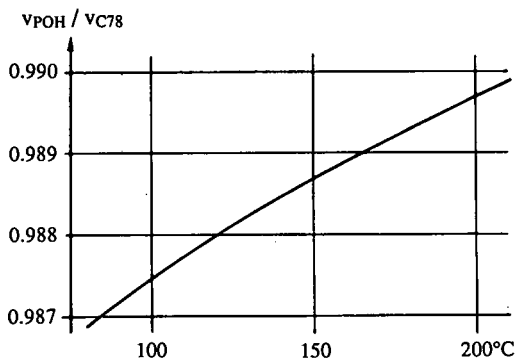


Fig. 3. Ratio of the molar volume of the POH and C78 stationary phases as a function of temperature.

For the preparation of column packings an exact amount of support (*ca.* 35 g, weighed with a precision of ± 0.01 g) was wetted with a 3% solution of the C78–POH mixture (*ca.* 2.22 g of mixture weighed with a precision of ± 1 mg) in cyclohexane (50 ml). Under a slow stream of argon (< 1 ppm of O_2) the solvent was evaporated at 60–70°C in a slowly rotating cylindrical evaporator, then the temperature was raised to 200°C for 10 h. Column packings were stored in an argon atmosphere. Columns (coiled Pyrex tubes, 330 cm \times 0.40 cm I.D.) were weighed before and after packing. The weight difference permitted the calculation of the column characteristics given in Table II. After packing the columns were filled with argon and those in use with oxygen-free helium.

TABLE II
CHARACTERISTICS OF THE CHROMATOGRAPHIC COLUMNS

ϕ_{POH} = Volume fraction of POH in the C78–POH mixture at 130°C; w_L = mass of this mixture in the column; P_L = percentage of L of the packing ($100w_L$ /total mass). In fact, ϕ_{POH} is temperature dependent but its variation is less than $\pm 0.1\%$ in the experimental temperature range (90–210°C).

$100\phi_{POH}$ (%)	Column	w_L (g)	P_L (%)
00.0	0–6	2.101	6.81
33.3	2–6	1.924	5.92
50.0	3–6	1.875	5.86
66.7	4–6	1.962	5.93
83.3	5–6	1.903	6.04
100.0	6–6	1.883	5.89

Apparatus

The gas chromatograph used for the determination of retention data is described in detail in refs. 10 and 13. In summary, a modified Packard-Becker (Delft, Netherlands) Model 439 gas chromatograph was used, equipped with two thermal conductivity detectors. The temperature in the oven was measured with a platinum sensor (100 Ω ; DIN 43710) and a Model S 1220 measuring device from Systemteknik (Lidingöe, Sweden). The platinum sensor was calibrated by the Eidg. Amt für Mass und Gewichte (Berne, Switzerland) between 0 and 400°C with a precision of ± 0.1 K. The temperature gradient in the oven was measured with chromel–alumel thermocouples at eight points. The mean column temperature was calculated by considering the temperature gradient as described in ref. 13.

Retention volume

The determination of the retention volume is described in detail in refs. 10 and 13. In summary, the helium carrier flow-rate was measured by means of a soap-film flow meter and the pressure at the inlet of the column was measured with a Model 710B precision device from Heise (Bassweiler, Germany). Retention time was determined at the peak maximum with a Hewlett-Packard Model 3390A integrator. The retention time of neon was used as the hold-up time for the calculation of net retention times. The inlet pressures never exceeded 1.5 bar, and it was assumed that gas-phase imperfections were negligible. The overall reproducibility of the retention volumes of neon was better than 1%.

Retention data were measured at 20-K intervals between 90 and 210°C at experimental temperatures as near as possible to the envisaged nominal temperature. The experimental temperature did not change more than 0.2 K during a working day. The first, last and mid-day chromatograms of a working day were obtained with a mixture of *n*-alkanes always containing the alkanes with $z = 5$ –10. Retention indices of all solutes were evaluated with the average net retention time of the alkanes if their individual values did not deviate by more than 1%. Otherwise, data for the working day were rejected.

After having measured all data on a given column, specific retention volumes of *n*-alkanes were converted into standard chemical potentials. With data determined near a given nominal temperature the following average was calculated:

$$\Delta\mu_z(\bar{T}_{\text{exp}}) = [\Delta\mu_z(T_{\text{exp},1}) + \dots + \Delta\mu_z(T_{\text{exp},n})]/n \quad (22)$$

where $T_{\text{exp},i}$ is the experimental temperature of the i th determination near a nominal temperature, n is the number of determinations and

$$\bar{T}_{\text{exp}} = (T_{\text{exp},1} + \dots + T_{\text{exp},n})/n \quad (23)$$

A quadratic regression was then fitted to each data set for an alkane measured on the same stationary liquid to give the dependence of the chemical potential on temperature, $\Delta\mu_z(T)$. Chemical potentials measured at T_{exp} were now corrected to T_{nom} by using the first derivative of the quadratic regression:

$$\Delta\mu_z(T_{\text{nom}}) = \Delta\mu_z(\bar{T}_{\text{exp}}) + [d\Delta\mu_z(T)/dT]_{T=\bar{T}_{\text{exp}}}(T_{\text{nom}} - \bar{T}_{\text{exp}}) \quad (24)$$

where $T_{\text{nom}} - \bar{T}_{\text{exp}}$ never exceeded ± 0.3 K.

Retention indices at nominal temperatures were calculated by the analogous iterative procedure. All successive calculations are based on these standard chemical potential differences of the n -alkanes and retention indices corrected for the nominal temperature, and they will be referred to as “experimental retention data”.

Solution data of n -alkanes as a function of the factors T (temperature), L (composition of the liquid stationary phase) and Z (carbon number of the n -alkanes).

Pentane–decane. As a first step, the standard

chemical potential differences of the n -alkanes pentane–decane ($z = 5$ – 10) were determined on the four stationary phases: 0–6, 2–6, 4–6 and 6–6 (see Table III) at intervals of 20 K in the temperature range 90–210°C to give a set of $6 \cdot 4 \cdot 7 = 168$ data points. Analysis of variance of this data set, shown in Table III, refers to the description of the experimental domain by eqn. 25 where $P_X^{(i)}$ is an orthogonal polynomial of the degree i related to the effect $X = T, L$ and Z and $b_X^{(i)}$ is the corresponding regression coefficient.

Results of the analysis of variance show that all terms of eqn. 25 are significant with the exception of those underlined. Indeed, in the analysis of variance two additional terms are significant (which are omitted in eqn. 25) corresponding to a quadratic and cubic dependence of $\Delta\mu_z^{A/P}$ on the carbon number of the n -alkane, hence we conclude that the dependence of standard chemical potentials at T^\dagger on Z is not purely linear. It is important to note that the error in the TL subspace is higher than the residual variance (error introduced by adjusting a new temperature or by changing the column). Therefore, effects in this subspace were tested against the residual variance of this subspace: “1st res.” (*cf.*, the analogous variance analysis in ref. 10).

In order to identify the relationship between the individual terms in eqn. 25 and the thermodynamic functions, let us develop the function $\Delta\mu_z^{A/P}$ around

$$\begin{aligned} \Delta\mu_z^{A/P} = & b^{(0)} + b_Z^{(1)}P_Z^{(1)} + b_T^{(1)}P_T^{(1)} + b_{T,Z}^{(1,1)}P_T^{(1)}P_Z^{(1)} + b_T^{(2)}P_T^{(2)} + b_{T,Z}^{(2,1)}P_T^{(2)}P_Z^{(1)} + \\ & + b_L^{(1)}P_L^{(1)} + b_{L,Z}^{(1,1)}P_L^{(1)}P_Z^{(1)} + \\ & + b_{T,L}^{(1,1)}P_T^{(1)}P_L^{(1)} + b_{T,L,Z}^{(1,1,1)}P_T^{(1)}P_L^{(1)}P_Z^{(1)} + b_{T,L}^{(2,1)}P_T^{(2)}P_L^{(1)} + b_{T,L,Z}^{(2,1,1)}P_T^{(2)}P_L^{(1)}P_Z^{(1)} + \\ & + b_L^{(2)}P_L^{(2)} + b_{L,Z}^{(2,1)}P_L^{(2)}P_Z^{(1)} + \underline{b_{T,L}^{(1,2)}P_T^{(1)}P_L^{(2)}} + \underline{b_{T,L,Z}^{(1,2,1)}P_T^{(1)}P_L^{(2)}P_Z^{(1)}} \end{aligned} \quad (25)$$

$$Y_z = Y_0 + z\delta Y_z \quad (26)$$

$$\begin{aligned} \Delta\mu_z^{A/P} = & \Delta\mu_0^{\dagger A} + z\delta\mu_z^{\dagger A} - \Delta T\Delta S_0^A - \Delta Tz\delta S_z^A - \Delta T^2 \cdot \frac{\Delta C_{P,0}^A}{2T^\dagger} - \Delta T^2z \cdot \frac{\delta C_{P,z}^A}{2T^\dagger} + \\ & + \varphi_P(\Delta\mu_0^{\dagger A/P} + m_0^{\dagger A/P}) + \varphi_Pz(\delta\mu_z^{\dagger A/P} - \delta\mu_z^{\dagger A} + \delta m_z^{\dagger A/P}) - \\ & \Delta T\varphi_P\Delta S_0^P - \Delta T\varphi_Pz(\delta S_z^P - \delta S_z^A) - \Delta T^2\varphi_P \cdot \frac{\Delta C_{P,0}^P}{2T^\dagger} - \Delta T^2\varphi_Pz \cdot \frac{\delta C_{P,z}^P - \delta C_{P,z}^A}{2T^\dagger} - \\ & \underline{\varphi_P^2 m_0^{\dagger A/P} - \varphi_P^2 z\delta m_z^{\dagger A/P} + \Delta T\varphi_P^2 \delta_0^{\dagger A/P} + \Delta T\varphi_P^2 z\delta \delta_z^{\dagger A/P}} \end{aligned} \quad (27)$$

TABLE III

ANALYSIS OF VARIANCE OF THE SET OF 168 STANDARD CHEMICAL POTENTIALS OF THE *n*-ALKANE SOLUTES WITH $5 \leq Z \leq 10$ IN THE TEMPERATURE RANGE 90–210°C AT FOUR COMPOSITIONS OF L

The source of variance is related to the orthogonal terms in eqn. 25. $X^{(i)}$ is the systematic polynomial variation of $\Delta\mu$ on the effects T (temperature), L (composition of the liquid stationary phase; 100 ϕ_p = 0.0, 33.3, 66.7 and 100.0%) and Z (carbon number of the solute). The subscripts in parentheses refer to the degree of the orthogonal polynomial: (1) linear; (2) quadratic; (3) cubic. SQ is the sum of squares, Φ is the number of degrees of freedom and $V' = V(\text{res.}) + v_X V(X)$ is the combined variance to be analysed by Fisher's F . The coefficients $b_X^{(i)}$ in eqn. 25 are also listed. The abbreviation "res." is for residual variance and "id" means that $V' = SQ/\Phi$ is equal to the corresponding SQ ($\Phi = 1$).

Source		SQ	Φ	V'	F	Significance (%)	$b_X^{(i)}$
X	(<i>i</i>)						
$\Delta\bar{\mu}$	(0)						26.2
T	(1)	90 460 075.6	1	id	$9.44 \cdot 10^5$	0.01	366.89
	(2)	53 555.9	1	id	$5.59 \cdot 10^2$	0.01	-5.154
	(res. T^*)	190.4	4	47.6	0.49	—)	
L	(1)	222 105.1	1	id	$2.32 \cdot 10^2$	0.01	32.521
	(2)	1717.8	1	id	$1.79 \cdot 10^1$	0.1	3.198
	(res. L^*)	936.6	1	id	9.78	1.0)	
TL	(1, 1)	448.7	1	id	4.68	5	-0.731
	(1, 2)	426.9	1	id	4.46	5	-0.797
	(2, 1)	158.3	1	id	1.65	20	0.251
	(res. TL^*)	789.1	15	52.6	0.55	—)	
1st res. ^a	(= ΣX^*)	1916.1	20	95.8			
Z	(1)	120 930 857.4	1	id	$8.98 \cdot 10^6$	0.01	-496.8
	(2) ^c	20 883.4	1	id	$1.55 \cdot 10^3$	0.01	4.469
	(3) ^c	544.5	1	id	$4.04 \cdot 10^1$	0.01	-0.548
	(res. Z^{**})	10.1	2	5.1	0.38	—)	
TZ	(1, 1)	970 242.4	1	id	$7.20 \cdot 10^4$	0.01	22.249
	(2, 1)	4673.0	1	id	$3.47 \cdot 10^2$	0.01	-0.891
	(res. TZ^{**})	1002.8	28	35.8	2.66	10)	
LZ	(1, 1)	1051.1	1	id	$7.80 \cdot 10^1$	0.01	1.309
	(2, 1)	212.1	1	id	$1.57 \cdot 10^1$	0.1	-0.658
	(res. LZ^{**})	344.9	13	26.5	1.9	20)	
TLZ	(1, 1, 1)	10.7	1	id	0.79	—	0.066
	(2, 1, 1)	52.1	1	id	3.87	5	0.084
	(1, 2, 1)	5.3	1	id	0.39	—	-0.052
	(res. TLZ^{**})	392.9	87	4.5	0.33	—)	
2nd res. ^b	(= ΣX^{**})	1750.7	130	13.5			

^a Sum of the residuals marked by one asterisk.

^b Sum of the residuals marked by two asterisks.

^c Quadratic and cubic levels of the factor Z are not included in eqn. 25.

the standard temperature T^\dagger by introducing $\Delta T = T - T^\dagger$, by assuming that the functions $Y = H_z, S_z, \delta_z$ and σ_z depend linearly on the carbon number in the *n*-alkane following eqn. 26, and by approximating the logarithmic expression multiplying ΔC_p by the first term of its Taylor series.

The calculation gives (see ref. 10) eqn. 27, where $\Delta\mu^\dagger = \Delta H - T^\dagger \Delta S$ is the chemical potential at the standard temperature and similarly $m^{\dagger, A/P} = \delta -$

$T^\dagger \sigma$. The visual arrangement of eqns. 25 and 27 facilitates the cross-identification of related terms. As an example, in the fourth line/second term (term 4/2) the coefficient $b_{L,Z}^{(2,1)}$ is related to $\delta m_z^{\dagger, A/P}$. The coefficient $b_{L,Z}^{(2,1)}$ is significant, meaning that the curvature of the standard chemical potential with composition shows a significant linear change with the carbon number of the alkanes.

The three underlined terms (third line/second

$$\begin{aligned}
 \Delta\mu_z^{A/P} &= 3\,465.8 - 510.49z + 9.712\Delta T + 1.2379\Delta Tz + 0.0043\Delta T^2 - 0.00244\Delta T^2z + \\
 \pm\sigma &= \begin{array}{cccccc} 25.4 & 2.60 & 76 & 77 & 7 & 7 \end{array} \\
 &+ 69.8\varphi_P + 3.77\varphi_{Pz} - 0.349\Delta T\varphi_P + 0.0134\Delta T\varphi_{Pz} + 0.0004\Delta T^2\varphi_P + 0.00016\Delta T^2\varphi_{Pz} - \\
 &\begin{array}{cccc} 7 & 7 & 1 & 1 & 1 & 1 \end{array} \\
 &81.9\varphi_A\varphi_P + 6.16\varphi_A\varphi_{Pz} + 0.282\Delta T\varphi_A\varphi_P \\
 &\begin{array}{ccc} 1 & 1 & 24 \end{array}
 \end{aligned} \tag{28}$$

term: 3/2 and also 3/3 and 4/4) are not significant, meaning that the entropy of the “methylene increment”, δS_z , is the same in the liquids C78 and POH (3.2), the partial molar heat capacity of a hypothetical “nullane”, $\Delta C_{P,0}$, is the same in C78 and POH (3.3) and the entropic term of the non-ideality of the “methylene increment” in C78–POH mixtures is negligible.

Pentane–tetradecane. In a second step, solution data of the alkanes pentane–decane were completed on two additional stationary phase mixtures: 3–6 and 5–6 (see Table III) to give for every alkane a set of $6 \cdot 7 = 42$ data. In addition, data for higher n -alkanes, hendecane–tetradecane, were measured on all six stationary phases in the temperature range 150–210°C to give for each of these alkanes a set of $6 \cdot 4 = 24$ data. Based on the variance analysis in Table III, it was now assumed that ΔH_z^A , ΔS_z^A , $\Delta C_{P,z}^A$ and δ_z are linear functions of the carbon number, z , and that the coefficient σ is independent of z . Imposing these constraints in eqns. 5 and 6, the set of 252 (lower alkanes) + 96 (higher alkanes) = 348 data were evaluated by fitting eqn. 3 by multiple regression to all data. The resulting regression coefficients are listed in Table IV.

Data in the solvent, idPOH, were calculated as follows. Using the coefficients listed in Table IV together with the molar volume of POH calculated with eqn. 21 (coefficients listed in Table I), the slope $\Delta'\mu_z^{\text{idP}}$ was calculated for every 10-K interval in the temperature range for a given alkane by using eqn. 7. Fitting eqn. 9 to these points, the data listed in Table IV were obtained. (Note that the direct extrapolation of $\Delta'H$, $\Delta'S$ and $\Delta'C_P$ is not applicable because of the dependence of the molar volume, v_{POH} , on temperature; e.g., direct extrapolation for dodecane with v_{POH} at 130°C would give $\Delta'H = 97 \text{ cal l mol}^{-2}$, $\Delta'S = -0.131 \text{ cal l mol}^{-2} \text{ K}^{-1}$ and $\Delta'C_P = -2.5 \text{ cal l mol}^{-2} \text{ K}^{-1}$ instead of 48, -0.252 and -2.8 , respectively.)

Numerical value of the “methylene increment”, $\delta\mu_z^{A/P}$. Because of the significance of a quadratic and cubic dependence of the standard chemical potential of the alkanes at T^\dagger on the carbon number, a linear dependence of ΔH_z^A , ΔS_z^A and $\Delta C_{P,z}^A$ was not imposed in the evaluation of the data of pentane–tetradecane as was described in the preceding section. However, inspection of the value of these functions listed in Table IV shows that they can be represented with very good precision as linear functions of z . Consequently, data for n -alkanes can be given by eqn. 28. The partial derivative of eqn. 28 with respect of the variable z is the “methylene increment”. Its value at $\varphi_P = 0$ and $\varphi_P = 1$ is given in eqns. 29 and 30:

$$\begin{aligned}
 \delta\mu_z^A &= -510.5 + 1.2379\Delta T - 0.00244\Delta T^2 \\
 \pm\sigma &= \begin{array}{ccc} 2.6 & 77 & 7 \end{array}
 \end{aligned} \tag{29}$$

$$\begin{aligned}
 \delta\mu_z^P &= -506.7 + 1.2513\Delta T - 0.00228\Delta T^2 \\
 \pm\sigma &= \begin{array}{ccc} 2.6 & 77 & 7 \end{array}
 \end{aligned} \tag{30}$$

Similarly, data for n -alkanes can be given by eqn. 31 on the ideal stationary phase, idPOH, at $[\text{OH}] = 1 \text{ mol l}^{-1}$ as

$$\begin{aligned}
 \Delta'\mu_z^{\text{idP}} &= 3\,448.9 + 9.602\Delta T + 0.0047\Delta T^2 - \\
 \pm\sigma &= \begin{array}{ccc} 25.8 & 77 & 8 \end{array} \\
 &496.57z + 1.2680\Delta Tz - 0.00217\Delta T^2z \\
 &\begin{array}{ccc} 2.59 & 78 & 8 \end{array}
 \end{aligned} \tag{31}$$

The first derivative of eqn. 31 with respect of z gives the corresponding methylene increment as

$$\begin{aligned}
 \delta'\mu_z^{\text{idP}} &= -496.6 + 1.2680\Delta T - 0.00217\Delta T^2 \\
 \pm\sigma &= \begin{array}{ccc} 2.6 & 78 & 8 \end{array}
 \end{aligned} \tag{32}$$

Solution data of solutes other than n -alkanes

Retention indices. These were determined at temperature intervals of 20 K on the four stationary phases: 0–6, 2–6, 4–6 and 6–6 (see Table III) in the temperature range indicated in Table IV to give in

general a set of 20 data. On this data set eqn. 15 was fitted with coefficients given in eqns. 16–18. In all instances the quadratic coefficients A_{TT} and $\mathcal{A}A_{TT}$ were non-significant even at the 20% significance level, with the exception of alcohols. In Table IV the six regression coefficients are listed for all substances even if they are not significant, whereas for alcohols all eight coefficients are given even if they are not significant (for the significance of the coefficients, see Results and Discussion).

Use of the resulting regression coefficients in eqn. 15, eqn. 21 for the calculation of the molar volume, and further eqns. 29 and 32 for the calculation of κ , retention indices were calculated at every 10-K interval for a solute in a solvent idPOH having a 1 molar concentration of interacting groups, X. The results are given in Table IV.

Thermodynamic data. For a given solute the experimental retention index data were converted one by one into standard chemical potentials by using eqn. 10 and the individual thermodynamic data for *n*-alkanes listed in Table IV. With the resulting data set, the coefficients in eqns. 3–6 were determined by multiple regression and are listed in Table IV.

Finally, a data set of retention indices was generated for 1 M idPOH solvent with the aid of coefficients listed in Table IV at every 10-K interval. These retention index data were converted into standard potentials and the coefficients $\Delta'H_j^{\text{idP}}$, $\Delta'S_j^{\text{idP}}$ and $\Delta'C_{p,j}^{\text{idP}}$ were determined by regression. The resulting coefficients with reference to the non-polar standard, $\mathcal{A}'H_j^{\text{idP}}$, $\mathcal{A}'S_j^{\text{idP}}$ and $\mathcal{A}'C_{p,j}^{\text{idP}}$, are listed in Table IV.

Conversion of thermodynamic data into reference states related to those of the distribution coefficient, K_D

Using the relationship given in eqn. A6 in the Appendix, a data set, $\Delta\mu^{\text{A/P}} - \Delta\mu^{(\text{D})\text{A/P}}$, was generated at 10-K intervals in the temperature range 90–210°C for the four mixtures $\varphi_{\text{POH}} = 0.000, 0.333, 0.667$ and 1.000. Molar volumes of the mixtures were calculated by assuming that C78 and POH form ideal mixtures and consequently

$$v_{\text{C78/POH}} = \varphi_{\text{C78}}v_{\text{C78}} + \varphi_{\text{POH}}v_{\text{POH}} \quad (33)$$

Fitting eqns. 3–6 to the resulting set of data, the necessary corrections were obtained for this conver-

sion, and they are listed in the next to the last line in Table IV.

In the last line in Table IV the necessary information is given to convert coefficients referring to pressures measured in atmospheres to those expressed in bars.

RESULTS AND DISCUSSION

Data listed in Table IV

Thermodynamic data for 156 solutes were measured on mixtures of two stationary phases, the paraffin C78 and its derivative POH. In the latter compound one of the methyl groups in C78 was substituted for a hydroxyl, resulting in a slightly polar stationary liquid with one primary alcohol as interacting group out of 78 heavy atoms. The alcohol concentration in the melt of pure POH is about 0.7 mol l⁻¹ at the temperatures of measurement (90–210°C). Interaction enthalpies between primary alcohols are known to be of the order of 5 kcal mol⁻¹. Therefore, even at the high temperatures of the gas chromatographic measurements there will be a considerable proportion of dimers in the melt of pure POH. Actually, at 130°C, as an example, about 24% of dimers were expected. In order to measure interaction free energies between monomers and solutes, we proposed to measure data at different alcohol concentrations in the stationary phase and to determine interaction energies by extrapolation to zero hydroxyl concentration.

The necessary precautions for the determination of molal Henry coefficients free of interfacial adsorption at the gas–liquid and liquid–support interfaces were discussed in ref. 14. In summary, in order to minimize retention by adsorption, a commercial support having a low specific surface area of about 0.56 m² g⁻¹ was chosen for the preparation of column packings. Also, the support was further deactivated by treatment with trimethyl(dimethylamino)silane but only to an extent such that the silylated support remained wettable by the non-polar C78. In fact, non-wettable supports result in a mixed retention mechanism and unusable data. In preliminary experiments the effect of adsorption on retention was evaluated by the method of Martin [15] by using packing materials with different C78 loadings and *n*-alkanes, primary alcohols, 1-nitroalkanes and 1-cyanoalkanes as test compounds. It

TABLE IV

RETENTION INDICES AND THERMODYNAMIC DATA OF 156 SOLUTES IN THE STATIONARY PHASES C78, POH AND idPOH AND THEIR MIXTURES; SOLUTES AT IDEAL DILUTION

Retention indices: I_{130} is the retention index at the reference temperature, $T^\dagger = 130 + 273.15$ K; for the meaning of the coefficients A , see eqns. 15-18. The constants in POH and a 1 M idPOH are given with reference to C78. *Thermodynamic functions:* ΔH and ΔS (ΔH and ΔS) are partial molar enthalpy and entropy differences at T^\dagger , ΔC_p (ΔC_p) is the mean partial molar heat capacity in the temperature range indicated. Reference states: Δ = ideal gas; Δ = ideal dilute solution in C78. Values designated by a prime are derivatives with respect of $[POH] = [OH]$ mol l⁻¹. At the end of the table additive corrections are listed *to convert data:* (A) to those related to the partition coefficients K_D (see eqn. A6) and (B) to those where pressures are measured in units of bar (instead of atm). Data for *n*-alkanes marked with a superscript, e, are extrapolated values. *Errors:* σ is the standard deviation around the regression. At the end of the table are listed standard deviations of coefficients and functions in units of the standard deviation around the regression $f(\text{coeff}) = \sigma(\text{coeff})/\sigma$. Data marked by superscript, s, are significant at the 10% significance level if tested against σ but considered to be significant on the basis of arguments in the Discussion. Data marked by one asterisk are at the 20% significance level those marked by double asterisks are under this limit.

No.	Compound	Temp. range	Retention index											
			C78			POH - C78			Mixture		id POH ([OH]=1) - C78			σ
			I_{130}	$10 \times A_T$	$100 \times A_{TT}$	ΔI_{130}	$10 \times \Delta A_T$	$100 \times \Delta A_{TT}$	A_L	$10 \times A_{LT}$	ΔI	$10 \times \Delta A_T$	$100 \times \Delta A_{TT}$	
(°C)	(K ⁻¹)	(K ⁻²)	(K ⁻¹)	(K ⁻²)	(K ⁻¹)	(K ⁻²)	(K ⁻¹)	(K ⁻¹)	(l mol ⁻¹)	(K ⁻¹)	(K ⁻²)	(K ⁻¹)		
HYDROCARBONS														
<i>n</i> -Alkanes														
00.05	Pentane	70	90-210	500	def.									
00.06	Hexane	70	90-210	600	def.									
00.07	Heptane	70	90-210	700	def.									
00.08	Octane	70	90-210	800	def.									
00.09	Nonane	70	90-210	900	def.									
00.10	Decane	70	90-210	1 000	def.									
00.11	Undecane	40	150-210	1 100	def.									
00.12	Dodecane	40	150-210	1 200	def.									
00.13	Tridecane	40	150-210	1 300	def.									
00.14	Tetradecane	40	150-210	1 400	def.									
<i>Isoalkanes</i>														
10.01	2,2-Dimethylbutane	20	90-170	540.9	+0.91	—**	0.3*	+0.23*	—**	- 1.7*	-0.12*	- 2.9 + 0.13	—**	0.52
10.02	2,3-Dimethylbutane	20	90-170	573.1	+0.92	—**	0.6*	+0.25*	—**	- 0.6*	-0.69 ^s	- 0.3 - 0.64	—**	0.46
10.03	2,2-Dimethylpentane	20	90-170	627.9	+0.87	—**	- 0.1*	+0.03*	—**	- 0.7*	-0.23*	- 2.1 - 0.29	—**	0.43
10.04	2,3-Dimethylpentane	20	90-170	679.4	+0.97	—**	0.5*	+0.14*	—**	- 0.4*	-0.05*	- 0.3 + 0.13	—**	0.33
10.05	2,4-Dimethylpentane	20	90-170	629.3	+0.53	—**	- 0.5*	-0.01*	—**	- 0.1*	-0.24*	- 1.1 - 0.37	—**	0.26
10.06	2,3-Dimethylhexane	20	90-170	765.6	+0.87	—**	0.3*	+0.04*	—**	- 0.5*	+0.16*	- 0.5 + 0.27	—**	0.24
10.07	2,4-Dimethylhexane	20	90-170	732.9	+0.52	—**	- 0.2*	+0.19 ^s	—**	+ 0.9	+0.30	+ 1.1 + 0.69	—**	0.17
10.08	3,4-Dimethylhexane	20	90-170	780.1	+1.04	—**	0.6*	+0.12*	—**	- 0.1*	+0.28*	+ 0.5 + 0.57	—**	0.29
10.09	2,2,3-Trimethylbutane	20	90-170	649.7	+1.22	—**	2.0*	+0.33 ^s	—**	+ 1.9	+0.05*	+ 6.1 + 0.6	—**	0.27
10.10	2,2,4-Trimethylpentane	20	90-170	694.1	+0.94	—**	0.2*	+0.13*	—**	+ 0.7*	+0.42*	+ 1.2 + 0.79	—**	0.36
10.11	2,3,4-Trimethylpentane	20	90-170	764.2	+1.29	—**	1.3*	+0.31*	—**	+ 1.7 ^s	+0.38*	+ 3.9 + 1.03	—**	0.42

No	Thermodynamic data											
	C78			POH - C78			Mixture		id POH([OH]=1) - C78			
	ΔH (cal mol ⁻¹)	ΔS (cal mol ⁻¹ K ⁻¹)	ΔC_p	ΔH (cal mol ⁻¹)	ΔS (cal mol ⁻¹ K ⁻¹)	ΔC_p	\bar{H} (cal mol ⁻¹)	σ (cal mol ⁻¹ K ⁻¹)	ΔH (cal mol ⁻²)	ΔS (cal mol ⁻² K ⁻¹)	ΔC_p	σ (cal mol ⁻¹)
HYDROCARBONS												
<i>n</i> -Alkanes												
00.05	- 5 507	-16.043	6.2	+ 203	+0.283	- 0.9	- 165	-0.282	+ 35	-0.043	- 1.3	4.7
00.06	- 6 505	-17.131	7.8	+ 202	+0.270	- 1.1	- 159	-0.282	+ 39	-0.070	- 1.7	4.7
00.07	- 7 517	-18.341	10.7	+ 200	+0.256	- 1.2	- 152	-0.282	+ 41	-0.102	- 1.8	4.2
00.08	- 8 517	-19.540	12.3	+ 197	+0.243	- 1.3	- 146	-0.282	+ 42	-0.129	- 2.0	3.9
00.09	- 9 531	-20.792	14.4	+ 196	+0.230	- 1.5	- 140	-0.282	+ 44	-0.158	- 2.3	4.4
00.10	-10 539	-22.035	15.8	+ 194	+0.216	- 1.6	- 134	-0.282	+ 45	-0.190	- 2.5	4.5
00.11	-11 561	-23.322	19.1	+ 193 ^e	+0.203 ^e	- 1.7 ^e	- 128 ^e	-0.282 ^e	+ 47	-0.221	- 2.6	4.7
00.12	-12 569	-24.581	20.5	+ 191 ^e	+0.189 ^e	- 1.8 ^e	- 122 ^e	-0.282 ^e	+ 48	-0.252	- 2.8	6.8
00.13	-13 576	-25.840	21.9	+ 190 ^e	+0.176 ^e	- 2.0 ^e	- 116 ^e	-0.282 ^e	+ 50	-0.281	- 3.1	6.7
00.14	-14 583	-27.099	23.3	+ 189 ^e	+0.163 ^e	- 2.1 ^e	- 109 ^e	-0.282 ^e	+ 54	-0.313	- 3.3	6.6
<i>Isoalkanes</i>												
10.01	- 5 709	-15.977	6.0	+ 255	+0.403	+ 3.5	- 177	-0.341	+ 90	+0.036	- 1.5	1.9
10.02	- 6 029	-16.322	6.4	+ 254	+0.407	+ 0.8**	- 318	-0.681	- 106	-0.422	- 1.1	2.7
10.03	- 6 603	-17.009	7.0	+ 211	+0.280	+ 3.4	- 201	-0.399	- 5	-0.217	- 0.9	1.8
10.04	- 7 102	-17.578	8.9	+ 224	+0.321	+ 1.2**	- 166	-0.319	+ 64	-0.042	- 1.6	1.7
10.05	- 6 689	-17.208	8.7	+ 203	+0.263	+ 0.7**	- 207	-0.407	- 29	-0.262	- 2.1	0.9
10.06	- 7 991	-18.678	11.2	+ 203	+0.262	+ 1.2 ^s	- 114	-0.203	+ 97	+0.014	- 2.4	0.8
10.07	- 7 738	-18.467	10.7	+ 234	+0.337	- 0.1**	- 96	-0.136 ^s	+ 169	+0.219	- 2.3	1.0
10.08	- 8 100	-18.761	10.3	+ 215	+0.296	+ 1.2**	- 91	-0.144**	+ 147	+0.143	- 1.7	1.5
10.09	- 6 750	-17.092	8.0	+ 247	+0.407	- 1.7 ^s	- 167	-0.285	+ 96	+0.128	- 1.9	1.1
10.10	- 7 256	-17.772	9.7	+ 223	+0.317	+ 0.5**	- 73*	-0.077**	+ 185	+0.273	- 2.4	1.9
10.11	- 7 889	-18.441	9.6	+ 250	+0.389	+ 1.5**	- 96*	-0.132**	+ 206	+0.338	- 1.7	2.2

(Continued on p. 240)

No	Thermodynamic data											
	C78			POH - C78			Mixture		id POH([OH]=1) - C78			
	ΔH (cal mol ⁻¹)	ΔS (cal mol ⁻¹ K ⁻¹)	ΔC_P	ΔH (cal mol ⁻¹)	ΔS (cal mol ⁻¹ K ⁻¹)	ΔC_P	Δ	σ (cal mol ⁻¹ K ⁻¹)	ΔH (cal mol ⁻²)	ΔS (cal mol ⁻² K ⁻¹)	ΔC_P	σ (cal mol ⁻¹)
<i>I-Alkenes</i>												
11.06	- 6 249	-16.679	8.3	+ 133	+0.145**	- 2.5**	- 300*	-0.666*	- 258	-0.790	- 2.2	5.8
11.07	- 7 276	-17.932	12.2	+ 140	+0.159	- 3.0 ^s	- 246	-0.509	- 163	-0.521	- 3.5	2.2
11.08	- 8 278	-19.138	12.5	+ 152	+0.180	- 1.1**	- 181	-0.363	- 58	-0.301	- 2.6	2.1
11.09	- 9 299	-20.404	14.0	+ 161	+0.195	- 1.0**	- 132	-0.246*	+ 16	-0.134	- 2.6	2.0
11.10	-10 314	-21.663	15.0	+ 155	+0.162	+ 0.6**	- 74**	-0.119**	+ 82	-0.015	- 2.6	2.2
<i>I-Alkynes</i>												
12.05	- 5 392	-15.969	7.1	+ 98	+0.217	- 1.1**	- 334	-0.629 ^s	- 296	-0.486	- 1.7	4.5
12.06	- 6 363	-16.945	8.6	+ 97	+0.208	- 3.1**	- 359	-0.717	- 343	-0.664	- 1.8	4.0
12.07	- 7 384	-18.168	11.9	+ 98	+0.204	- 3.7**	- 194*	-0.325**	- 115	-0.122	- 3.2	4.0
12.08	- 8 368	-19.325	12.9	+ 87	+0.166	- 2.8*	- 236	-0.441	- 195	-0.354	- 2.6	2.5
12.09	- 9 371	-20.544	15.3	+ 73	+0.119	- 2.1*	- 253	-0.493	- 239	-0.489	- 3.2	1.9
12.10	-10 389	-21.811	17.0	+ 85	+0.137	- 1.8**	- 237	-0.463	- 205	-0.435	- 3.4	2.2
<i>Alkynes</i>												
13.01	- 6 979	-17.758	9.3	+ 91	+0.180	- 3.7	- 335	-0.701	- 335	-0.714	- 0.7	2.2
13.02	- 6 838	-17.675	8.8	+ 49*	+0.052**	+ 0.4**	- 177 ^s	-0.360*	- 184	-0.444	- 0.9	2.3
13.03	- 8 667	-19.779	13.0	+ 42	+0.001**	+ 0.6**	- 253	-0.526	- 299	-0.745	- 1.4	1.9
<i>Monocyclic hydrocarbons</i>												
14.05	- 5 856	-15.694	6.3	+ 118	+0.096**	- 1.3**	- 389	-0.852	- 419	-1.157	- 1.5	4.7
14.06	- 6 791	-16.639	9.4	+ 179	+0.246	- 2.1**	- 79**	-0.088**	+ 103	+0.133	- 4.3	3.6
14.07	- 8 028	-17.876	10.6	+ 173	+0.234	- 0.6**	- 110*	-0.169**	+ 64	+0.029	- 4.2	2.4
14.08	- 9 168	-19.086	10.2	+ 155	+0.186*	+ 0.9**	+ 178**	+0.507**	+ 424	+0.871	- 3.9	5.7
14.10	-11 061	-21.115	16.3	+ 252*	+0.416*	- 2.9**	- 395	-0.932	+ 368	+0.701	- 7.2	4.6
<i>Bicyclic hydrocarbons</i>												
15.01	- 9 787	-19.749	14.7	+ 155*	+0.184**	+ 0.9**	+ 1**	+0.093**	+ 431	+0.908	- 7.7	3.2
15.02	- 9 554	-19.587	14.1	+ 185*	+0.245**	+ 3.1**	- 184*	-0.375*	+ 88	+0.013	- 6.3	3.5
15.03	-10 652	-20.434	13.0	+ 141*	+0.152**	+ 1.3**	- 404	-0.878	+ 26	-0.039	- 3.7	5.1
15.04	-10 399	-20.311	14.4	+ 212	+0.316*	- 1.1**	- 133*	-0.251**	+ 126	+0.124	- 5.2	2.8
<i>Methylcyclohexanes (MCH)</i>												
16.01	- 7 409	-17.342	9.1	+ 167	+0.201	+ 3.2	- 73*	-0.118**	+ 114	+0.073	- 2.9	1.6
16.02	- 8 396	-18.392	7.9	+ 167	+0.199	+ 4.4	- 27**	+0.015**	+ 186	+0.274	- 1.1	2.3
16.03	- 8 166	-18.202	7.8	+ 183	+0.235	+ 4.1	- 5**	+0.074**	+ 238	+0.400	- 1.3	2.4

(Continued on p. 242)

No.	Compound	Temp. range	Retention index												
			C78			POH - C78			Mixture		id POH ([OH]=1) - C78				
			<i>n</i>	<i>I</i> ₁₃₀	$\frac{10 \times}{A_T}$ (<i>K</i> ⁻¹)	$\frac{100 \times}{A_{TT}}$ (<i>K</i> ⁻²)	ΔI ₁₃₀	$\frac{10 \times}{\Delta A_T}$ (<i>K</i> ⁻¹)	$\frac{100 \times}{\Delta A_{TT}}$ (<i>K</i> ⁻²)	<i>A</i> _L	$\frac{10 \times}{A_{LT}}$ (<i>K</i> ⁻¹)	$\frac{\Delta I}{(I)}$ (<i>K</i> ⁻¹)	$\frac{10 \times}{\Delta A_T}$ (<i>K</i> ⁻¹)	$\frac{100 \times}{\Delta A_{TT}}$ (<i>K</i> ⁻²)	σ
16.04	<i>cis</i> -1,4-Di MCH	20	90-170	837.4	+3.37	—**	2.9	+0.07*	—**	+ 1.4*	+0.21*	+ 5.8	+ 0.46	—**	0.65
16.05	<i>trans</i> -1,4-Di MCH	20	90-170	816.0	+3.16	—**	2.5	+0.06*	—**	+ 1.8*	+0.23*	+ 5.7	+ 0.47	—**	0.60
<i>Cyclohexenes</i>															
17.01	Cyclohexene	20	90-170	704.4	+3.04	—**	7.1	+0.14*	—**	- 3.8	+0.75*	+ 4.2	+ 1.32	—**	0.66
17.02	1,3-Cyclohexadiene	20	90-170	688.6	+2.94	—**	11.6	+0.39*	—**	+ 2.7*	+0.78*	+ 19.8	+ 1.86	—**	0.62
17.03	1,4-Cyclohexadiene	20	90-170	724.9	+2.95	—**	11.4	+0.12*	—**	+ 1.0*	+0.12*	+ 17.5	+ 0.51	—**	0.57
<i>Alkylbenzenes</i>															
18.00	Benzene	20	90-170	675.0	+2.57	—**	17.0	+0.78*	—**	+ 5.1	+0.91*	+ 30.9	+ 2.72	—**	0.90
18.01	Toluene	20	90-170	784.0	+2.69	—**	16.9	+0.66*	—**	+ 4.5	+0.78*	+ 30.5	+ 2.35	—**	0.71
18.02	Ethylbenzene	20	90-170	874.0	+3.03	—**	16.4	+0.56*	—**	+ 4.6	+0.70*	+ 30.2	+ 2.08	—**	0.56
<i>Miscellaneous</i>															
19.01	Adamantane	16	130-210	135.3	+7.98	—**	11.0	-0.44*	—**	- 6.8	+2.39	+ 6.1	+ 2.86	—**	0.98
19.02	Naphthalene	16	130-210	213.7	+7.89	—**	34.0	-0.95*	—**	- 5.1	+2.68	+ 41.9	+ 2.87	—**	1.12
19.03	Azulene	16	130-210	329.7	+8.69	—**	35.7	-0.18*	—**	+21.1	-0.80*	+ 81.9	- 0.67	—**	1.66
ALKANE DERIVATIVES															
<i>1-Fluoroalkanes</i>															
20.05	1-Fluoropentane	20	90-170	557.1	+0.11*	—**	12.9	+0.15*	—**	+ 4.0*	-2.12	+ 26.1	- 2.61	—**	1.09
20.06	1-Fluorohexane	20	90-170	658.0	+0.08*	—**	13.0	+0.10*	—**	+ 3.7*	-2.06	+ 25.5	- 2.60	—**	1.03
20.08	1-Fluorooctane	20	90-170	859.6	+0.06*	—**	13.1	+0.17*	—**	+ 5.2	-0.96	+ 27.0	- 0.89	—**	0.59
<i>1,1,1-Trifluoroalkanes</i>															
21.08	1,1,1-Trifluorooctane	20	90-170	720.0	-2.26	—**	10.9	-0.41*	—**	+ 8.0	+0.01*	+ 29.9	- 0.29	—**	1.30
21.10	1,1,1-Trifluorodecane	20	90-170	918.5	-2.25	—**	11.3	-0.22*	—**	+ 8.6	+0.32*	+ 31.2	+ 0.41	—**	1.34
<i>1-Chloroalkanes</i>															
22.04	1-Chlorobutane	20	90-170	639.5	+1.69	—**	15.0	+0.21*	—**	+ 2.3	-0.88	+ 24.4	- 0.73	—**	0.47
22.05	1-Chloropentane	20	90-170	741.7	+1.41	—**	16.0	+0.61*	—**	+ 4.6	+0.36*	+ 29.7	+ 1.67	—**	0.30
22.06	1-Chlorohexane	20	90-170	842.9	+1.65	—**	16.4	+0.55*	—**	+ 5.8	-0.07*	+ 32.3	+ 0.99	—**	0.48
<i>1-Bromoalkanes</i>															
23.03	1-Bromopropane	20	90-170	627.1	+2.26	—**	17.2	+0.66*	—**	+ 4.9	-0.66*	+ 32.7	+ 0.29	—**	0.77
23.04	1-Bromobutane	20	90-170	730.4	+2.51	—**	17.5	+0.56*	—**	+ 6.5	-0.35*	+ 36.3	+ 0.63	—**	0.77

No	Thermodynamic data											
	C78			POH - C78			Mixture		id POH([OH]=1) - C78			
	ΔH (cal mol ⁻¹)	ΔS (cal mol ⁻¹ K ⁻¹)	ΔC_p	ΔH (cal mol ⁻¹)	ΔS (cal mol ⁻¹ K ⁻¹)	ΔC_p	Δ	σ (cal mol ⁻¹ K ⁻¹)	ΔH (cal mol ⁻²)	ΔS (cal l mol ⁻² K ⁻¹)	ΔC_p	σ (cal mol ⁻¹)
16.04	- 8 201	-18.281	9.2	+ 176	+0.220	+ 1.3**	- 124**	-0.214**	+ 55	-0.038	- 1.9	3.5
16.05	- 8 027	-18.123	10.0	+ 181	+0.230	+ 1.5**	- 126*	-0.213**	+ 60	-0.018	- 2.9	2.9
<i>Cyclohexenes</i>												
17.01	- 6 923	-16.812	7.7	+ 155	+0.228	+ 2.5**	+ 39**	+0.141**	+ 254	+0.477	- 2.7	3.3
17.02	- 6 776	-16.650	6.9	+ 158	+0.294	+ 2.6**	- 26**	+0.066**	+ 198	+0.539	- 2.1	2.9
17.03	- 7 150	-17.113	8.3	+ 108	+0.169	+ 1.5**	- 145*	-0.256**	- 44	-0.101	- 1.9	3.0
<i>Alkylbenzenes</i>												
18.00	- 6 717	-16.685	8.2	+ 190	+0.443	+ 3.8*	- 18**	+0.119**	+ 268	+0.860	- 3.7	3.5
18.01	- 7 793	-17.954	10.9	+ 157	+0.355	+ 1.0**	- 34**	+0.055**	+ 182	+0.605	- 4.8	2.7
18.02	- 8 641	-18.918	11.9	+ 137	+0.291	+ 0.7**	- 56**	-0.012**	+ 134	+0.445	- 4.4	2.4
<i>Miscellaneous</i>												
19.01	-10 541	-20.340	17.9	+ 189 ^s	+0.313 ^s	- 4.8*	+ 297	+0.690	+ 741	+1.548	-11.2	2.9
19.02	-11 305	-21.266	17.9	- 174**	-0.312**	- 3.3**	+ 332	+0.788	+ 334	+0.946	- 9.6	4.4
19.03	-12 443	-22.642	21.9	+ 207**	+0.633*	-14.4	- 496	-0.967	- 641	-1.045	-10.2	5.4
ALKANE DERIVATIVES												
<i>1-Fluoroalkanes</i>												
20.05	- 6 050	-16.603	9.5	+ 98 ^s	+0.214 ^s	- 7.6 ^s	- 671	-1.485	- 799	-1.773	- 2.3	5.4
20.06	- 7 073	-17.791	11.2	+ 84 ^s	+0.155*	- 5.4*	- 622	-1.387	- 758	-1.738	- 1.1	4.9
20.08	- 9 108	-20.255	14.3	+ 94	+0.151	- 2.2**	- 395	-0.839	- 411	-0.938	- 1.8	3.2
<i>1,1,1-Trifluoroalkanes</i>												
21.08	- 8 184	-19.747	16.3	- 1**	-0.082**	- 8.7 ^s	- 237*	-0.393**	- 311	-0.598	- 4.2	5.7
21.10	-10 174	-22.163	20.2	+ 34**	-0.013**	- 7.4*	- 172**	-0.256**	- 178	-0.326	- 5.4	6.2
<i>1-Chloroalkanes</i>												
22.04	- 6 543	-16.714	7.9	+ 93	+0.186	+ 1.5**	- 367	-0.772	- 371	-0.788	- 1.3	2.1
22.05	- 7 639	-18.109	10.2	+ 164	+0.367	+ 0.4**	- 124	-0.159*	- 79	+0.350	- 2.7	1.5
22.06	- 8 611	-19.234	12.1	+ 137	+0.297	- 0.7**	- 220	-0.397 ^s	- 96	-0.087	- 2.7	2.6
<i>1-Bromoalkanes</i>												
23.03	- 6 299	-16.268	6.3	+ 160	+0.393	- 2.8**	- 356	-0.709	- 244	-0.370	- 0.9	3.8
23.04	- 7 294	-17.406	11.3	+ 133	+0.325	- 5.8*	- 291	-0.547 ^s	- 207	-0.264	- 4.2	3.6

(Continued on p. 244)

TABLE IV (continued)

No.	Compound	Temp. range	Retention index											
			C78			POH - C78			Mixture		id POH ([OH]=1) - C78			σ
			n	I_{130}	$\frac{10 \times}{A_T}$ (K^{-1})	$\frac{100 \times}{A_{TT}}$ (K^{-2})	ΔI_{130}	$\frac{10 \times}{\Delta A_T}$ (K^{-1})	$\frac{100 \times}{\Delta A_{TT}}$ (K^{-2})	A_L	$\frac{10 \times}{A_{LT}}$ (K^{-1})	ΔI	$\frac{10 \times}{\Delta A_T}$ (K^{-1})	
(°C)										(l mol ⁻¹)	(K^{-1} mol ⁻¹)	(K^{-2} mol ⁻¹)		
23.05	1-Bromopentane	20 90-170	832.7	+2.59	—**	17.7	+0.63*	—**	+ 8.0	+0.24*	+ 38.8	+ 1.60	—**	0.84
<i>1-Cyanoalkanes</i>														
24.02	Cyanoethane	20 90-170	489.2	+0.69	—**	57.2	-0.47*	—**	+19.7	-3.11	+112.3	- 4.15	—**	1.41
24.03	1-Cyanopropane	20 90-170	587.9	+1.17	—**	55.9	-0.59*	—**	+15.2	-2.23	+104.2	- 3.11	—**	1.01
24.04	1-Cyanobutane	20 90-170	693.6	+1.30	—**	56.9	-0.37*	—**	+16.2	-1.32*	+107.1	- 1.44	—**	1.05
24.05	1-Cyanopentane	20 90-170	795.5	+1.38	—**	57.8	-0.24*	—**	+17.1	-0.99*	+109.2	- 0.78	—**	1.06
<i>1-Nitroalkanes</i>														
25.02	Nitroethane	20 90-170	567.8	+1.43	—**	47.3	+0.05*	—**	+13.2	-2.21	+ 88.7	- 2.30	—**	1.15
25.03	1-Nitropropane	20 90-170	661.9	+1.75	—**	45.6	+0.20*	—**	+13.4	-1.64 ^s	+ 86.9	- 1.29	—**	1.09
25.04	1-Nitrobutane	20 90-170	765.2	+2.01	—**	45.1	+0.31*	—**	+13.5	-1.74	+ 86.0	- 1.28	—**	1.07
25.05	1-Nitropentane	20 90-170	867.0	+2.14	—**	45.6	+0.37*	—**	+14.6	-1.46 ^s	+ 89.0	- 0.76	—**	1.12
<i>1-Acetoxyalkanes</i>														
26.03	1-Acetoxypropane	20 90-170	637.8	-0.58	—**	41.9	-0.63*	—**	+11.3	-1.25*	+ 76.9	- 2.01	—**	1.16
26.04	1-Acetoxybutane	20 90-170	739.5	-0.53	—**	42.9	-0.64*	—**	+12.2	-1.28*	+ 79.9	- 2.04	—**	1.05
26.05	1-Acetoxy-pentane	20 90-170	840.1	-0.41	—**	43.1	-0.73*	—**	+13.2	-1.22*	+ 82.2	- 2.07	—**	1.13
<i>1-Alkanols</i>														
27.04	1-Butanol	20 90-170	594.8	+0.87	+0.06*	66.3	-6.54	+0.56	+ 2.4	+0.06*	+ 99.2	- 8.37	+0.72	1.02
27.05	1-Pentanol	20 90-170	698.8	+0.89	+0.08*	67.9	-6.42	+0.57	+ 3.1	+0.47*	+102.5	- 7.57	+0.75	0.91
27.06	1-Hexanol	20 90-170	800.9	+1.11	+0.08*	68.6	-6.61	+0.60	+ 3.8	+0.18*	+104.6	- 8.24	+0.79	0.97
27.07	1-Heptanol	20 90-170	902.2	+1.19	+0.10 ^s	69.9	-6.68	+0.58	+ 4.0	+0.45*	+106.6	- 7.93	+0.77	1.02
<i>2-Alkanols</i>														
28.04	2-Butanol	20 90-170	545.4	+0.52	+0.07*	58.9	-5.05	+0.45	+ 3.6	-0.72*	+ 90.2	- 7.44	+0.59	1.25
28.05	2-Pentanol	20 90-170	643.8	+0.43	+0.07*	60.3	-4.82	+0.49	+ 5.9	-0.10*	+ 95.4	- 6.14	+0.66	1.03
28.06	2-Hexanol	20 90-170	744.7	+0.60	+0.04*	60.8	-4.85	+0.55	+ 5.3	-0.55*	+ 95.5	- 6.82	+0.74	0.99
28.07	2-Heptanol	20 90-170	845.0	+0.71	+0.05*	61.6	-4.94	+0.55	+ 5.6	-0.84*	+ 96.9	- 7.37	+0.73	1.19
<i>2-Methyl-2-alkanols</i>														
29.04	2-Methyl-2-propanol	20 90-170	471.0	+0.64	+0.20*	59.6	-5.85	+0.26	- 3.9	-1.54*	+ 80.4	- 9.91	+0.29	2.64
29.05	2-Methyl-2-butanol	20 90-170	597.9	+1.20	+0.15*	55.8	-5.02	+0.31	+ 1.0	-1.25*	+ 81.9	- 8.26	+0.38	1.50
29.06	2-Methyl-2-pentanol	20 90-170	690.9	+1.03	+0.12*	55.2	-4.82	+0.41	+ 2.2	-0.87*	+ 82.9	- 7.38	+0.53	1.16
29.07	2-Methyl-2-hexanol	20 90-170	786.1	+1.07	+0.13*	56.1	-4.80	+0.43	+ 3.1	-0.91*	+ 85.4	- 7.41	+0.56	1.02

TABLE IV (continued)

No	Thermodynamic data											
	C78			POH - C78			Mixture		id POH([OH]=1) - C78			
	ΔH (cal mol ⁻¹)	ΔS (cal mol ⁻¹ K ⁻¹)	ΔC_p (cal mol ⁻¹ K ⁻¹)	ΔH (cal mol ⁻¹)	ΔS (cal mol ⁻¹ K ⁻¹)	ΔC_p (cal mol ⁻¹ K ⁻¹)	\bar{H} (cal mol ⁻¹)	σ (cal mol ⁻¹ K ⁻¹)	ΔH (cal mol ⁻²)	ΔS (cal mol ⁻² K ⁻¹)	ΔC_p (cal mol ⁻² K ⁻¹)	σ (cal mol ⁻¹)
23.05	- 8 312	-18.624	12.2	+ 135	+0.323	- 5.9 ^s	- 175 [*]	-0.257 ^{**}	- 47	+0.121	- 4.4	3.9
<i>1-Cyanoalkanes</i>												
24.02	- 5 239	-15.536	8.8	- 482	-0.611	- 4.4 ^{**}	-1 076	-2.260	-1 981	-3.514	- 1.5	8.1
24.03	- 6 114	-16.339	11.2	- 508	-0.744	- 4.6 ^{**}	- 836	-1.733	-1 684	-2.999	- 1.5	5.4
24.04	- 7 169	-17.574	14.5	- 459	-0.636	- 5.0 ^{**}	- 621	-1.232	-1 345	-2.183	- 4.4	5.2
24.05	- 8 179	-18.768	14.5	- 448	-0.620	- 3.1 ^{**}	- 552	-1.065	-1 236	-1.945	- 3.0	5.6
<i>1-Nitroalkanes</i>												
25.02	- 5 853	-15.970	10.0	- 290	-0.293	- 4.9 ^{**}	- 796	-1.645	-1 363	-2.377	- 2.1	6.3
25.03	- 6 754	-16.954	12.6	- 232	-0.207 [*]	- 5.8 ^{**}	- 651	-1.333	-1 116	-1.853	- 3.7	5.8
25.04	- 7 743	-18.076	13.6	- 206	-0.166 [*]	- 5.2 ^{**}	- 652	-1.352	-1 105	-1.887	- 3.4	5.8
25.05	- 8 750	-19.282	15.9	- 204	-0.168 [*]	- 7.5 ^s	- 609	-1.249	-1 027	-1.702	- 4.6	5.6
<i>1-Acetoxyalkanes</i>												
26.03	- 7 008	-17.893	11.4	- 357	-0.576	+ 0.8 ^{**}	- 546	-1.098	-1 145	-2.043	- 0.3	6.7
26.04	- 8 021	-19.088	12.9	- 366	-0.596	- 0.8 ^{**}	- 544	-1.099	-1 168	-2.110	- 0.1	6.1
26.05	- 9 006	-20.252	15.1	- 393	-0.675	- 1.7 ^{**}	- 536	-1.082	-1 198	-2.205	- 0.7	6.2
<i>1-Alkanols</i>												
27.04	- 6 259	-16.592	9.5	-1 886	-4.049	+31.9	- 209 ^{**}	-0.365 ^{**}	-2 728	-5.675	+38.6	5.5
27.05	- 7 319	-17.865	12.9	-1 843	-3.944	+31.3	- 95 ^{**}	-0.102 ^{**}	-2 554	-5.256	+37.2	4.9
27.06	- 8 299	-18.990	14.3	-1 880	-4.049	+33.0	- 164 ^{**}	-0.275 ^{**}	-2 703	-5.654	+40.2	5.3
27.07	- 9 313	-20.224	17.4	-1 896	-4.087	+31.4	- 95 ^{**}	-0.122 ^{**}	-2 654	-5.547	+38.2	5.6
<i>2-Alkanols</i>												
28.04	- 5 842	-16.245	10.1	-1 494	-3.123	+24.7	- 465	-0.965 ^s	-2 443	-5.019	+31.2	6.9
28.05	- 6 858	-17.438	11.9	-1 436	-3.021	+26.8	- 276 ^s	-0.497 ^{**}	-2 205	-4.453	+32.9	5.3
28.06	- 7 839	-18.568	12.6	-1 433	-3.021	+28.3	- 346	-0.697 ^s	-2 329	-4.807	+36.2	5.1
28.07	- 8 828	-19.744	14.9	-1 460	-3.101	+28.7	- 389	-0.815 ^s	-2 444	-5.121	+35.8	5.9
<i>2-Methyl-2-alkanols</i>												
29.04	- 5 078	-15.379	14.2 [*]	-1 714	-3.651	+18.4 [*]	- 505 ^{**}	-1.172 ^{**}	-2 959	-6.377	+21.3	14.7
29.05	- 6 225	-16.464	12.8	-1 446	-3.098	+20.3	- 474 ^s	-1.043 ^s	-2 526	-5.395	+24.0	7.9
29.06	- 7 209	-17.696	14.5	-1 378	-2.951	+22.7	- 381	-0.815 ^s	-2 325	-4.929	+28.1	5.9
29.07	- 8 158	-18.829	16.5	-1 377	-2.955	+23.8	- 384	-0.822	-2 344	-4.989	+29.3	5.0

(Continued on p. 246)

TABLE IV (continued)

No.	Compound	Temp. range	Retention index											
			C78			POH - C78			Mixture		id POH ([OH]=1) - C78			σ
			I_{130}	$\frac{10 \times A_T}{(K^{-1})}$	$\frac{100 \times A_{TT}}{(K^{-2})}$	ΔI_{130}	$\frac{10 \times \Delta A_T}{(K^{-1})}$	$\frac{100 \times \Delta A_{TT}}{(K^{-2})}$	A_L	$\frac{10 \times A_{LT}}{(K^{-1})}$	ΔI	$\frac{10 \times \Delta A_T}{(K^{-1})}$	$\frac{100 \times \Delta A_{TT}}{(K^{-2})}$	
<i>n</i>	(°C)													
<i>1-Thiols</i>														
30.04	1-Butanethiol	20 90-170	718.9	+3.18	—**	16.6	-1.05*	—**	- 2.6	-0.07*	+ 20.6	- 1.43	—**	0.93
30.05	1-Pentanethiol	20 90-170	821.1	+3.34	—**	17.3	-0.98*	—**	- 3.2	-0.20*	+ 20.7	- 1.52	—**	0.82
30.06	1-Hexanethiol	20 90-170	922.0	+3.42	—**	18.6	-0.88*	—**	- 1.6*	-0.59*	+ 25.1	- 1.89	—**	1.24
<i>2-Alkanones</i>														
31.04	2-Butanone	20 90-170	537.5	+0.74	—**	46.1	-1.14*	—**	+ 9.0	-3.35	+ 79.1	- 5.77	—**	1.26
31.05	2-Pentanone	20 90-170	629.6	+0.79	—**	46.7	-1.04*	—**	+ 8.6	-2.56	+ 79.8	- 4.47	—**	1.31
31.06	2-Hexanone	20 90-170	731.4	+0.85	—**	47.9	-0.90*	—**	+ 9.9	-2.33	+ 82.6	- 3.91	—**	1.27
31.07	2-Heptanone	20 90-170	831.4	+0.91	—**	48.9	-0.87*	—**	+11.0	-2.14	+ 85.3	- 3.56	—**	1.37
<i>Aldehydes</i>														
32.05	Pentanal	20 90-170	647.8	+1.35	—**	41.9	-2.01	—**	+14.3	-0.83*	+ 79.5	- 3.38	—**	1.48
32.06	Hexanal	20 90-170	749.5	+1.31	—**	42.8	-1.88	—**	+14.0	-0.89*	+ 80.2	- 3.27	—**	1.32
32.07	Heptanal	20 90-170	851.0	+1.39	—**	43.2	-1.88	—**	+12.0	-1.07*	+ 78.2	- 3.55	—**	1.19
<i>Ethers</i>														
33.06	Dipropylether	20 90-170	656.8	+0.03*	—**	16.3	-0.55*	—**	+ 7.0	-0.65*	+ 33.3	- 1.42	—**	0.57
33.08	Dibutylether	20 90-170	854.9	+0.06*	—**	16.2	-0.50*	—**	+ 7.1	-0.69*	+ 34.0	- 1.41	—**	0.53
<i>Primary amines</i>														
34.04	Butylamine	20 90-170	609.4	+0.84	—**	63.1	-4.33	—**	-24.4	+2.17*	+ 55.4	- 2.60	—**	2.35
34.05	Pentylamine	20 90-170	711.8	+0.78	—**	63.6	-3.79*	—**	-27.0	+3.23*	+ 51.3	- 0.34	—**	3.04
34.06	Hexylamine	20 90-170	813.4	+0.86	—**	64.8	-3.59*	—**	-32.4	+2.89*	+ 43.8	- 0.61	—**	3.42
<i>Secondary amines</i>														
35.04	Diethylamine	20 90-170	548.9	-1.01*	—**	52.9	-4.13	—**	- 2.4	+0.27*	+ 73.6	- 4.91	—**	1.28
35.06	Dipropylamine	20 90-170	742.6	+0.37*	—**	41.3	-4.05	—**	- 1.9	+0.29*	+ 58.5	- 4.90	—**	1.30
<i>Tertiary amines</i>														
36.06	Triethylamine	20 90-170	673.6	+0.91	—**	27.6	-3.75	—**	-16.2	-1.18*	+ 16.6	- 6.99	—**	2.20
<i>Halomethanes</i>														
37.01	Dichloromethane	20 90-170	504.9	+1.37	—**	24.3	+0.71*	—**	13.4	+0.46*	+ 52.6	+ 2.17	—**	1.45
37.02	Trichloromethane	20 90-170	606.8	+2.17	—**	25.7	+0.39*	—**	11.5	-0.24*	+ 53.3	+ 0.72	—**	0.87
37.03	Tetrachloromethane	20 90-170	680.7	+3.19	—**	6.3	-0.04*	—**	1.5*	-0.27*	+ 5.5	- 0.39	—**	0.81
37.04	CF ₂ Br ₂	20 90-170	481.4	+1.01	—**	11.3	+1.83	—**	- 1.5*	-1.64	+ 15.0	+ 0.41	—**	0.74

No	Thermodynamic data											
	C78			POH - C78			Mixture		id POH([OH]=1) - C78			
	ΔH (cal mol ⁻¹)	ΔS (cal mol ⁻¹ K ⁻¹)	ΔC_p	ΔH (cal mol ⁻¹)	ΔS (cal mol ⁻¹ K ⁻¹)	ΔC_p	\bar{H} (cal mol ⁻¹)	σ (cal mol ⁻¹ K ⁻¹)	ΔH (cal mol ⁻²)	ΔS (cal mol ⁻² K ⁻¹)	ΔC_p	σ (cal mol ⁻¹)
<i>1-Thiols</i>												
30.04	- 7 043	-16.922	6.9	- 191	-0.497	- 0.5**	- 142**	-0.292**	- 472	-1.121	+ 0.3	4.8
30.05	- 8 042	-18.097	10.1	- 186	-0.488	- 0.1**	- 158**	-0.352**	- 491	-1.201	- 1.4	4.6
30.06	- 9 050	-19.330	14.6	- 178	-0.463	- 1.4**	- 244**	-0.561**	- 608	-1.467	- 4.1	6.5
<i>2-Alkanones</i>												
31.04	- 5 708	-16.031	10.1	- 515	-0.866	+ 1.4**	-1 028	-2.295	-1 973	-3.968	- 0.9	6.7
31.05	- 6 628	-17.063	12.2	- 493	-0.850	+ 1.2**	- 809	-1.781	-1 696	-3.362	- 1.1	6.4
31.06	- 7 649	-18.273	13.5	- 468	-0.794	+ 3.2**	- 750	-1.639	-1 583	-3.098	- 1.0	5.8
31.07	- 8 643	-19.462	14.9	- 476	-0.824	+ 4.6**	- 714	-1.549	-1 539	-3.007	- 1.0	5.9
<i>Aldehydes</i>												
32.05	- 6 700	-16.998	10.1	- 645	-1.306	+ 8.1*	- 484	-0.908 ^s	-1 463	-2.805	+ 0.1	6.7
32.06	- 7 738	-18.258	11.7	- 618	-1.243	+ 8.2 ^s	- 478	-0.916	-1 432	-2.766	+ 0.2	5.5
32.07	- 8 746	-19.469	14.1	- 626	-1.272	+ 7.3	- 488	-0.982	-1 466	-2.919	- 0.5	4.5
<i>Ethers</i>												
33.06	- 7 074	-17.803	9.9	- 79	-0.223	+ 1.5**	- 366	-0.712	- 590	-1.226	- 0.3	3.1
33.08	- 9 061	-20.196	13.8	- 71	-0.221	- 0.7**	- 359	-0.726	- 585	-1.283	- 0.9	2.8
<i>Primary amines</i>												
34.04	- 6 421	-16.798	6.7**	-1 352	-2.771	+ 6.6**	+ 529*	+1.101**	-1 065	-2.111	+ 2.2	12.2
34.05	- 7 468	-18.068	10.0*	-1 222	-2.472	+ 9.4**	+ 768*	+1.644*	- 548	-0.925	- 0.6	15.4
34.06	- 8 470	-19.259	13.7*	-1 189	-2.407	+14.5*	+ 749*	+1.523*	- 529	-1.013	- 2.7	15.0
<i>Secondary amines</i>												
35.04	- 6 218	-17.133	10.4	-1 226	-2.528	- 0.7**	- 156**	-0.288**	-1 698	-3.383	+ 0.4	7.5
35.06	- 7 858	-18.658	18.6	-1 064	-2.336	- 2.3**	- 74**	-0.120**	-1 534	-3.283	- 5.6	5.2
<i>Tertiary amines</i>												
36.06	- 7 049	-17.539	15.1	- 870	-2.033	+ 1.8**	- 272**	-0.779**	-1 572	-3.874	- 3.3	11.0
<i>Halomethanes</i>												
37.01	- 5 247	-15.326	4.1**	+ 126 ^s	+0.406	+ 7.4**	- 210**	-0.209**	- 17	+0.529	- 0.7	7.6
37.02	- 6 111	-16.068	7.7	+ 21**	+0.148 ^s	+ 2.3**	- 330	-0.556 ^s	- 365	-0.399	- 2.4	3.8
37.03	- 6 643	-16.422	5.7	+ 127	+0.147*	+ 5.3 ^s	- 210 ^s	-0.439*	- 117	-0.418	- 0.1	4.0
37.04	- 5 093	-15.274	5.3	+ 497	+1.178	- 4.7*	- 524	-1.188	- 31	+0.004	- 1.5	3.9

(Continued on p. 248)

TABLE IV (continued)

No.	Compound	Temp. range (°C)	Retention index												
			C78			POH - C78			Mixture		id POH ([OH]=1) - C78			σ	
			I_{130}	$10 \times A_T$ (K ⁻¹)	$100 \times A_{TT}$ (K ⁻²)	ΔI_{130}	$10 \times \Delta A_T$ (K ⁻¹)	$100 \times \Delta A_{TT}$ (K ⁻²)	A_L	$10 \times A_{LT}$ (K ⁻¹)	ΔI (l mol ⁻¹)	$10 \times \Delta A_T$ (K ⁻¹)	$100 \times \Delta A_{TT}$ (K ⁻²)		
HALOBENZENES															
38.01	Fluorobenzene	20	90-170	664.6	+2.23	—**	17.8	+0.39*	—**	+ 5.0	+0.42*	+ 34.2	+ 1.47	—**	0.92
38.02	Hexafluorobenzene	20	90-170	548.7	-2.14	—**	8.6	-0.30*	—**	+ 0.9*	-0.34*	+ 13.8	- 0.79	—**	0.62
38.03	Trifluoromethylbenzene	20	90-170	656.4	+0.22*	—**	17.4	+0.54*	—**	+ 4.0	-0.41*	+ 31.5	+ 0.49	—**	0.78
38.04	Chlorobenzene	20	90-170	864.5	+4.16	—**	20.0	+0.66*	—**	+ 4.5	+0.64*	+ 35.1	+ 2.19	—**	1.02
38.05	Bromobenzene	20	90-170	959.6	+5.34	—**	22.2	+0.76*	—**	+ 5.0	+0.35*	+ 37.7	+ 1.95	—**	1.15
ALKYLPYRIDINES															
39.01	Pyridine	20	90-170	723.4	+3.44	—**	63.4	-3.25	—**	+16.3	-1.09*	+113.8	- 5.23	—**	1.28
39.02	2-Picoline	20	90-170	802.2	+2.84	—**	64.8	-3.59	—**	+17.7	-1.91	+117.8	- 6.87	—**	1.24
39.03	3-Picoline	20	90-170	843.4	+3.45	—**	72.3	-3.98	—**	+23.6	-1.69*	+136.8	- 6.93	—**	1.47
39.04	4-Picoline	20	90-170	843.1	+3.63	—**	74.7	-3.94	—**	+18.9	-3.03	+134.4	- 8.85	—**	1.17
39.05	2,3-Lutidine	20	130-210	933.9	+3.27	—**	69.9	-3.49	—**	+20.7	-0.44*	+130.5	- 4.49	—**	1.57
39.06	2,4-Lutidine	20	130-210	919.5	+2.81	—**	72.8	-3.66	—**	+18.8	+0.78*	+132.1	- 2.96	—**	1.02
39.07	2,5-Lutidine	20	130-210	920.0	+2.76	—**	70.2	-3.26	—**	+17.0	-0.63*	+125.6	- 4.48	—**	1.18
39.08	2,6-Lutidine	20	130-210	870.1	+2.69	—**	63.4	-3.25	—**	+19.5	-2.27	+119.2	- 6.88	—**	0.97
39.09	3,4-Lutidine	20	130-210	982.8	+5.01	—**	86.1	-4.29	—**	+27.8	-1.23*	+164.0	- 6.48	—**	1.32
39.10	3,5-Lutidine	20	130-210	961.4	+4.26	—**	80.4	-3.64	—**	+26.1	-2.13	+153.3	- 6.94	—**	1.24
39.11	2-Ethylpyridine	20	130-210	886.9	+3.33	—**	54.9	-1.84	—**	+13.5	-0.60*	+ 98.6	- 2.61	—**	0.90
39.12	3-Ethylpyridine	20	130-210	938.6	+4.18	—**	70.4	-3.58	—**	+20.2	+1.63	+130.7	- 1.61	—**	0.95
39.13	4-Ethylpyridine	20	130-210	941.1	+4.33	—**	74.6	-3.92	—**	+18.3	-0.74*	+133.8	- 5.49	—**	1.60
39.14	2-Propylpyridine	20	130-210	976.5	+3.26	—**	54.1	-2.69	—**	+ 6.1	+3.18	+ 87.0	+ 1.50	—**	0.73
39.15	4-Propylpyridine	20	130-210	1032.3	+3.82	—**	73.7	-3.05	—**	+13.3	+2.78	+125.7	+ 0.76	—**	1.32
39.16	2,3,6-Collidine	20	130-210	1000.5	+2.74	—**	61.5	-2.65	—**	+19.6	-1.73*	+116.7	- 5.26	—**	1.48
39.17	2,4,6-Collidine	20	130-210	986.6	+2.28	—**	71.1	-4.09	—**	+18.4	+1.02*	+129.0	- 3.26	—**	1.04
39.18	4-tert-Butylpyridine	20	130-210	1067.3	+5.19	—**	75.7	-4.04	—**	+19.1	-0.08*	+136.6	- 4.71	—**	1.23
39.19	3-Chloropyridine	20	90-170	885.0	+4.47	—**	46.5	-1.45	—**	+16.3	-0.17*	+ 90.8	- 1.51	—**	0.93
ORGANOSILICON COMPOUNDS															
40.01	Tetramethylsilane	20	90-170	428.0	-0.46*	—**	- 0.8*	+0.74*	—**	+ 1.3*	-0.87*	- 2.4	- 0.20	—**	2.00
40.02	Hexamethyldisilane	20	90-170	685.9	+0.30	—**	- 0.5*	+0.30*	—**	+ 2.5*	-0.12*	+ 3.4	+ 0.29	—**	0.78
40.03	Hexamethyldisiloxane	20	90-170	597.4	-2.46	—**	- 0.3*	+0.50*	—**	+ 0.5*	-1.26*	+ 1.0	- 1.10	—**	1.23

No	Thermodynamic data											
	C78			POH - C78			Mixture		id POH([OH]=1) - C78			
	ΔH (cal mol ⁻¹)	ΔS (cal mol ⁻¹ K ⁻¹)	ΔC_p	ΔH (cal mol ⁻¹)	ΔS (cal mol ⁻¹ K ⁻¹)	ΔC_p	\bar{H} (cal mol ⁻¹)	σ (cal mol ⁻¹ K ⁻¹)	ΔH (cal l mol ⁻²)	ΔS (cal l mol ⁻² K ⁻¹)	ΔC_p	σ (cal mol ⁻¹)
HALOBENZENES												
38.01	- 6 680	-16.734	11.6	+ 94	+0.237	- 4.3**	- 128**	-0.150**	- 24	+0.191	- 6.0	4.5
38.02	- 6 474	-17.769	10.8	+ 51 ^s	+0.020**	+ 0.4**	- 244	-0.472 ^s	- 265	-0.615	- 2.8	3.3
38.03	- 7 029	-17.699	10.2	+ 135	+0.331	- 2.6**	- 281	-0.541 ^s	- 178	-0.229	- 2.1	4.2
38.04	- 8 308	-18.212	11.7	+ 119	+0.292	+ 1.0**	- 73**	-0.054**	+ 93	+0.411	- 5.5	4.4
38.05	- 9 036	-18.814	10.2	+ 122	+0.304	+ 5.2**	- 140**	-0.229**	+ 16	+0.212	- 3.7	4.5
ALKYLPYRIDINES												
39.01	- 7 032	-16.839	8.9	-1 112	-2.198	+ 7.9*	- 557	-1.078	-2 181	-4.196	+ 2.3	6.4
39.02	- 7 948	-18.105	11.3	-1 198	-2.413	+ 7.6*	- 746	-1.538	-2 545	-5.090	+ 3.0	6.2
39.03	- 8 242	-18.314	11.3	-1 352	-2.707	+ 9.6 ^s	- 764	-1.514	-2 747	-5.376	+ 3.2	7.0
39.04	- 8 199	-18.219	13.5	-1 374	-2.723	+ 5.9*	- 987	-2.123	-3 108	-6.293	+ 2.0	5.4
39.05	- 9 255	-19.678	13.0	-1 182	-2.321	+ 3.3**	- 418*	-0.718*	-2 139	-3.994	+ 2.4	7.5
39.06	- 9 182	-19.679	12.7	-1 244	-2.436	+ 3.4**	- 191**	-0.174**	-1 868	-3.297	+ 1.7	5.2
39.07	- 9 237	-19.807	13.8	-1 121	-2.164	+ 2.6**	- 417 ^s	-0.757*	-2 063	-3.862	+ 1.5	6.1
39.08	- 8 816	-19.387	14.8	- 917	-1.747	- 0.8**	- 704	-1.438	-2 407	-4.772	+ 0.5	4.5
39.09	- 9 535	-19.747	15.8	-1 416	-2.717	+ 2.8**	- 611	-1.117	-2 741	-5.116	+ 0.9	6.3
39.10	- 9 413	-19.719	14.6	-1 278	-2.438	+ 3.2**	- 764	-1.510	-2 777	-5.319	+ 2.8	6.2
39.11	- 8 770	-19.065	12.3	- 799	-1.546	+ 4.1**	- 372	-0.688	-1 436	-2.620	- 0.6	4.3
39.12	- 9 136	-19.324	12.7	-1 217	-2.401	+ 3.8**	- 81**	+0.119**	-1 555	-2.549	- 0.2	4.5
39.13	- 9 071	-19.133	11.1	-1 405	-2.811	+ 6.2**	- 464 ^s	-0.857*	-2 420	-4.654	+ 4.2	7.9
39.14	- 9 609	-20.024	11.7	- 998	-2.059	+ 6.2	+ 316	+0.927	- 587	-0.693	- 0.7	3.8
39.15	-10 169	-20.708	15.5	-1 155	-2.222	+ 4.2**	+ 224**	+0.772*	-1 031	-1.357	- 2.5	6.3
39.16	-10 063	-20.842	15.4	- 909	-1.761	+ 2.7**	- 609	-1.219	-2 122	-4.152	+ 2.3	7.3
39.17	- 9 982	-20.818	14.6	-1 378	-2.801	+ 6.2*	- 147**	-0.078**	-1 882	-3.402	+ 2.3	5.3
39.18	-10 219	-20.400	14.7	-1 489	-3.026	+ 7.5*	- 348 ^s	-0.581*	-2 247	-4.248	+ 1.2	5.9
39.19	- 8 455	-18.317	12.1	- 582	-1.116	+ 1.4**	- 372	-0.648 ^s	-1 208	-2.139	- 2.4	4.5
ORGANOSILICON COMPOUNDS												
40.01	- 4 894	-15.508	0.5**	+ 393	+0.717	+11.7*	- 407**	-0.853**	+ 18	-0.104	+ 4.0	11.3
40.02	- 7 308	-18.009	11.7	+ 268	+0.423	- 2.6**	- 209 ^s	-0.388*	+ 62	+0.003	- 3.6	3.9
40.03	- 7 019	-18.453	13.1	+ 313	+0.549	- 3.0**	- 442	-0.974 ^s	- 196	-0.626	- 4.9	6.6

(Continued on p. 250)

No	Thermodynamic data											
	C78			POH - C78			Mixture		id POH([OH]=1) - C78			
	ΔH (cal mol ⁻¹)	ΔS (cal mol ⁻¹ K ⁻¹)	ΔC_p	ΔH (cal mol ⁻¹)	ΔS (cal mol ⁻¹ K ⁻¹)	ΔC_p	\bar{H} (cal mol ⁻¹)	σ (cal mol ⁻¹ K ⁻¹)	ΔH (cal mol ⁻²)	ΔS (cal mol ⁻² K ⁻¹)	ΔC_p	σ (cal mol ⁻¹)
41.01	- 5 644	-14.938	7.5	+ 68 ^s	+0.049**	- 4.2*	- 238 ^s	-0.474*	- 243	-0.599	- 4.8	3.9
41.02	- 6 566	-17.231	5.0 ^s	+ 365	+0.708	+ 4.9**	- 143**	-0.223**	+ 332	+0.724	+ 0.4	5.3
41.03	- 6 157	-16.144	8.3	- 449	-0.843	+ 0.0**	- 657	-1.431	-1 467	-2.979	+ 0.5	3.8
41.04	- 6 684	-16.674	9.4	- 470	-0.785	- 2.3**	- 590	-1.229	-1 362	-2.520	- 0.3	3.2
41.05	- 6 743	-16.646	9.2	+ 53 ^s	+0.250	- 3.4*	+ 378	+0.956	+ 406	+1.339	- 5.1	3.2
41.06	- 7 279	-17.228	8.7	- 742	-1.313	+ 3.0**	- 482	-0.884*	-1 590	-2.772	+ 1.2	7.2
41.07	- 8 249	-18.189	7.0	- 784	-1.426	+ 3.7**	- 483	-0.904 ^s	-1 631	-2.912	+ 3.8	5.9
41.08	- 8 196	-18.075	9.5	-1 645	-3.507	+24.6	- 398	-0.755**	-2 701	-5.573	+29.2	8.3
41.09	- 6 704	-16.652	7.6**	-1 984	-3.912	+ 5.5**	+ 492**	+1.346*	-3 567	-7.124	+ 7.6	13.4
41.10	- 7 506	-17.527	12.2	-1 571	-3.261	+11.9 ^s	-1 020	-2.052	-3 416	-6.922	+ 3.7	7.7
41.11	- 9 891	-19.828	12.5	- 384	-0.641	+ 3.4	- 182	-0.211	- 571	-0.613	- 2.4	4.6
41.12	- 9 421	-19.512	10.6	-1 698	-3.404	+16.1	- 603	-1.211	-2 339	-4.656	+19.1	6.9
41.13	-10 183	-20.423	14.3	-1 403	-2.746	+ 8.6 ^s	- 609	-1.181	-2 240	-4.396	+ 8.9	5.6
41.14	- 9 032	-19.434	12.4	- 21**	+0.019**	- 1.4**	- 366	-0.689	- 568	-1.035	- 2.3	2.8
41.15	- 9 845	-20.587	13.4	- 196*	-0.412*	- 0.3**	- 52**	+0.041**	- 362	-0.533	- 2.0	3.6

ERROR OF THE COEFFICIENTS (STANDARD DEVIATION)

3.4	0.0061	0.10	4.7	0.0083	0.13	2.8	0.0061	6.6	0.0112	0.18
4.2	0.0102	0.49	4.7	0.0083	0.13	2.8	0.0061	6.6	0.0112	0.18
6.3	0.0154	0.44	8.6	0.0211	0.72	28.6	0.0711	12.0	0.0295	1.01
18.3	0.0486	0.49	31.9	0.0771	0.78	31.5	0.0711	44.6	0.1078	1.09

CONVERSIONS

A	550	7.799	0.9	- 2	+0.024	- 0.3	- 0	-0.001	- 2	+0.024	- 0.3
B	0	-0.026	0	0	0	0	0	0	0	0	0

was found that loadings of about 7% were required in order to obtain retention indices of the polar test compounds where the adsorption contributed less than 1 i.u. to retention. On such columns the specific

surface area of the stationary liquid was of the order of $s_L \approx 8 \text{ m}^2 \text{ g}^{-1}$.

The results are summarized in Table IV. The method of evaluation is discussed in detail under

Experimental. The principles of the calculations can be summarized in the following points.

(i) Thermodynamic data of *n*-alkanes were calculated from specific retention volumes whereas those of all other solutes were determined via retention indices, *i.e.*, relative to *n*-alkanes as reference compounds.

(ii) Data of *n*-alkanes were calculated by fitting eqns. 3–6 to experimental chemical potentials determined at different temperatures on C78–POH mixtures of the following composition: $100\phi_{\text{POH}} = 0.0, 33.3, 50.0, 66.7, 83.3$ and 100.0% . Data in idPOH at hydroxyl concentrations of $[\text{OH}] = 1 \text{ mol l}^{-1}$ were calculated by calculating standard chemical potentials at several temperatures by using eqns. 7 and 8 and fitting eqn. 9 to the resulting data set.

(iii) Retention indices of solutes were determined at several temperatures on C78–POH mixtures of the composition $100\phi_{\text{POH}} = 0.0, 33.3, 66.7$ and 100.0% . Retention indices at 130°C , I_{130}^A and $\Delta I_{130}^{\text{POH}}$, and the coefficients A and ΔA were calculated by fitting eqns. 15–18 to the experimental data set.

(iv) Retention indices on idPOH at $[\text{OH}] = 1 \text{ mol l}^{-1}$ were calculated for several temperatures by using eqn. 20 where the molar volume of POH, v_{POH} , was calculated with eqn. 21 and the value of κ with eqns. 29 and 32.

(v) Thermodynamic data for solutes other than *n*-alkanes were calculated by converting experimental retention indices point by point to standard chemical potentials (see eqn. 10) and by fitting eqns. 3–6 to the resulting data set.

(vi) Thermodynamic data for solutes other than *n*-alkanes in idPOH were calculated by generating points at different temperatures with retention index coefficients listed in Table IV, converting these indices into chemical potentials with the aid of thermodynamic functions of *n*-alkanes in idPOH and fitting eqn. 9 to the resulting data set.

From points iii–v it follows that regression equations describing the variations of retention indices are always based on experimental retention index data sets and those describing the variations of standard chemical potentials are always based on experimental standard chemical potential data (either directly measured or reconverted point by point from retention indices). The only exception are thermodynamic data on idPOH where, for obvious reasons, experimental retention indices are not

available (see point vi). Regression calculations in different spaces give slightly different results. Therefore, retention indices calculated with data listed under *Thermodynamic data* will slightly differ from those obtained by direct evaluation of retention index data sets listed under the heading *Retention indices*. In Table V retention indices calculated with eqn. 10 by using thermodynamic data are compared with those obtained with the experimental index data set, listed in Table IV, for the example of three chosen solutes. Differences in the coefficients obtained by fitting eqns. 15–18 directly to experimental data or to data sets generated by eqn. 10 are negligible. However, it is interesting that data generated by eqn. 10 cannot be described with high precision if quadratic terms are neglected. Indeed, the fitting error (residual around the regression) is of the same order of magnitude as the error when fitting eqn. 10 to experimental retention indices.

Significances of data listed in Table IV

The significance of the coefficients of solutes other than *n*-alkanes was always tested against the residual variance of the data set of the specific solute in

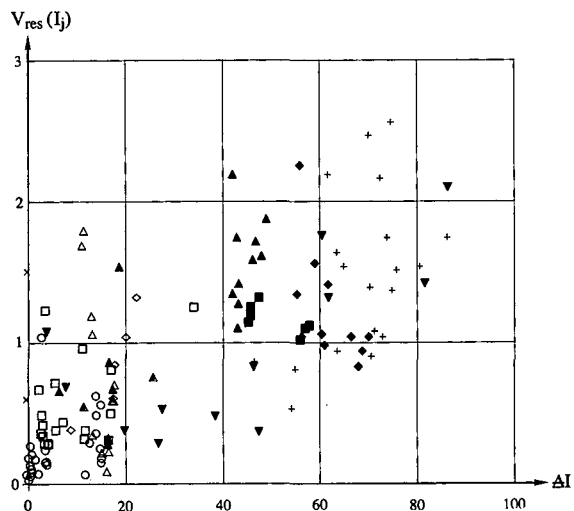


Fig. 4. Residual variance of retention index data sets around the regression equation as a function of the additional retention on the POH stationary phase, $\Delta I_{130}^{\text{POH}}$. ● = *n*-Alkane; ○ = hydrocarbons; □ = cyclic hydrocarbons and alkylbenzenes; △ = haloalkanes; ▽ = halomethanes; ◇ = halobenzenes; ■ = cyano- and nitroalkanes; ▲ = polar alkane derivatives (compounds 26.03–26.05 and 30.04–33.08 from Table IV); ◆ = alkanols; × = silanes; ▼ = miscellaneous (three alcohols).

TABLE V

RETENTION INDICES OF THREE SOLUTES CALCULATED BY FITTING EQNS. 15–18 TO DATA SETS OF DIFFERENT ORIGIN

T IV (same as in Table IV) = experimental retention indices; TD = data set generated with eqn. 10 by using thermodynamic data listed in Table IV, without ($A_{TT} = 0$) and with quadratic dependence. Temperature range = 90–170°C. Standard deviations of the coefficients are given in italics: T IV, experimental error; TD, fitting error (fitting eqns. 15–18 to data generated with eqn. 10).

Solute	Method	C78			POH-C78			Mixture			σ
		I_{130}	$A_T \cdot 10$ (K ⁻¹)	$A_{TT} \cdot 10^2$ (K ⁻²)	ΔI_{130}	$\Delta A_T \cdot 10$ (K ⁻¹)	$\Delta A_{TT} \cdot 10^2$ (K ⁻²)	A_L	$A_{LT} \cdot 10$ (K ⁻¹)	$A_{LTT} \cdot 10^2$ (K ⁻²)	
1-Chloropentane	T IV	741.7	+1.41		16.0	+0.61		4.6	+0.3		0.30
	$\pm\sigma$	<i>0.1</i>	<i>0.04</i>		<i>0.6</i>	<i>0.31</i>		<i>0.6</i>	<i>0.25</i>		
	TD 1	741.8	+1.42		16.3	+0.61		4.7	+0.34		0.27
	$\pm\sigma$	<i>0.1</i>	<i>0.04</i>		<i>0.8</i>	<i>0.27</i>		<i>0.5</i>	<i>0.19</i>		
	TD 2	741.7	+1.42	+0.000	15.9	+0.61	+0.001	4.8	+0.29	-0.016	0.03
	$\pm\sigma$	<i>0.0</i>	<i>0.01</i>	<i>0.002</i>	<i>0.1</i>	<i>0.03</i>	<i>0.013</i>	<i>0.1</i>	<i>0.02</i>	<i>0.009</i>	
2-Hexanone	T IV	731.4	+0.85		47.9	-0.90		9.9	-2.33		1.27
	$\pm\sigma$	<i>0.5</i>	<i>0.19</i>		<i>2.6</i>	<i>1.31</i>		<i>2.5</i>	<i>0.90</i>		
	TD 1	731.5	+0.86		48.2	-0.88		9.7	-2.43		0.85
	$\pm\sigma$	<i>0.4</i>	<i>0.11</i>		<i>2.4</i>	<i>0.87</i>		<i>1.7</i>	<i>0.60</i>		
	TD 2	731.4	+0.86	-0.000	47.9	-0.91	+0.004	9.7	-2.35	+0.020	0.03
	$\pm\sigma$	<i>0.0</i>	<i>0.01</i>	<i>0.002</i>	<i>0.2</i>	<i>0.03</i>	<i>0.002</i>	<i>0.1</i>	<i>0.02</i>	<i>0.010</i>	
Pyridine	T IV	723.4	+3.44		63.4	-3.25		16.3	-1.09		1.28
	$\pm\sigma$	<i>0.5</i>	<i>0.19</i>		<i>2.6</i>	<i>1.31</i>		<i>2.5</i>	<i>0.91</i>		
	TD 1	723.5	+3.46		63.9	-3.25		16.4	-1.16		0.78
	$\pm\sigma$	<i>0.3</i>	<i>0.12</i>		<i>2.2</i>	<i>0.79</i>		<i>1.5</i>	<i>0.55</i>		
	TD 2	723.4	+3.44	+0.003	63.4	-3.26	-0.001	16.4	-1.09	-0.020	0.03
	$\pm\sigma$	<i>0.0</i>	<i>0.00</i>	<i>0.002</i>	<i>0.1</i>	<i>0.03</i>	<i>0.012</i>	<i>0.1</i>	<i>0.02</i>	<i>0.009</i>	

question. A data set consisted in general of 20 data points. After calculation of eight regression coefficients the residual variance had twelve degrees of freedom. In Fig. 4, the residual variance of a solute data set around the regression equation is plotted as a function of the retention index difference of the solute at the standard temperature, $\Delta I_{130}^{\text{POH}}$. It is seen that there is a correlation between the residual variance and the ΔI value of the solutes. However, around the correlation residual variances vary as would be expected from variances of samples originating from the same population. On the basis of Fig. 4 we conclude that in the solute by solute evaluation of the experimental data sets the significance of the coefficients in eqns. 15–18 was seriously underestimated. In fact, variances of the coefficients were tested by the method of Fisher and Yates [16] against residual variances of a data set having twelve degrees of freedom, whereas these residual variances are themselves members of groups where an aver-

aging would be fully justified. Consequently, variances of coefficients should be tested against a variance of the same order of magnitude but having a much higher degree of freedom. In Fig. 4, classes could be formed at every 50-i.u. interval of ΔI with a resulting average residual variance of well over 100 degrees of freedom. Testing variance ratios against residual variances having over 100 instead of 12 degrees of freedom would considerably change their significance level. In particular, in Table IV all coefficients significant at the 10% significance level would become significant at the 5% level. On the basis of this discussion, such a coefficient will be considered to be significant and is designated by the subscript s.

Correlations

It was mentioned under Experimental that, with the exception of alcohols, retention indices could be described by six coefficients instead of eight needed

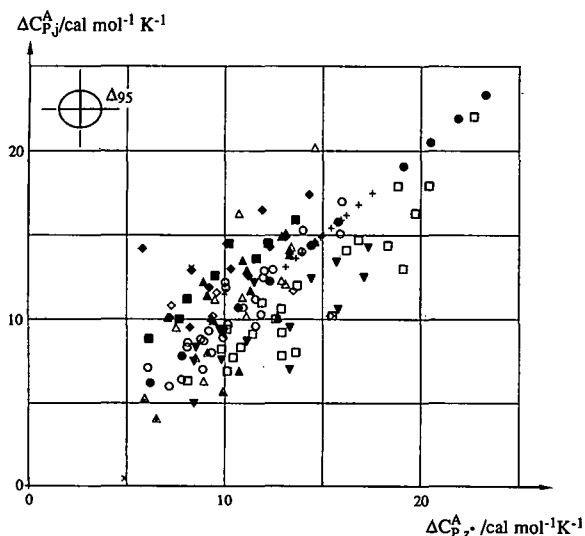


Fig. 5. Mean partial molar heat capacity differences of solutes, j , in the non-polar standard stationary phase, $\Delta C_{P,j}^A$, as a function of those of hypothetical n -alkanes with carbon numbers $z^* = I_{130}^A/100$. The inset marked Δ_{95} is the error ellipse of the individual value at the 95% confidence limit. Symbols as in Fig. 4.

for the description of the dependence of the standard chemical potential on temperature and composition.

Eqn. A12 shows that a non-linear temperature dependence of the index can have two reasons. First, it may be due to a difference in the slope of the numerator and denominator and, second, to a

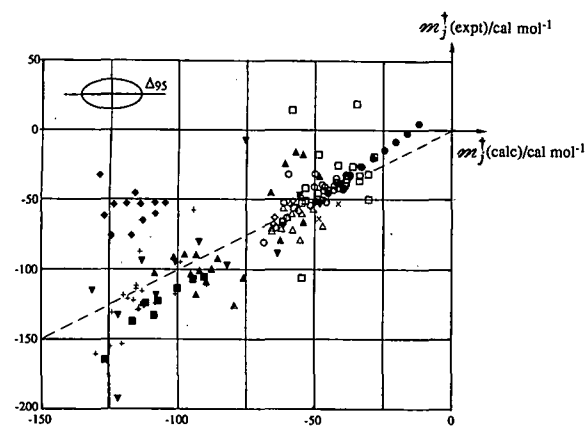


Fig. 6. Experimental coefficients of non-ideality (non-linearity) of the chemical potential-composition plot as a function of the same coefficient calculated with eqn. 34. Symbols as in Fig. 4. The dashed line marks the perfect correlation. The error ellipse is composed of the error of the experimental coefficients and the error of the correlation of the calculated coefficients.

difference in their curvature. The curvature introduced by the difference in the slope of the numerator and denominator is very slight for normal cases. A difference in their curvature is due to a difference of the partial molar heat capacity of the solute, $\Delta C_{P,j}$, and that of the n -alkanes bracketing the solute in the chromatogram. In Fig. 5, mean molar heat capacities of the solute in the standard non-polar stationary phase, $\Delta C_{P,j}^A$, are plotted as a function of an n -alkane with carbon number $z^* = I_{j,130}^A/100$. The approximate correlation ($r = 0.7451$) is sufficient to make non-significant the quadratic term in the functions $I_j(T)$ ($A_{TT} \approx 0$ in eqn. 16). Very high apparent molar heat capacities are observed for alcohols on the polar stationary phase, POH, effecting a significant curvature of the temperature dependence of their retention indices, I_j^{POH} .

In future work the most important correlation would be that permitting the prediction of the coefficient of non-ideality of the chemical potential of a solute, j , in the C78-POH mixtures, m_j . Knowledge of this coefficient is necessary for the calculation of the thermodynamic functions in stationary liquids with non-associated alcohol groups, idPOH. Its determination implies experimental determination of the thermodynamic functions on a

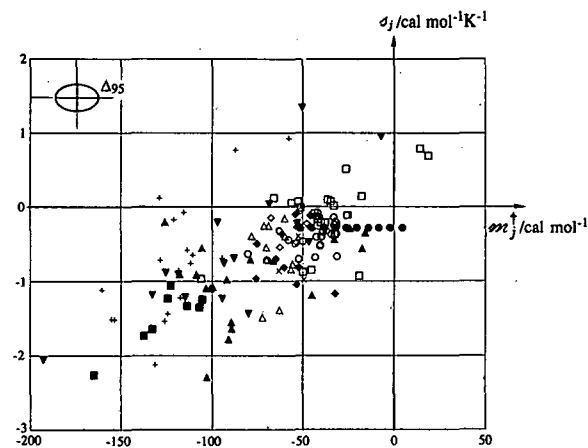


Fig. 7. Entropic component of the coefficient of non-ideality of a solute j , σ_j , as a function of the coefficient of non-ideality, m_j^{\dagger} , at the reference temperature $T^{\dagger} = 130 + 273.15$ K. The components of the error ellipse are the errors of the experimental determination of σ_j and m_j^{\dagger} . Correlation coefficient: 0.7169. Symbols as in Fig. 4.

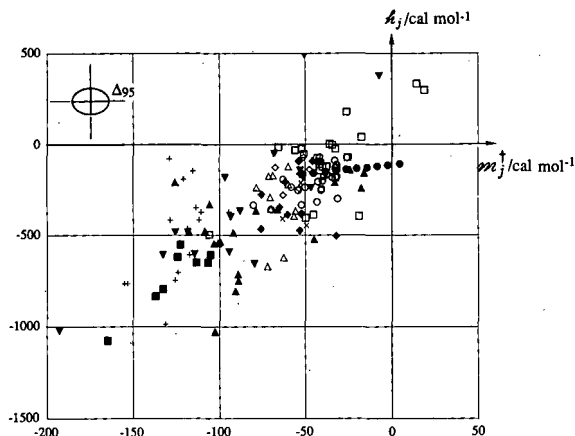


Fig. 8. Enthalpic component of the coefficient of non-ideality of a solute j , h_j^\dagger , as a function of the coefficient of non-ideality, m_j^\dagger , at the reference temperature $T^\dagger = 130 + 273.15$ K. The components of the error ellipse are the errors of the experimental determination of h_j^\dagger and m_j^\dagger . Correlation coefficient: 0.7345. Symbols as in Fig. 4.

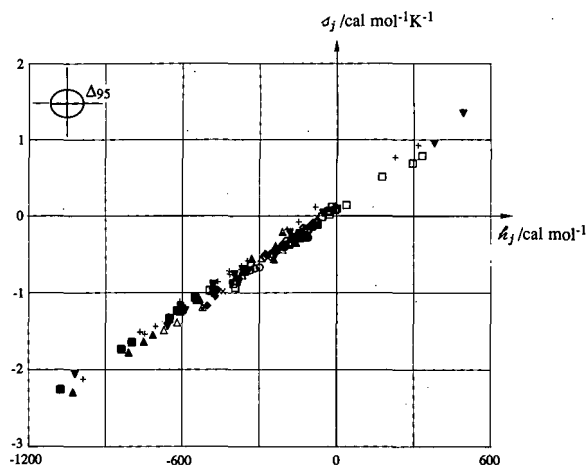


Fig. 9. Entropic component of the coefficient of non-ideality of a solute, σ_j , as a function of the enthalpic component, h_j . Correlation coefficient: 0.9941. Symbols as in Fig. 4.

least two liquid stationary phase mixtures, C78–POH, of different composition. Unfortunately, we cannot offer a good method of prediction. Eqn. 34 permits the prediction of the solutes with fair precision with the exception of alcohols:

$$m_j^\dagger = -0.0064 \Delta\mu_j^{\dagger,A} + 0.236 \Delta\mu_j^{\dagger,P} - 64.5 \quad (34)$$

Fig. 6 shows experimental coefficients of non-ideality as a function of those calculated with eqn. 34.

Knowledge of the coefficient of non-ideality of the thermodynamic data would permit an approximate prediction of its entropic and enthalpic com-

ponent as shown by the correlations depicted in Figs. 7 and 8. As pointed out by Krug *et al.* [17], the correlation between entropy and enthalpy can be excellent in spite of the lack of good correlations of enthalpy and entropy on the chemical potential. The latter correlation is shown in Fig. 9.

Finally, it should be noted that the present discussion is restricted to the presentation and criticism of the measured data. Their evaluation for the calculation of interaction free energies will be the subject of forthcoming publications.

SYMBOLS

The system adopted is as follows. *Superscripts* mean “at” or “in”: † = at the reference temperature; in A, A/P, L, P, idP. *Superscripts in parentheses* mean “referring to” or “of the degree”: (D) = referring to K_D ; (g), (h). *Subscripts* mean “of”: A, A/P, L, P, j , $z = 0, 1, \dots$, with the exception of the generally accepted symbols K_D , V_g , V_N , where the subscript is considered as part of the symbol. *Brackets*: [X] means molar concentration of X. Dimensions are given in *parentheses*.

A \equiv C78 (-)	The standard non-polar liquid
A-P (-)	Mixture of A and P
A (div.)	Coefficients in eqns. 16–18
$B = (1/2)(d\alpha/dT)(K^{-2})$	Temperature dependence of α
$\alpha (K^{-1})$	Isobaric coefficient of thermal expansion
b (div.)	Coefficients in eqn. 25
$C_{p,j} (\text{cal mol}^{-1} K^{-1})$	Partial molar heat capacity of j

Δ_α (div.)	Confidence limit at the $\alpha\%$ confidence level
$\Delta(-)$	Difference from the reference state, ideal gas
$\Delta(-)$	Difference from the reference state, ideal dilute solution in A
Δ' (l mol^{-1})	Partial derivative of $\Delta Y^{A/L}$ with respect to [X]
$\delta(-)$	Difference between the property of two substances in the same solvent
$F(-)$	Fisher's F
f (div.)	Factor to give the standard deviation of a coefficient as a function of standard deviation around the regression
$\Phi(-)$	Degrees of freedom
$\varphi(-)$	Volume fraction
g (atm kg mol^{-1})	Molal Henry coefficient
H_j (cal mol^{-1})	Partial molar enthalpy of j at T^\dagger
h (atm)	Molar Henry coefficient
h (cal mol^{-1})	Enthalpic coefficient in eqn. 6
$I(-)$	Retention index
idP (-)	Ideal solution of P in A
$i(-)$	Coefficient in eqn. 15
$j(-)$	A solute including n -alkanes
$K_D(-)$	Distribution coefficient
κ (l mol^{-1})	Coefficient defined in eqn. 20
L (-)	A stationary liquid
$L(-)$	"Factor" in the variance analysis of Table III (composition of the stationary phase)
M (g mol^{-1})	Molar mass
m (cal mol^{-1})	Coefficient in eqn. 3
μ (cal mol^{-1})	Chemical potential referring to g
$n(-)$	Number of moles
$n(-)$	Number of data in a set
P (atm)	Pressure
$P(-)$	A polar stationary liquid, monofunctional derivative of A
$P(-)$	Mass/total mass percent
R ($\text{cal mol}^{-1} \text{K}^{-1}$) and \mathcal{R} ($\text{atm l mol}^{-1} \text{K}^{-1}$)	Universal gas constant
ρ (g cm^{-3})	Density
S_j ($\text{cal mol}^{-1} \text{K}^{-1}$)	Partial molar entropy of j at T^\dagger
σ (div.)	Standard deviation
s ($\text{cal mol}^{-1} \text{K}^{-1}$)	Entropic coefficient in eqn. 6
T (K)	Thermodynamic temperature
$T(-)$	"Factor" in Table III referring to the temperature of an experiment
V (ml)	Volume
V_N (ml)	Net retention volume
V_g (ml g^{-1})	Specific retention volume
$V(y)$ (div.)	Variance of y
v (ml mol^{-1})	Molar volume
\tilde{v} (ml g^{-1})	Specific volume
w (g)	Mass
$X(-)$	Polar group in P
$Z(-)$	"Factor" in Table III referring to a dependence on z
$z(-)$	Carbon number of the n -alkane $\text{C}_z\text{H}_{2z+2}$
$z(-)$	n -Alkane solute with carbon number z

ACKNOWLEDGEMENTS

This paper reports on part of a project supported by the Fonds National Suisse de la Recherche Scientifique. The authors gratefully acknowledge the help of Dr. Ch. de Reyff in the evaluation of data and Dr. L. Jelinek for the determination of the specific surface area of the support.

APPENDICES

(A) Standard chemical potential of a solute at ideal dilution

In the absence of adsorption at the gas–liquid stationary phase and liquid stationary phase–solid support interfaces and if the interaction energy between the carrier and solute in the gas phase is negligible, eqn. A1 holds:

$$V_{g,j} = V_{N,j}/w_L = \tilde{v}_L K_{D,j} = \mathcal{R}T/(M_L h_j) = \mathcal{R}T/(1000 g_j) \quad (\text{A1})$$

where V_g and V_N (ml) is the specific and net retention volume respectively, K_D is the distribution coefficient and h (atm) and g (atm kg mol⁻¹) are the molar and molal Henry coefficients of the solute, j , in the stationary liquid L (= A or P or A–P mixture), w_L (g) is the mass of the stationary liquid in the column, M is the molar mass and \tilde{v} (ml g⁻¹) is specific volume. The standard chemical potential difference of the solute between the ideal gas phase and the ideal dilute solution in L can be given relative to K_D , h or g :

$$\Delta\mu_j^{(D)} = -RT \ln K_{D,j} \quad (\text{A2})$$

$$\Delta\mu_j^{(h)} = RT \ln [h_j/(\text{atm})] \quad (\text{A3})$$

$$\Delta\mu_j = RT \ln [g_j/(\text{atm kg mol}^{-1})] \quad (\text{A4})$$

In this paper, the chemical potential related to the molal Henry coefficient will be used if not stated otherwise. Application of Kirchhoff's approximation (*i.e.*, that the difference of the partial molar heat capacity between the two standard states, $\Delta C_{P,j}$, is constant in the experimental temperature domain) results in eqn. A5 for the temperature dependence of the function $\Delta\mu_j$ in a given solvent:

$$\Delta\mu_j^L = \Delta H_j^L - T\Delta S_j^L + \Delta C_{P,j}^L \left[T - T^\dagger - T \ln \left(\frac{T}{T^\dagger} \right) \right] \quad (\text{A5})$$

where ΔH_j and ΔS_j are the partial molar enthalpy and entropy difference, respectively, at the standard temperature $T^\dagger = 130 + 273.15$ K.

Combination of eqns. A1, A2 and A4 gives

$$\Delta\mu_j^L - \Delta\mu_j^{(D)L} = RT \ln (\mathcal{R}T\rho_L) \quad (\text{A6})$$

where ρ_L is the density of the solvent. Eqn. A6 is the necessary relationship for the conversion of the function $\Delta\mu_j$ to that related to the distribution coefficient, $\Delta\mu_j^{(D)}$. Obviously, a knowledge of ρ_L over the whole temperature range is necessary.

(B) Properties of A–P mixtures of liquids applied

Compounds depicted in Fig. 1 have the same molar volume and are slightly polar. Consequently, their mixture will be nearly ideal so that in eqn. A7 the molar volume of the pure liquids, v_A and v_P can be used instead of partial molar volumes:

$$V_{A/P} = V_A + V_P = n_A v_A + n_P v_P \quad (\text{A7})$$

where V is volume and n the number of moles. Division of eqn. A7 by $V_{A/P}$ gives

$$1 = \varphi_A + \varphi_P = ([A]v_A/1000) + ([P]v_P/1000) \quad (\text{A8})$$

where φ is the volume fraction and $[A]$ and $[P]$ are the molar concentrations of A and P in the A–P mixture. The polar-type compounds in Fig. 1 are monofunctional. Therefore, the molar concentration of the molar group $[X] \equiv [P]$. From eqn. A8 follows the relationship between the volume fraction and the molar concentration of the polar groups in the A–P mixture:

$$\varphi_P = v_P[P]/1000 = v_P[X]/1000 \quad (\text{A9})$$

(C) Standard chemical potential of a solute in A–P and A–idP mixtures

In the nearly ideal A–P mixtures the standard chemical potential difference of the solute will be given with sufficient precision by the symmetrical function (regular mixtures) given in eqn. 3. The derivative of eqn. 3 at constant temperature gives

$$\left(\frac{\partial \Delta\mu_j^{A/P}}{\partial \varphi_P} \right)_T = \Delta\mu_j^P + (\varphi_A - \varphi_P) m_j^{A/P} \quad (\text{A10})$$

where Δ refers to chemical potential differences between the ideal dilute solution in P with reference to that in the non-polar standard, A, and $m_j^{A/P}$ describes deviations from linearity of the function $\Delta\mu_j^{A/P}(\varphi_P)$. In ideal A–P mixtures $m_j^{A/P} = 0$.

The slope of $\Delta\mu_j^{A/P}$ at $[P] = [X] = 0$ is calculated by using eqns. A9 and A10 to give eqn. 7 in the Introduction. The chemical potential in an ideal liquid P with reference to the standard non-polar liquid, A, is given by eqn. 8.

(D) Retention index in terms of chemical potential differences

The retention index is defined as

$$I_j^L = 100 \cdot \frac{\log V_{N,j}^L - \log V_{N,z}^L}{\log V_{N,z+1}^L - \log V_{N,z}^L} + 100z \quad (\text{A11})$$

where the net retention volumes of the n -alkanes with carbon numbers z and $z+1$, $V_{N,z}$ and $V_{N,z+1}$, are neighbours of the net retention volume of the solute, $V_{N,j}$. Substitution of either eqn. A1 or A2 or A3 and eqn. A4 in eqn. A11 results in the relationship of eqn. 10 in the Introduction.

(E) Retention index in A–P and A–idP mixtures

The retention index in A–P mixtures as a function of temperature and composition is given by the polynomial expression of eqn. 15 (see also eqns. 16–18). The relationship between retention index and thermodynamic functions is found by combination of eqns. 3, 10 and 11:

$$I_j^{A/P} = 100 \cdot \frac{\delta\mu_{jjz}^A + \varphi_P(\delta\mu_{jjz}^P - \delta\mu_{jjz}^A) + \varphi_A\varphi_P\delta m_{jjz}^{A/P}}{\delta\mu_z^A + \varphi_P(\delta\mu_z^P - \delta\mu_z^A) + \varphi_A\varphi_P\delta m_z^{A/P}} + 100z \quad (\text{A12})$$

It is important to stress that the retention index is not a linear function of the composition even in ideal A–P mixtures (all m_k are zero). The retention index in A–idP mixtures is found by combination of eqns. 9 and 10 to give

$$I_j^{A/idP} = 100 \cdot \frac{\delta\mu_{jjz}^A + [P](\delta'\mu_{jjz}^{idP} - \delta'\mu_{jjz}^A)}{\delta\mu_z^A + [P](\delta'\mu_z^{idP} - \delta'\mu_z^A)} + 100z$$

The functions in parentheses are marked with a prime, δ' , as they are formally the first derivative of a chemical potential with respect to $[P]$, and consequently their dimension (cal l mol^{-2}) is different from that of those without a prime. However, note that the numerical value of $\delta'\mu^A = \delta\mu^A$ and $\delta'\mu^{idP} = \delta\mu^{idP}$ ($[P] = 1 \text{ mol l}^{-1}$). The slope of the function $I_j^{A/idP}$ can now be calculated at constant temperature to give

$$\left(\frac{\partial I_j^{A/idP}}{\partial [P]}\right)_T = 100 \cdot \frac{\delta\mu_z^A \delta'\mu_{jjz}^{idP} - \delta\mu_{jjz}^A \delta'\mu_z^{idP}}{(\delta\mu_z^A)^2 (1 + [P]\kappa)^2} \quad (\text{A14})$$

where for simplicity

$$\kappa = (\delta'\mu_z^{idP} - \delta'\mu_z^A) / \delta\mu_z^A \quad (\text{A15})$$

In our mixtures the value of κ is very small. The value of the slope at $[P] = 0$ is given by

$$\begin{aligned} \left(\frac{\partial I_j^{A/idP}}{\partial [P]}\right)_{T,[P]=0} &= \left(\frac{\partial I_j^{A/P}}{\partial [P]}\right)_{T,[P]=0} \\ &= 100 \cdot \frac{\delta\mu_z^A \delta'\mu_{jjz}^{idP} - \delta\mu_{jjz}^A \delta'\mu_z^{idP}}{(\delta\mu_z^A)^2} \end{aligned} \quad (\text{A16})$$

Case 1. $\delta\mu_z^A$ and $\delta'\mu_z^{idP}$ (and consequently κ), I_j^A and the value of the slope of the retention index as a function of $[P]$ calculated from the polynomial of eqn. 15 (see eqn. 19) are known. In order to calculate the value of I_j^{idP} let us first rearrange eqn. A12 at $[P] = 0$ as follows:

$$100 \delta\mu_{jjz}^A = \delta\mu_z^A (I_j^A - 100z) \quad (\text{A17})$$

Combination of eqns. A17 and A16 gives, after rearrangement,

$$100 \delta'\mu_{jjz}^{idP} = \delta\mu_z^A \left(\frac{\partial I_j^{A/P}}{\partial [P]}\right)_{T,[P]=0} + \delta'\mu_z^{idP} (I_j^A - 100z) \quad (\text{A18})$$

Substitution of eqns. A17 and A18 in eqn. A13 gives, after simplifications, the necessary relationship for the calculation of I_j^{idP} at $[P] = 1$:

$$\mathcal{A}I_j^{idP} = \left(\frac{\partial I_j^{A/P}}{\partial [P]}\right)_{T,[P]=0} \frac{[P]}{1 + [P]\kappa} \quad (\text{A19})$$

Case 2. The A–P mixture is ideal ($m = 0$) and I_j^A and $\mathcal{A}I_j^P \equiv \mathcal{A}I_j^{idP}$ ($[P] = 1000/v_P$) are known. Substitution of $[P] = 1$ and $[P] = 1000/v_P$ in eqn. A19 and combination of the results gives the necessary relationship for the calculation of $\mathcal{A}I_j^{idP}$ from data in ideal A–P mixtures:

$$\mathcal{A}I_j^{idP} = \mathcal{A}I_j^P \frac{(v_P/1000) + \kappa}{1 + \kappa} \quad (\text{A20})$$

REFERENCES

- 1 G. A. Huber and E. sz. Kováts, *Anal. Chem.*, 45 (1973) 1155.
- 2 J. H. Hildebrand and R. L. Scott, *The Solubility of Non-electrolytes*. Reinhold. New York. 3rd ed.. 1950.

- 3 E. A. Guggenheim, *Mixtures*, Oxford University Press, Oxford, 1952.
- 4 P. J. Flory, *J. Chem. Phys.*, 9 (1941) 660.
- 5 P. J. Flory, *J. Chem. Phys.*, 10 (1942) 51.
- 6 P. J. Flory, *J. Chem. Phys.*, 12 (1944) 425.
- 7 M. L. Huggins, *J. Chem. Phys.*, 9 (1941) 440.
- 8 M. L. Huggins, *Ann. N.Y. Acad. Sci.*, 43 (1942) 1.
- 9 M. L. Huggins, *Ann. N.Y. Acad. Sci.*, 44 (1943) 431.
- 10 G. Défayes, D. F. Fritz, T. Görner, G. Huber, C. de Reyff and E. sz. Kováts, *J. Chromatogr.*, 500 (1990) 139.
- 11 R. Cloux, G. Défayes, K. Foti, J.-Cl. Dutoit and E. sz. Kováts, in preparation.
- 12 G. Körösi and E. sz. Kováts, *J. Chem. Eng. Data*, 26 (1981) 323.
- 13 D. F. Fritz, A. Sahil and E. sz. Kováts, *J. Chromatogr.*, 186 (1979) 63.
- 14 K. S. Reddy and E. sz. Kováts, *Chromatographia*, 30 (1990) 493.
- 15 R. L. Martin, *Anal. Chem.*, 33 (1961) 347.
- 16 R. A. Fisher and F. Yates, *Statistical Tables*, Oliver and Boyd, Edinburgh, 6th ed., 1963.
- 17 R. R. Krug, W. G. Hunter and R. A. Grieger, *J. Phys. Chem.*, 80 (1976) 2341.

Factor analysis and experimental design in high-performance liquid chromatography

XIII.★ Correspondence factor analysis of the heterogeneity of the behaviour of congeneric solutes series studied on homogeneous OV phases in gas chromatography

Jacques R. Chrétien

Laboratoire de Chimimétrie, Université d'Orléans, 45046 Orléans Cédex (France) and Institut de Topologie et de Dynamique des Systèmes, Associé au CNRS UA 34, Université Paris VII, 1 Rue Guy de la Brosse, 75005 Paris (France)

Michel Righezza

Laboratoire de Chimimétrie, Université d'Orléans, 45046 Orléans Cédex (France)

Aicha Hassani and Brahim Y. Meklati

Laboratoire d'Analyse Organique Fonctionnelle Systématique, Institut de Chimie, USTHB, El-Alia BP 32, Bab Ezzouar, Algiers (Algeria)

(Received March 13th, 1992)

ABSTRACT

A correspondence factor analysis (CFA) of gas chromatographic retention data, *i.e.*, Kováts retention indices, is presented. The data matrix correspond to aromatic congeneric solutes series, monosubstituted benzenes, benzaldehydes or acetophenones, studied on the same type of stationary phases, namely phenylmethylsilicone with various percentages of the phenyl substituent (0–75%). CFA of three reduced submatrices gives a trend analysis of the relative behaviour of solutes and of the relative influence of stationary phases and temperatures. CFA was found to be a sensitive detector of the relative heterogeneity between solutes and/or chromatographic systems, even for the study of congeneric compound series studied on stationary phases of the same type.

INTRODUCTION

Most often principal component analysis (PCA) is used to search for similarities in the chromato-

graphic behaviour of heterogeneous series of compounds [1]. However, PCA is not suitable for the analysis of closely similar data, such as chromatographic retention data relative to homogeneous or congeneric series of compounds. When there is a major factor that governs the chromatographic retention, *e.g.*, the vapour pressure in gas-phase chromatography, the contributions of the remaining factors are hidden. In such types of factor analysis,

Correspondence to: Dr. J. R. Chrétien, Laboratoire de Chimimétrie, Université d'Orléans, 45046 Orléans Cedex, France.

★ For part XII see B. Walczak, M. Dreux and J. R. Chrétien, *Chromatographia*, 31 (1991) 575–582 and for part. XI see ref. 11.

about 99% of the information content of the data matrix is taken into account with the first axis [2] and all the variables are strongly correlated.

The less often used correspondence factor analysis (CFA) is more appropriate for the analysis of homogeneous populations [2,3]. It can be used just as a classical clustering technique or as a detector of fine physico-chemical effects influencing the chemical activity of the studied compounds and/or of the selectivity of the stationary phases. CFA has been used, for example, for the analysis of a large set of Kováts retention indices of esters [2] and hydrocarbons [3]. In the latter instance, interesting results were obtained for simulation of the catalysis of hydrocarbons, for comparison of the interactions of zinc and nickel ions with alkenes, the data later being made more precise by topological analysis [4–6]. Such studies partially explain the interest devoted to factor analysis and to CFA in chromatographic structure–activity relationships (CSAR) with their extension to the field of liquid chromatography [4,7].

It must be emphasized that, like polarity, the heterogeneity of solutes and/or stationary phases is a relative concept. CFA has proved to be a valuable tool for evaluating the heterogeneities nested in a chromatographic retention data matrix [3], but it must be questioned whether this technique is able also to detect potential heterogeneity of more homogeneous chromatographic systems. For example, let us consider the previous example of esters [2]. This involves a large set of 1450 Kováts retention indices of 175 saturated and unsaturated aliphatic esters determined of fourteen polysiloxane stationary phases which were analysed by factor analysis. The series of compounds was congeneric, but variation in the polarity of the stationary phases was obtained with different percentages of different types of substituent groups, phenyl, cyanoethyl, trifluoroalkyl, trifluorophenyl, etc. The question now arises of whether the application of CFA could have been extended to the case of a homogeneous series of stationary phases by varying only the percentage of the same substituent to obtain phases of different polarities.

To go beyond the practical limit of application of CFA presented so far, for a homogeneous series of compounds, we selected a data matrix of Kováts retention indices of aromatic compounds deter-

mined on a homogeneous series of seven OV phenyl stationary phases. This matrix corresponds to 35 unsubstituted or monosubstituted benzene, aldehyde and acetophenone compounds, studied at different temperatures. A systematic chemometric analysis of heterogeneity inside homogeneous systems is presented with progressive CFA analysis of this large data set. The study of three complementary matrices will offer the possibility of explaining more subtle chromatographic factors.

DATA

The 35 compounds, presented Fig. 1, were eleven monosubstituted benzenes [including the unsubstituted benzaldehyde (AH) and acetophenone (CH)], fourteen *o*-, *m*- and *p*-substituted aldehydes and ten *o*-, *m*- and *p*-substituted acetophenones. These compounds were studied on seven OV methylphenyl-silicone phases. The phenyl compounds were studied in the range 80–140°C and the disubstituted phenyl compounds in the range 120–160°C [8,9].

Three different data matrices were studied. The first corresponds to 33 compounds of the three subseries: benzenes, aldehydes and acetophenones derivatives, that is, except the two compounds labelled BF and AoOM. These compounds were studied on all the OV stationary phases, except OV-22. The temperatures considered were 120°C for all these six phases plus 130 and 140°C for OV-11 and 130°C for OV-25. Hence this first data matrix regroups the data relative to 33 compounds studied in nine different chromatographic systems, including six different stationary phases and three temperatures effects.

The other two data matrices correspond to more homogeneous data sets. In the second matrix, the temperature is limited to 120°C. This matrix corresponds to all 35 compounds indicated in Fig. 1. In the third matrix, the subseries of compounds is limited to all the aldehydes and acetophenones, *i.e.*, to 26 compounds including the unsubstituted aldehyde (AH) and acetophenone (AC). This last case offers the possibility of treating the largest set of the chromatographic system, the seven OV phases considered at four different temperatures, 120, 130, 140 and 160°C, minus OV-25 at 140°C, that is, 27 different chromatographic systems.

a

Substituents:

X	H	F	CH ₃	Cl	OCH ₃	Br	OH	OC ₂ H ₅	NO ₂
Label:	H	F	M	Cl	OM	Br	OH	OE	NO

Compounds:

B :	BH	BF	BM	BCl	BOM	BBr	BOH	BOE	BNO
A :	AH	AoF AmF ApF	AoM AmM ApM	AoCl AmCl ApCl	AoOM AmOM ApOM	AoBr AmBr			
C :	CH	CoF CpF	CoM CmM CpM	CoCl CpCl		CpOM CpBr	CoOH		

B = X-C₆H₅ **A** = X-C₆H₄-CHO **C** = X-C₆H₄-CO-CH₃

b

MATRIX 1

T°C	OV101	OV3	OV7	OV11	OV17	OV25	OV22
120	B	AC	B	AC	B	AC	B
130	AC	AC	AC	AC	AC	AC	AC
140	AC	AC	AC	AC	AC	AC	AC
160	AC	AC	AC	AC	AC	AC	AC

MATRIX 2

T°C	OV101	OV3	OV7	OV11	OV17	OV25	OV22
120	B	AC	B	AC	B	AC	B
130	AC	AC	AC	AC	AC	AC	AC
140	AC	AC	AC	AC	AC	AC	AC
160	AC	AC	AC	AC	AC	AC	AC

MATRIX 3

T°C	OV101	OV3	OV7	OV11	OV17	OV25	OV22
120	B	AC	B	AC	B	AC	B
130	AC	AC	AC	AC	AC	AC	AC
140	AC	AC	AC	AC	AC	AC	AC
160	AC	AC	AC	AC	AC	AC	AC

B: benzene series
A: benzaldehyde series
C: acetophenone series

Fig. 1. (a) The 35 substituted phenyl compounds: benzenes (B), benzaldehydes (A) and acetophenones (C). The label for a compound consists of the label of its substructure A, B or C, plus the position of the substituent, *ortho* (*o*), *meta* (*m*) or *para* (*p*) for the disubstituted ones, plus the label of the substituent X. (b) Table of the experimental design: chromatographic system and considered data matrices. The columns of the matrix indicate the stationary phase type and the rows indicate the temperature. The compounds series are indicated by their labels A, B or C. The submatrices submitted to CFA are indicated by a dashed-line box for the first, a solid-line box for the second and a dot-dashed-line box for the third.

DATA PROCESSING

Factor analysis is particularly effective as a method of extracting information from large data sets. Among the variants of this technique CFA, devel-

oped by Benzécri [10], is more suitable for the analysis of relatively homogeneous series of data. The basic principles of CFA have been presented previously [3] and will not be repeated here. Owing to the normalizations used in this method, the compounds

The study of this large set of compounds and phases used with some temperatures effects shows that differences in behaviour can be detected at different levels. The CFA detects differences with an average behaviour calculated from the experimental data matrix. The compounds or phases that have this average behaviour are projected at the centre of the graph. The compounds or phases that can be deduced from each other by a proportionality relationship have the same projection. In Fig. 2, the compounds or phases that have different projections, *i.e.*, with no proportionality relationships between them, are significantly different.

The projection area of the benzene derivatives is more scattered than that for the other two subséries of carbonylated compounds. However, the temperature effects must also be taken into account. These temperature effects partially hide the potential structural variations between aldehydes and acetophenones.

A second matrix without temperature effects must be considered. This matrix includes the six OV phases used at the same temperature of 120°C. The corresponding CFA is presented Fig. 3 in the form of the first factorial plane. This factorial plane in-

cludes 79% of the information content, 57% for axis 1 and 22% for axis 2. The information content of the similar first factorial plane for the preceding matrix was 67% owing to a greater dispersion of the information induced by two supplementary temperatures corresponding to three supplementary chromatographic systems (OV-11 at 130 and 140°C and OV-25 at 130°C). This graph, corresponding only to Kováts retention indices determined at 120°C, shows the same trends. Axis 1, determined by OV-101 and OV-25, reflects polarity. The projection order of compounds on the first axis is similar. The greatest variations of dipolar moment are for the substituted benzenes. They induce a greater dispersion of the representative points of the compounds. Axis 2 offers a better discrimination of the three series of compounds. The most deactivated compounds, *i.e.*, benzaldehydes, acetophenones and nitrobenzene, are on the right-hand part of the diagram and the less polar compounds, with donor substituents, are on the left.

To improve the sensitivity of the CFA analysis for the partially hidden disubstituted compounds, a new matrix will be considered. The set of mono-substituted benzenes which contribute the most to

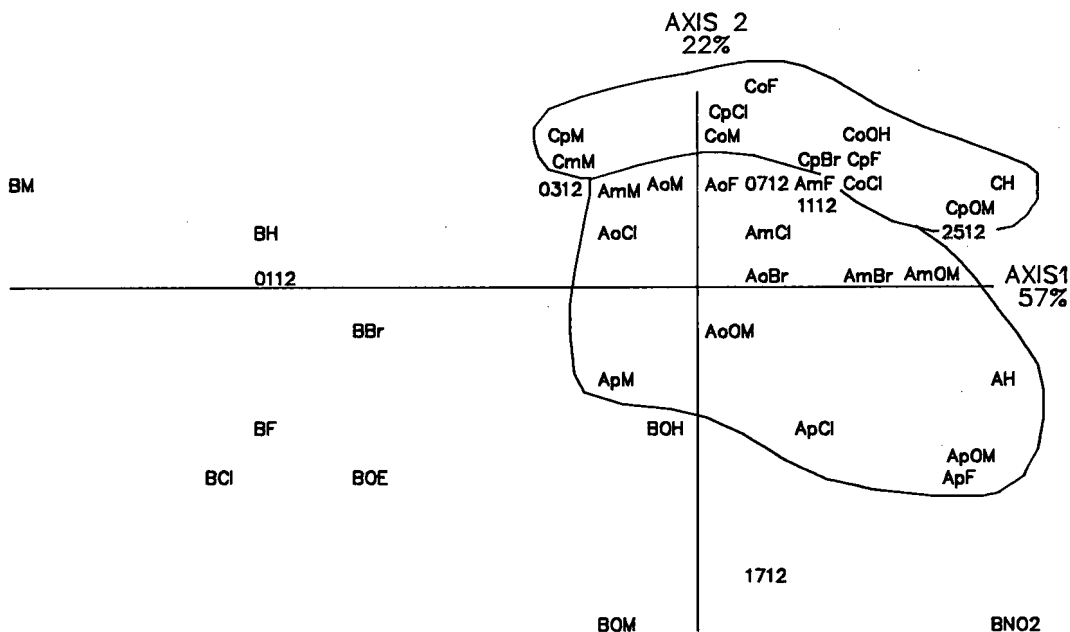


Fig. 3. CFA of the second matrix including the three subséries without temperature effects. The projection on the first factorial plane shows a better discrimination between the two substituted series, acetophenone and benzaldehyde.

the information content in the two previous analyses are removed. Then only the two more similar carbonylated subseries remain. A more extensive study of temperature effects can be envisaged simultaneously.

The third matrix is then based on a more homogeneous population including only carbonylated compounds, *i.e.*, substituted benzaldehydes or acetophenones. It includes a wider heterogeneity dealing with temperature effects by using the seven stationary phases OV-101, OV-3, OV-7, OV-11, OV-17, OV-22 and OV-25 at four temperatures, 120, 130, 140 and 160°C, except for OV-25 at 140°C. This represents a set of 26 compounds studied in 27 different chromatographic systems.

Projection on the first factorial plane is given Fig. 4. The plane includes 72% of the information content, 45% according to the first and 27% according to the second axis. This graph presents an interesting relationship order. A clear separation of the two

series of compounds is observed. Comparison with Fig. 3, corresponding to the second matrix, shows an apparent rotation of about 45° of the compound clusters due to the absence of monosubstituted phenyl compounds. The comparison of Figs. 3 and 4 shows that the first axis is rotated counterclockwise. The better separation of the two series is due to the absence of the levelling effect of the monosubstituted phenyl series, with its important variation of the electronic effects of the substituent reflected in the variation of the dipolar moments.

The two populations, aldehydes and acetophenones, constitute two clouds admitting the origin of the axes 1 and 2 as a centre of symmetry, or, more precisely, the first bisector as an axis of symmetry. The better separation of the two chemical series according to their corresponding cloud is given by the first bisector. The variation of the polarity of the stationary phases is introduced by the second bisector, from the non-polar OV-101 up to the most po-

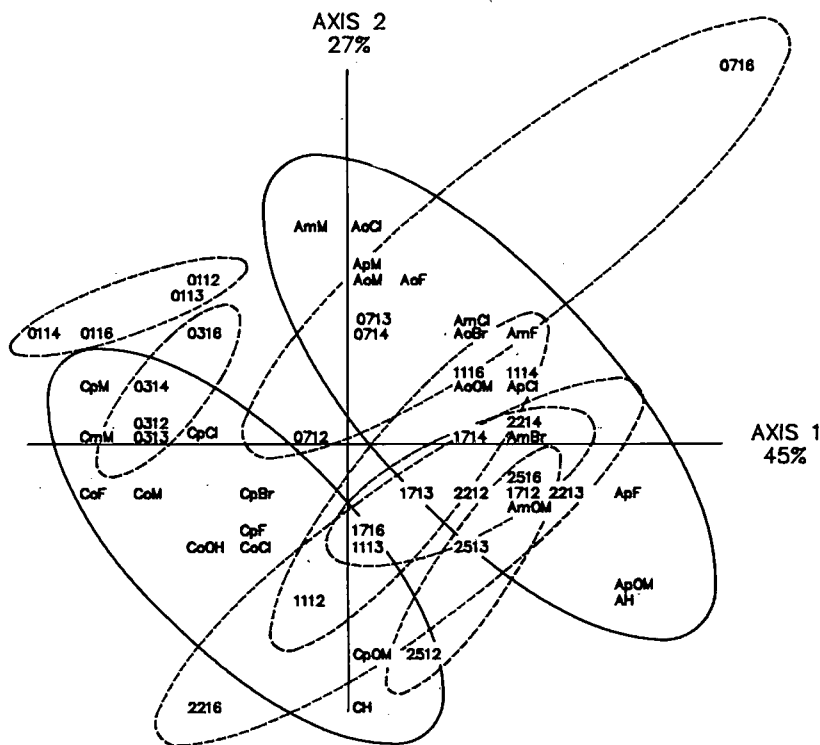


Fig. 4. CFA of the third matrix limited to carbonylated compounds with maximum temperature effects. Projection on the first factorial plane. A total discrimination is observed between the two disubstituted series acetophenone and benzaldehyde, circled with solid lines. Temperature effects, circled with dashed lines, are oriented according to the first bisector.

lar OV-25. Comparison of Figs. 2 and 4 shows that axes 1 and 2 in Fig. 2 play a similar role to the first and second bisectors, respectively. We have shown in Fig. 2 that the temperature effect with OV-11 was parallel to axis 2. In Fig. 4, the temperature effect is parallel to the corresponding first bisector. The general trends of the temperature effects are directed according to the first bisector. Increasing temperatures are noticed in this direction except for the non-phenyl-substituted OV-101, a methylsilicone, and for OV-22 studied at 160°C, labelled 2216, which shows a relatively large Df/dT variation in the range 140–160°C. For these two exceptions the directions of these temperatures effects are opposite to the preceding ones.

We could have considered also a “supplementary” Fig. 2, not given here, which corresponds to a CFA of the first matrix but with a projection on the second factorial plane, defined by factorial axes 3 and 4. The analogy between this “supplementary” figure and Fig. 4 must be stressed. In Fig. 2, the major contribution of the monosubstituted phenyl derivatives to the information content is taken into account by axes 1 and 2. Hence the resulting information corresponding to the two disubstituted phenyl derivative series is given chiefly and more clearly in the “supplementary” Fig. 2. In Fig. 4 the corresponding data matrix is strictly independent of the monosubstituted benzene series. This first factorial plane is a pure contribution of the aldehydes and acetophenones studied at different temperatures. Despite three supplementary temperatures (OV-11 at 130 and 140°C and OV-25 at 130°C) in Fig. 2, the level of similarities between the CFA of matrices 1 and 3, that is, between the “supplementary” Fig. 2 and Fig. 4, was not so evident, *a priori*.

The influence of a relatively limited effect on Kováts retention indices, such as the temperature effect, introduced only by three supplementary temperature effects can produce non-negligible perturbation. On comparing Fig. 2 and 3, a modification of the ordering of the three chemical series is observed. In Fig. 3, the cluster of acetophenones is lost among the aldehydes. The contribution of axis 3, *i.e.*, factorial plane 2-3, must be considered also to observe a clear separation between these three chemical series.

CONCLUSION

Despite the strong homogeneity of the data matrix, due to the choice of congeneric series of aromatic solutes analysed on the same type of phenylsilicone stationary phases, the present study demonstrate that CFA is a sensitive detector of the relative heterogeneity between solutes and/or stationary phases. The so-called heterogeneity corresponds to deviations from proportionality between rows or columns of the data matrix, that is, between particular compounds or between particular chromatographic variables.

The possibility of taking homogeneous systems, such as congeneric compound series and stationary phases of the same type, offers the possibility of identifying weak structural, electronic, polarity or temperature effects. To emphasise this point, let us consider the case of another experimental design, with a higher degree of heterogeneity of the compounds and/or of the stationary phases. The projection of the compounds considered here would have been much less scattered and the corresponding factors, detected here, more or less hidden.

A progressive study with CFA of particularly chosen submatrices helps to delineate more precisely the abstract and/or the real factors which govern the chromatographic process.

REFERENCES

- 1 G. Musumarra, G. Scarlata, G. Romano, S. Clementi and S. Wold, *J. Chromatogr. Sci.*, 22 (1984) 538–547.
- 2 K. Szymoniak and J. R. Chrétien, *J. Chromatogr.*, 404 (1987) 11–22.
- 3 R. F. Hirsch, R. J. Gaydosh and J. R. Chrétien, *Anal. Chem.*, 52 (1980) 723.
- 4 J. R. Chrétien, *Trends Anal. Chem.*, 6 (1987) 275–278.
- 5 J. R. Chrétien, J. E. Dubois, R. F. Hirsch and R. J. Gaydosh, *J. Chromatogr.*, 207 (1981) 115–130.
- 6 J. R. Chrétien, K. Szymoniak, J. E. Dubois, R. F. Hirsch and R. J. Gaydosh, *J. Chromatogr.*, 294 (1984) 1–14.
- 7 R. J. Kalishan, *Quantitative Structure Chromatographic Retention Relationships*, Wiley, New York, 1987, p. 224.
- 8 A. Hassani and B. Y. Meklati, *Chromatographia*, 33 (1992) 267–272.
- 9 A. Hassani and B. Y. Meklati, in preparation.
- 10 J. P. Benzécri, *L'Analyse des Données*, Vol. 2, Dunod, Paris, 1973.
- 11 M. Righezza and J. R. Chrétien, *J. Chromatogr.*, 556 (1991) 169–180.

Liquid jet evolution from a gas chromatographic injector

J. Qian[☆], C. E. Polymeropoulos and R. Ulisse

Department of Mechanical and Aerospace Engineering, Rutgers University, P.O. Box 909, Piscataway, NJ 08855-0909 (USA)

(Received March 6th, 1992)

ABSTRACT

Liquid particles from the breakup of liquid jets produced by a gas chromatographic syringe autoinjection system were observed and measured experimentally. The particle size depended on the motion of the syringe plunger. Very large, fast-moving particles were observed during accelerating periods of the liquid jet. The injection test chamber temperature affected the downstream particle size by heating the liquid before it left the needle and by evaporation into the hot gas. The particles produced by the water and heptane samples used were large and did not lend themselves to rapid vaporization within the gas stream of the gas chromatographic inlet port. Under such conditions, total sample vaporization must be considered either on the hot inlet port wall or on inserts within the inlet port.

INTRODUCTION

A common method of sample introduction into a gas chromatograph is injection via a microliter syringe into a heated inlet port. The liquid jet from the needle breaks down into particles which evaporate in the carrier gas stream, by interaction with inserts within the inlet port or in contact with the hot inlet port wall. Reproducible rapid vaporization and uniform mixing of the resulting sample vapor with the carrier gas are important for proper separation of the liquid sample components and for determining or minimizing different discrimination errors. Rapid sample vaporization may, however, result in pressure excursions within the inlet port, which can alter the flow-rate through the column [1].

The evaporation rate of the liquid particles produced during an injection depends on their initial size and velocity. The mechanism of liquid jet breakup and particle formation from a sample

injector is therefore the first step in the study of inlet port injection performance, and constitutes the subject of this investigation. As it turns out, the size of the particles produced is relatively large and does not lend itself to the commonly perceived flash vaporization process within the carrier gas stream, even at high inlet port temperatures. This leaves interaction with the hot wall or with inserts as the dominant mechanism for vaporization. Additional considerations are that the injection process using a syringe involves plunger motions which are not smooth, resulting in liquid jets with intermittent or variable injection speeds, and that the mechanical motion of the plunger may result in needle tip oscillation producing jets with large lateral motions.

This investigation is the first in a series aimed at examining liquid jet breakup from a commonly used autoinjection system. The specific aims of this work were to record the liquid injection process and to measure the size of particles injected into a simulated inlet port. A needle support system that eliminated large-amplitude lateral motion of the needle tip, and of the emerging liquid jet, allowed conclusions on the ability to generate particles for different fluids and ambient temperatures and on the general requirements for sample vaporization. The sample size used was large (5 μ l) to permit a clear identification of the

Correspondence to: Dr. C. E. Polymeropoulos, Department of Mechanical and Aerospace Engineering, Rutgers University, P.O. Box 909, Piscataway, NJ 08855-0909, USA.

[☆] Present address: Graduate Program, Department of Mechanical Engineering, Princeton University, Princeton, NJ 08544, USA.

different periods during autoinjection. In addition, elevated temperature results were obtained by preheating the gas stream in addition to the wall. Although preheating the gas stream is not part of the chromatographic system under consideration, its use in the present experimentation resulted in a uniform test section environment and permitted easier interpretation of the experimental findings. The majority of the present data were with pure heptane and water as sample liquids to provide variation in surface tension and latent heat of vaporization.

The breakup of a laminar liquid jet issuing from a small orifice has been the subject of numerous experimental and analytical investigations because of its practical importance in the understanding of liquid droplet formation in sprays, in the generation of controlled droplet streams, etc. Several reviews [2,3] can be consulted for treatment of different aspects of the process. Of primary interest has been the amplification of disturbances and drop formation in laminar jets [4–8], jet breakup length [9–11], the influence of ambient and liquid properties and the aerodynamic effect of the surrounding gas [5,8,12–15], etc. Results from these and other previous works will be used as necessary in the discussion of the experimental findings of this work.

EXPERIMENTAL

Fig. 1 is a schematic diagram of the experimental apparatus. The sample injection process employed an autoinjector (Model 7673A automated sampler; Hewlett-Packard) discharging into a heated test section at ambient pressure. Both the test section and the injector were bolted on to a heavy brass plate mounted on a movable platform. A low-speed (18 cm/s), heated air flow was maintained through the test section, which was also equipped with

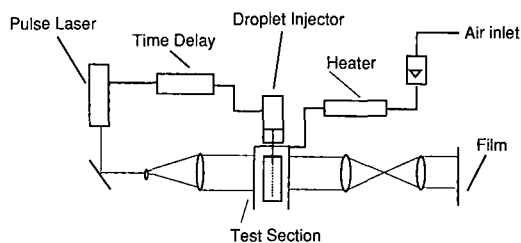


Fig. 1. Schematic diagram of the experimental apparatus.

windows for photographic observation of the liquid jet and of the resulting particles. The photographic system employed parallel light from a pulsed (17-ns pulse duration) ruby laser which was triggered via a time delay connected to the control box of the automated injector. The photographic set-up could also be used to record in-line holograms to avoid depth of field problems with measuring small-sized particles at different object distances from the plane of focus. For this work the negatives were evaluated manually using appropriate enlarging optics with a video camera and monitor. Holograms were reconstructed using a helium–neon laser and then evaluated using the same video–monitor system.

Fig. 2 is a more detailed diagram of the test section showing the position of the syringe needle during injection. The needle used was 5 cm × 150 mm I.D. × 650 mm O.D. For the flow-rate and fluids tested, this resulted in fully developed flow at the needle exit. The test section I.D. was 6 cm, and was equipped with two sets of 4 cm wide and 5 cm long quartz windows for photographic observation of the liquid jet and of the resulting particles. The windows were positioned so that one set allowed observation of the liquid in the vicinity of the needle exit, where the jet breakup occurred, and the second set was used for observation of liquid particles to a maximum distance of 15 cm from the needle tip. As shown in Fig. 2, the needle entered the test section through an opening (1 mm in diameter) machined into a 2.5 cm diameter and 3.5 cm long aluminum cylinder attached to the top of the test section. The purpose of this cylinder was to support two rubber

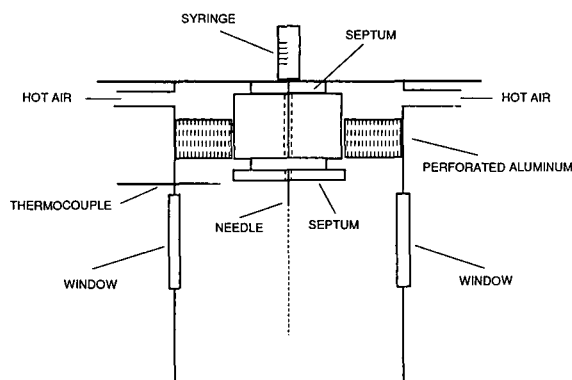


Fig. 2. Test section inlet.

septa 3 mm in diameter and 0.7 mm thick as shown in Fig. 2. The septa sealed the test section entrance, and also provided damping of lateral vibrations of the needle. The needle length was 4 cm and its tip extended 3 mm beyond the second septum.

Air was introduced through the test section using two 4 mm diameter inlet ports and a perforated aluminum plate positioned downstream from the inlets to smooth the gas flow. Two bare thermocouples were used for temperature monitoring and control of the air heater and of the heating tapes which were wrapped around the test section wall. This resulted in almost isothermal conditions within the injection environment. This was verified using a separate movable thermocouple probe with which the maximum temperature difference between any two points within a radius of 2 cm along the test section axis was found to be 2%. The range of temperatures tested was between 20 and 270°C, and the liquids injected were pure heptane and pure water.

Heat transfer from the test section resulted in an increase in the temperature of the syringe and of the fluid inside the sample vial. A separate set of thermocouples were used to check the injector and vial temperatures, which were found to be *ca.* 25°C higher than ambient at the highest test section temperature used. In addition, for the present test conditions, the needle required 100 ms before it reached its final position inside the test section. The combination of higher syringe and fluid temperatures together with the heating of the sample as it passed through the heated syringe during injection will be considered in the interpretation of the experimental results. The liquid speed at the needle exit was calculated from the speed of the syringe plunger, which was recorded on 16-mm film using a high-speed motion picture camera.

RESULTS AND DISCUSSION

Injection periods

Fig. 3 shows the temporal variation of the mean liquid jet speed at the needle exit. For the incompressible liquids used the jet speed was calculated from the measured speed of the syringe plunger motion (also shown in Fig. 3) and the known ratio of plunger to syringe diameter. Fig. 3 shows three distinct periods during the 61-ms injection process,

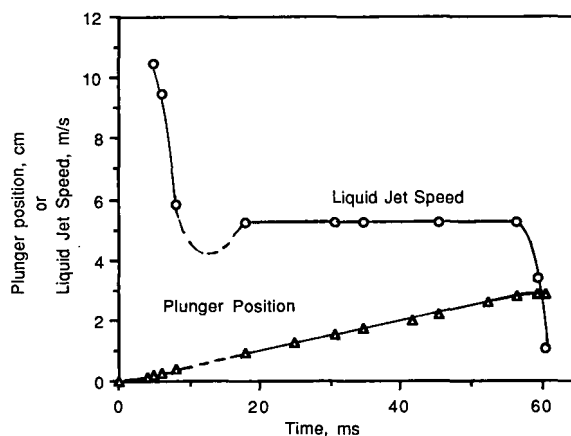


Fig. 3. Syringe plunger position and liquid jet speed during injection.

which are attributed to interactions among the electromechanical components of the injector: (a) an initial unsteady period (0–20 ms) where the jet speed first increased to a maximum of about 10.5 m/s within the first 5 ms and then changed irregularly for the next 15 ms; (b) a steady injection period lasting about 38 ms, where the jet speed was 5.3 m/s; and (c) a final short, *ca.* 3 ms period where the speed dropped to zero as the liquid was depleted. The data for the period between about 10 and 18 ms were insufficient to resolve accurately the shape of the liquid speed curve, and the dashed line was drawn to reflect the observed liquid jet behavior from photography. It should be noted that superimposed on the relatively long time-scale speed variations shown in Fig. 3, the liquid jet was also subjected to small-amplitude, high-frequency disturbances from the injector electromechanical system and from the laboratory environment. These disturbances were amplified resulting in the jet breakup, as will be discussed in the following sections.

Table I gives a summary of the experimental parameters tested and of the steady injection period jet Reynolds and Weber numbers calculated using the steady speed of the jet. The Reynolds numbers at 20°C show that both the water and heptane jets were laminar. At the higher temperature shown (70°C), the Reynolds numbers were near the upper limit of the laminar regime and the jets would be expected to show sensitivity to hydrodynamic disturbances. The Weber numbers for water were sufficiently low for

TABLE I
SUMMARY OF EXPERIMENTAL CONDITIONS

Sample liquids	Water, heptane	
Sample size	5 μ l	
Jet diameter, D_j	150 μ m	
Injection time	60 ms	
Test section pressure	1 atm	
Test section temperature	20–270°C	
Jet Reynolds number, $V_j D_j / \nu$, at:	20°C	70°C
Water	760	1900
Heptane	1300	2000
Jet Weber number, $\rho D_j^2 / \sigma$, at:	20°C	70°C
Water	0.07	0.07
Heptane	0.26	0.26

Rayleigh breakup [2] of the jet, meaning breakup by the growth of axisymmetric oscillations induced by surface tension. For heptane, the larger Weber numbers place the jet breakup mode within the regime where aerodynamic forces augment the effect of surface tension [2]. The resulting oscillations wavelengths and droplet sizes produced are therefore expected to be smaller for heptane samples [2].

In the following sections, findings related to the initial unsteady and steady-state periods are discussed. The final short, unsteady period at the end of the injection involves a relatively small fraction of the sample and will be examined in future work.

Initial unsteady injection period

Fig. 4a and b show a heptane jet 3 ms after the beginning of injection for 20 and 212°C test section temperatures, respectively. The acceleration of the

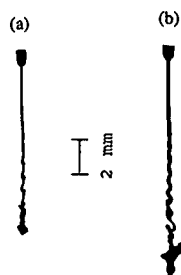


Fig. 4. Heptane jet, initial unsteady period, 3 ms after beginning of injection. (a) 20°C test section temperature; (b) 265°C test section temperature. The needle tip is visible at the top of the photograph.

liquid noted in Fig. 3 resulted in the formation of a large liquid particle at the leading edge of the jet. In addition, during the accelerating period at the beginning of injection, the syringe plunger motion caused intermittent lateral oscillations of the needle tip which show as high-frequency sinuous disturbances on the emerging jet. The speed of the jet leading edge, and of the large particle formed, were around 10 m/s as measured using photographs taken at different times from the beginning of injection.

For the heptane jets in Fig. 4, the leading edge particle (with initial typical major dimension of 1000 μ m) had an irregular shape and tended to disintegrate into smaller particles as it travelled downstream. For water jets (not shown), the higher surface tension of water maintained integrity of the large leading edge particle as it travelled through the test section. Particle Weber numbers based on the major particle dimension were *ca.* 6 for heptane and 1.5 for water, and confirm the observed difference in the disintegration process. Additional large particles were also observed during the period between 15 and 20 ms during the irregular motion of the plunger, which is indicated by the dashed line in Fig. 3. The production of such particles was attributed to rapid changes in the jet speed during this period.

The implications of these observations are that the unsteady jet period can produce appreciably sized particles which move at high speeds, *i.e.*, which are not amenable to rapid vaporization, at least within the air stream. Such large particles may also be a significant fraction of the sample size, especially for small injected samples. In such cases rapid vaporization within the inlet port must be accomplished using liquid contact with heated insert surfaces.

Steady injection period

Fig. 5a shows the initial breakup of a water jet in 20°C ambient gas, and Fig. 5b shows the resulting droplets at a mean distance of 12 cm from the needle tip. Fig. 5c and d show similar photographs for a heptane jet. Fig. 5a and c show that the jet breakup was the result of the growth of capillary waves arising from disturbances in the injector environment. The size of the particles produced depended on the wavelength before breakup and both main and satellite droplets were observed. Fig. 5a and c also show evidence of coalescence of droplets after

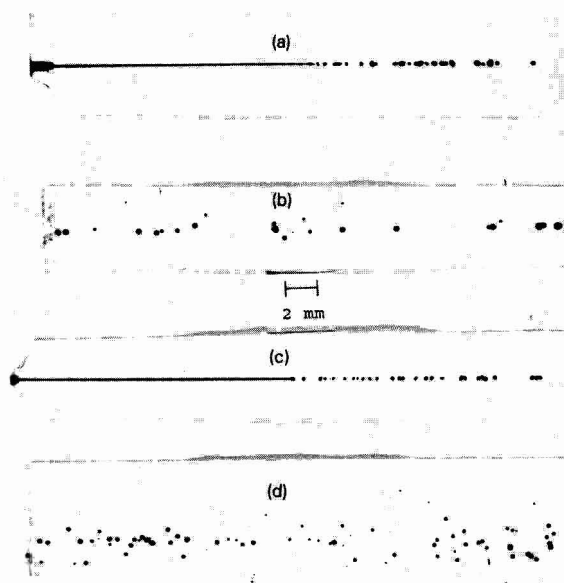


Fig. 5. Steady-state period, 20°C test section temperature. (a) Water jet, 40 ms after the beginning of injection; (b) water particles, 12.5 cm from needle tip, at 50 ms; (c) heptane jet, 50 ms; (d) heptane particles, 12.5 cm from needle tip, 45 ms.

breakup. Fig. 5b and d show that around 12 cm from the needle tip the heptane jet droplets were smaller and showed considerably more radial dispersion than water droplets. The larger droplets from the water jet were due to coalescence between particles moving along the same axis. As is indicated in Fig. 5d, heptane droplets tended to disperse by several millimeters in the radial direction, thus minimizing the probability of coalescence. The magnitude of the observed particle radial dispersion was of the order of the inside radius of typical inlet port inserts. This suggests that during a chromatographic injection significant sample vaporization takes place on the hot insert wall. In addition, lateral oscillations of the needle during injection (such oscillations were mostly suppressed in this work) will promote wall vaporization.

Fig. 6 presents measured mean particle sizes as a function of distance from the needle tip for a 20°C test section temperature. The data are for at least 100 particles per point measured from different photographs taken using the same time delay after the start of injection, and the size of non-spherical

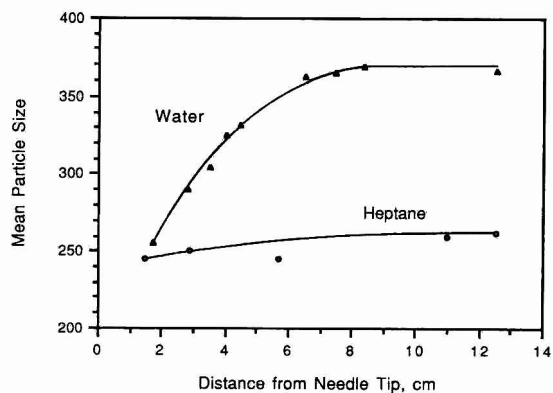


Fig. 6. Variation of arithmetic mean particle size with distance from the needle tip, at 20°C test section temperature. Mean particle size in μm .

particles was recorded as the mean of two major dimensions. For water the coalescence effect shows as a gradual increase in the size of the droplets. There was a very small size increase for heptane particles. Fig. 6 also shows that the mean particle size right after the jet breakup was 256 μm for water. This compares favorably with the value of 260 μm predicted from axisymmetric stability theory at the wavelength of maximum disturbance amplification [16]. For heptane the mean measured particle size near the jet breakup was 245 μm , which is smaller than that for water. The difference is due to the higher jet Weber number for heptane (Table I), which, according to calculations from stability theory, including the aerodynamic influence of the ambient gas [16], yields a slightly shorter wavelength for maximum disturbance amplification.

Fig. 7 shows a typical breakup of a heptane jet for a test section temperature of 265°C. It is noted that the jet surface before breakup was irregular at high temperature and that this resulted in segmentation of the jet. This behavior was typical at elevated test section temperatures and was also observed with water samples. The irregular appearance of the jet

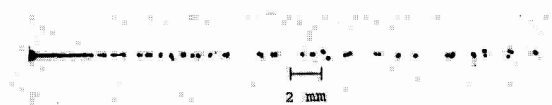


Fig. 7. Heptane jet, at 265°C test section temperature, 40 ms after the beginning of injection.

TABLE II
ESTIMATION OF DROPLET PREHEAT TIME

Liquid	Initial droplet diameter (μm)	Temperature ($^{\circ}\text{C}$)	Preheat time (ms)
Water	284	265	73
Heptane	278	265	7

surface at elevated test section temperatures is attributed to increased sensitivity of the jet to hydrodynamic disturbances as the jet Reynolds number was increased due heating of the fluid during injection (Table II). Liquid heating during the injection process is influenced by the temperature reached during the initial 100 ms period as the needle enters the heated test section and by the convection process within the syringe as the liquid is pushed out. It is currently difficult to make an accurate prediction of the liquid temperature at the needle exit because of lack of reliable data on the time-varying heat transfer coefficient between the needle outside surface and the hot ambient gas. It is possible, however, to demonstrate that significant heating takes place inside the needle by using a sample fluid of relatively low boiling point and showing that, at a sufficiently high test section temperature, there is evidence of boiling at the needle exit. Fig. 8a and b show a hexane sample

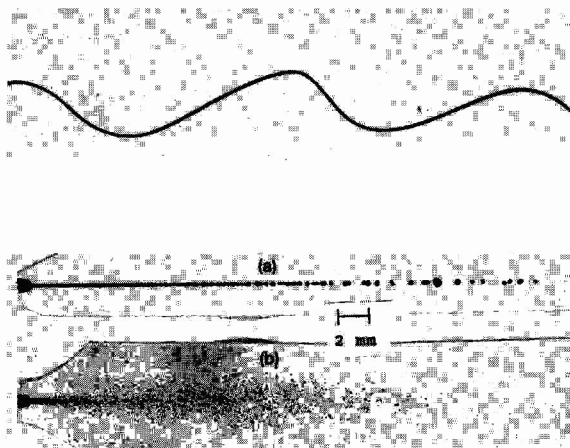


Fig. 8. Hexane jet, 50 ms after the beginning of injection. (a) 20 $^{\circ}\text{C}$ test section temperature; (b) 300 $^{\circ}\text{C}$ test section temperature.

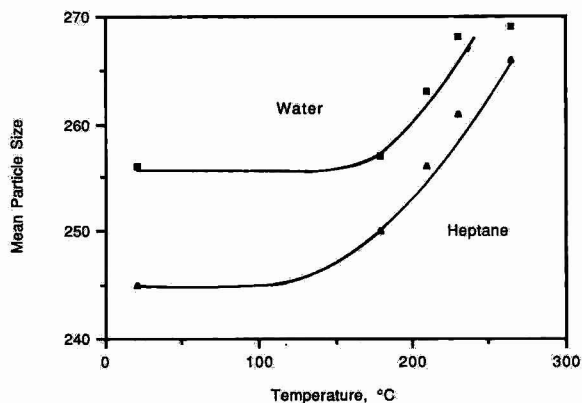


Fig. 9. Variation of the arithmetic mean particle size near the jet breakup with test section temperature. Mean particle size in μm .

injected into the test section at 20 and 300 $^{\circ}\text{C}$, respectively. The large number of small droplets evolving at the needle exit for the high test section temperature is attributed to boiling conditions within the needle. For hexane this means a temperature of at least 68.7 $^{\circ}\text{C}$, which is the normal boiling point of hexane.

The appearance and amplification of irregular disturbances on the jet resulted in jet segmentation, which is evident in Fig. 7. The liquid segments subsequently collapsed into large particles with the net result that the mean particle size after breakup increased as the test section temperature increased. This is indicated in Fig. 9, where the test section

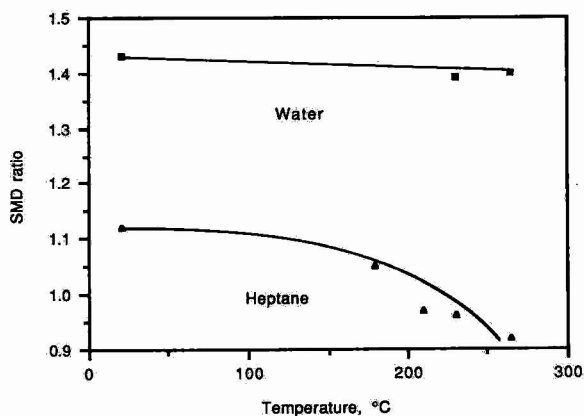


Fig. 10. Ratio of particle Sauter mean diameter at a distance of 12.5 cm from the needle tip to that at jet breakup, as a function of test section temperature.

temperature is plotted against the arithmetic mean particle size for both liquids tested.

The downstream development of particle size at elevated temperatures is suggested by the results in Fig. 10, where the ratio of the Sauter mean diameter 12.5 cm from the needle tip to that after breakup is plotted against the test section temperature (the Sauter [2] mean diameter is used here because it is appropriate for evaporating particles). At low temperatures, this ratio was larger than unity for both samples tested, which is consistent with the results in Fig. 4. As the test section temperature was increased the Sauter mean diameter ratio for water particles increased whereas that for heptane decreased. This is because for the water samples coalescence, which increased the particle size, predominated over the decrease in size due to evaporation. For heptane particles, however, vaporization predominated, resulting in a net decrease in particle size. It is not possible to separate the opposing effects of coalescence and vaporization on particle size. An estimate of incipient vaporization can, however, be furnished by estimating the preheat time, which is the time needed for a water or heptane droplet to reach its equilibrium temperature. This can then be compared with the residence time in the hot environment to estimate the time available for vaporization. Table II shows estimated droplet preheat times calculated using the relationships shown in the Appendix. The preheat times were *ca.* 73 ms for water and only 7 ms for heptane for conditions appropriate to a 265°C test section temperature. The particle residence time travelling at a speed of 5 m/s within the 12.5-cm test section distance is calculated to be *ca.* 24 ms. This shows that the heptane particles were subjected to steady-state vaporization conditions for about 17 ms, whereas water particles did not reach conditions for significant vaporization.

CONCLUSIONS

The breakup of water and heptane liquid jets under conditions encountered with sample auto-injection in a gas chromatograph injection port was examined experimentally using 5- μ l samples injected in 61 ms. The specific aims of this work were to measure the size of particles produced with different injection port temperatures in the range 20–270°C and to relate the measurements to conditions relevant to actual sample injections.

It was shown that the motion of the syringe plunger during injection is of primary importance. The initial unsteady (0–20 ms) period of unsteady plunger motion produced large, fast-moving particles which were not subject to rapid vaporization. The subsequent (20–59 ms) steady-state injection period produced particles which conformed to jet breakup stability theory at low test section temperatures. Radial dispersion of the heptane particles was significant, and of the order of a gas chromatographic insert diameter, indicating the importance of liquid vaporization on the insert wall during injection.

At high temperatures, heating of the liquid during injection increased the jet Reynolds number to near the upper limit for laminar jet flow. This resulted in irregular breakup and segmentation of the jet, producing larger particles after the jet as the test section temperature was increased. For heptane samples injected into high test section temperatures, the particle size decreased with distance from the needle tip, while particles from water samples increased in mean size under the same conditions. This was shown to be the result of the competing effects of coalescence and evaporation.

This work is being extended to include examination of various parametric effects, such as sample size, injection speed and sample type, on the particles produced. The work will also include high-speed motion pictures of the liquid jets and of the particles produced, and a more detailed examination of liquid heating inside the syringe and the needle.

ACKNOWLEDGEMENT

We acknowledge the support of Hewlett-Packard, Avondale Division, for providing equipment necessary for carrying out this work.

APPENDIX

Determination of droplet preheat time

Heat transferred into a liquid droplet which is introduced into a hot environment initially increases the liquid temperature and also contributes to liquid vaporization. Eventually the droplet may reach equilibrium conditions where the temperature remains constant with time and all the heat transferred is used for quasi-steady vaporization. For the relatively large water droplets and ambient conditions

considered, vaporization during the unsteady heat-up period is negligible and calculation of the heat-up time can be carried out using a constant-diameter sphere. Under the assumption of a uniform droplet temperature $T(t)$, an energy balance for a droplet of diameter D initially at temperature T_0 moving inside a hot environment at T_a yields the following relationship for the time, t , to reach different droplet temperatures [17]:

$$t = \frac{\rho C_1}{6K_g(2 + 0.6Re^{0.5})} \cdot D_0^2 \ln \left(\frac{T_a - T_0}{T_a - T} \right) \quad (\text{A1})$$

where ρ and C_1 are the liquid density and specific heat, respectively, K_g is the gas thermal conductivity, $Re = VD/\nu$ is the droplet Reynolds number based on the droplet speed, V , and ν is the kinematic viscosity of the gas. Eqn. A1 is solved for the preheat time, t_s , for which the droplet temperature reaches its equilibrium value, T_s , given by the following equation for quasi-steady vaporization [18]:

$$\frac{Y_s}{1 - Y_s} = \frac{C_g(T_a - T_s)}{L} \quad (\text{A2})$$

where C_g is the vapor specific heat at constant pressure, L is the latent heat of vaporization and Y_s the equilibrium vapor mass fraction, is given by the Clausius-Clapeyron equation:

$$Y_s = \frac{W_1}{W} \cdot \exp \left[\frac{L}{R} \left(\frac{1}{T_b} - \frac{1}{T_s} \right) \right] \quad (\text{A3})$$

T_b is the liquid boiling point, W_1 is the molecular weight of the liquid and W is the molecular weight of the vapor mixture at the liquid surface.

REFERENCES

- 1 A. E. Kaufman and C. E. Polymeropoulos, *J. Chromatogr.*, 454 (1988) 23.
- 2 A. A. Lefebvre, *Atomization and Sprays*, Hemisphere, New York, 1989.
- 3 L. R. Utreja and D. B. Harmon, American Institute of Aeronautics paper No. 90-1616, Seattle, WA, 1990.
- 4 W. S. Rayleigh, *Proc. London Math. Soc.*, 4 (1878) 10.
- 5 E. Goedde and M. C. Yuen, *J. Fluid Mech.*, 40 (1970) 495.
- 6 A. M. Sterling and C. A. Steicher, *J. Fluid Mech.*, 68 (1975) 477.
- 7 D. B. Bogoy, *Annu. Rev. Fluid Mech.*, 11 (1979) 207.
- 8 H. Q. Yang, American Institute of Aeronautics paper No. 91-0693, Reno, NV, 1991.
- 9 R. P. Grant and S. Middleman, *AIChE J.*, 12 (1966) 669.
- 10 M. J. McCarthy and N. A. Molloy, *Chem. Eng. J.*, 7 (1974) 1.
- 11 H. Eroglu and N. Chigier, *Phys. Fluids A*, 3 (1990) 303.
- 12 C. Weber, *Z. Angew. Math. Mech.*, 11 (1931) 136.
- 13 V. Levich, *Physicochemical Hydrodynamics*, Prentice Hall, Englewood Cliffs, NJ, 1962.
- 14 R. E. Phiney, *Phys. Fluids*, 16 (1973) 193.
- 15 R. D. Reitz and F. V. Bracco, *Phys. Fluids*, 22 (1979) 1064.
- 16 Q. Jun, *M.S. Thesis*, Rutgers University, New Brunswick, NJ, 1991.
- 17 F. P. Incropera and D. P. De Witt, *Foundations of Heat Transfer*, Wiley, New York, 1990.
- 18 M. Kanury, *Introduction to Combustion Phenomena*, Gordon & Breach, New York, 1975.

Investigation of a scyllitol-derived (saturated) disc-shaped liquid crystal stationary phase in capillary gas chromatography[☆]

A. Kraus, U. Schumann and G. Kraus

Institute of Analytical Chemistry, Martin-Luther-Universität Halle, O-4010 Halle (Saale) (Germany)

B. Kohne and K. Praefcke

Institute of Organic Chemistry, Technische Universität Berlin, W-1000 Berlin 12 (Germany)

(First received July 10th, 1991; revised manuscript received April 23rd, 1992)

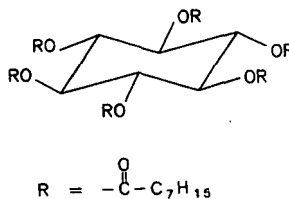
ABSTRACT

Hexa-O-octanoyl-*scyllo*-inositol, a scyllitol-derived disc-shaped liquid crystal, was tested as a stationary phase in gas chromatography. The retention indices of series of isomers selected as test substances differing in chemical structure, molecular geometry and physico-chemical properties were measured, and conclusions about the mechanism of interaction between the stationary phase and the test molecules are discussed. The polarity of the phase was measured according to Rohrschneider. The determination of the phase transition temperatures using the capacity factor in the heating and cooling cycles showed that the liquid crystal can be supercooled.

INTRODUCTION

Rod-shaped and polymeric liquid crystals of various structures are being widely investigated and used as stationary phases in gas chromatography (GC). Little information is available on the properties and separation mechanisms of discotic liquid crystalline stationary phases. In 1984 Witkiewicz *et al.* [1] investigated discotic nematic triphenylene derivatives and in 1988 Zhang and Wang [2] used rufigallol hexaalkanoates.

We became interested in filling this gap by studying the discogen **1**, a hexaester [3-5] of the naturally



Hexa-O-octanoyl-*scyllo*-inositol (**1**).

occurring *scyllo*-inositol (scyllitol)^{**} with an extremely wide discotic mesophase ($\Delta T \approx 120$ K), as a stationary phase in capillary GC to broaden our knowledge about the mechanisms of interaction between such a phase and various test molecules and about structure selectivities [7,8]. **1** has the following melting and clearing temperatures

Correspondence to: Dr. G. Kraus, Institute of Analytical Chemistry, Martin-Luther-Universität Halle, O-4010 Halle (Saale) Germany.

[☆] Part 66 on liquid-crystalline compounds of the Berlin research group; Part 65: K. Praefcke, B. Kohne, S. Diele, G. Pelzl and A. Kjaer, *Liq. Cryst.*, 11 (1992) 1-8.

^{**} *scyllo*-Inositol is one of the possible eight stereoisomers of inositol [6] having all hydroxyl groups in equatorial positions with the result of a totally flat structure.

K → D _{ho}	79.6°C
D _{ho} → Is	119.3°C

where K indicates crystalline, D_{ho} indicates discotic hexagonal orthorhombic, and Is indicates isotropic state. Between these temperatures the compound is a discotic hexagonal orthorhombic liquid crystal. Between these temperatures the compound is a discotic hexagonal orthorhombic liquid crystal.

EXPERIMENTAL

The measurements were carried out using a modified gas chromatograph, GCHF 18.3 (ZWG/Chromatron), equipped with a flame ionization detector and split injector. Nitrogen was used as the carrier gas. The glass capillary column was made of soft glass (25 m × 0.25 mm I.D.). After etching with gaseous HCl and deactivating with Carbowax 20M, the capillary was coated dynamically with a solution of 10% of the liquid crystal I in dichloromethane. The efficiency of the column was 66 500 theoretical plates for *o*-methylanisole with capacity factor, $k' = 2.89$.

RESULTS AND DISCUSSION

Transition temperatures

The GC determination of the transition temperatures using the k' values of methylanisoles in the heating and cooling cycles shows that the phase can be supercooled to 61.5°C (Fig. 1) and that a change of phase in the wide discotic range of temperature can be excluded, as no jumps can be observed. Comparing the transition temperatures determined by GC with the values obtained with a polarization microscope we conclude that there are higher deviations for disc- than for rod-shaped liquid crystals [7,8].

The ratio of the capacity factors at the melting point ($\Delta k'$ high) and at the clearing temperature ($\Delta k'$ relatively small) correlates with the ratio of the transition enthalpies of the phase at these temperatures, as determined by differential scanning calorimetry [5]:

K → D _{ho}	$\Delta H = 43.30$ kJ/mol
D _{ho} → Is	$\Delta H = 9.47$ kJ/mol

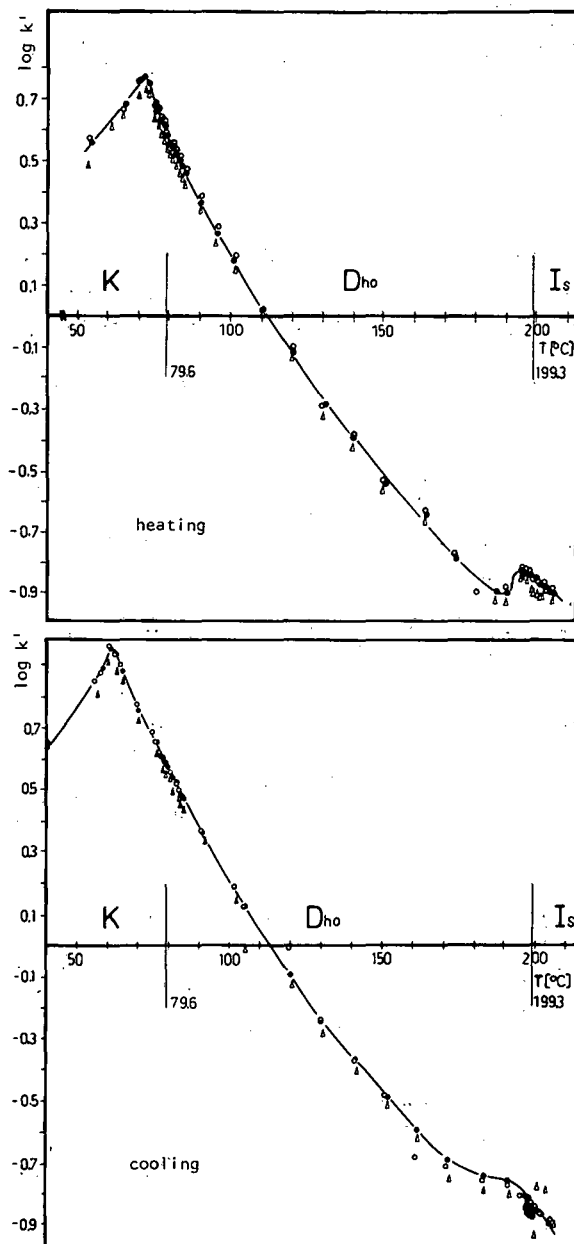


Fig. 1. Dependence of capacity factors, k' , on temperature (on heating and cooling) for isomeric methylanisoles. ● = *p*-; ○ = *m*-; △ = *o*-methylanisole.

Structure selectivity and retention behaviour

Generally, stationary phases consisting of rod-shaped liquid crystals are (more or less) suitable for

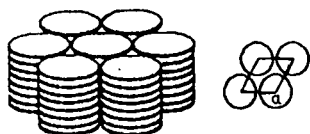


Fig. 2. Structure of a discotic columnar D_{ho} phase.

separating close-boiling geometrical isomers according to their length-to-breadth ratio, taking advantage of the ordered structure in the liquid crystalline state [7,8]. This so-called structure selectivity (α) leads to, for instance, $\alpha_{p/m} > 1$ for disubstituted benzenes.

To elucidate possible separation effects caused by the liquid crystal structure of the used discotic phase (Fig. 2), several types of substances with different molecular structures and space requirements were used. Taking into account the rule "like dissolves like", we assumed, for example, stronger interactions of the cyclohexane structures with the stationary phase than of the other substances used.

The Kováts retention indices, determined in the mesophase range, in the isotropic liquid phase and in the supercooled state, show that the elution order mainly follows the order of the boiling temperatures of the test substances (Figs. 3-8). As expected,

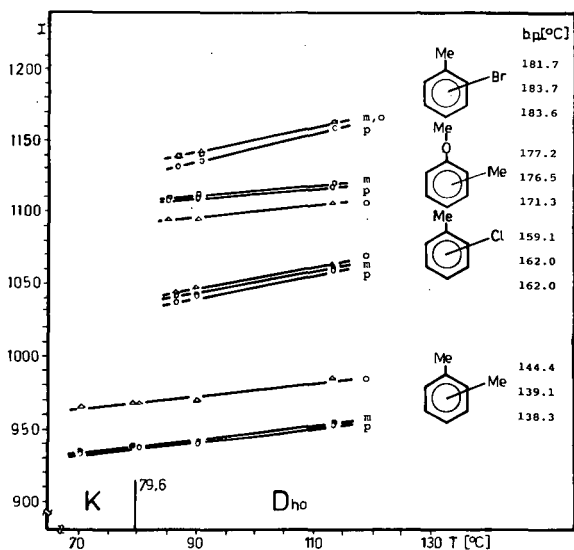


Fig. 3. Dependence of retention indices (I) of isomeric benzene derivatives on temperature. Me = Methyl.

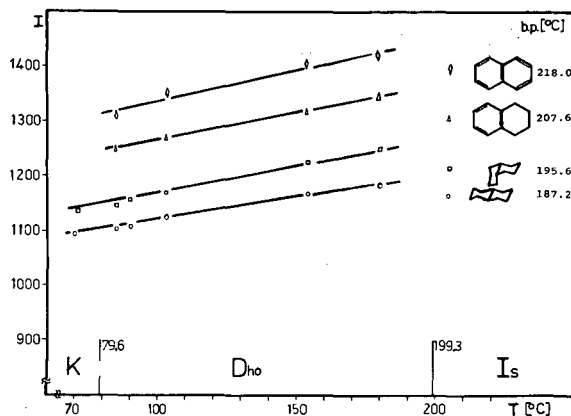


Fig. 4. Dependence of retention indices of naphthalene, tetralin and decalines on temperature.

ed, no structure selectivity concerning the length-to-breadth ratio is observed for the isomeric disubstituted benzenes ($\alpha_{p/m} < 1$) and *cis*- and *trans*-decalines (Figs. 3 and 4). Deviations from the elution or-

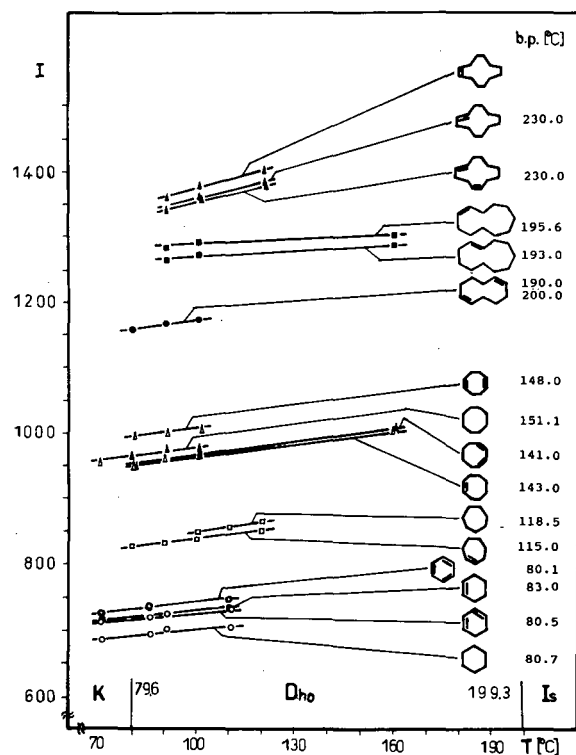


Fig. 5. Dependence of retention indices of cyclic hydrocarbons on temperature.

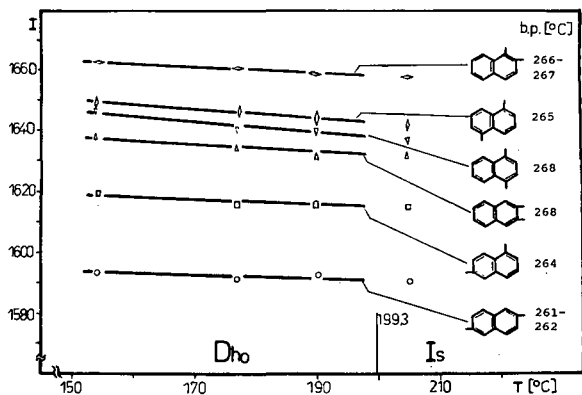


Fig. 6. Dependence of retention indices of isomeric dimethylnaphthalenes on temperature.

der according to boiling points can be observed for the elution of cyclohexane, -hexene and -hexadiene and benzene and for the pair cyclooctane (b.p. 151.1°C) and *cis,cis*-cycloocta-1,5-diene (b.p. 148°C) (Fig. 5).

In addition to the supporting effect of the polarity of the stationary phase, the probable reason seems to be that interactions of the substrate molecules take place only within the gaps (e.g., the empty spaces between the columns) of the hexagonal columnar discotic phase (Fig. 2) with parts of the radical-symmetrical arranged lateral functions of

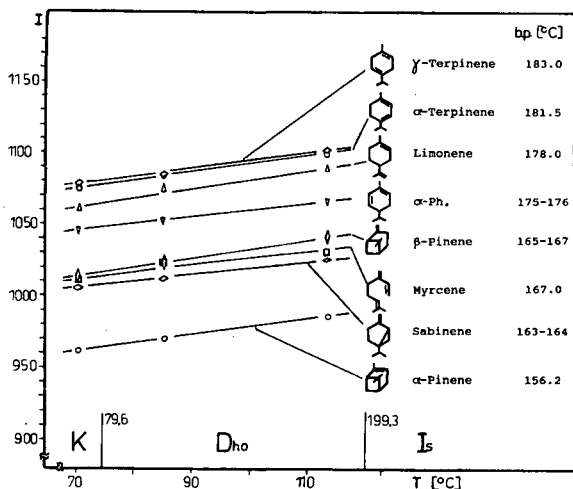


Fig. 7. Dependence of retention indices of terpenes on temperature. α -Ph = α -phellandrene.

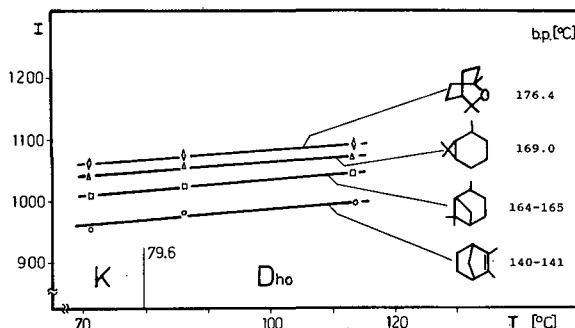


Fig. 8. Dependence of retention indices of 1,8-cineole, carane, pinane and santene on temperature.

the disc, but not with or between the centres of the discotic molecules of columnar structure. Therefore, the results confirm the structural attributes of this discotic phase, discussed by Kohne and Praefcke [4,5]. These are perfect space filling (minimum dead space in the centre of the discotic molecule) and an optimum coverage of the area in the periphery of the "core", which can become slightly puckered by the radical-symmetrical arranged lateral functions.

This interaction characteristic would explain the retention of the six-membered hydrocarbons, where the flatter cyclohexadiene (b.p. 80.5°C) is eluted after cyclohexane (b.p. 80.7°C) and nearly co-eluted with the higher boiling cyclohexene (b.p. 83.0°C). The lowest boiling benzene with the flattest structure is eluted last. This can also explain the lack of selectivity of the discotic phase concerning the length-to-breadth ratio (e.g., xylenes). The dimethylnaphthalenes (Fig. 6) are eluted as on normal low-polarity stationary phases [9,10].

Unexpectedly, the *o*-halotoluenes with the lowest boiling temperatures are eluted after or together with the corresponding *meta* isomers (Fig. 3). Comparing our results with the measurements of Witkiewicz *et al.* [1], we find a corresponding elution order of the test substances used in both instances. The elution of *n*-nonane before cyclooctane, considered by Witkiewicz *et al.* to characterize their discotic phases and for comparison also tested in our measurements, seems to be normal. It follows the boiling points and the rules of GC polarity established by Schomburg [11].

In general, the explanation of the retention mechanism given by Witkiewicz *et al.* does not contradict

our suggestions, because the structures of the investigated discotic stationary phase differ considerably.

Polarity

The polarity values of **I** were determined according to Rohrschneider: benzene, $x = 0.85$; ethanol, $y = 1.53$; 2-butanone, $z = 1.23$; nitromethane, $u = 1.64$; pyridine, $s = 1.30$. In the discotic hexagonal columnar state, the phase is of low polarity like a methylsilicone substituted by a small proportion of phenyl groups.

CONCLUSIONS

Taking into consideration the structure of the investigated *scyllo*-inositol derivative [4,5], which shows perfect space filling in the centre of the molecule and an optimum coverage of the area in the periphery of the “core” which can become slightly puckered by radical-symmetrical arranged lateral functions (yielding a “flexible super disc”), we can conclude that the interactions of the test com-

pounds take place favourably within the empty spaces between the columns of the columnar structure with random parts of the lateral substituents but not between the centres of the discotic molecules.

REFERENCES

- 1 Z. Witkiewicz, J. Szulz and R. Dabrowski, *J. Chromatogr.*, 315 (1984) 145.
- 2 P. Zhang and L. Wang, *Kexue Tongbao (Foreign Lang. Ed.)*, 33 (1988) 1171; *Chem. Abstr.*, 110 (1989) 105610s.
- 3 B. Kohne, K. Praefcke, W. Stephan and P. Nürnberg, *Z. Naturforsch., B: Chem. Sci.*, 40 (1985) 981.
- 4 B. Kohne and K. Praefcke, *Chem. Ztg.*, 109 (1985) 121.
- 5 B. Kohne and K. Praefcke, *Angew. Chem.*, 96 (1984) 70; *Angew. Chem., Int. Ed. Engl.*, 23 (1984) 82.
- 6 Th. Pasternak, *Les Cyclitols*, Hermann, Paris, 1962.
- 7 Z. Witkiewicz, *J. Chromatogr.*, 251 (1982) 311.
- 8 G. Kraus, *Habilitation*, Martin-Luther-Universität Halle, Halle, 1983.
- 9 W. Engewald, *Habilitation*, Universität Leipzig, Leipzig, 1978.
- 10 F. Hahne, *Dissertation*, Martin-Luther-Universität Halle, Halle, 1990.
- 11 G. Schomburg, *J. Chromatogr.*, 23 (1966) 18.

Separation and identification of all isomeric *n*-nonadecenes by capillary gas chromatography on a mesogenic stationary phase with Fourier transform infrared and mass spectrometric detection

L. Soják, I. Ostrovský and R. Kubinec

Chemical Institute, Faculty of Natural Sciences, Comenius University, Mlynská Dolina, 842 15 Bratislava (Czechoslovakia)

G. Kraus and A. Kraus

Department of Chemistry, Martin-Luther University, Weinbergweg 16, 4020 Halle/Saale (Germany)

(Received February 24th, 1992)

ABSTRACT

High-resolution capillary gas chromatography (HRGC) with an isomeric selective liquid crystal as stationary phase permits a better separation of the seventeen possible *n*-nonadecene isomers and *n*-nonadecane than a separation system with a non-mesogenic stationary phase. For the identification of the separated isomers, structure–retention correlations based on extrapolation of the dependence of homomorphous factors on the number of carbon atoms for homologous series of *n*-alkenes and the different temperature dependences of the retention indices of geometrical isomers were used. Identification was confirmed by a combination of HRGC with Fourier transform infrared and mass spectrometric detection on the basis of infrared spectra which are distinctly different for the geometrical isomers. The rule of the alternation retention of *cis*- and *trans*-alkenes with an odd number of carbon atoms separated on a mesogenic stationary phase was reformulated.

INTRODUCTION

n-Alkenes represent an interesting model for the study of gas chromatographic (GC) isomeric selectivity concerning positional and geometrical isomerism. They are also technologically important materials obtained as complex mixtures of isomers by catalytical dehydrogenation of *n*-alkanes with a wide range of carbon numbers.

In GC separations of higher *n*-alkenes, a favourable effect of the polarity of stationary phase is compensated for by the interfacial adsorption of

isomers on the polar stationary phase–gas interface, this effect being inversely proportional to the polarity of the individual isomers [1]. Separation systems combining the high efficiency of capillary columns with the isomeric selectivity of liquid crystals as stationary phases permit improved separations of complex mixtures of isomers, including those with very similar physico-chemical properties [2].

In previous work [3], the separation of isomeric C₁₇ and C₁₈ *n*-alkenes and *n*-alkanes was studied on a high-efficiency capillary column with 4',5-*n*-hexylpyrimidin-2-yl-phenyl 4-*n*-propylbenzoate (PrBHP) liquid crystal as stationary phase. The separation was optimized with respect to the stationary phase film thickness and column temperature. This separation system permits better and faster separa-

Correspondence to: Dr. L. Soják, Chemical Institute, Faculty of Natural Sciences, Comenius University, Mlynská Dolina, 842 15 Bratislava, Czechoslovakia.

tions of isomeric *n*-heptadecenes and *n*-octadecenes compared with previously obtained separations on non-mesogenic and mesogenic stationary phases.

The aim of this work was the separation and identification of all isomeric *n*-nonadecenes and *n*-nonadecane using the separation system with PrBHP liquid crystal as stationary phase coupled with Fourier transform infrared (FT-IR) and mass spectrometric (MS) detection. The contribution of the mesogenic stationary phase used to the separation of isomeric *n*-nonadecenes is based on a comparison with their separation on the non-mesogenic phase Apolane-87 in a capillary column with an efficiency of about 500 000 plates [4].

EXPERIMENTAL

As a model mixture, the product of the catalytic dehydrogenation of *n*-nonadecane, in which the *n*-alkene content was enriched by displacement liquid chromatography with 2-propanol, was used. It contains a mixture of the seventeen possible isomeric *n*-nonadecenes and *n*-nonadecane.

GC measurements were carried out with a Hewlett-Packard GC-FT-IR-MS system. The model mixture was separated in a glass capillary column with liquid crystalline PrBHP (synthesized by Dr. K. D. Scherf, Martin-Luther University, Halle, Germany) as stationary phase, having a mesophase range from 65 to 170°C and possible supercooling to about 28°C. The capillary column was prepared from Unihost glass (Kavalier, Teplice, Czechoslovakia). After etching with gaseous hydrogen chloride, the glass capillary was coated statically with a solution of PrBHP in dichloromethane. The effective efficiency of a prepared column of 90 m × 0.25 mm I.D. for the studied compounds was about 200 000 plates (film thickness 0.03 μm, column temperature 100°C, average linear velocity of carrier gas 40 cm s⁻¹). The selectivity coefficient (relative retention), α , for *p*- and *m*-xylene at 50°C was 1.16.

RESULTS AND DISCUSSION

The chromatograms of isomeric *n*-nonadecenes and *n*-nonadecane obtained with the PrBHP liquid crystal separation system and those obtained with Apolane-87 (from Ref. 4) are shown in Fig. 1. Retention indices and their temperature coefficients of

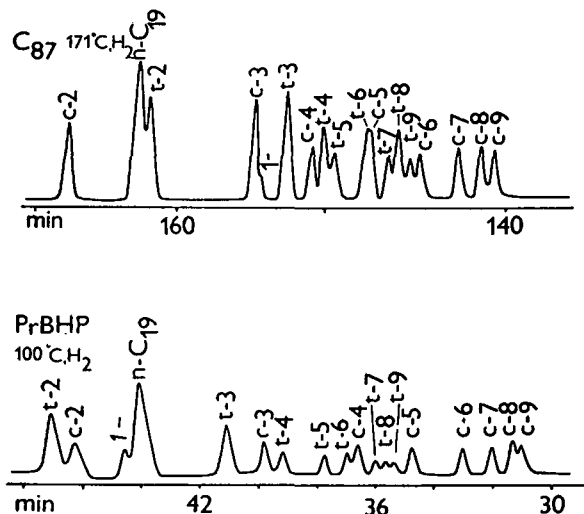


Fig. 1. Separation of isomeric *n*-nonadecenes and *n*-nonadecane using a 90 m × 0.25 mm I.D. column with PrBHP ($N \approx 200\,000$ plates) and a 200 m × 0.25 mm I.D. column with Apolane-87 ($N \approx 500\,000$ plates). c = *cis*; t = *trans*; 1 = 1-nonadecene; n-C₁₉ = *n*-nonadecane.

TABLE I

RETENTION INDICES OF *n*-NONADECENES AND THEIR TEMPERATURE COEFFICIENTS ON PrBHP AT 100°C AND ON APOLANE-87 AT 170°C

dI^{PrBHP}/dT values were measured within the temperature range 90–100°C and dI^{Ap-87}/dT values within the range 170–190°C.

<i>n</i> -Nonadecene	I_{100}^{PrBHP}	dI/dT	I_{170}^{Ap-87}	dI/dT
<i>cis</i> -9-	1839.2	0.57	1860.3	0.12
<i>cis</i> -8-	1840.4	0.50	1861.7	0.12
<i>cis</i> -7-	1844.8	0.51	1864.4	0.11
<i>cis</i> -6-	1850.3	0.48	1869.0	0.11
<i>cis</i> -5-	1859.1	0.42	1874.7	0.10
<i>trans</i> -9-	1862.1	0.39	1870.4	0.09
<i>trans</i> -8-	1863.5	0.37	1871.3	0.08
<i>trans</i> -7-	1865.2	0.33	1872.8	0.08
<i>cis</i> -4-	1868.3	0.37	1881.3	0.08
<i>trans</i> -6-	1869.9	0.30	1875.3	0.07
<i>trans</i> -5-	1873.7	0.29	1878.9	0.06
<i>trans</i> -4-	1880.1	0.23	1879.9	0.04
<i>cis</i> -3-	1882.4	0.23	1887.9	0.06
<i>trans</i> -3-	1888.3	0.17	1884.6	0.01
1-	1902.0	0.07	1887.1	0.04
<i>cis</i> -2-	1908.3	0.24	1907.6	0.06
<i>trans</i> -2-	1910.9	0.10	1899.0	0.00

n-nonadecenes on PrBHP and Apolane-87 are given in Table I.

Individual *n*-nonadecene isomers were identified by extrapolation of the dependence of the homomorphy factors, *H*, on the number of carbon atoms (n_c) for the homologous series of C_{15} – C_{18} *n*-alkenes, on the basis of previously measured retention indices [3]. The characteristic monotonous dependence of homomorphy factors, $H = f(n_c)$, for homologues on a non-mesogenic stationary phase does not apply on mesogenic stationary phases because it is influenced by the alternation of retention in homologous series when homologous with the orientation of the carbon chain more in the direction of the molecular axis have increased retention

[3,5]. In connection with alternation of retention, in some instances an opposite retention order of isomers with the double bond in the middle of the carbon chain and their neighbouring positional isomers on mesogenic, in comparison with their separation on non-mesogenic, stationary phases has been found. Therefore, for the identification of isomeric *n*-nonadecenes separated on PrBHP, further means were used.

The identification of *cis* and *trans* isomers was confirmed on the basis of the different temperature dependences of their retention indices. The data in Table I show that the dI/dT values on PrBHP are higher for *cis* than for *trans* isomers by an average of 0.14 i.u./°C. On Apolane-87 the corresponding

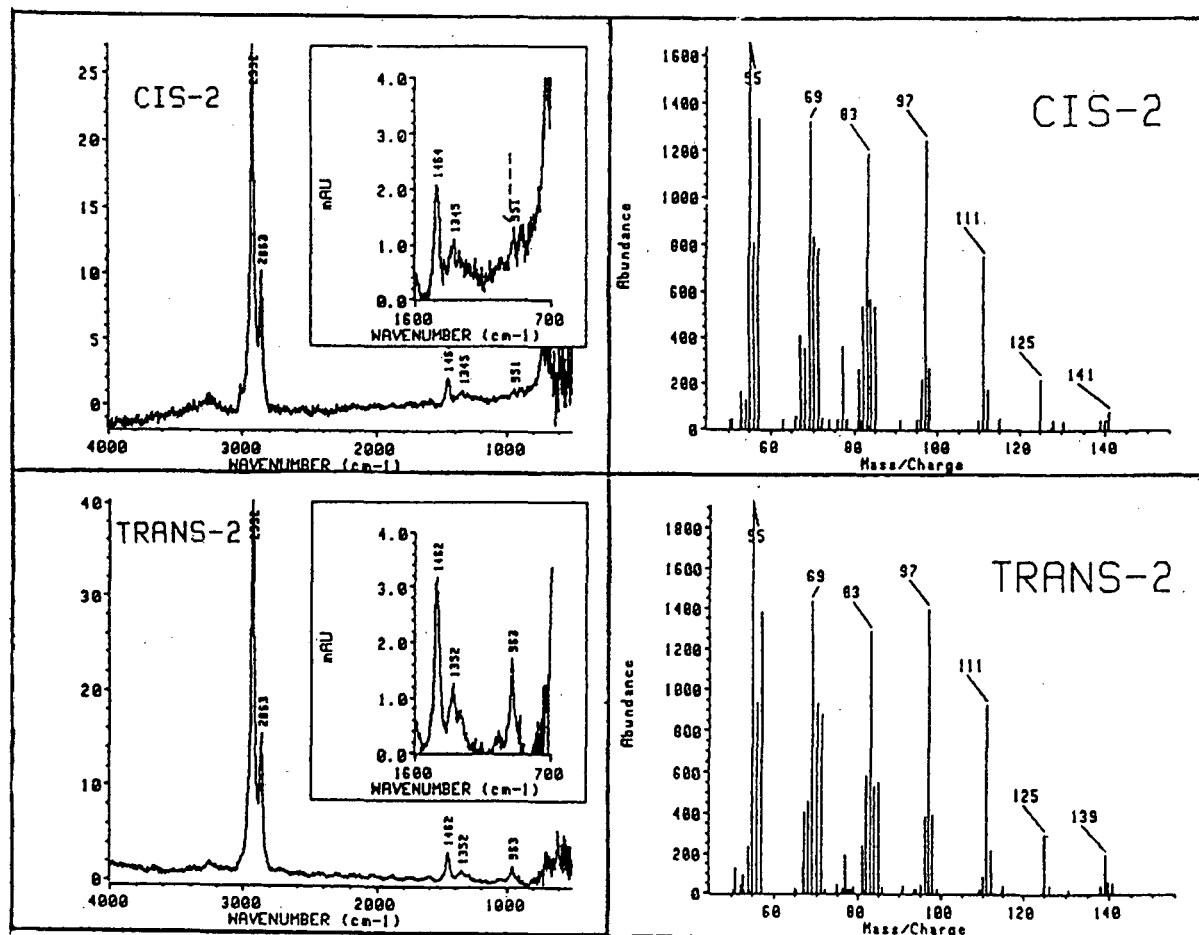


Fig. 2. Mass and IR spectra of *cis*-2- and *trans*-2-nonadecene.

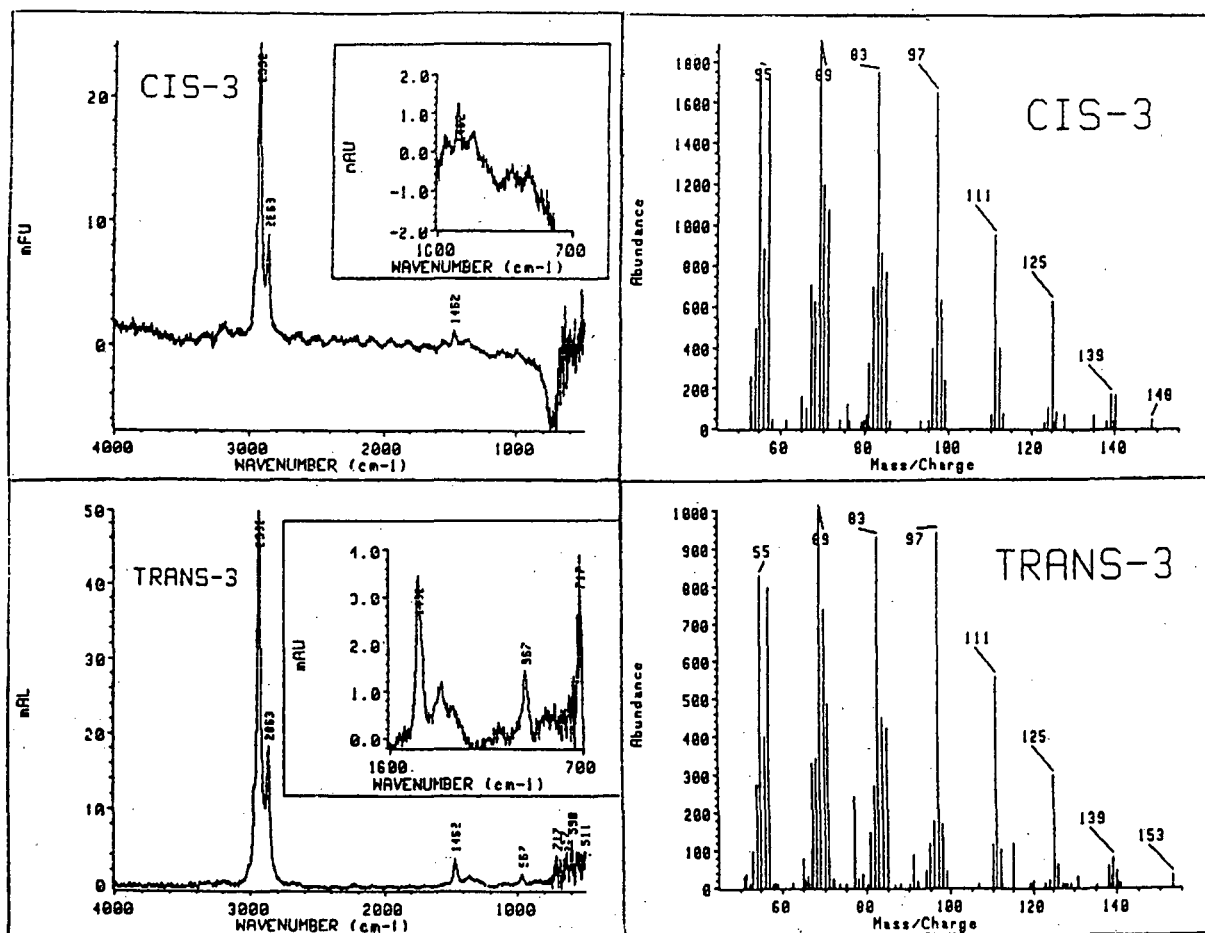


Fig. 3. Mass and IR spectra of *cis*-3- and *trans*-3-nonadecene.

difference is 0.05 i.u./°C; therefore, easier temperature optimization of their separation is possible on the PrBHP column.

The identification of isomeric *n*-nonadecenes carried out on the basis of structure–retention correlations was confirmed by FT-IR and MS detections of the eluates from the PrBHP capillary column. The results for the peaks identified as *cis*-2- and *trans*-2-nonadecenes and *cis*-3- and *trans*-3-nonadecenes are shown in Figs. 2 and 3, respectively. The geometrical and positional isomers of *n*-nonadecenes produce very similar mass spectra, and therefore their use for identification purposes is problematic. However, the infrared spectra of the geometrical isomers are distinctly different [6]. In contrast

to *cis* isomers, the *trans* isomers show a characteristic absorption at 963 cm^{-1} for *trans*-2-nonadecene and at 967 cm^{-1} for *trans* isomers with the double bond located closer to the middle of the carbon chain of the molecule (*trans*-3- up to *trans*-9-nonadecene).

The dependence of the difference in the retention indices of neighbouring positional *cis*- and *trans*-*n*-nonadecene isomers (δI values) on the position of the double bond, in comparison with those obtained on Apolane-87, is shown in Fig. 4. The δI values of positional *cis* and *trans* isomers increase with a shift of the double bond from the middle to the end of the carbon chain. The δI values on PrBHP are generally higher, with the exception of

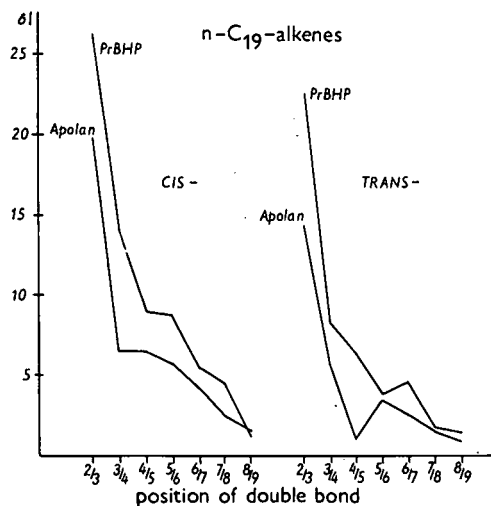


Fig. 4. Dependence of difference in retention indices of neighbouring positional *cis*- and *trans*-nonadecene isomers on the position of the double bond for PrBHP and Apolane-87.

the pair *cis*-8-*cis*-9-nonadecene, even taking into consideration the different column temperatures used with PrBHP and Apolane-87. This is in agreement with the fact that the selectivity of liquid crystals for positional isomers increases with a shift of the double bond from the middle to the end of the carbon chain [5]. Hence the selectivity increases in the same direction as the retention of positional isomers, and therefore their separation is more favoured on a liquid crystal than on a non-mesogenic stationary phase. The comparison of the retention indices of *n*-nonadecenes measured on PrBHP and those measured on Apolane-87 shows a higher retention range of the studied compounds (66.1 i.u.) relative to Apolane-87 (47.3 i.u.). As is shown in Fig. 1, using a column with PrBHP the separation of all isomeric *n*-nonadecenes was achieved at a 2.5-fold lower efficiency in comparison with the Apolane-87 column.

The lower δI value for the pair *cis*-8-*cis*-9-nonadecene on PrBHP than on Apolane-87 is connected with the alternation of retention of positional *n*-alkene isomers on mesogenic phases. From the data in Fig. 4, it follows that on a mesogenic phase *cis*-nonadecenes with an odd position of the double bond and *trans*-nonadecenes with an even position of the double bond show an increased retention, as follows from the regular decrease in retention with a

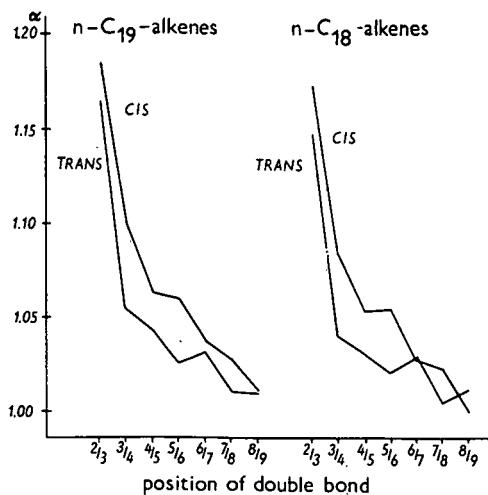
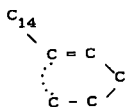


Fig. 5. Dependence of relative retention values on the position of the double bond for neighbouring positional *cis* and *trans* isomers of *n*-octadecenes and *n*-nonadecenes on PrBHP.

shift of the double bond from the end to the middle of the carbon chain. However, previously [3,5], on the basis of results on alternation of retention for homologous series of *n*-alkenes on a mesogenic phase, the increased retention of *n*-alkenes with an odd number of carbon atoms for *cis*-alkenes with an even position of the double bond and for *trans*-alkenes with an odd position of the double bond was proposed.

The dependence of the relative retention values, α , on the position of the double bond for neighbouring position *cis*- and *trans*-nonadecenes and -octadecenes on PrBHP is shown in Fig. 5. It seems that trends of these dependences are similar to those in Fig. 4. This means that the alternation of the retention of *n*-alkanes (as standards in the Kováts retention index system) on PrBHP does not affect the trends of the alternation retention of positional *trans*- and *cis*-nonadecene isomers. These results and also similar results obtained for C₁₃, C₁₅ and C₁₇ *n*-alkenes confirm the formulated trends of alternation of the retention of *cis*- and *trans*-*n*-alkenes with an odd number of carbon atoms on mesogenic stationary phases. Previously formulated trends of alternation of retention of these *n*-alkenes were distorted by the effect of the alternation of retention of *n*-alkenes with an even number of carbon atoms in homologous series.

A low δI value was found on Apolane-87 for the pair *trans*-4-/*trans*-5-nonadecene (Fig. 4), the separation of which on Apolane-87 is worse than the separation of isomeric pairs of *trans*-nonadecenes having a more central position of the double bond in the carbon chain. This result is connected with the propyl effect experienced by the *trans*-4-isomer. The propyl effect is an intramolecular interaction between the propyl group and the π -electron system of the double bond [4,5]:



which causes a lower retention of this isomer of *ca.* 3 i.u. Therefore, this isomer is eluted more closely to the *trans*-5-isomer, as could be predicted from the regularity of the dependence of the retention of the

positional *trans* isomers on the position of the double bond. On PrBHP in connection with alternation of retention, the increased retention of *trans*-4-nonadecene leads to the partial elimination of the effect of a propyl group on the retention dependence (see Fig. 4). It is evident from the measurements on Apolane-87 that the propyl effect is present also at relatively high temperatures, *e.g.* 190°C.

REFERENCES

- 1 L. Soják, J. Krupčík and J. Janák, *J. Chromatogr.*, 195 (1980) 224.
- 2 J. Mazur and Z. Witkiewicz, *LC · GC*, 3 (1990) 38.
- 3 L. Soják, I. Ostrovský, R. Kubinec, G. Kraus and A. Kraus, *J. Chromatogr.*, 520 (1990) 75.
- 4 L. Soják, I. Ostrovský and P. Skalák, *Ropa Uhlie*, 22 (1980) 490.
- 5 L. Soják, G. Kraus, P. Farkaš and I. Ostrovský, *J. Chromatogr.*, 249 (1982) 29.
- 6 M. Hesse, H. Meier and B. Zech, *Spektroskopische Methoden in der Organischen Chemie*, Georg Thieme, Stuttgart, New York, 1987, p. 41.

Gas chromatographic identification of halogenated hydrocarbons by using the correlation between their retention and boiling points

T. C. Gerbino[☆], G. Castello and G. D'Amato

Istituto di Chimica Industriale, Università, Corso Europa 30, 16132 Genova (Italy)

(First received February 24th, 1992; revised manuscript received May 18th, 1992)

ABSTRACT

The correlation between relative retention values of halogenated hydrocarbons (methanes, ethanes and ethenes with different halogen atoms in the molecule) and their boiling points at atmospheric pressure was found to be linear, and was used for identification purposes in gas chromatography. Absolute and relative retention values were measured on non-polar (OV-1) and polar (SP-1000) packed columns; the linear correlations found with the boiling points as a function of the number of hydrogen, chlorine, bromine and iodine atoms permits peak identification starting from known boiling points. Calculation of the boiling points of trace compounds starting from gas chromatographic data or linear interpolation to predict both the retentions and the boiling points of substances whose standards are not available are also possible.

INTRODUCTION

When complex mixtures of organic compounds have to be analysed in industrial or environmental samples, gas chromatographic (GC) techniques are often used, and the identification of the various unknown substances is carried out by using specific detectors or mass spectrometry (GC-MS). When conventional GC detectors are used, the identification can be achieved by comparing the retention values of the unknown peaks with those of a target compound list on columns having different polarities. Unexpected compounds, often present in polluted environmental samples, may remain unidentified with this procedure, as a proper reference standard is not available.

The GC-MS technique takes into account the retention times on a capillary column (often non-po-

lar or low polarity) and the comparison of the mass spectra with those listed in a standard library. Some differences in the actual and literature spectra, due to the background, different ionization conditions, etc., often do not permit the identification of the sample [1]. Further, in order to obtain a sensitivity similar to that of specific detection methods such as electron-capture detection (ECD), MS should be applied in the single ion monitoring (SIM) mode and the information contained in a full-scan spectrum is therefore lost. The use of a GC-MS system with ion-trap detection (ITD), which permits the identification to be carried out with full-scan spectra on 10 pg of sample [2,3], can solve the sensitivity problem, but expensive and delicate MS equipment generally cannot be applied in routine and field analysis.

When authentic standards are not available, neither the use of specific GC detectors nor mass spectra permit the tentative identification of unknown compounds, but an indication of the identity of a given peak can be obtained by using correlation rules between the retention data and the physical

Correspondence to: Dr. G. Castello, Istituto di Chimica Industriale, Università, Corso Europa 30, 16132 Genova, Italy.

[☆] Present address: Laboratorio Chimico, Castalia SpA, Via Borzoli 76, 16161 Genova, Italy.

and structural properties of the compounds [4–7]. A relatively simple spectrum search restricted to a few compounds or the injection of authentic samples on to different columns can achieve the final identification.

In a previous paper [8], it was shown that a linear correlation exists between the relative retention, r , and the vapour pressure of halogenated hydrocarbons, and that it can be used to precalculate the retention times of compounds for which standard samples are not available. The dependence of the retention data on the vapour pressure is more rigorous from the theoretical point of view [9], but in practice the boiling point values (T_B) which are more readily available in handbooks, catalogues, etc., can be used with satisfactory results. The correlation between boiling point and retention data was noted in early days of chromatography [10] and was mainly used for the identification of hydrocarbons [11] and for simulated distillation purposes. Less attention has been devoted to the study of retention–boiling point correlations for other homologous series, but correlations between chromatographic behaviour and physico-chemical properties of many compounds have been observed [12–15].

In this paper, we confirm the existence of regular correlations between the T_B and r values of halogenated hydrocarbons, and the possibility of using these rules to predict the retention behaviour of compounds for which standards are not available and conversely, the vapour pressures and boiling points through GC analysis.

EXPERIMENTAL

Packed columns having different polarities were used: non-polar OV-1 and polar SP-1000, both 10% (w/w) on Chromosorb W DMCS (80–100 mesh), each 3 m × 2 mm I.D.

In order to evaluate the effect on retention of interfacial adsorption and support activity, two columns of each type were used, filled with stationary phases prepared in the same way but from different batches of support, and made from stainless steel and Pyrex glass. The differences in adjusted retention times, t_R , were restricted to the second decimal figure and were mainly attributed to differences in flow-rates. The relative retention values were in fact reproducible to the third decimal figure (relative

standard deviation less than 1%) and no appreciable difference in the shape, width and tailing factor of the peaks was observed. This is probably due to the relatively high percentage of liquid phase, the efficient deactivation due to DMCS silanization, and the low “polarity” of the compounds analysed.

A Varian (Palo Alto, CA, USA) Model 3760 gas chromatograph was used with thermal conductivity detection (TCD). The small differences in the responses of TCD to halogenated compounds with different numbers of carbon atoms in the molecule permit the preparation of standard mixtures containing comparable amounts of each compound. Specific detection methods, such as ECD, currently used for the determination of low concentrations of halogenated compounds in the environment, require very different amounts of each substance to be injected in order to obtain peaks of comparable area, and this may influence the width, shape, retention time and resolution of some peaks. The chromatogram may also be complicated by the presence of impurities that, nearly undetected at low concentration by TCD, show large peaks using ECD, due to their great electron affinity. Helium was used as the carrier gas at a flow-rate of 30 cm³ min⁻¹.

The samples used (see Table I) included chloro-, bromo- and iodo-methanes, -ethanes and -ethenes with one or more identical or different halogen atoms in the molecule. They were analysed at 50, 75, 100 and 125°C on both columns. The following discussion is based on the retention values measured at 100°C, but the conclusions can easily be applied to analyses carried out at different temperatures.

THEORY

A detailed discussion of the theoretical background of the work was published previously [8], and is briefly summarized below.

For many homologous series, the boiling point, T_B , the vapour pressure, p^0 , the activity coefficient, γ , and the number of structural units in the molecule, n , are linearly correlated [9,12–14]:

$$\log p^0 = K_3 + K_4 n = K_1 + K_2 T_B \quad (1)$$

$$\log \gamma = K_5 + K_6 n = K_5 - (K_3 K_6 / K_4) + (K_6 / K_4) \log p^0 \quad (2)$$

$$\log r_{s,q} = \log(p_q^0 / p_s^0) + \log(\gamma_q / \gamma_s) \quad (3)$$

where the K are constant for each homologous series at constant temperature, $r_{s,q}$ is the relative retention of substance s with respect to a reference compound q and subscripts q and s on p^0 and γ have the same meaning.

By taking into account the equation for the retention volume, V_R :

$$V_R = N_1 RT / \gamma p^0 \quad (4)$$

where N_1 is the number of moles of stationary phase in the column, the following equations are obtained:

$$\log V_R' = \log (N_1 RT) - Z \quad (5)$$

and

$$\log r_{s,q} = \log(p_q^0 \gamma_q) - Z \quad (6)$$

where

$$Z = K_5 - (K_3 K_6 / K_4) + [(K_6 / K_4) + 1] / (K_1 + K_2 T_B) \quad (7)$$

showing that for homologous series the behaviour of r values is as linear as that of V_R' values as function of T_B . This linearity was confirmed experimentally [8].

When neither the p^0 nor T_B values for a given compound are available, but it belongs to a homologous series and its number of structural units, n_s , is known, the T_B value being linearly correlated with n_s [9], a linear relationship is found:

$$\log r_{s,q} = \log(p_q^0 \gamma_q) - (K_3 + K_5) - (K_4 + K_6)n_s \quad (8)$$

also when the structural units considered are not methylenic groups or carbon atoms, but are halogen atoms, substituent groups, etc. [8,9,16]. The above equations will apply exactly when the retention is due only to gas-liquid partitioning. Interfacial adsorption in different columns would produce different although similar results. The experiments carried out with different columns, as described under Experimental, showed that no appreciable difference in the results is found when the concentration of liquid phase on the silanized support is not lower than 10%. Lower percentages of liquid phase or the use of a less deactivated support may influence the results as the effect of adsorption can become appreciable with respect to that of partition.

RESULTS AND DISCUSSION

Table I lists the compounds analysed, their adjusted retention times, t_R' , measured at 100°C, the r values measured with respect to 1-chloro-2-bromoethane [8] and the boiling points taken from literature [17], T_B (w).

The correlation between the $\log r$ values of halomethanes listed in Table I on the non-polar OV-1 column and T_B (w) is shown in Fig. 1. The various halomethanes lie on different straight lines depending on the number of hydrogen atoms in the molecule and on the type of halogen atom. It has been shown previously [8] that when the correlation between $\log r$ and $\log p^0$ is considered, all the halomethanes lie on four straight lines that depend on the number of hydrogen atoms in the molecule, independent of the type of substituted halogen atom.

Fig. 1 also shows that compounds with different halogen atoms linearly interpolate those with the same halogen: CH_2ClI is between CH_2Cl_2 and CH_2I_2 ; CH_2ClBr between CH_2Cl_2 and CH_2Br_2 ; CHCl_2Br and CHCl_2Br_2 between CHCl_3 and CHBr_3 ; and CCl_3Br between CCl_4 and CBr_4 . It can therefore be accepted as a general rule that molecules that contain two different halogens lie on the straight line connecting the three halomethanes with the same number of hydrogen atoms and a

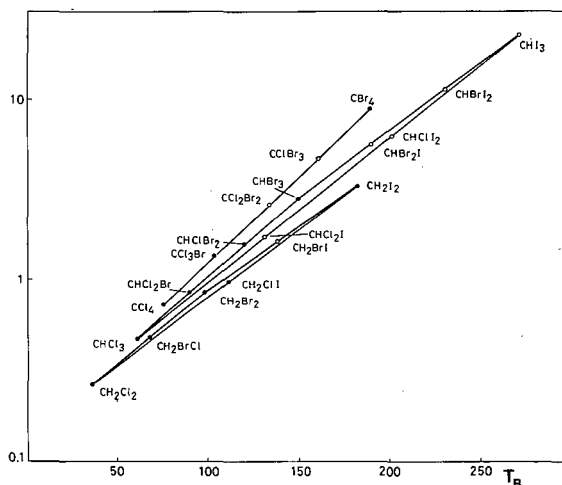


Fig. 1. Retention of halomethanes on OV-1 relative to 1-chloro-2-bromoethane, r , as a function of the boiling point at 760 Torr, T_B . ● = Experimental data; ○ = calculated values (see text).

TABLE I

HALOGENATED COMPOUNDS ANALYSED, LISTED IN ORDER OF DECREASING NUMBER OF HYDROGEN AND Cl, Br, I ATOMS, THEIR RETENTIONS RELATIVE TO 1-CHLORO-2-BROMOETHANE, \bar{r} , ON NON-POLAR AND POLAR COLUMNS AT 100°C AND THEIR BOILING POINTS AT 760 TORR TAKEN FROM REF. 17, T_B (w)

Compound	OV-1		SP-1000		T_B (w)
	t'_R	r	t'_R	r	
<i>Halomethanes</i>					
CH ₃ I	0.60	0.27	0.77	0.11	42.4
CH ₂ Cl ₂	0.58	0.27	1.65	0.24	40
CH ₂ ClBr	1.05	0.48	3.44	0.50	68.1
CH ₂ ClI	2.12	0.98	8.55	1.24	109
CH ₂ Br ₂	1.84	0.85	7.00	1.02	97
CH ₂ I ₂	7.22	3.33	44.58	6.49	182
CHCl ₃	1.04	0.48	2.84	0.41	61.7
CHCl ₂ Br	1.90	0.87	6.48	0.94	90
CHClBr ₂	3.40	1.57	14.57	2.12	119.5
CHBr ₃	6.02	2.77	32.55	4.73	149.5
CHI ₃	49.50	22.81	—	—	218
CCl ₄	1.58	0.73	1.35	0.20	76.5
CCl ₃ Br	2.97	1.37	3.92	0.57	104
CBr ₄	18.79	8.66	112.80	16.42	190
<i>Haloethanes</i>					
CH ₃ CH ₂ Cl	0.3	0.15	0.33	0.05	12.3
CH ₃ CH ₂ Br	0.60	0.28	0.70	0.10	38.4
CH ₃ CH ₂ I	1.12	0.52	1.34	0.19	72.3
CH ₃ CHCl ₂	0.81	0.37	1.34	0.19	57.28
CH ₂ ClCH ₂ Cl	1.30	0.60	3.86	0.56	83.5
CH ₂ ClCH ₂ Br	2.17	1	6.87	1	107
CH ₂ BrCH ₂ Br	3.69	1.70	12.13	1.76	131.4
CH ₂ ICH ₂ I	14.20	6.54	—	—	200
CH ₃ CCl ₃	1.37	0.63	1.37	0.20	74.1
CH ₂ ClCCl ₃	4.95	2.28	11.60	1.69	130.5
CHCl ₂ CHCl ₂	6.76	3.11	45.34	6.60	146
CHBr ₂ CHBr ₂	60.4	27.83	—	—	243.5
CHCl ₂ CCl ₃	11.15	5.14	30.02	4.37	162
CCl ₃ CCl ₃	21.64	9.97	30.12	4.38	186
<i>Haloethenes</i>					
CH ₂ =CCl ₂	0.56	0.26	0.52	0.08	37
ClCH=CHCl, <i>trans</i>	0.76	0.35	1.10	0.16	47.5
ClCH=CHCl, <i>cis</i>	1.00	0.46	2.41	0.35	60.3
ClCH=CCl ₂	1.91	0.88	2.54	0.37	87
Cl ₃ C=CCl ₂	4.12	1.90	3.18	0.46	121
BrCH=CHBr, <i>cis</i>	3.06	1.41	10.83	1.58	112.5
BrCH=CHBr, <i>trans</i>	2.53	1.17	5.58	0.81	108

unique type of halogen (CH₂Cl₂, CH₂Br₂, CH₂I₂; CHCl₃, CHBr₃, CHI₃; CCl₄, CBr₄, Cl₄). When the boiling point is known, the linear interpolation of these straight lines will permit the r values of all the possible halomethanes to be calculated. On the other hand, as the boiling points of many uncommon

compounds are unknown or only approximate, the interpolation from measured r values should permit more correct values to be obtained.

In a previous paper [8], the correlation between r and $\log p^0$ was found to give satisfactory precision, p^0 being calculated with Antoine-type equations.

TABLE II

COMPARISON OF RELATIVE RETENTION VALUES ON THE NON-POLAR OV-1 COLUMN PREVIOUSLY MEASURED AND CALCULATED FROM REF. 8, r_p , CALCULATED FROM LITERATURE $T_B(w)$ VALUES, r_w AND GRAPHICALLY INTERPOLATED WITH THE TRIANGLE RULE, r_g

Compound	r_p	r_w	r_g
CH_2BrI	1.64	1.64–1.72	1.64
CHCl_2I	1.73	2.65	1.71
CHClI_2	6.29	14.61	6.22
CHBr_2I	5.59	9.63	5.56
CHBrI_2	11.30	34.0	11.27
CCl_2Br_2	2.52	1.89	2.52
CClBr_3	4.69	4.44	4.66

Table II shows that the correspondence between the r_p values, measured experimentally and calculated starting from p^0 , and r_w values, calculated from the $T_B(w)$ values listed in ref. 17, is small. This may depend on the low precision of the tabulated $T_B(w)$ of uncommon compounds. In fact, eqn. 1 shows that for homologous series the boiling point is linearly correlated with n , and this is confirmed in Figs. 1–4 for di-, tri- and tetrahalomethanes. By interpolation in Figs. 2–4, the values of the boiling points $T_B(g)$ shown in Table III were calculated.

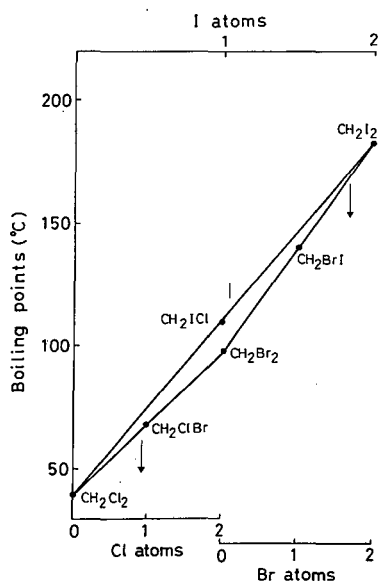


Fig. 2. Linear behaviour of the boiling points as a function of the number of structural units (Cl, Br or I atoms) in dihalomethane molecules.

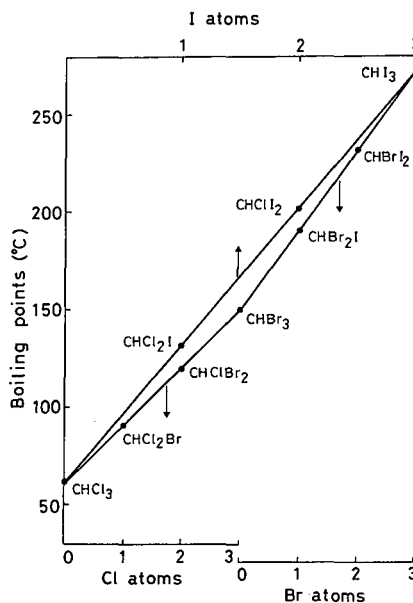


Fig. 3. Linear behaviour of the boiling points as a function of the number of structural units (Cl, Br or I atoms) in trihalomethane molecules.

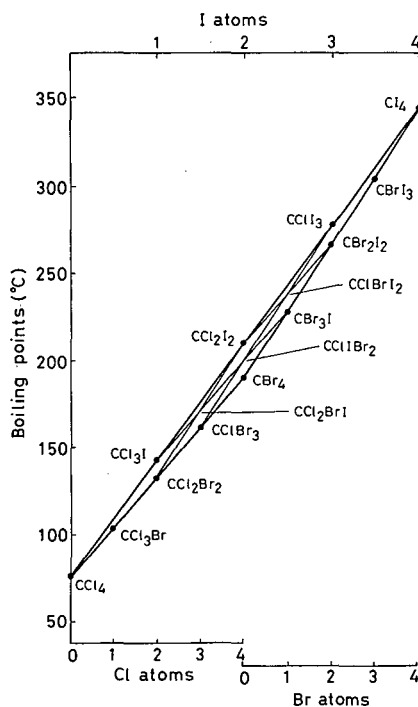


Fig. 4. Linear behaviour of the boiling points as a function of the number of structural units (Cl, Br or I atoms) in tetrahalomethane molecules. Thin lines in the inner part of the triangle show the fine structure that permits the calculation of r or T_B values for molecules with three different halogen atoms.

TABLE III
BOILING POINTS OF HALOGENATED METHANES FOUND IN THE LITERATURE [17], $T_B(w)$, AND CALCULATED BY INTERPOLATION WITH THE TRIANGLE RULE $T_B(g)$

Compound ^a	$T_B(w)$	$T_B(g)$
CH ₂ BrI	138–141	138
CHCl ₃	61.7	62
CHCl ₂ Br	90	90
CHCl ₂ I	131	131
CHClBrI	–	160
CHClI ₂	200	201
CHBr ₃	149.5	150
CHBr ₂ I	–	190
CHBrI ₂	–	231
CHI ₃	218	272
CCl ₃ Br	104	104
CCl ₃ I	142	142
CCl ₂ Br ₂	120	133
CCl ₂ BrI	–	166
CCl ₂ I ₂	–	210
CClBr ₃	158–159	161
CClBr ₂ I	–	200
CClBrI ₂	–	235
CClI ₃	–	276
CBr ₄	190	190
CBr ₃ I	–	228
CBr ₂ I ₂	–	266
CBrI ₃	–	304
Cl ₄	–	344

^a The compounds are listed in order of decreasing number of hydrogen, chlorine and bromine atoms.

Some of the predicted values are very different from the literature values, but in our opinion this is due to the imperfect knowledge of the physical data for uncommon compounds, which may also decompose when heated.

Literature data on the boiling points of the three compounds CCl₃Br (104°C), CCl₂Br₂ (120°C) and CClBr₃ (160°C) show that on replacement of Cl with Br atoms an increase of 16 and 40°C, respectively, is observed. A regular behaviour is more probable, and a ΔT_B of $(160 - 104)/2 = 28^\circ\text{C}$ leads to a value of $104 + 28 = 132^\circ\text{C}$ for the boiling point of CCl₂Br₂, closer to the value predicted by the proposed method.

As another example, the difference in literature T_B on replacement of a Cl with a I atom between CHI₃ (218°C) and CHClI₂ (200°C) is only 18°C, whereas a difference of 69°C is observed between

CHClI₂ and CHCl₂I (131°C), and a difference of 65.5°C between CCl₃I (142°C) and CCl₄ (76.5°C). The predicted value of 272°C or for CHI₃ therefore seems more reliable.

By using the $T_B(g)$ values shown in Table III, the r_g values shown in the last column of Table II were obtained. The good correspondence between these values and those calculated with the more rigorous approach of the vapour pressure is evident. The linear correlation of the r values with the boiling points therefore being confirmed, the retention times can be deduced from known boiling points and *vice versa* (Fig. 1).

When both r and T_B are known for three compounds having only chlorine, bromine or iodine atoms in the molecule, these compounds can be plotted as the three apices of a triangle while compounds with mixed halogens lie at regular intervals on the three sides of the same triangle. This simple "triangle rule" therefore permits one to obtain by linear interpolation or by simple arithmetic proportions the r and T_B values of any compound belonging to the considered homologous series.

The general rule states in fact that when the r and T_B values of the three halomethanes having the formula CH₂X_m (Fig. 5), where X may be Cl, Br or I, are known, it is possible to calculate the T_B or the r values of all the compounds having the formula

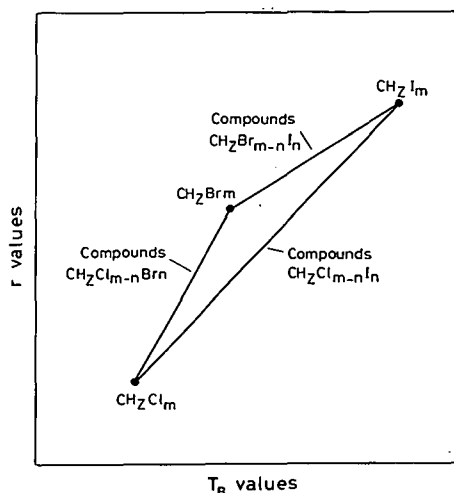


Fig. 5. Schematic diagram of the "triangle rule" for halomethanes. $z = 0, 1, 2$ or 3 ; $m = 4 - z$; $n < m$. The compounds with different halogen atoms lie on the sides of the triangle at constant intervals whose number depends on the z value.

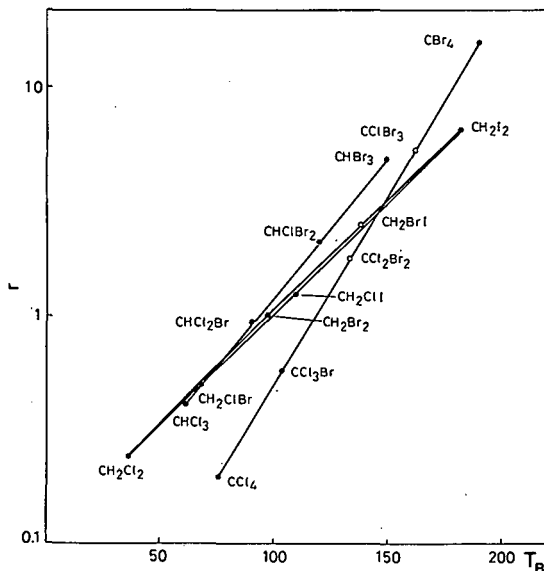


Fig. 6. Retention of some halomethanes on the polar SP-1000 column relative to 1-chloro-2-bromoethane, r , as a function of the boiling point at 760 Torr, T_B . ● = Experimental data; ○ = calculated values (see text).

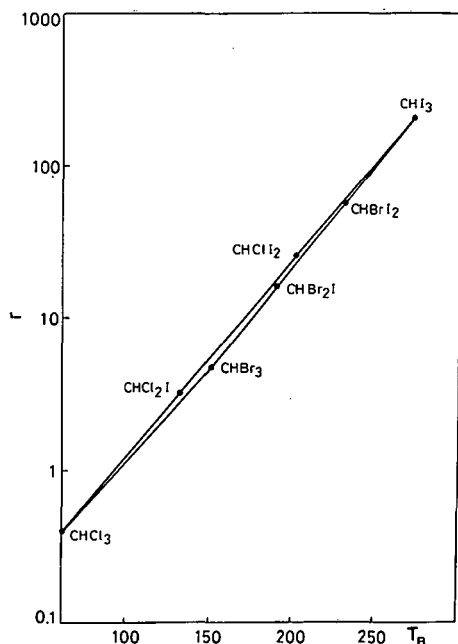


Fig. 7. Retention of all the trihalomethanes on the polar SP-1000 column relative to 1-chloro-2-bromoethane, r , as a function of the boiling points at 760 Torr, T_B .

TABLE IV

COMPARISON OF RELATIVE RETENTION VALUES ON THE POLAR SP-1000 COLUMN PREVIOUSLY MEASURED AND CALCULATED FROM REF. 8, r_p CALCULATED FROM LITERATURE $T_B(w)$ VALUES, r_w AND GRAPHICALLY INTERPOLATED WITH THE TRIANGLE RULE, r_g

Compound	r_p	r_w	r_g
CH_2BrI	2.56	2.48–2.65	2.48
CHCl_2I	3.25	6.43	3.18
CHClBrI	—	—	6.90
CHClI_2	25.6	102.9	21.9
CHBr_2I	16.51	43.5	16.4
CHBrI_2	57.6	411.5	57.5
CHI_3	202	—	—
CCl_2Br_2	1.77	1.07	1.77
CClBr_3	5.32	4.82	5.32

$\text{CH}_z\text{X}_m\text{-}_n\text{Y}_n$, where Y is a halogen different from X. It is obvious that when $z = 3$, i.e., with compounds having the general formula CH_3X , the triangle is reduced to a straight line where the three halomethanes lie.

The compounds with three different halogen atoms lie within the triangle and, belonging to homologous series, follow a linear behaviour. It is possible to calculate their r and Bp values, as shown with thin lines in the centre of the triangle in Fig. 4.

The correlation between r and T_B values shows the same behaviour on the polar liquid phase SP-1000, as shown in Fig. 6. The triangle rule can also be applied in this instance, as shown for trihalomethanes CHX_3 in Fig. 7. In Table IV the r_g values calculated from the graphically extrapolated T_B (g) are compared with the r_w values obtained from tabulated $T_B(w)$ and with those previously calculated from the vapour pressures, r_p [8]. The r_p and r_g values correspond reasonably well whereas the r_w values sometimes being very different, confirm that some values of the boiling points deduced from uncertain experimental data can be replaced with those obtained by GC analysis.

The haloethanes and -ethenes also show regular behaviour. Fig. 8, obtained from analysis on the non-polar column, shows that these compounds lie on three straight lines. A fine triangular structure is also present, that cannot be seen on the scale of Fig. 8. but permits the calculation of data for various

Determination of trace amounts of carboxylic acids in ambient air by capillary gas chromatography–mass spectrometry

Stefan Sollinger, Karsten Levsen and Monika Emmrich

Fraunhofer Institute for Toxicology and Aerosol Research, Nikolai-Fuchs-Strasse 1, D(W)-3000 Hannover 61 (Germany)

(First received January 17th, 1992; revised manuscript received April 23rd, 1992)

ABSTRACT

A method for the determination of organic acids in ambient air using an ion-exchange resin in a bifunctional manner is presented. The ion-exchange resin is used as an adsorbent for sampling and subsequently as catalyst for the methylation of the adsorbed acids by methyl formate. The methyl esters are analysed by gas chromatography or gas chromatography–mass spectrometry. This method can be used to monitor workplace atmospheres and to analyse other ambient air samples.

INTRODUCTION

Organic acids are important compounds in chemical industry and are encountered in solvents, plastics and food processing. They are known as ubiquitous odour pollutants with a very low odour threshold (below 1 ppb in air). Moreover, fatty acids are released in considerable amounts into the atmosphere by biogenic sources. Hence methods for the determination of trace amounts of organic acids in the gaseous phase with low detection limits are desirable.

Some methods for the determination of carboxylic acids in ambient air have been reported. All these methods have in common that they require specialized analytical techniques and instrumentation or, if gas chromatography (GC) is used, special column phases. Simon *et al.* [1] reported a method using Florisil as adsorbent for sampling followed by ion chromatographic detection. Brocco and Tappa [2] also used ion chromatography, but collected air-

borne acids using filters impregnated with potassium hydroxide. The “scrubber” technique has been described in combination with ion chromatography [3]. Alternative approaches utilized liquid chromatographic procedures for detection. Samples have been collected on charcoal tubes, desorbed by sodium hydroxide with subsequent injection into a liquid chromatograph using a cation-exchange resin and a sulphuric acid mobile phase [4]. This technique has been termed ion-moderated partition chromatography [5]. For high-performance liquid chromatography with UV detection, derivatization by *p*-bromophenacyl bromide has been proposed, where sampling is achieved again by adsorption on charcoal [6]. An 18-crown-6 ether was useful for improvement of the conversion of the corresponding alkali metal salts into their bromophenacyl derivatives [7]. Liquid chromatographic approaches may also include ion-exclusion columns [8]. The GC determination of free organic acids was performed using analytical columns packed with 0.3% FFAP + 0.3% H₃PO₄ [9,10].

If a FFAP column is not available, derivatization of the acids will be necessary, and different methods have been reported [11–15]. Boron trifluoride in

Correspondence to: Dr. S. Sollinger, Fraunhofer Institute for Toxicology and Aerosol Research, Nikolai-Fuchs-Strasse 1, D(W)-3000 Hannover 61, Germany.

TABLE I
CONDITIONS FOR THE DETERMINATION OF VOLATILE ORGANIC ACIDS BY MASS SPECTROMETRY

Time (min)	Ion monitored (m/z)	Methyl ester of	Abbreviation
5 -8	88	Propionic acid	C ₃
8 -10.2	74	Butanoic acid	C ₄
	100	Methacrylic acid	METH
10.2-13.5	74	Methoxyacetic acid	MEAC
	74	Pentaic acid	C ₅
13.5-15.5	74	Hexanoic acid	C ₆
	117, 119	Trichloroacetic acid	TRIC
> 15.5	74	Heptanoic acid	C ₇
	74	Octanoic acid	C ₈
	74	Nonanoic acid	C ₉

methanol is a common derivatization reagent but with the disadvantage of column degradation if the methylation solution is injected without removal of the boron trifluoride. Another drawback is the relatively high boiling point of the solvent methanol, thus not allowing for the baseline GC separation of the lower homologues of fatty acid esters.

In this paper, a method is proposed in which the acids are adsorbed on different adsorbents and determined by GC after derivatization with methyl formate in the presence of a cation-exchange resin in the protonated form. The cation-exchange resin acts as an acidic catalyst to drive the methylation of the acids. GC can be carried out using common columns with methyl- or methyl/phenylsilicone phases.

EXPERIMENTAL

Instruments

A Hewlett-Packard Model 5890 gas chromatograph coupled with a Hewlett-Packard MSD 5970 mass spectrometer and a modified thermal desorption unit (Chrompack, Middelburg, Netherlands) was used. Baseline GC separation was achieved using an RTx-Volatiles capillary column (30 m × 0.25 mm I.D., 1.0- μ m film thickness) (Restek). Other columns with methyl- or methyl/phenylsilicone phases can also be used. The temperature was maintained at 35°C for 5 min and then raised at 10°C/min to 200°C. The gas chromatograph was equipped with a thermal desorption unit (Chrompack) modified as described previously [16]. The mass spectrometer was operated in the total-ion

mode (33-175u) and in the selected ion monitoring (SIM) mode (low-resolution option). The ions monitored under SIM conditions are listed in Table I.

Sampling

Gaseous samples were collected by adsorption on silica gel, activated charcoal and Amberlyst or their combinations. Fig. 1 shows the apparatus used for the generation of gaseous samples of the acids, consisting of a mass flow controller, a humidifier, a heated injector and a thermostated adsorption tube. The recovery experiments were carried out with gaseous samples of the acids produced as described in Fig. 1 with the exception of methoxyacetic acid and trichloroacetic acid, which were injected directly onto the adsorption tube.

Derivatization

Volumes of 2 ml of methyl formate were placed in glass vials (160 mm × 16 mm O.D.), which were closed by a screw-cap sealed with a silicone-rubber septum. The adsorbent loaded with organic acids

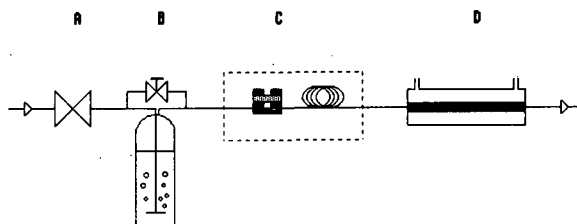


Fig. 1. Arrangement of standard gas and sampling equipment. A = Mass flow controller; B = humidifier; C = heated injector; D = thermostat for the sampling tubes.

and the Amberlyst cation-exchange resin (400 mg) was added to these vials. The tightly closed vials were heated at 90°C for 30 min by immersing them 40 mm deep in a stirred oil-bath. Before opening the vials they were chilled with water to prevent losses of the volatile esters. Volumes of 1–100 μ l of the solution were injected into a stainless-steel tube filled with Tenax TA. The compounds were transferred to the gas chromatograph by thermal desorption after purging the solvent.

Thermal desorption

To purge the solvent, the oven of the thermal desorption unit was kept at 50°C for 8 min, maintaining a helium flow of 5 ml/min through the Tenax tube [160 mm \times 6 mm I.D., containing 120 mg of Tenax TA (60–80 mesh)]. Thermal desorption was carried out by heating at 250°C for 10 min while a cryotrap capillary arranged in series was kept at –100°C. The analytes, now cryofocused, were then transferred to the analytical column by heating the cryotrap ballistically at 15°C/min to 200°C.

Chemicals

The acids, methyl formiate and the Amberlyst R 15 ion-exchange resin [17] were purchased from Aldrich (Steinheim, Germany). All reagents were of special grade. Before use the ion-exchange resin was washed several times with methanol until the methanol phase remained colourless and then extracted with methanol overnight using a mechanical shaker.

Silica gel (type G) and charcoal adsorption tubes (type B) were obtained from Dräger (Lübeck, Germany). Tenax TA (60–80 mesh) was purchased from Chrompack.

RESULTS AND DISCUSSION

Methylation

A mixture of ten organic acids (listed in Table I) consisting of 200 or 2000 μ g of each compound (not dissolved in any solvent) was methylated as described above (eight consecutive methylations were carried out). Methoxyacetic acid was added to the acid mixture immediately before the addition of the methylation suspension. Thus, the concentrations of the acids in 2 ml of the methylation solution were 0.1 and 1.0 mg/ml, respectively. A typical chro-

matogram is shown in Fig. 2a for the total-ion mode and in Fig. 2b for the SIM mode. Recoveries were determined by external calibration. Within the reproducibility of the experiment the yield of the methylation step for each organic acid tested is >80%, with the possible exception of trichloroacetic acid, showing a slightly lower recovery. As chloroform was identified by GC–mass spectrometry (MS) in the methylation suspension, it is assumed that the lower recovery in the case of trichloroacetic acid is due to the formation of chloroform as a competitive process. According to Christensen *et al.* [18], trichloroacetic acid decomposes to chloroform when heated. The temperature and depth of immersion of the vial in the oil-bath have to be chosen carefully in order to control this competitive effect. As the methylation was performed with two different concentrations of the acids (four times at each concentration), it was found that the methylation was nearly independent of the acid concentration, which is explained by the excess of ion-exchange resin and methyl formiate (the results are summarized in Table II).

Recovery including sampling

Activated charcoal tubes, silica gel tubes and ion-exchange resin tubes (Pasteur pipettes containing 800 mg of Amberlyst R 15 ion-exchange resin) were tested. A 1-ml volume of the mixture of ten acids was used to generate a gaseous sample of vaporized acids employing the apparatus shown in Fig. 1. Ten litres of humidified nitrogen (relative humidity 45%) were drawn through the tubes, maintaining a flow-rate of 150 ml/min. The contents of the tubes were then transferred into vials containing the methylation suspension (see Experimental). The reference solution was prepared by direct injection of 1 μ l of the acid mixture into a second vial also containing the methylation suspension. The methylation of both solutions was carried out as described under Experimental. The experiment was repeated three times. The recoveries, shown in Fig. 3, depend on the individual adsorbent and acid under investigation. The recovery is \geq 85% for the organic acids containing four or five carbon atoms, independent of the adsorbent chosen (standard deviation <14%). For the higher homologues a decrease in recovery was found with increasing boiling point, the decrease being greater for activated char-

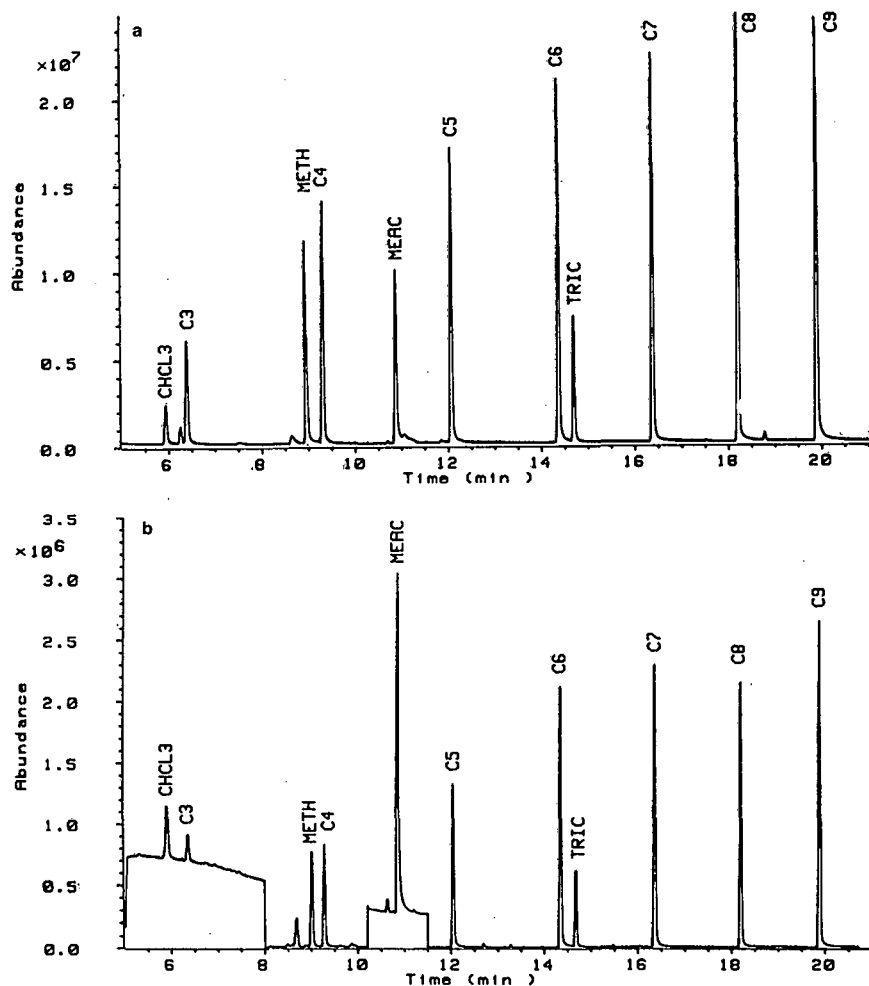


Fig. 2. (a) Typical total-ion chromatogram and (b) typical SIM chromatogram. For abbreviations, see Table I.

coal than for silica gel or Amberlyst. This decrease in recovery is also observed, if activated charcoal is added to the reference suspension after methylation of the acids and an additional heating period, thus leading to the conclusion that this reduced recovery is due to irreversible adsorption of esters of the higher homologues.

Amberlyst gave recoveries $>80\%$ for all acids, with the exception of propionic acid, the most volatile acid studied. Keeping this in mind, a combination of two adsorbents is recommended if quantitative sampling of all organic acids listed in Table I is desired. To test this, a combination of 500 mg of

Amberlyst and 100 mg of activated charcoal arranged in series was investigated. The recoveries with both adsorbents were determined separately. As Table III reveals, only short-chain acids break through the Amberlyst adsorbent, leading to low recoveries if only Amberlyst is used. If the recoveries from both adsorbents determined separately are added, a value close to 100% is achieved also for the very volatile acids.

Detection limits, blanks

Detection limits (signal-to-noise ratio = 3) are shown in Table IV. If detection occurs by mass

TABLE II
RECOVERY (%) AND REPRODUCIBILITY OF METHYLATION USING METHYL FORMATE AND AN ION-EXCHANGE RESIN AS REAGENTS
Concentration of each acid in the methylation solution = 0.1 or 1 mg/ml.

Compound	0.1 mg/ml acid				1 mg/ml acid							
	Replicate No.				Replicate No.							
	1	2	3	4	1	2	3	4				
Propionic acid	100.0	99.7	99.8	98.1	99.4	0.9	98.0	96.4	101.3	105.2	100.2	3.9
Methacrylic acid	97.1	104.4	99.1	96.4	99.3	3.6	102.3	98.4	97.6	95.5	98.7	2.5
Butanoic acid	105.9	114.4	107.2	98.4	106.5	6.6	105.1	96.3	99.1	103.8	96.3	7.7
Methoxyacetic acid	100.4	103.3	101.0	99.7	101.1	1.6	106.1	97.3	86.4	97.2	96.8	8.1
Pentanoic acid	109.8	114.4	105.0	101.0	107.6	5.8	97.9	95.4	103.9	103.1	100.0	4.1
Hexanoic acid	95.4	96.6	100.0	102.3	98.6	3.2	105.0	101.6	103.8	99.8	102.6	2.3
Trichloroacetic acid	80.1	79.2	85.3	86.1	82.7	3.5	77.1	78.4	82.7	85.3	80.9	3.8
Heptanoic acid	87.6	86.7	87.1	89.2	87.7	1.1	84.5	89.2	85.4	90.2	87.3	2.8
Octanoic acid	81.3	80.8	81.7	82.5	81.6	0.7	86.2	80.9	84.5	89.1	85.2	3.4
Nonanoic acid	82.6	85.5	83.4	84.3	84.0	1.2	84.7	85.3	81.3	87.6	84.7	2.6

^a R.S.D. = relative standard deviation.

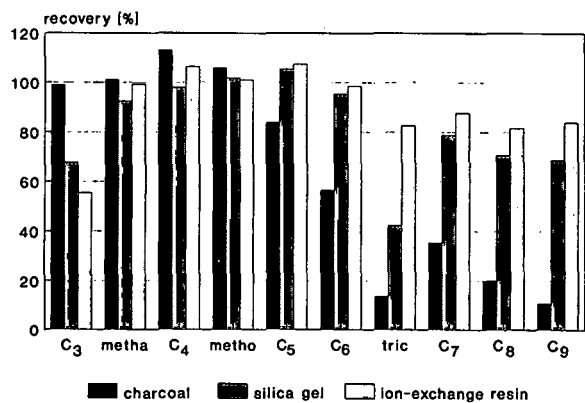


Fig. 3. Recoveries using different adsorbents. For abbreviations, see Table I.

spectrometry in the total-ion mode, detection limits from 0.1 to 2.4 $\mu\text{g}/\text{l}$ are achieved. They are lower by a factor of 5–10 if the mass spectrometer is operated under SIM conditions. The detection limit depends on the molecular weight, *i.e.*, higher homologues exhibit lower detection limits, which is due to a higher detector response. The detection limits can be further reduced by applying an additional pre-concentration step (*i.e.*, by injecting larger volumes of the methylation solution onto Tenax adsorbent followed by thermal desorption after purging the solvent as described under Experimental). This procedure exhibits a high reproducibility for most of the methyl esters, with the exception of methyl propionate, which shows a lower recovery due to a

TABLE III
RECOVERY USING A COMBINATION OF AMBERLYST AND ACTIVATED CHARCOAL

Compound	Recovery (%)					
	Replicate 1			Replicate 2		
	Amberlyst	Charcoal	Total	Amberlyst	Charcoal	Total
Acetic acid	31.3	62.2	93.5	40.1	60.4	90.5
Propionic acid	55.4	42.5	97.9	57.4	42.9	100.3
Butanoic acid	85.1	13.5	98.6	89.8	8.6	98.4

TABLE IV
DETECTION LIMITS

Compound	Total ion mode: without additional preconcentration		SIM			
			Without additional preconcentration		With additional preconcentration	
	$\text{ng}/\mu\text{l}^a$	ng/l^b	$\text{pg}/\mu\text{l}^a$	ng/l^b	$\text{pg}/\mu\text{l}^a$	ng/l^b
Propionic acid	4.3	861	850	170	11.5	2.3
Methacrylic acid	3.4	672	880	176	10.1	2.0
Butanoic acid	4.7	948	900	180	13	2.6
Methoxyacetic acid	12.3	2464	1020	204	18	3.6
Pentanoic acid	3.4	696	905	181	11	2.2
Hexanoic acid	2.6	520	157	31.5	1.7	0.3
Trichloroacetic acid	n.d. ^c	n.d. ^c	282	56.4	4.3	0.8
Heptanoic acid	1.2	232	16	3.2	0.3	0.06
Octanoic acid	0.70	142	6.5	1.3	0.09	0.02
Nonanoic acid	0.56	112	4.2	8.4	0.05	0.01

^a In methylation suspension.

^b In air sample.

^c Not determined.

TABLE V
RECOVERY AND REPRODUCIBILITY OF REPLICATE PRECONCENTRATIONS

Methyl ester of	Recovery (%)					Mean	R.S.D. (%)
	Replicate No.						
	1	2	3	4	5		
Propionic acid	73.8	69.9	61.6	58.4	60.4	64.8	6.7
Methacrylic acid	115.8	90.1	88.7	97.3	95.9	97.6	10.8
Butanoic acid	119.8	86.5	116.7	84.2	84.3	98.3	9.0
Methoxyacetic acid	118.7	93.4	92.4	91.2	90.2	97.2	12.1
Pentanoic acid	113.8	97.7	96.7	96.2	95.1	99.9	7.8
Hexanoic acid	114.7	112.7	103.3	103.9	113.3	109.6	5.5
Trichloroacetic acid	91.9	89.9	73.6	75.2	78.1	81.7	8.5
Heptanoic acid	105.6	97.7	98.1	101.2	101.6	100.8	3.2
Octanoic acid	98.8	101.3	105.4	96.7	97.1	99.8	3.6
Nonanoic acid	100.9	110.9	101.9	103.4	104.4	104.3	3.9

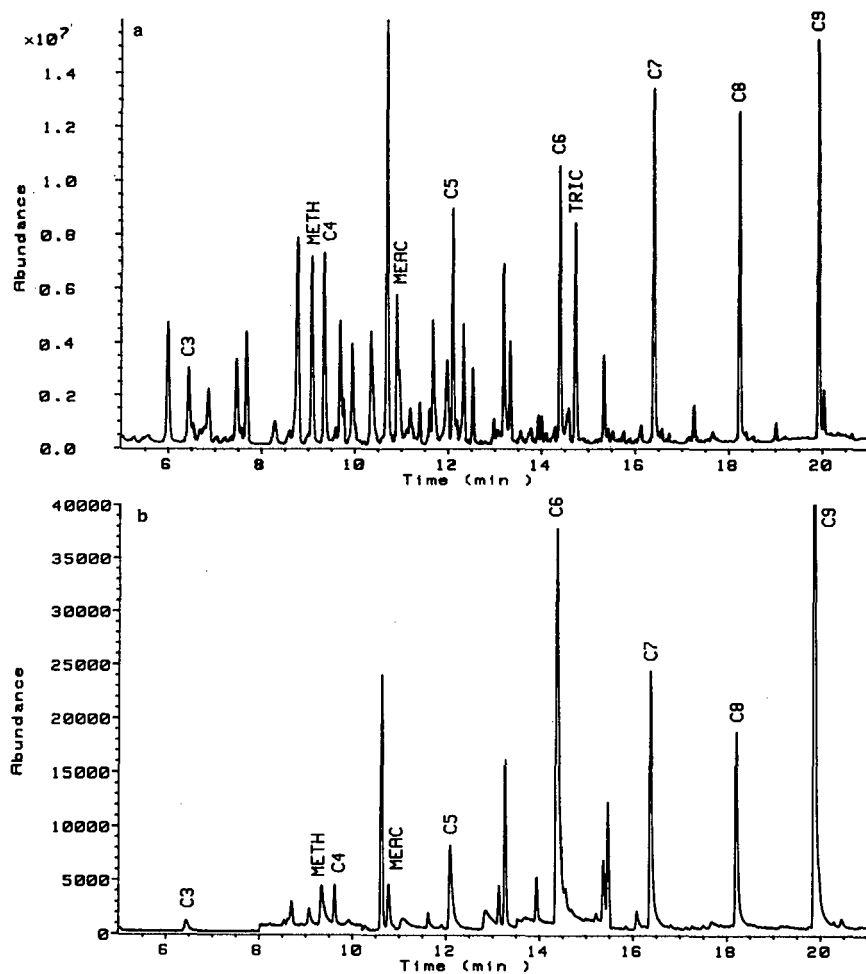


Fig. 4. (a) Typical total-ion chromatogram and (b) typical SIM chromatogram obtained after preconcentration in the thermal desorption unit. For abbreviations, see Table I. Additional peaks are due to impurities in the methylation reagent.

higher volatility, and trichloroacetic acid, due to thermal instability (see Table V). Two chromatograms obtained after preconcentration are shown in Fig. 4a (total-ion mode) and Fig. 4b (SIM mode). A further increase in sensitivity is also achievable by on-column injection of larger volumes using the retention gap technique [19]. Blank values were below the detection limit for the acids under investigation.

CONCLUSIONS

The method described for sampling and determining trace amounts of gaseous carboxylic acids shows a high repeatability and high recovery. The sample volume required is ≤ 10 l. The acids are collected on an adsorbent (Amberlyst cation-exchange resin), which also catalyses the methylation of the acids. Derivatization and GC separation of the carboxylic acids require no special equipment and are completed within 50 min. Damage to the analytical column by a derivatization reagent is eliminated as the solid catalyst settles at the bottom of the vial after the derivatization step. Detection limits reach the lower ppt level.

Further simplification of the procedure is suggested by carrying out the derivatization directly in an adsorption tube containing the bifunctional adsorbent, followed by thermal desorption into the GC-MS system.

REFERENCES

- 1 P. Simon, F. Brand and C. Lemacon, *J. Chromatogr.*, 479 (1989) 445.
- 2 D. Brocco and R. Tappa, *J. Chromatogr.*, 367 (1986) 240.
- 3 W. R. Hartmann, M. O. Andrae and G. Helas, *Atmos. Environ.*, 23 (1989) 1531.
- 4 R. E. Pauls and G. J. Weight, *J. Chromatogr.*, 254 (1983) 171.
- 5 *Ion-Moderated Partition Chromatography*, Bio-Rad Labs., Richmond, CA, 1980.
- 6 S. Vainiotalo, P. Pfäffli and A. Zitting, *J. Chromatogr.*, 258 (1983) 207.
- 7 K. Kuwata and S. Tanaka, *J. Chromatogr.*, 455 (1988) 425.
- 8 D. Grosjean, A. van Neste and S. S. Parmar, *J. Liq. Chromatogr.*, 12 (1989) 3007.
- 9 Y. Hoshika, *Anal. Chem.*, 54 (1982) 2433.
- 10 Y. Hoshika, *Analyst (London)*, 106 (1981) 166.
- 11 A. Di Lorenzo, *J. Chromatogr.*, 55 (1971) 303.
- 12 H. Iwase, T. Kimura and T. Sugiyama, *Bunseki Kagaku*, 24 (1975) 272.
- 13 A. Anton, *Anal. Chem.*, 40 (1968) 1116.
- 14 R. G. Ackman and S. N. Hooper, *Lipids*, 5 (1970) 417.
- 15 E. Hantala and M. L. Weaver, *Anal. Biochem.*, 30 (1969) 32.
- 16 S. Sollinger and K. Levsen, *Fresenius' Z. Anal. Chem.*, submitted for publication.
- 17 *Technical Information Bulletin Number AL-142, Ion-Exchange Resins and Related Polymeric Adsorbents*, Aldrich, Milwaukee, WI, 1991.
- 18 J. M. Christensen, K. Rasmussen and B. Køppen, *J. Chromatogr.*, 442 (1988) 317.
- 19 K. Grob, G. Karr and M. L. Riekkola, *J. Chromatogr.*, 334 (1985) 129.

CHROM. 24 334

Determination of sulphurated compounds in *Tagetes patula* cv. *nana* essential oil by gas chromatography with mass spectrometric, Fourier transform infrared and atomic emission spectrometric detection

Carlo Bicchi, Carlotta Frattini, Gloria Pellegrino and Patrizia Rubiolo

Dipartimento di Scienza e Tecnologia del Farmaco, Via P. Giuria 9, 10125 Turin (Italy)

Vittorio Raverdino and George Tsoupras

Hewlett Packard SA, P.O. Box 365, CH-1217 Meyrin 1, Geneva (Switzerland)

(First received February 3rd, 1992; revised manuscript received May 5th, 1992)

ABSTRACT

The determination of the sulphurated compounds in the essential oil of *Tagetes patula* cv. *nana* by gas chromatography (GC)–mass spectrometry with different ionization techniques (electron impact and positive- and negative-ion chemical ionization), GC–Fourier transform infrared spectrometry and GC–atomic emission spectrometry is reported. *Tagetes* essential oils contain a series of acetylenic thiophenes in various amounts; the most abundant have already been described in the literature, whereas the structures of some others, especially trace components, are still unknown. These compounds are known to be repellent to insects. The contribution that these combined techniques can make to the identification and structure elucidation of acetylenic thiophene compounds in the essential oil of *T. patula* cv. *nana* is discussed.

INTRODUCTION

The identification of the components of a complex mixture, such as an essential oil, is generally carried out by combining a separation technique [mainly gas chromatography (GC)] with a structure identification technique, of which the best established are mass spectrometry (MS) and Fourier transform infrared spectrometry (FT-IR).

The coupling between GC and atomic emission spectrometry (AES) has recently been made available commercially for the routine analysis of complex mixtures. The use of microwave-induced helium plasma (MIP)–AES at low pressure for GC

detection has been known since 1965 [1,2]. In 1976, Beenakker [3,4] described an atmospheric pressure helium plasma with a new cavity concept which was immediately successful. More recently, new commercial instruments have become available which combine an atmospheric Beenakker-like plasma with a photodiode-array detector as a multi-channel detector [5]. The main feature of MIP–AES is the multi-element selective detection, which permits the calculation of the elemental formulae of the components separated by GC [6–8].

During a study on the composition of the essential oils of some ornamental plants [9], we focused our attention on the flowers of a cultivar of *Tagetes patula*, in particular *Tagetes patula* cv. *nana* Furia. A class of compounds characteristic of these species is the acetylenic thiophenes, a group of minor com-

Correspondence to: Professor C. Bicchi, Dipartimento di Scienza e Tecnologia del Farmaco, Via P. Giuria 9, 10125 Turin, Italy.

ponents which are relatively abundant in the early vegetation stages of the plant. Acetylenic thiophenes constitute an important group of secondary metabolites, found in many species of Asteraceae [10–12]. These compounds are widely studied for their biological activity, in particular as photoinduced insecticides, nematocides, fungicides and bactericides. Extracts of *Tagetes* are used in folk medicine to treat ailments which include conjunctivitis, mumps, sore eyes, coughs and dysentery [13].

This paper describes the contribution that combined techniques (GC–MS with different ionization modes, GC–FT-IR, GC–AES) can make to the identification and structure elucidation of acetylenic thiophenes in complex mixtures such as *T. patula* cv. *nana* essential oils without the need for preliminary isolation.

EXPERIMENTAL

Essential oil samples

T. patula cv. *nana* was identified and supplied by Professor E. Cappelletti (Dipartimento di Biologia, Università di Padova, Padova, Italy). The essential oils were obtained by submitting dried flowers to steam distillation, either in a modified Marcusson apparatus (100 g) [14] or in a modified Marcusson microapparatus, developed in the authors' laboratory (10 g) [15].

Capillary gas chromatographic (cGC) analysis

cGC analyses were carried out on a fused-silica open tubular (FSOT) capillary column (23 m × 0.25 mm I.D., film thickness $d_f = 0.3 \mu\text{m}$) coated with OV-1, installed in a Carlo Erba Mega 5360 gas chromatograph provided, with both flame ionization (FID) and sulphur-selective detection (SSD) [16]. The operating conditions were as follows: column temperature, increased from 50°C (held for 1 min) to 220°C at 3°C/min; carrier gas, hydrogen; flow-rate, 1.6 ml/min; injection system, split; splitting ratio, 1:30; and detector temperature, 250°C. cGC data were processed by a Hewlett-Packard 3393A integrator.

cGC–MS analysis

cGC–MS analyses were carried out on a Hewlett-Packard Model 5988A GC–MS system. The same column as for cGC analysis was used, with cGC

conditions as above except that the carrier gas was helium. Positive-ion (PICI) and negative-ion chemical ionization (NICI) were carried out with methane at an ion source temperature of 100°C and a pressure of 0.7 Torr.

cGC–FT-IR analysis

A Hewlett-Packard Model 5965 xGC–IR system was used. A 1- μl volume of the essential oil diluted 1:100 in hexane was injected. cGC analysis was carried out on the FSOT column and under the chromatographic conditions described above.

The FT-IR conditions were as follows: cGC–FT-IR interface, 100- μl light-pipe (10 cm length × 1.2 mm I.D.); temperature, 240°C; make-up gas, nitrogen; flow-rate, 0.2 ml/min; time resolution (repetition rate), 3 scans/s at 8 cm^{-1} resolution. In most cases five interferograms were added in real time, resulting in an effective time slice of about 2 s. The FT-IR detector was an HgCdTe type of narrow band width (4000–750 cm^{-1}).

cGC–AES analysis

The MIP system was an HP 5921 AES instrument coupled with an HP 5890 gas chromatograph provided with an autosampler (HP 7673A). The same column as for cGC analysis was used, with the cGC conditions as described above except that the carrier gas was helium. AES was used to measure the C:S ratio at the wavelengths C = 193 nm and S = 181 nm. The AES conditions were as follows: cavity temperature, 270°C; spectrometer purge flow, nitrogen at 2 l/min; scavenger gases, oxygen and hydrogen; make-up flow, helium at 60 ml/min; window purge helium at 30 ml/min.

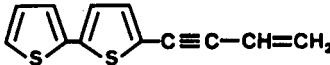
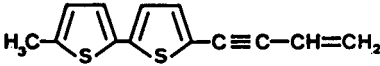
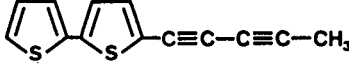
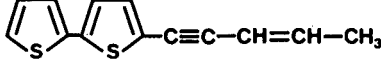
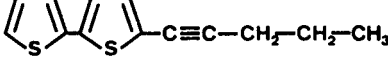
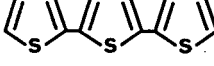
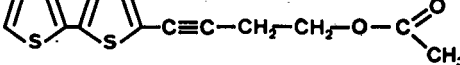
RESULTS AND DISCUSSION

Acetylenic thiophenes constitute a classical example of constituents of a complex mixture that are quantitatively minor but of high biological interest. Recently, Hathcock *et al.* [17] reported the presence of two of them (compounds **6** and **7** in Table I) in the essential oils of *Tagetes minuta*, together with a brief discussion of the techniques for their identification. To the authors' knowledge, compounds belonging to this class have never been reported before in *Tagetes* essential oils.

Table I gives the elemental formulae, structural

TABLE I

ELEMENTAL FORMULAE, STRUCTURAL FORMULAE AND SYSTEMATIC NAMES OF THE ACETYLENIC THIOPHENES IDENTIFIED IN *T. PATULA* CV. *NANA* FLOWERS ESSENTIAL OIL

Compound No.	MW	Elemental formula	Structural formula	Systematic
1	216	C ₁₂ H ₈ S ₂		5-(3-Buten-1-ynyl)-2,2'-bithienyl
2	230	C ₁₃ H ₁₀ S ₂		5'-Methyl-5-(3-buten-1-ynyl)-2,2'-bithienyl
3	228	C ₁₃ H ₁₀ S ₂		5-(1,3-Pentadiynyl)-2,2'-bithienyl
4	230	C ₁₃ H ₁₀ S ₁		5-(3-Penten-1-ynyl)-2,2'-bithienyl
5	232	C ₁₃ H ₁₄ S ₂		5-(1-Pentynyl)-2,2'-bithienyl
6	248	C ₁₂ H ₈ S ₂		α-Terthienyl
7	276	C ₁₄ H ₁₂ S ₂ O ₂		5-(4-Acetoxy-1-butynyl)-2,2'-bithienyl

formulae and names of the sulphurated compounds identified in the essential oil of *T. patula* cv. *nana* flowers. These compounds must be identified through coupled techniques when their isolation is impossible, as here, where the plant material was scarce and the essential oil content low. The classical methods of detection (FID) and identification [electron impact (EI) MS] can often be insufficient for identification for several reasons, e.g., the complexity of the essential oils in question, the small amounts of the compounds under investigation, the compounds under investigation elute in very complex

parts of the gas chromatogram and the compounds under investigation elute very close to quantitatively major components.

Fig. 1 reports the cGC–EI–MS pattern of the *T. patula* essential oil.

The first problem to deal with is the qualitative location of acetylenic thiophenes within the cGC pattern and their quantitative evaluation, if necessary. This was achieved by simultaneous FID–SSD [16]. Fig. 2 shows the cGC–SSD pattern of the sample previously reported, where seven sulphurated compounds are detected.

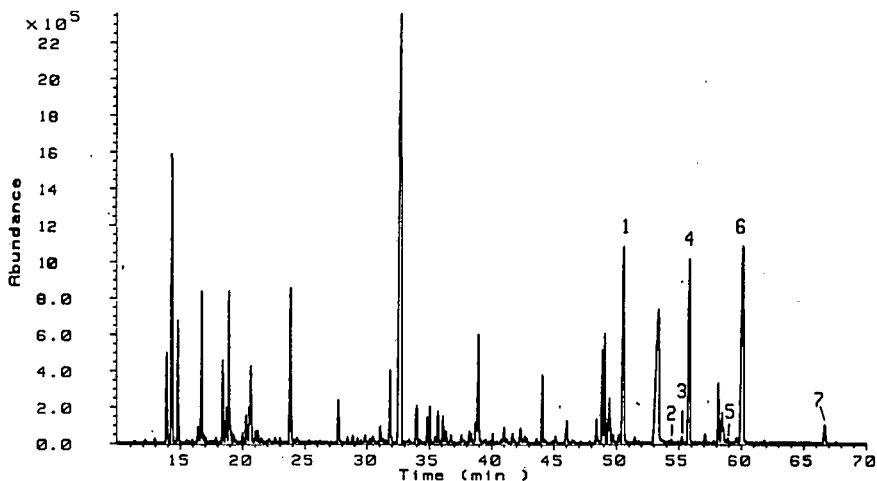


Fig. 1. cGC-EI-MS pattern of the *T. patula* cv. *nana* flower essential oil.

SSD also affords quantitative results, although these are affected by the quadratic detector response related to the excited species *S_2 produced in SSD. Retention indices were used to identify the acetylenic thiophenes in the various combined GC-identification techniques patterns.

Identification of sulphur-containing compounds can also be achieved by GC-MIP-AES. This technique provides not only information that is multi-element sensitive, selective, qualitative and linearly quantitative, but also information about the elemental formulae of the eluting components.

Elemental formulae can be calculated from GC-AES results through the following element-to-carbon (E/C) ratio expression [18]:

$$\frac{E}{C} = \frac{E \text{ at. in ref. } E (\text{area of uk.}) C (\text{area of ref.})}{C \text{ at. in ref. } E (\text{area of ref.}) C (\text{area of uk.})}$$

where at. = atoms, ref. = reference and uk. = unknown.

As the original molecular structure of the analytes could influence the element responses [7,8,18], one of the acetylenic thiophene components unambiguously identified in the sample (compound 7) through its IR and EI mass spectra was used as a reference for calculation. One of the most critical points for the determination of the empirical formula is a reliable and unambiguous evaluation of the peak area of each element in the formula: this requires a baseline cGC separation of the peaks under investigation and a careful selection of the integration codes. For complex mixtures such as those under investigation, a cGC column coated with a different stationary phase can often be necessary to obtain a baseline separation of the components in question.

Table II reports the C:S ratios calculated for acetylenic thiophenes detected in the essential oil under investigation. Fig. 3 shows those parts of the S and C AES patterns where the acetylenic thiophenes elute. This example clearly shows the reason why the C:S ratio for compound 1 is in very good agreement with the supposed elemental formula whereas the C:S ratios for compounds 2, 4 and 6 are not particularly close to the theoretical values. In these

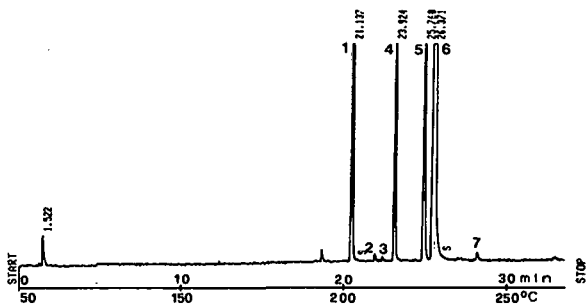


Fig. 2. cGC-SSD pattern of the *T. patula* cv. *nana* flower essential oil.

TABLE II
C:S RATIOS CALCULATED FOR ACETYLENIC THIOPHENES DETECTED IN THE ESSENTIAL OIL OF *TAGETES PATULA* CV. *NANA* FLOWERS

Compound No.	MW	Elemental formula	C:S ratio	
			Theoretical	Experimental
1	216	C ₁₂ H ₈ S ₂	0.166	0.164
2	230	C ₁₃ H ₁₀ S ₂	0.154	0.175
4	230	C ₁₃ H ₁₀ S ₂	0.154	0.160
6	248	C ₁₂ H ₈ S ₃	0.25	0.261
7	276	C ₁₄ H ₁₂ S ₂ O ₂	0.142	Reference

instances, an exact C peak-area value is difficult to determine because of overlapping with major or equally abundant peaks. Moreover, the C pattern at 193 nm in the part of the chromatogram where the acetylenic thiophenes elute is very complex, and compounds 3 and 5 are present only in trace amounts; as a consequence, their C peak areas do not provide a correct calculation of the C:S ratio.

AES results are very useful for identification, and

often also to calculate the elemental formula, but they do not provide any structural information. Structure elucidation without isolation can only be carried out using GC-MS with different ionization mode and GC-FT-IR.

The EI mass spectra of acetylenic thiophenes are characterized by a very intense molecular ion M⁺, which is often the base peak of the spectrum; other less intense but diagnostic ions corresponding to the acetylenic thiophene structure are, for instance, the fragments at *m/z* [M - HS]⁺, *m/z* 215 ([C₁₂H₇S₂)⁺ and *m/z* 171 ([C₁₁H₇S]⁺). The fragmentation patterns of the acetylenic thiophenes identified here are in agreement with that reported by Hartough [19] and Horn and Lambertson [20].

GC-MS with both PICI and NICI using methane as reactant gas produces high-intensity diagnostic ions affording the confirmation of the molecular weight of acetylenic thiophenes. Methane PICI-MS gives a high-intensity quasi-molecular ion [M + 1]⁺ due to a proton addition, while methane NICI-MS produces high-intensity molecular ions (M⁻) as a consequence of an electron-capture phenomenon. In the essential oil under investigation, the electron-capture phenomenon associated with methane

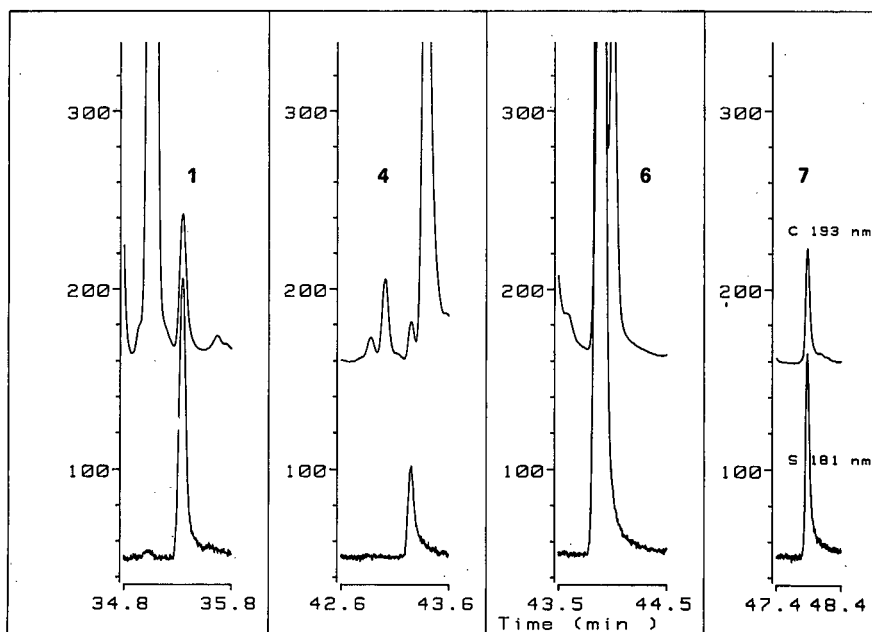


Fig. 3. S and C AES patterns of compounds 1, 4, 6 and 7.

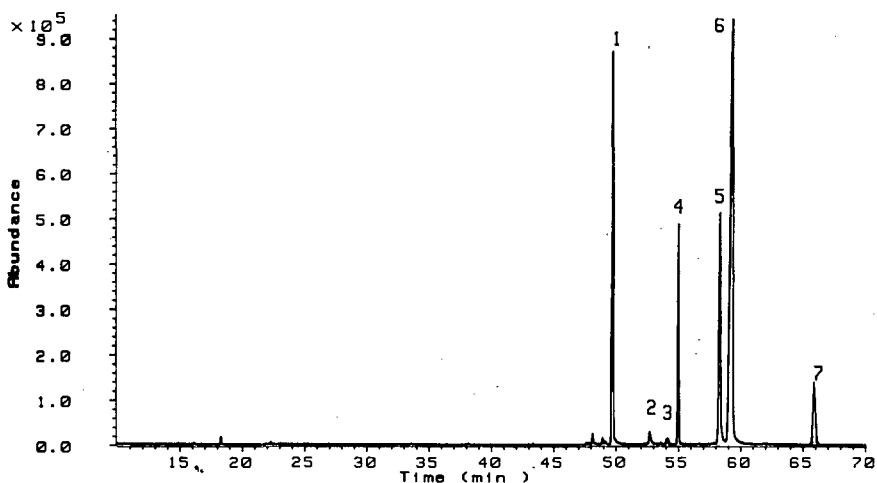


Fig. 4. cGC-methane NICI-MS pattern of *T. patula* cv. *nana* flower essential oil.

NICI-MS is specific for the acetylenic thiophenes, and is complementary to GC-SSD and to GC-AES for their correct identification in the total chromatogram. Fig. 4 reports the cGC-methane NICI-MS pattern of *T. patula* cv. *nana* essential oil. In both the CI and EI mass spectra, the peaks at m/z M^+ and $[M+2]^+$ exhibit the characteristic intensity ratio peculiar to ions containing sulphur. Fig. 5 reports the EI, NICI and PICI mass spectra of compound 1. Table III reports the main CI- and EI-MS ions characteristic of the acetylenic thiophenes present in the essential oil under investigation.

GC-FT-IR also gives significant spectra useful and complementary to MS for an unambiguous identification of acetylenic thiophenes. They can be identified by their characteristic absorptions in the following regions [19–22]: 3080 cm^{-1} , medium-high-intensity band, CH = stretch in the thiophene ring; 2195 cm^{-1} , medium-low-intensity band, $-\text{C}\equiv\text{C}-$ stretch of the acetylenic triple bond; 1505 , 1415 , 1380 cm^{-1} , medium-low-intensity bands, substitution in position 2 of the thiophene ring; and 835 , 795 cm^{-1} , high-intensity band characteristic of the thiophene ring.

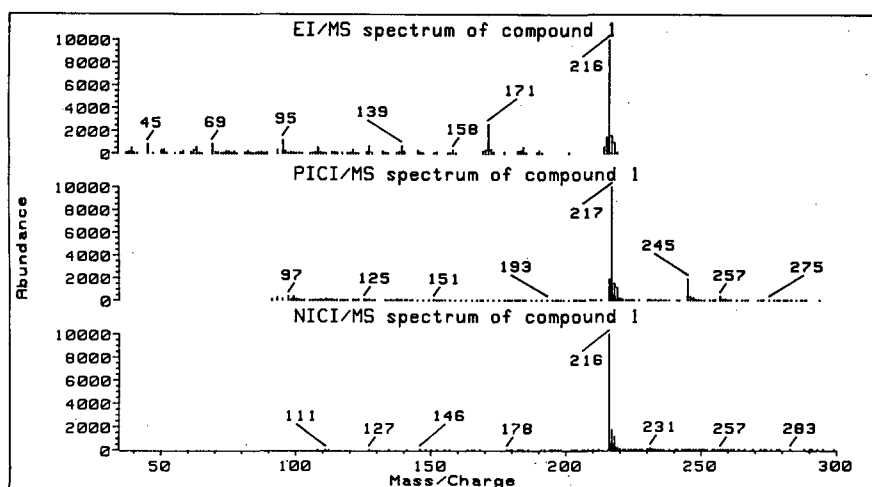


Fig. 5. EI, NICI and PICI mass spectra of compound 1.

TABLE III

EI- AND CI-MS IONS CHARACTERISTIC OF THE ACETYLENIC THIOPHENES PRESENT IN THE ESSENTIAL OIL OF *TAGETES PATULA* CV. *NANA* FLOWERS

Compound No.	MW	Ionization mode	Main fragments (<i>m/z</i> , %)
1	216	EI	45(8.38), 69(10.15), 95(10.31), 127(6.13), 139(6.43), 171(26.32), 172(3.67), 173(1.35), 215(12.57), 216(100), 217(14.83), 218(9.55)
2	230		39(4.71), 45(5.47), 83(15.60), 102(6.33), 121(4.25), 152(6.09), 184(4.78), 197(22.36), 229(36.07), 230(100), 231(18.10), 232(11.38)
3	228		45(1.39), 69(5.32), 121(3.92), 139(5.99), 141(5.01), 169(4.27), 183(4.78), 195(18.71), 227(34.78), 228(100), 229(17.72), 230(11.40)
4	230		39(9.64), 45(10.23), 69(8.32), 115(6.86), 165(5.76), 171(7.20), 184(7.15), 197(10.75), 229(25.94), 230(100), 231(17.48), 232(9.82)
5	232		41(53.38), 43(62.52), 83(31.30), 84(100), 97(28.89), 111(22.15), 149(16.35), 203(19.72), 231(14.69), 232(49.56), 233(9.01), 234(8.46)
6	248		45(13.96), 69(10.92), 121(5.71), 124(6.33), 127(13.49), 171(10.23), 190(4.12), 203(16.35), 247(5.93), 248(100), 249(15.75), 250(13.82)
7	276		43(24.56), 45(4.32), 69(5.52), 171(9.44), 203(12.41), 215(5.06), 216(100), 217(15.77), 218(9.76), 276(8.45), 277(1.42), 278(0.75)
1	216	NICI	216(100), 217(17), 218(11), 231(1.47)
2	230		230(100), 231(189), 232(12)
3	228		228(100), 229(25), 230(17), 243(1.39)
4	230		230(100), 231(18), 232(119), 245(1.56)
5	232		232(100), 233(16), 234(11)
6	248		248(100), 249(18), 250(16), 263(1.90)
7	276		276(100), 277(18), 278(16)
1	216	PICI	216(18.99), 217(M+1) (100), 218(15.11), 219(11.55), 245(18.96)
2	230		230(24.68), 231(M+1) (100), 232(20.32), 233(13.59), 259(15.12)
3	228		Non-significant spectrum
4	230		230(25.05), 231(M+1) (100), 232(17.90), 233(11.57), 259(16.81)
5	232		233(M+1) (100), 234(14.70), 235(10.03), 261(14.16)
6	248		248(23.74), 249(M+1) (100), 250(17.34), 251(13.96), 277(16.25)
7	276		217(37.11), 277(M+1) (100), 278(14.15), 279(10.97), 305(10.06)

Fig. 6 reports the FT-IR spectra of **1** and **6**. The two spectra clearly show that the IR spectra contribute to the characterization of the thiophenic part of the structure, with absorptions near 3083, 1509,

1414, 1385, 841 and 795 cm^{-1} for **1**, and with those near 3080, 1503, 1418, 1379, 832 and 796 cm^{-1} for **6**. In addition, **1** exhibits the absorptions characteristic of the acetylenic group, with the absorption at 2195

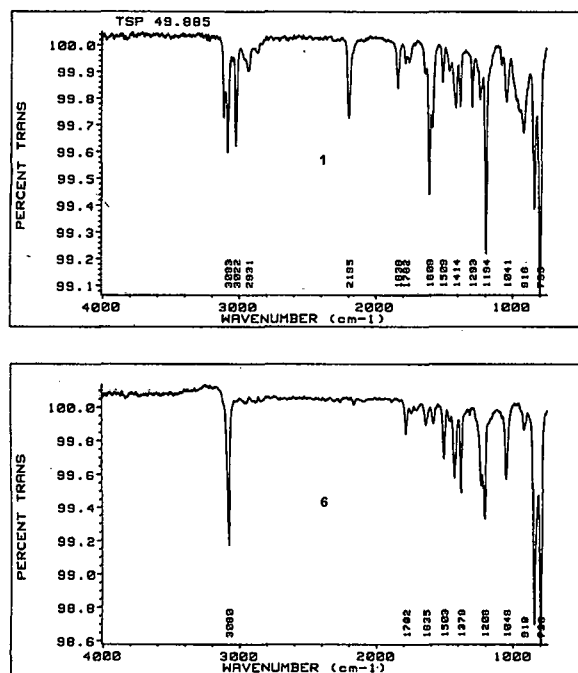


Fig. 6. FT-IR spectra of compounds 1 and 6.

cm^{-1} and those at 3100, 3022 and 2931 cm^{-1} characteristic of the substituent in position 2 on the thiophene ring.

Table IV reports the characteristic absorptions

TABLE IV

CHARACTERISTIC ABSORPTIONS FOR THE ACETYLENIC THIOPHENES PRESENT IN THE ESSENTIAL OIL OF *TAGETES PATULA* CV. *NANA* FLOWERS

Compound No.	Molecular mass	IR band position (cm^{-1}) ^a
1	216	3083(m), 3022(m), 2931(w), 2195(m), 1838(m), 1782(w), 1509(w), 1414(w), 1380(w), 1194(s), 830(m), 798(s)
2	230	3110(w), 3081(m), 3025(w), 2940(w), 2205(w), 1615(w), 798(s)
4	230	3079(m), 3040(w), 3016(m), 2932(s), 2869(m), 2231(w), 1747(w), 1621(s), 1516(w), 1443(w), 1383(w), 1194(m), 910(m), 798(s)
6	248	3080(s), 1782(w), 1635(w), 1503(w), 1420(m), 1396(m), 1206(s), 1046(w), 918(s), 835(s), 798(s)

^a m = medium; s = strong; w = weak.

for the acetylenic thiophenes present in the essential oil under investigation. FT-IR also afforded an unambiguous distinction between the two isomers at MW 230 (2 and 4), which cannot be distinguished by MS. Compound 2 actually shows medium-low-intensity bands at 3040, 2870 and 2748 cm^{-1} , corresponding to the stretching of a methyl substituent in position 4 of the thiophene ring [19,22]. The lower sensitivity of GC-FT-IR than GC-MS allowed us to record significant IR spectra only for four of the seven detected acetylenic thiophenes.

ACKNOWLEDGEMENTS

C.B., C.F., G.P. and P.R. thank the Ministero dell'Università e della Ricerca Scientifica e Tecnologica (60% and 40% research funds), CNR (Progetto Finalizzato Chimica Fine 2) and Assessorato Agricoltura Foreste e Ambiente Naturale della Regione Autonoma Valle d'Aosta for financial support to the laboratory.

REFERENCES

- 1 A. J. McCormick, S. C. Tong and W. D. Cook, *Anal. Chem.*, 37 (1965) 1470.
- 2 C. A. Bache and D. J. Lisk, *Anal. Chem.*, 37 (1965) 1477.
- 3 C. I. M. Beenakker, *Spectrochim. Acta, Part B*, 31 (1976) 483.
- 4 C. I. M. Beenakker, *Spectrochim. Acta, Part B*, 32 (1977) 173.
- 5 P. L. Wylie and D. B. Quimby, *J. High Resolut. Chromatogr.*, 12 (1989) 813.

- 6 J. J. Sullivan and D. B. Quimby, *J. High Resolut. Chromatogr.*, 12 (1989) 282.
- 7 P. L. Wylie, J. L. Sullivan and D. B. Quimby, *J. High Resolut. Chromatogr.*, 13 (1990) 499.
- 8 J. Th. Jelink and A. Venema, *J. High Resolut. Chromatogr.*, 13 (1990) 447, and references cited therein.
- 9 C. Bicchi, C. Frattini, G. Pellegrino, P. Rubiolo, E. M. Cappelletti and R. Caniato, in preparation.
- 10 F. Bohlmann, T. Burkhardt and C. Zdero, *Naturally Occurring Acetylenes*, Academic Press, London, 1973.
- 11 F. Bohlmann and C. Zdero, in S. Gronwitz (Editor), *The Chemistry of Heterocyclic Compounds, Vol. 44, Thiophene and Its Derivatives, Part 1*, Wiley, New York, 1985, p. 251.
- 12 L. P. Christensen and J. Lam, *Phytochemistry*, 30 (1991) 11.
- 13 G. H. N. Towers and D. E. Champagne, in J. Lam, H. Breteler, T. Arnason and L. Hansen (Editors), *Chemistry and Biology of Naturally-Occurring Acetylenes and Related Compounds*, Elsevier, Amsterdam, 1988, p. 139, and references cited therein.
- 14 H. Kaiser and W. Lang, *Dtsch. Apoth.-Ztg.*, 175 (1951) 163.
- 15 C. Bicchi, A. D'Amato, C. Frattini and G. M. Nano, *J. Chromatogr.*, 279 (1983) 409.
- 16 C. Bicchi, A. D'Amato and M. Galli, *J. High Resolut. Chromatogr.*, 12 (1989) 349.
- 17 L. Hathcock, C. Wells and W. Bertsch, in P. Sandra (Editor), *Proceedings of the 13th International Symposium on Capillary Chromatography, Riva del Garda, May 1991*, Hüthig, Heidelberg, 1991, p. 1427.
- 18 P. C. Uden, Y. Yoo, T. Wang and Z. Cheng, *J. Chromatogr.*, 468 (1989) 319.
- 19 H. D. Hartough, in A. Weissberger (Editor), *Chemistry of Heterocyclic Compounds*, Interscience, New York, 1952, pp. 3 and 130.
- 20 D. H. S. Horn and J. A. Lambertson, *Aust. J. Chem.*, 16 (1963) 475.
- 21 F. Bohlmann, C. Zdero and W. Gordon, *Chem. Ber.*, 100 (1967) 1193.
- 22 N. B. Colthup, L. H. Daly and S. E. Wiberley, *Introduction to Infrared and Raman Spectroscopy*, Academic Press, London, 1964.

Chromatographic analysis of *cis*- and *trans*-mevinphos in poisoned wildlife

William J. Allender

Chemistry Branch, Biological and Chemical Research Institute, P.M.B. 10, Rydalmere, 2116 New South Wales (Australia)

James Keegan

Department of Chemistry, University of Technology, Sydney, P.O. Box 123, Broadway, 2007 New South Wales (Australia)

(First received December 9th, 1991; revised manuscript received May 19th, 1992)

ABSTRACT

A method is described for the analysis of the *cis*- and *trans*-isomers of mevinphos in baits and avian tissues. The procedure involves extraction of the mevinphos isomers with acetone–dichloromethane (1:1) followed by clean-up on alumina. Bait samples were initially screened by thin-layer chromatography and identity of extracts confirmed by infrared spectrophotometry and gas chromatography–mass spectrometry.

INTRODUCTION

Mevinphos, methyl 3-(dimethoxyphosphinyloxy) but-2-enoate, is the active component of the insecticide Phosdrin. The technical product contains approximately 60% (w/w) of the *E* or (*cis*) isomer and the balance of the *Z* or (*trans*) isomer (or α and β isomers, respectively, Fig. 1) [1,2]. The *cis* isomer is much more biologically active than the corresponding *trans* isomer [3,4].

Mevinphos is a systemic insecticide and acaricide with contact, respiratory and stomach action. It is formulated as an emulsifiable spray concentrate for the control of chewing and sucking insects and spider mites over a wide range of crops. Generally, mevinphos has little effect on wildlife in practice as it is rapidly broken down to less toxic decomposition products [5]. However, over the years, misuse of agricultural chemicals, pesticides in particular,

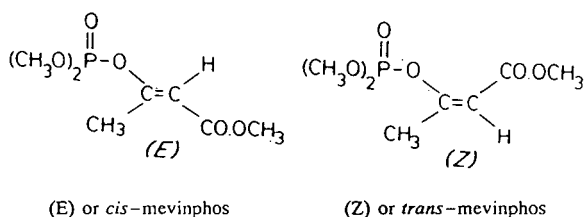


Fig. 1. Chemical structures for the isomers of mevinphos.

have resulted in poisoning of native wildlife [6–11]. Mevinphos is also quite toxic to birds with an acute oral LD₅₀ of 0.75–7 mg/kg [2].

Native birds are protected by law, however, some cases of deliberate poisonings occur as they may be still considered pests when they compete with man for food and attack his livestock.

A number of methods have been developed to determine mevinphos (and other organophosphorus pesticides) such as thin-layer chromatography (TLC), cholinesterase inhibition and gas chromatography (GC) [12–15]. Of these, GC procedures are more specific and less time-consuming.

Correspondence to: W. J. Allender, Chemistry Branch, Biological and Chemical Research Institute, P.M.B. 10, Rydalmere, 2116 New South Wales, Australia.

The present paper describes a specific and robust GC and GC–mass spectrometric (MS) procedure for the determination of the *cis* and *trans* isomers (or α and β isomers) of mevinphos in the tissues of poisoned native wedge-tailed eagles (*Aquila audax*).

EXPERIMENTAL

Reagents

Mevinphos (99.0% purity) was obtained from Ajax Chemicals (Sydney, Australia). Standard solutions of mevinphos contained the *cis* (α) and *trans* (β) isomers in the proportions of 60:40. A standard stock solution (10 $\mu\text{g/ml}$) was prepared in *n*-hexane and refrigerated (*ca.* 4°C). This solution was used to prepare a working standard (1.0 $\mu\text{g/ml}$) in hexane, in addition to serving as a spiking media for placing mevinphos into the bird tissues at known concentrations. Clean-up was performed using alumina (Brockman activity II, BDH, Poole, UK) previously heated at 600°C, cooled overnight and then deactivated with water (5%, w/w) before use.

All other chemicals used such as acetone, hexane dichloromethane, etc. were either nanograde or chromatographic grade.

Gas chromatography

The chromatographic analyses were carried out on a Varian Aerograph Model 3700 gas chromatograph equipped with a thermionic specific (ceramic-alkali) detector, and a 1.8 m \times 2.0 mm I.D. glass column containing 10% Carbowax 20M on Gas-Chrom II (80–100 mesh) was used. The column, injector and detector temperatures were 155, 200 and 300°C, respectively. Nitrogen (high purity) was the carrier gas at a flow-rate of 30 ml/min. Mevinphos concentrations (*cis* and *trans* isomers) were determined by external quantitation with standard solutions of mevinphos using a Varian Model 4400 integrator interfaced to the gas chromatograph and attenuated at 8 mV full-scale deflection (attenuation 2 \uparrow 3).

Gas chromatography–mass spectrometry

The GC–MS analyses were carried out on a Hewlett-Packard HP5890 gas chromatograph interfaced to a HP 5970 MSD mass spectrometer system. A 25 m \times 0.22 mm I.D. BP20 (a bonded-phase Carbowax 20M) column was used to separate the mevin-

phos isomers and obtain electron-impact spectra of each. The injector was cool on column, with the oven temperature programmed from 50°C (1 min) to 250°C at 25°C/min. The helium (high purity) carrier gas pressure was set at 100 kPa. The pressure in the ion source (electron-impact mode) was between 10^{-5} and $5 \cdot 10^{-6}$ Torr, the ionising potential 70 eV, and the accelerating voltage 5kV. The mass range examined in the extracts was between 40 to 300 amu.

Sample preparation

Two dead wedge-tail eagles *Aquila audax* were seized from a rural property by a National Parks and Wildlife Service ranger, along with a quantity of Phosdrin found at the site. The liver, crop and gizzard tissues were dissected from each of the poisoned birds, weighed and then cut into small pieces. All tissue samples were stored at -20°C prior to analysis. The tissues were then accurately weighed (5–15 g) into Sorvall cups, and 50 ml of acetone–dichloromethane (1:1) solvent mixture were added to each. The mixtures were then blended at medium speed (No. 5) using a Sorvall omni-mixer for about 2 min and then filtered through a Whatman No. 1 filter into a Kuderna–Danish flask. The samples were re-extracted with a further 25 ml of solvent mixture and the residue was washed several times with the same solvent and passed through the filter into the flask. The combined solvent extracts were then concentrated to *ca.* 2 ml. A 1-ml volume of *n*-decane was added as a “keeper” and the remainder of the solvent removed under a gentle stream of nitrogen to a final volume of 1 ml.

Column clean-up

A slurry of 10 g of prepared alumina in hexane was poured into a 300 mm \times 15 mm I.D. glass column plugged with glass wool, and 5 g of anhydrous sodium sulphate were added on top of the adsorbent. The columns were covered with aluminium foil to prevent ultraviolet irradiation conversion of *trans* isomer to *cis* isomer [4]. The residue extracts were transferred with two 1-ml portions of hexane and placed on top of the prepared columns. The columns were then washed with a 50-ml portion of hexane to remove any lipophilic co-extractives in the extracts. After discarding the eluate, the mevinphos (*cis* and *trans* isomers) was eluted from

the column with 100 ml of 20% (v/v) acetone in hexane into a 100-ml volumetric flask and diluted to volume with hexane. This fraction was subsequently diluted further with hexane depending upon the initial screening of the eluate.

Recoveries

A standard additions procedure was followed as no control eagle tissue was available. Recoveries of mevinphos were determined from representative, previously analysed minced eagle liver spiked at 5-10 $\mu\text{g/g}$ mevinphos.

RESULTS AND DISCUSSION

Analysis by GC and GC-MS

Several columns were investigated for separating and detecting the two isomers of mevinphos. Only polar columns such as Carbowax 20M and diethy-

lene glycol succinate (DEGS) gave satisfactory separation with sharp, symmetrical peak responses.

Typical GC-MS total ion current chromatograms of the reference standard mevinphos (*cis* and *trans* isomers) and a liver extract from a poisoned eagle *Aquila audax* are shown in Fig. 2. The mevinphos isomers gave the following retention times: *cis* 9.56 min and *trans* 9.78 min under the GC conditions described. The peaks of *cis*- and *trans*-mevinphos were analysed by GC-MS, the mass spectra of which are shown in Fig. 3. For screening and identification purposes, the ions m/z 127 and 192 were monitored.

The method detection limit for mevinphos (*cis* and *trans* isomers) in the liver tissues was estimated at 0.04 $\mu\text{g/g}$. The liver recoveries ($n = 4$) averaged 76.0%, with a relative standard deviation (R.S.D.) of 4.3%, and were somewhat lower than expected; whilst recoveries of the standard corresponding to

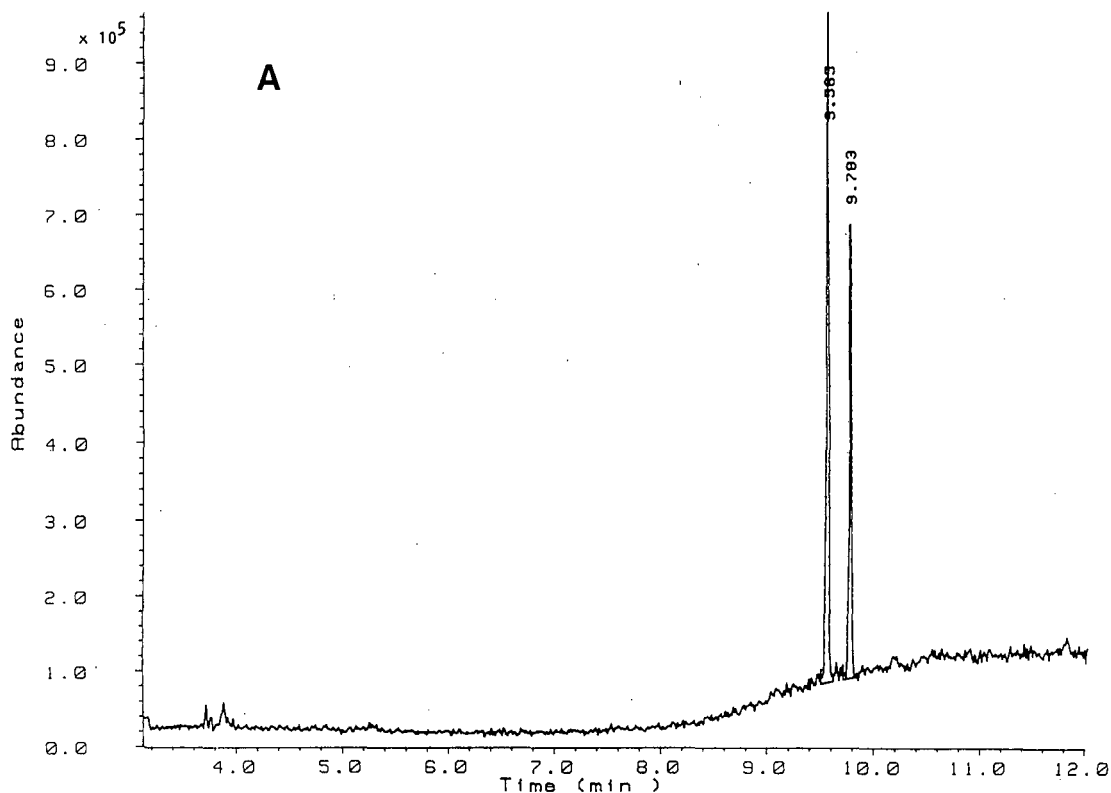


Fig. 2.

(Continued on p. 318)

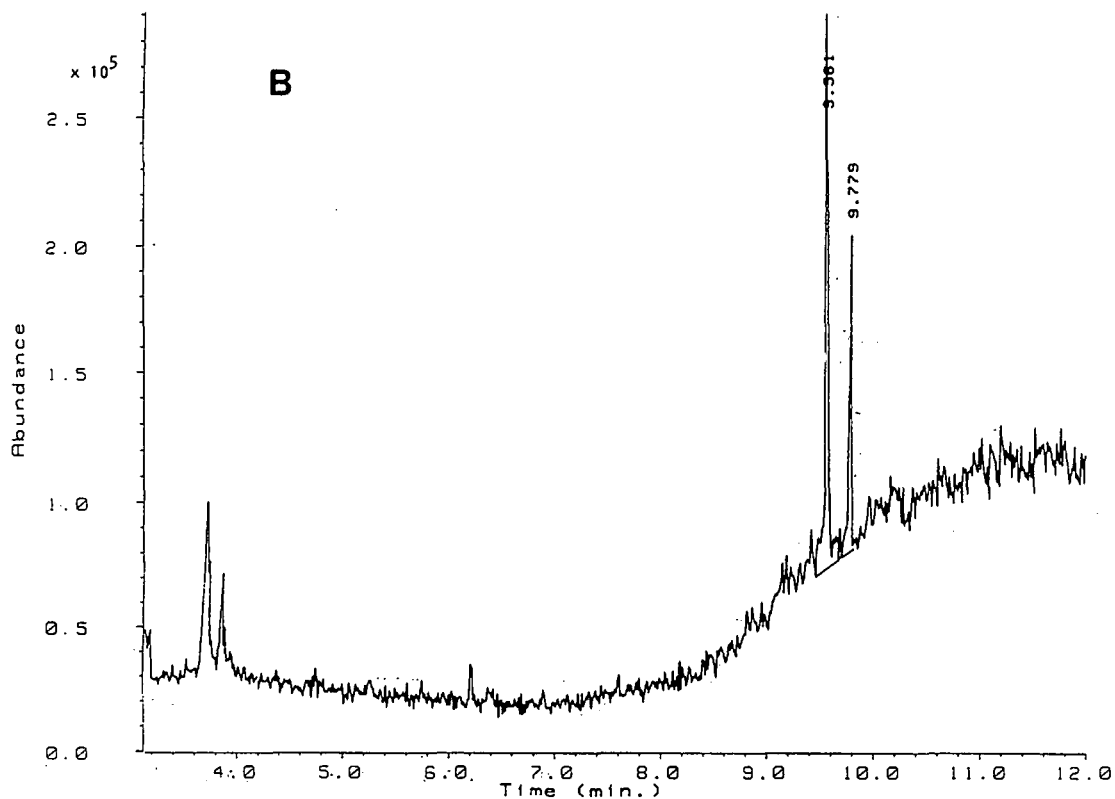


Fig. 2. GC-MS total ion current chromatograms of (A) *cis*- and *trans*-mevinphos reference standard and (B) a liver extract from a poisoned eagle *Aquila audax*.

10 µg/g. were 95.5% (R.S.D. 3.5%). This may be due to losses of mevinphos from tissues before extraction and clean-up rather than during the procedure.

Infrared spectrophotometry

Infrared spectrophotometry was used to confirm the identity of the peaks in the bait extract found in one eagle's beak. Fig. 4 shows the infrared spectrum

TABLE I

MEVINPHOS RESIDUES FOUND IN TISSUES OF POISONED WEDGE-TAILED EAGLES *AQUILA AUDAX*

Bird No.	Tissue	Total mevinphos (<i>cis</i> + <i>trans</i>) found in tissue "as received" (mg/kg)	Ratio of <i>cis</i> to <i>trans</i> isomer found in tissue
1	Food found in beak	32.0	58:42
1	Crop and gizzard	16.8	58:43
1	Liver	1.7	62:38
2	Crop	4.6	58:42
2	Gizzard	4.5	58:42
2	Liver	0.8	61:39

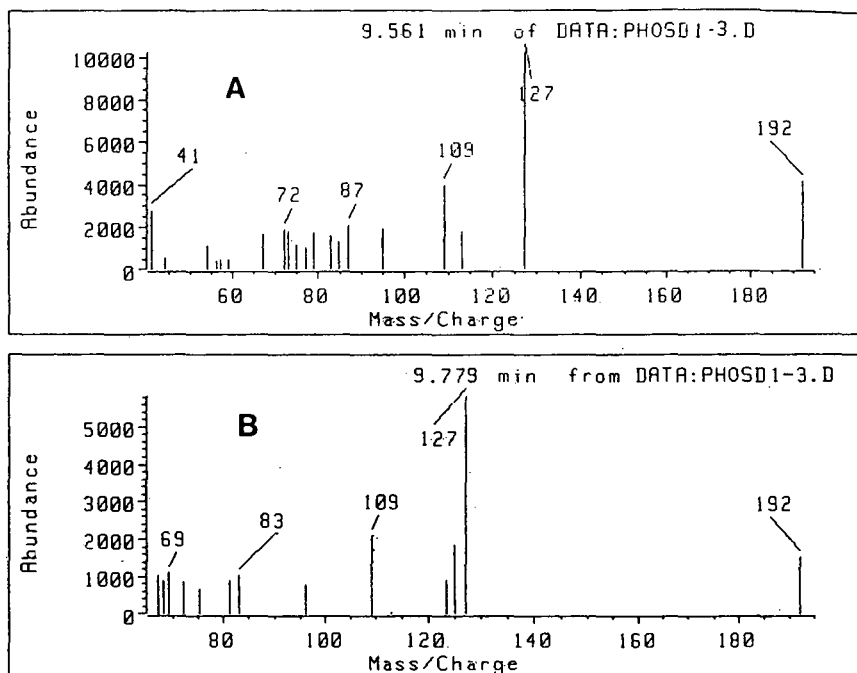


Fig. 3. Electron-impact mass spectrum of (A) *cis*- and (B) *trans*-mevinphos isomers.

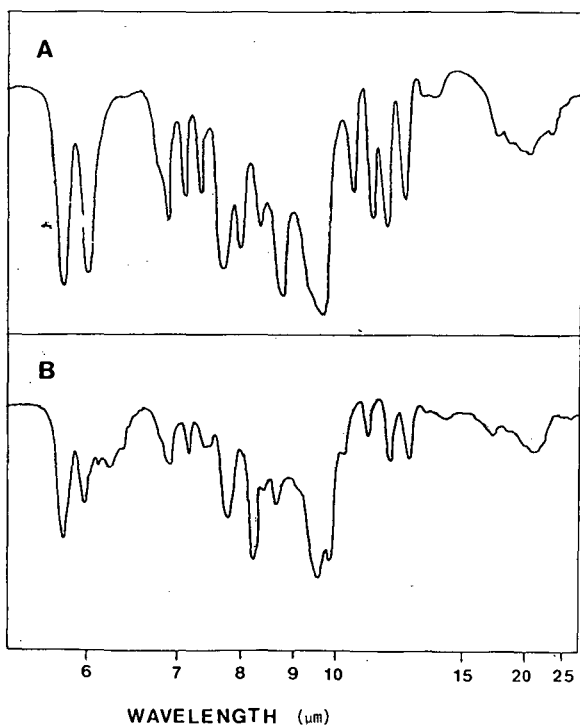


Fig. 4. Infrared spectra of (A) *cis* (or α) and *trans* (or β) isomers of mevinphos.

of both isomers separated and collected by preparative TLC (based on the work of Mendoza *et al.* [16]) and rechromatographed by GC. These data correspond with those reported by Stiles *et al.* [1].

Application to a baiting incident

The Phosdrin pesticide found at the site was found to contain 62% (w/v) of mevinphos with an isomeric *cis/trans* ratio of 59:41. Table I shows the tissue concentrations of mevinphos in the dead eagles found at the site.

In one of the birds (No. 1), death had apparently occurred quite rapidly as a portion of the poisoned meat was still present in the bird's beak. The *cis* and *trans* (α/β) isomeric ratios were little different from the Phosdrin found at the site. The *trans* (β) isomer of mevinphos is known to be less active as a cholinesterase inhibitor being some 22 times less toxic than the *cis* isomer [4,17]. Morello *et al.* [18] showed that *trans*-mevinphos (β -mevinphos) was degraded faster than the *cis* (α) isomer by mouse liver homogenates at approximately 3 and 2 μmol , respectively. This may also occur in birds of prey and would account for the slightly increased isomeric ratio of *cis* to *trans* in the livers of the poisoned eagles.

REFERENCES

- 1 A. R. Stiles, C. A. Reilly, G. R. Pollard, C. H. Tieman, L. F. Ward, D. D. Soloway and R. R. Whetsone, *J. Org. Chem.*, 26 (1961) 3960–3968.
- 2 C. R. Worthing and S. B. Walker (Editors), *The Pesticide Manual — A World Compendium*, British Crop Protection Council, London, 7th ed., 1983, p. 381.
- 3 F. W. Seume and R. O. O'Brien, *Toxicol. Appl. Pharmacol.*, 2 (1960) 495–503.
- 4 E. Y. Spencer, *Can. J. Biochem. Physiol.*, 39 (1961) 1790–1792.
- 5 K. I. Beynon, D. H. Hutson and A. N. Wright, *Residue Rev.*, 47 (1973) 8796.
- 6 G. A. Hamilton, K. Hunter, A. S. Ritchie, A. D. Ruthven and P. I. Stanely, *Pesticide Sci.*, 7 (1976) 175–183.
- 7 P. M. Brown, P. J. Bunyan and P. I. Stanley, *J. Forensic. Sci. Soc.*, 17 (1977) 211–221.
- 8 G. A. Hamilton, A. D. Ruthven, E. Findlay, K. Hunter and D. A. Lindsay, *Biol. Conserv.*, 21 (1981) 315–326.
- 9 R. L. Reece and P. Handson, *Vet. Rec.*, 111 (1982) 453–455.
- 10 W. J. Allender, *J. Chromatogr.*, 508 (1990) 199–202.
- 11 W. J. Allender, *J. Anal. Toxicol.*, 14 (1990) 45–49.
- 12 W. Winterlin, C. Mourer and H. Beckman, *J. Agric. Food. Chem.*, 18 (1970) 401–404.
- 13 H. P. Burchfield and E. E. Storrs, *J. Chromatogr. Sci.*, 13 (1975) 202–211.
- 14 A. D. Martin, G. Norman, P. I. Stanley and G. E. Westlake, *Bull. Environ. Contamin. Toxicol.*, 26 (1981) 775–780.
- 15 K. W. Edgell, E. L. Jenkins, V. Lopez-Avila and J. E. Longbottom, *J. Assoc. Off. Anal. Chem.*, 74 (1991) 295–309.
- 16 C. E. Mendoza, P. J. Wales, H. A. McCleod and W. P. McKinley, *Analyst*, 93 (1968) 173–177.
- 17 M. H. Clear, F. R. Fowler, S. R. B. Solly and A. R. Ritchie, *N. Z. J. Sci.*, 20 (1977) 221–224.
- 18 A. Morello, A. Vardanis and E. Y. Spencer, *Biochem. Pharmacol.*, 17 (1968) 1795–1802.

Comparison of methods to prevent restrictor plugging during off-line supercritical extraction

Mark D. Burford, Steven B. Hawthorne and David J. Miller

Energy and Environmental Research Center, University of North Dakota, Grand Forks, ND 58202 (USA)

Terry Braggins

Meat Industry Research Institute of New Zealand, P.O. Box 617, Hamilton (New Zealand)

(First received February 12th, 1992; revised manuscript received May 26th, 1992)

ABSTRACT

Real-world environmental samples which contain high concentrations of water and/or extractable matrix components frequently cause intermittent or irreversible plugging of capillary flow restrictors during off-line supercritical fluid extraction. Heating the entire restrictor at 50°C produces a constant extraction flow-rate (± 0.03 ml/min) for such samples, but poor collection efficiencies (30–65% recovery for polycyclic aromatic hydrocarbons) were obtained because the supercritical fluid could not be depressurized directly into the collection solvent. While the collection efficiency was improved (80–90%) by nebulizing an organic solvent with the restrictor effluent, a simpler method was to heat all but the last 3 cm of the restrictor and to depressurize the extract directly in the collection solvent. Depending on the sample matrix, restrictor heater temperatures ranging from 50 to 200°C were required to avoid restrictor plugging. With proper heating, constant extraction flow-rates (± 0.07 ml/min) and high collection efficiencies (90–100%) for polycyclic aromatic hydrocarbons and *n*-alkanes as volatile as *n*-octane were achieved.

INTRODUCTION

Efforts to reduce the use of potentially hazardous solvents and decrease sample preparation time has led to supercritical fluid extraction (SFE) becoming a popular alternative to conventional solvent extraction methods. A good deal of emphasis has been placed on the applications of SFE, but less has been reported about poor SFE flow rates which can occur from restrictor plugging during extraction and low collection efficiencies which can be associated with the methods (*e.g.*, heating) used to avoid restrictor plugging. Restrictor plugging can often occur during off-line SFE when the sample matrices

contain high concentrations of water or extractable matrix components. Since the depressurization occurs at the restrictor tip and inside the restrictor [1], the reduction of the extraction fluid density within the restrictor can cause a decrease in the solubility of the analytes. The decrease in analyte solubility, combined with the Joule-Thomson cooling effect of the expanding extraction fluid at the restrictor exit, produces a subcritical solvent which may lead to analytes precipitating and, ultimately, plugging the inside of the restrictor. For example, cuticle waxes precipitate when supercritical CO₂ (99 atm, 40°C) is cooled to a subcritical liquid (69 atm, 0°C) [2]. In order to prevent such plugging, the restrictor can be heated to counteract Joule-Thomson cooling or constructed to minimize the pressure drop from the extraction cell to the restrictor outlet. Heating the restrictor may also increase the extraction fluid solubility of analytes having some volatility, since ex-

Correspondence to: Dr. S. B. Hawthorne, Energy and Environmental Research Center, University of North Dakota, Grand Forks, ND 58202, USA.

traction fluid solubility (at a given density) generally mirrors analyte vapor pressure [3].

The most practical and popular method to prevent plugging during off-line SFE is to heat the restrictor using a linear flow restrictor generally consisting of silica capillary tubing [4–9] or a mechanical and/or electric feedback regulator [10–13]. The advantage of using an electric feedback regulator [12,13] is the reproducible flow achieved with a variable orifice. However, the equipment is expensive and not amenable to direct collection of extracted analytes in a small volume of organic solvent. Conversely, the simple linear restrictor has the advantage of being inexpensive and disposable, available with several inner diameters to achieve desired flow-rates, and the extracted analytes can be collected in a variety of collection systems. Unfortunately, the linear restrictors are more susceptible to plugging during the extraction of complex samples and are, therefore, frequently heated either directly with a heating element [4–9] or indirectly by warming the collection device [14]. Alternative methods include combining an organic solvent with the pressurized [15] or depressurized [16] extraction fluid, or maintaining the density of the extraction fluid in the linear restrictor by using a nitrogen- or argon-pressurized collection vessel [17–19].

In this study, three methods of heating a linear restrictor and their effects on analyte collection efficiencies were evaluated based on the criteria that the ideal system would eliminate restrictor plugging using cheap, disposable, fused silica restrictors which could easily be changed to vary the extraction flow-rate, but still produce quantitative collection efficiencies (*e.g.*, >90%) of the extracted analytes using only a few milliliters (2.5 to 5.0 ml) of organic collection solvent. The extraction flow rates and collection efficiencies of the various heater designs were determined by spiking polycyclic aromatic hydrocarbons (PAHs) onto silanized glass beads and performing SFE. The final design was further tested with a series of *n*-alkanes. The ability of the system to prevent restrictor plugging from the matrix components was ascertained by monitoring the SFE flow-rate while extracting several samples known to cause restrictor plugging.

EXPERIMENTAL

Supercritical fluid extractions

Supercritical fluid extractions were performed using SFC-grade carbon dioxide (Scott Gases; Plumsteadville, PA, USA) and an ISCO Model 260D syringe pump (ISCO, Lincoln, NE, USA) operated at 400 atm. The extraction cell and pre-equilibration coil [1 m × 0.76 mm I.D. × 1.6 mm (1/16 in.) O.D. coiled stainless-steel tubing placed before the extraction cell to pre-warm the CO₂ to the extraction temperature] were maintained at 50°C using a thermostatically-controlled tube heater. Extractions were performed using a 0.5-ml (30 mm × 4.6 mm I.D.) extraction cell from Keystone Scientific (Bellefonte, PA, USA). The flow-rate of the supercritical fluid through the extraction cell was measured as liquid CO₂ at the pump and was controlled by 11-cm-long restrictors (28 μm or 32 μm I.D. × 140 μm O.D.) cut from fused-silica tubing (Polymicro Technologies, Phoenix, AZ, USA).

Three restrictor heater designs were investigated. The first design was similar to the commercially available Dionex restrictor heater used in their model SFE-703 instrument [9] and consisted of a stainless-steel tube (110 mm × 0.25 mm I.D.), partially wrapped in flexible electrical heating tape which was insulated with Lytherm insulating material (Lydall, Rochester, NH, USA) and electrical insulation tape (Fig. 1). The heating system was regulated with a J thermocouple and a temperature controller unit (Model 6102; Omega, Stamford, CT, USA). The heating tape covered 9 cm of the 11-cm stainless-steel tubing, and the last 2 cm of tubing was heated only by conduction. All but the last 2 mm of the restrictor was encased in the heated stainless-steel tubing.

Extracted analytes were collected in a 7.4-ml collection vial (60 mm height × 10 mm I.D. neck) capped with a screw cap (possessing a hole) and two 15-mm diameter PTFE-faced silicone septa, into which was placed a 61-mm-long (5 mm O.D. × 3 mm I.D.) glass tube insert and a vent tube (Hypodermic needle, Stubs gauge 18), as shown in Fig. 1. No attempt was made to control the collection solvent temperature during SFE. Methylene chloride (5 ml, pesticide grade from Fisher, Springfield, NJ, USA) was the collection solvent. The solvent volume was maintained during SFE by introducing ad-

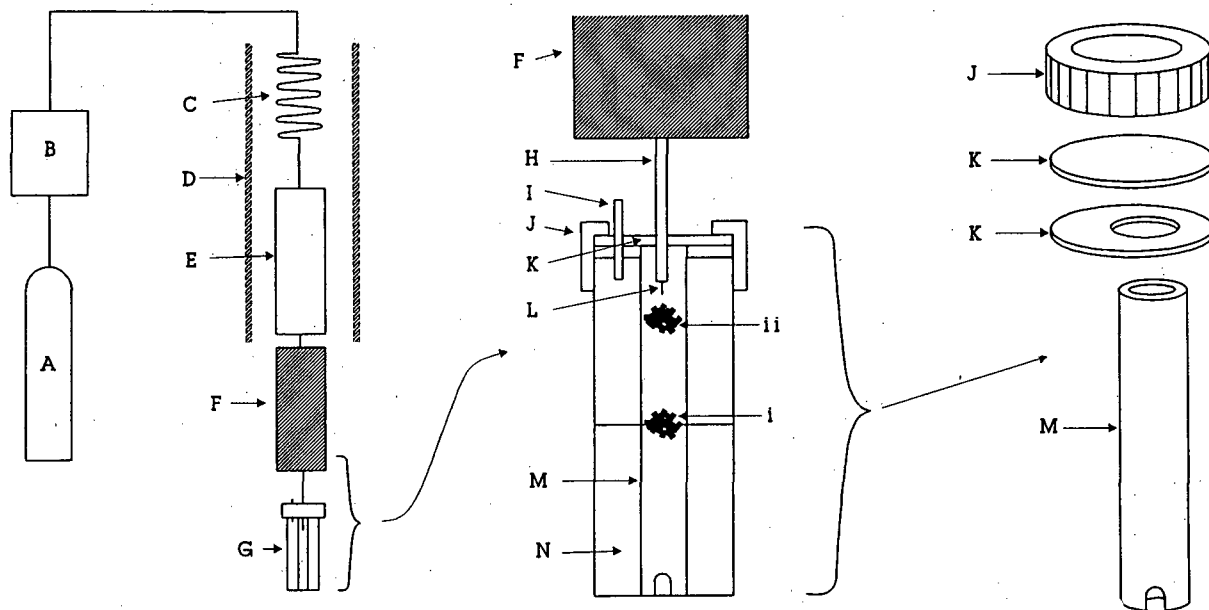


Fig. 1. SFE and restrictor heater apparatus. Components of extraction system are (A) CO₂ cylinder, (B) syringe pump, (C) pre-equilibration coil, (D) heating tube, (E) extraction cell, (F) heating tape wrapped around stainless-steel tubing and insulated with Lytherm insulating material and electrical insulating tape, (G) 7.4-ml collection vial, (H) stainless-steel tubing, (I) vent (hypodermic needle) (J) hole cap, (K) septum, (L) fused-silica restrictor, (M) glass tube, (N) 5 ml methylene chloride. Analytes deposit at points (i) and (ii) depending on the restrictor heater temperature, as discussed in the text.

ditional solvent through the septum with a hypodermic syringe. Using this arrangement, the restrictor effluent passed through the glass tube insert, into the collection solvent, and out the vent. To ensure a gas-tight seal between the insert and the collection vial septum, the glass tube was made *ca.* 1 mm longer than the length of the vial, thus, when the lid was screwed on, pressure was applied to the septum, forming a gas-tight seal.

The second restrictor heater design also encased the majority of the restrictor in heated stainless-steel tubing, using the same heating method as the first design. With the second design, an organic solvent was introduced at the tip of the restrictor and nebulized by placing a plastic tee-piece (3 cm long \times 0.6 cm I.D.) between the restrictor and the glass tube. The three ends of the tee-piece were sealed with 6-mm rubber septa (Fig. 2). A single-piston reciprocating minipump (LDC Analytical, Riviera Beach, FL, USA) delivered organic solvent (0.3 ml/min) to the tee-piece. Extracted analytes were collected in the nebulized solvent which was transport-

ed through a 61-mm-long (5 mm O.D. \times 3 mm I.D.) glass tube into a 7.4-ml collection vial (60 mm height \times 10 mm I.D. neck) containing 5 ml methylene chloride (Fig. 2). The addition of the nebulizing solvent at 0.3 ml/min approximately balanced the collection solvent loss so that no further solvent addition was required during the extraction (solvent volume remained *ca.* 5 ml during SFE). No attempt was made to control the collection solvent temperature.

The third heated restrictor design (Fig. 3) used an insulated aluminum block (75 mm long \times 20 mm diameter) with an electric cartridge heater (50 W, 40 mm long \times 6 mm diameter). The temperature was regulated with a J thermocouple and a temperature controller unit (Model 6102, Omega). The restrictor was heated by inserting the fused-silica tubing through a 1-mm-diameter hole drilled through the heating block. Analytes were collected in a 3.7-ml collection vial (45 mm height \times 8 mm I.D. neck) containing 2.5 ml of methylene chloride. Collection solvent volume was maintained by small additions

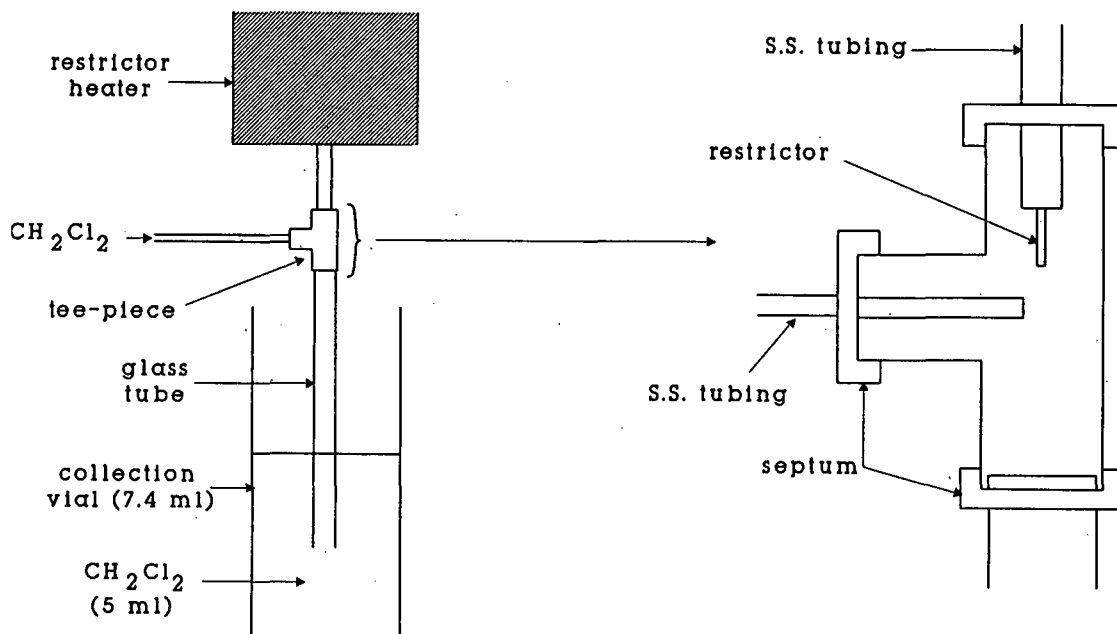


Fig. 2. Solvent nebulizer apparatus used in conjunction with the restrictor heater in Fig. 1 to introduce organic solvent (methylene chloride) to the tip of the capillary restrictor. See text for additional information. S.S. = stainless-steel.

of solvent during SFE. The collection vial was either free-standing in air (*i.e.*, no attempt to control collection solvent temperature) or placed in an aluminum block which contained a water-filled hole (26 mm deep \times 23 mm I.D.) to accommodate the collection vial.

Standards and samples

Standards containing six PAHs ranging from naphthalene to chrysene (*ca.* 2.5 mg/ml each) or C₇ to C₃₀ *n*-alkanes (*ca.* 1.7 mg/ml each) were prepared in methylene chloride and stored at -10°C until used. Spiking quantities for the individual PAHs and *n*-alkanes were at *ca.* 12.5 μg and 17 μg of each compound, respectively. Collection efficiencies were determined by filling the extraction cell with *ca.* 0.7 g of 70–80-mesh silanized glass beads (Analab, Norwalk, CT, USA) and spiking the PAH mixture (5 μl) or *n*-alkane mixture (10 μl) onto the top of the beads. The cell was immediately sealed to prevent any loss of the volatile components, placed inside the tube heater, equilibrated for 5 min, and then extracted for 10 min with CO₂ at 400 atm and 50°C. At the end of the extraction, the collection solvent

was spiked with 5 μl (20 μg) of the internal standard *n*-heptadecane (for the PAHs) or 10 μl (26 μg) of the internal standard phenanthrene (for the *n*-alkanes) and analyzed using capillary gas chromatography (GC) with flame ionization detection (FID).

Five real-world samples with differing physical and chemical properties were chosen to test the ability of the restrictor heater to avoid restrictor plugging. The samples included railroad bed soil (Hastings, MN, USA), pine needles (Grand Forks, ND, USA), petroleum waste sludge (British Petroleum, USA), marine sediment standard reference material (SRM) 1941 [National Institute of Standards and Technology (NIST), Gaithersburg, MD, USA], and elemental sulfur (99.999% pure, Aldrich, Milwaukee, WI, USA). Prior to SFE, the railroad bed soil was air-dried and sieved to <2 mm to remove any sticks and other debris, and 0.8 g of soil was placed in the extraction cell. The pine needles were freshly picked and cut into 10-mm lengths, and 0.35 g were immediately placed into the extraction cell. For the petroleum sludge, the extraction cell was initially half-filled with 70–80-mesh silanized glass beads and then filled with *ca.* 200 mg of sample. This ar-

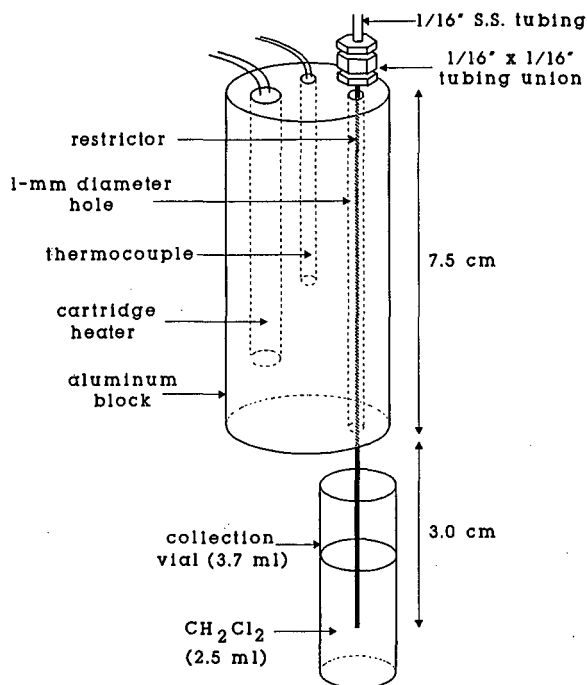


Fig. 3. Aluminum block restrictor heater apparatus. Fused-silica restrictor (11 cm long) was inserted through a 1-mm-diameter hole drilled through the aluminum heater block. The heater block was insulated with Lytherm insulating material and electrical insulating tape (for clarity, the insulating material and tape were omitted from the diagram). See text for additional information. S.S. = stainless-steel; " = inch.

range was required to prevent plugging of the 0.5 μm extraction cell frit, not the restrictor. The marine sediment (0.35 g) and elemental sulfur (0.4 g) were extracted without any preparation.

Gas chromatographic analysis

All GC analyses were done with a Hewlett-Packard 5890 gas chromatograph with FID and hydrogen as the carrier gas. The injections were performed in split mode with a 20:1 split ratio into a wide-bore (25 m \times 0.32 mm I.D., 0.17 μm film thickness) HP-5 fused-silica capillary column. The injector and detector temperatures were maintained at 300°C. The oven temperature for the PAH analysis was 80°C at injection, followed by a temperature ramp at 8°C/min to 320°C. For the *n*-alkane analysis the oven temperature at injection was 35°C for 2 min followed by a temperature ramp at 8°C/min to 320°C.

RESULTS AND DISCUSSION

Depending on the nature of the sample, two different types of plugging have been encountered when using unheated capillary restrictors placed in a collection solvent. With some wet samples (more than *ca.* 1% water), the restrictor blocks as water freezes at the cooled restrictor outlet. Plugging from frozen water has previously been eliminated by maintaining the collection solvent temperature at 5°C with a thermostatically-controlled collection vial heating block [20]. The second type of plugging results from precipitated analytes and extracted matrix materials, and mostly occurs with samples containing very high concentrations of extractable components. Maintaining consistent SFE flow-rates with such samples requires the restrictor to be heated. Such heating has previously been achieved with a heat gun and produced reasonable extraction flow-rates, but also resulted in 20–50% loss of semi-volatile analytes [20].

In an effort to improve analyte collection efficiencies, a more controllable means of regulating the temperature of the restrictor was investigated by using a thermostatically-controlled restrictor heater with three restrictor heater designs (Figs. 1–3). The ability of the three designs to prevent restrictor plugging was assessed by extracting spiked PAHs from silanized glass beads. Since the spikes extracted very rapidly (within 2 or 3 void volumes of extraction system) and were present at a relatively high concentration (75 μg total PAHs), an unheated restrictor plugged very quickly upon commencing SFE. The PAH spike, therefore, proved to be a useful test for the ability of each restrictor heater design to prevent restrictor plugging. All three designs were able to maintain the extraction flow-rate, which could easily be varied by using the appropriate capillary restrictor. However, collection efficiencies varied for the three methods as discussed below.

Design 1, heating the whole restrictor

The initial restrictor heater design (Fig. 1) heated the whole restrictor (although the last 2 cm was indirectly heated as described in the experimental section). This eliminated restrictor plugging using either high (150°C) or low (50°C) restrictor heater temperatures. Reasonably constant extraction flow-

rates (*ca.* 0.75 ± 0.03 ml/min with the restrictor heater at 50°C) were obtained with a $28\text{-}\mu\text{m}$ I.D. restrictor, but the collection efficiencies were unacceptably low (*ca.* 30–65% recovery for the spiked PAHs), irrespective of analyte volatility or restrictor heater temperature (Table I). Visual inspection of the collection device indicated that the poor collection efficiencies were caused by the extraction fluid not depressurizing directly in the collection solvent, which led to some of the analytes depositing in the glass tube of the collection vial rather than in the collection solvent (i and ii in Fig. 1). Removing the crystallized analytes from the glass tube proved to be difficult as the collection vial had to be dismantled and the glass tube manually rinsed and/or sonicated with solvent. Simply shaking the vial to resolvent the analytes proved impractical as the solvent would leak out of the holes in the septum made by the restrictor heater and collection vial vent. The solvent rinse was combined with the collection solvent to produce a final collection volume of *ca.* 8 ml, and the combined solvent was used to obtain the collection efficiency values in Table I. Such deposition was most prevalent at the lower

restrictor heater temperatures (50°C) where the majority of the analytes crystallized on the inside of the glass tube. In these instances, the tube was also sonicated in the collection solvent to remove the precipitated analytes.

Interestingly, the location of the crystallized analytes (i and ii in Fig. 1) was related to the physical state of the depressurizing extraction fluid. As the restrictor heater temperature was increased, the analytes were deposited further down the glass tube and further away from the restrictor outlet. Heating the restrictor heater above 100°C dramatically increased the effluent temperature (Fig. 4) and caused the disappearance of frozen CO_2 present at lower restrictor heater temperatures at the restrictor tip. The sudden increase in the restrictor effluent temperature corresponds to a previously reported [1] CO_2 phase change from a two-phase region of gas and solid to a single gaseous phase on expansion at temperatures of *ca.* $>100^\circ\text{C}$. In the gas phase (restrictor heater 150°C), the analytes form very small solute particles ($<0.2\ \mu\text{m}$ [6]), leading to the formation of an aerosol. The aerosol is apparently swept along the glass tube until it reaches the cooled glass at the solvent boundary; at this location (Fig. 1, i), the less volatile analytes precipitated (*ca.* 20% fluoranthene and 40% chrysene precipitated in the glass tube; the rest of the PAHs including *ca.* 10% fluoranthene and 1% chrysene were recovered in the collection solvent). At lower restrictor heater temperatures (50°C), the majority of the analytes condensed in the glass tube near the restrictor outlet (Fig. 1, ii), and the collection solvent contained only the most volatile analytes (*ca.* 60% naphthalene and 45% acenaphthylene trapped in the collection solvent, the rest of the PAHs including *ca.* 5% acenaphthylene precipitated in the glass tube). It was also noted that small reversible changes in the flow-rate were obtained by heating the restrictor (Fig. 4), indicating that the restrictor heater has some potential to act as a fine SFE flow controller.

The restrictor heater design shown in Fig. 1 provides sufficient heat so that the collection solvent temperature was not significantly lowered during SFE (solvent temperature *ca.* 8°C after 10 min of extraction with the restrictor heater at 50 or 150°C), and resulted in an increase in solvent evaporation that may have caused the volatile analytes to be purged from the collection solvent. Because of the

TABLE I

COLLECTION EFFICIENCIES OF PAHs INTO METHYLENE CHLORIDE AT VARIOUS RESTRICTOR HEATER TEMPERATURES USING A $28\text{-}\mu\text{m}$ I.D. RESTRICTOR WITH THE GLASS TUBE INSERT COLLECTION VIAL (FIG. 1) OR THE SOLVENT NEBULIZER (FIG. 2)

PAH	Percent collected (R.S.D.) ^a			
	50°C^b	100°C^b	150°C^b	$50^\circ\text{C}/\text{CH}_2\text{Cl}_2^c$
Naphthalene	55 (2)	63	64	95 (5)
Acenaphthylene	43 (4)	41	30	88 (5)
Fluorene	46 (13)	50	35	83 (4)
Phenanthrene	50 (16)	55	30	84 (3)
Fluoranthene	55 (12)	67	29	81 (3)
Chrysene	50 (1)	66	43	83 (3)

^a Value in parentheses is the percent relative standard deviation (R.S.D.) of triplicate 10-min extractions. Recoveries for 100°C and 150°C restrictor heater temperatures were based on one extraction.

^b Collection efficiencies achieved using the glass tube insert collection vial (Fig. 1). The recovery values were obtained from the combined solvent rinse and collection solvent. See text for additional information.

^c Collection efficiencies obtained using the solvent nebulizer (Fig. 2).

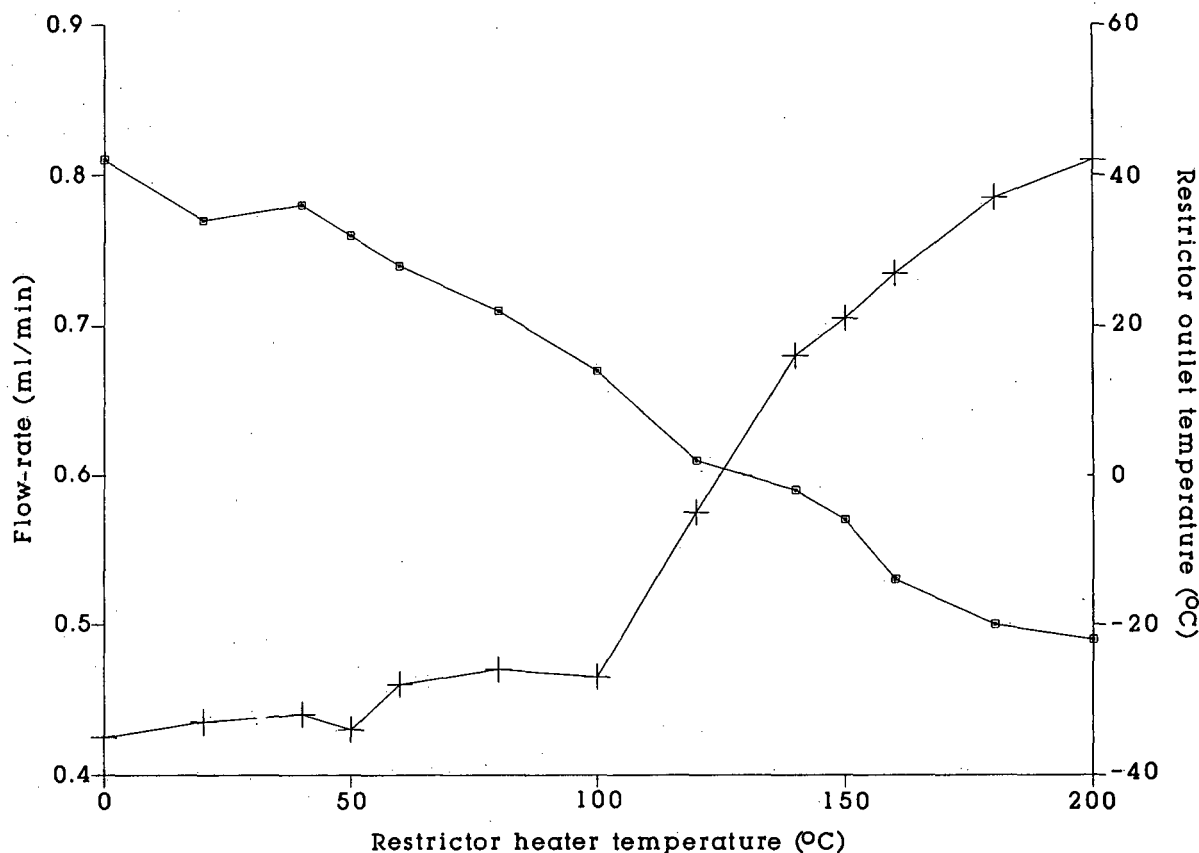


Fig. 4. Effect of restrictor heater temperature on the restrictor outlet temperature (+) and extraction flow-rate (□) using the glass tube insert collection vial (Fig. 1). Outlet temperature was measured with a J thermocouple placed at the restrictor exit. The large increase in restrictor outlet temperature corresponded to a phase change in the CO_2 exiting the restrictor. At restrictor heater temperatures of *ca.* $> 100^\circ\text{C}$, the CO_2 was a gas, and at lower temperatures, the CO_2 was a mixture of gas and solid. SFE was performed at 400 atm and 50°C with a heated $11\text{ cm} \times 28\ \mu\text{m}$ I.D. capillary restrictor and a 0.5-ml Keystone extraction cell filled with silanized glass beads (70–80 mesh).

dimensions of the glass tube (3 mm I.D.), the extraction effluent escaped into the solvent as large bubbles. The formation of large bubbles in conjunction with a high gas flow (*ca.* 0.7 ml/min liquid CO_2 , resulting in a gas flow of *ca.* 360 ml/min) and the small collection solvent volume (5 ml), apparently caused the poor trapping efficiencies. This was confirmed by analytes found deposited in the collection vial vent. A narrower glass tube insert (2 mm I.D.) was utilized in an attempt to reduce the bubble size; however, no improvement in collection efficiencies was obtained. A similar commercial system used by Dionex was able to obtain high collection efficiencies for PAHs (97% recovery for naphthalene [9]), using a larger solvent volume (15 ml), precooling of

the collection solvent (cooled to *ca.* 0°C before the extraction), and lower extraction flow-rates (270 ml/min, *ca.* 0.5 ml/min liquid CO_2). Since the restrictor heater design shown in Fig. 1 did not meet all of the goals of good collection efficiencies, low solvent volumes and simplicity, other restrictor heater designs were investigated.

Design 2, post-extraction solvent nebulizer

The second design introduced an organic solvent (0.3 ml/min) at the tip of the restrictor (Fig. 2) in an attempt to increase solute/solvent contact, and increase the amount of analyte transported to the bulk collection solvent. The design also allowed for a simplified collection vial which only required a

relatively small (5 ml) collection solvent volume. The restrictor effluent nebulized the solvent introduced into the tee-piece to form a fine mist which was swept down the glass tube and into the bulk collection solvent. Using this method, no analyte deposition was seen along the glass tube and no additional solvent was required to maintain the solvent volume in the collection vial (solvent volume remained *ca.* 5 ml during SFE). The collection efficiencies for the PAHs were greatly improved (81–95%, Table I) and were attributed to increased solvent contact with the depressurized extract at the restrictor outlet. Low (50°C) restrictor heater temperatures were still sufficient to avoid restrictor plugging, since the solvent did not come in direct contact with the restrictor, thus reducing restrictor cooling. The nebulizer design produced constant extraction flow-rates (*ca.* 0.7 ± 0.05 ml/min) at low restrictor heater temperatures (50°C), but still did not meet the goals of simplicity (*i.e.*, an additional pump was required) and quantitative collection efficiencies (*e.g.*, >90%).

Design 3, heated restrictor placed in collection solvent

In an attempt to improve the collection efficiencies and further simplify the collection apparatus, the third design placed the restrictor directly into the collection solvent without any transfer device

(Fig. 3). To minimize the non-heated zone of the restrictor (*i.e.*, the restrictor tip in the collection solvent), the restrictor length was kept to a minimum (11 cm), high restrictor heater temperatures (100 to 200°C) were applied, and small (3.7 ml) collection vials with small collection solvent volumes (2.5 ml) were used. This design used an aluminum heating block to heat the restrictor, as the heating block was less of a fire hazard in the presence of evaporating solvents than the heating tape used in designs 1 and 2.

The restrictor block heater produced reasonable extraction flow-rates (0.7 ± 0.07 ml/min) for the spiked PAHs, but required higher restrictor heater temperatures (100–150°C) to eliminate restrictor plugging due to Joule–Thomson cooling of the restrictor tip in the collection solvent. Quantitative collection efficiencies (*ca.* 90–95%, Table II) were obtained, presumably because direct depressurization of the extraction fluid into the collection solvent increased the solute–solvent contact and greatly reduced the solvent evaporation as the collection solvent temperature was quickly lowered to below 0°C during the extraction (Fig. 5). Very small bubbles were observed at the restrictor outlet, the increased viscosity of the cooled solvent possibly reducing the size of the bubbles which increases the solute–solvent resonance time [21]. Increasing the extraction flow-rate from 0.6 to 0.7 ml/min liquid

TABLE II

COLLECTION EFFICIENCIES OF PAHs INTO METHYLENE CHLORIDE AT VARIOUS RESTRICTOR HEATER TEMPERATURES AND SFE FLOW-RATES BY DIRECT DEPRESSURIZATION OF THE EXTRACTION FLUID INTO THE COLLECTION SOLVENT (FIG. 3)

PAH	Percent collected ^a					
	28- μ m I.D. restrictor ^b			32- μ m I.D. restrictor ^c		
	50°C	100°C	150°C	50°C	100°C	150°C
Naphthalene	Blocked ^d	Blocked	90.8 (1.3)	Blocked	89.9 (2.1)	91.1 (3.0)
Acenaphthylene	Blocked	Blocked	94.0 (0.9)	Blocked	91.7 (2.1)	90.8 (5.1)
Fluorene	Blocked	Blocked	93.7 (3.0)	Blocked	93.1 (1.8)	91.9 (5.1)
Phenanthrene	Blocked	Blocked	95.5 (1.6)	Blocked	95.3 (0.2)	94.1 (1.4)
Fluoranthene	Blocked	Blocked	95.7 (1.8)	Blocked	95.6 (0.5)	99.4 (2.0)
Chrysene	Blocked	Blocked	90.1 (1.1)	Blocked	96.1 (2.1)	92.4 (2.0)

^a Value in parentheses is the percent relative standard deviation of triplicate 10-min extractions.

^b Flow-rate *ca.* 0.61 ml/min liquid CO₂ at pump.

^c Flow-rate *ca.* 0.85 ml/min at restrictor heater temperature of 100°C and *ca.* 0.69 ml/min at restrictor temperature of 150°C.

^d Restrictor becomes blocked after a few minutes so that no flow is present.

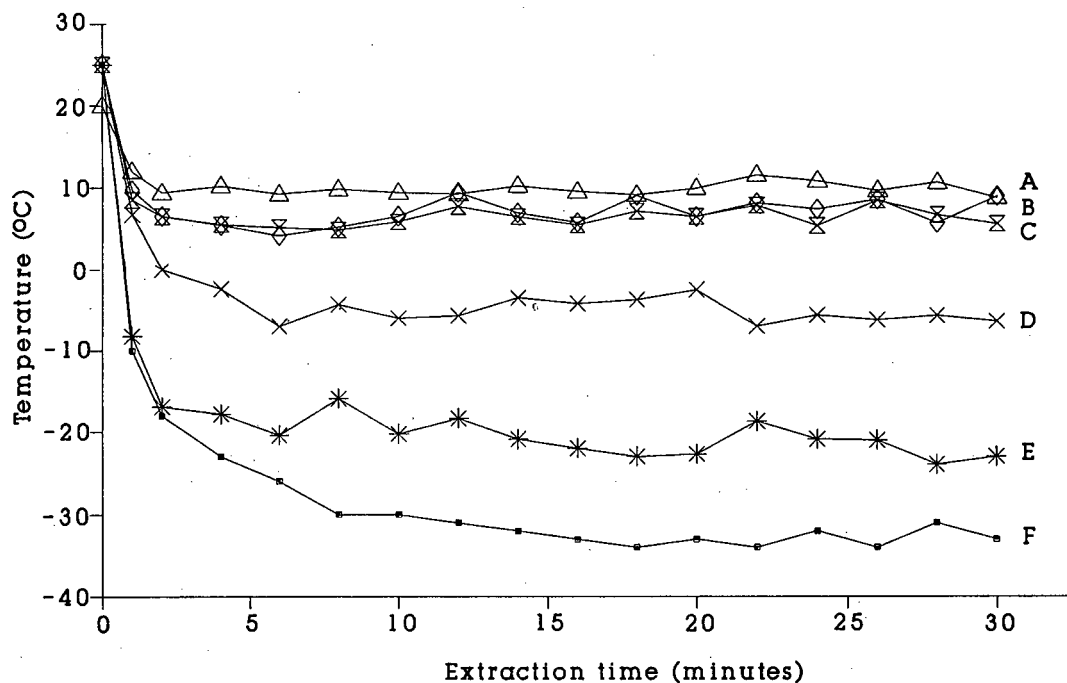


Fig. 5. SFE collection solvent temperature at various restrictor heater temperatures, with the extraction fluid being directly depressurized into the collection solvent (Fig. 3). Temperature profiles are shown for the collection solvent (2.5 ml) in a 3.7-ml vial standing in water with an 11 cm \times μ m I.D. restrictor heated to 200°C (A), restrictor heated to 100°C (B), no restrictor heating (C), or with the collection solvent vial in air with an 11 cm long \times 28 μ m I.D. restrictor heated to 200°C (D), restrictor heated to 100°C (E), and no restrictor heating (F).

CO₂ (*i.e.*, using 28- and 32- μ m I.D. restrictors, respectively) enabled a lower restrictor heater temperature (100°C) to be used, which still eliminated restrictor plugging and produced quantitative (*ca.* 90–95%) collection efficiency (Table II).

The collection efficiencies using the restrictor block heater were further investigated using a test mix of *n*-alkanes possessing a large range of volatilities. At low restrictor heater temperatures (50 and 100°C) analytes as volatile as *n*-octane could be efficiently collected (>90%). However, at higher restrictor heater temperatures (200°C), *n*-decane was the most volatile species that was efficiently collected (Table III). The decrease in collection efficiencies with increasing restrictor temperature was presumed to be due to an increase in aerosol formation at the restrictor outlet and purging of volatile components due to an increase in the collection solvent temperature (Fig. 5).

Since previous work had shown that maintaining

the solvent temperature above 0°C improved the extraction flow-rate for wet samples [20], a collection vial water bath was combined with the restrictor heater to assess the influence of collection solvent temperature on collection efficiencies. By placing the collection vial in a container of water initially at room temperature, the cooling effect of the expanding fluid in the solvent was reduced, so that the collection solvent temperature was stabilized at *ca.* 5–10°C (Fig. 5), and reasonable flow-rates were attained. Maintaining the collection solvent temperature at 5–10°C significantly reduced the collection efficiencies of the very volatile analytes (*ca.* 40% recovery for *n*-heptane, Table III) and also increased solvent evaporation. However, *n*-decane could still be efficiently trapped (*ca.* 90%) at all the restrictor heater temperatures investigated, even with the collection solvent temperature maintained above 0°C.

Since depressurizing the heated restrictor directly

TABLE III

COLLECTION EFFICIENCIES OF *n*-ALKANES INTO METHYLENE CHLORIDE (2.5 ml) AT VARIOUS RESTRICTOR HEATER TEMPERATURES USING A 28- μ m I.D. RESTRICTOR DEPRESSURIZED DIRECTLY INTO THE COLLECTION SOLVENT (FIG. 3)

Collection vial in	<i>n</i> -Alkane		Percent collected ^a				
			No heating ^b	50°C	100°C	150°C	200°C ^c
Air	Heptane	(C ₇)	78.1 (1.8)	73.9 (3.3)	71.8 (6.9)	71.5 (5.9)	56.5 (15.9)
	Octane	(C ₈)	90.6 (0.8)	92.3 (1.5)	90.8 (7.9)	88.7 (6.3)	79.9 (9.3)
	Nonane	(C ₉)	94.8 (0.9)	92.4 (2.1)	*93.3 (8.7)	94.5 (5.2)	89.4 (6.9)
	Decane	(C ₁₀)	98.2 (0.7)	96.1 (3.0)	96.6 (8.7)	97.7 (3.5)	93.8 (6.2)
	Pentadecane	(C ₁₅)	97.1 (1.6)	101.5 (5.3)	99.0 (7.7)	95.5 (3.4)	93.2 (2.9)
	Eicosane	(C ₂₀)	97.7 (2.2)	103.4 (3.7)	102.3 (5.2)	95.1 (2.8)	95.0 (3.4)
	Pentacosane	(C ₂₅)	100.8 (1.1)	104.5 (2.0)	98.4 (5.0)	98.3 (3.2)	94.0 (9.1)
Water	Heptane	(C ₇)	44.0 (13.1)	42.2 (15.7)	38.1 (8.0)	34.0 (8.6)	34.2 (16.2)
	Octane	(C ₈)	73.0 (5.8)	71.8 (6.8)	71.9 (5.3)	68.8 (3.8)	70.0 (7.0)
	Nonane	(C ₉)	85.6 (2.9)	85.5 (5.9)	88.1 (4.7)	81.5 (4.0)	86.4 (5.0)
	Decane	(C ₁₀)	94.2 (1.7)	90.7 (5.0)	93.0 (4.4)	87.9 (4.2)	92.2 (3.9)
	Pentadecane	(C ₁₅)	97.5 (2.7)	97.0 (4.1)	96.0 (5.5)	92.8 (2.2)	93.4 (1.7)
	Eicosane	(C ₂₀)	97.0 (1.4)	97.7 (5.3)	93.1 (6.8)	94.0 (0.9)	96.5 (2.5)
	Pentacosane	(C ₂₅)	99.0 (3.6)	93.8 (3.3)	101.3 (3.7)	100.0 (3.8)	95.5 (4.4)

^a Value in parentheses is the percent relative standard deviation of triplicate 10 minute extractions.

^b Flow-rate *ca.* 0.81 ml/min liquid CO₂.

^c Flow-rate *ca.* 0.59 ml/min liquid CO₂.

into the collection solvent appeared to meet the goals of simplicity, small collection solvent volumes (*ca.* 2.5 ml), quantitative collection efficiencies, and reasonable extraction flow-rates (*ca.* 0.7 ± 0.07 ml/min), a range of environmental samples was chosen to assess the restrictor heater's ability to avoid restrictor plugging. The samples were selected from over a hundred different samples, and the majority represented the worst cases of restrictor plugging encountered during past studies. The samples included (i) an air-dried railroad bed soil (*ca.* 1%, w/w, water) which is fairly typical of soils in regard to restrictor plugging; (ii) pine needles (*ca.* 80%, w/w, water) containing cuticle wax and producing intermittent restrictor plugging; (iii); petroleum waste sludge (*ca.* 45%, w/w, water) contaminated with *ca.* 10% (w/w) extractable hydrocarbons and causing intermittent/complete blockage of the restrictor; (iv) a NIST marine sediment (SRM 1941) with *ca.* 2% elemental sulfur [22] and causing intermittent/complete blockage of the restrictor; and (v) elemental sulfur which causes rapid blocking of an unheated restrictor.

For the majority of the samples, a continuous flow was achieved by heating the restrictor to the experimentally-determined temperature, which in some cases was as high as 200°C (Table IV). To avoid restrictor plugging, none of the samples except elemental sulfur required the collection solvent to be temperature controlled by placing the collection vial in water, which is advantageous since allowing the collection solvent temperature to drop below 0°C during the extraction improves the collection efficiencies of very volatile analytes, as shown in Table III. A constant flow (0.7 ± 0.1 ml/min) was attained for most of the test samples during the 30-min extraction (Fig. 6). However, for the petroleum waste sludge which contained a large concentration of extractable material, the flow-rate initially decreased and then stabilized with time. Reasonable flow-rates were also obtained for samples containing large amounts of water, such as fresh pine needles (80%, w/w, water) and petroleum waste sludge (45%, w/w, water). It appeared that the temperature inside the heated restrictor was sufficient to avoid water freezing at the restrictor tip,

TABLE IV

EFFECT OF RESTRICTOR HEATER TEMPERATURE ON SFE FLOW-RATES WITH SEVERAL SAMPLES KNOWN TO CAUSE RESTRICTOR PLUGGING USING A 30- μm I.D. RESTRICTOR DEPRESSURIZED DIRECTLY INTO THE COLLECTION SOLVENT (FIG. 3)

Sample	Qualitative flow ^a				
	No heating	50°C	100°C	150°C	200°C
Railroad bed soil	Blocked	Continuous	Continuous	Continuous	Continuous
Pine needles	Blocked	Blocked	Continuous	Continuous	Continuous
Marine sediment	Blocked	Blocked	Intermittent	Continuous	Continuous
Petroleum waste sludge	Blocked	Blocked	Blocked	Intermittent	Continuous
Elemental sulfur	Blocked	Blocked	Blocked	Blocked	Continuous ^b

^a The flow-rates are assessed as continuous (constant flow \pm 0.1 ml/min), intermittent (flow varies and may temporarily stop for 1 or 2 s), or blocked (no flow). SFE conditions: 0.5-ml Keystone extraction cell filled with sample, exposed for 30 min to 400 atm and 50°C CO₂ with a heated 11 cm \times 30 μm I.D. capillary restrictor. Collection vial in air unless otherwise indicated.

^b Collection vial in water (initially at room temperature).

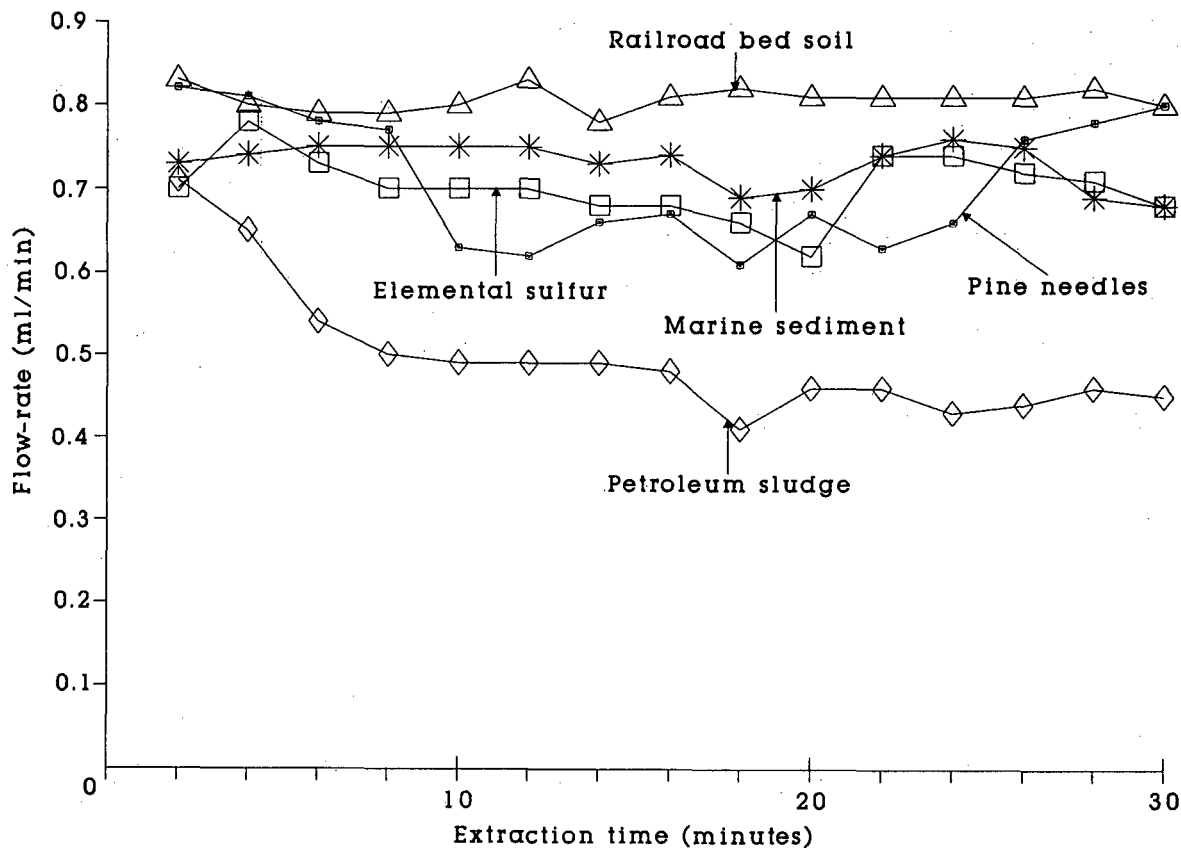


Fig. 6. Changes in flow-rate during SFE of railroad bed soil (0.8 g), marine sediment (0.35 g) and petroleum sludge (200 mg), with the extraction fluid being directly depressurized into the collection solvent (Fig. 3). SFE was performed at 400 atm and 50°C with a heated (150°C) 11 cm \times 30 μm I.D. capillary restrictor and a 0.5-ml Keystone extraction cell. Flow-rate measured as liquid CO₂ at pump.

even when the collection vial was not placed in water and the collection solvent was allowed to cool below 0°C.

In this study, there was no evidence of thermal degradation of analytes, as no qualitative differences could be found between SFE extracts obtained with and without a heated restrictor. Since the time spent in the heated restrictor is short, thermal degradation seems unlikely, particularly for species that are thermally stable enough to be analyzed by GC. In the worst case, where no density decrease along the restrictor is assumed, an analyte requires only *ca.* 10^{-2} s to be transported through an 11 cm \times 28 μ m I.D. restrictor at 0.5 ml/min liquid CO₂ flow-rate (this value may be halved if the density decrease along the restrictor is included [1]). In the unlikely event that thermal degradation does become a problem for extremely sensitive analytes, then the nebulizer design which operated at lower restrictor heater temperatures (50°C) may be more appropriate. The results of this study demonstrate that the restrictor heater design which allowed direct depressurization of the SFE extract into the collection solvent best achieved the goals of simplicity, low collection solvent volume, quantitative collection efficiencies, and the elimination of restrictor plugging.

ACKNOWLEDGEMENTS

The financial support of the US Environmental Protection Agency, EMSL-LV (Las Vegas), Shell Development Corporation, and the US Department of Energy is gratefully acknowledged. The authors would also like to thank ISCO (Lincoln, NE, USA) for instrument loans, and Sheryl Schmidt (British Petroleum, USA) for the petroleum waste sludge sample.

REFERENCES

- 1 R.D. Smith, J. H. Fulton, R. C. Petersen, A. J. Kopriva and B. W. Wright, *Anal. Chem.*, 58 (1986) 2057.
- 2 E. Stahl, K. W. Quirin, D. Gerard and G. Rau, *Ber. Bunsen Ges. Phys. Chem.*, 88 (1984) 900.
- 3 M. E. Paulaitis, V. J. Krukonis, R. T. Kurnik and R. C. Reid, *Rev. Chem. Eng.*, 1 (1983) 179.
- 4 J. M. Wong, N. Y. Kado, P. A. Kuzmicky, H.-S. Ning, J. E. Woodrow, D. P. H. Hsieh and J. N. Seiber, *Anal. Chem.*, 63 (1991) 1644.
- 5 H. M. McNair and J. O. Frazier, *Am. Lab.*, 23, No 11 (1991) 24D.
- 6 B. W. Wright, C. W. Wright, R. W. Gale and R. D. Smith, *Anal. Chem.*, 59 (1987) 38.
- 7 J. Wisser, Suprex Corporation, Pittsburgh, PA, personal communication.
- 8 *Applications Bulletin No. 71*, ISCO, Lincoln, NE, 1991.
- 9 B. Jones, Dionex Corporation, Salt Lake City, UT, personal communication.
- 10 E. Stahl, W. Schilz, E. Schütz and E. Willing, *Angew. Chem., Int. Ed. Engl.*, 17 (1978) 731.
- 11 R. M. Campbell, D. M. Meunier and H. J. Cortes, *J. Microcol. Sep.*, 1 (1989) 302.
- 12 M. Saito, T. Hondo and Y. Yamauchi, in R. M. Smith (Editor), *Supercritical Fluid Chromatography*, RSC Chromatography Monographs, London, 1989, p. 203.
- 13 *Application Note 228-138*, Hewlett-Packard, Avondale, PA, 1991.
- 14 P. Sandra, F. David and E. Stottmeister, *J. High Resolut. Chromatogr.*, 13 (1990) 284.
- 15 C. A. Thomson and D. J. Chesney, *J. Chromatogr.*, 543 (1991) 187.
- 16 M. Takeuchi and T. Saito, *J. High Resolut. Chromatogr.*, 14 (1991) 347.
- 17 R. M. Campbell and M. L. Lee, *Anal. Chem.*, 58 (1986) 2247.
- 18 R. E. Jentoft and T. H. Gouw, *Anal. Chem.*, 44 (1972) 681.
- 19 P. Subra and P. Boissinot, *J. Chromatogr.*, 543 (1991) 413.
- 20 J. J. Langenfeld, M. D. Burford, S. B. Hawthorne and D. J. Miller, *J. Chromatogr.*, 594 (1992) 297.
- 21 N. L. Porter, E. R. Campbell, A. R. Rynaski, B. J. Murphy, R. B. Nielsen and B. E. Richter, *Proceedings of the International Symposium on Supercritical Fluid Chromatography and Extraction, Park City, UT, January 14–17, 1991*, p. 127.
- 22 M. M. Schantz, B. A. Benner, Jr., S. N. Stephen, C. B. J. Koster, K. E. Hehn, S. F. Stone, W. R. Kelly, R. Zeisler and S. A. Wise, *Fresenius' J. Anal. Chem.*, 338 (1990) 501.

Supercritical fluid extraction of nitrated polycyclic aromatic hydrocarbons and polycyclic aromatic hydrocarbons from diesel exhaust particulate matter

Thomas Paschke^{*}, Steven B. Hawthorne and David J. Miller

University of North Dakota, Energy and Environmental Research Center, Box 8213, University Station, Grand Forks, ND 58202 (USA)

Bernd Wenclawiak

Analytische Chemie I, Universität Siegen, Adolf Reichwein Strasse, 5900 Siegen (Germany)

(First received March 9th, 1992; revised manuscript received June 9th, 1992)

ABSTRACT

Polycyclic aromatic hydrocarbons (PAHs) and nitrated PAHs (nitro-PAHs) were extracted from diesel exhaust particulates and diesel soot using supercritical CHClF_2 (freon-22), CO_2 , and CO_2 with added modifiers. Pure CO_2 was able to extract 1-nitropyrene spiked on air sampling filters, but did not yield quantitative extractions from diesel exhaust particulates [standard reference material (SRM) 1650 of the National Institute of Standards and Technology (Gaithersburg, MD, USA)]. 1-Nitropyrene could be quantitatively extracted in 45 min using either pure CHClF_2 or 10% toluene in CO_2 as a modifier, whereas 10% mixtures of CHClF_2 or methanol in CO_2 yielded only moderate recoveries. Supercritical CHClF_2 also yielded quantitative extraction of PAHs from SRM 1650. Various nitro-PAHs could be determined in soot collected from the exhaust pipe of a bus after extraction with CO_2 modified with CHClF_2 or toluene.

INTRODUCTION

Diesel exhaust particulate matter contains a wide variety of nitrated polycyclic aromatic hydrocarbons (nitro-PAHs), of which 1-nitropyrene is by far the most abundant [1,2]. Tests with the Ames short-term bioassay for detection of chemical mutagens prove that 1-nitropyrene is a direct mutagen causing spontaneous mutations in *Salmonella typhimurium* bacteria [3–6]. For the determination of nitro-PAHs, diesel particulates are usually extracted for

24 h with methylene chloride with a Soxhlet apparatus [4]. The use of a supercritical fluid could reduce the extraction time to less than an hour while greatly reducing the amount of liquid solvent required. It has been shown previously that PAHs can be quantitatively extracted with pure CO_2 or CO_2 -methanol (95:5) [7] using relatively long (*e.g.* 90 min) extraction times, and the extraction of nitro-PAHs from sorbents has been reported [8,9]. However, little is known about the extraction behavior of nitro-PAHs from complex matrices such as diesel exhaust particulates. Under many supercritical fluid extraction (SFE) conditions, supercritical extractions of polar compounds from a complex matrix like diesel exhaust particulates often yields poor recoveries when pure CO_2 is used. Experiments with incinerator fly ash and sediment samples indicate that of-

Correspondence to: Dr. S. B. Hawthorne, University of North Dakota, Energy and Environmental Research Center, Box 8213, University Station Grand Forks, ND 58202, USA.

* Present address: Analytische Chemie I, Universität Siegen, Adolf Reichwein Strasse, 5900 Siegen, Germany.

TABLE I
COMPARISON OF PROPERTIES OF SUPERCRITICAL FLUIDS

Compound	Critical temperature, T_c (°C)	Critical pressure P_c (atm)	Dipole moment (Debye)
CO ₂	31.3	72.9	0.0
Methanol	239.5	81.0	1.7
Methanol–CO ₂ (10:90) ^a	51.5	74.2	–
CHClF ₂	96.1	49.1	1.4
CHClF ₂ –CO ₂ (10:90) ^a	38.2	69.6	–
Toluene	318.8	41.4	0.4
Toluene–CO ₂ (10:90) ^a	67.2	67.9	–

^a The critical data of the 10% mixtures were calculated with SF-Solver by ISCO, Lincoln, NE, USA.

ten the solubility of the analyte is not the limiting factor for quantitative extractions [10–13]. Instead, it appears that strong interactions between the analyte and the matrix exist which must be overcome by a stronger solvent than CO₂ [10–13].

The most common way to increase the solvent strength of CO₂ is the use of methanol as a modifier. Because of its high critical temperature of 240°C, pure methanol is not a suitable solvent for supercritical extractions under mild conditions. CHClF₂ provides a dipole moment similar to methanol, but has more moderate critical data (Table I). CHClF₂ (freon-22) has been used by Li and co-workers [14,15] as a mobile phase for supercritical fluid chromatography (SFC) of steroids and phenols and for the extraction of steroids. Compared to CO₂, CHClF₂ showed much shorter retention times for these polar compounds. (CHClF₂ is also much more desirable from the environmental standpoint than fully-halogenated freons because it degrades more rapidly in the lower atmosphere and therefore has a low potential for ozone destruction and global warming. In addition, CHClF₂ is being suggested as the future coolant in home air conditioning systems [16].) Besides CHClF₂ and methanol-modified CO₂, which are expected to yield better extraction results than CO₂ because of their higher dipole moment, toluene was also used as a modifier. Toluene-modified CO₂ has been reported to increase the extraction of dioxins from fly ash, presumably because of its aromatic character [13].

This study compares pure CO₂, pure CHClF₂, and CO₂ modified with 10% toluene, methanol,

and CHClF₂ for their ability to extract nitro-PAHs from diesel exhaust particulates and soot.

EXPERIMENTAL

Samples

The diesel exhaust particulate sample (standard reference material, SRM 1650) was supplied by NIST (National Institute of Standards and Technology, Gaithersburg, MD, USA), and is considered to be representative for cumulative sampling of heavy-duty engines for shorter periods of time [4]. SRM 1650 contains 19 ± 2 µg/g 1-nitropyrene according to NIST based on Soxhlet extractions. The diesel soot sample was collected from the exhaust pipe of a bus which had a 6.9-l International diesel engine (1985). All samples were stored in the dark at 4°C until used.

Supercritical fluid extractions

Supercritical extractions were performed with ISCO 260D or 100D syringe pumps (ISCO, Lincoln, NE, USA) using SFC-grade CO₂ or >99.9% purity CHClF₂ (Scott Specialty Gases, Plumsteadville, PA, USA). For generating modified CO₂ two pumps were connected with a mixing tee and two backpressure control valves following the manufacturer's instructions (Fig. 1). SRM 1650 diesel exhaust particulate (25 mg) or diesel exhaust pipe soot (250 mg) were extracted in 0.5 ml or 2.2 ml extraction cells, respectively (Keystone Scientific, Bellefonte, PA, USA). The extraction pressure was 400 atm (405 bar) during all extractions. The extraction

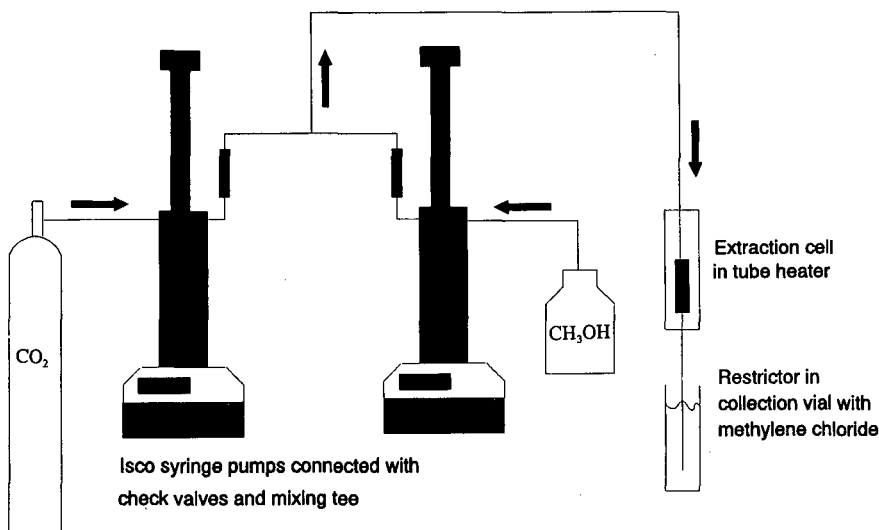


Fig. 1. Schematic diagram of the SFE system using CO₂ with an organic modifier (e.g., methanol). Arrows indicate the direction of extraction fluid flow. Details on the individual system components are given in the text.

temperature was maintained by placing the cell in a thermostatically controlled tube heater. Because of the different critical temperatures of the various pure and modified fluids used, the extraction temperature was 40°C with pure CO₂, 100°C with pure CHClF₂, 80°C with CO₂–methanol, 60°C with CO₂–CHClF₂ modifier, and 100°C with CO₂–toluene.

Supercritical fluid flow rates were maintained at ca. 0.3 ml/min (measured as liquid at the pump) using capillary restrictors with an internal diameter of 19–23 μm (Polymicro Technologies, Phoenix, AZ, USA). Plugging of the restrictor occurred occasionally when CO₂–methanol or pure CHClF₂ were used, because of freezing water at the outlet of the restrictor or precipitated analytes inside the restrictor. In these cases, the restrictor was briefly heated with a heat gun to maintain flow. When CHClF₂ was the supercritical fluid, restrictors tended to break more frequently and were, therefore, replaced after every extraction.

All extracts were collected in 5 ml methylene chloride placed in a 70 mm long × 18 mm I.D. glass vial. During extraction, methylene chloride had to be added from time to time because of evaporation losses. After the extraction, the solvent was evaporated with nitrogen to a volume of 1 ml. The sam-

ple was then transferred into an autosampler vial and the internal standard (deuterated chrysene) was added. HPLC-grade methanol used as a modifier was briefly sonicated for degasification before use. All other organic solvents were pesticide grade (“Optima”; Fisher Scientific, USA).

In order to determine the trapping efficiency of the extracted analytes in the 5 ml methylene chloride, air particulate sampling filters (10 × 40 mm pieces of Whatman QM-A quartz microbore filters) were spiked with 0.2 ml of a solution containing 50 to 90 μg/g each of phenanthrene, 1-nitronaphthalene and 1-nitropyrene in methanol. The solvent was evaporated for 10 min, the filter was transferred immediately into an extraction cell, and extracted with CO₂.

Gas chromatographic analysis

The extracts from the spiked samples were analyzed by gas chromatography with flame ionization detection (GC–FID) using a Hewlett-Packard Model 5890 equipped with an HP 7673 automatic sampler, an HP 3396A integrator, and an HP-5 capillary column (25 m × 320 μm I.D., 0.17 μm film thickness). Hydrogen was used as the carrier gas. Samples were injected at a split ratio of 1:30. The GC oven temperature for all analyses was 60°C fol-

lowed by a temperature ramp at 8°C/min to 330°C.

All diesel particulate extracts were analyzed by GC-MS (HP 5988) in the selected ion monitoring mode using the molecular ion for each species and the same capillary column that was used for the FID analyses. The carrier gas was helium. Because of limited sample availability, only 25-mg amounts of SRM 1650 were extracted and the samples had to be injected splitless to achieve the required sensitivity. Diesel particulate extracts contained a high amount of nonvolatile organic compounds, so the injection port liner had to be changed daily. Extracts from the diesel bus exhaust pipe soot were injected at a split ratio of 1:40 because larger (250 mg) samples were extracted and nitro-PAH concentrations in this soot sample were significantly higher than in the SRM sample. Certified standards of nitro-PAHs in methanol (NIST SRM 1587) were used for quantitative standards and to confirm the retention times of the individual nitro-PAHs. Each sample extract and quantitative standard was spiked with 90 ng of [²H₁₂]chrysene as an internal standard, and all quantitations were based on the ratios of the individual peak areas to those of the internal standard.

RESULTS AND DISCUSSION

Extractions from spiked filters

As shown in Table II, 1-nitropyrene was quantitatively extracted in 30 min from spiked quartz filters with pure supercritical CO₂ at a pressure of 400 atm and a temperature of 40°C. In addition to demonstrating that 1-nitropyrene has sufficient solubility in CO₂ to be efficiently extracted, these results demonstrate that the chosen trapping conditions allowed recoveries better than 95% for 1-nitropyrene

TABLE II

SFE RECOVERIES FROM SPIKED QUARTZ FIBER FILTERS WITH PURE CO₂

Compound	Recovery (%)	SD ^a (%)
Phenanthrene	97.4	4
1-Nitronaphthalene	95.4	2
1-Nitropyrene	98.9	2

^a Standard deviations are based on 5 extractions.

as well as for the more volatile compounds 1-nitronaphthalene and phenanthrene.

GC-MS analysis of diesel exhaust particulate extracts

Extracts from diesel particulates contain such a broad variety of organic compounds that neither FID nor electron-capture detection were selective enough to analyze these extracts for nitro-PAHs without additional sample treatment. With GC-MS, the most intense peaks in the total ion current chromatogram of the unfractionated diesel exhaust particulate extracts were identified as high-molecular-mass (ca. C₁₈ to C₂₈) alkanes. When the GC-MS is operated in the selected ion monitoring (SIM) mode, the selectivity was sufficient to quantitate the nitro-PAHs, the PAHs (except for those with *m/z*

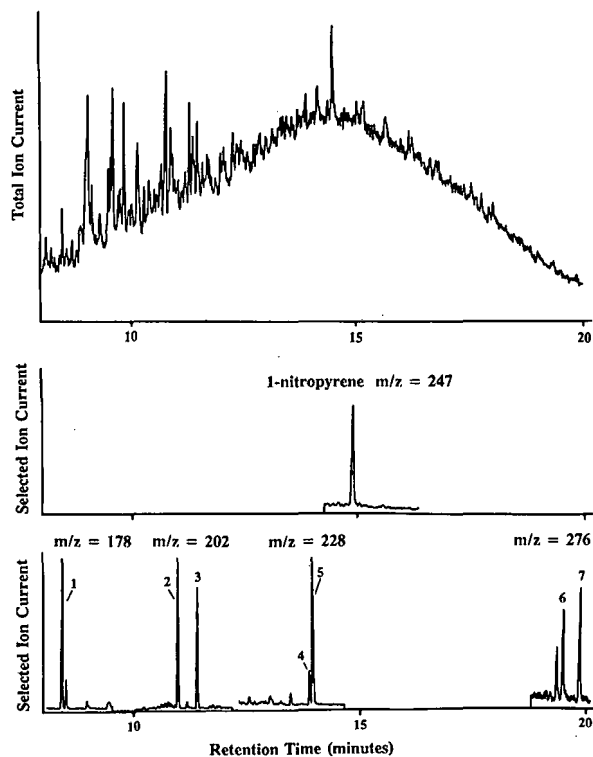


Fig. 2. Comparison of the total ion current chromatogram (scan range 50–350 amu) of an unfractionated CHClF₂ extract of diesel exhaust particulate with the selected ion current chromatograms for 1-nitropyrene and phenanthrene (peak 1), fluoranthene (peak 2), pyrene (peak 3), benz[*a*]anthracene (peak 4), chrysene (peak 5), indeno[1,2,3-*cd*]pyrene (peak 6), and benzo[*ghi*]perylene (peak 7).

252 because of interfering ions), and the internal standard (deuterated chrysene) as shown in Fig. 2 by a comparison between a total ion and a selected ion chromatogram of an unfractionated extract. With the extraction of a 25-mg sample, concentration of the extract to 1 ml, and a splitless injection of 1 μ l, the method detection limit was *ca.* 1 ng of 1-nitropyrene per mg of soot using SIM.

Extraction kinetics of 1-nitropyrene from bus soot

To determine a reasonable extraction time, preliminary extractions of the bus soot with CO₂-methanol (90:10) were performed and fractions were collected after 5, 10, 15, 25, 35, 45, 60, 90 and 120 min. As shown in Fig. 3, more than 95% of the extractable 1-nitropyrene was extracted after 45 min. Based on these results, the extraction time for all subsequent extractions was set to 45 min.

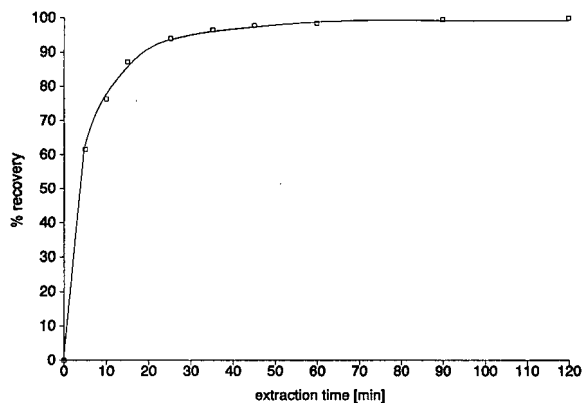


Fig. 3. SFE extraction kinetics of 1-nitropyrene from 250 mg of diesel bus exhaust pipe soot using CO₂ modified with 10% methanol. Fractions were collected after 5, 10, 15, 45, 60, 90, and 120 min of extraction and analyzed as described in the text. The extraction yield was normalized to the final value obtained after 120 min of extraction.

TABLE III
EXTRACTION EFFICIENCIES OF 1-NITROPYRENE FROM NIST DIESEL EXHAUST PARTICULATES USING VARIOUS SUPERCRITICAL FLUIDS

Supercritical fluid	Concentration (μ g/g)	Recovery ^a (%)	Average recovery ^a \pm S.D. (%)
CO ₂	3.3	18	25 \pm 9
	3.3	17	
	6.2	32	
	6.3	33	
CO ₂ -methanol (90:10), set 1	5.8	31	28 \pm 3
	5.4	28	
	4.6	24	
	5.9	31	
CO ₂ -methanol (90:10), set 2	5.1	27	32 \pm 8
	5.5	29	
	5.4	28	
	8.3	44	
CHClF ₂	22.0	116	117 \pm 7
	20.9	110	
	23.6	124	
CO ₂ -CHClF ₂ (90:10)	7.2	38	43 \pm 7
	7.8	41	
	7.2	38	
	10.1	53	
CO ₂ -toluene (90:10)	19.8	104	97 \pm 8
	18.4	97	
	16.9	89	

^a Recoveries compared to 19 \pm 2 μ g/g 1-nitropyrene based on Soxhlet extractions as certified by NIST.

Extractions from Standard Reference Material 1650

The first extraction of the diesel exhaust particulates (SRM 1650) was performed with the most common supercritical fluid, CO₂. After 45 min at 400 atm and 40°C, only 25% of the 1-nitropyrene reported by NIST was extracted (Table III). These results indicate that solubility is not the limiting factor for supercritical extraction of nitro-PAHs from exhaust particulate samples, since 1-nitropyrene could easily be extracted from spiked filters (Table II). Extraction with CO₂ containing 10% methanol modifier did not increase the recovery considerably, and only *ca.* 30% of the 1-nitropyrene was extracted. Since methanol modifier has previously been reported to increase the recoveries of moderately polar analytes, these results were somewhat surprising. To verify these low recoveries, a second set of samples were extracted under identical conditions and yielded similar recoveries (Table III).

In contrast to the extraction with pure CO₂ and methanol-modified CO₂, SFE with pure CHClF₂ yielded excellent recoveries (117%) *versus* the Soxhlet extraction value (19 ± 2 µg/g) certified by NIST, possibly because of its high dipole moment (1.4 Debye). Since the capillary restrictors sometimes broke when using pure CHClF₂ as the extraction fluid (and because of possible environmental objections to using freons as extraction fluids), CHClF₂ was also used as a modifier in CO₂ in the hopes of maintaining the high extraction efficiencies while reducing the total amount of CHClF₂ used. With CO₂-CHClF₂ (90:10), extraction efficiencies were only slightly better than the CO₂ and CO₂-methanol

(90:10) results, *i.e.*, only 43% of the 1-nitropyrene was extracted.

Because of the potential of toluene to break π-bonding interactions between the diesel exhaust particulate matrix and the nitro-PAHs, toluene-modified CO₂ was also tested as an extraction fluid. As shown in Table III, CO₂-toluene (90:10) yielded good recoveries (97%). The ability of toluene modifier to extract nitro-PAHs from diesel exhaust particulate is likely a result of its aromatic character rather than its low dipole moment of only 0.4 Debye.

Extractions from the bus exhaust pipe soot

1-Nitropyrene is the only nitro-PAH in the SRM sample that is reported with a certified value. Other nitro-PAHs are present in considerably lower concentrations, but, because of limited sample availability, quantitations of additional nitro-PAHs could not be performed. Much larger quantities of the bus soot were available, which allowed additional nitro-PAHs to be quantitated from the extraction of 250-mg samples. The extractions were performed with CO₂-CHClF₂ (90:10) and CO₂-toluene (90:10) as supercritical fluids, which gave the best recoveries from the SRM sample (with the exception of pure CHClF₂).

As shown in Table IV, several additional nitro-PAHs besides 1-nitropyrene were extracted from diesel soot using either CHClF₂ or toluene as modifiers in CO₂. A comparison of the diesel exhaust particulate extracts (Table III) and the diesel soot (Table IV) shows two interesting differences. First,

TABLE IV
NITRO-PAHs EXTRACTED FROM BUS SOOT

Compounds	Extracted with CO ₂ -CHClF ₂ (90:10)		Extracted with CO ₂ -toluene (90:10)	
	µg/g	SD ^a (µg/g)	µg/g	SD ^a (µg/g)
2-Nitrofluorene	27	7	28	2
9-Nitroanthracene	63	12	62	7
3-Nitrofluoranthene	10	1	11	2
1-Nitropyrene	450	70	540	50
7-Nitrobenz[a]anthracene	10	2	12	1
6-Nitrochrysene	4	2	4	1

^a Standard deviations based on 4 extractions.

the bus soot contains much higher concentrations of 1-nitropyrene. Additionally, the amount of each nitro-PAH extracted from the bus soot using CO₂-CHClF₂ (90:10), was nearly identical to that extracted using CO₂-toluene (90:10). While CO₂-CHClF₂ (90:10) only extracted 44% as much of the 1-nitropyrene from the diesel exhaust particulate sample (compared to the CO₂-toluene (90:10) extraction, Table III), the extraction of the bus soot sample with CO₂-CHClF₂ (90:10) yielded 83% as much 1-nitropyrene as the CO₂-toluene extraction (Table IV).

The large differences in 1-nitropyrene concentrations found in the exhaust particulates and the exhaust pipe soot samples might be explained by the differences in the sources and collection of the two samples. The NIST diesel exhaust particulate sample was collected from the exhaust stream in the heat exchangers of a dilution tube facility, while the diesel soot sample was collected directly from the exhaust pipe of a bus. If it is assumed that the nitro-PAHs were formed at the same time when the particle growth took place, nitro-PAHs would be found inside the NIST-particles as well as on the surface. For quantitative extractions, the supercritical fluid must extract the analyte not only from the surface, but from the inside of a particle as well. Based on the recoveries shown in Table III, this was possible with pure CHClF₂ or CO₂-toluene modifier (90:10), whereas CHClF₂-modifier was too weak as a solvent. Since all of the fluids tested in Table II

[except pure CHClF₂ and CO₂-toluene (90:10)] yielded similar amounts of extracted 1-nitropyrene from the NIST diesel exhaust particulate sample, it appears that *ca.* 30% of the 1-nitropyrene was located in "easier" (*e.g.*, surface) sites for extraction. In contrast, the bus soot was present in the exhaust pipe for an extended period of time. During operation of the bus, nitro-PAHs from the exhaust stream could have been adsorbed on the surface of the soot, or it is also possible that the soot acted as a catalyst for the formation of additional nitro-PAHs from PAHs and nitrogen oxides. As a result, the bus soot is more likely to contain high concentrations of nitro-PAHs adsorbed on the surface than the NIST exhaust particulate sample and, therefore, the bus soot has a higher proportion of the nitro-PAHs which are easier to extract than the NIST exhaust particulate sample. While no additional direct evidence exists for this explanation, the results shown in Tables III and IV clearly indicate that even relatively small changes in sample matrix can have significant effects on the extraction efficiencies obtained when the extraction conditions are not sufficiently strong.

Recoveries of PAHs from NIST diesel exhaust particulate

Although the major emphasis of this paper was to develop SFE conditions for the quantitative recovery of nitro-PAHs, the NIST diesel exhaust particulate extracts generated using pure CHClF₂,

TABLE V
RECOVERIES OF PAHs FROM NIST DIESEL EXHAUST PARTICULATE

	NIST ($\mu\text{g/g}$) ^b	% Recovery versus NIST Values ^a		
		CHClF ₂	CO ₂ -CHClF ₂	CO ₂ -toluene
Phenanthrene	71	82 ± 12	61 ± 12	68 ± 4
Fluoranthene	51 ± 4	92 ± 11	66 ± 13	81 ± 3
Pyrene	48 ± 4	89 ± 9	61 ± 13	79 ± 2
Benz[<i>a</i>]anthracene	6.5 ± 1.1	106 ± 8	38 ± 9	97 ± 2
Chrysene	22	115 ± 11	41 ± 10	101 ± 1
Indeno[1,2,3- <i>cd</i>]pyrene	2.3	105 ± 27	7 ± 5	40 ± 9
Benzo[<i>ghi</i>]perylene	2.4 ± 0.6	104 ± 16	5 ± 4	70 ± 9

^a Percent recoveries versus the NIST values ± one standard deviation unit based on triplicate extractions for the CHClF₂ and CO₂-toluene (90:10), and quadruplicate extractions for the CO₂-CHClF₂ (90:10).

^b Concentrations reported by NIST based on Soxhlet extraction. The values for phenanthrene, chrysene, and indeno[1,2,3-*cd*]pyrene are given by NIST as informational values without standard deviations. All other values are certified by NIST.

CO₂-CHClF₂ (90:10), and CO₂-toluene (90:10) were also analyzed for PAHs to determine if similar trends in extraction efficiencies were obtained. As shown in Table V, the PAH recoveries were similar to those shown in Table III for the 1-nitropyrene from the same sample. Extraction with pure CHClF₂ yielded the best recoveries of the PAHs compared to the Soxhlet extraction values reported by NIST, while toluene-modified CO₂ also yielded reasonably good recoveries. As was the case for the 1-nitropyrene, the use of CHClF₂ as a modifier in CO₂ did not yield as high recoveries of the PAHs as either pure CHClF₂ or toluene-modified CO₂.

CONCLUSIONS

SFE with pure CHClF₂ yielded the highest recoveries of both nitro-PAHs and PAHs from diesel exhaust particulates, although CO₂ modified with toluene also yielded good extraction efficiencies. Even though extraction with pure CO₂ yielded quantitative recoveries of nitro-PAHs from spiked air sampling filters, only 30% recoveries of 1-nitropyrene were achieved from diesel exhaust particulates. These results demonstrate that quantitative extraction of nitro-PAHs from diesel exhaust particulates requires extraction fluids that can overcome matrix-analyte interactions as well as simply solvate the analyte.

ACKNOWLEDGEMENTS

The authors would like to thank the United

States Environmental Protection Agency, EMSL-LV (Las Vegas) for financial support. SFE pump loans from ISCO are also gratefully acknowledged.

REFERENCES

- 1 M.C. Paputa-Peck, R. S. Marano, D. Schuetzle, T. L. Riley, C. V. Hampton, T. J. Prater, L. M. Skewes, T. E. Jensen, P. H. Ruehle, L. C. Bosch and W. P. Duncan, *Anal. Chem.*, 55 (1983) 1946–1954.
- 2 D. Schuetzle, T. L. Riley, T. J. Prater, T. M. Harvey, D. F. Hunt, *Anal. Chem.*, 54 (1982) 265–271.
- 3 J. N. Pitts, *Atmos. Environ.*, 21 (1987) 2531–2547.
- 4 D. Schuetzle, T. E. Jensen, J. C. Ball, *Environment International*, 11 (1985) 169–181.
- 5 I. T. Salmeen, A. M. Pero, R. Zator, D. Schuetzle and T. L. Riley, *Environ. Sci. Technol.*, 18 (1984) 375–382.
- 6 D. Schuetzle, F. S.-C. Lee, T. J. Prater and S. B. Tejada, *Intern. J. Environ. Anal. Chem.*, 9 (1981) 93–144.
- 7 S. B. Hawthorne, D. J. Miller, *J. Chromatogr. Sci.*, 24 (1986) 258–264.
- 8 B. W. Wright, C. W. Wright, R. W. Gale and R. D. Smith, *Anal. Chem.*, 59 (1987) 38–44.
- 9 J. M. Wong, N. Y. Kado, P. A. Kuzmicky, J. E. Woodrow, D. P. H. Hsieh and J. N. Seiber, *Anal. Chem.*, 63 (1991) 1644–1650.
- 10 S. B. Hawthorne, *Anal. Chem.*, 62 (1990) 633A–642A.
- 11 F. I. Onuska and K. A. Terry, *J. High Resolut. Chromatogr.*, 12 (1989) 357–361.
- 12 S. B. Hawthorne, D. J. Miller, J. J. Langenfeld, *J. Chromatogr. Sci.*, 28 (1990) 2–8.
- 13 N. Alexandrou and J. Pawliszyn, *Anal. Chem.*, 61 (1989) 2770–2776.
- 14 S. F. Y. Li, C. P. Ong, M. L. Lee, H. K. Lee, *J. Chromatogr.*, 515 (1990) 515–520.
- 15 C. P. Ong, H. K. Lee and S. F. Y. Li, *Anal. Chem.*, 62 (1990) 1389–1391.
- 16 P. S. Zurer, *Chem. Eng. News*, July 24 (1989) 7.

High-performance thin-layer chromatographic mobility of porphyrins and their copper complexes on different adsorbents

Koichi Saitoh, Rie Kashiwa, Ryota Tada, Chikara Kiyohara and Nobuo Suzuki

Department of Chemistry, Faculty of Science, Tohoku University, Sendai, Miyagi 980 (Japan)

(First received October 14th, 1991; revised manuscript received April 23rd, 1992)

ABSTRACT

The R_f values of twelve synthetic porphyrins including porphine and phenyl- and alkyl-substituted porphines, and also of their copper complexes, were obtained on thin-layer chromatographic plates coated with silica gel, cellulose, NH_2 -bonded silica gel and octadecyl-bonded silica gel (ODS) with different developing solvents. On the first three plates, the mobilities (R_f values) of each porphyrin were always smaller than those of the corresponding copper complex, whereas the opposite occurred on the last plate. With an identical solvent, the mobilities of both a porphyrin and its copper complex increase in the following order of polar adsorbents: silica gel < NH_2 -silica < cellulose. *meso*-Tetra(4-pyridyl)porphine was adsorbed so strongly on every polar adsorbent that it hardly migrated from the origin, whereas a large migration with the $R_f \approx 0.9$ occurred on an ODS plate specifically with *N,N*-dimethylformamide.

INTRODUCTION

The convenience of thin-layer chromatography (TLC) has been applied to the isolation or preliminary identification of porphyrins and porphyrin esters by many investigators [1,2]. High-performance TLC (HPTLC) has promised to give higher resolution and reproducibility than conventional TLC for the separation of porphyrins and related compounds. Only a limited number of papers have dealt with systematic studies of the HPTLC behaviour of porphyrins and metalloporphyrins.

In our laboratory, a series of fundamental studies have been carried out on the HPTLC migration behaviour of metal complexes of various porphyrins, such as *meso*-tetraphenylporphine [3,4], *meso*-tetraakis(4-tolyl)porphine [5] and etioporphyrin [6], using

both normal- and reversed-phase separation modes, and porphine [7], haematoporphyrin [8] and pheophorbide-a and -b (not of the porphyrin but the chlorin family) [9] only using the reversed-phase mode. As these studies were not always carried out under identical conditions, the mobilities of different porphyrins and metalloporphyrins could not be easily compared with each other.

This paper describes the comparison of the mobilities of different porphyrins in the forms of the free acids (H_2P) and copper(II) complexes [$\text{Cu}(\text{P})$] under identical conditions of adsorbent and solvent. The HPTLC study covered twelve synthetic porphyrins, including porphine, which is the compound with the most basic structure of porphyrin, and its analogues substituted with alkyl, *para*-substituted-phenyl or pyridyl groups. The $\text{Cu}(\text{P})$ s were taken as model metalloporphyrins. Four kinds of adsorbents, *viz.*, silica gel, cellulose, aminopropyl-bonded silica gel (NH_2 -silica) and ODS, were used.

Correspondence to: Dr. K. Saitoh, Department of Chemistry, Faculty of Science, Tohoku University, Sendai, Miyagi 980, Japan.

EXPERIMENTAL

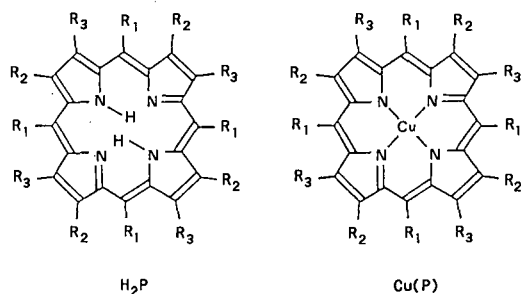
Porphyrins and their copper complexes

Fig. 1 shows the porphyrins studied. The preparations of H₂POR [7], H₂TPP [3], H₂TPP [5] and H₂ETIO [6] have been described in previous papers. H₂TMP [10] and H₂TPyP [11] were prepared by literature methods, respectively. Other porphyrins were synthesized by the general method of Adler *et al.* [12], in which pyrrole reacted, in refluxing propionic acid, with a suitable aromatic aldehyde, *e.g.*, fluorobenzaldehyde for H₂TFPP. These porphyrins were purified according to the procedures of Barnett *et al.* [13]. H₂OEP was obtained commercially (Strem Chemicals, Newburyport, MA, USA).

All Cu(P)s were prepared by the reaction of the porphyrin with ten times the equivalent amount of copper(II) acetylacetonate in refluxing chloroform [14]. They were then purified by alumina column chromatography followed by recrystallization.

HPLC

Commercially available HPTLC plates (10 × 10 cm) (Merck, Darmstadt, Germany) precoated with



Porphyrin (H ₂ P)	Abbr. P	R ₁	R ₂	R ₃
porphine	POR	H	H	H
meso-tetramethylporphine	TMP	CH ₃	H	H
meso-tetraphenylporphine	TPP	ph-H	H	H
meso-tetrakis(4-tolyl)porphine	TTP	ph-CH ₃	H	H
meso-tetrakis(4-methoxyphenyl)porphine	TMPP	ph-OCH ₃	H	H
meso-tetrakis(4-fluorophenyl)porphine	TFPP	ph-F	H	H
meso-tetrakis(4-chlorophenyl)porphine	TCPP	ph-Cl	H	H
meso-tetrakis(4-nitrophenyl)porphine	TNPP	ph-NO ₂	H	H
meso-tetrakis(4-biphenyl)porphine	TBPP	ph-ph-H	H	H
meso-tetrakis(4-pyridyl)porphine	TPyP	4-pyridyl	H	H
etioporphyrin I	ETIO	H	C ₂ H ₅	CH ₃
octaethylporphyrin	OEP	H	C ₂ H ₅	C ₂ H ₅

ph = para-substituted phenyl; -(C₆H₄)_n.

Fig. 1. The H₂P and Cu(P) species studied.

silica gel (silica gel 60), cellulose, NH₂-silica (NHY₂ F254S), and ODS (RP-18 F254S), all from Merck, were used. The silica gel plate was cleaned by development with methanol and then activated prior to use by heating at 110°C for 30 min followed by cooling in a silica gel desiccator for 2 h. The other plates were used without preliminary treatment. A portion of the thin-layer coating was preliminarily scraped off each plate so that the development would stop automatically when the solvent front had migrated 75 mm from the origin.

A sample solution of an H₂P or Cu(P) was prepared at a concentration of 0.1 mM or less in chloroform. A 0.5-μl portion of the solution was charged with the aid of a glass capillary micropipette (Drummond Scientific, Broomall, PA, USA) on to the sample origin located 5 mm from the edge of the TLC plate. All porphyrins or their copper complexes were spotted on identical plates so that their mobilities could be compared with each other.

The chromatogram was developed horizontally in a Camag (Muttens, Switzerland) Model 28510 sandwich-type chamber in a room thermostated at 25°C. After the migration of the solvent front had automatically stopped at the preset distance (75 mm), the development was allowed to continue for an additional 5 min so that the irregularity of the amount of solvent particularly in the vicinity of the solvent front was reduced. The chromatogram was recorded spectrophotometrically at the absorption maximum wavelength of the Soret band of each compound (about 500 nm) with a Shimadzu (Kyoto, Japan) Model CS-920 densitometer.

RESULTS AND DISCUSSION

One sharp spot was detected for each compound in the chromatogram on all the chromatographic plates used. The *R_F* values obtained for H₂P and Cu(P) on different HPTLC plates are given in Tables I and II, respectively. For discussing the mobility of each compound, the migration factor *R_M* calculated from the following equation is used hereafter:

$$R_M = \log\left(\frac{1}{R_F} - 1\right) \quad (1)$$

For convenience, *R_M* values above 1.7 or below -1.7 will be entered on the graphs as 1.7 or -1.7, respectively.

TABLE I

 $R_F \times 100$ VALUES OF H_2P

Plate	Solvent	$R_F \times 100$											
		POR	TMP	TPP	TTP	TMPP	TFPP	TCPP	TNPP	TBPP	TPyP	ETIO	OEP
Silica gel	Carbon tetrachloride	2	0	5	2	0	3	10	0	1	0	1	0
	<i>m</i> -Xylene	42	8	85	87	6	97	SF ^a	8	90	0	17	39
	Benzene	54	14	97	SF	21	SF	SF	24	SF	0	21	48
	Trichloroethylene	15	2	25	21	0	33	59	0	17	0	4	8
	1,2-Dichloroethane	97	4	SF	SF	66	SF	SF	78	SF	0	40	64
Cellulose	Hexane	25	9	21	14	0	5	7	0	0	0	16	24
	Cyclohexane	39	11	43	34	0	8	18	0	0	0	14	32
	Methylcyclohexane	—	14	52	39	—	—	38	—	—	0	23	37
	Carbon tetrachloride	SF	64	SF	SF	75	87	96	7	84	0	92	SF
NH ₂ -silica	Methylcyclohexane	—	0	3	3	—	—	3	—	—	0	2	4
	Carbon tetrachloride	15	13	53	57	6	51	67	0	24	0	32	48
	<i>m</i> -Xylene	55	52	91	97	41	97	SF	23	86	0	79	91
	Trichloroethylene	43	57	93	98	43	95	SF	17	88	0	82	94
	Carbon disulphide	12	5	27	24	0	22	43	0	9	0	8	11
	Benzene	74	72	SF	SF	82	SF	SF	59	SF	0	92	SF
ODS	Methanol	42	11	10	7	13	20	5	47	3	0	10	12
	Ethanol	57	19	44	35	36	60	39	80	26	0	26	33
	1-Propanol	55	23	63	63	66	72	60	92	49	0	69	76
	1-Butanol	64	48	86	98	76	91	82	SF	81	0	95	SF
	Acetone	94	78	81	75	91	90	78	97	80	0	76	77
	Acetonitrile	42	7	10	10	19	17	4	42	2	0	2	2
	Ethyl acetate	SF	SF	SF	SF	SF	SF	SF	SF	SF	0	91	95
	DMF	90	82	75	61	83	80	72	89	76	89	63	44

^a SF = Moved with the solvent front.

Silica gel plate

With an identical solvent, H_2P generally has a larger R_M value than corresponding $Cu(P)$; an example of the comparison of the R_M values is shown in Fig. 2. This implies that the chelation of the nitrogen atoms in the porphyrin nucleus with a copper ion weakens the interaction between the porphyrin nucleus and the active sites (presumably silanol groups) on the surface of the silica gel.

In both series of H_2P and $Cu(P)$ with *meso*-substituted porphyrin structures, the mobility tends to decrease in the order of porphyrin ligands $TPP > POR > TMP > TPyP$, which means that the adsorption increases in the reverse of this order of the porphyrins.

In the H_2TPP molecule, four phenyl groups are bonded with four *meso*-carbons in the porphyrin nucleus, with rotation out of the porphyrin plane by more than 60° [15]. Such a steric configuration of

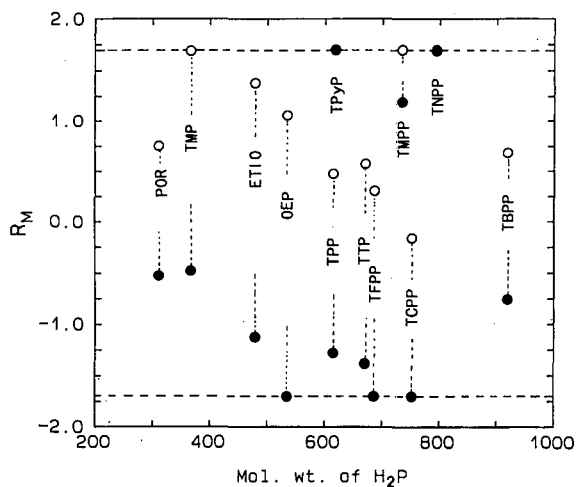


Fig. 2. R_M values of (○) H_2P and (●) $Cu(P)$ on a silica gel plate with trichloroethylene. The broken line indicates $R_M = -1.7$ or 1.7.

TABLE II

 $R_f \times 100$ VALUES OF Cu(P)

Plate	Solvent	$R_f \times 100$											
		POR	TMP	TPP	TTP	TMPP	TFPP	TCPP	TNPP	TBPP	TPyP	ETIO	OEP
Silica gel	Cyclohexane	4	0	0	0	0	0	0	0	0	0	1	2
	Carbon tetrachloride	37	18	44	42	0	54	77	0	18	0	25	50
	<i>m</i> -Xylene	93	88	SF ^a	SF	32	SF	SF	24	SF	0	SF	SF
	Toluene	—	87	SF	SF	—	—	SF	—	—	0	SF	SF
	Trichloroethylene	77	75	95	96	6	SF	SF	2	85	0	93	SF
Cellulose	Hexane	35	13	24	22	0	6	4	0	0	0	18	32
	Cyclohexane	47	19	44	43	3	9	12	2	0	0	21	41
	Methylcyclohexane	—	27	60	60	—	—	24	—	—	0	26	54
	Carbon tetrachloride	SF	95	SF	SF	80	82	94	11	87	0	97	SF
NH ₂ -silica	Cyclohexane	4	0	4	4	0	3	5	0	0	0	4	7
	Carbon tetrachloride	43	53	76	82	16	77	88	0	49	0	76	88
	<i>m</i> -Xylene	82	84	98	SF	64	SF	SF	32	95	0	SF	SF
	Trichloroethylene	80	88	SF	SF	64	SF	SF	26	SF	0	SF	SF
	Carbon disulphide	52	54	80	84	8	69	91	0	48	0	70	79
ODS	Methanol	17	5	5	4	7	10	4	34	0	0	2	3
	Ethanol	32	10	28	21	31	43	20	70	15	0	12	20
	1-Propanol	36	16	47	44	54	63	51	85	36	0	26	41
	1-Butanol	45	25	67	64	75	81	70	SF	58	0	42	60
	Acetone	79	59	72	64	75	81	70	SF	58	0	42	60
	Acetonitrile	19	7	3	0	5	6	0	25	0	0	4	4
	Ethyl acetate	89	74	SF	98	SF	SF	SF	SF	SF	0	85	91
	DMF	91	77	73	55	84	77	68	88	53	87	50	40

^a SF = Moved with the solvent front.

phenyl groups presumably increases the distance separating the porphyrin plane from the silica gel surface. The bulky phenyl moieties weaken the adsorption of H₂TTP and Cu(TTP) compared with H₂POR and Cu(POR), respectively. With TMP, the methyl groups bonded to the porphyrin nucleus are relatively compact so that the groups interfere little with the interaction between the porphyrin nucleus and the silica gel surface. The enhancement of charge density localization in the porphyrin nucleus due to the bonding of electron-donating methyl groups with the porphyrin nucleus is regarded as one of the factors contributing to the stronger adsorption of H₂TMP than H₂POR and also Cu(TMP) than Cu(POR). H₂TPyP and Cu(TPyP) were adsorbed so strongly that they hardly migrated from the origin with a variety of solvents. Strong interaction between pyridyl group(s) [basic nitrogen atom(s) in particular] and acidic silanol group(s) on the surface of silica gel is suggested as the reason.

In the series of *meso*-tetrakis(*para*-substituted-phenyl)porphyrins and also of their copper complexes, the mobility tends to decrease in the order of porphyrin ligands TCPP > TFPP > TTP ≥ TTP > TBPP > TMPP > TNPP, although some irregularities are found with different solvents. A few examples of the plots of R_M versus the Hammett constant σ_p of the substituent group [16] bonded to the *para*-position of the phenyl moiety of such a porphyrin are shown in Fig. 3.

Fig. 3 shows that the adsorption of both H₂P and Cu(P) tends to be weakened, approximately in proportion to the increase in the electron-withdrawing ability of the substituent group, except for NO₂, bonded with the phenyl moieties of the TPP structure. It is concluded that the substituent group affects indirectly the electron density and its localization on the porphyrin nucleus interacting with the active site on the surface of silica gel. The nitro group is the most polar of the substituents of pres-

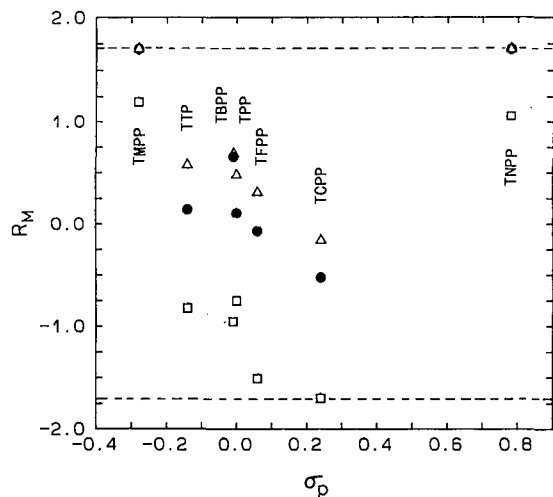


Fig. 3. Plots of the R_M of (■ and △) *para*-substituted tetraphenylporphyrines and (●) the copper complex versus the Hammett constant σ_p of the substituent. HPTLC plate: silica gel. Solvents: □ = *m*-xylene; △ = trichloroethylene; ● = carbon tetrachloride. The broken line indicates $R_M = -1.7$ or 1.7 .

ent interest, and electron resonance occurs between the nitro and phenyl groups. The strong adsorption of H_2TNPP and $Cu(TNPP)$ on silica gel is presumably attributable to the direct interaction of the nitro group with the active sites on the surface of silica gel in addition to the interaction between the porphyrin nucleus and silica gel.

In the series of alkylated porphyrins, such as H_2TMP , H_2ETIO and H_2OEP , and also of their copper complexes, the mobility tends to increase with increase in the bulk of the alkyl moieties of the porphyrin molecule.

Cellulose plate

The mobilities of both H_2P and $Cu(P)$ on a cellulose plate were larger, in most instances, than those on both silica gel and NH_2 -silica plates with an identical solvent. H_2TPyP and $Cu(TPyP)$ were so strongly adsorbed on cellulose that they did not leave the origin with any of the solvents tested. The mobility of a H_2P was smaller than that of $Cu(P)$ with an identical solvent.

NH_2 -silica plate

The chromatographic migration characteristics of H_2P and $Cu(P)$ on an NH_2 -silica plate are similar

to those found on both silica gel and cellulose in the following respects: (1) the mobility of H_2P is smaller than that of $Cu(P)$ with an identical solvent; (2) the mobilities of H_2TNPP and H_2TMPP are smaller than those of other *para*-substituted tetraphenylporphyrines, and analogous mobility trends are found with their copper complexes; (3) both H_2TPyP and $Cu(TPyP)$ are adsorbed so strongly that they hardly move with any of the solvents tested; (4) the mobility of alkylated porphyrins increases with increasing the bulk of the alkyl substituent group, *i.e.*, $TMP < ETIO < OEP$. Fig. 4 shows typical mobility trends for H_2P and $Cu(P)$ on an NH_2 -silica plate.

The mobility of H_2P on an NH_2 -silica plate was between those on silica gel and cellulose plates with an identical solvent, and similar mobility trends were found also for $Cu(P)$.

ODS plate

The mobility of H_2P was larger than that of the corresponding $Cu(P)$ with an identical solvent. TPP analogues substituted with polar groups, such as methoxy [H_2TMPP and $Cu(TMPP)$] and nitro [H_2TNPP and $Cu(TNPP)$], showed larger mobilities than the parent compounds [H_2TTP and $Cu(TTP)$]. These migration trends are the reverse of those found on polar adsorbents, such as silica gel, cellulose and NH_2 -silica.

The migration sequences of the different H_2Ps

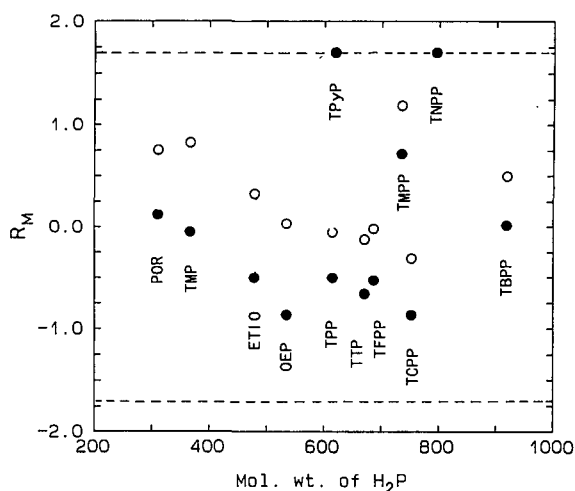


Fig. 4. R_M values of (○) H_2P and (●) $Cu(P)$ on an NH_2 -silica plate with carbon tetrachloride. The broken line indicates $R_M = -1.7$ or 1.7 .

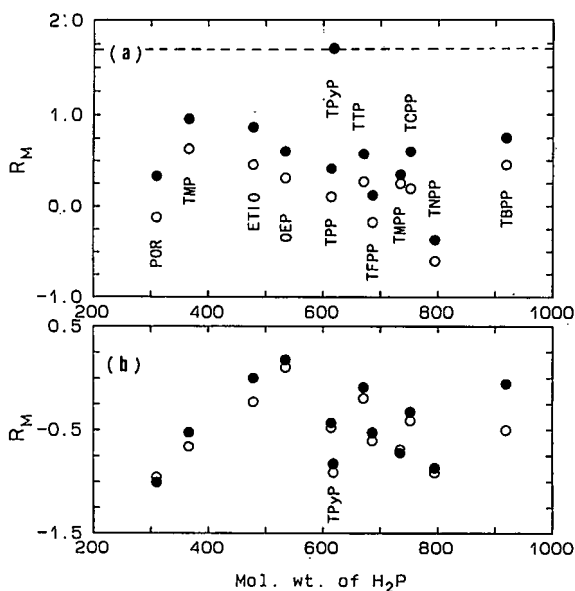


Fig. 5. R_M values of (O) H_2P and (●) $Cu(P)$ on an ODS plate with (a) ethanol and (b) DMF. The broken line indicates $R_M = 1.7$.

and also of the $Cu(P)$ s depended on the solvent used. The mobility trends for porphyrins observed with ethanol and dimethylformamide (DMF) are compared in Fig. 5. It is noted that both H_2TPyP and $Cu(TPyP)$ do not leave the origin with various polar solvents, whereas they can migrate close to $R_F = 0.9$ with DMF.

The dependence of the mobility trend of alkylated porphyrins on the solvent is complicated. The increasing orders of mobility are as follows: $H_2ETIO \approx H_2TMP \approx H_2OEP$ in methanol; $H_2TMP < H_2ETIO < H_2OEP$ in alcohols, such as ethanol, 1-propanol and 1-butanol; $H_2ETIO \approx H_2OEP < H_2TMP$ in aprotic solvents such as acetone, ethyl acetate and acetonitrile; and $H_2OEP < H_2ETIO < H_2TMP$ in DMF. Further, the mobility order $Cu(TMP) < Cu(ETIO) < Cu(OEP)$ is found with acetone, ethyl acetate and alcohols other than methanol, whereas the reverse order occurs with DMF. Solvent effects on the dimerization or aggregation of alkylated porphyrins, the solvation of the alkyl moiety of ODS and the interaction with unalkylated sites on the surface of ODS are possible reasons, but not clear evidence sufficient for an explanation has yet been obtained.

CONCLUSIONS

It has been confirmed that the mobilities of H_2Ps and $Cu(P)$ s depend considerably on the thin-layer adsorbent and on the developing solvent used. Each porphyrin always has a smaller mobility than its copper complex on the HPTLC plates coated with polar adsorbents, such as silica gel, cellulose and NH_2 -silica, whereas the reverse tendency occurs on an ODS plate. Both H_2TPyP and $Cu(TPyP)$ show small mobilities on all the HPTLC plates tested with different solvents, whereas they show specifically large mobilities with the combination of an ODS plate and DMF.

The difference in mobilities between H_2Ps and $Cu(P)$ s on a silica gel plate is greater than those observed on other plates. Accordingly, silica gel is recommended as an effective adsorbent for the HPTLC separation of a $Cu(P)$ from the corresponding H_2P . For the separation of porphyrins or their copper complexes, the most effective combination of the adsorbent and solvent should be chosen according to the compounds to be separated. The migration behaviour of alkylated porphyrins on an ODS plate in particular depends considerably on the solvent used.

ACKNOWLEDGEMENT

This study was supported by a Grant-in-Aid for Scientific Research from the Ministry of Education, Science and Culture.

REFERENCES

- 1 J.-H. Fuhrhop and K. M. Smith, in K. M. Smith (Editor), *Porphyrins and Metalloporphyrins*, Elsevier, Amsterdam, 1975, pp. 858-859.
- 2 W. I. White, R. C. Bachmann and B. F. Burnham, in D. Dolphin (Editor), *The Porphyrins*, Vol. I, Academic Press, New York, 1978, pp. 553-576.
- 3 K. Saitoh, M. Kobayashi and N. Suzuki, *Anal. Chem.*, 53 (1981) 2309.
- 4 N. Suzuki, K. Saitoh and Y. Shibata, *J. Chromatogr.*, 504 (1990) 179.
- 5 M. Kobayashi, K. Saitoh and N. Suzuki, *Chromatographia*, 20 (1985) 49.
- 6 S. Miyake, K. Saitoh and N. Suzuki, *Chromatographia*, 20 (1985) 417.
- 7 Y. Wakui, K. Saitoh and N. Suzuki, *Chromatographia*, 22 (1986) 160.

- 8 N. Suzuki, K. Saitoh and Y. Sugiyama, *Chromatographia*, 21 (1986) 509.
- 9 K. Adachi, K. Saitoh and N. Suzuki, *J. Chromatogr.*, 457 (1988) 99.
- 10 I. Tabushi, K. Sakai, K. Yamamura, *Tetrahedron Lett.*, 21 (1978) 1821.
- 11 E. B. Fleischer, *Inorg. Chem.*, 1 (1962) 493.
- 12 A. D. Adler, F. R. Longo, J. D. Finavelli, J. Goldmacher, J. Assour and L. Korsakoff, *J. Org. Chem.*, 32 (1967) 476.
- 13 G. H. Barnett, M. F. Hudson and K. M. Smith, *J. Chem. Soc., Perkin Trans. 1*, (1975) 1401.
- 14 J. W. Buchler, in K. M. Smith (Editor), *Porphyrins and Metalloporphyrins*, Elsevier, Amsterdam, 1975, pp. 182–184.
- 15 S. J. Silvers and A. Tulinsky, *J. Am. Chem. Soc.*, 89 (1967) 3331.
- 16 D. D. Perrin, B. Dempsey and E. P. Serjeant, *pK_a Prediction for Organic Acids and Bases*, Chapman and Hall, London, 1981, pp. 109–126.

Identification and determination of mellein in cultures of the fungus *Septoria nodorum* (Berk.) by thin-layer and high-performance liquid chromatography

Jutta Sachse

Swiss Federal Research Station for Agronomy, Reckenholz, CH-8046 Zurich (Switzerland)

(First received December 10th, 1991; revised manuscript received May 19th, 1992)

ABSTRACT

In order to select *in vitro* wheat embryos with a high level of resistance to the fungal pathogen *Septoria nodorum* (Berk.), extracts from *Septoria* cultures grown on infected wheat grains were prepared. One of their toxins, mellein, was identified by thin-layer chromatography and its content determined by high-performance liquid chromatography using UV light and fluorescence detection. Synthetic (\pm)mellein was used as standard. We investigated two techniques of *Septoria* cultivation, different methods of mellein extraction and the stability of the extracted mellein. In these experiments, the content of mellein in fresh fungal cultures amounted to 46 mg/kg, but in the dry material only 21 mg per kg of dry matter were recoverable.

INTRODUCTION

Fungal infection is a cause of significant yield losses in grain crops. The fungus *Septoria nodorum*, a prominent wheat parasite [1,2], retards germination and growth of seeds and young plants and suppresses carbon dioxide assimilation [3–7]. A high level of resistance to this pathogen is, therefore, an important selection criterion for wheat breeders. Because determination of resistance using traditional techniques is a lengthy process, the development of *in vitro* methods to test embryos or plant tissues using extracts of *Septoria* cultures or of one of its identified toxins was undertaken.

Previously, we have tested extracts from infected wheat plantlets, prepared by the Kietreiber test method [8]. The extracts were separated using thin-layer chromatography (TLC) [7] and the biological activity of some of the bands visible with UV light

was examined. We could confirm growth suppression of coleoptiles and roots of germinating wheat grains.

For our biological assays, a pure fungus toxin with a known content in *Septoria* cultures is necessary as a standard. Since none of the *Septoria* toxins was commercially available, mellein (3,4-dihydro-8-hydroxy-3-methylisocoumarin), which is well known and synthesizable, was chosen. For the identification and determination of mellein, we decided to use TLC and high-performance liquid chromatography (HPLC), respectively, an elegant alternative to biological tests for determining the content of numerous mycotoxins. This technique has been used particularly for the isolation and purification of mycotoxins needed for tests on plant material. As yet, no determinations of *Septoria* toxins by HPLC have been reported in the literature. However, there is one publication on the determination of mellein and other toxins in filtrate cultures of *Aspergillus ochraceus* [9]. Filtrates of cultures contain fewer interfering substances than extracts from wheat grains infected with *S. nodorum*. Therefore,

Correspondence to: Dr. J. Sachse, Swiss Federal Research Station for Agronomy, Reckenholz, CH-8046 Zurich, Switzerland.

we first had to develop a method suited to our research; this is the subject of this paper.

EXPERIMENTAL

Cultivation of S. nodorum on wheat grains

Two procedures were used for the cultivation of *S. nodorum*:

(a) According to Fried [10], yielding a brown, finely crushed, dry powder (cultivation *a*).

(b) According to Kietreiber [8], consisting of fungus grown on grains germinating on a substrate of wet filter paper (cultivation *b*).

Extraction

(a) A 30-g aliquot of dry powder (water content 12.75%) was extracted for at least 8 h (or preferably overnight) with 450 ml of ethyl acetate in a Soxhlet apparatus. For the biological test, 100 g of the powder must be extracted and processed. It may be necessary first to remove lipids from the material by extraction with petroleum ether (b.p. 40/70°C) for 3 h.

(b) The wet grains and the filter paper from two dishes were cut into pieces of approximately 1 cm², crushed in a mortar and extracted in a Soxhlet apparatus.

The extracts were concentrated under vacuum at 50°C to an oily consistency. Residues of ethyl acetate, free acetic acid and oxygen were removed with a stream of nitrogen. The concentrated extract was then flushed with ethyl acetate into a 25- or 100-ml measuring flask, depending on the amount of the extracted material. If necessary, the solution was diluted prior to measurement.

Identification of mellein

Thin-layer chromatography. As a standard, (\pm) mellein, synthesized by Fluka (Buchs, Switzerland) (m.p. 38–40°C) was used. It had a purity of 98% (gas chromatography) and absorption maxima at 246 and 314 nm in ethanol, with molar extinction coefficients of 6740 and 4350, respectively. These data correspond to those in the literature [11,12].

Thin-layer plates (10 × 20 cm) were prepared with silica gel (Art. 7731; Merck, Darmstadt, Germany) and with silica gel with fluorescence indicator (Art. 7730, Merck) as follows: 2.75 g of silica gel suspended in ethanol–water (9:1, v/v) were poured

onto the plate. The eluent was light petroleum (b.p. 40–70°C)–ethyl acetate (60:40, v/v); the R_F of 10 μ g of mellein is 0.62. For polyamide plates (10 × 20 cm), 1 g of polyamide Woelm (ICN Pharmaceuticals, Eschwege, Germany) with an addition of 0.2 g of cellulose MN 300 (Macherey–Nagel, Düren, Germany) was suspended in 6 ml of 96% ethanol and dispersed on the plate. The eluent was ethanol–water (40:60, v/v), R_F 0.38. On thin-layer plates, mellein was detected with the following spray reagents: 1 M sodium hydroxide, ammonia, ferric chloride (1% in water) and reagents according to Krebs *et al.* [13], Nos. 3, 91, 108 and 230. For two-dimensional TLC, 20 × 20 cm plates were used with twice the amount of the sorbents mentioned above and the same eluents.

High-performance liquid chromatography. The experimental conditions for mellein determination were as follows: pump series 3B; UV detector LC 75 with autocontrol, 246 nm, 16 a.u.f.s.; fluorescence detector LS-3B, excitation 326 nm, emission 458 nm (Perkin-Elmer, Norwalk, CT, USA); sample injector 7125 with 20- μ l loop (Rheodyne, Cotati, CA, USA); recorder W + W 320 (Scientific Instruments, Münchenstein, Switzerland); integrator 4290 (Spectra-Physics, San Jose, CA, USA); column ODS Hypersil 5 μ m, 250 × 4 mm I.D. (Hewlett-Packard, Corvallis, OR, USA); eluent acetonitrile (Merck Art. 14291), double-distilled water (proportions below), Fontavapor 285 (Büchi Laboratoriums-Technik, Flawil, Switzerland), flow-rate 1 ml/min, chart speed 10 cm/h.

A 0.5- μ g aliquot of pure mellein was eluted by acetonitrile–water (80:20, v/v) in 3 min. However, for its detection in the above-mentioned extracts, an acetonitrile–water ratio of 30:70 (v/v) was necessary. Its retention time in this case amounts to 21 min (see Fig. 1). Prior to injection, the extracts were filtered through a 0.5- μ m filter FHL P 01300 (Millipore, Bedford, MA, USA). The mellein peak is identified in four ways: by comparison with an extract from non-infected wheat grains, by addition of pure mellein to an extract, by recording the absorption spectrum with the UV detector and the autocontrol and fluorescence detection.

Determination of mellein content

A plot of the extinction at 246 nm of 10–50 μ g of mellein per ml of ethanol results in a straight line.

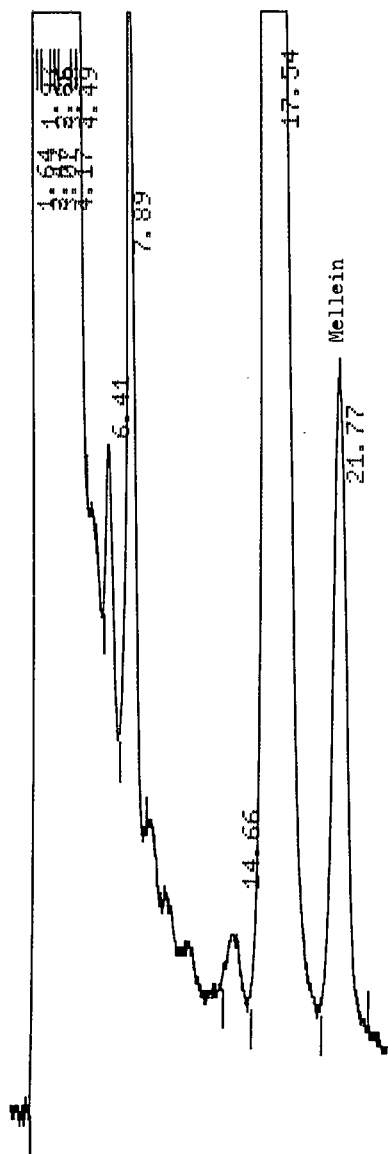


Fig. 1. HPLC of a *Septoria* extract from cultivation *a*. A 100-g aliquot of powder extracted 15 h according to Soxhlet. The concentrate was dissolved in 50 ml of ethyl acetate and diluted 1:10. Detection by fluorescence. For chromatographic conditions, see the Experimental section. Numbers at peaks indicate retention times in min.

But in this investigation, the more intensive and specific fluorescence was preferred. Here, a linear response is obtained between 0.01 and 1 μg of mellein per ml of ethanol. The detection limit was 5 ng

at a signal-to-noise ratio of 2. As the external standard 0.2 μg of mellein was chosen for peak integration.

RESULTS AND DISCUSSION

For mellein extraction, ethyl acetate is superior to more polar and non-polar solvents. An extractant with a boiling point above 75°C and a medium polarity is indicated. Under such conditions, the sample must be extracted in a Soxhlet apparatus for at least 8 h, or preferably overnight. Prior extraction with petroleum ether does not cause a loss of mellein. Extraction by stirring at room temperature or at 50°C gives significantly smaller mellein yields from cultivation *a*. The isolation of mellein from fungal cultures on wheat grains depends on their consistency. Extraction is more difficult from the powder obtained by cultivation method *a* than from the wet material of method *b*. Stirring the latter at room temperature for 4 h yields more mellein than a Soxhlet procedure of equal duration. The result is different when the material is carefully dried in a desiccator before extraction. Then, despite grinding, mellein from the fungus culture *b* is less easily extracted. This is apparently because of shrinking of the grains, resulting in a stronger bond or destruction of the toxin (Table I).

The detection, identification and determination of mellein by TLC and HPLC is more handicapped by interference by other substances—possibly resulting from oxidation during the drying process—when cultivation *a* is used. Thus, for this material, it is necessary to carry out a two-dimensional TLC in the same eluent or to use silica gel plates 35 cm long. With cultivation *b* there are fewer problems with both techniques.

The quick technique of TLC was used for preliminary investigations of the possible occurrence of mellein. To date, only the unspecific reagent ferric chloride has been applied to detect mellein on thin-layer plates. We were interested in identifying mellein with a higher degree of certainty using different colour reactions. On thin-layer plates mellein is visible as a white-blue spot under long-wave UV light and it quenches the fluorescence on plates with a fluorescence indicator. With ammonia, it appears cornflower blue; with ferric chloride violet-red; with Echtblausalz B No. 91 [13] brown-orange; with

TABLE I

CONTENT OF MELLEIN IN FUNGUS CULTURES OF *SEPTORIA NODORUM* (BERK.), CULTIVATED ON WHEAT GRAINS (mg PER kg OF DRY MATTER)

The values are the results of 2–4 total analyses.

Extraction procedure and duration	Cultivation <i>a</i>		Cultivation <i>b</i> with filter paper ^a				
	Sample amount (g)	Dried and ground	Sample amount (g)	Wet and crushed	Dried	Dried and ground	
Soxhlet 4 h	100	10.5	13.5 ^b	29.2		68.9 Extraneous infection	
			20.25				
	100	15.4	13.5	45.9		37.2	
			20.0				
15 h	30	20.4	6.75				
	15	20.9					
Stirring for 4 h	100	1.6	13.5	32.3	19.5	19.9	
							25°C
							50°C

^a The whole filter paper with wheat grains was cut into 1-cm² pieces before each subsequent treatment.

^b Pro plastic sheet 200 grains = 6.75 g.

aluminum chloride No. 3 [13] intensive blue. With Folin–Ciocalteus reagent No. 108 [13] a weak greyish-blue spot develops slowly. The most suitable indicator is Pauly's reagent No. 230 [13], which stains mellein yellow, like sunflowers. Such a spot changes to brown with 1 *M* sodium hydroxide solution. Thus, mellein is detectable successively by four colour tests on the same plate: UV light, ammonia, Pauly's reagent (after drying the plate) and, finally, by sodium hydroxide solution.

The experimental conditions described for HPLC were optimal for the determination of mellein. Using methanol instead of acetonitrile as eluent, altering the acetonitrile–water proportion or the flow-rate, or substituting the ODS Hypersil column by a LiChrospher RP-18 did not improve the separation of mellein from the other substances in the crude extract.

Mellein is most stable in concentrated oily extracts treated with nitrogen and stored at –20°C in the dark. Mellein is not volatile under vacuum (water-jet pump) and is thermostable. The nitrogen treatment removes ethyl acetate, free acetic acid and oxygen residues; without this treatment, only 60% of the mellein content can be determined. Half

the mellein was lost within a week when the extracts were diluted with ethyl acetate and stored in the refrigerator or at room temperature in day light or in the dark.

Using the described methods, the mellein content of the analysed material amounted to 21 mg per kg of dry matter from cultivation *a*, but 46 mg/kg from cultivation *b*. The latter material is less homogeneous; its mellein content depends on the degree of *Septoria* infection of the single grain, the fungus growth and the mellein production. The mellein content of cultivation *b* is considerably increased when the grains are infected with other fungi in addition to *Septoria* (Table I). The relative standard deviations of the determination of pure mellein, within and between extracts, are shown in Table II. Recovery tests were performed with uninfected wheat grains spiked with different amounts of mellein: 96% recovery was obtained from 20 mg of mellein per kg of wheat, 94% from 5 mg/kg and 89% from 1 mg/kg (*n* = 3; relative standard deviation 1.85, 2.46, 3.74%, respectively). The detection limit was 500 µg of mellein per kg of wheat at a signal-to-noise ratio of 2. Mellein is not detectable on heavily infected wheat grains without *Septoria*

TABLE II
PRECISION AND ACCURACY OF MELLEIN DETERMINATION

Amounts of mellein	Relative standard deviation (%) ($n = 3$)	
	Within extracts	Between extracts
Pure mellein		
50 ng per 20 μ l of ethanol	1.40	
100 ng per 20 μ l of ethanol	1.35	
200 ng per 20 μ l of ethanol	1.32	
Extracts from		
Cultivation <i>a</i>		
10 mg per kg of dry matter	2.90	5.85
15 mg per kg of dry matter	2.75	5.79
20 mg per kg of dry matter	2.67	5.70
Cultivation <i>b</i>		
20 mg per kg of dry matter	2.59	8.35
30 mg per kg of dry matter	2.55	8.10
45 mg per kg of dry matter	2.50	7.65

cultivation. This result and those in Table I show that mellein is produced in the mycelium and is destroyed to different degrees when the mycelium perishes.

REFERENCES

- 1 M. Schmiedknecht, *Nachrichtenbl. Dtsch. Pflanzenschutzd. Berlin, N.F.*, 21 (1967) 54.
- 2 Z. Eyal, A. L. Scharen, J. M. Prescott and M. van Ginkel, in G. P. Hettel (Editor), *The Septoria Diseases of Wheat: Concepts and Methods of Disease Management*, D. F. Cimmyt, Mexico, 1987.
- 3 M. Devys, J.-F. Bousquet, A. Kollmann and M. Barbier, *C. R. Acad. Sci. Paris, Ser. C*, 286 (1978) 457.
- 4 J.-F. Bousquet, H. Belhomme de Franqueville, A. Kollmann and R. Fritz, *Can. J. Bot.*, 58 (1980) 2575.
- 5 J.-F. Bousquet, M. Skajennikoff, O. Bethenod and O. Chartier, *Ann. Phytopathol.*, 9 (1977) 503.
- 6 J.-F. Bousquet, M. Skajennikoff, O. Bethenod and O. Chartier, *C. R. Acad. Sci. Paris, Ser. D*, 283 (1976) 1053.
- 7 J.-F. Bousquet and M. Skajennikoff, *Phytopath. Z.*, 80 (1974) 355.
- 8 M. Kietreiber, *Seed Sci. Technol.*, 9 (1981) 717.
- 9 I. Delgadillo, *Mycotoxin Res.*, 2 (1986) 9.
- 10 P. M. Fried, in P. M. Fried (Editor), *Septoria of Cereals, Proceedings, Third International Workshop on Septoria Diseases of Cereals*, Swiss Federal Research Station for Agronomy, Zurich-Reckenholz, 1989, p. 28.
- 11 J. Blair and G. T. Newbold, *J. Chem. Soc.*, (1955) 2871.
- 12 L. M. Harwood, *J. Chem. Soc., Chem. Commun.*, (1982) 1120.
- 13 K. G. Krebs, D. Heusser and H. Wimmer, in E. Stahl (Editor), *Dünnschichtchromatographie*, Springer, Berlin, Heidelberg, New York, 1967, p. 813.

Critical thin-layer chromatography as a novel method for the determination of the molecular weight and compositional inhomogeneity of block copolymers

B. G. Belenkii, E. S. Gankina, V. N. Zgonnik, I. I. Malchova and E. U. Melenevskaya

Institute for Analytical Instrumentation, Russian Academy of Sciences, Rijsky Prospect 26, 198103 St. Petersburg (Russia)

(First received September 9th, 1991; revised manuscript received March 5th, 1992)

ABSTRACT

The mechanism of the fractionation of two-block AB copolymers (BC), consisting of polystyrene (PS) as block A and poly(*tert.*-butyl methacrylate) (PtBMA) as block B, was studied by thin-layer chromatography (TLC). It is shown that under the critical conditions for TLC [critical TLC (CTLC)], the PS blocks of BC are fractionated by the mechanism of exclusion TLC (ETLC) of the PS block (whereas the PtBMA block of BC is chromatographically invisible) and the PtBMA blocks of BC are fractionated by ETLC of the PtBMA block (whereas the PS block of BC is chromatographically invisible). The molecular weights (MW) of BC were determined by the ETLC method and those of PS and PtBMA blocks under the conditions of CTLC (PtBMA)–ETLC (PS) and CTLC (PS)–ETLC (PtBMA). The calculated compositions of the analysed BC correspond to the data calculated from the kinetics of copolymerization and micro-column exclusion chromatography.

INTRODUCTION

The molecular weight distribution (MWD) and compositional inhomogeneity (CI) of block copolymers (BC) are the main characteristics that disclose the synthesis mechanism and make it possible to predict their properties.

The analysis of the CI of BC is considered in many investigations in which classical and chromatographic methods of fractionation have been used (for reviews see refs. 1–3).

When BC exhibit complex heterogeneity (with respect to MWD and CI), the only method for their reliable analysis is based on cross-fractionation [1]. When the compositional distribution of BC is narrow, their MWD may be determined relatively precisely by using one-dimensional fractionation, *e.g.*, by using dual-detector exclusion chromatography

(with continuous determination of the fractional composition) [4].

The chromatographic cross-fractionation of BC may be carried out most effectively by using chromatography under critical conditions, which is the most selective type of polymer chromatography. On the basis of modern concepts of the theory of critical phenomena in the adsorption of macromolecules on porous adsorbents, a theory of liquid chromatography of polymers has been developed in recent years. This theory shows that exclusion (EC) and adsorption (AC) chromatography are separated from each other at a critical point at which the first-order phase transition takes place with a distribution coefficient $K_d = 1$ and the macromolecules pass from the adsorbed state into solution with a very slight change in eluent composition or temperature [5–9]. It has been shown theoretically [10,11] that conditions of critical chromatography (CC) exist under which heteropolymers (copolymers and functional oligomers) can differ only in the size (molecular weight, MW) of one of the components,

Correspondence to: B. G. Belenkii, Institute for Analytical Instrumentation, Russian Academy of Sciences, Rijsky Prospect 26, 198103 St. Petersburg, Russia.

whereas the second component is under the critical conditions and is chromatographically “invisible”, *i.e.*, it is in the state in which its K_d is independent of MW. As applied to BC, CC may be used for separation according to the size (MW) of one of the blocks (chromatographically “visible”). The fractions obtained may be characterized according to the MWD with the aid of other chromatographic methods, *e.g.*, EC, which makes it possible to obtain a complete picture of BC heterogeneity (MWD and CI).

THEORETICAL

We shall now consider some theoretical aspects of BC chromatography. The composition of a two-block AB copolymer will be characterized by the fraction of component A:

$$\xi_A = \frac{N_A}{N_A + N_B} \quad (1)$$

where N is the unit number. Let us assume that the units of the B type are “tacky”, *i.e.*, they are adsorbed on the pore surface, whereas those of the A type are adsorptionally inactive and, hence, are in the pore volume. The theory shows that at a fixed interaction energy between BC segments and the adsorbing surface, $-\varepsilon_A$ and $-\varepsilon_B$ in kT units (where k is Boltzmann’s constant and T is the temperature in kelvin), a critical BC composition, ξ_A^{cr} , exists at which all chains with $\xi_A < \xi_A^{cr}$ are adsorbed and all chains with $\xi_A > \xi_A^{cr}$ are in solution (in the mobile phase). In this instance the change in the Gibbs energy of BC with $\xi_A = \xi_A^{cr}$ (in kT units), $-\Delta G_{BC}$, is equal to zero. Under these conditions, the distribution coefficient of the macromolecule is $K_d = \exp(-\Delta G) = 1$. The result of the change in $-\Delta G$ in chromatography is the chromatographic mobility, R_F :

$$R_F = \frac{1}{1 + (V_p/V_o)\exp(-\Delta G)} \quad (2)$$

where V_p and V_o are the pore and the interparticle volumes, respectively, of the sorbent.

Fig. 1 shows the dependence of the Gibbs energy, $-\Delta G_{BC}$, of adsorption of BC that contain B blocks with the same dimensions ($MW_B = \text{constant}$) on the interaction energy (in kT units) with the surface of the segments of the more “tacky” block B, $-\varepsilon_B$

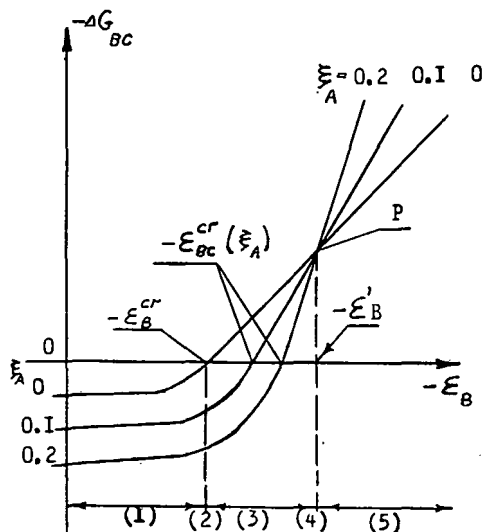


Fig. 1. Gibbs energy of BC adsorption ($-\Delta G_{BC}$) versus energy of interaction of a segment of block B with the adsorbent surface ($-\varepsilon_B$).

($-\varepsilon_B > -\varepsilon_A$). BC differ in composition ξ_A (block A size). The curve for $\xi_A = 0$ corresponds to the homopolymer B, and the curves for $\xi = 0.1$ and $\xi_A = 0.2$ correspond to BC for which the MW of block A is 10% and 20% of that of block B, respectively. When $-\varepsilon_B$ is increased (by decreasing the displacer content in the eluent), the following successive chromatographic conditions may be distinguished (they are characterized in Fig. 1 by figures in parentheses):

(1) Exclusion chromatography of BC ($-\varepsilon_B < -\varepsilon_B^{cr}$) with exclusion separation of BC according to the size of the macromolecule (proportional to $MW_{BC} = MW_A + MW_B$).

(2) Critical chromatography of block B ($-\varepsilon_B = -\varepsilon_B^{cr}$) with exclusion separation of BC according to the size MW of block A (block B is chromatographically “invisible”^a).

^a The conditions of pre-critical (PTLC) and near-critical (NTLC) TLC of block B [around point (2): $-\varepsilon_B = -\varepsilon_B^{cr}$] could also be distinguished but they are not of interest from the analytical standpoint. The purpose of the present work was to carry out experimentally all the above chromatographic regimes of TLC and to apply these TLC variants to the determination of the polydispersity of the PS-PtBMA [polystyrene-poly(*tert.*-butyl methacrylate)] block copolymers.

(3) Pre-critical chromatography of block A ($-\varepsilon_B^{Cr} < -\varepsilon_B < -\varepsilon_B'$), where $-\varepsilon_B'$ is the energy that corresponds to eluent composition critical for block A ($-\varepsilon_A = -\varepsilon_A^{Cr}$). In this instance adsorption separation of block B according to length occurs with the exclusion effect for block A (with increasing MW_A the value of $-\Delta G_{BC}$ decreases and the R_F value of BC increases).

(4) Critical chromatography of block A ($-\varepsilon_A = -\varepsilon_A^{Cr}$ at $-\varepsilon_B > -\varepsilon_B^{Cr}$). In this instance the BC curves with different ξ_A intersect at point P, at which only adsorption separation according to the length of block B can occur (block A is chromatographically “invisible”).

(5) Near-critical chromatography of block A ($-\varepsilon_A > -\varepsilon_A^{Cr}$, $-\varepsilon_B = -\varepsilon_B'$, $-\varepsilon_B \gg -\varepsilon_B^{Cr}$). In this instance separation according to the lengths of blocks A and B (with increasing MW_A the value of $-\Delta G_{BC}$ increases and the R_F value of BC decreases).

It can be seen from Fig. 1 that if the value of $-\varepsilon_B$ is varied from $+\infty$ to $-\varepsilon_B^{Cr}$ (by increasing the displacer content in the eluent), gradual desorption of BC will occur each time when we have $-\Delta G_{BC}(\xi_A) = 0$ ($K_d = 1$) with a gradually increasing content of the “adhesive” block B (with decreasing ξ_A). The

homopolymer B is desorbed last (at the point $-\varepsilon_B = -\varepsilon_B^{Cr}$). The selectivity of this process increases with decreasing pore size of the adsorbent [10,11].

EXPERIMENTAL

Preparation of block copolymers

PS–PtBMA block copolymers of the AB type were obtained by successive anionic polymerization in an all-sealed vacuum system (10^{-6} Torr) [12–14]. The PS precursors of BC were synthesized under conditions that make it possible to obtain linear narrow-disperse homopolymers [11]. After the completion of PS polymerization with tBMA, samples were collected from the reaction system. They were reference samples of PS blocks of each BC. According to the conditions of synthesis, BC can contain homo-PS as a result of the reaction of the “living” PS chains with possible impurities in the second monomer (tMBA), but should not contain homopolymers of the methacrylic monomer (PtBMA).

The MW of the PS precursors of BC were determined by microcolumn exclusion chromatography (MEC) [15].

Table I gives the MW of PS precursors of BC, PtBMA and BC according to the data from MEC

TABLE I

MW OF BLOCK COPOLYMERS; PC PRECURSORS, PtBMA; PS AND PtBMA BLOCKS OF BC

Method of determination	MW $\times 10^{-3}$										
	Block copolymers					PS precursors of BC			PtBMA		
	BC-31	BC-21	BC-53	BC-41	BC-52	PS-30 ^a	PS-50 ^a	PS-20 ^a	1	2	3
From polymerization conditions	130	95	75	65	27	64.5	13.5	80	20	80	200
TLC	127	97	78	69	30	66	15	83	24	81	250
PS block from polymerization conditions	64.5	80	13.5	5	13.5						
TLC	60	85	11	5	11						
PtBMA block from polymerization conditions	64.5	15	60	60	13.5						
TLC	60	13	60	60	13						

^a Determined by microcolumn exclusion chromatography (MEC).

and TLC and those calculated from the polymerization conditions.

Thin-layer chromatography

TLC was carried out by using commercial plates on a glass support with KSKG silica gel (pore diameter 120 Å, 5–20- μm fraction) Reakhim (Moscow, Russia) [16] with silica sol [16] as binder, or plates prepared manually by the same procedure [16] with LiChrospher Si 300 silica gel (pore diameter 300 Å, 10- μm fraction) (Merck, Darmstadt, Germany). Prior to coating, the glass plates were washed in a dichromate–sulphuric acid mixture, then thoroughly washed with tap water and after coating they were activated at 120°C for 30 min. The samples were spotted from solutions (at a concentration of 5 mg/ml) of PS in carbon tetrachloride and of PtBMA and BC in chloroform in amounts of 2–3 μg for BC.

The plate with the samples was saturated in eluent vapour for 1 h, developed in the ascending mode in an appropriate eluent and dried in an oven at 180°C for 15–20 min. Detection was carried out by spraying the plates with a 3.3% solution of potassium permanganate in concentrated sulphuric acid with subsequent heating at 180°C for 15–20 min. The polymer zones developed as black spots on a white background.

PS standards from Waters (Milford, MA, USA) were used.

RESULTS AND DISCUSSION

Exclusion TLC. Evaluation of the MW of block copolymers, their PS pressures and PtBMA by ETLC

According to the ETLC data in methyl ethyl ketone (MEK), calibration dependences of R_F on $\log M$ were plotted for PS standards on silica gels with pore diameters of 120 Å (Si 120) and 300 Å (Si 300). These dependences were linear on silica gel Si 120 in the M range from $5 \cdot 10^3$ to $50 \cdot 10^3$ (exclusion limit $50 \cdot 10^3$) and on silica gel Si 300 in the M range from $50 \cdot 10^3$ to $500 \cdot 10^3$. By using these dependences, the MW of BC, the PS precursors of BC and PtBMA were determined with the aid of ETLC. The results are given in Table I. It is clear that the MW of BC obtained by ETLC, calculated from the polymerization conditions and obtained by the MEC are in good agreement.

Critical TLC for PtBMA–exclusion TLC for PS [CTLC(PtBMA)–ETLC(PS)]

For plates with silica gels Si 120 and Si 300, the conditions of CTLC of PtBMA (eluent composition) under which the PS samples undergo ETLC were established. Under these conditions of CTLC (PtBMA)–ETLC(PS), two pairs of BC with similar MW of the PS blocks but differing in the MW of the PtBMA blocks were chromatographed. Fig. 2 shows that on silica gel Si 120 PtBMA with different MW (points 1 and 2) have the same R_F values that

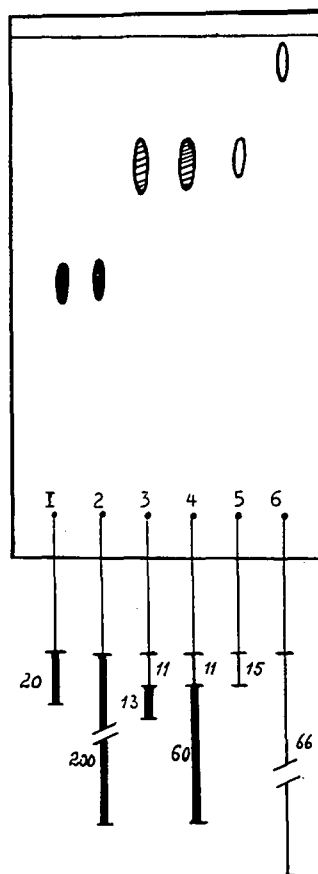


Fig. 2. CTLC(PtBMA)–ETLC(PS) on silica gel Si 120. Eluent: cyclohexane–toluene–MEK (9:1:2.3). (1,2) PtBMA with MW (1) $20 \cdot 10^3$ and (2) $200 \cdot 10^3$; (3) BC-52; (4) BC-53; (5) PS-50; (6) PS-30. Figs. 2–6 show schematically homopolymers and BC in the form of zones (open zones, PS; black zones, PtBMA; hatched zones, BC), and their compositions as lines, the length of which corresponds to the MW of polymers (figures indicate the MW of polymers and BC blocks according to TLC data): — PS; — PtBMA.

correspond to $K_d = 1$ (the proof of CTLC conditions for PtBMA). In this instance BC (points 3 and 4) with the same MW of the PS block ($13.5 \cdot 10^3$) and different MW of the PtBMA blocks ($13.5 \cdot 10^3$ and $60 \cdot 10^3$) have the same R_F values ($K_d < 1$) corresponding to the MW of the PS precursor (5) with MW $13.5 \cdot 10^3$. These results were confirmed by CTLC(PtBMA)–ELC(PS) on silica gel Si 300. In this instance BC with MW of the PS blocks equal to $64.5 \cdot 10^3$ and $80 \cdot 10^3$ and the MW of the PtBMA blocks equal to $64.5 \cdot 10^3$ and $15 \cdot 10^3$ have R_F values corresponding to those of PS precursors with MW of $64.5 \cdot 10^3$ and $80 \cdot 10^3$. These experiments showed that under the conditions of CTLC (PtBMA)–ETLC(PS) the MW of the PtBMA block does not affect the chromatographic behaviour of BC which undergo chromatography under conditions analogous to the ETLC of PS which correspond to the MW of their PS blocks. The MW of PS blocks of BC determined under the conditions of CTLC(PtBMA)–ETLC(PS) are given in Table I.

Critical TLC for PS and adsorption TLC for PtBMA

The conditions of CTLC(PS)–ATLC(PtBMA) for BC with the same MW of the PtBMA blocks correspond to point 4 in Fig. 1. However, under the CTLC conditions for PS on silica gel, even for relatively low MW PtBMA, we have $K_d \gg 1$, and the PtBMA zones remain at the start. Under these conditions, it is impossible to distinguish chromatographically BC differing in the MW of the PtBMA blocks. If pyridine, which has a high affinity for silanol hydroxyl groups, is added to the eluent, it is possible to perform dynamic modification of the silica gel, which converts it into an analogue of the phenyl silica gel. The affinity of the phenyl silica gel for PS exceeds that for PtBMA [3]. By varying the amount of pyridine, it is possible to achieve the conditions of CTLC(PS)–ATLC(PtBMA), whereas at a lower content, pre-critical TLC (PTLC) may be achieved and at a higher content near-critical TLC (NTLC) for PS and ATLC for PtBMA are achieved (Fig. 1, states 3, 4 and 5, respectively). Finally, by adding a still greater amount of pyridine to the eluent, it is possible to invert the chromatogram completely and to obtain CTLC(PS)–ETLC (PtBMA) conditions.

Conditions for CTLC(PS)–ATLC(PtBMA) and NCTLC(PS)–ATLC(PtBMA)

Figs. 3, 4 and 5 show the chromatograms corresponding to the conditions for CTLC(PS)–ATLC (PtBMA), PCTLC(PS)–ATLC(PtBMA) and NCTLC(PS)–ATLC(PtBMA), respectively, which are easily determined from the natural arrangement of the chromatographic zones of PS and BC with PS blocks of different MW. In Fig. 3 the PS zones with different MW are on the same level (CTLC of PS). Under these conditions BC with PS blocks of

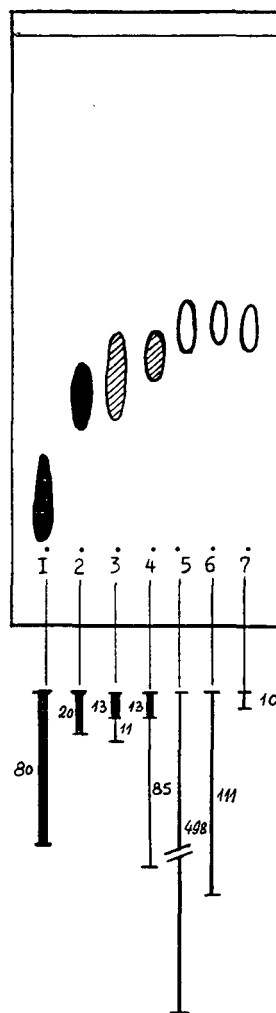


Fig. 3. CTLC(PS)–ATLC(PtBMA) on silica gel Si 120. Eluent: cyclohexane–toluene–MEK–pyridine (9:0.4:1.8:1). (1,2) PtBMA with MW (1) $80 \cdot 10^3$ and (2) $20 \cdot 10^3$; (3) BC-52; (4) BC-21; (5–7) PS with MW, (5) $498 \cdot 10^3$, (6) $111 \cdot 10^3$ and (7) $10 \cdot 10^3$.

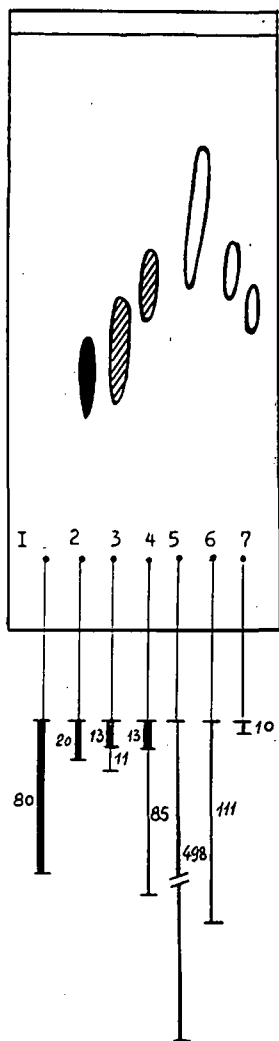


Fig. 4. PCTLC(PS)-ATLC(PtBMA) on silica gel Si 120. Eluent: cyclohexane-toluene-MEK-pyridine (9:0.4:1.7:1). For (1-7) see Fig. 3.

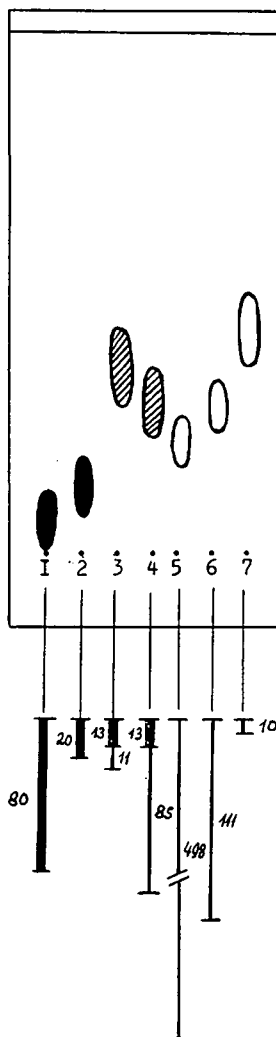


Fig. 5. NCTLC(PS)-ATLC(PtBMA) on silica gel Si 120. Eluent: cyclohexane-toluene-MEK-pyridine (9:0.4:1.3:1.2). For (1-7) see Fig. 3.

different MW and PtBMA blocks of the same MW are also on the same level (have identical R_F values). In Fig. 4 the R_F value of PS zones increases with increasing MW (PCTLC of PS). In this instance BC with the PS block of higher MW is placed higher (has a higher R_F value). Fig. 5 shows the decrease in the R_F value of PS with increasing MW because adsorption on silica gel increases (NCTLC of PS). Correspondingly, the R_F value for BC ($MW_{PtBMA} =$

constant) depends on the length of the PS block; with increasing length of this block, R_F decreases.

Critical TLC for PS-exclusion TLC for PtBMA [CTLC(PS)-ETLC(PtBMA)]

Fig. 6 shows the TLC of BC under the conditions of CTLC(PS)-ETLC(PtBMA). It is clear that PS 1 and 2 of different MW migrate at the same level (the proof of CTLC for PS). The BC pairs 3-4 and 5-6

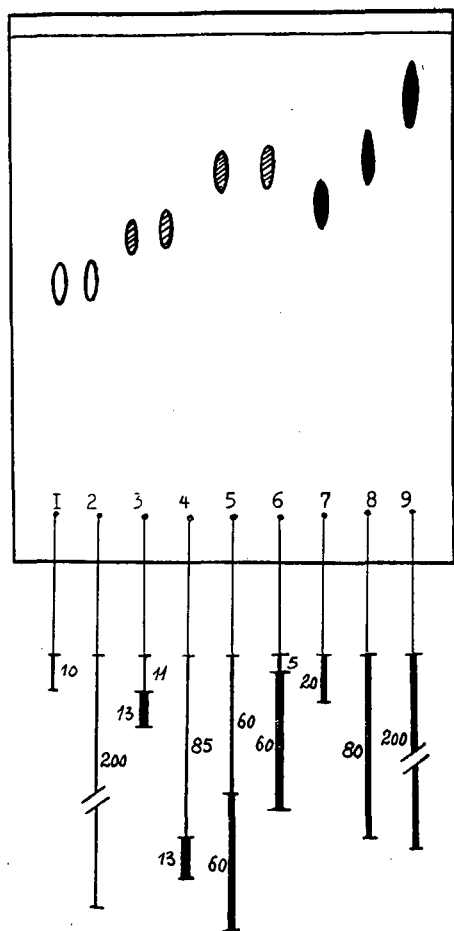


Fig. 6. CTLC(PS)-ETLC(PtBMA) on silica gel Si 300. Eluent: cyclohexane-toluene-MEK-pyridine (9:0.4:0.4:4). (1,2) PS with MW (1) $10 \cdot 10^3$ and (2) $200 \cdot 10^3$; (3) BC-52; (4) BC-21; (5) BC-31; (6) BC-41; (7-9) PtBMA with MW (7) $20 \cdot 10^3$, (8) $80 \cdot 10^3$ and (9) $200 \cdot 10^3$.

with similar MW of the PtBMA blocks ($13.5 \cdot 10^3$, $15 \cdot 10^3$ and $64.5 \cdot 10^3$, $60 \cdot 10^3$, respectively) but with different MW of the PS block have the same R_f values for each pair determined by the MW of the PtBMA blocks. This can be seen if these R_f values are compared with those for PtBMA with MW equal to $20 \cdot 10^3$ and $80 \cdot 10^3$.

Hence, in this instance the conditions of CTLC (PS)-ETLC(PtBMA) are observed, the PS block of BC is chromatographically invisible and the comparison with the ETLC of PtBMA makes it possible to evaluate the MW of the PtBMA block.

The values of MW for the investigated BC and their PS and PtBMA blocks obtained according to the TLC data (Table I) show that they are in good agreement with each other and with the data obtained from the polymerization conditions and MEC.

In many instances BC are inhomogeneous and contain homopolymer admixtures. They can be removed under the conditions of pre-critical TLC in which the impurities of a more "tacky" homopolymer are more intensively absorbed than BC (their R_f value is lower than that for BC). Homopolymer admixtures may be separated from BC by using stepwise TLC [17]. The authors separated PS from BC with the aid of ETLC on a dry plate in chloroform. Under the chosen polymerization conditions, the investigated BC did not contain homopolymer admixtures. If necessary, PtBMA may be separated from BC with the aid of precipitation TLC by using an appropriate solvent.

It may be assumed that the proposed method of analysis of composition inhomogeneity of BC is universal, and the mechanism of carrying out the analysis under the conditions described here by normal-phase and reversed-phase (with dynamic modification of the silica gel) TLC is relatively easy. A procedure for the determination of BC compositional inhomogeneity on the basis of this method may be proposed.

REFERENCES

- 1 V. A. Miagchenkov and S. Ya. Frenkel, *Compositional Inhomogeneity of Copolymers* (in Russian), Khimiya, Leningrad, 1988.
- 2 S. Mori, *J. Appl. Polym. Sci.*, 38 (1989) 95.
- 3 G. Glockner and A. H. E. Muller, *J. Appl. Polym. Sci.*, 38 (1989) 1761.
- 4 V. D. Krasikov, V. V. Nesterov, B. G. Belenkii, V. N. Zgonnik and B. L. Erusalimskii, *Vysokomol. Soedin., Ser. A*, 31 (1989) 204.
- 5 B. G. Belenkii, E. S. Gankina, M. B. Tennikov and L. Z. Vilenchik, *Dokl. Akad. Nauk SSSR*, 231 (1976) 1147.
- 6 M. B. Tennikov, P. P. Nefedov, M. A. Lazareva and S. Ya. Frenkel, *Vysokomol. Soedin., Ser. A*, 19 (1977) 657.
- 7 A. M. Skvortsov, B. G. Belenkii, E. S. Gankina and M. B. Tennikov, *Vysokomol. Soedin., Ser. A*, 20 (1978) 678.
- 8 A. A. Gorbunov and A. M. Skvortsov, *Vysokomol. Soedin., Ser. A*, 28 (1986) 2170.
- 9 S. G. Entelis, V. V. Evreinov and A. V. Gorshkov, *Adv. Polym. Sci.*, 76 (1986) 129.
- 10 A. A. Gorbunov and A. M. Skvortsov, *Vysokomol. Soedin., Ser. A*, 21 (1979) 339.

- 11 A. A. Gorbunov and A. M. Skvortsov, *Vysokomol. Soedin., Ser. A*, 30 (1988) 895.
- 12 M. A. Eremina, V. N. Erenburg, V. N. Zgonnik, E. Yu. Melenevskaya, E. P. Levingagen and R. I. Palchik, *Vysokomol. Soedin., Ser. A*, 27 (1985) 1308.
- 13 A. H. E. Muller, in T. E. Hogen Esch (Editor), *Recent Advances in Anionic Polymerization*, Elsevier, Amsterdam, 1987, p. 205.
- 14 A. H. E. Muller, *Makromol. Chem.*, 182 (1981) 2863.
- 15 B. G. Belenkii, M. S. Bello, J. J. Kever and E. M. Koroleva. *Synthesis, Structure and Properties of Polymers* (in Russian). Nauka, Leningrad, 1989, p. 253.
- 16 B. G. Belenkii, E. S. Gankina, L. S. Litvinova, I. I. Malahova, V. E. Vaskovskii, S. V. Khotimchenko and V. P. Dikarev, *Bioorg. Khim.*, 10 (1984) 244.
- 17 E. S. Gankina, I. I. Malahova, J. J. Kever and B. G. Belenkii, *Talanta*, 34 (1987) 167.

Theoretical aspects of chiral separation in capillary electrophoresis

II. The role of organic solvent

Stephen A. C. Wren and Raymond C. Rowe

Pharmaceutical Department, ICI Pharmaceuticals, Macclesfield SK10 2NA (UK)

(First received March 25th, 1992; revised manuscript received June 15th, 1992)

ABSTRACT

Previous work in chiral capillary electrophoresis has shown that the addition of methanol to the buffer can lead to either an increase or decrease in separation. This behaviour is explained by a mathematical model. The proposed model is supported by new work on the chiral separation of propranolol enantiomers using buffer systems containing methanol or acetonitrile.

INTRODUCTION

Capillary electrophoresis (CE) is a rapidly expanding separation technique which has been successfully employed in a wide range of analytical problems. One area of great promise is the field of chiral analysis. In this area separation is achieved by the use of a range of chiral selectors which are added to the buffer [1–9] or trapped in a gel matrix [10].

An interesting feature seen in several of the reports is the variation in the degree of separation of the two enantiomers as the concentration of chiral selector is varied. In particular the separation increases with chiral selector concentration until a maximum value is achieved. Further increases in chiral selector concentration result in a decline in separation. In an earlier paper we proposed a model which explains this type of behaviour [11]. This model was supported by experimental data on the separation of propranolol using β -cyclodextrin and a methyl substituted β -cyclodextrin.

In several of the reports the addition of organic solvent to the buffer was also shown to have an important effect on the separation. The reason for this has been investigated in this paper by the use of the separation model mentioned above. In addition further work on the separation of the enantiomers of propranolol involving the addition of methanol and acetonitrile to the buffer is presented.

MODEL

In a previous paper [11] a model of the chiral separation process was proposed as a working hypothesis. The model is summarised below:



where μ_1 is the electrophoretic mobility of the analyte in free solution, μ_2 is the electrophoretic mobility of the analyte chiral selector complex and K_1 and K_2 are equilibrium constants. A and B are a pair of enantiomers which have the same electrophoretic mobility in free solution. They interact with a chiral selector C dissolved in the buffer to form the enantiomer–chiral selector complexes AC and BC. If the size of the chiral selector molecule is large in comparison to that of the analyte it seems likely that AC and BC will have similar size and shape, and hence, as a first approximation, the same electrophoretic mobility. If the exchange of A between the free and bound forms is very rapid then the apparent electrophoretic mobility of A, $\bar{\mu}_a$, will be a function of the proportion of the time A is free and the time it is complexed, *i.e.*

$$\bar{\mu}_a = \frac{([A])}{([A] + [AC])}\mu_1 + \frac{([AC])}{([A] + [AC])}\mu_2 \quad (1)$$

Manipulation of eqn. 1 and a similar expression which describes the apparent electrophoretic mobility of B leads to an equation which describes the apparent mobility difference between the two enantiomers (see eqn. 2).

$$\mu = \frac{[C](\mu_1 - \mu_2)(K_2 - K_1)}{1 + [C](K_1 + K_2) + K_1K_2[C]^2} \quad (2)$$

From eqn. 2 it is clear that the apparent mobility difference will be zero if $K_1 = K_2$ or $\mu_1 = \mu_2$. In addition the apparent mobility difference will be zero if $[C] = 0$ or $[C]$ is very large. This implies that between these two extremes some value of $[C]$ will give a maximum apparent mobility difference and hence a maximum separation of the two enantiomers.

Eqn. 2 can be investigated by the substitution of some plausible values for the equilibrium constants, the electrophoretic mobilities $\mu_1 = 2 \cdot 10^{-4} \text{ cm}^2/\text{V} \cdot \text{s}$ and $\mu_2 = 1 \cdot 10^{-4} \text{ cm}^2/\text{V} \cdot \text{s}$ and a chiral selector concentration range covering the values typically seen in the literature.

Fig. 1 was generated by this procedure and shows the apparent mobility difference as a function of chiral selector concentration for three sets of equilibrium constants. In each of these sets K_2 is 10% larger than K_1 . It is clear that the optimum chiral selector concentration depends upon the size of the equilib-

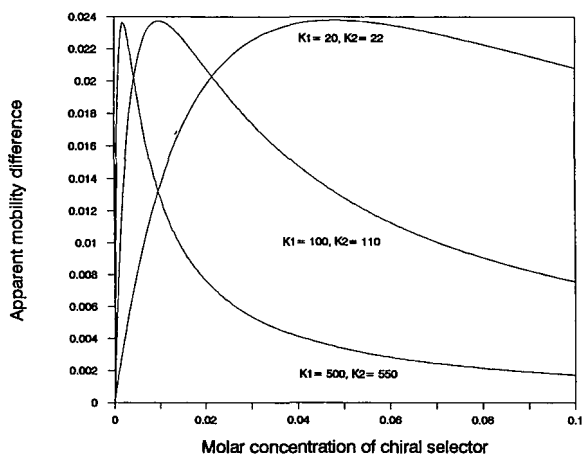


Fig. 1. Theoretical curves generated from eqn. 2 using $\mu_1 = 2 \cdot 10^{-4} \text{ cm}^2/\text{V} \cdot \text{s}$, $\mu_2 = 1 \cdot 10^{-4} \text{ cm}^2/\text{V} \cdot \text{s}$ and three sets of equilibrium constants. From ref. 11.

rium constants. The greater the affinity of the analyte for the chiral selector the lower is the optimum concentration. This means that the best chiral selector concentration for one analyte is unlikely to be the best for another.

BACKGROUND

Guttman *et al.* [10] used β -cyclodextrin in a gel matrix to separate the D and L forms of dansylated amino acids. They found that the selectivity changed when 10% of methanol was added to the buffer. For three of the amino acids the selectivity decreased whereas for the other nine it increased. The selectivity increase for the aromatic amino acids was noted in particular.

Fanali [5] used a buffer containing 40 mM of β -cyclodextrin to separate the enantiomers of the β -blocker propranolol. Methanol was added to the buffer in proportions ranging from 0 to 40%. The resolution at 0% was zero and the best value was obtained at 30%.

These two results can be examined with the aid of the proposed model.

With cyclodextrins it is assumed that the hydrophobic portion of the analyte sits inside the hydrophobic cavity. Therefore addition of methanol would be expected to reduce the affinity of the analyte for the cyclodextrin and increase it for the bulk buffer, *i.e.* to reduce the size of the equilibrium

constants K_1 and K_2 . Whether this change in equilibrium constants leads to an increase or decrease in the apparent mobility difference (and hence separation) will depend upon whether the concentration of cyclodextrin is above or below the optimum value for the original system. This can be seen from Fig. 1.

Suppose for the first case we have a buffer with a chiral selector concentration of 40 mM and equilibrium constants of $K_1 = 500$ and $K_2 = 550$. If methanol were then added such that the new equilibrium constants were now $K_1 = 100$ and $K_2 = 110$ then the apparent mobility difference, and hence separation, would increase by about a factor of three.

In the second case suppose that we have a chiral selector concentration of 10 mM and the equilibrium constants for the two enantiomers were $K_1 = 100$ and $K_2 = 110$. If then another buffer was examined which contained the same chiral selector concentration but enough methanol such that the equilibrium constants were $K_1 = 20$ and $K_2 = 22$, then the apparent mobility difference would decrease to about half of the original value leading to a decrease in separation.

According to the model, therefore, in Fanali's [5] work the addition of methanol led to an increase in the separation of propranolol enantiomers as the concentration of β -cyclodextrin was above the optimum for a methanol free buffer.

The model also predicts that the addition of methanol could also lead to the opposite result, *i.e.* a decrease in separation of the propranolol enantiomers. This would happen if the original cyclodextrin concentration was at or below the optimum value for an organic solvent free buffer.

It was therefore decided to test this prediction by the examination of the separation of the enantiomers of propranolol (1-[(1-methylethyl)amino]-3-1-naphthalenyloxy)-2-propanol in buffers which contained different amounts of methanol or acetonitrile along with 40 mM lithium phosphate and 3.7 mM "methyl"- β -cyclodextrin (MeBCD). In a previous paper [11] it was shown that 3.7 mM MeBCD was below the concentration for the optimum separation.

EXPERIMENTAL

Experiments were carried out on PACE 2100 or PACE 2000 systems (Beckman Instruments, High Wycombe, UK). The separation capillary was fused silica with an internal diameter of 75 μm , a total length of 57 cm and a length of 50 cm from inlet to the detector. The samples were loaded by a 2-s pressure injection and separated at 25°C using a voltage of 20 kV. The data were recorded at 200 nm using a 2 Hz collection rate.

Racemic propranolol was made at ICI Pharmaceuticals, and MeBCD was a gift from Waker Chemicals (Halifax, UK). The MeBCD had the 2-, 3- and 6-hydroxy groups partially substituted with methoxy ones with the average degree of substitution being 1.8.

The buffers were all 40 mM in lithium phosphate (from lithium hydroxide and orthophosphoric acid) and were prepared by mixing stock solutions of 50 mM lithium phosphate at pH 3.0; 370 mM MeBCD in water; methanol or acetonitrile; and water in the appropriate proportions. The buffers were degassed ultrasonically and filtered through 0.2 μm filters. Propranolol was dissolved in water at 0.01 mg ml^{-1} .

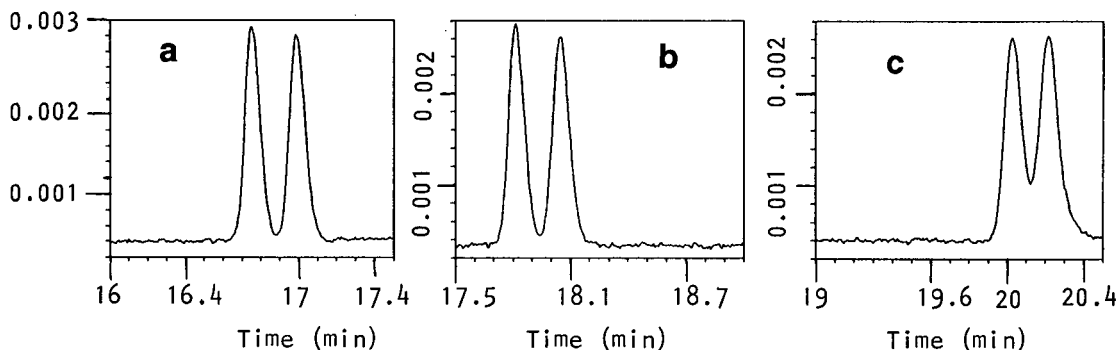


Fig. 2. The change in the separation of propranolol enantiomers with changing methanol concentration: (a) 0%, (b) 5%, (c) 19%.

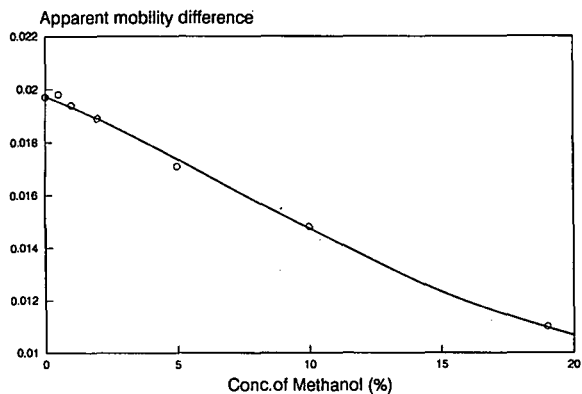


Fig. 3. The electrophoretic mobility difference ($10^{-4} \text{ cm}^2/\text{V} \cdot \text{s}$) between propranolol enantiomers as a function of methanol concentration.

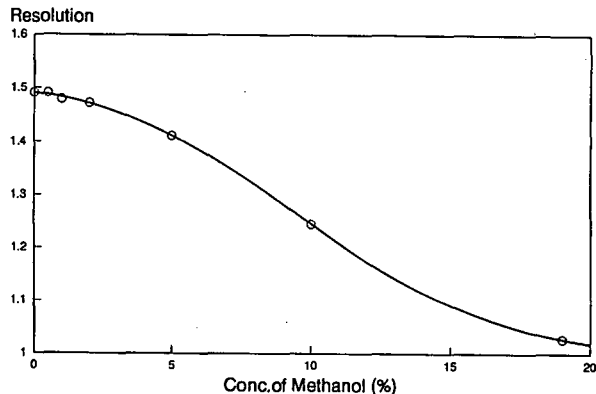


Fig. 4. The change in resolution between propranolol enantiomers as a function of methanol concentration.

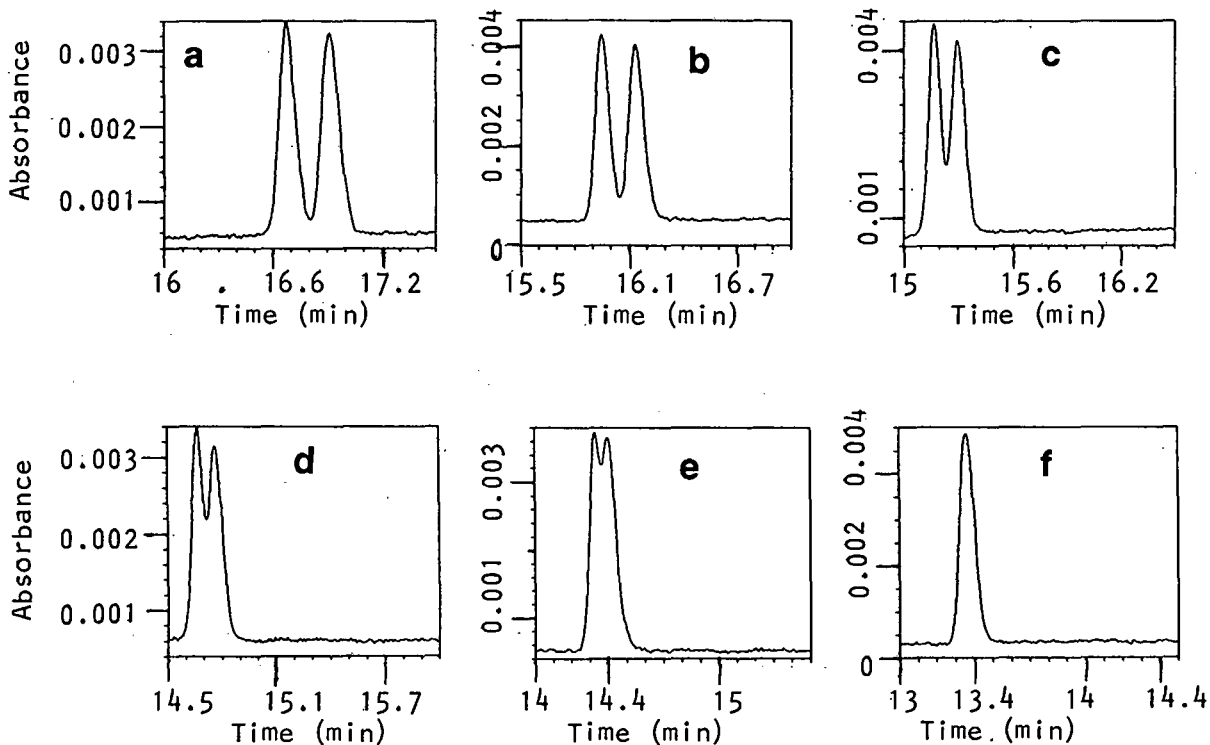


Fig. 5. The change in the separation of propranolol enantiomers with changing acetonitrile concentration: (a) 0%, (b) 2%, (c) 6%, (d) 8%, (e) 10%, (f) 15%.

Duplicate injections were made and the migration times typically varied by less than 1%.

RESULTS AND DISCUSSION

In Fig. 2 the separation at three of the seven methanol concentrations are shown. It is clear that, as expected from the proposed model, increasing the methanol content leads to a significant decline in the separation of the two propranolol enantiomers. The reason for this is the decline in apparent mobility difference. This can be seen in Fig. 3 where the measured apparent mobility difference is plotted against the methanol concentration.

The resolution (R_s) between the two propranolol enantiomers can be measured using eqn. 3.

$$R_s = 1.177 \times \frac{(t_2 - t_1)}{(W_{a\frac{1}{2}} + W_{b\frac{1}{2}})} \quad (3)$$

where t_1 = migration time of the first enantiomer and $W_{a\frac{1}{2}}$ = peak width at half height of the first enantiomer.

Fig. 4 shows how the resolution measured using eqn. 3 decreases from the baseline value of 1.5 at 0% methanol to a value of just over 1 at 19% methanol. Fig. 2 also shows that the migration times of both enantiomers increases with increasing methanol concentration.

The same experiments were also carried out using acetonitrile as the organic solvent instead of methanol. Acetonitrile is less polar than methanol and so

might be expected to bring about a larger reduction in the equilibrium constants. The results obtained at six of the seven acetonitrile concentrations are shown in Fig. 5. The trend is even more pronounced than that seen with methanol. As the acetonitrile concentration increases from 0 to 15% the resolution declines from baseline to zero. The measured apparent mobility difference is shown in Fig. 6 and from this it is clear that the loss of resolution is caused by the loss of apparent mobility difference. In contrast to the results with methanol (Fig. 2) it can be seen from Fig. 5 that the addition of acetonitrile leads to a decrease in migration times. The reason for this is probably a combination of differences in viscosity [12] and the different amounts of time spent as free propranolol and the more slowly moving propranolol–cyclodextrin complex.

CONCLUSIONS

The influence of organic solvent on separation in chiral CE has been investigated using a simple mathematical model. The model was strongly supported by new work on the separation of propranolol in buffer systems containing methanol or acetonitrile.

Further work is under way to check the applicability of this model to other chiral molecules.

REFERENCES

- 1 H. Nishi, T. Fukuyama, M. Matsuo and S. Terabe, *J. Microcolumn. Sep.*, 1 (1989) 234.
- 2 R. O. Cole, M. Sepaniak and W. L. Hinze, *J. High Resolut. Chromatogr.*, 13 (1990) 579.
- 3 K. Otsuka and S. Terabe, *J. Chromatogr.*, 515 (1990) 221.
- 4 S. Fanali, *J. Chromatogr.*, 474 (1989) 441.
- 5 S. Fanali, *J. Chromatogr.*, 545 (1991) 437.
- 6 G. Persson, S. Palmarsdottir, A. Walhagen and L. E. Edholm, presented at the 15th International Symposium on Column Liquid Chromatography, Basle, June 3–7, 1991, poster.
- 7 H. Nishi, T. Fukuyama and S. Terabe, *J. Chromatogr.*, 553 (1991) 503.
- 8 K. Otsuka, J. Kawahara, K. Tatekawa and S. Terabe, *J. Chromatogr.*, 559 (1991) 209.
- 9 J. Snopek, H. Soini, M. Novotny, E. Smolkova-Keulemansova and I. Jelinek, *J. Chromatogr.*, 559 (1991) 215.
- 10 A. Guttman, A. Paulus, A. S. Cohen, N. Grinberg and B. L. Karger, *J. Chromatogr.*, 448 (1988) 41.
- 11 S. A. C. Wren and R. C. Rowe, *J. Chromatogr.*, 603 (1992) 235.
- 12 S. J. Van der Wal, *Chromatographia*, 20 (1985) 274.

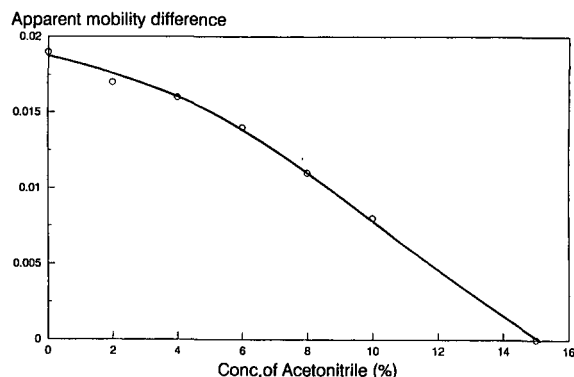


Fig. 6. The electrophoretic mobility difference ($10^{-4} \text{ cm}^2/\text{V} \cdot \text{s}$) between propranolol enantiomers as a function of acetonitrile concentration.

Effect of addition of glucose on micellar electrokinetic capillary chromatography with sodium dodecyl sulphate

Takashi Kaneta[☆], Shunitz Tanaka, Mitsuhiko Taga and Hitoshi Yoshida

Department of Chemistry, Faculty of Science, Hokkaido University, Kita-ku, Sapporo 060 (Japan)

(First received December 13th, 1991; revised manuscript received April 28th, 1992)

ABSTRACT

Glucose was investigated as a possible additive for the improvement of resolution in micellar electrokinetic capillary chromatography. Addition of glucose to the micellar solution facilitated the complete separation of a mixture of nine nucleosides by both extending the elution range and changing the selectivity. Extension of the elution range can be attributed to an increase in the electrophoretic mobility of the micelle. It is also apparent that glucose selectively reduces the distribution coefficients for solutes containing a hydrophilic functional group. This effect was valuable in the separation of some solutes with hydrophilic functional groups and large capacity factors.

INTRODUCTION

Micellar electrokinetic capillary chromatography (MECC), which was first introduced by Terabe and co-workers [1,2], is an excellent separation technique. In MECC, neutral species are separated on the basis of their differential partitioning between an electroosmotically pumped aqueous mobile phase and an electrophoretically retarded micellar pseudo-phase. Commonly, micelles are formed from charged surfactants such as sodium dodecyl sulphate (SDS). Because of its high efficiency and resolving power, MECC makes it possible to achieve excellent separations of many mixtures, *e.g.*, phenylthiohydantoin-derivatized amino acids [3], ingredients of antipyretic analgesics [4] and catechols [5–7]. However, in an early study, Terabe *et al.* [2] indicated that the separation of solutes having low or high capacity factors was difficult in MECC. To

separate these solutes several techniques have been studied, including the addition to the background electrolyte solution of additives such as cyclodextrin [8], tetraalkylammonium salts [9] and many others [10–12]. These additives are found to facilitate the separation of compounds by means of a direct interaction between additive and solutes and by modifying partitioning between the two phases.

Balchunas and Sepaniak [13] discussed the resolution of MECC in terms of the elution range. The elution range of MECC is determined by the elution time of the bulk solution (t_0) and of the micelles (t_{mc}). All neutral solutes are eluted within the range defined by t_0 and t_{mc} . The ratio t_0/t_{mc} is utilized as a guide to the length of the elution range. A decrease in the value indicates that the elution range has been extended and therefore the resolution increased [2]. Extension of the elution range and improvement in the resolution of MECC can be accomplished by making t_0 smaller or t_{mc} larger. By making the electroosmotic mobility smaller or the electrophoretic mobility of micelles larger, t_{mc} can be increased because the net flow velocity of micelles is the sum of the electroosmotic mobility and the opposing electrophoretic mobility. The simplest

Correspondence to: Dr. M. Taga, Department of Chemistry, Faculty of Science, Hokkaido University, Kita-ku, Sapporo 060, Japan.

[☆] Present address: Faculty of Engineering, Kyushu University, Hakozaki, Fukuoka 812, Japan.

method to increase the electrophoretic mobility of micelles is to increase the SDS concentration [2]. However, the higher the SDS concentration, the larger is the current required for applying a given voltage because of the increased conductivity of the bulk solution. A consequence to this larger current is a degradation in the separation efficiency. To increase the electrophoretic mobility of the micellar phase without increasing its concentration, Balchunas and Sepaniak [13] attempted to use sodium decyl sulphate, which has a higher mobility than that of SDS because of its short alkyl chain, but this gave poor reproducibility of the solute retention time.

Another approach to extending the elution range involves adjustment of another important factor, the electroosmotic mobility. Because it influences both t_0 and t_{mc} , the control of the electroosmotic mobility does not necessarily lead to an extension of the elution range. The electroosmotic mobility is dependent on the pH of the solution, the solvent and the state of the capillary inner wall. Some studies have reported the use of an organic solvent to control the electroosmotic mobility [14–16]. Several modifications of the inner surface of fused-silica capillaries have been attempted in capillary zone electrophoresis or MECC [17,18]. We recently reported that the use of a cationic surfactant was effective in controlling the electroosmotic mobility, *i.e.*, adsorption of a cationic surfactant controlled the net charge on the capillary inner surface [19].

In this paper, we describe a new approach to improving the resolution of MECC, that is, the use of glucose as an additive. The addition of glucose to the background electrolyte significantly improved the separation of nine nucleosides. This enhanced resolution can be explained by an extended elution range and a change in selectivity. Glucose was found to decrease the distribution coefficients of some solutes into the micellar phase. Distribution coefficients are selectively decreased for solutes having hydrophilic functional groups. The usefulness of this glucose effect is demonstrated in the separation of phenanthroline analogues possessing high capacity factors.

EXPERIMENTAL

Apparatus

Fused-silica capillary tubes of 50 μm I.D. were

obtained from Gasukuro Kogyo (Tokyo, Japan). A high-voltage power supply, the Shimadzu (Kyoto, Japan) IP-1B isotachophoretic analyser, was used for applying the voltage. A CV⁴ variable-wavelength absorbance detector (ISCO, Lincoln, NE, USA) was utilized to measure absorbance. Detection was carried out by measuring the absorbance at 210 nm on the column at a position 20 cm from the negative end of the capillary tube. A sample was injected by moving the injection end of the capillary to the sample reservoir and raising it above the other end for a constant time. The electroosmotic velocities of the bulk solution and the electrophoretic velocities of micelles were evaluated from the respective measurement of the methanol peak, which is insoluble in the micellar phase, and the Sudan III peak, which is completely soluble in it.

Conditioning of a new capillary followed the method reported by Lauer and McMannigill [20]. The capillary was filled with 0.1 M KOH overnight, then flushed for 15 min with water and finally operated with buffer only before an experiment was performed. After finishing the experiments the capillary was flushed and filled with the operating buffer not containing surfactant.

Reagents

All reagents were of analytical-reagent grade and used as received. Adenosine (Ad), guanosine (Gu), cytidine (Cy), uridine (Ur), thymidine (Th), 2'-deoxyadenosine (dAd), 2'-deoxyguanosine (dGu), 2'-deoxycytidine (dCy) hydrochloride and deoxyuridine (dUr) were obtained from Tokyo Kasei Kogyo (Tokyo, Japan). Sample solutions were prepared by diluting to 100 ml with doubly distilled, deionized water after dissolving a stoichiometric amount of each reagent in 20 ml of 0.1 M HCl. All other reagents were obtained from Wako (Osaka, Japan).

The background electrolyte solution was prepared as follows. The required amounts of SDS and glucose were dissolved in water and then 1–2.5 ml of 1 M phosphoric acid were added to the solution. The pH of the solution was adjusted to 7.0 by adding 1 M NaOH, and finally the solution was diluted to 50 ml.

RESULTS AND DISCUSSION

In MECC, which is based on the partitioning between aqueous and micellar phases, the separa-

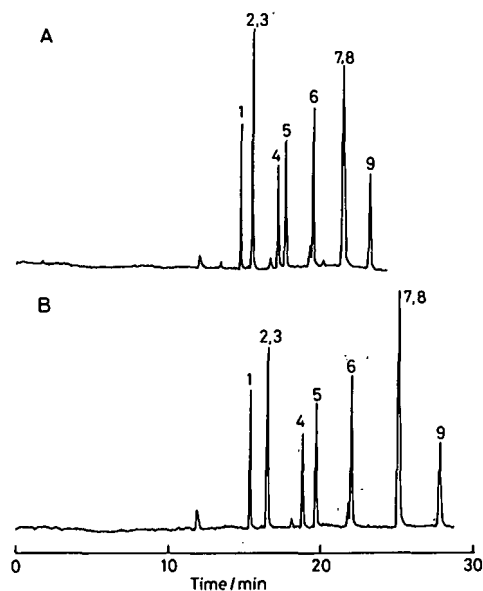


Fig. 1. Chromatograms of the test mixture of nine nucleosides. 1 = Ur; 2 = Cy; 3 = dUr; 4 = dCy; 5 = Th; 6 = Gu; 7 = Ad; 8 = dAd; 9 = dGu. Capillary length, 700 mm; effective length, 500 mm; buffer, 50 mM phosphate (pH 7.0); temperature, constant at 20°C. (A) 150 mM SDS, 35 μ A (12.2 kV); (B) 200 mM SDS, 45 μ A (12.4 kV).

tion of solutes that are either only slightly soluble (having low capacity factors) or completely soluble (having high capacity factors) in the micellar phase is difficult. Therefore, additional techniques are required to separate these solutes with MECC. We first tried to separate nine nucleosides with low capacity factors.

In Fig. 1A, a chromatogram of the nine nucleosides under ordinary MECC conditions is shown. Utilizing 150 mM SDS solution, seven nucleosides were separated but Cy–dUr and Ad–dAd could not be separated. The simplest technique for the extension of the elution range is to increase the SDS concentration. The elution range with 200 mM SDS solution (Fig. 1B) is larger than that with 150 mM SDS (Fig. 1A), but the separation between Cy–dUr and Ad–dAd is not improved. A higher concentration of SDS makes the conductivity of the bulk solution higher, which is liable to generate a deleterious amount of Joule heat. Extension of the elution range by increasing the SDS concentration is limited by this effect.

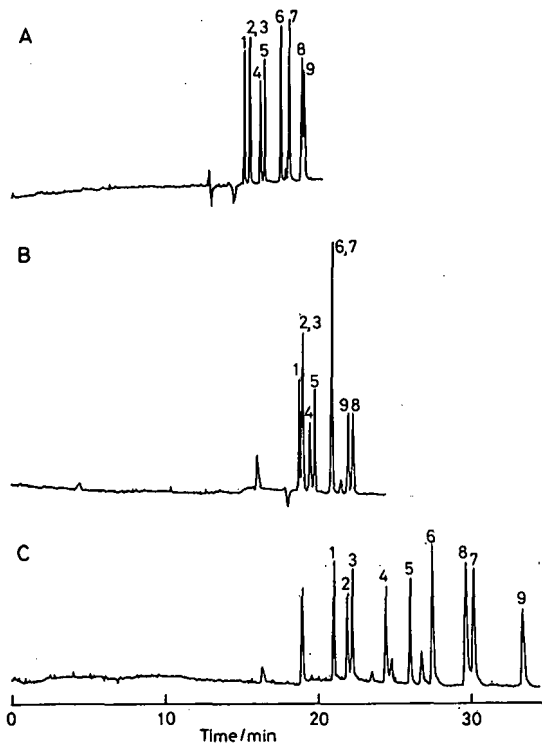


Fig. 2. Effect of additives on the chromatograms: (A) 10% methanol, applied voltage 13.5 kV; (B) 20% methanol, applied voltage 15.8 kV; (C) 1.0 M glucose, applied voltage 17.8 kV. SDS concentration, 150 mM; current, constant at 35 μ A. Other conditions and solutes as in Fig. 1.

Otsuka *et al.* [21] reported that the addition of methanol to the background electrolyte was effective in expanding the elution range and changing the selectivity in MECC, so the effect of methanol was investigated. As shown in Fig. 2A and B, the addition of methanol improved the separation of Ad and dAd but it was not effective in the separation of Cy and dUr. The separation window of the nine nucleosides is narrow and the difference in the retention time between nucleosides is very short. This leads to the conclusion that the addition of methanol is effective for the separation of solutes possessing high capacity factors [21] but not those with low capacity factors.

Fig. 2C is the chromatogram obtained by utilizing a solution containing 150 mM SDS and 1 M glucose. The addition of glucose causes the separation window to become wider and the voltage to become larger than the same separation without glucose

TABLE I

ELECTROOSMOTIC MOBILITY, ELECTROPHORETIC MOBILITY OF THE MICELLE AND THE ELUTION RANGE, t_0/t_{mc} , AT VARIOUS CONCENTRATIONS OF GLUCOSE

Capillary length, 500 mm; effective length, 300 mm; buffer, 20 mM phosphate containing 100 mM SDS (pH 7.0); temperature, 23°C.

Concentration of glucose (M)	Electroosmotic mobility ($10^{-4} \text{ cm}^2 \text{ s}^{-1} \text{ V}^{-1}$)	Electrophoretic mobility of micelle ($10^{-4} \text{ cm}^2 \text{ s}^{-1} \text{ V}^{-1}$)	t_0/t_{mc}
0	5.4	-4.2	0.23
0.25	4.5	-3.6	0.21
0.5	4.0	-3.3	0.17
1.0	3.0	-2.6	0.12

(Fig. 1A). It is readily apparent that the addition of glucose improves the resolution of the Cy-dUr and Ad-dAd peaks. However, a longer separation time is observed compared with the other chromatograms. Galactose and ribose showed the same effects as glucose but sorbitol gave a slightly smaller effect.

In Table I, the effect of glucose on the electroosmotic mobility, the electrophoretic mobility of the micelle at 100 mM SDS and the elution range (t_0/t_{mc}) are shown. The ratio t_0/t_{mc} is related to the electroosmotic mobility, μ_{eo} , and the electrophoretic mobility of the micelle, μ_{mc} , by

$$\frac{t_0}{t_{mc}} = 1 + \frac{\mu_{mc}}{\mu_{eo}} \quad (1)$$

where $0 > \mu_{mc}/\mu_{eo} > -1$. With increasing concentration of glucose both the electroosmotic mobility and the electrophoretic mobility of micelles are reduced. Most of this decrease will be explained in the terms of an increase in the viscosity of the bulk solution with an increase in glucose concentration. However, the increasing in viscosity is not effective in extending the elution range as shown in eqn. 1, because the mobilities are inversely proportional to the viscosity of the solution. The decrease in the electrophoretic mobility of the micellar phase generally makes the elution range narrow, but nevertheless the elution range appears to be extended. This may be because the addition of glucose caused the electrophoretic mobility of the micellar phase to decrease but not as much as the electroosmotic mobility, which indicates that the increase in t_{mc} was larger than that in t_0 .

When the critical micellar concentration (CMC)

was examined in the presence of glucose, it was found that at glucose concentrations of 0, 0.5 and 1 M the CMC of SDS was 8.1 (close to the established value), 7.4 and 6.5 mM, respectively. This experiment was carried out by conductimetric titration of each glucose solution at 25°C with 50 mM SDS solution containing the same glucose concentration as the sample. The decrease in CMC is also caused by the addition of inorganic salts [22] and alcohols [23]. With sodium chloride addition, the aggregation number increases with increasing concentration of sodium chloride [22]. It is speculated that a decrease in the CMC will increase the micelle aggregation number and the concentration of aggregated surfactant. Generally, the electrophoretic mobility of the micelle increases with an increase in the micellar concentration in MECC [2]. It is considered that the extension of the elution range is caused by the increase in the electrophoretic mobility of the micelle with increasing aggregated surfactant concentration. However, the improvement in the resolution for the nucleoside mixture by the addition of glucose cannot be understood only in terms of extension of the elution range because there is no improvement, as shown in Fig. 1.

Reversal of the elution order of Ad and dAd was observed on the addition of glucose, compared with the chromatogram obtained utilizing a 150 mM SDS solution without glucose and applying a higher voltage (14.5 kV). This reversal of elution order means that there has been a change in the separation selectivity, *i.e.*, a selective change in the distribution coefficients in the presence of glucose. We undertook an investigation of the distribution coefficients

TABLE II
DEPENDENCE OF DISTRIBUTION COEFFICIENTS ON
THE CONCENTRATION OF GLUCOSE

Conditions as in Table I except for the SDS concentration.

Solute	Concentration of glucose (M)			
	0	0.25	0.50	1.0
Phenol	41.2	42.6	41.1	36.2
Benzene	88.3	92.3	92.3	91.0
Toluene	248	257	258	257
1-Naphthol	602	560	506	443
Naphthalene	1172	1155	1092	1014

for several solutes with relatively high capacity factors.

The capacity factor, k' , is defined as the ratio of the total moles of the solute in the micellar phase to that in the aqueous phase, and it can be expressed as [2]

$$k' = \frac{t_R - t_0}{t_0(1 - t_R/t_{mc})} \quad (2)$$

and

$$k' = K \cdot \frac{V_{mc}}{V_{aq}} \quad (3)$$

where t_R is the retention time of the solute, K is the distribution coefficient and V_{mc} and V_{aq} are the volumes of micellar and aqueous phases, respectively. When the micellar concentration is low, the equation may be approximated by

$$k' = K\nu(C_{sf} - CMC) \quad (4)$$

where ν is the partial specific volume of the SDS micellar phase and C_{sf} is the SDS concentration. Assuming that ν is constant, the distribution coefficients of solutes were calculated from the plot of k' vs. SDS concentration. However, nucleosides are very hydrophilic and their distribution coefficients were too small to determine. Therefore, we used some aromatic compounds as test solutes. The dependence of the distribution coefficients for the test solutes on the concentration of glucose is shown in Table II. The distribution coefficients of benzene and toluene were not changed by addition of glucose (the relative standard deviations were about 2%).

However, the distribution coefficients of phenol and naphthalene were decreased by about 12% and that of 1-naphthol was decreased by *ca.* 25% in the presence of 1 M glucose. It seems that this effect is selective for solutes having high capacity factors and hydrophilic functional groups such as nucleosides, phenol and naphthol. The improvement in the resolution for the nucleoside mixture could be attributed to the selective decrease in distribution coefficients.

Fig. 3 shows the chromatograms of a mixture of several solutes having some hydrophilic functional groups such as pyridyl and hydroxyl and high capacity factors in a buffer containing 20 mM SDS without glucose (Fig. 3A) and with 1.0 M glucose (Fig. 3B). In Table III, the capacity factors and the separation selectivities of the solutes in Fig. 3 are shown (the separation selectivity, α , is the ratio of the capacity factors of the two components). The capacity factors of all solutes decreased on the addition of glucose, but the extent of the decrease was not uniform. Compounds such as 2,9-dimethyl-

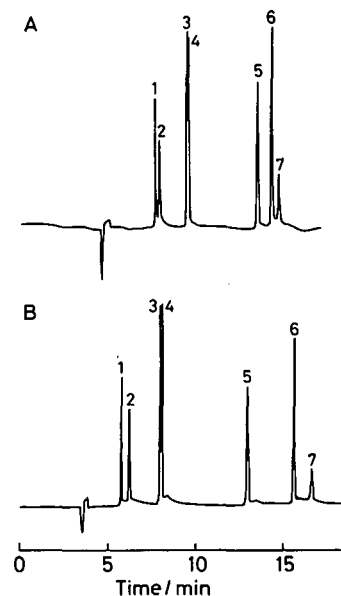


Fig. 3. Chromatograms of a test mixture. Capillary length, 500 mm; effective length, 300 mm; buffer, 20 mM phosphate containing 20 mM SDS (pH 7.0); temperature, 24°C. 1 = 4,4'-Bipyridyl; 2 = 2,2'-bipyridyl; 3 = 1-naphthol; 4 = 2-naphthol; 5 = 2,9-dimethyl-1,10-phenanthroline; 6 = phenanthrene; 7 = Sudan III. (A) Without glucose, current 5 μ A (9.6 kV); (B) with 1.0 M glucose, current 15 μ A (19.5 kV).

TABLE III
CAPACITY FACTORS, k' , AND SEPARATION SELECTIVITY, α , OF TEST SOLUTES

Solute	Without glucose		1.0 M glucose	
	k'	α	k'	α
2,2'-Bipyridyl	1.09		0.88	
4,4'-Bipyridyl	1.23	1.13	1.13	1.28
1-Naphthol	2.43		2.18	
2-Naphthol	2.52	1.04	2.26	1.04
2,9-Dimethyl-1,10-phenanthroline	20.89		11.38	
Phenanthrene	65.19	3.12	53.59	4.71

1,10-phenanthroline exhibited a large decrease in comparison with others such as naphthols. The addition of glucose allowed phenanthrene to be sufficiently separated from Sudan III and increased the separation selectivity between 2,2'-bipyridyl and 4,4'-bipyridyl from 1.13 to 1.28 and between 2,9-dimethyl-1,10-phenanthroline and phenanthrene from 3.12 to 4.71. The specific decrease in the capacity factor of 2,9-dimethyl-1,10-phenanthroline seems to be due to its hydrophilic functional group.

The detailed mechanism of the decrease in the capacity factor on addition of glucose is not clear. However, it is postulated that the distribution of a solute to the micellar phase is suppressed by the displacement of water from around the hydrophilic functional group by glucose. In conclusion, glucose, as an additive in MECC, seems to offer an interesting modification to the separation selectivity.

CONCLUSIONS

The addition of glucose to the background electrolyte in MECC resulted in an extension of the elution range and improved separation selectivity, thereby allowing the complete separation of a mixture of nine nucleosides with low capacity factors. The addition of glucose brings about a decrease in the distribution coefficients of solutes with high capacity factors and hydrophilic functional groups. Utilization of carbohydrates such as glucose is expected to provide a new technique for the control of the separation selectivity in MECC. This is a preliminary report and therefore the mechanism is not well understood; however, efforts are being made to characterize completely the action of carbohydrate additives.

REFERENCES

- 1 S. Terabe, K. Otsuka, K. Ichikawa, A. Tsuchiya and T. Ando, *Anal. Chem.*, 56 (1984) 111.
- 2 S. Terabe, K. Otsuka and T. Ando, *Anal. Chem.*, 57 (1985) 834.
- 3 K. Otsuka, S. Terabe and T. Ando, *J. Chromatogr.*, 332 (1985) 219.
- 4 S. Fujiwara and S. Honda, *Anal. Chem.*, 59 (1987) 2773.
- 5 R. A. Wallingford and A. G. Ewing, *Anal. Chem.*, 60 (1988) 258.
- 6 R. A. Wallingford and A. G. Ewing, *J. Chromatogr.*, 441 (1988) 299.
- 7 R. A. Wallingford and A. G. Ewing, *Anal. Chem.*, 61 (1989) 98.
- 8 S. Terabe, H. Ozaki, K. Otsuka and T. Ando, *J. Chromatogr.*, 332 (1985) 211.
- 9 H. Nishi, N. Tsumagari and S. Terabe, *Anal. Chem.*, 61 (1989) 2434.
- 10 S. Terabe and T. Isemura, *Anal. Chem.*, 62 (1990) 650.
- 11 A. Cohen, S. Terabe, J. A. Smith and B. L. Karger, *Anal. Chem.*, 59 (1987) 1021.
- 12 S. A. Swedberg, *J. Chromatogr.*, 503 (1990) 449.
- 13 A. T. Balchunas and M. J. Sepaniak, *Anal. Chem.*, 59 (1987) 1466.
- 14 A. T. Balchunas and M. J. Sepaniak, *Anal. Chem.*, 60 (1988) 617.
- 15 M. M. Bushey and J. W. Jorgenson, *Anal. Chem.*, 61 (1989) 491.
- 16 M. M. Bushey and J. W. Jorgenson, *J. Microcol. Sep.*, 1 (1989) 125.
- 17 S. Terabe, H. Utsumi, K. Otsuka, T. Ando, T. Inomata, S. Kuze and Y. Hanaoka, *J. High Resolut. Chromatogr. Chromatogr. Commun.*, 9 (1986) 666.
- 18 R. M. McCormick, *Anal. Chem.*, 60 (1988) 2322.
- 19 T. Kaneta, S. Tanaka and H. Yoshida, *J. Chromatogr.*, 538 (1991) 385.
- 20 H. H. Lauer and D. McMannigill, *Anal. Chem.*, 58 (1986) 166.
- 21 K. Otsuka, S. Terabe and T. Ando, *Nippon Kagaku Kaishi*, 7 (1987) 950.
- 22 J. N. Phillips, *Trans. Faraday Soc.*, 51 (1955) 561.
- 23 K. Shinoda, *J. Phys. Chem.*, 58 (1954) 1136.

Capillary electrophoretic analysis of oxindole alkaloids from *Uncaria tomentosa*

Hermann Stuppner and Sonja Sturm

Institute of Pharmacognosy, University of Innsbruck, Innrain 52, A-6020 Innsbruck (Austria)

Günther Konwalinka

Department of Internal Medicine, University of Innsbruck, Innsbruck (Austria)

(First received March 27th, 1992; revised manuscript received June 9th, 1992)

ABSTRACT

The main oxindole alkaloids from the root bark of *Uncaria tomentosa* were separated by capillary electrophoresis. The electrophoretic parameters for the separation of the six alkaloids were optimized by studying the impact of the buffer composition, the ionic strength and the pH and the applied electric field on the separation efficiency of the analytical system. The best separation was achieved with a fused-silica capillary tube and 20 mM phosphate running buffer (pH 5.6) at a constant voltage of 10 kV. The determination of oxindole alkaloids in a crude methanolic extract of *Uncaria tomentosa* demonstrates the applicability of this method.

INTRODUCTION

Capillary electrophoresis (CE) is a powerful separation technique that has become an important analytical and micropreparative tool in peptide and protein chemistry [1]. In addition to its special selectivity, the CE method provides short separation times, small sample requirements and virtually no waste production. Therefore, it can be considered as an ideal complement to high-performance liquid chromatography (HPLC). In spite of these advantages, few papers have been published so far describing the application of CE to the separation of natural plant constituents [1,2]. In this paper, the separation and determination of oxindole alkaloids in *Uncaria tomentosa* with CE is reported.

Uncaria tomentosa (Willd.) DC. (Rubiaceae), commonly known as “una de gato”, is a woody

liana growing in South America. Decoctions of the root bark are used in traditional Peruvian medicine for the treatment of arthritis, gastritis, cancer and certain epidermic diseases [3]. Phytochemical studies of the root bark have shown the presence of triterpenes, some minor constituents and six main oxindole alkaloids, which previously have been identified as pteropodine, isopteropodine, mitraphylline, isomitraphylline, speciophylline and uncarine F (Fig. 1) [4–7]. Because of the wide range of pharmacological and biological activities of these compounds, their separation and determination are of considerable interest.

So far, analyses for oxindole alkaloids have been accomplished by thin-layer and gas-liquid chromatography and HPLC [5,8,9]. The application of these methods to the separation of the stereoisomeric oxindole alkaloids from *Uncaria tomentosa* however, led to unsatisfactory resolution of adjacent pairs of alkaloids. In this work, a CE method for the rapid separation and determination of oxindole alkaloids in *Uncaria tomentosa* extracts was

Correspondence to: Dr. Herman Stuppner, Institute of Pharmacognosy, University of Innsbruck, Innrain 52, A-6020 Innsbruck, Austria.

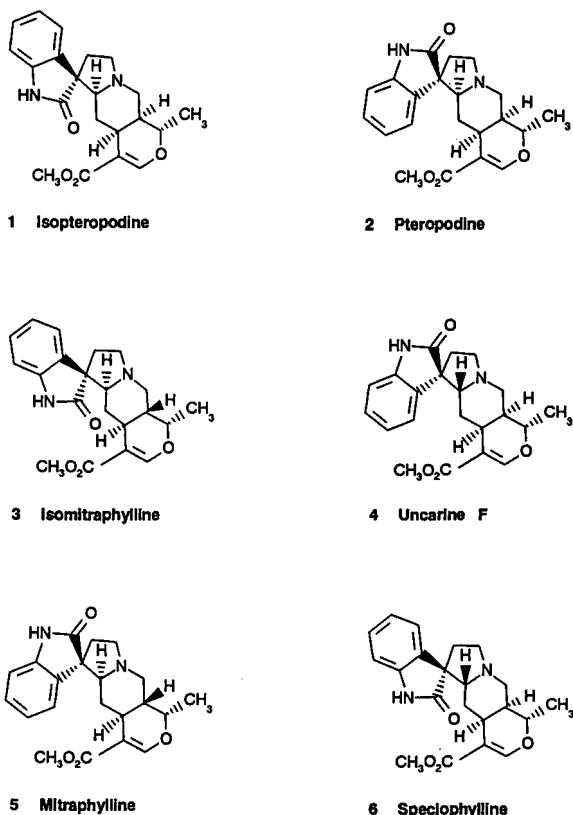


Fig. 1. Structures of the investigated oxindole alkaloids.

developed. The influence of pH, the ionic strength of the buffer and the applied voltage on the resolution of oxindole alkaloids from *Uncaria tomentosa* is discussed.

EXPERIMENTAL

Materials

Methanol, mesityl oxide, Na_2HPO_4 and KH_2PO_4 were purchased from Merck (Darmstadt, Germany). The reference alkaloids 1–6 (Fig. 1) were a gift from Professor J. D. Phillipson (University of London). Plant material of *Uncaria tomentosa* (root bark) was obtained from Mr. K. Kepplinger (Innsbruck, Austria). A voucher specimen is deposited in the Institute of Pharmacognosy, University of Innsbruck.

Sample preparation

Alkaloids 1–6 (0.75–3.15 mg) were dissolved in 1 ml of methanol and diluted with the eluent buffer (1:5) in order to give final concentrations of 15–63 $\mu\text{g}/\text{ml}$. Exhaustive extraction of 1.0 g of *Uncaria tomentosa* root bark material was carried out with a Soxhlet apparatus using methanol as solvent. For qualitative and quantitative analyses the extract obtained was evaporated to dryness and the residue dissolved in 1.00 ml methanol and diluted with phosphate buffer (20 mM, pH 5.6) in a ratio of 1:5. Mesityl oxide (diluted 1:1250 with water) was added to all sample solutions as a neutral marker (0.1 ml/ml).

Calibration

The calibration graph was obtained from standard solutions containing the alkaloid 1 in concentrations between 0.005 and 0.300 mg/ml in methanol–eluent buffer (1:5).

Analytical method

A Beckman CZE System 2000 (Model P/ACE) equipped with a UV detector, an automatic injector, a temperature-controlled column cartridge (57 cm x 75 μm I.D.) (Beckman No. 338427), an auto-sampler and a printer was used. The detection wavelength was 254 nm. All experiments were carried out at 25°C at a constant voltage of 10 kV. When studying the effect of electric field on electrophoretic mobilities, voltages between 5 and 20 kV were used. Injections were made using the pressure mode for 1 s each. When investigating the influence of the sample volume on the resolution, sampling times of 1, 3 and 5 s were used.

Phosphate buffer solutions (10–25 mM) were prepared by dissolving appropriate amounts of Na_2HPO_4 and KH_2PO_4 in doubly distilled water. The pH of each buffer solution was checked with a pH meter. All sample and buffer solutions were filtered through 0.45- μm filters (Sartorius, Göttingen, Germany). Between runs, the capillary was washed with 0.1 M NaOH for 3 min, followed by equilibration with running buffer (3 min).

RESULTS AND DISCUSSION

The electropherogram of a model mixture of the alkaloids isopteropodine (1), pteropodine (2), iso-

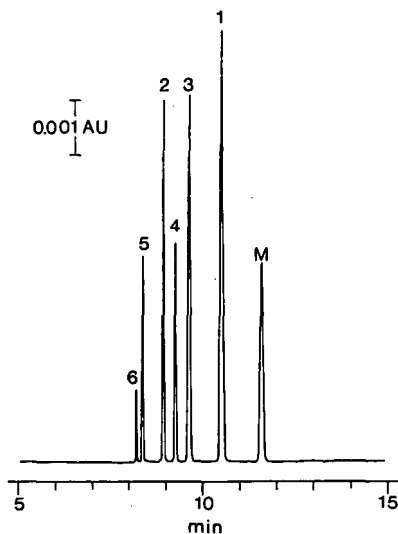


Fig. 2. Electropherogram of a model mixture of the alkaloids isopteropodine (1), pteropodine (2), isomitraphylline (3), uncarine F (4), mitraphylline (5) and speciophylline (6). M is the neutral marker mesityl oxide. Buffer, 20 mM phosphate buffer (pH 5.6); column, fused silica (570 × 0.075 mm I.D.); injection, pressure mode, 1 s (4.8 nl); injected amounts (ng), (1) 0.32, (2,3) 0.30, (4) 0.16, (5) 0.15, (6) 0.07, (M) 0.30; voltage, 10 kV; current, 17 μ A; detection, UV at 254 nm; temperature, 25°C.

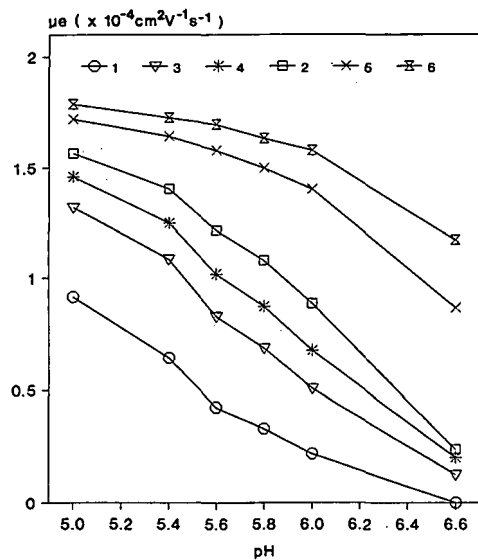


Fig. 3. Effect of pH on electrophoretic mobilities (μ_e) of alkaloids 1–6. pH, 5.0–6.6; other conditions same as in Fig. 2.

mitraphylline (3), uncarine F (4), mitraphylline (5) and speciophylline (6) is shown in Fig. 2. Baseline separation of the six compounds could be achieved in less than 15 min using a fused-silica capillary tube with phosphate buffer (20 mM, pH 5.6) as running electrolyte at a constant voltage of 10 kV. UV detection was performed at 254 nm. In this system the alkaloids are positively charged and migrate faster to the cathode than the neutral marker mesityl oxide.

Optimization of the parameters was carried out by investigating the influence of electrolyte composition, pH, electric field and ionic strength on the mobilities of 1–6. The parameter with the strongest influence on the mobilities of the alkaloids is pH. As alkaloids are weak bases, an acidic buffer system was chosen in order to ensure an adequate degree of dissociation. Fig. 3 shows the mobilities of the analytes at different pH values of the phosphate buffer. The true electrophoretic mobility (μ_e) was calculated using the equation

$$\mu_e = (L/V) [(1/t_m) - (1/t_{co})] \quad (1)$$

where L is the total capillary length (cm), l the distance from injection to the detector (cm), V the applied voltage (V), t_m the solute migration time (s) and t_{co} the hold-up time of the electroosmotic flow marker mesityl oxide (s) [10]. The reproducibility of the solute mobilities was good. Six analyses of the standard mixture gave a relative standard deviation of 0.66%.

It is evident from Fig. 3, that the alkaloids with higher pK_a values are eluted faster than those with lower values [11,12]. The lower mobilities of the alkaloids at higher pH values are due to the increased electroosmotic flow. Excellent resolution (R_s) of adjacent pairs of alkaloids was observed at pH of 5.6 (Fig. 4).

The influence of the electric field strength on resolution is shown in Fig. 5. As the number of theoretical plates is proportional to the applied voltage, resolution was enhanced up to an electric field strength of 175 V/cm [13]. Beyond this point, the resolution decreased as the voltage was increased further. This is due to Joule heating effects [13,14].

Fig. 6 shows the effect of ionic buffer strength on the separation efficiency of the system at a constant voltage of 10 kV and a pH value of 5.6. In addition to the higher current, increasing the buffer concen-

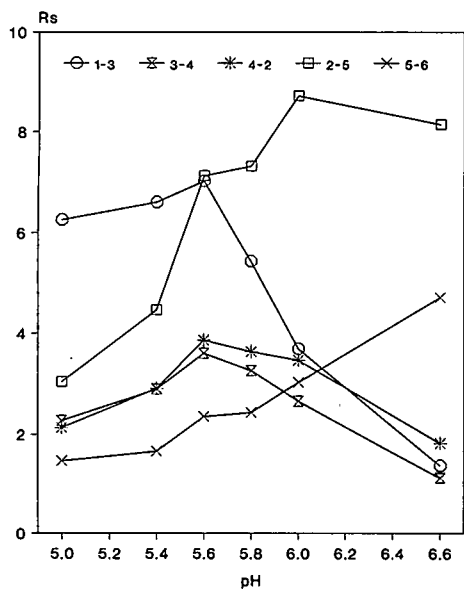


Fig. 4. Effect of pH (5.0–6.6) on resolution (R_s) of the alkaloid pairs 1–3, 3–4, 4–2, 2–5 and 5–6. Conditions as in Fig. 3.

tration resulted in an increased spread of the electrophoretic mobilities between the investigated alkaloids. The alkaloids 1–4 exhibited faster and alkaloids 5–6 slower migration. In addition, peak broadening was significantly reduced. The best sep-

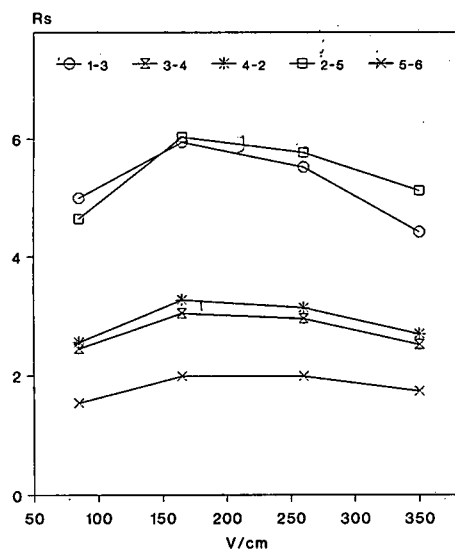


Fig. 5. Effect of electric field strength (V/cm) on resolution (R_s) of the alkaloid pairs 1–3, 3–4, 4–2, 2–5 and 5–6. Voltage, 5–20 kV; other conditions as in Fig. 2.

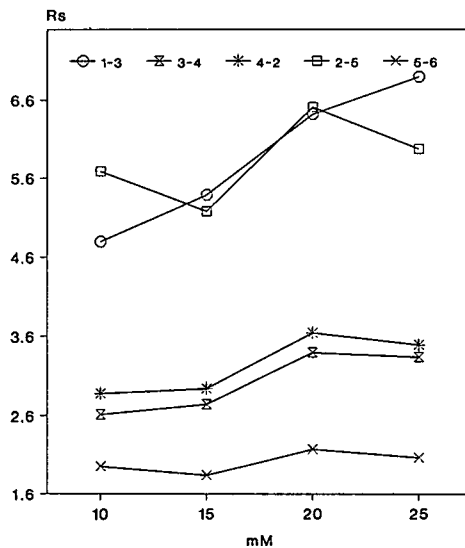


Fig. 6. Effect of buffer concentration on resolution (R_s) of the alkaloid pairs 1–3, 3–4, 4–2, 2–5 and 5–6. Buffer, 10–25 mM phosphate buffer; other conditions as in Fig. 2.

aration of all compounds was achieved with a buffer concentration of 20 mM. In contrast to the other alkaloid pairs, the resolution of the pair 2–5 decreased on increasing the buffer concentration from 10 to 15 mM and from 20 to 25 mM.

The effect of injection volume on CE performance has already been reported [15]. Accordingly, zone distortion and band broadening are only avoided if the sample volumes are kept as small as possible (< 1% of the total capillary volume). Table I shows the number of theoretical plates (N) and the resolution (R_s) obtained on increasing the sample volume, the actual amount of sample introduced being kept constant (sampling times of 1, 3 and 5 s). Both N and R_s decreased with increasing injection time.

To confirm the applicability of the proposed separation method, a crude methanolic extract of *Uncaria tomentosa* was investigated. CE yielded a baseline separation within 15 min. Peaks 1–6 were identified by comparison with standards. Quantitative information was obtained by using the external standard method. As the investigated oxindole alkaloids are stereoisomers with very similar UV molar absorptivities (ϵ) [8], calibration was performed only with compound 1. The graph obtained was lin-

TABLE I
EFFECT OF INJECTION TIME ON NUMBER OF THEORETICAL PLATES AND RESOLUTION

Sampling times: 1, 3 and 5 s. Other conditions as in Fig. 2.

Injection time (s)	Compound	Concentration ($\mu\text{g/ml}$)	Plates per metre, $N (\times 10^5)$	R_s
1	1	66.09	1.260	
	3	61.95	2.194	6.42
	4	39.13	2.858	3.39
	2	61.95	3.149	3.62
	5	32.17	3.541	6.50
	6	14.78	4.680	2.17
3	1	22.03	0.800	
	3	20.65	1.037	4.70
	4	13.04	1.136	2.19
	2	20.65	1.321	2.29
	5	10.72	1.452	4.14
	6	4.93	1.748	1.36
5	1	13.22	0.316	
	3	12.39	0.379	3.10
	4	7.83	0.456	1.37
	2	12.39	0.471	1.30
	5	6.43	0.671	2.78
	6	2.96	0.920	1.09

ear in the range of 5–300 $\mu\text{g/ml}$ ($y = 0.14298x + 0.00204$; $r^2 = 0.998$). The detection limit was *ca.* 1.2 $\mu\text{g/ml}$. The results of the quantification are shown in Table II. The relative standard deviation (six experiments) was between 1.2 and 5.3% for all compounds studied.

In conclusion, the described CE technique represents an excellent method for the qualitative and quantitative analysis of *Uncaria tomentosa* for stereoisomeric oxindole alkaloids.

ACKNOWLEDGEMENTS

We gratefully acknowledge Beckman Instruments Austria for providing the Beckman System 2000 (Model P/ACE) for these investigations. We also thank Professor J. D. Phillipson (Department of Pharmacognosy, University of London) for the generous gift of the oxindole alkaloid standards, as Mr. K. Kepplinger (Innsbruck) for the *Uncaria tomentosa* plant material and Mr. A. Vorndran (In-

TABLE II
RESULTS OF THE DETERMINATION OF ALKALOIDS IN A CRUDE METHANOLIC EXTRACT OF *Uncaria tomentosa*
Average results (g per 100 g) \pm S.D. for six analyses.

Compound	Calibration	Concentration (g per 100 g)
1	$y = 0.14298x + 0.00204$ ($r^2 = 0.998$)	0.0285 ± 0.0012
2	Calculated with eqn. 1	0.0551 ± 0.0028
3	Calculated with eqn. 1	0.0186 ± 0.0006
4	Calculated with eqn. 1	0.0104 ± 0.0001
5	Calculated with eqn. 1	0.0276 ± 0.0007
6	Calculated with eqn. 1	0.0142 ± 0.0003
Total		0.1544 ± 0.0036

stitute of Radiochemistry, University of Innsbruck) for helpful suggestions and technical advice.

REFERENCES

- 1 Z. Deyl and R. Struzinsky, *J. Chromatogr.*, 569 (1991) 63.
- 2 P. G. Pietta, P. L. Mauri, A. Rava and G. Sabattini, *J. Chromatogr.*, 549 (1991) 367.
- 3 F. W. Ostendorf, *Suriname Bull.*, 79 (1962) 199.
- 4 R. Cerri, R. Aquino, F. De Simone and C. Pizza, *J. Nat. Prod.*, 51 (1988) 257.
- 5 H. Wagner, B. Kreutzkamp and K. Jurcic, *Planta Med.*, 51 (1985) 419.
- 6 S. Montenegro de Matta, F. Delle Monache, F. Ferrari and G.B. Marini-Bettolo, *Il Farmaco*, 31 (1976) 527.
- 7 S. Sturm, H. Stuppner and G. Konwalinka, in preparation.
- 8 J. D. Phillipson and S. R. Hemingway, *J. Chromatogr.*, 105 (1975) 163.
- 9 J. D. Phillipson, N. Supavita and L.A. Anderson, *J. Chromatogr.*, 244 (1982) 91.
- 10 A. S. Cohen, A. Paulus and B. L. Karger, *Chromatographia*, 24 (1987) 15.
- 11 N. Finch and W. I. Taylor, *J. Am. Chem. Soc.*, 84 (1962) 3871.
- 12 K. C. Chan, F. Morsingh and G. B. Yeoh, *J. Chem. Soc. C*, 24 (1961) 2245.
- 13 J. W. Jorgenson and K.D. Lukacs, *Anal. Chem.*, 53 (1981) 1298.
- 14 H. J. Issaq, G. M. Janini, I. Z. Atamna and G. M. Muschik, *J. Liq. Chromatogr.*, 14 (1991) 817.
- 15 J. Jorgenson and K. D. Lukacs, *Science*, 222 (1983) 266.

Determination of C₈–C₂₀ saturated anionic and cationic surfactant mixtures by capillary isotachopheresis with conductivity detection

C. Tribet and R. Gaboriaud

Laboratoire d'Énergétique et Réactivité aux Interfaces, Université Paris VI, 4 Place Jussieu, 75231 Paris Cedex 05 (France)

P. Gareil

Laboratoire de Chimie Analytique de l'École Supérieure de Physique et de Chimie Industrielles de la Ville de Paris, 10 Rue Vauquelin, 75231 Paris Cedex 05 (France)

(First received January 23rd, 1992; revised manuscript received April 22nd, 1992)

ABSTRACT

Isotachopheresis combined with conductivity detection was systematically investigated as an alternative method for the determination of various classes of C₈–C₂₀ saturated ionic surfactants, including sulphates, sulphonates and quaternary ammonium cations. Its major interest is the ability to perform separations in free electrolyte media (*i.e.*, without any stationary phase) and in capillaries of fairly large inner diameter (typically 0.5 mm), which reduces the possibility of deleterious adsorption, often encountered in other techniques with ionic surfactants. Methanol–water mixtures of appropriate compositions were used to prevent micellization of the surfactant from occurring, thus yielding separations according to their free-form electrophoretic mobilities. Compounds differing in one carbon atom only can be fully resolved. The steady-state zone stability was ascertained by plotting analyte zone lengths *versus* injected amounts and by determinations of separation capacities for standard binary mixtures in various proportions. Conductimetry provides a convenient and universal detection method, with acceptable detection limits (*ca.* 0.1–1 nmol for a 10- μ l volume injected), owing to the absence of background electrolyte in analyte zones, inherent in isotachopheretic principles. The determination of the quaternary ammonium ions contained in an industrial surfactant formulation is presented as an example.

INTRODUCTION

During the last decade, surface-active compounds have gained widespread applications that now encompass much more than detergency. They are involved, generally as mixtures, in many industrial separation processes (liquid–liquid extraction, flotation of ore minerals, enhanced oil recovery) and in many formulations of products of agricultu-

ral, food, pharmaceutical or health interest such as body creams and vesicle encapsulation of medicines. They even have entered the class of fine reagents for analytical purposes to promote ion-pair or micellar pseudo-phase formation. A wide variety of surface-active agents, both ionic and non-ionic, are becoming commercially available to meet these needs and, consequently, this places great demands on high-performance analytical methods capable of discriminating homologues, isomers or any other small structural differences.

Chromatographic techniques overall have been considered to meet these requirements, especially for the non-ionic class of the most often oligomeric

Correspondence to: Dr. C. Tribet, Laboratoire d'Énergétique et Réactivité aux Interfaces, Université Paris VI, 4 Place Jussieu, 75231 Paris Cedex 05, France.

or polymeric surfactants, such as the derivatized polyoxyethylenes [1–4].

In contrast, less has been published on the various classes of ionic surfactants with chain lengths ranging from eight to about twenty carbon atoms, whether they are anionic (alkyl sulphates and sulphonates, carboxylates) or cationic (trimethylalkylammonium, alkylimidazolium ions), probably because of increased difficulties owing to their ionic character. Apart from when previous derivatization of the ionic moiety is applied [4], these products cannot be submitted to capillary gas (GC) or supercritical fluid chromatography (SFC) owing to their low volatility. Moreover, their poor solubility in supercritical carbon dioxide makes the use of a polar modifier necessary in SFC and precludes one of the major advantages of this techniques, *viz.*, its compatibility with flame ionization detection. Thus, only the separation of C₈–C₂₄ even carbon number free fatty acids on a packed microbore column has been reported so far [5]. In addition to their ionic character, the amphiphilic properties make the choice of suitable phase systems in liquid chromatography (LC) that would prevent strong or even irreversible adsorption on a stationary phase difficult. The most successful techniques reported are reversed-phase [6,7] and ion-pair [8–14] chromatography.

Various modes of detection have been combined with the LC separations of ionic surfactants. The most common, direct UV absorbance, is virtually restricted to alkylbenzene sulphates and sulphonates [8], imidazolines [9] or ester derivatives [7]. Indirect UV absorbance was used for qualitative detection of ammonium ion with xylene sulphonate as a UV-absorbing counter-ion [13]. On-line extraction of a postcolumn-formed, UV-absorbing [10] or fluorescent [6] ion pair was also implemented for cationic [10] and anionic [6] surfactants, but required complex equipment. Differential refractive index monitoring would constitute a versatile means of detection [8,14], but suffers from a lack of sensitivity. Light scattering appears to be well adapted to the detection of heavy compounds, but is not consistent with separations under ion-pairing conditions. Hence its use is limited to non-ionic surfactants or a mere class separation of the ionic and non-ionic types under reversed-phase conditions [15]. Finally, ion-pair chromatography associated with conduc-

tivity detection has been reported for aliphatic and olefinic anionic surfactants, but a device allowing the suppression of the mobile phase ions is necessary in order to obtain a level of detectability of practical interest [11]. This device considerably reduces the choice of compatible counter ions and gives a certain degree of complexity to the method. None of these LC methods has turned out to be completely satisfactory because of limitations in either the separation itself or the detection modes. Few quantitative determinations have been reported [5,6,14], which is a hint that they remain a problem. Detection limits are commonly in the 1–10 nmol range for *ca.* 10–20- μ l injections [7,10,11,13] and more seldom in the 0.1–1 nmol range [5,6].

The purpose of this work was to develop and assess an alternative method for the determination of the various classes of C₈–C₂₀ saturated anionic and cationic surfactants, based on electrophoresis in its isotachophoretic mode combined with conductivity detection. The interest in this approach is first, the ability to perform separations in free electrolyte solutions, *i.e.*, without any stationary phase, often responsible for strong adsorption, and second, the acceptable sensitivity of conductivity detection when used in the absence of a background electrolyte medium, as in the case with isotachopheresis (ITP), the displacement mode of electrophoresis. Further no specific sample treatment or derivatization should be required. Nevertheless, the application of ITP to surfactant analysis has remained uncommon and no method allowing the total determination of C₈–C₂₀ saturated alkyl sulphates or ammonium ions has been proposed. Previous work in this direction dealt with C₁–C₈ [16] or C₁–C₁₈ [17] fatty acids, decyl and dodecyl sulphonates and inorganic ions in shampoo formulations [18] and complex alkyl sulphonate mixtures formed in the peroxodisulphate-initiated polymerization of butadiene [19]. All of them seem very promising. This is why we carried out a systematic investigation of the operational electrolyte systems, including various aqueous–organic solvent mixtures, to assess better the performances of ITP with respect to surfactant mixture analysis. The optimum conditions found for cationic surfactants were applied to trimethylalkylammonium ion mixture of industrial interest synthesized by alkylation of natural copra oil.

EXPERIMENTAL

Apparatus and products

The separations were performed with an LKB 2127 Tachophor apparatus (Pharmacia–LKB, Uppsala, Sweden) fitted with solvent-resistant poly-methylpentene (TPX) pieces in direct contact with the solutions. A single column configuration was used with 22 cm × 0.55 mm I.D. polytetrafluorethylene (PTFE) tubing. The separation unit was equipped with a conductivity detector, comprising linear and differential signal outputs, and a UV absorbance detector operated with a 254-nm wavelength filter. The signals were recorded on a Kipp and Zonen (Delft, Netherlands) BD 100 three-channel chart recorder. The driving current was delivered by the Tachophor power supply unit and a laboratory-made pilot unit capable of delaying the start of the recorder and switching the current intensity to a lower value a short time before the solutes migrate past the detector cell.

The electrolytes were prepared from ultrapure deionized water (18 MΩ cm resistivity) produced by a Millipore Milli-Q system and from high-performance liquid chromatographic-grade solvents (methanol, 1- and 2-propanol, acetonitrile) purchased from Prolabo (Paris, France). Buffer solutions were prepared from the highest available grades of analytical reagents, used as received. The standard surfactants studied were supplied by Fluka (Buchs,

Switzerland) or Lancaster Synthesis (Morecambe, UK) and used as received after solubilization in water or methanol. Noramium, an industrial mixture of quaternary ammonium ions manufactured by CECA (Paris La Défense, France), was kindly provided by Orsan (Orsay, France). All solutions were degassed for 10–15 min in an ultrasonic bath.

Electrolyte preparation

The leading solutions were prepared from 0.1 M stock buffer solutions of potassium acetate–acetic acid or L-histidine–hydrochloric acid in the appropriate proportions and in various aqueous organic solvent mixtures. A 5-ml volume of these stock solutions were added to 1 ml of pure (99%) tetraethylene glycol (Aldrich) and adjusted to 50 ml with the appropriate aqueous organic solvent mixture to obtain the desired 10 mM leading electrolyte solutions. The pH of the final electrolyte solutions was measured using a classical pair of glass and reference electrodes for aqueous media. For methanol, the effect of organic solvent proportion was studied between 0 and 80% (v/v). The terminating electrolyte solutions were prepared simply by dissolving the appropriate weight of reagent in the same solvent mixture as that of the leading electrolyte. The compositions of the electrolytes yielding the best results for the sulphates, sulphonates and ammonium ions are given in Table I.

TABLE I.

OPERATING ELECTROLYTE SYSTEMS FOR ANIONIC (SULPHATES AND SULPHONATES) AND CATIONIC (AMMONIUM IONS) ANALYSIS OF SATURATED C₈–C₂₀ SURFACTANT MIXTURES

Parameter	Anionic separations	Cationic separations
Leading electrolyte		
Leading ion	Cl ⁻ 10 mM	K ⁺ 10 mM
Counter ion	L-Histidine 13.3 mM ^a	Acetate 20 mM ^a
pH	4.88 ^b	5.64 ^b
Additive	Tetraethylene glycol 2% (v/v)	Tetraethylene glycol 2% (v/v)
Terminating electrolyte	Picolinic acid 10 mM	Creatinine 10 mM
Solvent composition ^c	Methanol–water (80:20)	Methanol–water (50:50)

^a Total concentration of acidic and basic forms.

^b The unusual pH values of the L-histidine and acetate buffers can be accounted for by the acid–basic pK shifts in methanol–water mixtures. The pK of acetate is greatly increased whereas that of histidinium remains roughly unchanged. In addition, the purely aqueous feature of the electrode filling solutions is stressed here (see Experimental).

^c For both the leading and terminating electrolytes.

Running parameters

Volumes of 5 μl of sample mixtures were normally injected into the separation unit at the interface between the leading and the terminating electrolytes. A high voltage was then applied. The separations were performed under a driving current intensity of 120–130 μA for a typical time of 10 min. Then the current was switched to 20–30 μA just prior to zone recording. The total analysis time varied between about 20 and 30 min, according to the sample.

RESULTS AND DISCUSSION

Constraints arising from micellization phenomena

Industrially, ionic surfactants are mainly employed in neat aqueous media. It is therefore nat-

ural to seek purely aqueous separation conditions for their analysis by ITP, as first proposed earlier [18,19]. This approach is well documented by the values of absolute electrophoretic mobilities in water, m^0 , available in the literature, which vary from $27.1 \cdot 10^{-5}$ to $20.6 \cdot 10^{-5} \text{ cm}^2 \text{ V}^{-1} \text{ s}^{-1}$ on going from octyl- to octadecyltrimethylammonium ions and from $30.1 \cdot 10^{-5}$ to $24.9 \cdot 10^{-5} \text{ cm}^2 \text{ V}^{-1} \text{ s}^{-1}$ (at 25°C) on going from octyl to dodecyl sulphate [20]. From these mobility values, the possibility of separating surfactants differing in one carbon atom only can be contemplated.

For the case of cationic surfactants, a leading electrolyte consisting of an aqueous potassium acetate–acetic acid buffer was first tested. The interest in this buffer lies in the fact that, as soon as the voltage is applied, the analyte, most often in the

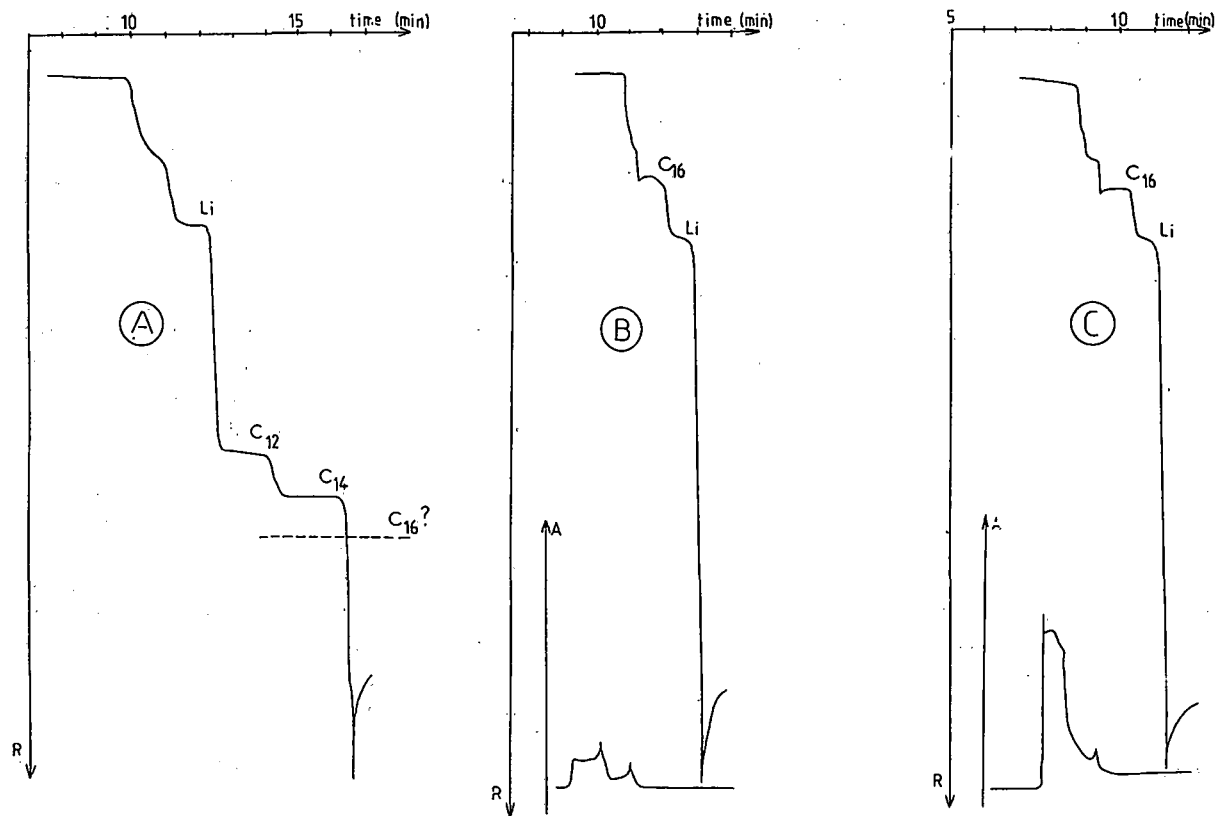


Fig. 1. Isotachopheretic migration of alkyltrimethylammonium ions with a purely aqueous electrolyte system. (A) C_{12} – C_{14} mixture; (B) C_{16} -ammonium ion; (C) C_{16} ion in the presence of cerol orange. Li^+ ion was added to all analyte solutions as a reference mobility marker. Leading electrolyte, 10 mM K^+ , acetate buffer (pH 4.7), terminating electrolyte, 10 mM acetic acid; detection current, 20 μA ; samples, 20 nmol each of C_{12}^+ , C_{14}^+ and C_{16}^+ -ammonium surfactants, 5 nmol Li^+ , 2 nmol cerol orange (injected volume 5 μl). Dashed line: expected step height of the C_{16} -ammonium ion.

form of an iodide or bromide salt in the samples, exchanges its counter ion for acetate, which greatly improves its solubility. As the analytes remain fully ionized over in whole operational pH range, pH is not a key parameter from the viewpoint of separability. Therefore the pH was adjusted to 4.7, which enables one simply to use acetic acid as the terminating electrolyte, with H^+ as the terminating ion. Likewise, promising results were easily obtained with dodecyl- and tetradecyltrimethylammonium ions, as shown in Fig. 1A. However, for alkyl chain lengths of 16 or more carbon atoms, apparently inconsistent isotachopherograms were obtained, insofar as the corresponding surfactant zones were detected before that of lithium ion used as a reference mobility marker ($m^0 = 40.1 \cdot 10^{-5} \text{ cm}^2 \text{ V}^{-1} \text{ s}^{-1}$ at 25°C [20]), and with a lower step height (Fig. 1B). This phenomenon can be attributed to the formation of a more mobile species in equilibrium with the free surfactant, *i.e.*, to the micellization of the long-chained surfactants. Using an ITP steady-state simulation program [21] and ignoring micellization phenomena, the equilibrium concentration of the hexadecyltrimethylammonium ion was evaluated to be 4.93 mM, while the critical micellar concentration (CMC) of the C_{16} -ammonium ion with acetate as counter ion was previously determined to be 1.6 mM. Under these conditions, the apparent mobility of the C_{16} -ammonium ion is much higher than those of both the C_{14} and C_{12} ions, and the prediction of the C_{16} step height derived from the measurements of the corresponding C_{12} and C_{14} step heights no longer holds true (Fig. 1A and B). Further, it has been shown that the electrophoretic mobility of an ionic micelle is *ca.* 2–3 times higher than that of the free ionic surfactant [22]. The presence of the aggregates was confirmed by injecting a mixture of hexadecyltrimethylammonium ion and cerol orange, a very slightly water-soluble neutral dye that can be solubilized by micelles (Fig. 1C). The UV detector trace revealed the presence of a UV-absorbing species in the zone of the C_{16} surfactant, which indicates that the neutral dye had migrated inside the hydrophobic micelle cavity (it should be noted that a constant delay was observed between the records of the UV absorbance and conductivity signals, owing to the distance between the location of the sensing cells, along the capillary). Further investigations on the isotachopheretic behaviour of

ionic micelles, reported elsewhere [23], have shown that ITP turns out to be a technique well adapted to the characterization of such micelles and the study of micellization phenomena.

As the purpose of this work was the determination of free surfactants, conditions preventing the formation of aggregates had to be designed. In this respect, Abe *et al.* [18] chose simply to lower the concentration of their leading ion to 5 mM, so that the equilibrium concentration of dodecyl sulphate in its zone would not reach the CMC of this species of *ca.* 8 mM. However, this approach is limited insofar as the concentration of the leading ion cannot be easily lowered to a sufficient extent to match the CMC values of longer alkyl-chain surfactants. This prompted us to explore the possibilities of using binary aqueous organic mixtures as solvents for the leading electrolyte. Methanol, 1- and 2-propanol and acetonitrile were successively tested in various proportions. For quaternary ammonium ions, mixtures containing up to 70% of methanol were required to prevent micellization below 10 mM with alkyl chain lengths up to C_{20} . The free surfactants can then be separated in the order of their electrophoretic mobilities.

Selection of the operating conditions

The optimization of the operating conditions is aimed at minimizing the zone disturbances mainly caused by electroosmotic flow or analyte adsorption on the capillary surface. Electroosmotic flow is usually suppressed in ITP by adding 0.1–0.3% of a neutral polymeric surfactant to the leading electrolyte. This solution is not applicable with ionic surfactant analytes, which could interact with these additives. However, electroosmosis is almost entirely suppressed, without the need of a neutral surfactant, when using electrolytes containing large proportions of methanol. Working under low pH conditions may further improve electroosmosis suppression, but the final choice of pH was mainly dictated by the solubilizing properties of the counter ion and by elimination of deleterious adsorption effects.

Hence, for quaternary ammonium ions, use of an acetate buffer was maintained with aqueous–organic electrolytes for the solubility reason already discussed. For alkyl sulphates, analyte adsorption on the capillary surface and subsequent mixing with

the terminating zone occurs when using a low pH leading electrolyte (e.g., a β -alanine buffer with an aqueous pH of 3.7). Such a phenomenon was avoided with a pH 5.5 aqueous histidine buffer. This improvement can be explained by the better protective role played by the increased number of fixed negative charges on the capillary surface at higher pH, as is apparent from the observation of the sharp resulting separation boundary between the last surfactant zone and the terminating zone. This boundary can be conveniently checked by systematically using a UV-absorbing species for the terminating

ion such as creatinine for cationic separations and picolinic acid for anionic separations.

Under the optimized operating conditions given in Table I, the ionic surfactants are separated into well defined, classical isotachophoretic zones, displaying increasing electrical resistance with increasing alkyl chain length. These conditions provide satisfactory qualitative resolution of any class of saturated C_8 - C_{20} alkyl-chain ionic surfactants, as shown in Fig. 2. The resolving power of the technique enables one to distinguish surfactants differing in one carbon atom only, as is the case for the

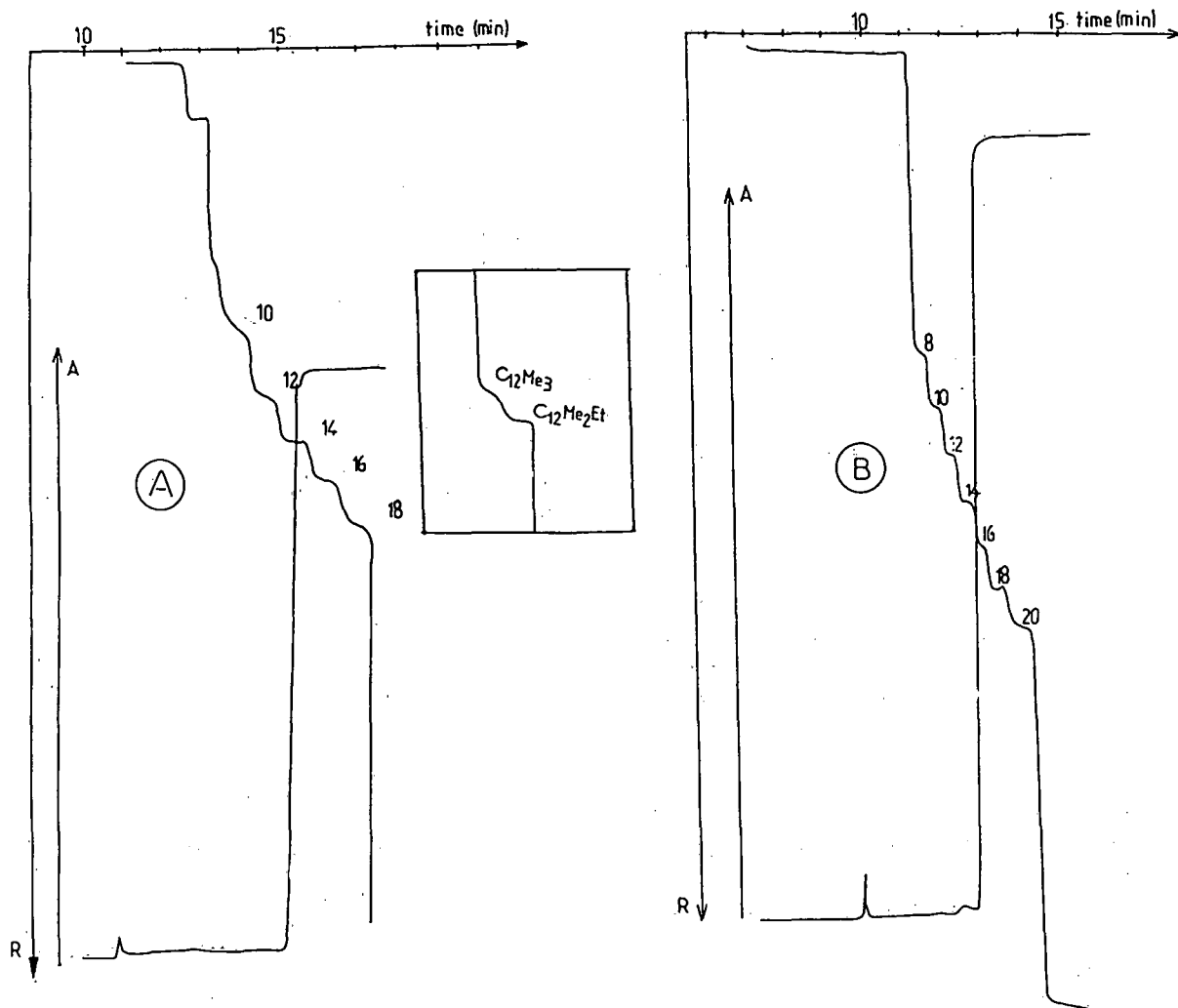


Fig. 2. ITP separation of C_8 - C_{20} alkyltrimethylammonium ions (A) and sulphonates (B). Electrolyte systems as in Table I. Detection current, $30 \mu A$; sample, standard mixtures containing 5 nmol of each surfactant ($5 \mu l$ injected). Inset: separation of dodecyltrimethylammonium and dodecylethyldimethylammonium ions under conditions identical with those for the above ammonium ions.

dodecyltrimethylammonium and dodecylethyldimethylammonium ions (see inset in Fig. 2). However, in practice the mass of the species seems to act as the major discriminating parameter, as surfactant ions of equal mass but different organic structures, such as the cetylpyridinium and benzyldimethyldodecylammonium ions (common MW 304.5), are not resolved from one another. This constitutes a limitation to the method performance compared with that of GC, which is capable of separating branched-chain isomers. In an attempt to define the discriminating principle better, the migration behaviour of perfluorooctyl sulphonate (MW 499) was investigated and compared with that of octyl sulphonate (MW 193). No resolution was observed using the conditions for anionic separations given in Table I. This result shows that the sizes of the CH_2 and CF_2 moieties are about the same, which in turn can only be explained by strong solvation of the carbonaceous chains. In conclusion, the actual basic discriminating parameter is not the mass, but rather the size of the surfactants, including solvation effects, even if size is uniquely related to mass or number of carbon atoms for the most commonly encountered hydrocarbonaceous chains. In addition, an improvement in the resolution of branched-chain isomers might be expected from these results by using solvents or electrolyte additives capable of inducing interactions directly related to chain length. However, this approach was not successful as neither investigations on organic solvents (such as 1- and 2-propanol and acetonitrile) nor the replacement of acetate counter ion by longer chain carboxylates (such as propanoate, butyrate, valerate and hexanoate) provided a noticeable improvement in the separation performances.

Quantitative aspects

The quantitative aspects of the method were first studied by injecting various amounts (0–50 nmol) of pure compounds. The linear relationship between amount injected and zone length was verified for octyl, dodecyl and eicosyl sulphate and also for decyl- and dodecyltrimethylammonium ions (Fig. 3A and B). It is noteworthy that the slopes of the straight standardization lines obtained are all of the same order of magnitude and differ only slightly for close homologous surfactants. This behaviour is in agreement with the approximate theoretical equa-

tion between zone length, l_i , and injected amount, n_i , of a solute i [21]:

$$l_i = [F U / I] [1 + m_c^0 / m_i^0] n_i \quad (1)$$

where F is the Faraday constant, U the chart speed of the recorder, I the current intensity at the time of detection and m_c^0 and m_i^0 the absolute mobilities of the counter ion c and solute i , respectively. Eqn. 1

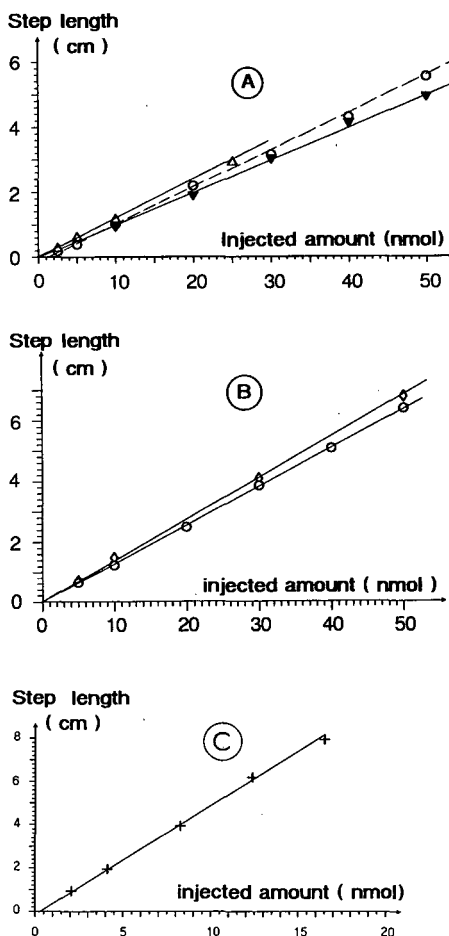


Fig. 3. Experimental plot of recorded step length versus amount of single solute injected for (A) alkyl sulphate and (B) ammonium surfactants. Electrolyte conditions as in Table I. Detection current, 30 μA ; recorder chart speed, 10 mm/min. (C) Extended precision plot relative to dodecyltrimethylammonium ion for a reduced range of injected amount. Operating conditions as for (A) and (B), except that the purely aqueous electrolyte system was used with 20 μA as detection current and 20 mm/min as recorder chart speed. (A) \blacktriangledown = Octyl sulphate; \circ = dodecyl sulphate; \triangle = eicosyl sulphate; (B) \diamond = $\text{C}_{12}\text{H}_{25}\text{N}(\text{CH}_3)_3 \text{Br}$; \circ = $\text{C}_{10}\text{H}_{21}\text{N}(\text{CH}_3)_3 \text{Br}$.

further indicates a slight increase in zone length with decreasing solute mobility, *i.e.*, with increasing chain length. This point was also supported by the experimental results (Fig. 3A and B). Hence conductivity detection provides the advantage over direct or indirect absorbance, often used in LC, that a single calibration point, realized with any surfactant standard of roughly intermediate chain length, suffices for a first estimate of the proportions of an unknown mixture. Moreover, to obtain an accurate analysis of a previously identified mixture, the availability of a reference mixture containing all the components of the mixture to be determined in known proportions is not required, as effective mobility is the only solute parameter influencing the zone length. For this purpose, only the plot between zone length and step height needs to be determined, and this can be done using a few commercially available surfactants belonging to the same class.

Separation capacity

A well known practical limitation of any ITP system is the finite amount of sample mixture that the system can separate. This limitation corresponds to the theoretical concept of separation capacity. If the injected amounts of two closely migrating solutes are beyond the respective capacities for these solutes, an ITP steady state is not reached at the time of detection and only a partial separation occurs, leaving an unresolved mixed zone. Thus, an intermediate conductivity step is detected between those of the pure species. In practice, pure and mixed zones can be differentiated by injecting two widely differing amounts of the sample mixture: when a mixed zone is still present, its length varies with the amount injected whereas the lengths of the resulting pure zones remain constant in length. The separation capacity, n_s , was experimentally determined for the model binary mixture of C_{12} - and C_{14} -sulphates and -trimethylammonium ions; n_s is defined as the maximum amount of the more mobile C_{12} surfactant that can be separated from the less mobile C_{14} surfactant under given isotachophoretic conditions (capillary dimensions, leading electrolyte composition and binary mixture proportions). Fig. 4 shows that linear plots were obtained for the inverse of the separation capacity, $1/n_s$, versus the ratio of molar C_{14} of C_{12} amounts injected, δ . This result is in agreement with theoretical expectations [21] and is

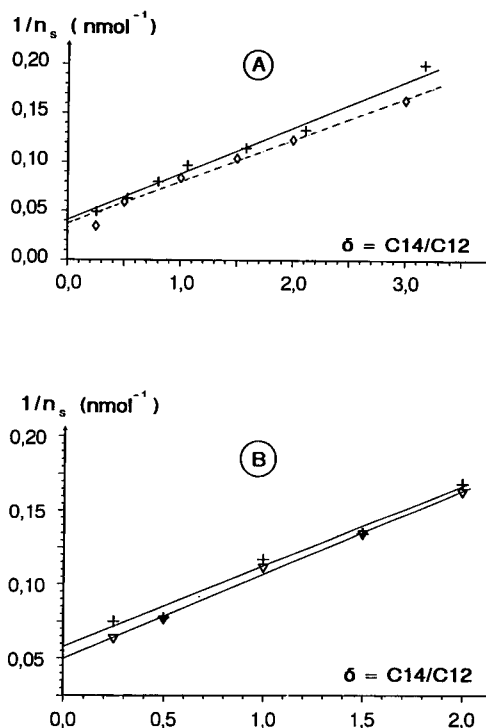


Fig. 4. Plot of the inverse of separation capacity, n_s , versus the molar ratio of C_{14} to C_{12} -alkyl surfactant amounts injected, δ . (A) Alkyltrimethylammonium ions; (B) alkyl sulphates. Electrolyte systems as in Table I, except for the solvent compositions: (A) \times = water; \diamond = water-methanol (50:50); (B) ∇ = water-methanol (20:80); \times = water-methanol (40:60).

a proof that both anionic and cationic surfactants exhibit normal ITP behaviour. Fig. 4 also shows that the percentage of methanol in the electrolyte has only a very slight influence on the separation capacity, which remains of the order of 10 nmol for equimolar binary mixtures. In contrast, it was ascertained that 1- or 2-propanol in place of methanol is very unfavourable with respect to separation capacity and hence separability. This phenomenon can be attributed to the fact that solvation of surfactant alkyl chains is stronger with 1- or 2-propanol than with methanol, resulting in more hindered, heavier structures. Consequently, the difference in electrophoretic mobilities of two close homologues such as the C_{12} and C_{14} surfactants tends to level off. These results again illustrate the significant role played by solvation effects in discriminating carbonaceous chains.

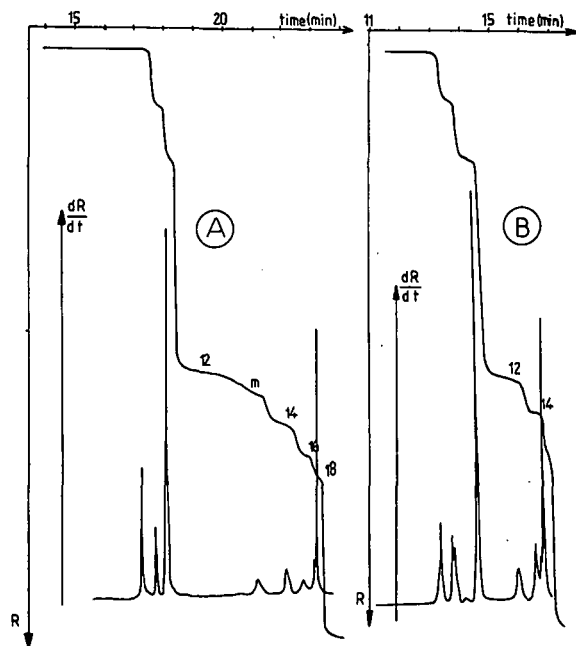


Fig. 5. Determination of the minor (A) and major (B) components of Noramium, a commercial quarternary ammonium surface-active agent. Electrolyte systems: see Table I but diluted to $6 \cdot 10^{-2} M$. Sample: (A) $5 \mu\text{l}$ of a 2.915 mg/ml Noramium solution in water; (B) $5 \mu\text{l}$ of a 1.615 mg/ml solution. The symbol *m* denotes a mixed zone between the C_{12} and C_{14} surfactants.

Application to the analysis of an industrial cationic surfactant formulation

The above ITP method was applied to the analysis of Noramium, a complex commercial formulation of quaternary ammonium ions of industrial in-

terest. This surface-active agent is available as a viscous concentrated solution containing 49–51% quarternary ammonium ions, 13–15% water and 35–37% 2-propanol (mass percent), according to the technical sheet provided by the manufacturer. It is derived from copra oil and its composition may vary according to season and the origin of the oil. Hence the proportion of some components may vary within 10% and only a mean distribution in the quaternary ammonium ions is available from the manufacturer. To analyse this sample accurately, we carried out four calibrations with pure standards of C_{12} – C_{18} surfactants. The analysis was carried out in two steps. First, a sample size corresponding to an overall dilution of 2.915 mg/ml in water was injected, in order to determine the proportions in minor components, mainly the C_{16} - and C_{18} -alkyltrimethylammonium ions, with good accuracy. It can be seen from Fig. 5A that neither the C_8 nor the C_{10} component was detected under such conditions, so the concentration of each of them can be evaluated to be less than 1% in the mixture, from the minimum detectable amount of the method. For such a sample size, an intermediate zone between those of dodecyl- and tetradecyltrimethylammonium ions was detected and further identified as a mixed zone of these components. Second, a sample of 1.652 mg/ml was injected in the same manner (Fig. 5B), which enabled one to determine the major C_{12} and C_{14} components in the absence of their mixed zone. Table II shows that the results afforded by the isotachophoretic method are in

TABLE II

COMPARISON BETWEEN THE MOLAR PERCENTAGE COMPOSITION OF NORAMIUM IN ALKYLTRIMETHYLAMMONIUM IONS DETERMINED BY ITP (THIS WORK) AND THE AVERAGE CORRESPONDING COMPOSITION GIVEN BY THE MANUFACTURER

The determination "without calibration" is simply the ratio of the step length of the corresponding compound to the sum of the lengths of all the surfactant steps.

Components (alkyltrimethylammonium ions)	ITP determination without calibration (mol%)	ITP determination with complete calibration (mol%)	Average composition according to the manufacturer (mol%)
C_8 and C_{10}	<1	<1	3.5 and 6
C_{12}	59.6	59.8	60
C_{14}	23.2	23.1	16–20
C_{16}	10.8	10.0	6–10
C_{18}	6.1	6.2	5

good agreement with the average composition given by the manufacturer. Further, the zone length calibration enabled us to determine the number of moles and then the mass of each component contained in the 1.652 mg/ml Noranium sample. The total mass of quaternary ammonium ions in this solution, and then the total mass percentage, can be derived. The result obtained, 49.7–50.7% of surfactant (in the chloride form) in the crude Noranium, suffers only from a 1% uncertainty, according to the precision of the method, and are in excellent agreement with the manufacturer's specification. Moreover, we ascertained the absence of free fatty amines by comparing an analysis in acidic medium (Table I) with the same one realized with a β -alanine-KOH buffer in 50% methanol (pH 10.6), which gave an identical result.

CONCLUSION

The absence of any stationary phase, a fairly large capillary inner diameter (*ca.* 0.5 mm) and a proper choice of electrolyte pH and additives has resulted in tail-free, stable steady-state ITP zones with any of the ionic surfactant classes. Although the separation capacity might be further improved by the finding of a still more suitable solvent composition or electrolyte additive, the above isotachophoretic method, associated with conductivity detection, affords analytical performances comparable to those of the classical chromatographic methods. Surfactants differing in only one carbon atom can be separated within an analysis time of *ca.* 20–30 min. The mass limit of detection is of the order of 0.5 nmol for about 10 μ l injected, which gives a concentration limit of detection of *ca.* $5 \cdot 10^{-5}$ M. However, promising experiments have shown that, by using electrokinetic sample introduction and applying ITP principles, volumes of a few hundred microlitres of dilute samples could be preconcentrated at the inlet of a capillary having such dimensions. This should allow the concentration limit of detection to be lowered by at least a factor of 10.

For the purpose of these analyses, our efforts were aimed at avoiding micelle formation, so that

only free surfactants can be present. In addition, the preliminary results on the isotachophoretic behaviour of ionic micelles presented here have suggested a new application area for ITP as a method for the determination of ionic micelle characteristics, such as CMC, charge ratio or neutral solute solubility. Likewise, ITP can be expected to become a method very well adapted to the characterization of small ionic polymers. Work is in progress in both directions.

REFERENCES

- 1 K. Noguchi, Y. Yanagihara, M. Kosai and B. Katagama, *J. Chromatogr.*, 461 (1989) 365.
- 2 P. L. Desbène, B. Desmazières and J. J. Basselier, *J. Chromatogr.*, 461 (1989) 305.
- 3 P. Varughese, M. E. Gangoda and R. K. Gilpin, *J. Chromatogr.*, 499 (1990) 469.
- 4 P. Sandra and F. David, *J. High Resolut. Chromatogr.*, 13 (1990) 414.
- 5 Y. Liu, F. Yang and C. Pohl, *J. Microcol. Sep.*, 2 (1990) 245.
- 6 F. Smedes, J. C. Kraak, C. E. Werkhoven-Goewie, U. A. Th. Brinkman and R. W. Frei, *J. Chromatogr.*, 247 (1982) 123.
- 7 M. Kudoh and K. Tsuji, *J. Chromatogr.*, 294 (1984) 456.
- 8 D. Thomas and J. L. Rocca, *Analisis*, 7 (1979) 386.
- 9 J. Kawase, Y. Takao and K. Tsuji, *J. Chromatogr.*, 262 (1983) 408.
- 10 J. Kawase, Y. Takao and K. Tsuji, *J. Chromatogr.*, 262 (1983) 293.
- 11 J. Weiss, *J. Chromatogr.*, 353 (1986) 303.
- 12 G. R. Bear, *J. Chromatogr.*, 371 (1986) 387.
- 13 C. J. Dowle, W. C. Campbell and B. G. Cooksey, *Analyst*, 114 (1989) 883.
- 14 R. Caesar, H. Weightman and G. R. Mintz, *J. Chromatogr.*, 478 (1989) 191.
- 15 G. R. Bear, *J. Chromatogr.*, 459 (1988) 91.
- 16 T. Barth, *Anal. Chem.*, 59 (1987) 2232.
- 17 M. Koval, D. Kaniansky, M. Hutta and R. Lacko, *J. Chromatogr.*, 325 (1985) 151.
- 18 M. Abe, T. Yamaguchi, M. Nakaname, K. Watanabe and K. Ogino, *Yukagaku*, 37 (1988) 1000.
- 19 J. L. Ammerdorffer, A. A. G. Lemmens, A. L. German and F. M. Everaerts, *Polymer Commun.*, 31 (1990) 61.
- 20 R. C. Weast (Editor), *Handbook of Chemistry and Physics*, CRC Press, Boca Raton, FL, 68th ed., 1988.
- 21 D. Mosset, P. Gareil, J. Desbarres and R. Rosset, *J. Chromatogr.*, 390 (1987) 69.
- 22 K. Otsuka, S. Terabe and T. Ando, *J. Chromatogr.*, 332 (1985) 219.
- 23 C. Tribet, R. Gaboriaud and P. Gareil, *Electrochim. Acta*, 37 (1992), in press.

Short Communication

Reversed-phase high-performance liquid chromatographic and derivative UV spectrophotometric determination of α -phenylethylamine in phosphomycin

Gabriella Gazzani, Giovanna Stoppini and Carlo Gandini

Department of Pharmaceutical Chemistry, University of Pavia, Viale Taramelli 12, 27100 Pavia (Italy)

Antonio Bettero

Institute of Pharmaceutical and Toxicological Chemistry, University of Milan, Milan (Italy)

(First received December 30th, 1991; revised manuscript received May 12th, 1992)

ABSTRACT

Two sensitive and selective methods were developed for the evaluation of α -phenylethylamine (α -PEA), an impurity possibly present in the antibiotic phosphomycin (PHO). The reversed-phase high-performance liquid chromatographic method uses a LiChrosorb NH₂ column with acetonitrile–0.1 M NaH₂PO₄ · H₂O buffer as eluent and allows the simultaneous detection of PHO and α -PEA in a complex matrix such as pharmaceutical preparations. The amine gives a linear detection response over the range 15–85 μ g/ml. The derivative spectrophotometric method can specifically discriminate the amine in the range 230–280 nm. The α -PEA concentration is determined by measuring the distance between the maximum at 250 nm and the adjoining minimum at 248 nm in the second-derivative spectrum. A linear correlation was found in the concentration range 15–160 μ g/ml. For both procedures, no sample pretreatment is required.

INTRODUCTION

(+)- α -Phenylethylamine (α -PEA) is used as a reagent in the synthesis of phosphomycin (PHO) to separate it, as (+)- α -phenylethylammonium (–)-*cis*-1,2-epoxypropylphosphonate, from its isomer [1,2]. For this reason, the antibiotic may contain this bioactive amine [3,4] as an impurity. Different methods, based on thin-layer chromatographic [5],

gas chromatographic [6–8] and high-performance liquid chromatographic (HPLC) [9–11] techniques, are available for the simultaneous detection of this amine in fermented foods in which it occurs naturally. The methods proposed are generally complex and time consuming, and hence they are not suitable for the routine analysis needed for the quality control of pharmaceutical, parapharmaceutical and food products.

The aim of this investigation was to develop simple, high-resolution methods for the detection of α -PEA in raw materials and in pharmaceutical preparations containing PHO.

Correspondence to: G. Gazzani, Department of Pharmaceutical Chemistry, University of Pavia, Viale Taramelli 12, 27100 Pavia, Italy.

EXPERIMENTAL

Reagents and chemicals

Sodium dihydrogenphosphate monohydrate ($\text{NaH}_2\text{PO}_4 \cdot \text{H}_2\text{O}$), sodium hydroxide and hydrochloric acid of analytical-reagent grade and acetonitrile of HPLC quality (LiChrosolv) were purchased from Merck (Darmstadt, Germany). Phosphomycin, calcium and disodium salts, and α -phenylethylamine were obtained from Sigma (St. Louis, MO, USA).

HPLC

All separations were carried out isocratically at room temperature using a Merck–Hitachi (Tokyo, Japan) Model 655A-11 liquid chromatograph, equipped with a Rheodyne (Cotati, CA, USA) Model 7125 injector (20- μl loop), a Model 655A variable-wavelength UV detector and a D2000 Chromato-integrator (Merck–Hitachi). A stainless-steel LiChrosorb NH_2 (particle size 10 μm) column (250 \times 4 mm I.D.) and a LiChrocart NH_2 guard-column (4 \times 4 mm I.D.) were obtained from Merck. The mobile phase was acetonitrile–0.1 M $\text{NaH}_2\text{PO}_4 \cdot \text{H}_2\text{O}$ buffer solution (pH 7.5) (35:65, v/v). Water for preparing buffer solutions was doubly distilled in an all-glass apparatus. All solvents were filtered through Millipore (Milford, MA, USA) HA filters (0.45 μm) and degassed ultrasonically before use. The flow-rate was 1.5 ml/min and the column effluent was monitored at 255 nm. Before analysis all samples were filtered through Millipore HV filters (0.45 μm).

Spectrophotometry

A Perkin-Elmer (Oak Brook, IL, USA) Model 552 double-beam spectrophotometer, a Model 561 recorder and 10-mm quartz cells were used. Normal and second-derivative parameters were range 380/190 nm, 1.0 ± 0.2 a.u.f.s., 0.5 response, scanning speed 120 nm/min and recorder chart speed 20 nm/cm.

Stock solutions

Standard solutions were prepared by dissolving 30–40 mg of α -PEA in a 50-ml volumetric flask with doubly distilled water. These solutions were then diluted to obtain solutions containing 5–200 $\mu\text{g}/\text{ml}$ of the amine. Standard α -PEA solutions were em-

ployed to prepare synthetic mixtures containing PHO disodium salt at a concentration of 50 mg/ml. All freshly prepared solutions were stored at 4°C; under these conditions they were stable for 1 week.

Samples

PHO disodium salt. Approximately 2 g of each sample were dissolved in doubly distilled water and diluted to 50 ml.

PHO calcium salt. Approximately 2 g of each sample were dispersed in 45 ml of doubly distilled water, mixed thoroughly for 30 min and centrifuged; the supernatant was filtered through Whatman 40 paper and diluted to 50 ml.

Antibiotic tablets. Twenty tablets of each commercial product were finely powdered. Approximately 4 g of each sample were dispersed in 45 ml of doubly distilled water and treated as described for the preparation of PHO calcium salt samples.

Calibration

Stock solutions of α -PEA and α -PEA with PHO were used to construct the calibration graphs. Linear least-squares regression was used. Using a Cartesian coordinate system, the α -PEA concentrations ($\mu\text{g}/\text{ml}$) were plotted on the abscissa and the corresponding analytical responses on the ordinate. The amounts of the amine present were evaluated either as the peak areas, as estimated by the integrator, when the HPLC method was used, or the distances

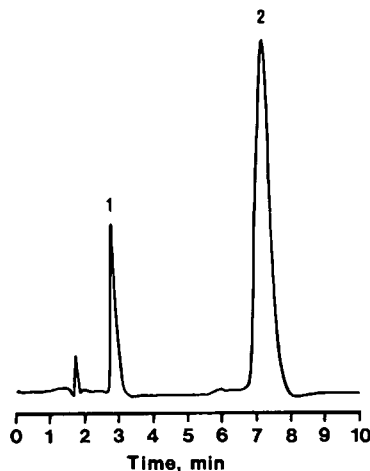


Fig. 1. RP-HPLC separation of (1) α -PEA (80 $\mu\text{g}/\text{ml}$) and (2) PHO (50 mg/ml).

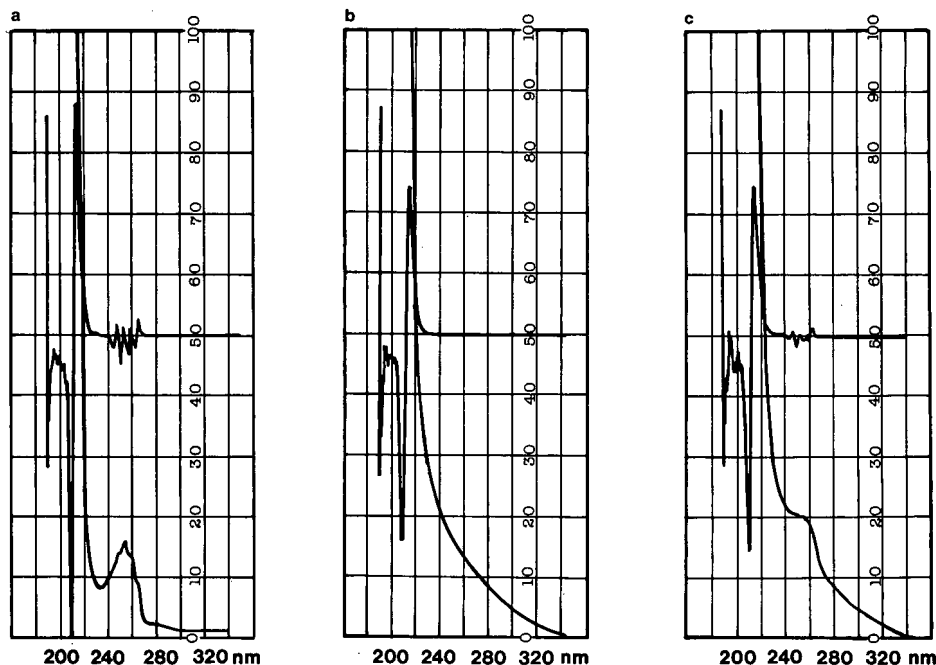


Fig. 2. Normal and second-derivative spectra of (a) α -PEA, (b) PHO and (c) a mixture of PHO (50 mg/ml) and α -PEA (0.1%).

measured as mm, between the maximum at 250 nm and the adjacent minimum at 248 nm, when the spectrophotometric method was applied. The calibration graphs constructed with α -PEA alone or in presence of PHO obeyed the same regression equations ($y = 199.315x$, $r = 0.999$, for the RP-HPLC method, and $y = 0.034x$, $r = 0.998$, for the spectrophotometric method). With both methods the intercepts did not differ statistically from zero.

RESULTS AND DISCUSSION

HPLC method

Fig. 1 shows the chromatograms obtained on analysing the standards of α -PEA and PHO. Statistical analysis did not reveal significant differences ($p < 0.01$) between the calibration graphs obtained using solutions containing the standard of amine alone or solutions containing the amine and a fixed

TABLE I

STATISTICAL ANALYSIS OF THE RESULTS OBTAINED ON ANALYSING A SYNTHETIC MIXTURE (50 mg/ml PHO)

Method	α -PEA concentration ($\mu\text{g/ml}$)	α -PEA found ^a ($\mu\text{g/ml}$)	Mean error (%)	S.D. ^b	R.S.D. ^c (%)
RP-HPLC	65.6	65.9	0.56	1.03	1.56
Second-derivative	68.0	68.7	1.03	1.25	1.82

^a Mean of six determinations.

^b S.D. = standard deviation.

^c R.S.D. = relative standard deviation.

concentration of phosphomycin. A linear detection response was obtained between peak area and concentration of α -PEA over the range 15–85 $\mu\text{g}/\text{ml}$ (corresponding to 0.3–1.7 μg injected), the detection limit for the impurity being 2 $\mu\text{g}/\text{ml}$ (twice the signal-to-noise ratio). The accuracy and precision of the method are shown in Table I.

The method was used for the analysis of several commercial samples of PHO disodium and calcium salts and several pharmaceutical preparations containing the antibiotic. Only one sample of PHO calcium salt was shown to contain unquantifiable traces of the amine.

Spectrophotometric method

Fig. 2a and b show the absorbance spectra and the second-derivative traces in the wavelength range 300–190 nm obtained for standards of α -PEA and PHO, respectively. The second-derivative UV profile of a mixture of the two compounds (0.1% α -PEA) is shown in Fig. 2c.

It is clear that the second-derivative method can discriminate the amine in the wavelength region 230–280.

Using this method there were no significant differences ($p < 0.01$) in the calibration graphs obtained with standard solutions of the amine and the amine plus an excess amount of the antibiotic. This confirms the absence of a matrix effect. A linear correlation was found in the concentration range 15–160 $\mu\text{g}/\text{ml}$. The detection limit was 4 $\mu\text{g}/\text{ml}$ (twice the signal-to-noise ratio). The precision and the accuracy of this method are reported Table I. The effectiveness of the resolution with this method was evaluated by analysing the same samples as tested with the HPLC method. The results confirmed the presence of trace amounts of the amine in one sample of phosphomycin calcium salt.

CONCLUSIONS

Two sensitive and specific methods have been developed for the accurate determination of α -phenyl-

ethylamine. Both methods are rapid and, further, they do not require preliminary extraction treatments; the samples are simply dissolved in water and the solutions must be filtered only if the matrix is not hydrosoluble. The HPLC method allows the simultaneous detection of PHO and its impurity in complex matrices such as pharmaceutical preparations.

The second-derivative spectrophotometric method is suitable for the determination of α -PEA in simple matrices. It is very rapid and does not involve destruction of the matrix, hence it is very useful for the validation of raw material batches or for stability studies.

ACKNOWLEDGEMENT

This work was supported by a grant from the Ministero dell'Università e della Ricerca Scientifica e Tecnologica.

REFERENCES

- 1 E. J. Glamkowski, G. Gal, A. J. Davison and M. Sleztinger, *J. Org. Chem.*, 35 (1970) 3510–3512.
- 2 T. Otsuki, Y. Okamoto and H. Sakurai, *Synthesis*, (1983) 811–813.
- 3 J. Luthy and C. Schlatter, *Z. Lebensm.-Unters.-Forsch.*, 177 (1983) 439–443.
- 4 W. Lovemberg, *Toxicants Occurring Naturally in Foods*. Publication No. 1354, National Academy of Science, Washington, D.C., 1970.
- 5 K. D. H. Chin and P. E. Koeler, *J. Food. Sci.*, 48 (1983) 1826–1828.
- 6 W. F. Staruszhievicz and J. F. Bond, *J. Assoc. Off. Anal. Chem.*, 30 (1981) 584–591.
- 7 S. Yamamoto, H. Itano, H. Kataoka and N. Mekital, *J. Agric Food. Chem.*, 30 (1981) 435–439.
- 8 G. B. Baker, J. T. F. Wong, R. T. Coutts and F. M. Pasutto, *J. Chromatogr.*, 392 (1987) 317–331.
- 9 C. Buteau, C. L. Duitschaever and G. C. Ashton, *J. Chromatogr.*, 284 (1984) 201–210.
- 10 H. M. L. J. Joosten and C. Olieman, *J. Chromatogr.*, 356 (1986) 311–319.
- 11 M. A. J. S. Van Boekel and A. P. Arentsen-Stasse, *J. Chromatogr.*, 389 (1987) 267–272.

Short Communication

High-performance liquid chromatographic method for the enantiomeric separation of the chiral metabolites of midazolam

J. Drewe

Departments of Anaesthesia and Research, University Clinic/Kantonsspital, CH-4031 Basle (Switzerland)

E. Küsters

Chemical Process and Research Development, Sandoz Pharma Ltd., CH-4002 Basle (Switzerland)

(First received April 27th, 1992; revised manuscript received June 19th, 1992)

ABSTRACT

The enantiomeric resolution of the chiral metabolites of midazolam, 4-hydroxymidazolam and 1,4-dihydroxymidazolam, by high-performance liquid chromatography on a chiral stationary phase containing immobilized ovomucoid is described (no derivatization was necessary). Large separation factors (up to $\alpha = 2.9$) were obtained by varying the type and amount of organic modifier in the mobile phase. The system so far developed is recommended for monitoring possible differences in the stereoselective metabolism of midazolam.

INTRODUCTION

Different bioactive properties of enantiomers of pharmaceutical racemates have often been outlined [1]. As a consequence, pharmacological and pharmacokinetic studies of a new drug are nowadays carried out only on single enantiomers. Whereas much attention has been focused on the different properties of chiral drugs, less attention has been paid to the stereoselective properties of chiral metabolites, especially when the drug itself is achiral.

The achiral short-acting benzodiazepine midazo-

lam is commonly used as preanaesthetic medication and in the induction and maintenance of anaesthesia [2,3]. The metabolic pathway of midazolam is shown in Fig. 1. The main metabolic route of the drug in humans is the hepatic formation of the achiral metabolite 1-hydroxymethylmidazolam (1-OH) [4], which is further conjugated to form the inactive 1-OH-glucuronide. From the stereochemical point of view, the metabolic pathways, which include the formation of 4-hydroxymidazolam (4-OH) and 1,4-dihydroxymidazolam (1,4-diOH), are of interest. These metabolites contain an asymmetric centre, and therefore some additional pharmacological routes are theoretically possible, especially in different disease states.

Analytical assays for midazolam and its metabo-

Correspondence to: Dr. Jürgen Drewe, Departments of Anaesthesia and Research, University Clinic/Kantonsspital, Hebelstrasse 20, CH-4031, Basle, Switzerland.

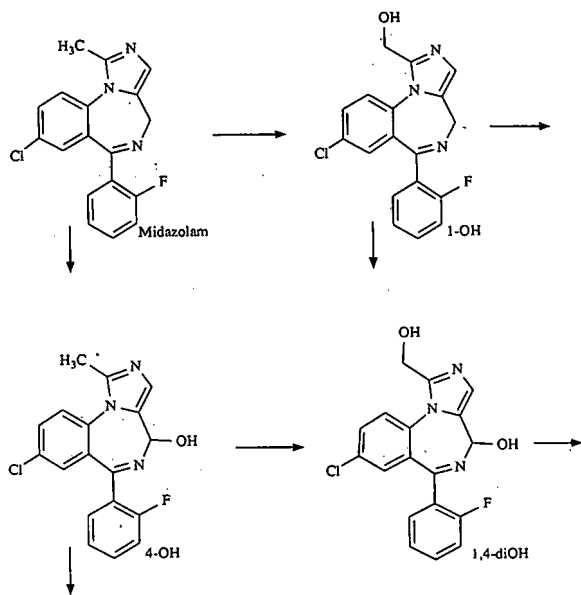


Fig. 1. Structures of midazolam and its main metabolites, 1-hydroxymidazolam, 4-hydroxymidazolam and 1,4-dihydroxy midazolam.

lites include gas chromatography [5-12] and high-performance liquid chromatography (HPLC) [7,11,13-17]. No cited approach considers stereochemical aspects.

For monitoring possible differences in the stereoselective metabolism it is necessary to develop

analytical methods, that allow the enantiomeric separation of 4-OH and 1,4-diOH. The aim of this publication is to show the enantiomeric separation of 4-OH and 1,4-diOH using HPLC with a chiral stationary phase.

EXPERIMENTAL

Materials

4-OH and 1,4-diOH were kindly provided by Hoffmann-La Roche (Basle, Switzerland). Acetonitrile and ethanol were of analytical grade.

Apparatus

A Kontron HPLC pump (Model 420) was used in conjunction with a variable-wavelength Kontron UV detector (Model 430). The separation was performed on an ovomucoid-based HPLC column (Ultron ES-OVM, 5 μ m particle size with 100- Å pores, 15 \times 0.46 cm I.D.; Shinwa Chemical Industries, Kyoto, Japan). Mobile phase and chromatographic parameters are given in the legends of Figs. 2 and 3.

RESULTS AND DISCUSSION

The present investigations were made with a column containing immobilized ovomucoid. Its use for enantiomeric separation has been reported by Miwa *et al.* [18,19]. The advantages of this ovomucoid column for chiral HPLC separations include good

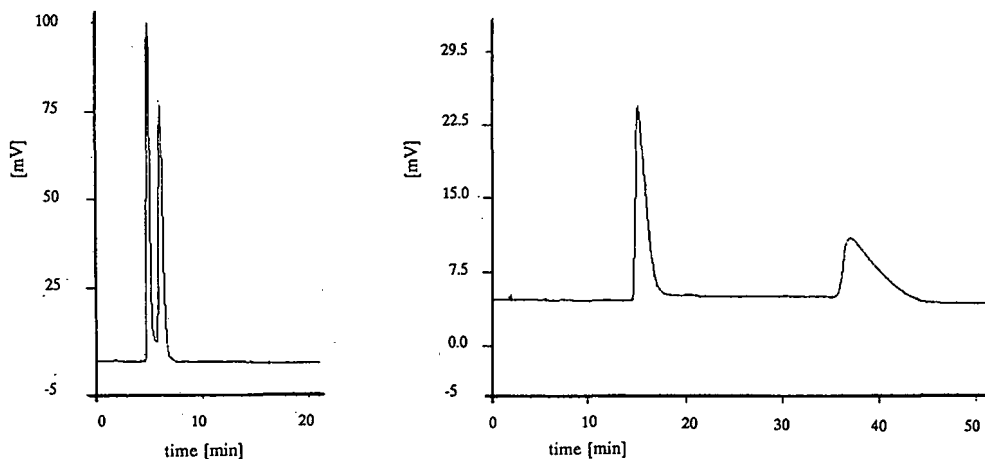


Fig. 2. Enantiomeric separation of 4-hydroxymidazolam. Mobile phase: 20 mM ammoniumphosphate buffer with 20% acetonitrile (left curve) and 10% acetonitrile (right curve), with phosphoric acid adjusted to pH 7. Flow-rate: 1.0 ml/min. UV detection: 220 nm. Injected volume: 20 μ l (containing 2 μ g of metabolites).

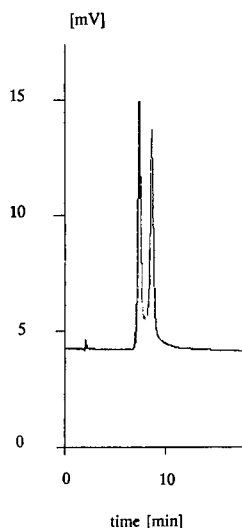


Fig. 3. Enantiomeric separation of 1,4-dihydroxymidazolam. Mobile phase: 10% acetonitrile with phosphoric acid adjusted to pH 7; other parameters as in Fig. 2.

stability to changes in temperature, pH, organic solvent composition and antitrypsin activity [20]. Systematic procedures have recently been developed by Kirkland *et al.* [21] and Wada *et al.* [22].

The aim of the present study was to achieve baseline separations of the enantiomers of both 4-OH and 1,4-diOH with capacity factors below 15 for all four components in a single run. A buffer concentration of 20 mM was used because lower ionic strengths are expected to give higher k' -values [22]. The pH value was maintained at 7 and the temperature at 25°C. Changes were made only with respect to the type and amount of uncharged modifier. The influence of organic modifier is shown in Table I for

TABLE I
INFLUENCE OF ORGANIC MODIFIER ON k' AND SEPARATION FACTOR (α)

Modifier	k_1	k_2	α
<i>4-Hydroxymidazolam</i>			
10% Ethanol	No separation within 2 h		
10% Acetonitrile	7.8	19.3	2.5
20% Ethanol	3.8	11.1	2.9
20% Acetonitrile	2.6	3.3	1.2
<i>1,4-Dihydroxymidazolam</i>			
10% Acetonitrile	3.6	4.2	1.2

the enantiomeric separation of 4-OH. The chromatograms are displayed in Fig. 2 (for 4-OH) and Fig. 3 (for 1,4-diOH). As expected from an earlier work by Kirkland *et al.* [21], large decreases in α and k' -values were observed with increasing amounts of acetonitrile and ethanol. The retention times and the separation factor obtained with ethanol are significantly larger than those obtained with acetonitrile. Not having the pure enantiomers as a reference, the separations were confirmed only with diode-array detection. Owing to its less hydrophobic character, the retention of 1,4-diOH is lower than that of 4-OH.

For a simultaneous determination of the enantiomers of 4-OH and 1,4-diOH, 10% acetonitrile should be chosen as organic modifier. With this chromatographic system studies involving stereoselective pharmacokinetics and/or metabolism could be achieved.

REFERENCES

- 1 E. J. Ariëns, *Eur. J. Clin. Pharmacol.*, 26 (1984) 663.
- 2 R. J. Fragen, F. Gahl and N. Calowell, *Anesthesiology*, 49 (1978) 41.
- 3 I. Helci, R. Lupolover, J.-P. Buch and R. Amrein, *Arzneim.-Forsch.*, 31 (1981), 2284.
- 4 I. F. I. De Kroon, P. N. J. Langendijk and P. N. F. C. De Goede, *J. Chromatogr.*, 491 (1989) 107.
- 5 R. M. Arendt, D. J. Greenblatt and W. A. Garland, *Pharmacology*, 29 (1984) 158.
- 6 P. Coassolo, C. Aubert, Y. Sumitapura and J.P. Cano, *J. High Resolut. Chromatogr. Chromatogr. Commun.*, 5 (1982) 31.
- 7 J. X. De Vries, R. Judie, I. Walter-Sack and R. Conradi, *Biomed. Chromatogr.*, 4 (1990) 28.
- 8 P. Heizmann, J. C. Jordan and B. Ludwig, *J. Chromatogr.*, 415 (1987) 170.
- 9 P. Heizmann and R. von Alten, *J. High Resolut. Chromatogr. Chromatogr. Commun.*, 4 (1981) 266.
- 10 M. Sunzel, *J. Chromatogr.*, 491 (1989) 455.
- 11 J. Vasiliades and C. Owens, *J. Chromatogr.*, 182 (1988) 439.
- 12 P. Crevat-Pisano, S. Dragna, C. Granthil, P. Coassolo and J. P. Cano, *J. Pharmacol.*, 38 (1986) 578.
- 13 G. B. Kraus, R. G. Gruber, R. Knoll, U. Danner, *Anaesthetist*, 38 (1988) 658.
- 14 J. Vasiliades and T. H. Sahawnd, *J. Chromatogr.*, 228 (1982) 195.
- 15 C. V. Puglisi, J. Pao, F. J. Ferrara and J. A. de Silva, *J. Chromatogr.*, 344 (1985) 199.
- 16 J. Vasiliades and T. H. Sahawnd, *J. Chromatogr.*, 225 (1981) 266.
- 17 T. B. Vree, A. M. Baars, L. H. D. Booij and J. J. Driessen, *Arzneim.-Forsch.*, 31 (1981) 2215.

- 18 T. Miwa, T. Miyakawa and M. Kayano, *Chem. Pharm. Bull.*, 35 (1987) 682.
- 19 T. Miwa, T. Miyakawa and M. Kayano, *J. Chromatogr.*, 408 (1987) 316.
- 20 M. D. Melamed, in A. Gottschalk (Editor), *Glycoproteins*, Elsevier, New York, 1966, p. 317.
- 21 K. M. Kirkland, K. L. Neilson and D. A. McCombs, *J. Chromatogr.*, 545 (1991) 43.
- 22 H. Wada, H. Fujima and J. Haginaka, presented at the *15th International Symposium on Liquid Chromatography, HPLC '91, Basle, Switzerland, 1991*, poster.

Short Communication

Determination of folic acid in an elemental diet by high-performance liquid chromatography with UV detection

Hiroshi Iwase

Ajinomoto Co., Inc., Kawasaki Factory, 1-1 Suzuki-cho, Kawasaki-ku, Kawasaki (Japan)

(First received March 11th, 1992; revised manuscript received June 3rd, 1992)

ABSTRACT

Determination of folic acid (550 ng/g) in an elemental diet containing 46 compounds at concentrations at least $0.02 \cdot 10^6$ times higher than that of folic acid was performed by high-performance liquid chromatography with ultraviolet detection at 360 nm using acetonitrile–water (pH 2.1, adjusted with phosphoric acid) (9:91) with the addition of 1 mM ethylenediaminetetraacetic acid disodium salt as the mobile phase. This method is suitable for the determination of folic acid in an elemental diet, because it is simple, rapid, sensitive and reproducible. The calibration graph was linear in the range 0–0.6 μg . Recovery of folic acid was about 95% by the standard addition method. There was good agreement between the indicated and found folic acid concentrations.

INTRODUCTION

Numerous methods have been developed for the analysis of folic acid, including spectrophotometry [1,2], a microbiological method [3] and high-performance liquid chromatography (HPLC) [4–6]. The content of folic acid in human blood from cancer patients is less than in normal subjects [6].

The measurement of folic acid in an elemental diet (commercial name Elental, Ajinomoto, Kawasaki, Japan) containing 46 compounds (*e.g.* amino acids, vitamins, organic acids, soybean oil, dextrin, minerals) at concentrations at least $0.02 \cdot 10^6$ times higher than that of folic acid [7] has proved to be valuable for process control, quality control purposes and clinical chemistry.

Spectrophotometry is not suitable for complex sample matrices. Microbiological methods have generally been used for the routine determination of vitamins. However, this method is tedious and time-consuming [3,8]. The analysis of folic acid has been performed by HPLC. However, HPLC cannot be used for the routine determination of folic acid in complex sample matrices such as Elental, because experimental conditions for the sample preparation such as concentration of trace amounts of folic acid and removing interferences caused by the complex sample matrices have not been investigated in detail.

Previous papers [8,9] have reported the routine analysis of cyanocobalamin and ascorbic acid in Elental. The present paper deals with the routine determination of folic acid (550 ng/g) in Elental. Routine determination of folic acid was performed by HPLC with UV detection at 360 nm, a wavelength that is quite specific to folic acid, using aceto-

Correspondence to: Dr. H. Iwase, Ajinomoto Co., Inc., Kawasaki Factory, 1-1 Suzuki-cho, Kawasaki-ku, Kawasaki, Japan.

nitrile–water (pH 2.1, adjusted with phosphoric acid) (9:91) with addition of 1 mM ethylenediaminetetraacetic acid disodium salt (Na_2EDTA) as the mobile phase.

EXPERIMENTAL

Reagents and materials

Folic acid used in this study was of Japanese Pharmacopeia standard. Acetonitrile (Wako, Osaka, Japan) was of HPLC grade. Other reagents were all of analytical grade.

Apparatus and conditions

A Model 655 A-11 high-performance liquid chromatograph (Hitachi, Tokyo, Japan) equipped with a Model 655 A variable-wavelength detector (Hitachi, Tokyo, Japan) set at 360 nm was used. The samples were applied by a Rheodyne Model 7125 sample loop injector with an effective volume of 2 ml. HPLC was carried out on a 25 X 0.46 cm I.D. column of Capcellpak C_{18} (5 μm) (Shiseido, Tokyo, Japan) using acetonitrile–water (pH 2.1, adjusted with phosphoric acid) (9:91) with 1 mM Na_2EDTA as the mobile phase at a flow-rate of 0.6 ml/min and a column temperature of 35°C. A Shimadzu UV-2100 UV variable-wavelength recording spectrophotometer (Shimadzu, Kyoto, Japan) was used for the absorption spectra.

Sample preparation

To a solution of Elental (20 g) dissolved completely in deionized water (60 ml) on a water bath at 50°C was added sodium chloride (10 g). After this solution was allowed to stand at room temperature for 30 min, it was accurately diluted to 100 ml with deionized water and then this solution was extracted with hexane (10 ml) for 3 min to remove oils. This aqueous layer was used for the test sample. An aliquot (2 ml) was injected into the chromatograph.

Folic acid was stable in aqueous solution at 50°C for 1 h.

RESULTS AND DISCUSSION

Chromatography

Not only folic acid, but also other vitamins, amino acids and organic acids absorb in UV region. Folic acid shows UV absorbance at around 280 and

360 nm. The absorbance at 360 nm is quite specific to folic acid. Riboflavin and cyanocobalamin also have absorbance at around 360 nm.

The first choice of wavelength to achieve highly sensitive detection of folic acid was 280 nm. However, many unknown overloading peaks were observed on the chromatogram, and folic acid could not be identified.

The second choice was 360 nm in order to eliminate co-existing compounds from the chromatograms. In addition, the effect of adding Na_2EDTA to the mobile phase on the determination of folic acid was also examined. Overloading peaks were practically eliminated in this way and folic acid could be observed on the chromatogram. When no Na_2EDTA was added to the mobile phase, the folic acid peak was slightly broadened and an unknown peak with a slight inflection was observed on the chromatogram. This may mean that folic acid and unknown compounds chelate with co-existing metals. On the other hand, peaks of folic acid and unknown compounds with sufficient intensity were obtained by adding Na_2EDTA to the mobile phase (Fig. 1), because metals could be masked with Na_2EDTA .

From the above, it is clear that the addition of Na_2EDTA to the mobile phase was necessary to obtain sharp peaks. Complete elution required about 25 min. Despite the large injection volume (2 ml), folic acid was concentrated on a Capcellpak C_{18} column, separated and then detected at 360 nm without interference from any other compounds. It was necessary to inject 2 ml of sample solution for the determination because folic acid in Elental is present in a very small amount. As a possible modification of this method, sample enrichment at the top of column might be considered. A similar technique has been used in ion chromatography. For the identification of folic acid in Elental, a freshly prepared model solution containing 45 compounds with no added folic acid was examined by this method. No folic acid peak was observed on the chromatogram. Thus, the procedure used here might be considered advantageous for the routine determination of folic acid in complex mixtures.

Determination of folic acid

The calibration graph for folic acid was constructed by plotting the peak height against the

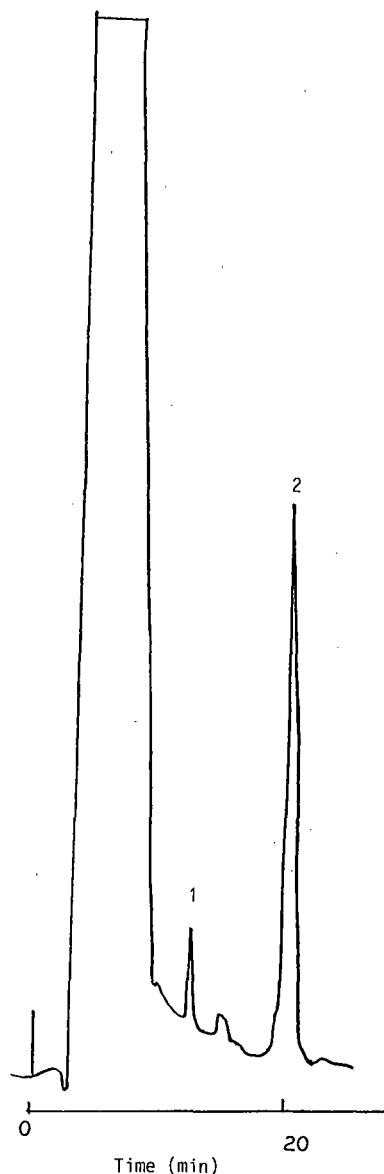


Fig. 1. Chromatogram of folic acid in Elental with UV detection at 360 nm. Amount of folic acid injected, 0.22 μg in 2 ml. Mobile phase: acetonitrile–water (pH 2.1, adjusted with phosphoric acid) (9:91) with 1 mM Na_2EDTA . Peaks: 1 = folic acid; 2 = unknown.

amount of folic acid and satisfactory linearity was obtained in the range 0–0.6 μg .

A known amount of folic acid was added to Elental and overall recovery was estimated by the standard addition method. The recovery of folic acid

TABLE I

ANALYTICAL DATA FOR FOLIC ACID IN ELEN TAL

Relative standard deviation = 1.8% ($n = 5$) with no addition of folic acid.

Concentration indicated (mg per 100 g)	Analytical data (mg per 100 g)	Recovery (%)
0.055	0.053	96.4
	0.052	94.5
	0.054	98.2
	0.052	94.5
	0.052	94.5

was about 95% with a relative standard deviation (R.S.D.) of 1.8% with no addition of folic acid.

Table I shows the analytical data for folic acid in Elental. There was good agreement between the indicated and found folic acid concentrations.

In conclusion, HPLC with detection at 360 nm, using acetonitrile–water (pH 2.1, adjusted with phosphoric acid) (9:91) with addition of 1 mM Na_2EDTA as a mobile phase, seems very useful for the determination of folic acid because it is satisfactory with respect to selectivity, rapidity and accuracy. It is simple and convenient, and therefore applicable to the routine analysis of folic acid in Elental.

Application of the proposed method to the determination of compounds in other elemental diets such as Elental P and Hegan ED and of drugs in biological fluids is also being studied.

REFERENCES

- 1 *The United States Pharmacopeia*, XXII Revision, US Pharmacopial Convention, Rockville, MD, 1990, p. 592.
- 2 *The Pharmacopeia of Japan*, Hirokawa Publishing, Tokyo, 12th ed., 1992, p. C-226.
- 3 T. Suzuki and S. Muraoka, *Bitamine Aminosan no Biseibutsuteiryoho*, Nanzando Publishing, Tokyo, 1956, p. 101.
- 4 R. B. H. Wills, C. G. Shaw and W. R. Day, *J. Chromatogr. Sci.*, 15 (1977) 262.
- 5 M. Amin and J. Reusch, *Analyst (London)*, 112 (1987) 989.
- 6 T. Ichinose, M. Nakajima, M. Toyama, N. Yominaga and Y. Hayashi, *The 40th Annual Meeting of the Japan Society for Analytical Chemistry, Hiyoshi, 1991*, The Japan Society for Analytical Chemistry Publishing, Tokyo, 1991, p. 117.
- 7 S. Ogoshi (Editor), *Elental Diet*, Nankodo Publishing, Tokyo, 1983.
- 8 H. Iwase, *J. Chromatogr.*, 590 (1992) 187.
- 9 H. Iwase, *J. Chromatogr.*, 606 (1992) 277.

Short Communication

Isolation and identification via high-performance liquid chromatography and thin-layer chromatography of benzoxazolinone precursors from *Consolida orientalis* flowers

Seçkin Özden

Faculty of Science, Karadeniz Technical University, 61080 Trabzon (Turkey)

Tuncel Özden

Faculty of Education, Karadeniz Technical University, 61335 Söğütlü/Trabzon (Turkey)

Imren Attila

Faculty of Science, Karadeniz Technical University, 61080 Trabzon (Turkey)

Mustafa Küçükislamoglu

Faculty of Education, Karadeniz Technical University, 61335 Söğütlü/Trabzon (Turkey)

Arslan Okatan

Faculty of Forestry, Karadeniz Technical University, 61080 Trabzon (Turkey)

(First received December 24th, 1991; revised manuscript received June 30th, 1992)

ABSTRACT

From the flowers of *Consolida orientalis* (Ranunculaceae) benzoxazolinone (BOA) and 2,4-dihydroxy-1,4-benzoxazin-3-one (DI-BOA) were isolated and identified by thin-layer chromatography, high-performance liquid chromatography, infrared spectroscopy and ¹H nuclear magnetic resonance. Also, the presence of 2-O-glucosyl-2,4-dihydroxy-1,4-benzoxazin-3-one was confirmed by thin-layer chromatography and high-performance liquid chromatography. These compounds are reported for the first time from the Ranunculaceae family.

Correspondence to: Professor Dr. S. Özden, Faculty of Science, Karadeniz Technical University, 61080 Trabzon, Turkey.

INTRODUCTION

Benzoxazolinone (BOA) was first isolated from rye seedlings; it possesses antifungal, anti-inflammatory and plant growth activities [1–3]. It is reported to be a degradation product produced by heating the hydroxamic acid, 2,4-dihydroxy-1,4-benzoxazine-3-one (DIBOA). DIBOA also exists in the plant as its 2-glucoside form [4–8]. The sugar is enzymatically removed during the isolation procedure. The reactions responsible for the formation of DIBOA and BOA can be summarized as shown in Fig. 1.

BOA, DIBOA and its glucoside have also been found in certain species of Gramineae and Acanthaceae [1,3–5,7,9]. *Consolida orientalis* (Gay) Schröd (synonym: *Delphinium orientale*) is one of the 23 *Consolida* species found widely in Turkey [10]. *Delphinium* and *Consolida* species are used in folk medicine as pediculicides, insecticides for cattle and as antirheumatics [11]. These plants are rich sources of alkaloids, and there are many studies of their alkaloids [12]. There is only one report on the organic acids [13] and anthocyanins [14] of *C. orientalis*.

After isolating and identifying BOA from the flowers of *C. orientalis*, because this product is derived from DIBOA and its glucoside, we also searched for these products. In this study, BOA, DIBOA and its glucoside were identified by thin-layer chromatography (TLC) and high-performance liquid chromatography (HPLC). In the identification, standard materials used were isolated from the seeds of *Secale cereale* L [4,5]. After identification, BOA and DIBOA were isolated by using column chromatography and preparative TLC and their structures were elucidated by their m.p. and IR and ^1H NMR spectra. These compounds have been isolated from the Ranunculaceae species for the first time.

Plant material from *C. orientalis* was collected from two different parts of Turkey and it was found that both types contained DIBOA and its glucoside.

EXPERIMENTAL

Plant material

C. orientalis was collected from Ankara-Ayaş and from Gümüşhane-Bayburt in July–August 1990, and *Aquilegia olympica* from Maçka-Trabzon, *Delphinium formosum* from Arsin-Trabzon and *Consolida glandulosa* from Gümüşhane-Bayburt were collected in July 1990.

Secale cereale L., used as a source of standard materials, was collected from Trabzon in August 1990.

Chemicals

Methanol (LiChrosolv) and acetic acid were obtained from Merck (Darmstadt, Germany). ^1H NMR solvents and authentic BOA were purchased from Aldrich (Milwaukee, WI, USA).

General procedure

All melting points were determined on an electrothermal digital melting point apparatus and are not corrected. ^1H NMR spectra were obtained using a Bruker AC 200 FT NMR spectrometer, using $[\text{D}_6]\text{dimethyl sulphoxide}$ (DMSO- d_6) as the solvent and tetramethylsilane (TMS) as internal standard. IR spectra were determined on a Perkin-Elmer 177 IR spectrophotometer in potassium bromide pellets. TLC and preparative TLC were performed on silica gel 60 G and HF₂₅₄ (1:1) (Merck), thickness 0.25 and 0.5 mm (Camag instruments, Muttens, Switzerland).

The solvent systems were as follows: (I) chloroform–methanol–water (75:25:3, v/v/v); (II) *n*-butanol saturated with water; (III) ethyl acetate–methanol–water (100:13.5:10, v/v/v); (IV) chloroform–

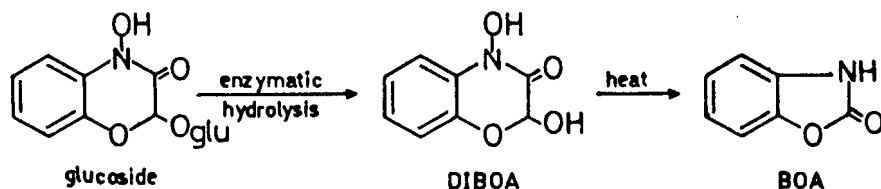


Fig. 1. Formation of DIBOA and BOA.

acetic acid (90:10, v/v). The spots were visualized under short-wavelength UV light and ferric chloride was used for the determination of hydroxamic acids. Column chromatography was carried out using silica gel 60 (70–230 mesh) (Merck).

The HPLC system consisted of a Shimadzu (Tokyo, Japan) liquid chromatograph fitted with two Model LC 9A solvent delivery systems, a Model SPD 6AV UV absorbance detector, a Model C-R5A computing integrator and a Rheodyne 7125 injector valve with a 20- μ l sample loading loop. Chromatography was carried out on a Shim-pack CLC-ODS (M) silica stainless-steel column (150 \times 4 mm I.D., 5 μ m particle size) (Shimadzu) eluted with water–methanol–acetic acid (73:27:3, v/v) at 254 nm and flow-rate was 0.8 ml/min. The sample volume injected was 20 μ l and separations were performed at ambient temperature under normal laboratory lighting conditions. The mobile phase was degassed with helium and chromatographic analysis was performed isocratically.

Extraction and isolation of compounds

Extraction of DIBOA and BOA from C. orientalis flowers. A 50-g aliquot of plant material was ground with water in a Waring blender (300 ml) after standing for 3 h at room temperature to allow enzymatic hydrolysis of the glucoside, heated on a water bath for 1 h at 70°C and filtered. The filtrate (approximately 250 ml) was extracted successively with several portions of *n*-hexane and diethyl ether and combined diethyl ether extracts were dried over anhydrous magnesium sulphate and evaporated to dryness on a rotary evaporator under reduced pressure. The residue was placed on a silica gel column and eluted successively with *n*-hexane, *n*-hexane–chloroform (90:10 to 50:50), chloroform and chloroform–diethyl ether (90:10 to 80:20). Fractions of 25 ml were collected and examined by TLC and HPLC.

In some fractions BOA and DIBOA were identified and their R_F values and retention time were identical to the authentic BOA and DIBOA isolated from *S. cereale* L. From these fractions DIBOA and BOA were isolated by preparative TLC using solvent system I. The identities of BOA and DIBOA were confirmed by m.p. and IR and ^1H NMR spectra.

BOA: m.p. 138°C (*n*-hexane–diethyl ether); IR (cm^{-1}) 3234, 1885, 1778, 1731, 1484, 1372, 1011, 941,

698, ^1H NMR (DMSO- d_6), δ (ppm) 7.31 (s, 4H Ar-H), 9.04 (s, 1H, N-H).

DIBOA: m.p. 155°C (diethyl ether); IR (cm^{-1}) 3200, 2870, 1650, 1590, 1475, 1270, 1210, 1085, 1052, 1030, 973, 825, 747. ^1H NMR (DMSO- d_6), δ (ppm) 7.10 (s, 4H, Ar-H), 8.17 (s, 1H, OH), 10.90 (s, 1H, N-OH).

Extraction of glucoside from C. orientalis flowers. A 5-g aliquot of dried plant material was ground in a Waring blender with methanol (150 ml), refluxed for 6 h and the slurry filtered through filter paper. The extract was evaporated to dryness under reduced pressure. The residue was taken up in water and then extracted successively with *n*-hexane, diethyl ether and *n*-butanol. The combined *n*-butanol phases were evaporated to dryness under reduced pressure and the residue (0.05 g) was dissolved in methanol. From the methanolic solution, glucoside was determined by co-chromatography with standard material isolated from *S. cereale* in both TLC and HPLC. At the same time both this glucoside and the DIBOA glucoside isolated from *S. cereale* gave the same colours with ferric chloride reagent in TLC.

RESULTS AND DISCUSSION

Two different extracts of *C. orientalis*, with water and methanol, were prepared and both of the extracts were tested on TLC with authentic BOA and DIBOA obtained from *S. cereale*.

In the water extract, the amount of BOA and DIBOA was higher, because of the heat and enzymatic hydrolysis. In the methanol extract, the amount of the glucoside was higher, but there was a small amount of DIBOA since boiling methanol destroys the enzymes.

In TLC, the spots of DIBOA and its glucoside were easily detected as dark zones at 254 nm UV light and visualized with ferric chloride reagent, which gives a violet colour with hydroxamic acids. Thus, it is apparent that BOA does not occur naturally in *C. orientalis* flowers but is a degradation product of DIBOA as mentioned in the literature [4–8].

After isolating DIBOA, it was heated in water and confirmed by HPLC that it turns to BOA.

BOA and DIBOA were isolated from column and preparative TLC. Since it is well known that

TABLE I

TLC R_f VALUES AND HPLC RETENTION TIMES OF BOA, DIBOA AND DIBOA GLUCOSIDE

Compound	TLC R_f values in system				Colour with ferric chloride	Retention time (min)
	I	II	III	IV		
BOA	0.80	0.91	0.77	0.48	—	20.73
DIBOA	0.44	0.88	0.63	0.18	Violet	11.89
Glucoside	0.11	0.59	0.14	—	Violet	9.47

DIBOA occurs in intact plants as its 2-O-glucosyl derivative, and since the presence of BOA and DIBOA was confirmed by spectroscopic methods, the identification of the glucoside was made only with TLC and HPLC.

The spectroscopic data and m.p. were identical to those of authentic BOA and DIBOA isolated from *S. cereale* and also fit the results reported previously [4,6,7,15,16].

The R_f values obtained by TLC and retention times obtained by HPLC of BOA, DIBOA and its glucoside are given in Table I.

The HPLC separation of the mixture of these three compounds is shown in Fig. 2.

In this study, the complete separation of these three products with a CLC-ODS silica column using UV detection (254 nm) and the solvent system water-methanol-acetic acid (73:27:3, v/v) is also realized for the first time. The method is simple and easily applicable.

DIBOA and its glucoside were also sought in *Aquilegia olympica*, *Consolida armeniaca*, *Delphinium formosum* and *Consolida glandulosa* flowers by co-chromatography with standards in both TLC and HPLC, but it was found that they are not present in these plants.

ACKNOWLEDGEMENT.

This study was supported by the Research Fund of Karadeniz Technical University.

REFERENCES

- 1 A. I. Virtanen and P. K. Hietala, *Acta Chem. Scand.*, 9 (1955) 1453.
- 2 H. Otsuka, Y. Hirai, T. Nagao and K. Yakasaki, *J. Nat. Prod.*, 51 (1988) 4.
- 3 R. B. Wolf, G. F. Spencer and R. O. Plattner, *J. Nat. Prod.*, 48 (1985) 59.
- 4 A. I. Virtanen and P. K. Hietala, *Acta Chem. Scand.*, 14 (1960) 499.
- 5 P. K. Hietala and A. I. Virtanen, *Chem. Scand.*, 14 (1960) 502.
- 6 E. Honkanen and A. I. Virtanen, *Acta Chem. Scand.*, 14 (1960) 504.
- 7 C. L. Tipton, J. A. Klun, R. R. Husted and M. D. Pierson, *Biochemistry*, 6 (1967) 2866.
- 8 J. A. Klun, C. L. Tipton, J. F. Robinson, D. L. Ostrem and M. Beroza, *J. Agr. Food Chem.*, 18 (1970) 663.
- 9 D. J. Milles, *J. Nat. Prod.*, 49 (1986) 355.
- 10 P. H. Davis, *Flora of Turkey and the East Aegean Islands*, Vol. 1, University Press, Edingburgh, 1965.
- 11 T. Baytop, *Türkiye'de Bitkilerle Tedavi*, İst. Üniv. Yayınları No. 3255, İstanbul, 1984.

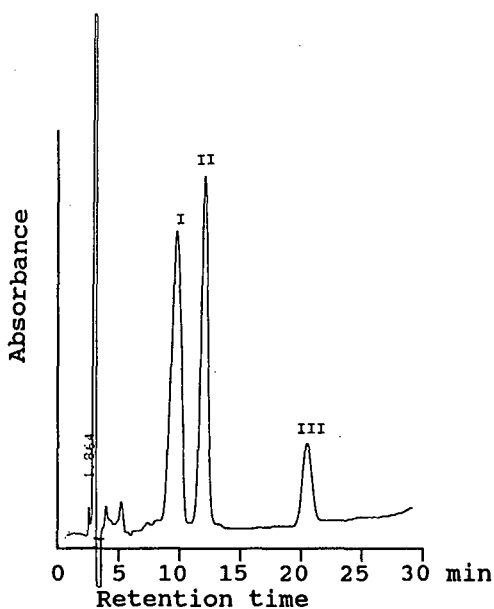


Fig. 2. Chromatogram of an artificial mixture of purified BOA (III), DIBOA (II) and its glucoside (I). Injection volume, 20 μ l.

- 12 W. S. Pelletier, *Alkaloids, Chemical and Biological Perspectives*, Wiley, New York, 1984.
- 13 I. Atilla, A. Baysal, M. Tüfekçi, Y. Gök and S. Özden, *Plant Med. Phytother.*, 24 (1990) 224.
- 14 G. Sulyok and J. Balint, *Stud. Org. Chem.*, 23 (1986) 261.
- 15 J. Sam and J. L. Valentine, *J. Pharm. Sci.*, 58 (1969) 1043.
- 16 C. J. Pouchert, *The Aldrich Library of Infrared Spectra*, Aldrich, Milwaukee, WI, 2nd ed., 1975.

Short Communication

Application of two rapid techniques of column chromatography to separate the pungent principles of ginger, *Zingiber officinale* Roscoe

Rafael Zarate, Sukrasno and Michael M. Yeoman

Institute of Cell and Molecular Biology, University of Edinburgh, Daniel Rutherford Building, Mayfield Road, Edinburgh EH9 3JH, Scotland (UK)

(First received March 3rd, 1992; revised manuscript received June 1st, 1992)

ABSTRACT

Two rapid techniques of column chromatography, flash chromatography and vacuum chromatography, together with solvent systems differing in polarity, have been used to separate the pungent principles (gingerols and shogaols) of an extract of ginger powder. Gingerols consist of a homologous series of aldols each containing a phenolic group which together with shogaols, showing similar structure, give the pungency of ginger. Thin-layer chromatographic analysis of the fractions collected from both chromatographic techniques showed that the main gingerol homologues are separated satisfactorily from the other compounds only using vacuum chromatography. These compounds were eluted with hexane–diethyl ether (30:70) and (20:80) respectively. The results obtained with flash chromatography, on the other hand, were not satisfactory.

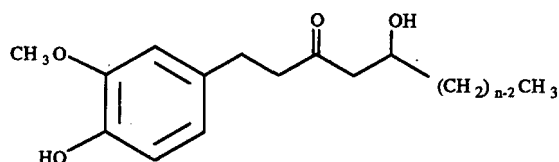
INTRODUCTION

The rapid and successful separation of selected compounds from a plant extract containing a myriad of substances is a problem facing the plant biochemist. It is therefore important to effect a crude separation of the plant components before more sophisticated procedures are employed. Such separation may include extraction using selected solvents, partition into two immiscible solvents (liquid–liquid extraction) and vacuum or flash chromatography [1–4]. Apart from the speed of the chromatographic process, vacuum and flash chromatography

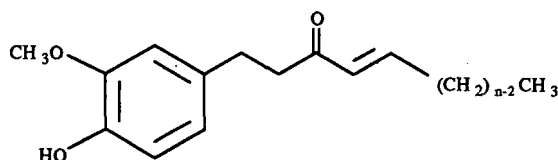
also offer a high loading capacity. Their use is of course not limited to the crude separation of the components of plant extracts, as they have been used successfully for the purification and separation of compounds in mixtures containing few components, such as products of chemical synthesis. A wide range of packing materials have been employed with both techniques, with silica gel used most frequently, but others, such as cellulose, polyamide, and bonded silica (reversed-phase particles) have also been used [5].

Attempts have been made to isolate gingerols (Fig. 1) from a crude extract of ginger by Shoji *et al.* [6] and Farthing and O'Neill [7]. Shoji *et al.* [6] partitioned the methanol extract between ethyl acetate–water, and *n*-hexane–methanol, followed by repetitive column chromatography (six times) on

Correspondence to: R. Zarate, Institute of Cell and Molecular Biology, University of Edinburgh, Daniel Rutherford Building, Mayfield Road, Edingburgh EH9 3JH, Scotland, UK.



[n]-Gingerol



[n]-Shogaol

Fig. 1. Molecular structure of gingerol and shogaol.

silica gel eluted with benzene-ethyl acetate, while Farthin and O'Neill [7] used the same liquid-liquid extraction [6], followed by counter current chromatography, which gave good separation of the gingerol homologues.

In this paper a comparison is made between flash and vacuum column chromatography and their effectiveness assessed in separating the gingerols the main components of the pungent principle of *Zingiber officinale* Roscoe.

EXPERIMENTAL

Preparation of extract (stock solution)

Freeze-dried ginger rhizome powder (20 g) was extracted with acetone (analytical-reagent grade; BDH, Poole, U.K.) according to the method described by Spiro and Kandiah [8]. The acetone extract was evaporated to dryness on a water bath at 35°C using a rotary evaporator and the residue dissolved in 50 ml of 80% methanol. The resultant solution was subjected to liquid-liquid extraction 3 times with 50 ml hexane. The hexane fraction which contains mainly waxy materials, volatile oils and higher amount of shogaols than in the ether phase,

was analysed on thin-layer chromatography (TLC) (see Fig. 3) and then discarded. To the 80% methanol fraction, a mixture of diethyl ether and water (2:1, v/v) was added to produce two layers, the organic and aqueous phases. The pungent principles were mainly present in the ether fraction which was then dried with anhydrous sodium sulphate, evaporated to dryness as before, dissolved in 10 ml methanol and stored as the stock solution.

Thin-layer chromatography

TLC was used to evaluate the products of fractionation and eluates of flash and vacuum column chromatography. TLC was carried out on Silica gel 60, 20 × 20 cm plates, layer thickness 0.2 mm (Merck No. 5553, Darmstadt, Germany), under saturated conditions in a glass tank (Panglas, Shandon, TLC chromatank, Runcorn, UK). The solvent system was toluene-methanol (80:5), a variation of that of Bhagya [9]. Visualization of the compounds on the plates was achieved after spraying with Folin-Ciocalteu reagent (BDH). Using this method gingerols, which constitute the main part of the pungent principle in ginger, displayed R_F values of 0.24-0.29 and shogaols, the minor component, showed R_F values of 0.45-0.50 as shown in Fig. 3.

Flash chromatography

The equipment used for flash chromatography was a glass chromatography column 135 cm in length with an inside diameter of 2.0 cm, supplied by Aldrich (Gillingham, UK), as described by Still *et al.* [3]. To prepare the column 9.5 g of silica gel 60 (40-60 μm, Merck 9385) was added slowly while tapping continuously to produce even packing, to give an effective column length of 15 cm, then an 0.8-cm layer of 40-100 mesh sand (BDH) was carefully placed on the flat top of the dry gel bed. Initially, 40 ml of the solvent system, as used for TLC, was added to the column and pressure applied from a cylinder containing nitrogen to remove the solvent from the silica, remove any trapped air and produce a compact column. Finally, an extra 200 ml of solvent was run through, to achieve an even compact column. To the column a 2-ml sample, obtained by evaporating 2 ml of stock solution in methanol in a stream of nitrogen and redissolving the residue in 2 ml of eluent, was applied. The sample was drawn into the silica by applying pressure from a nitrogen

cylinder. After the whole sample had been adsorbed by the column, 200 ml of eluent was added, pressure applied to produce a flow-rate of 50 mm per min (read from the decrease in the level of the solvent above the column bed) and 20 fractions of a volume of 10 ml collected. The compounds in each fraction were analysed by TLC following the method described above.

Vacuum chromatography

A Buchner flask (100 ml) fitted with a sintered filter funnel with an inside diameter of 3.5 cm was connected to a water pump. To the funnel, a similar amount (9.5 g) of silica gel 60, as used in flash chromatography, was added slowly to obtain an evenly packed silica column, 3 cm in length.

A 3-ml volume of the stock solution of ginger extract was added to 2 g of silica gel 60 and dried by means of a rotary evaporator over a warm water bath at 35°C. The dried powder containing the sample was then spread evenly over the top of the silica

column. A piece of filter paper (Whatman No. 1, Maidstone, UK) with the same diameter as the inside diameter of the funnel was placed on top of the sample to prevent damage to the column during addition of the solvent. Hexane (25 ml) was added slowly, and the solvent allowed to penetrate the whole column, then the atmosphere in the flask was sucked out to facilitate rapid elution and the eluent collected as the first fraction. Further elution was carried out using 20 aliquots of 25 ml of solvent mixtures with increasing polarity, composed of hexane–diethyl ether and diethyl ether–methanol, as shown in Fig. 2. The individual eluates of 25 ml were transferred to a test tube, evaporated to a volume of 10 ml in a stream of nitrogen and then analysed by TLC.

RESULTS AND DISCUSSION

Preliminary separation

The TLC chromatograms of the fractionation

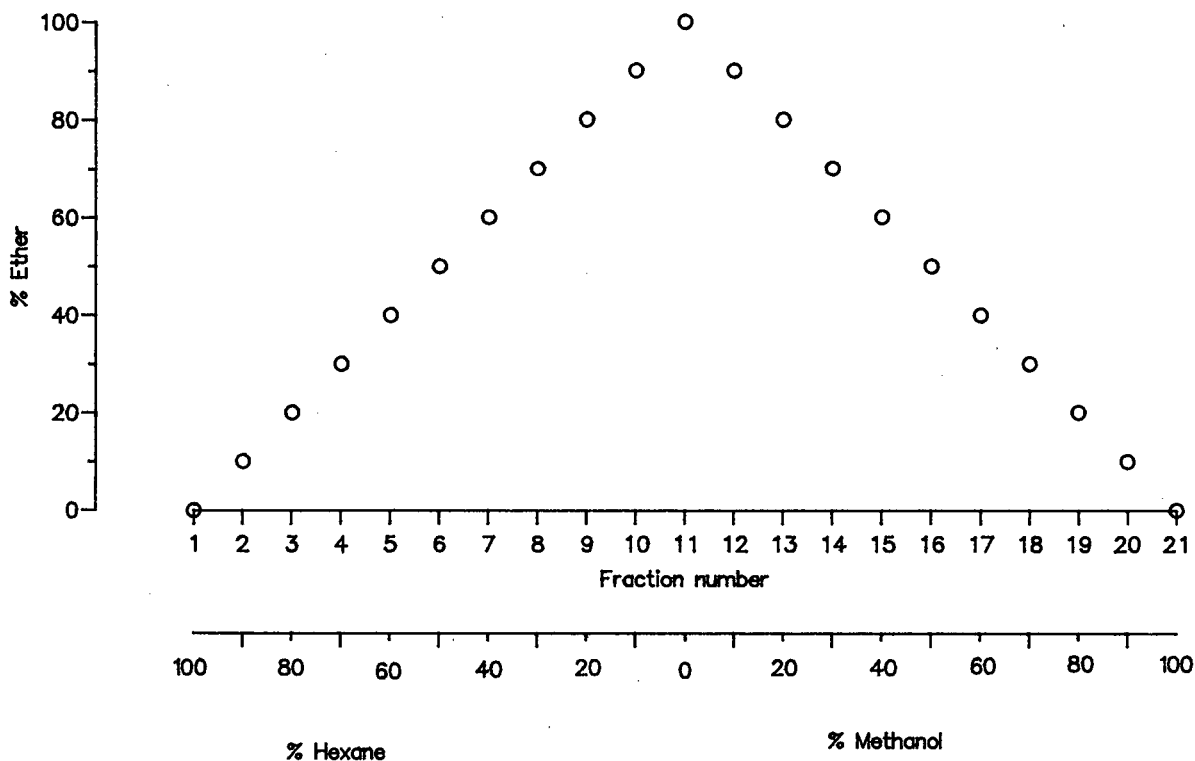


Fig. 2. Composition of the solvent system used in vacuum chromatography (21 different aliquots).

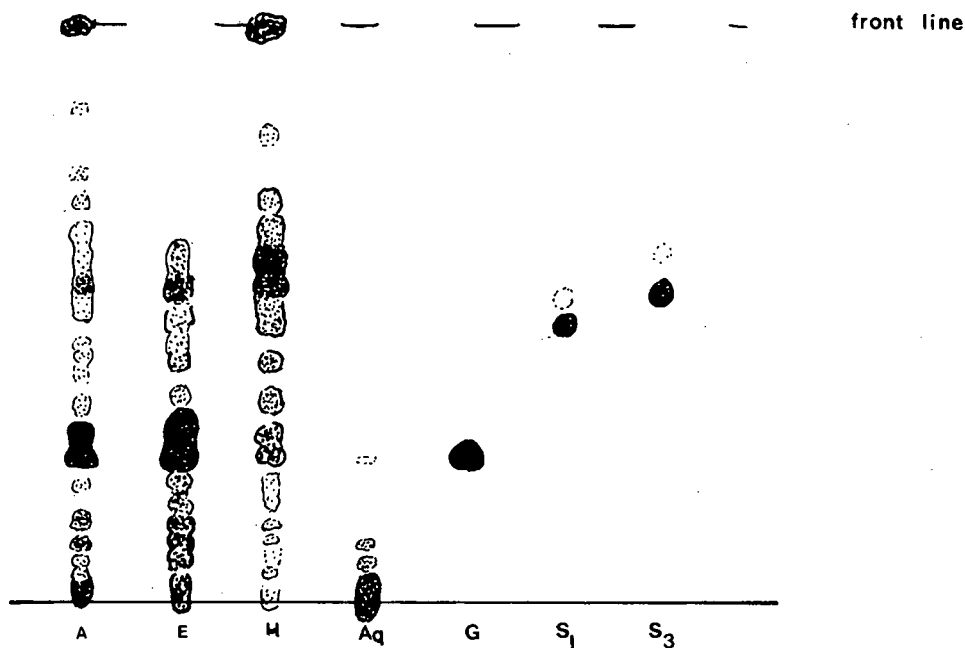


Fig. 3. TLC of the fractions obtained from the liquid–liquid extraction. A = total acetone extract (5 μ l), B = ether phase (10 μ l), H = hexane phase (10 μ l), Aq = aqueous phase (10 μ l), G = [6]-gingerol (2 μ l = 70 μ g), S₁, S₃ = shogaol homologues (2 μ l = 25 μ g). The amount of sample loaded is indicated in brackets, as for Figs. 4–6.

products are presented in Fig. 3. As predicted, the pungent principles are present mainly in the ether fraction, with a higher amount of shogaol in the hexane phase. In the aqueous fraction, compounds

which react with Folin–Ciocalteu reagent were also present. These compounds, however, are unlikely to be the pungent components of ginger, since they do not run far from the origin in the TLC system used.

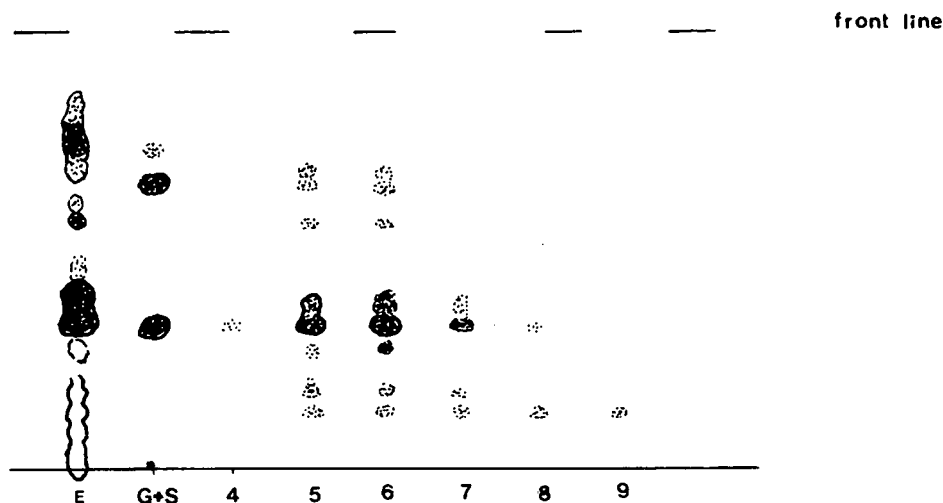


Fig. 4. TLC of the 10-ml fractions obtained using flash chromatography with toluene–methanol (80:5) as solvent. Numbers indicate the different fractions collected (10 μ l), E = ether phase (10 μ l), G + S = [6]-gingerol (2 μ l = 70 μ g), shogaol (2 μ l = 25 μ g). Only fractions which were known to contain the compounds under investigation were loaded onto the TLC plates.

Flash chromatography

This is a moderate-resolution, preparative technique usually carried out in a column-overload condition, using the same solvent system as with TLC. It has been reported that compounds which differ in R_F value by only 0.15 can be separated satisfactorily using flash chromatography [3,5]. Therefore, it was expected that, using this technique, gingerols the major components of the pungent principle in ginger and shogaols, would be clearly separated because the difference between their R_F values is greater than 0.15 (ca. 0.20–0.25).

The results, however, presented in Fig. 4 show that most of the components of the pungent principle (gingerols, shogaols) were present in the same fractions (5 to 7). Overloading does not seem to be the cause, because the loading capacity of the column used [3] is approximately 400 mg, while the amount of sample loaded was less than 200 mg. Different lengths of the bed column (10–15 cm) and different flow-rates (50–100 mm per min) were tested, as well as the solvent system hexane–diethyl ether (30:70) employed in vacuum chromatography which gave clear separation of the gingerols. How-

ever, less satisfactory results were obtained as all the components of the pungent principle appear in fractions H₂–H₄ (see Fig. 6). The silica gel employed for the development of the TLC was 15 μ m (Merck No. 5553), while for flash chromatography it was 40–60 μ m. (Merck No. 9385). If the silica gel used for both forms of chromatography had been the same, as suggested by Majors and Enzweiler [5], it would have simplified comparison of the results. It is also possible that the number of compounds present in the plant extract may also affect the efficiency of the column.

Vacuum chromatography

It was surprising that although the technique of vacuum chromatography is much simpler than flash chromatography, the main pungent components of ginger, the gingerols, are almost completely resolved from the shogaols, present in fractions 8 and 9 (see Fig. 5). Using this technique the length of the column was only 3 cm, much shorter than the column used for flash chromatography (15 cm), with a wider inside diameter of the column which provides a high loading capacity. It appears that the solvent

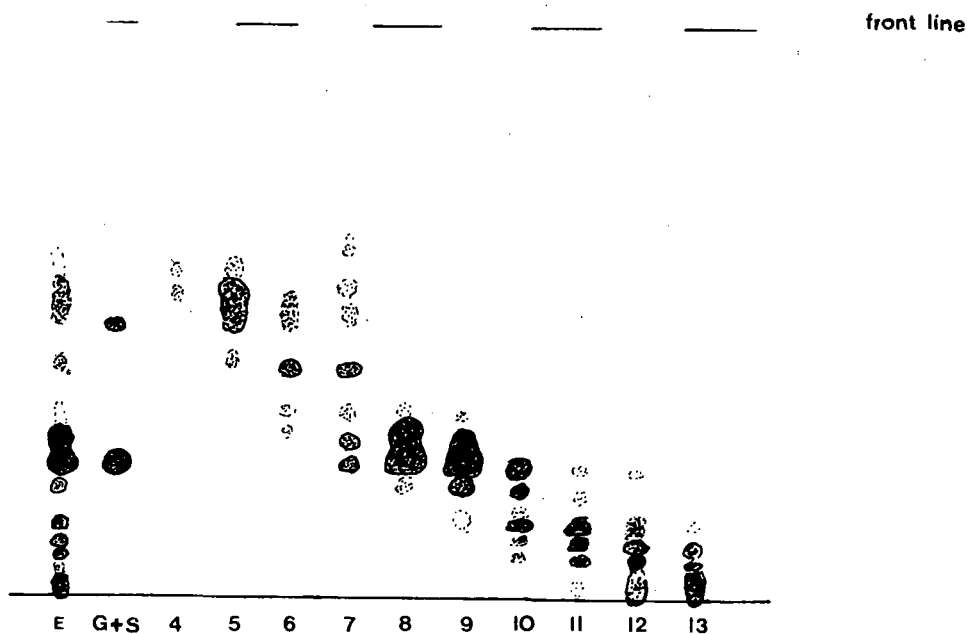


Fig. 5. TLC of the 10-ml fractions obtained using vacuum chromatography, when a solvent gradient was employed. Numbers indicate the different fractions collected, 4–13 (10 μ l); E = ether phase (10 μ l); G + S = [6]-gingerol (2 μ l = 70 μ g); shogaol (2 μ l = 25 μ g). Only fractions which were known to contain the compounds under investigation were loaded onto the TLC-plates.

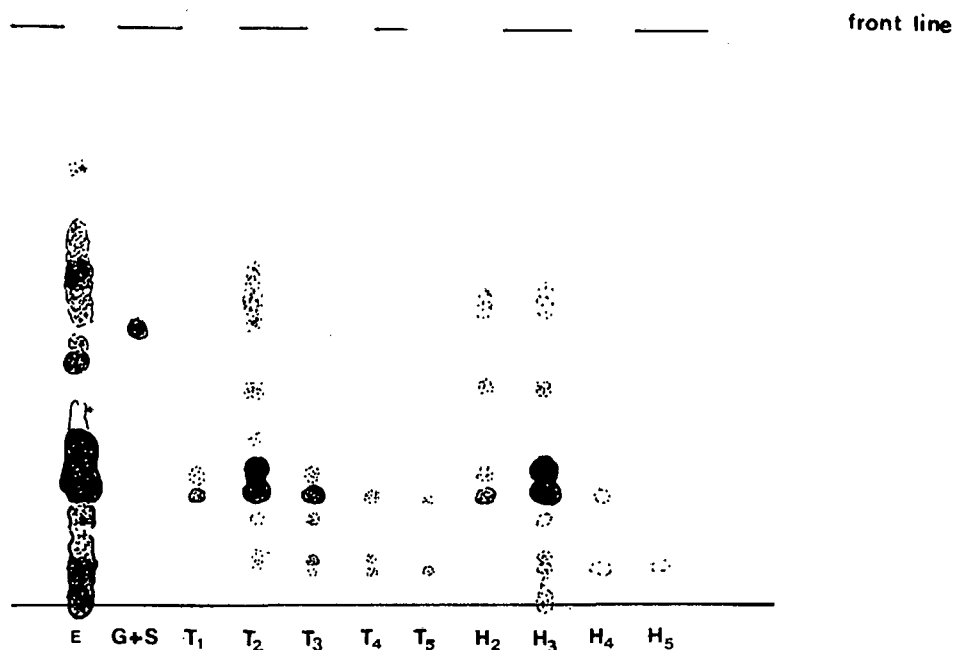


Fig. 6. TLC of the 10 ml fractions obtained using flash chromatography with hexane-diethyl ether (30:70) as solvent system, fractions H₂-H₄ (10 μ l) and the 10-ml fractions collected in vacuum chromatography when an isocratic solvent system toluene-methanol (80:5) was used, fractions T₁-T₅ (10 μ l); E = ether phase (10 μ l); G + S = [6]-gingerol (2 μ l = 70 μ g); shogaol (2 μ l = 25 μ g). Only fractions which were known to contain the compounds under investigation were loaded onto the TLC plates.

gradient plays a major part in this chromatographic technique. Indeed, isocratic elution using the solvent system developed for TLC has also been tried. However, a satisfactory separation was not achieved (see Fig. 6). Similar results were obtained in an attempt to isolate the steroid (23,24-dimethylcholesta-5,22-dien-3 β -ol) from a petroleum ether extract of *Crescentia cujete* bark (unpublished observation). It is unlikely that the method of application of the sample to the column has any significant effect on the efficiency of separation because the results presented in Fig. 6 (fractions T₁-T₅) show that the separation achieved using an isocratic system was inferior to that with a gradient (see Fig. 5) with the same loading arrangement used for both solvent systems.

Of course, solvent gradients can also be employed in flash chromatography, but then the technique becomes long and tedious, with the simple equipment employed for the above experiments. These results suggest that a number of advantages are offered by vacuum column chromatography. 1) The equipment is of low cost and easily assem-

bled using components available in most laboratories. 2) A solvent system can easily be developed by mixing two solvents with different polarities in different proportions. 3) This method may also be used for purification by increasing the polarity of the gradient more slowly and eluting smaller volumes for each fraction.

A much more complicated system of vacuum liquid chromatography has been developed by Targett *et al.* [4] using a longer column, maintained under vacuum, with isocratic elution as for flash chromatography. Therefore, results similar to those of flash chromatography might be expected since isocratic elution is used, but would appear to be less favourable for a preliminary separation of the component of plant extracts.

ACKNOWLEDGEMENTS

We would like to thank Dr. G. Wallace for use of the flash column chromatography equipment, Dr. M. Kuroyanagi for a supply of the gingerol and shogaol standards. Dr. S. C. Fry for constructive

discussion of the manuscript, and the Cabildo Insular de Tenerife, Spain for financial support.

REFERENCES

- 1 J. C. Coll, S. J. Mitchell and G. J. Stokie, *Aust. J. Chem.*, 30 (1977) 1859.
- 2 B. F. Bowden, J. C. Coll, S. J. Mitchell and G. J. Stokie, *Aust. J. Chem.*, 31 (1978) 1303.
- 3 W. C. Still, M. Kahn and A. Mitra, *J. Org. Chem.*, 43 (1978) 2923.
- 4 N. M. Targett, J. P. Kilcoyme and B. Green, *J. Org. Chem.*, 44 (1979) 4962.
- 5 R. E. Majors and T. Enzweiler, *LC · GC Int.*, 2 (1989) 10.
- 6 N. Shoji, A. Iwasa, T. Takemoto, Y. Ishida and Y. Ohizumi, *J. Pharm. Sci.*, 71 (1982) 1174.
- 7 J. E. Farthing and M. O'Neill, *J. Liq. Chromatogr.*, 13 (1990) 941.
- 8 M. Spiro and M. Kandiah, *Int. J. Food Sci. Techn.*, 24 (1989) 589.
- 9 Bhagya, *J. Food Sci. Techn.*, 14 (1977) 176.

Short Communication

Gas chromatographic separation of polycyclic aromatic hydrocarbons on a mesomorphic copolysiloxane stationary phase

Hongju Wang, Tongmou Gen, Rounong Fu, Jiya Zhu, Xiuzhen Wei, Hueisheng Li and Jihua Liu

Department of Chemical Engineering, Beijing Institute of Technology, P.O. Box 327, Beijing 100081 (China)

(First received November 7th, 1991; revised manuscript received May 26th, 1992)

ABSTRACT

A mesomorphic copolysiloxane was prepared and used as a selective stationary phase for capillary column gas chromatography. It was found to have an operating temperature range of 70–280°C and unique selectivity for some isomeric compound separations such as those of three-, four- and five-ring polycyclic aromatic hydrocarbons.

INTRODUCTION

The gas chromatographic (GC) analysis of samples consisting of isomeric solutes with nearly identical vapour pressures remains a challenge. Moreover, the problem is often compounded by the complexity of mixtures containing classes of materials such as polycyclic aromatic hydrocarbons (PAHs) [1]. Thus, even with columns of the highest available efficiency, it is fair to say even today that the resolution of isomers such as five-ring PAHs (including, e.g., the carcinogenic benzo[*a*]pyrene) is not entirely satisfactory [2].

In contrast, it has been recognized for some time that liquid-crystalline (mesomorphic) stationary phases provide enhanced GC separations of many

isomeric compounds, including PAHs, on the basis of solute geometry [2]. As a result, a number of liquid-crystalline phase have been introduced [3–5], the best known being the commercially available materials developed by Janini and co-workers [6–9]. An example of the remarkable shape selectivity of nematic mesophases is that they yield baseline separations of most parent PAHs, which was achieved for the first time with packed columns containing BMBT [N,N'-bis(*p*-methoxybenzylidene)- α,α' -bi-*p*-toluidine] stationary phase [6].

However, the utility of such low-molecular-weight liquid-crystalline phases is limited by the excessive column bleeding at elevated temperatures, the moderate column efficiency and the restricted useful mesomorphic temperature ranges. As a result, the coupling of liquid crystal functional groups on to a polysiloxane backbone via a flexible alkyl spacer has been successfully accomplished [10,11]. The methylene spacers between the liquid-crystal-

Correspondence to: Prof. R. Fu, Department of Chemical Engineering, Beijing Institute of Technology, P.O. Box 327, Beijing 100081, China.

line substituents and the polysiloxane help to preserve the original characteristics of the liquid crystals [12]. Significant improvements in efficiency and thermal stability over the monomeric stationary phases were obtained with the development of these polysiloxane phases. In addition, Markides *et al.* [13] have shown that they provide good resolution, *e.g.*, of PAHs, with open-tubular columns.

Copolymers composed of two different liquid-crystalline moieties have been reported. Biphenyl-carboxylic esters of polysiloxanes constitute a large group of liquid-crystalline copolymers [11,13,14] and several procedures for their synthesis of chromatographic applications have been described [13–16]. Not only nematic but also smectic–nematic and smectic copolymers are suitable as stationary phases [11,14,17]. Polymers with the cholesteric mesophase are also known [11] although to a much smaller extent. The mesomorphic copolysiloxanes usually show a wider range of the mesophase than their corresponding homopolymers. These copolymers have high thermal resistance and show good behaviour of the column; further improvement in their properties is possible by cross-linking in the column [15].

In this paper, the synthesis of a mesomorphic copolysiloxane stationary phase that can be used over a wide temperature range is described and its chromatographic properties as a capillary GC stationary phase are discussed. The selectivity for isomeric PAHs is also demonstrated.

EXPERIMENTAL

A Model SP-3700 gas chromatograph (Beijing Analytical Instrument Factory, Beijing, China) equipped with a capillary split injection system and a flame ionization detector was used for evaluation of retention behaviour. All chemicals used for synthesis were of analytical-reagent grade.

Synthesis

For the synthesis of the mesomorphic copolysiloxane, 4-[(4'-(allyloxy)phenylmethylacetyl]-4'-methoxybiphenyl (0.891 g, 2.475 mmol), 0.073 g (0.275 mmol) of N-(4-allyloxy benzylidene)-4'-methoxyphenylamine, 0.16 g (containing 2.5 mmol of Si–H) of poly(methylsiloxane) and 40 ml of dry toluene were mixed. The mixture was heated to

110°C under a nitrogen atmosphere and stirred for 24–72 h until no absorption band of Si–H was detectable by IR spectrometry (2140 cm^{-1}). The resulting copolymer was purified by filtration or precipitation with methanol. The copolymer was collected by centrifugation at 9000 rpm (13 000 g) for 25 min and dried in a vacuum oven to give a white solid. The copolymer side-chain proportions were governed by the starting molar proportions of the reactants. Table I shows the structures and the phase transition temperatures of the mesomorphic copolysiloxane and its corresponding homopolymers (Allyloxy)phenylmethylacetyl]-4'-methoxybiphenyl and N-(allyloxy benzylidene)-4'-methoxyphenylamine were both prepared in the laboratory. Poly(methylsiloxane) was obtained from the Merck-Schuchardt (Munich, Germany).

Column preparation

Fused-silica capillary columns (0.28 mm I.D.) (Yongnian Optical Fibre Factory, Hebei, China) were purged with dry nitrogen at 220°C for 5 h before coating. The mesomorphic copolysiloxane was dissolved in methylene chloride (35°C) at a concentration of about 4.0 mg/ml, which gave a film thickness of 0.33 μm using the static coating procedure. Before filling the capillary, the coating solution was carefully filtered through a glass filter.

RESULTS AND DISCUSSION

Table II gives the characteristics of four fused-silica capillary columns coated with this copolymer. The stationary phase provides satisfactory column efficiencies (3650 plates/m, anthracene solute; 250°C) owing to the flexibility of the polysiloxane backbone and the concomitant low surface tension, which facilitate the homogeneous coating of the mesomorphic copolysiloxane phase on the untreated fused-silica columns. Column 5 coated with 90:10 I–II (see Table I) mixed stationary phase was used for comparison.

The selectivity and polarity of mesomorphic copolysiloxane are represented by McReynolds constants. These parameters and average polarities are given in Table III. These parameters are also listed for PEG-20M for comparison. The average polarity of the copolymer is lower than that of PEG-20M. It is a medium-polar stationary phase. Rohrschneider

TABLE I

STRUCTURES AND PHASE TRANSITION TEMPERATURES OF THE COPOLYMER STUDIED AND ITS CORRESPONDING HOMOPOLYMER

Transition temperatures were measured by hot-stage light-polarized microscopy.

Polymer ^a	Phase transitions (°C) ^b
$\left[\text{CH}_3 - \underset{\text{O}}{\overset{ }{\text{Si}}} - (\text{CH}_2)_3 - \text{O} - \text{C}_6\text{H}_4 - \text{COO} - \text{C}_6\text{H}_4 - \text{C}_6\text{H}_4 - \text{OCH}_3 \right]_{27}$	90%
$\left[\text{CH}_3 - \underset{\text{O}}{\overset{ }{\text{Si}}} - (\text{CH}_2)_3 - \text{O} - \text{C}_6\text{H}_4 - \text{CH}=\text{N} - \text{C}_6\text{H}_4 - \text{OCH}_3 \right]_{27}$	10%
$\left[\text{CH}_3 - \underset{\text{O}}{\overset{ }{\text{Si}}} - \text{O} - (\text{CH}_2)_3 - \text{O} - \text{C}_6\text{H}_4 - \text{COO} - \text{C}_6\text{H}_4 - \text{C}_6\text{H}_4 - \text{OCH}_3 \right]_x$	c78n276i
$\left[\text{CH}_3 - \underset{\text{O}}{\overset{ }{\text{Si}}} - \text{O} - (\text{CH}_2)_3 - \text{O} - \text{C}_6\text{H}_4 - \text{CH}=\text{N} - \text{C}_6\text{H}_4 - \text{OCH}_3 \right]_x$	n138n287i
$\left[\text{CH}_3 - \underset{\text{O}}{\overset{ }{\text{Si}}} - (\text{CH}_2)_3 - \text{O} - \text{C}_6\text{H}_4 - \text{CH}=\text{N} - \text{C}_6\text{H}_4 - \text{OCH}_3 \right]_y$	n102n140i

^a 27 is the degree of polymerization of poly(methylsiloxane).^b c = crystalline; n = nematic; i = isotropic.

[20] and McReynolds [21] proposed that liquid-crystalline stationary phases have low or medium polarities as determined by the sum of the retention indices of test substances that react in different ways with the stationary phase. It is known, however, that the interaction of the liquid-crystalline stationary phase with the chromatographed substances depends not only on the polarity of the phase but also on the interaction of the substance with the ordered structure of the liquid crystal. Therefore, for a more complete characterization of the liquid-crystalline stationary phase, additional substances such as xylenes [22], diethylbenzene and ethylbenzene isomers, toluene, ethylbenzene, *n*-propylbenzene and *n*-butylbenzene [23] should be tested.

To determine the effect of temperature on column efficiency, the height equivalent to a theoretical plate (HETP) was measured at different temperatures and a constant flow-rate of the carrier gas. Fig. 1 shows a plot of HETP vs. column temperature (*t*) for anthracene on the two mesomorphic

copolysiloxane capillary columns. It is clear that the column efficiency increases with increasing temperature.

TABLE II

CHARACTERISTICS OF THE MESOMORPHIC COPOLY-SILOXANE CAPILLARY COLUMNS USED

Test compound: anthracene.

Column No. ^a	Column dimensions (length × I.D.)	Column efficiency (plates/m)	Column temperature (°C)
1	10 m × 0.28 mm	2060	205
2	10 m × 0.28 mm	2070	218
3	19 m × 0.28 mm	3650	250
4 ^b	13 m × 0.28 mm	1720	220
5	10 m × 0.25 mm	810	225

^a The capillary film thicknesses are about 0.28–0.33 μm.^b DCUP (dicumyl peroxide) 10% and V4 [tetra(methylvinyl)cyclotetrasiloxane] 4.4% cross-linked column. The method of cross-linking was similar to that of Liu *et al.* [18].

TABLE III
SELECTIVITIES AND POLARITIES OF THE MESOMORPHIC COPOLYSILOXANE STUDIED

Stationary phase	McReynolds constant (ΔJ) ^a					
	X'	Y'	Z'	U'	S'	Mean
Copolymer	251	264	330	429	420	339
PEG-20 ^b	322	536	368	572	510	461

^a X' = Benzene; Y' = butanol; Z' = 2-pentanone; U' = nitropropane; S' = pyridine.

^b From ref. 19.

Fig. 2 shows chromatograms of three-ring PAH isomers on capillary columns coated with a non-polar stationary phase (SE-30), with the mesomorphic copolymer and with a mixed stationary phase. The resolution is best when the liquid-crystalline copolymer is used. This is a result of both the high selectivity of the column and its high chromatographic efficiency. Columns can be easily coated with the copolymer to produce efficient columns that lead to the narrow peaks.

To illustrate the practical utility of the mesomor-

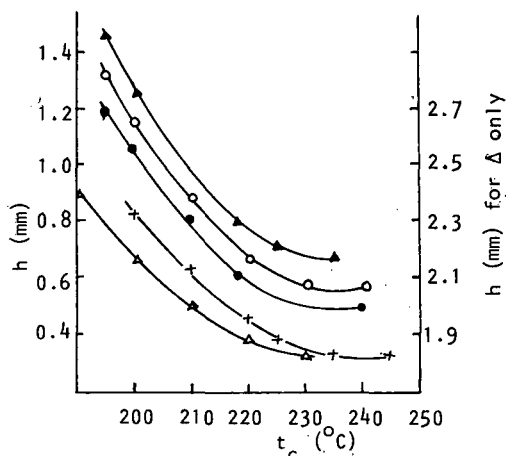


Fig. 1. Plot of HETP against temperature for anthracene on (○) column 1, (●) column 2, (×) column 3, (▲) column 4 and (Δ) column 5 (see Table II).

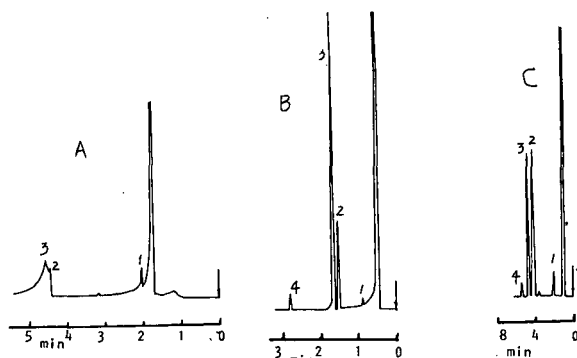


Fig. 2. Chromatograms of isomeric three-ring PAHs on (A) SE-30, (B) copolymer (column 1) and (C) mixed column (column 5). Column temperature, 225°C. Peaks: 1 = fluorene; 2 = anthracene; 3 = phenanthrene; 4 = carbazole.

phic copolysiloxane solvents, we present as examples the separation of three-, four- and five-ring PAHs with this copolymer in Fig. 3. The resolution of isomers such as anthracene-phenanthrene, benzo[*a*]anthracene-triphenylene-chrysene and benzo[*a*]pyrene-benzo[*e*]pyrene-pyrene with "slightly polar" phases such as SE-52 and SE-54 is not entirely satisfactory [24,25], whereas isomers of four-ring PAHs were separated here on a 10-m column with a film thickness of 0.33 μm . Fig. 4 shows the temperature-programmed separation of a mixture

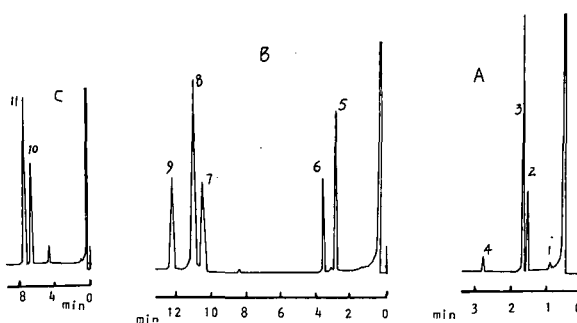


Fig. 3. Separations of (A) three-, (B) four- and (C) five-ring PAHs with the mesomorphic copolysiloxane stationary phase. Peaks: 1 = fluorene; 2 = phenanthrene; 3 = anthracene; 4 = carbazole; 5 = fluoranthene; 6 = pyrene; 7 = triphenylene; 8 = benzo[*a*]anthracene; 9 = chrysene; 10 = benzo[*e*]pyrene; 11 = benzo[*a*]perylene. Column temperatures: (A) 225°C (column 1); (B) 240°C (column 2); (C) 280°C (column 4).

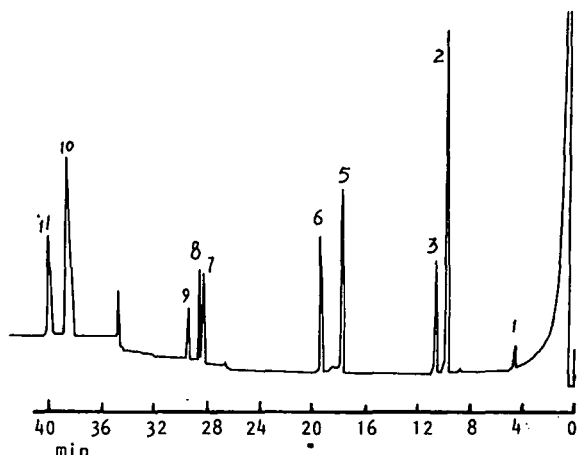


Fig. 4. Temperature-programmed separation of PAHs on column 3. Column temperature, 150°C for 3 min, then increased to 280°C at 4°C/min. Solutes as in Fig. 3.

of ten of the three- to five-ring PAHs encountered most frequently in environmental samples.

We note in passing that the elution order of the five-ring PAHs with conventional polymeric liquid phases is benzo[*e*]pyrene followed by benzo[*a*]pyrene [10]. In contrast, the elution pattern of these solutes with mesomorphic polysiloxanes is consistent with the degree of their rod-like geometry, the more rod-like being retained longer. Thus, benzo[*e*]pyrene elutes first with this copolymer, followed by benzo[*a*]pyrene.

CONCLUSIONS

A mesomorphic copolysiloxane was successfully synthesized and can be easily coated on capillary columns to give high thermal stability, high column efficiencies and high selectivity for the separation of PAHs. This copolymer reveals a wider range of the mesophase than its corresponding monomeric liquid crystals.

ACKNOWLEDGEMENT

This work was supported by the National Natural Science Foundation of China.

REFERENCES

- 1 L. C. Sander and S. A. Wise, *Adv. Chromatogr.*, 25 (1986) 139.
- 2 G. M. Janini, G. M. Muschik, H. J. Issaq and R. J. Laub, *Anal. Chem.*, 60 (1988) 1119.
- 3 G. M. Janini, *Adv. Chromatogr.*, 17 (1979) 231.
- 4 M. S. Vigdergauz, R. V. Vigalok and G. V. Dmitrieva, *Usp. Khim.*, 50 (1981) 943.
- 5 Z. Witkiewicz, *J. Chromatogr.*, 251 (1982) 311.
- 6 G. M. Janini, K. Johnston and W. L. Zielinski, Jr., *Anal. Chem.*, 47 (1975) 670.
- 7 G. M. Janini, G. M. Muschik and W. L. Zielinski, Jr., *Anal. Chem.*, 48 (1976) 809.
- 8 G. M. Janini, G. M. Muschik, J. A. Schroer and W. L. Zielinski, Jr., *Anal. Chem.*, 48 (1976) 1879.
- 9 W. L. Zielinski, Jr. and G. M. Janini, *J. Chromatogr.*, 186 (1979) 237.
- 10 H. Finkelmann, R. J. Laub, W. L. Roberts and C. A. Smith, in M. Cooke, A. J. Dennis and G. L. Fischer (Editors), *Polynuclear Aromatic Hydrocarbons: Physical and Biological Chemistry*, Battelle Press, Columbus, OH, 1982, p. 275.
- 11 B. A. Jones, J. S. Bradshaw, M. Nishioka and M. L. Lee, *J. Org. Chem.*, 49 (1984) 4947.
- 12 H. Finkelman, in A. Ciferri, W. R. Krigbaum and R. B. Meyer (Editors), *Polymeric Liquid Crystals*, Academic Press, New York, 1982, p. 35.
- 13 K. E. Markides, N. Nishioka, B. J. Tarbet, J. S. Bradshaw and M. L. Lee, *Anal. Chem.*, 57 (1985) 1296.
- 14 J. S. Bradshaw, C. Schregenberger, K. H.-C. Chang, K. E. Markides and M. L. Lee, *J. Chromatogr.*, 358 (1986) 95.
- 15 K. E. Markides, H. C. Chang, C. M. Schregenberger, B. J. Tarbet, J. S. Bradshaw and M. L. Lee, *J. High Resolut. Chromatogr. Chromatogr. Commun.*, 8 (1985) 516.
- 16 M. A. Apfel, H. Finkelmann, G. M. Janini, R. J. Laub, B. H. Luhmann, A. Price, W. L. Roberts, T. J. Shaw and C. A. Smith, *Anal. Chem.*, 57 (1985) 651.
- 17 M. Nishioka, B. A. Jones, B. J. Tarbet, J. S. Bradshaw and M. L. Lee, *J. Chromatogr.*, 357 (1986) 79.
- 18 H.-W. Liu, A.-Q. Zhang, Y.-H. Jin and R.-N. Fu, *J. High Resolut. Chromatogr.*, 12 (1989) 533.
- 19 H. C. K. Chang, K. E. Markides, J. S. Bradshaw and M. L. Lee, *J. Chromatogr. Sci.*, 26 (1988) 280.
- 20 L. Rohrschneider, *J. Chromatogr.*, 39 (1969) 383.
- 21 W. O. McReynolds, *J. Chromatogr. Sci.*, 39 (1969) 383.
- 22 M. S. Vigdergauz, R. K. Gabbitova, R. V. Vigalok and I. R. Novikova, *Zavod. Lab.*, 45 (1979) 894.
- 23 J. Szulc, *Doctoral Thesis*, Military Technical Academy, Warsaw, 1982.
- 24 A. Bjorsth (Editor), *Handbook of Polycyclic Aromatic Hydrocarbons*, Marcel Dekker, New York, 1983.
- 25 M. L. Lee, M. Novotny and K. D. Bartle, *Analytical Chemistry of Polycyclic Aromatic Compounds*, Academic Press, New York, 1981.

Short Communication

Thin-layer chromatography on polyacrylonitrile

V. Consideration of separation mechanisms of some aliphatic and aromatic amines

T. J. Janjić, D. M. Milojković, A. Broćović, Ž. J. Arbutina and M. B. Čelap

Faculty of Chemistry, University of Belgrade, Studentski trg 16, P.O. Box 550, 11001 Belgrade (Yugoslavia)

(First received March 23rd, 1992; revised manuscript received June 11th, 1992)

ABSTRACT

The chromatographic behaviour of ten aliphatic and aromatic amines on thin layers of polyacrylonitrile sorbent was investigated using seven aqueous solvent systems. It was established that an increase in the hydrophobic part of the amines results in their increased retention on this sorbent. A positive linear dependence between the number of carbon atoms in the *n*-alkyl groups of primary aliphatic amines and the corresponding R_M values was also established. The separation of the investigated amines was assumed to be based on non-specific hydrophobic interactions between their non-polar parts and the hydrocarbon chains of the sorbent.

INTRODUCTION

In previously published papers of this series [1-4] the application of polyacrylonitrile sorbent (PANS), as a bifunctional adsorbent consisting of polar cyano groups and non-polar hydrocarbon chains, to the separation of several classes of compounds was described and the corresponding separation mechanisms were considered. Thus, in the separation of isomeric *cis-trans* complexes of cobalt(III) [1] it was assumed that hydrogen bonds form between the cyano groups of this sorbent and N-hydrogens of the sorbate, and also that the sorbent

retains cationic complexes on the basis of ion-dipole interactions. It was further assumed that the separations of some food-stuff dyes [2], *tris*(β -diketonato) complexes of transition metals [3] as well as *tris*(alkylxanthato)cobalt(III) complexes [4] by means of aqueous solvent systems are based on non-specific interactions between the non-polar parts of the sorbent and the sorbates (reversed-phase chromatography). However, under conditions used for normal-phase chromatography, namely the application of non-aqueous solvent systems for the separation of *tris*(β -diketonato) complexes of cobalt(III), chromium(III) and ruthenium(III), which do not contain aromatic rings in their molecules [3], and *tris*(alkylxanthato)cobalt(III) complexes [4] it was assumed that these substances are sorbed on PANS by the mechanism of hydrogen bond formation between methyne hydrogen atoms

Correspondence to: Dr. T. J. Janjić, Faculty of Chemistry, University of Belgrade, Studentski trg 16, P.O. Box 550, 11001 Belgrade, Yugoslavia.

of the sorbent and highly electronegative atoms of the sorbates. Finally, in investigations of the chromatographic behaviour of tris(β -diketonato) complexes of transition metals, containing aromatic rings in their molecules [3] using non-aqueous solvents, it was assumed that the sorption of these substances on PANS is based on donor–acceptor interactions of the π -electron systems of the sorbates and the cyano groups of the sorbent.

Continuing our investigations of the separation mechanisms of different sorbates on PANS, in this paper we wanted to examine the chromatographic behaviour of hydrochlorides of some aliphatic and aromatic amines by the application of aqueous solvent systems. Under these conditions amines occur in the form of positively charged cations containing various hydrophobic parts and may be expected to exhibit an interesting chromatographic behaviour. At the same time, these investigations may serve as a check and confirmation of the previously assumed possible interactions between PANS and different sorbates.

EXPERIMENTAL

The preparation of PANS, its application to microscope slides and development of chromatograms are described in our first paper [1]. The investigated *n*-butylamine, *n*-hexylamine, *n*-octylamine and *n*-decylamine (Merck, Darmstadt, Germany), *n*-dodecylamine, dihexylamine, N-isopropylcyclohexylamine (Fluka, Buchs, Switzerland) and N-alkylaryl amines (synthesized and analysed by Mr. Milovan Ivanović, IHTM, Belgrade, Yugoslavia, according to procedures described in the literature [5]) were

first, before being spotted on PANS layers, converted into the corresponding substituted ammonium chlorides by means of 6 mol dm⁻³ hydrochloric acid. To measured volumes of the latter solutions, whose concentration was about 2 mmol cm⁻³ and pH about 2, an equivalent volume of ethanol was added. In all the investigated cases the plates were spotted with 0.2 μ l of freshly prepared solutions.

All components of the chromatographic solvent systems used (Table I) were of analytical grade.

The detection of amines was performed by exposing developed plates to iodine vapour for 10 min.

RESULTS AND DISCUSSION

As can be seen from Table I, seven solvent systems were used for the separation of the investigated substances. These solvent systems, which mainly contain water, was selected above all because the investigated substances are water-soluble salts. In addition, the selected systems also contain Brønsted acids, which prevent protolysis of the sorbate cations.

The R_F values measured are listed in Table II. As may be seen from the table, the results obtained for primary aliphatic amines (substances 1–5) show that elongation of the alkyl group of the amines results in increased retention on PANS. This trend also holds for other cases where the hydrophobic part of a molecule is increased, illustrated by the following sequences:

- (a) $R_F(6) < R_F(2)$;
 (b) $R_F(10) < R_F(9) < R_F(8)$

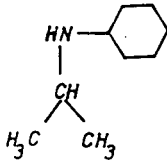
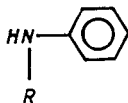
where the numbers in brackets correspond to the ordinal numbers of amines in Table II.

TABLE I

COMPOSITION OF THE CHROMATOGRAPHIC SOLVENT SYSTEMS USED AND THE CORRESPONDING DEVELOPMENT TIMES

No.	Solvent system	Volume ratio	Development time (min)
1	1 M hydrochloric acid	—	35
2	1.25 M hydrochloric acid–ethanol	80:20	45
3	0.125 M hydrochloric acid–ethanol	80:20	45
4	0.1 M perchloric acid	—	30
5	0.125 M perchloric acid–ethanol	80:20	40
6	1 M ammonium chloride	—	35
7	1.25 M ammonium chloride–ethanol	80:20	45

TABLE II
 R_F VALUES OF THE INVESTIGATED AMINES

No.	Amine	Solvent system ^a						
		1	2	3	4	5	6	7
	$\text{CH}_3-(\text{CH}_2)_n-\text{NH}_2$							
1	$n = 3$	79	86	84	79	87	81	85
2	$n = 5$	64	78	76	58	78	67	71
3	$n = 7$	36	71	58	23	54	50	56
4	$n = 9$	18	63	46	9	30	36	41
5	$n = 11$	10	46	25	0	17	24	27
6	$[\text{CH}_3-(\text{CH}_2)_5]_2\text{NH}$	47	53	31	11	28	39	47
7		88	90	86	79	86	83	91
8	 R = 2-propyl	81	87	81	71	79	78	88
9	R = 2-butyl	75	82	79	68	78	68	78
10	R = cycloheptyl	67	76	75	64	77	50	67

^a See Table I.

In addition, from Table II it may be seen that in all the investigated cases relatively smaller R_F values were established for the amine 8, which contains one aromatic ring, in comparison with the amine 7, in which this ring is completely hydrogenated.

Taking into account the chemical nature of PANS and that of the investigated substituted ammonium salts, the following most probable separation mechanisms can be assumed:

(1) The formation of hydrogen bonds between the cyano groups of the sorbent and N-hydrogens of a sorbate.

(2) Ion exchange of the investigated cations on carboxylic groups of the sorbent [1].

(3) Non-specific hydrophobic interactions between the hydrocarbon moieties of the investigated amines and the non-polar chains of PANS.

In the case of alkyl amines, however, the first interaction above is inconsistent with the obtained results, *i.e.*, if this interaction is predominant, a sequence of R_F values opposite to that observed should be expected. As is known, the positive inductive effect, which increases with elongation of an alkyl group, would decrease the effective positive charge on the hydrogen atoms of an alkyl-substituted ammonium group. This will weaken hydrogen bonds. The same effect would cause increased steric hindrance with chain elongation.

On the other hand, under conditions of ion-exchange chromatography of amines on different ion exchangers it has been established by other authors [6,7] that an increase in the non-polar part of amines results in their increased retention. Therefore, if this mechanism is relevant for the investigat-

ed process a sequence of aliphatic amine R_F values would be similar to that observed in this work. However, as is known [1], ion exchange on carboxylic groups is not possible when strongly acidic solvents are used (in our case solvents 1–5, Table I). Consequently, as the results obtained in this paper using these solvents are not significantly different from those established with the solvents containing salts, it seems that the ion-exchange mechanism in the latter case is not predominant.

From all the aforesaid it may be assumed that the separation of these substances takes place in a reversed-phase mode, *i.e.* by hydrophobic interactions [8], where, as it is known, an increase in the hydrophobicity of the sorbate results in increased retention. Such an assumption is supported by the fact that all the solvent systems used are similar to those applied in reversed-phase chromatography and by the observation that a decrease in the water content of a solvent system leads to an increase in the R_F value [9,10]. Similar behaviour has been observed on cyanopropyl-modified silica (which also contains cyano groups and hydrocarbon chains) by chromatography of some steroids using aqueous solvents [10] and was explained by the presence of non-polar hydrocarbon chains between the silica gel skeleton and the cyano groups.

Finally, a possible explanation for the observed sequence of amines 7 and 8 could be the fact that amine 8, which contains a benzene ring with planar configuration, exhibits a greater sorbate–sorbent contact surface than amine 7, which contains a non-planar cyclohexane ring [11]. A greater retention for benzene than cyclohexane was also established in adsorption gas chromatography on graphite, where the retention is exclusively based on dispersive sorbate–sorbent interactions.

In addition, a linear dependence between the number of carbon atoms in a n -alkyl group of primary aliphatic amines and the corresponding R_F values was established (Fig. 1).

On the basis of all the aforesaid it may be concluded that the results obtained in this work make more probable the hydrophobic interaction mechanism for the separation of other substances on PANS, proposed in our earlier papers [2–4], since it could be applied also to explain the chromatographic behaviour of amines investigated in this paper.

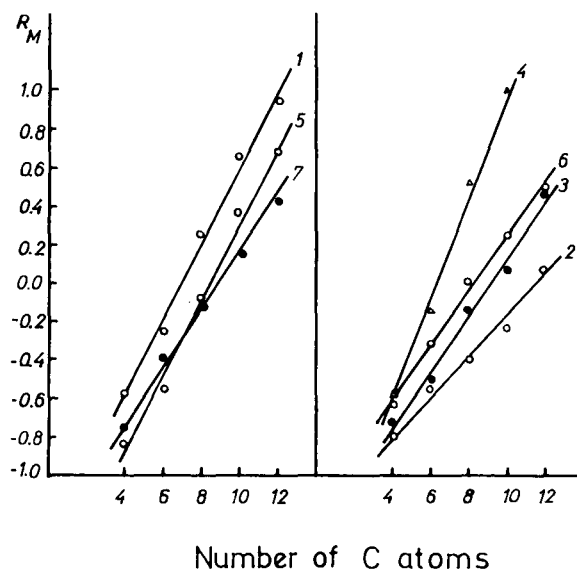


Fig. 1. Relation between the number of carbon atoms in a n -alkyl group of primary aliphatic amines and the corresponding R_M values. The numbers on the lines refer to the solvent system used given in Table I.

ACKNOWLEDGMENTS

The authors are grateful to the Serbian Republic Research Fund for financial support and to Mr. Milovan Ivanović, who kindly supplied us with the samples of some of the investigated amines.

REFERENCES

- 1 T. J. Janjić, D. M. Milojković, Ž. J. Arbutina, Ž. Lj. Tešić and M. B. Čelap, *J. Chromatogr.*, 481 (1989) 465.
- 2 T. J. Janjić, D. M. Milojković, Ž. J. Arbutina and M. B. Čelap, *J. Serb. Chem. Soc.*, 56 (1991) 33.
- 3 T. J. Janjić, D. M. Milojković, Ž. Lj. Tešić and M. B. Čelap, *J. Planar Chromatogr.*, 3 (1990) 495.
- 4 T. J. Janjić, D. M. Milojković, G. N. Vučković, Ž. J. Arbutina and M. B. Čelap, *J. Chromatogr.*, 596 (1992) 91.
- 5 I. V. Mićović, M. D. Ivanović, D. M. Piatak and V. Dj. Bojić, *Synthesis*, (1991) 1043.
- 6 L. Lepri, P. G. Desideri and V. Coas, *J. Chromatogr.*, 79 (1973) 129.
- 7 F. Gelferikh, *Ionity*, Izdatelstvo Inostrannoi Literatury, Moscow, 1962, p. 167.
- 8 Cs. Horváth, W. Melander and I. Molnar, *J. Chromatogr.*, 125 (1976) 129.
- 9 P. Jandera, *J. Chromatogr.*, 314 (1984) 13.
- 10 W. Jost, H. E. Hauck and W. Fischer, *Chromatographia*, 21 (1986) 375.
- 11 E. Leibnits and Kh. G. Shtrupp, *Rukovodstvo po Gazovoi Khromatografii*, Vol. 1, Mir, Moscow, 1988, p. 306.

Short Communication

Determination of hypericin and pseudohypericin by thin-layer chromatography–densitometry

Th. Kartnig and I. Göbel

Institute of Pharmacognosy, Karl-Franzens-University, Universitätsplatz 4/I, A-8010 Graz (Austria)

(First received April 21st, 1992; revised manuscript received June 26th, 1992)

ABSTRACT

The accuracy and reproducibility of the determination of hypericin and pseudohypericin by measuring the emitted fluorescence *in situ* on thin-layer chromatography plates can be improved significantly by using appropriate dipping reagents. The effects of pyridine, polyethylene glycol 4000, paraffins, silicone oil and Triton X-100 in various solvents and combinations on the intensity and stability of emitted fluorescence are described. Using the test conditions established by this investigation, hypericin can be quantified exactly within the range 5–50 ng and pseudohypericin within the range 20–200 ng. The relative standard deviation for the quantification under the given conditions is less than 1.5% for both substances.

INTRODUCTION

Thin-layer chromatography (TLC)–densitometry is still an appropriate method of determining hypericin and pseudohypericin in plant and plant tissue extracts as well as in pharmaceutical formulations [1]. Several TLC systems for the separation of hypericin and pseudohypericin are described [1–5].

The exact and reproducible quantification of TLC-separated hypericins by measuring the emitted fluorescence *in situ* depends on intensifying and stabilizing the fluorescence. This may be achieved by spraying or dipping the TLC plate with appropriate reagents after development. A review on the use of fluorescence enhancement reagents in TLC is given in ref. 6. In systematic investigations we tested sub-

stances reported to increase the intensity of fluorescence of various plant constituents [2,3,7–12]. Finally, we improved the conditions of quantification significantly so that an exact determination of hypericin within the range 5–50 ng and of pseudohypericin within the range 20–200 ng with a relative standard deviation of less than 1.5% was achieved.

EXPERIMENTAL

Chemicals

Hypericin was obtained from Roth (Karlsruhe, Germany, product No. 7929 and was used as follows: 1 mg in 100 ml of methanol (solution A), 1 ml of solution A diluted with 3 ml of methanol (solution B) (2 μ l of solution B = 5 ng of hypericin). Pseudohypericin was obtained from Hämosan (Graz, Austria) and was used as follows: 1 mg in 100 ml of methanol (2 μ l = 20 ng of pseudohypericin). (Hypericin and pseudohypericin solutions

Correspondence to: Universitäts-Professor Dr. Theodor Kartnig, Institute of Pharmacognosy, Karl-Franzens-University, Universitätsplatz 4/I, A-8010 Graz, Austria.

have to be kept in the dark and at low temperature.)

The other chemicals were as follows: pyridine (Merck, Darmstadt, Germany, product No. 9728), polyethylene glycol (PEG) 4000 (Merck, product No. 807490), viscous paraffin (Merck, product No. 7160), liquid paraffin (Merck, product No. 7162), highly liquid paraffin (Merck, product No. 7174), paraffin in block form (Merck, product No. 7150), silicone oil (Merck, product No. 7742), Triton X-100 (Merck, product No. 8603)

Thin-layer chromatography

The TLC plates were 10 × 20 cm TLC aluminium sheets coated with silica gel 60 (without fluorescent indicator) (Merck, product No. 5553) and were developed in unsaturated tanks (Desaga, Heidelberg, Germany, product No. 12 01 73). Test solutions and plant extracts were applied as bands of 6 mm (micropipette by HAACK, Vienna, Austria). The mobile phase was toluene-ethylformate-formic acid (5:4:1) [3,4]. After development over 8 cm, solvent was quickly evaporated in a warm airstream and the plate dried for 10 min at 60°C.

Detection was with UV light at 366 nm. Hyper-

icin ($R_F = 0.58$) and pseudohypericin ($R_F = 0.63$) are separated sufficiently and with sharp boundaries.

Equipment

A Shimadzu CS 9000 dual-wavelength flying-spot scanner was used with the following settings: beam size 0.4 × 10 mm; wavelength = 313 nm; delta "y" = 0.04 mm, filter 4, zero set mode at start.

Sample preparation

A 30- to 50-mg aliquot of powdered (sieve 180, European Pharmacopoeia) *Hypericum* leaves or herbs was extracted with 5 ml of methanol at room temperature using a magnetic stirrer for 1 h. Extraction of plant material was repeated twice with 5 ml of methanol for 5 min. The combined filtrates were evaporated to dryness and the residue dissolved in 2.00 ml of methanol. The solution was filtered again prior to application to the TLC plate.

Preparation of the plate for fluorodensitometric determinations

The developed and dried plate was first dipped into a solution of 10% pyridine in diethyl ether (so-

TABLE I

EFFECTS OF VARIOUS SUBSTANCES ON THE INTENSITY AND STABILITY OF THE FLUORESCENCE OF HYPERICIN AND PSEUDOHYPERICIN

The stabilizing effect is expressed as the decrease in fluorescence achieved within 30 min: - = >25%; (+) = 20-25%; + = <20%; +++ = <3%.

Substance	Fold increase in intensity	Stabilizing effect	Concentration of substance; solvent
Pyridine [2,3]	2-5	-	10%; diethyl ether, acetone
PEG 4000 [7]	2-4	(+)	5%; ethanol
Pyridine + PEG 4000	2-5	-	5% pyridine, 5% PEG, ethanol
Highly liquid paraffin [7-11]	3-10	(+)	20-70%; diethyl ether, <i>n</i> -hexane, toluene
Liquid paraffin [7-11]	3-10	+	20-70%; diethyl ether, <i>n</i> -hexane, toluene
Viscous paraffin [7-11]	3-10	+++	20-70%; diethyl ether, <i>n</i> -hexane, toluene
Block form paraffin	6-8	-	4-8%; toluene
Block form + viscous paraffin	8-12	+	3-4% block form, 25-50% viscous paraffin; diethyl ether
Pyridine + highly liquid paraffin	7-10	-	1-10% pyridine, 50-70% paraffin, diethyl ether, <i>n</i> -hexane
Pyridine + liquid paraffin	7-12	-	1-10% pyridine, 50-70% paraffin, diethyl ether, <i>n</i> -hexane
Pyridine + viscous paraffin	7-15	(+)	1-10% pyridine, 50-70% paraffin, diethyl ether, <i>n</i> -hexane
Silicone oil [7]	2-10	(+)	30-70%; diethyl ether
Pyridine + silicone oil	10-12	(+)	5% pyridine, 30-70% silicone oil, diethyl ether
Triton X-100 [9-12]	2-3	(+)	1-33%; <i>n</i> -hexane, chloroform, toluene

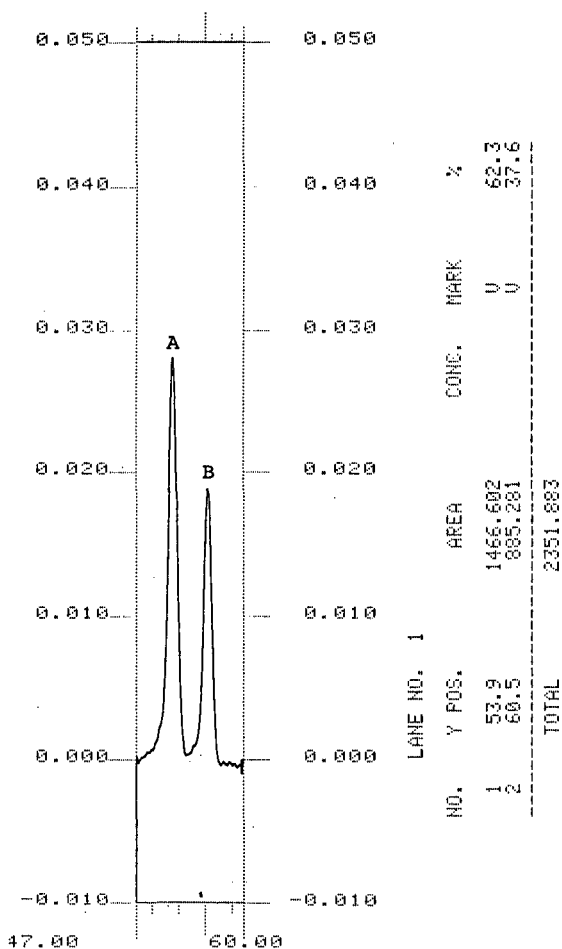


Fig. 1. Scanning profile of a methanolic extract of *Hypericum perforatum* herbs. A = Pseudohypericin; B = hypericin.

lution 1) in a dipping tank (Desaga, product No. 12 41 52). After the diethyl ether had evaporated (ca. 3 min) the plate was dipped into a homogeneous mixture of two volumes of viscous paraffin and one volume of diethyl ether (solution 2), also in a dipping tank.

Subsequently, the plate was placed vertically on a flat surface in the dark for 1 h and the emitted fluorescence was then measured.

Calculations

The contents of hypericin and pseudohypericin are calculated from the formulae:

$$\text{Hypericin (ng)} = \frac{45 (A_t - A_1) + 5 (A_2 - A_1)}{A_2 - A_1}$$

$$\text{Pseudohypericin (ng)} = \frac{180 (A_t - A_1) + 20 (A_2 - A_1)}{A_2 - A_1}$$

where A_t is the area of the sample curve, A_1 is the area of the curve of 5 ng of hypericin and 20 ng of pseudohypericin, and A_2 is the area of the curve of 50 ng of hypericin and 200 ng of pseudohypericin.

Standards of hypericin and pseudohypericin were measured with every determination.

RESULTS AND DISCUSSION

Fluorodensitometric quantification of hypericins *in situ* without application of fluorescence enhancing and stabilizing reagents produces only imprecise and non-reproducible results. The reason for this phenomenon is on the one hand a relatively weak fluorescence and on the other hand insufficient stability of fluorescence intensity [7].

To optimize the quantification of hypericin and pseudohypericin we checked all the steps of the procedure. Extracting plant material in the way described dissolves out the hypericins quantitatively.

TLC separation is better achieved by the suggested system [2,3] than by using RP-8 plates and acetonitrile [1]. The spots are separated well and exhibit sharp margins, as the scanning profile shows (Fig. 1).

To increase fluorescence intensity and improve stability, we tested several substances in various concentrations and combinations as well as in various solvents (see Table I).

Homogeneous application of the reagents to the plate is only guaranteed by dipping and not by spraying [7]. The best effect was achieved with 10% pyridine in diethyl ether as the first dipping solution. After removing diethyl ether from the plate in a warm airstream, other solutions were applied as second reagents (see Table II).

Finally, we found the best effect using consecutive applications of 10% pyridine in diethyl ether as the first dipping solution and 66% viscous paraffin in diethyl ether as the second dipping solution.

To conserve solvents, the dipping procedure should be carried out in dipping tanks. The TLC plate has to be held with forceps. Immediately after withdrawing the plate from the second solution, it

TABLE II

EFFECTS OF VARIOUS SUBSTANCES APPLIED AFTER A BASIC TREATMENT WITH 10% PYRIDINE IN METHANOL

The stabilizing effect is expressed as the decrease in fluorescence achieved within 30 min. - = >25%; (+) = 20-25%; + = <20%; + + + = <3%.

Substance	Fold increase in intensity	Stabilizing effect	Concentration of substance; solvent
PEG 4000	2	-	5%; ethanol
Liquid paraffin	12-14	+	70%; diethyl ether
Viscous paraffin	6-15	+ + +	50-70%; diethyl ether
Blijock form paraffin	6-8	-	4-8%; toluene
Bock form + viscous paraffin	10-12	-	3-4% block form, 25-50% viscous paraffin; diethyl ether
Silicone oil	10	-	70%; diethyl ether
Triton X-100	2-3	-	1-33%; n-hexane, chloroform, toluene

should be placed vertically on a flat surface, e.g. on the turned over metal cover of a TLC tank (Desaga, product No. 12 01 02), in the dark for 1 h. During this time the diethyl ether evaporates and the excess paraffin flows down the plate. After 1 h fluorescence is sufficiently stable for measurements to be made.

To maintain exact results with every TLC plate, 5 and 50 ng of hypericin as well as 20 and 200 ng of pseudohypericin have to be determined as calibration substances. In numerous determinations of identical samples we observed that, in spite of strict adherence to the protocol, there were small differences from experiment to experiment. These differences can be avoided by using hypericin and pseudohypericin standards on the same plate.

The accuracy of the fluorodensitometric measurement of hypericin and pseudohypericin in the procedure described is expressed as the relative standard deviation and is less than 1.5%. The reproducibility of the determination of hypericin and pseudohypericin from plant material is also expressed as the relative standard deviation and is less than 3.5%.

ACKNOWLEDGEMENT

We thank Firma Hämosan (Graz, Austria) for generously providing pseudohypericin.

REFERENCES

- 1 M. Vanhaelen and R. Vanhaelen-Fastre, *J. Chromatogr.*, 281 (1983) 263.
- 2 H. Wagner, S. Bladt, and E.-M. Zgainski, *Drogenanalyse, Dünnschichtchromatographische Analyse von Arzneidrogen*, Springer, Berlin, 1983.
- 3 *Deutscher Arzneimittel-Codex (Ergänzung zum Arzneibuch)*, Govi-Verlag, 1979.
- 4 R. Berghöfer and J. Hölzl, *Dtsch. Apoth. Ztg.*, 126 (1986) 2569.
- 5 P. Pachaly, *Dtsch. Apoth. Ztg.*, 124 (1984) 2159.
- 6 C. F. Poole, S. K. Poole, T. A. Dean and N. M. Chirco, *J. Planar Chromatogr.*, 2 (1989) 180.
- 7 H. Jork, W. Funk, W. Fischer and H. Wimmer, *Dünnschichtchromatographie. Reagenzien und Nachweismethoden*, Band 1a, VCH Verlagsgesellschaft 1989.
- 8 S. Uchiyama and M. Uchiyama, *J. Chromatogr.*, 153 (1978) 135.
- 9 S. Uchiyama and M. Uchiyama, *J. Chromatogr.*, 262 (1983) 340.
- 10 B. Lin Ling, W. R. G. Baeyens, H. Marysael, K. Stragier and P. de Moerloose, *J. Liq. Chromatogr.*, 12 (1989) 3135.
- 11 S. Uchiyama and M. Uchiyama, *J. Liq. Chromatogr.*, 3 (1980) 681.
- 12 S. S. J. Ho, H. T. Butler and C. F. Poole, *J. Chromatogr.*, 281 (1983) 330.

Short Communication

Salting-out thin-layer chromatography of transition metal complexes

I. Investigation of the behaviour of mixed aminocarboxylato cobalt(III) complexes on silica gel

Gordana Vučković, Diana Miljević, Tomislav J. Janjić and Milenko B. Čelap

Faculty of Chemistry, University of Belgrade, P.O. Box 550, 11001 Belgrade (Yugoslavia)

(First received April 13th, 1992; revised manuscript received July 1st, 1992)

ABSTRACT

Twenty-four mixed aminocarboxylato cobalt(III) complexes of anionic and neutral types, containing nitro ligands with or without ammonia ligands and belonging to six homologous series, were investigated by salting-out thin-layer chromatography on silica gel, using seven ammonium sulphate solutions in water. In most cases it was established that a decrease in the R_F values of the complexes accompanied increasing salt concentration of the solvent systems used. A positive linear dependence between the R_M [$\log(1/R_F - 1)$] values of the complexes and the mol percent (mol fraction $\times 100$) of ammonium sulphate in the solvent systems used was found. Finally, a positive linear dependence between the R_M values of the complexes of a homologous series and the number of carbon atoms in the hydrophobic part of a complex was also established. To explain these results, a mechanism based on hydrophobic interaction between the sorbate and the sorbent is proposed.

INTRODUCTION

In several recently published papers by Lederer and co-workers [1–4] the effect of the salt concentration in the water developer on the R_F values of many classes of organic compounds obtained by paper chromatography and thin-layer chromatography (TLC) on cellulose was investigated. It was found that increasing the salt concentration de-

creased the R_F values of the studied compounds (salting-out TLC). The same effect has been also investigated on some transition metal complexes using paper chromatography [5–6] and TLC on silica gel [7], but in these cases a similar trend was not observed. For this reason we wanted to determine if a salting-out effect can also occur in the case of transition metal complexes. To this end we chromatographed on silica gel some of complexes containing hydrophobic hydrocarbon moieties with ammonium sulphate solutions in water in a wide range of concentrations. Silica gel was chosen because, as established in an earlier paper [8], this sorbent is capable of non-specific hydrophobic interac-

Correspondence to: Assistant Professor Gordana Vučković, Faculty of Chemistry, University of Beograd, P.O. Box 550, Studentski trg 16, 11001 Beograd, Yugoslavia.

tions with some metal acetyl-acetonato complexes from water–organic solvents [8].

EXPERIMENTAL

The syntheses of the complexes were performed according to procedures given in the literature (Table I), and the chromatographic procedure is described in an earlier paper [9]. The solutions of different concentrations of ammonium sulphate

(Merck, Darmstadt, Germany) in water were used for chromatographic development. The chromatography was carried out at $20 \pm 2^\circ\text{C}$.

RESULTS AND DISCUSSION

The results obtained are given in Table I. They show that the investigation was carried out with eleven neutral and thirteen anionic mixed cobalt (III) complexes, belonging to six homologous se-

TABLE I
 $R_f \times 100$ VALUES OF THE INVESTIGATED COMPLEXES

No.	Complex ^a	Optical activity ^b	Ref. for synth.	Ammonium sulphate content in solvent system used						
				1.1 0.63	2.2 1.14	3.3 1.69	4.4 2.20	5.5 2.66	6.6 3.10	7.7 3.48 mol/dm ³
<i>cis</i> -(NO ₂), <i>trans</i> (N)-[Co L ₂ (NO ₂) ₂] ⁻										
1	L = gly		10	99	99	99	97	98	95	97
2	L = S-ala	+	10	96	94	89	87	82	78	73
3	L = S-abu	+	11	88	82	76	70	62	51	45
4	L = S-nva	+	11	73	66	58	44	31	22	21
5	L = S-nle	+	11	52	46	32	17	12	9	6
<i>cis</i> (NO ₂), <i>trans</i> (N)-[Co L ₂ (NO ₂) ₂] ⁻										
6	L = iabu		11	89	84	79	70	60	49	44
7	L = S-val	+	11	78	73	63	53	40	29	25
8	L = S-leu	+	11	60	53	44	29	19	12	11
9	L = S-ile	+	11	68	51	47	32	22	15	12
<i>cis</i> (O), <i>trans</i> (NH ₂)-[Co L ₂ (NO ₂)NH ₃]										
10	L = gly		12	98	99	99	97	98	97	99
11	L = S-ala	+	12	92	92	89	85	84	83	79
12	L = S-abu	+	13	79	80	69	63	62	61	46
13	L = S-nva	+	13	55	52	46	31	21	18	11
14	L = S-val	+	13	61	59	56	44	36	31	24
<i>mer</i> -[Co L(NO ₂) ₃ NH ₃] ⁻										
15	L = gly		14	98	98	97	97	97	97	97
16	L = S-ala	-	14	97	96	95	93	93	93	89
17	L = S-abu	-	14	95	93	91	85	82	79	70
18	L = S-nva	-	14	92	87	82	74	65	60	52
<i>cis</i> (NO) ₂ , <i>trans</i> (NH ₂ , NH ₃)-[Co L(NO ₂) ₂ (NH ₃) ₂]										
19	L = gly		12	98	96	97	97	97	97	98
20	L = S-ala	+	12	97	92	95	94	93	93	87
21	L = S-abu	+	12	94	88	90	85	83	76	75
<i>trans</i> (NO ₂), <i>cis</i> (NH ₃)-[Co L(NO ₂) ₂ (NH ₃) ₂]										
22	L = gly		12	99	95	97	97	97	96	97
23	L = S-ala	+	12	98	94	94	93	93	91	91
24	L = S-abu	+	12	93	89	89	83	82	77	76

^a gly = glycine; S-ala = (s)-alanine; S-abu = (s)-aminobutyric acid; S-nva = (s)-norvaline; S-nle = (s)-norleucine; iabu = isoaminobutyric acid; S-val = (s)-valine; S-leu = (s)-leucine; S-ile = (s)-isoleucine.

^b Sign of optical rotation at 589 nm.

ries, using seven solvent systems comprising ammonium sulphate solutions of various concentrations in water. From Table I it is seen that, under the experimental conditions applied, in 80% of the cases increasing of the salt concentration in the solvent system resulted in a decrease in the R_F values of the complexes. This decrease is in accordance with the results obtained by salting-out TLC of numerous organic compounds on cellulose [1–4]. Considering the composition of the complexes that do not exhibit the aforementioned effect, it may be noted that they contain the glycinato anion as an aminocarboxylato ligand. On this basis it could be assumed that the absence of the aforementioned ef-

fect is due to a small hydrophobic part of such complexes, which results in insufficient non-specific hydrophobic interaction between such sorbates and the siloxane groups of the sorbent, which are hydrophobic, unlike to silanol groups [15]. This assumption is in accordance with the fact that this effect increases with the degree of chain branching in aminocarboxylato ligands in a homologous series of the investigated complexes [16].

In addition, we established in most cases a linear dependence of the R_M [$\log(1/R_F - 1)$] values of the complexes on the mol percent (mol%) of ammonium sulphate in the solvent system used for cases for which $R_M > -1.00$ (see Fig. 1). This allows the

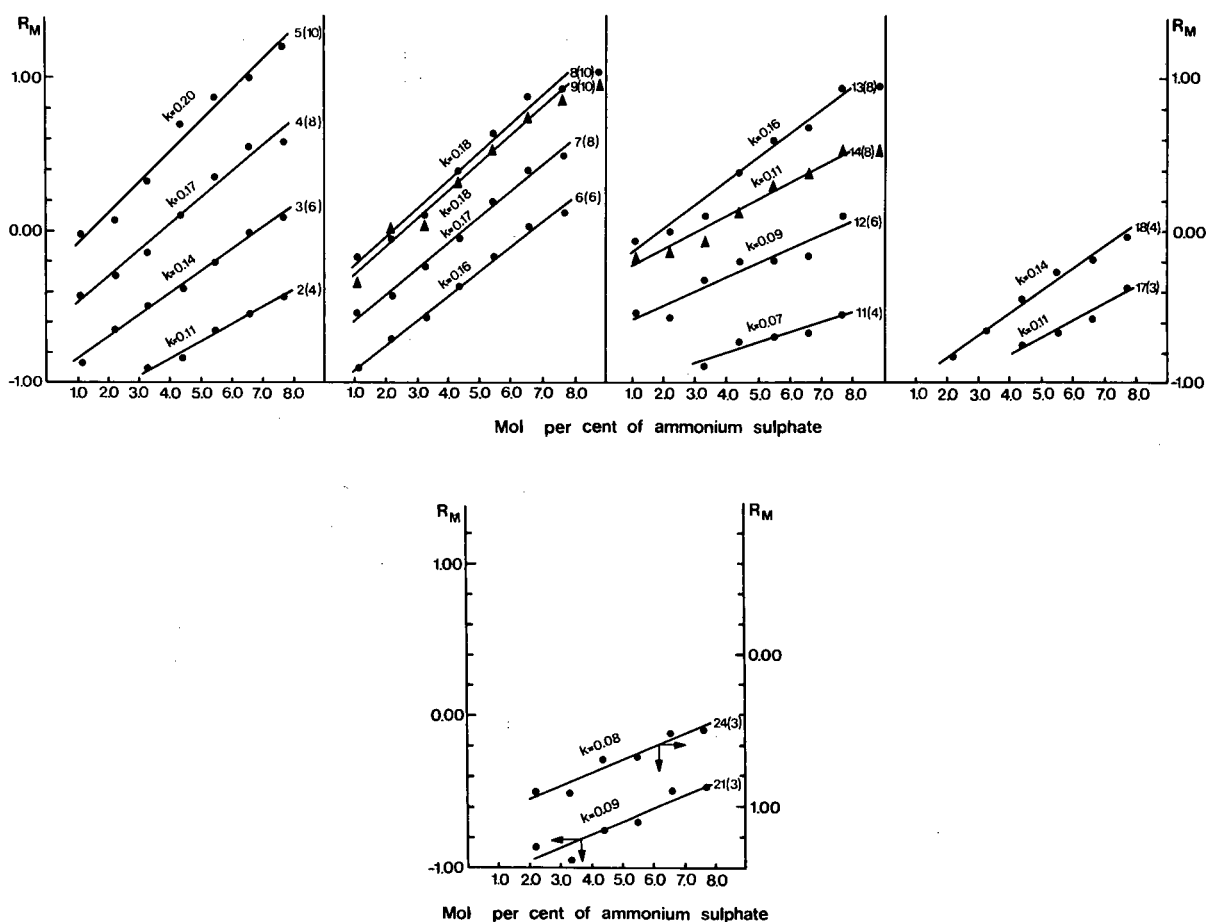


Fig. 1. Dependence of the R_M values of the complexes on ammonium sulphate mol%. Numbers beside the lines represent the complexes used from Table I and the number of the corresponding carbon atoms in the hydrophobic part of a complex (given in brackets); k refers to the corresponding slopes.

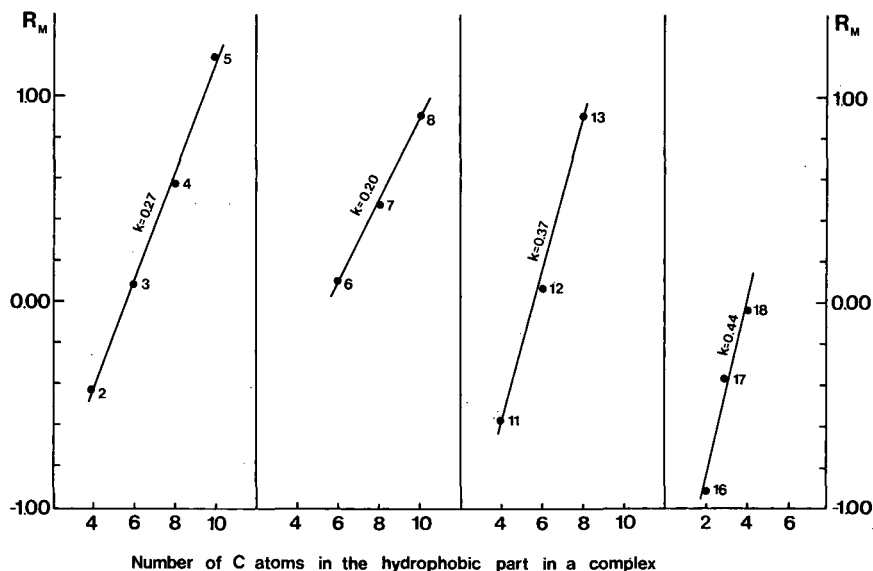


Fig. 2. Dependence of the R_M values of the complexes on the number of carbon atoms in the hydrophobic part in a complex obtained with 7.7 mol% ammonium sulphate solution. Numbers on the lines represent the complexes used from Table I. k as in Fig. 1.

possibility of using the slopes of the resultant straight lines as a determinant of salting-out efficiency. From Fig. 1 it is seen that the slopes of the straight lines increase within a homologous series, which is in accordance with the increase in the hydrophobic part of the molecules in the series.

A linear dependence of the R_M values on the number of carbon atoms in the hydrophobic part of the complexes of the same homologous series, shown in Fig. 2, was also found. From Fig. 2 it is seen that the slopes of the individual straight lines are different. This means that a change of one carbon atom results in a different change in the R_M value in different homologous series of the complexes depending on the other constituents of the complex and their distribution. The aforementioned correlations represented in Figs. 1 and 2 are similar to those previously obtained by column liquid chromatography [17–20], in which linear plots of $\log k'$ capacity factor versus the number of repeated units in a sorbate or the modifier or additive concentration in the mobile phase have been reported.

Finally, we compared the selectivities obtained using the most diluted and the most concentrated solutions of ammonium sulphate (1.1 and 7.7 mol%, respectively). For this reason, in Fig. 3 we have shown the mutual dependence of the R_M val-

ues obtained with these two solutions for three series of complexes for which suitable values for such a presentation were obtained. The linear correlation shown on the figure is a consequence of the previously described linear correlation between $\log k'$ (R_M) and the number of the sorbate repeated units [17–20]. Since the slopes of all three straight lines are greater than 1, this means that the log of the separation factor [8] for two adjacent members in

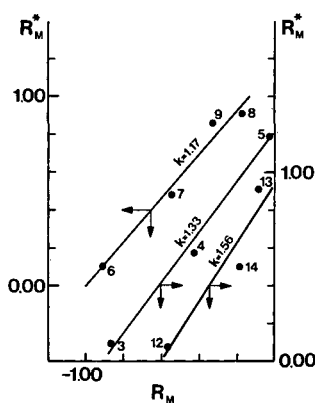


Fig. 3. Dependence of the R_M values of the investigated complexes obtained with 1.1 (R_M) and 7.7 mol% (R_M^*) ammonium sulphate solution. Numbers on the lines represent the complexes from Table I. k as in Fig. 1.

all three series of complexes is greater for more concentrated ammonium sulphate solutions.

On the basis of all the above it may be concluded that silica gel can be also applied for salting-out TLC, in spite of considerable differences between the properties of this sorbent and those of earlier applied cellulose. In addition, it may be concluded that salting-out TLC on silica gel can also be applied for the separation of transition metal complexes.

ACKNOWLEDGEMENT

The authors are grateful to the Serbian Republic Research Fund for financial support.

REFERENCES

- 1 M. Lederer, *J. Chromatogr.*, 194 (1980) 270.
- 2 A. O. Kuhn and M. Lederer, *J. Chromatogr.*, 406 (1987) 389; and references cited therein.
- 3 A. O. Kuhn and M. Lederer, *J. Chromatogr.*, 440 (1988) 165.
- 4 A. O. Kuhn, M. Lederer and M. Sinibaldi, *J. Chromatogr.*, 469 (1989) 253.
- 5 F. Basolo, M. Lederer, L. Ossicini and K. H. Stephen, *J. Chromatogr.*, 10 (1963) 262.
- 6 R. K. Ray and G. Kauffman, *J. Chromatogr.*, 442 (1988) 381.
- 7 T. Baba, H. Yoneda and M. Muto, *Bull. Chem. Soc. Jpn.*, 41 (1968) 1965.
- 8 Ž. Lj. Tešić, T. J. Janjić and M. B. Čelap, *J. Chromatogr.*, 585 (1991) 359.
- 9 M. B. Čelap, Gordana N. Vučković, T. J. Janjić, M. J. Malinar and P. N. Radivojša, *J. Chromatogr.*, 196 (1980) 59.
- 10 M. B. Čelap, D. J. Radanović, T. I. Nikolić and T. J. Janjić, *Inorg. Chim. Acta*, 2 (1968) 52.
- 11 M. B. Čelap, R. G. Denning, D. J. Radanović and T. J. Janjić, *Inorg. Chim. Acta*, 5 (1976) 175.
- 12 M. B. Čelap, M. J. Malinar and T. J. Janjić, *Rev. Chim. Min.*, 13 (1976) 175.
- 13 M. B. Čelap and M. J. Malinar, *Rev. Roum. Chim.*, 22 (1977) 569.
- 14 M. B. Čelap, M. J. Malinar and T. J. Janjić, *Z. Anorg. Allg. Chem.*, 383 (1971) 341.
- 15 B. A. Bidlingmeyer, J. K. Del Rios and J. Korpl, *Anal. Chem.*, 54 (1982) 442.
- 16 A. R. Timerbaev and O. M. Petrukhin, *Zhidkostnaya Adsorbtsionaya Khromatografiya Khelatov*, Nauka, Moscow, 1989, p.68.
- 17 S.-T. Lai, L. Sangermano and D. C. Locke, *J. Chromatogr.*, 312 (1984) 313.
- 18 P. Jandera and J. Rozkošná, *J. Chromatogr.*, 362 (1986) 325.
- 19 P. Jandera, *J. Chromatogr.*, 449 (1984) 361.
- 20 P. Jandera, *J. Chromatogr.*, 314 (1984) 13.

Book Review

High-performance liquid chromatography, by S. Lindsay, Wiley, Chichester, 2nd ed., 1992, XXII + 337 pp., price £ 17.50 (paperback), £ 39.95 (hardcover), ISBN 0-471-93115-2 (paperback); 0-471-93180-2 (hardcover).

This book is a volume in the ACOL series *Analytical Chemistry by Open Learning*, a project of Thames Polytechnic in London. The texts in this series are intended to be used by students and others who want to learn not only by reading a text but also by answering questions which are presented throughout the book. There is open space which allows the answers to be noted down directly in the book. The correct and detailed answers are presented at the end of each chapter. Approximately one third of the total pages are used for questions (nicely presented in grey boxes), empty space and answers. This may seem to be a high percentage, but in fact the problems themselves present a lot of very instructive material which could not be dealt with in the preceding text. It is also very helpful that the reader is told what he or she should know now by the presentation of "learning objectives", often followed by a number of references which give a deeper insight into a special topic.

The first edition of this high-performance liquid chromatography (HPLC) text was published in 1987. That edition was not really satisfactory because it was too short and many important topics were not mentioned at all. This second edition is an almost new text which can be fully recommended, although it does not replace a good textbook on HPLC (as no ACOL book is intended to be used without background information). The individual chapters are: (1) Introduction; (2) Retention and

peak dispersion; (3) Solvent delivery and sample injection; (4) Columns; (5) Detectors; (6) The mobile phase; (7) Column packings and modes of HPLC; (8) Method development; (9) Some practical aspects of HPLC; and (10) Some additional topics. Perhaps the theoretical background of the method has been dealt with too briefly; Chapter 2 is only 14 pages long, excluding the pages used for questions and answers. Some figures are too schematic, but there are also many very instructive chromatograms. The reviewer was especially impressed by the clear and detailed sections about the diode-array detector, electrochemical detectors, mobile phase optimization and method development. The "practical aspects" presented in Chapter 9 relate to column packing and testing, mobile phase preparation and some practical procedures with columns and samples. Chapter 10 brings the book to a good completion with sections on small-bore columns, fast LC, separation of enantiomers, flash chromatography, preparative HPLC, supercritical fluid chromatography (too short with less than a page) and LC-mass spectrometry. Very helpful are some tables with units of measurement and the index.

As an ACOL text the book is intended for individual use, and those who work through it will benefit enormously.

Berne (Switzerland)

Veronika R. Meyer

Author Index

- Allender, W. J. and Keegan, J.
Chromatographic analysis of *cis*- and *trans*-mevinphos in poisoned wildlife 609(1992)315
- Arbutina, Ž. J., see Janjić, T. J. 609(1992)419
- Armstrong, D. W., see Feng, Z. 609(1992)187
- Attila, I., see Özden, S. 609(1992)402
- Bárcena, J. A., see Martínez-Lara, E. 609(1992)141
- Belenkii, B. G., Gankina, E. S., Zgonnik, V. N., Malchova, I. I. and Melenevskaya, E. U.
Critical thin-layer chromatography as a novel method for the determination of the molecular weight and compositional inhomogeneity of block copolymers 609(1992)355
- Bettero, A., see Gazzani, G. 609(1992)391
- Bicchi, C., Frattini, C., Pellegrino, G., Rubiolo, P., Raverdino, V. and Tsoupras, G.
Determination of sulphurated compounds in *Tagetes patula* cv. *nana* essential oil by gas chromatography with mass spectrometric, Fourier transform infrared and atomic emission spectrometric detection 609(1992)305
- Booth, C. K., Nixon, P. F. and Winzor, D. J.
Gel chromatographic evaluation of the binding constant for the interaction of thiamin diphosphate with magnesium ion 609(1992)83
- Braggins, T., see Burford, M. D. 609(1992)321
- Brinkman, U. A. T., see Ståb, J. A. 609(1992)195
- Broćović, A., see Janjić, T. J. 609(1992)419
- Burford, M. D., Hawthorne, S. B., Miller, D. J. and Braggins, T.
Comparison of methods to prevent restrictor plugging during off-line supercritical extraction 609(1992)321
- Butler, E. C. V. and Dal Pont, G.
Liquid chromatography-electrochemistry procedure for the determination of chlorophenolic compounds in pulp mill effluents and receiving waters 609(1992)113
- Castello, G., see Gerbino, T. C. 609(1992)289
- Čelap, M. B., see Janjić, T. J. 609(1992)419
- Čelap, M. B., see Vučković, G. 609(1992)427
- Chang, Y.-W., see Hsu, M.-C. 609(1992)181
- Chrétien, J. R., Riguezza, M., Hassani, A. and Meklati, B. Y.
Factor analysis and experimental design in high-performance liquid chromatography. XIII. Correspondence factor analysis of the heterogeneity of the behaviour of congeneric solutes series studied on homogeneous OV phases in gas chromatography 609(1992)261
- Christie, W. W., see Nikolova-Damyanova, B. 609(1992)133
- Cofino, W. P., see Ståb, J. A. 609(1992)195
- Dal Pont, G., see Butler, E. C. V. 609(1992)113
- D'Amato, G., see Gerbino, T. C. 609(1992)289
- Davies, M., Smith, K. D., Harbin, A.-M. and Hounsell, E. F.
High-performance liquid chromatography of oligosaccharide alditols and glycopeptides on a graphitized carbon column 609(1992)125
- Drewe, J. and Küsters, E.
High-performance liquid chromatographic method for the enantiomeric separation of the chiral metabolites of midazolam 609(1992)395
- Dutoit, J.-C., see Reddy, K. S. 609(1992)229
- Emmrich, M., see Sollinger, S. 609(1992)297
- Feibush, B., see Zhou, F.-X. 609(1992)103
- Felinger, A. and Guiochon, G.
Optimization of the experimental conditions and the column design parameters in displacement chromatography 609(1992)35
- Feng, Z., Gollamudi, R., Han, G., Tang, Y. and Armstrong, D. W.
Chiral separation of nipecotic acid amides 609(1992)187
- Fisher, D., see Walter, H. 609(1992)219
- Fitos, I., Visy, J., Simonyi, M. and Hermansson, J.
Chiral high-performance liquid chromatographic separations of vinca alkaloid analogues on α , -acid glycoprotein and human serum albumin columns 609(1992)163
- Frattini, C., see Bicchi, C. 609(1992)305
- Fu, R., see Wang, H. 609(1992)414
- Gaboriaud, R., see Tribet, C. 609(1992)381
- Gandini, C., see Gazzani, G. 609(1992)391
- Gankina, E. S., see Belenkii, B. G. 609(1992)355
- Gareil, P., see Tribet, C. 609(1992)381
- Gazzani, G., Stoppini, G., Gandini, C. and Bettero, A.
Reversed-phase high-performance liquid chromatographic and derivative UV spectrophotometric determination of α -phenylethylamine in phosphomycin 609(1992)391
- Gen, T., see Wang, H. 609(1992)414
- Gerbino, T. C., Castello, G. and D'Amato, G.
Gas chromatographic identification of halogenated hydrocarbons by using the correlation between their retention and boiling points 609(1992)289
- Göbel, I., see Kartnig, T. 609(1992)423
- Gollamudi, R., see Feng, Z. 609(1992)187
- Guiochon, G., see Felinger, A. 609(1992)35
- Guiochon, G., see Ma, Z. 609(1992)19
- Han, G., see Feng, Z. 609(1992)187
- Harbin, A.-M., see Davies, M. 609(1992)125
- Hassani, A., see Chrétien, J. R. 609(1992)261
- Hawthorne, S. B., see Burford, M. D. 609(1992)321
- Hawthorne, S. B., see Paschke, T. 609(1992)333
- Hermansson, J., see Fitos, I. 609(1992)163
- Herslof, B. G., see Nikolova-Damyanova, B. 609(1992)133
- Honda, F., Honda, H. and Koishi, M.
Application of non-porous silica ultramicrospheres to high-performance liquid chromatographic column packings 609(1992)49
- Honda, H., see Honda, F. 609(1992)49
- Hounsell, E. F., see Davies, M. 609(1992)125

- Hsu, M.-C., Chang, Y.-W. and Lee, Y.-T.
Column liquid chromatography and microbiological assay compared for determination of cefadroxil preparations 609(1992)181
- Hughbanks, D., see Singhal, R. P. 609(1992)147
- Iwase, H.
Determination of folic acid in an elemental diet by high-performance liquid chromatography with UV detection 609(1992)399
- Janjić, T. J., Milojković, D. M., Broćović, A., Arbutina, Ž. J. and Čelap, M. B.
Thin-layer chromatography on polyacrylonitrile. V. Consideration of separation mechanisms of some aliphatic and aromatic amines 609(1992)419
- Janjić, T. J., see Vučković, G. 609(1992)427
- Jelínek, I., see Snopek, J. 609(1992)1
- Kaliszan, A., see Kaliszan, R. 609(1992)69
- Kaliszan, R., Kaliszan, A., Noctor, T. A. G., Purcell, W. P. and Wainer, I. W.
Mechanism of retention of benzodiazepines in affinity, reversed-phase and adsorption high-performance liquid chromatography in view of quantitative structure-retention relationships 609(1992)69
- Kaneta, T., Tanaka, S., Taga, M. and Yoshida, H.
Effect of addition of glucose on micellar electrokinetic capillary chromatography with sodium dodecyl sulphate 609(1992)369
- Kartnig, T. and Göbel, I.
Determination of hypericin and pseudohypericin by thin-layer chromatography–densitometry 609(1992)423
- Kashiwa, R., see Saitoh, K. 609(1992)341
- Keegan, J., see Allender, W. J. 609(1992)315
- King, J.-K. and Pinto, N. G.
Short fibrous supports for preparative chromatographic separations of biomolecules 609(1992)61
- Kiyohara, C., see Saitoh, K. 609(1992)341
- Kohne, B., see Kraus, A. 609(1992)277
- Koishi, M., see Honda, F. 609(1992)49
- Konwalinka, G., see Stuppner, H. 609(1992)375
- Kováts, E. sz., see Reddy, K. S. 609(1992)229
- Kraus, A., Schumann, U., Kraus, G., Kohne, B. and Praefcke, K.
Investigation of a scyllitol-derived (saturated) disc-shaped liquid crystal stationary phase in capillary gas chromatography 609(1992)277
- Kraus, A., see Soják, L. 609(1992)283
- Kraus, G., see Kraus, A. 609(1992)277
- Kraus, G., see Soják, L. 609(1992)283
- Krull, I. S., see Zhou, F.-X. 609(1992)103
- Kubinec, R., see Soják, L. 609(1992)283
- Küçükislamoglu, M., see Özden, S. 609(1992)402
- Küstern, E., see Drewe, J. 609(1992)395
- Lai, F. and Sheehan, T.
Enhancement of detection sensitivity and cleanup selectivity for tobramycin through pre-column derivatization 609(1992)173
- Lee, Y.-T., see Hsu, M.-C. 609(1992)181
- Levsen, K., see Sollinger, S. 609(1992)297
- Li, H., see Wang, H. 609(1992)414
- Liu, J., see Wang, H. 609(1992)414
- López-Barea, J., see Martínez-Lara, E. 609(1992)141
- Ma, Z. and Guiochon, G.
Shock layer thickness in the case of wide bands of single components and binary mixtures in non-linear liquid chromatography 609(1992)19
- Malchova, I. I., see Belenkii, B. G. 609(1992)355
- Martínez-Lara, E., Pascual, P., Toribio, F., López-Barea, J. and Bárcena, J. A.
Rapid method for the determination of glutathione transferase isoenzymes in crude extracts 609(1992)141
- Meklati, B. Y., see Chrétien, J. R. 609(1992)261
- Melenevskaya, E. U., see Belenkii, B. G. 609(1992)355
- Meyer, V. R.
High-performance liquid chromatography (by S. Lindsay) (Book Review) 609(1992)432
- Miljević, D., see Vučković, G. 609(1992)427
- Miller, D. J., see Burford, M. D. 609(1992)321
- Miller, D. J., see Paschke, T. 609(1992)333
- Milojković, D. M., see Janjić, T. J. 609(1992)419
- Nikolova-Damyanova, B., Herslof, B. G. and Christie, W. W.
Silver ion high-performance liquid chromatography of derivatives of isomeric fatty acids 609(1992)133
- Nixon, P. F., see Booth, C. K. 609(1992)83
- Noctor, T. A. G., see Kaliszan, R. 609(1992)69
- Okada, T.
Automated analyses of non-ionic surfactants in terms of hydrophobic and polyoxyethylated chain lengths 609(1992)213
- Okatan, A., see Özden, S. 609(1992)402
- Ostrovský, I., see Soják, L. 609(1992)283
- Özden, S., Özden, T., Attila, I., Küçükislamoglu, M. and Okatan, A.
Isolation and identification via high-performance liquid chromatography and thin-layer chromatography of benzoxazolinone precursors from *Consolida orientalis* flowers 609(1992)402
- Özden, T., see Özden, S. 609(1992)402
- Paschke, T., Hawthorne, S. B., Miller, D. J. and Wenclawiak, B.
Supercritical fluid extraction of nitrated polycyclic aromatic hydrocarbons and polycyclic aromatic hydrocarbons from diesel exhaust particulate matter 609(1992)333
- Pascual, P., see Martínez-Lara, E. 609(1992)141
- Pellegrino, G., see Bicchi, C. 609(1992)305
- Pinto, N. G., see King, J.-K. 609(1992)61
- Pirkle, W. H., see Welch, C. J. 609(1992)89
- Polymeropoulos, C. E., see Qian, J. 609(1992)269
- Praefcke, K., see Kraus, A. 609(1992)277
- Purcell, W. P., see Kaliszan, R. 609(1992)69
- Qian, J., Polymeropoulos, C. E. and Ulisse, R.
Liquid jet evolution from a gas chromatographic injector 609(1992)269
- Raverdino, V., see Bicchi, C. 609(1992)305
- Raymond, F. D., see Walter, H. 609(1992)219
- Reddy, K. S., Dutoit, J.-C. and Kováts, E. sz.
Pair-wise interactions by gas chromatography. I. Interaction free enthalpies of solutes with non-associated primary alcohol groups 609(1992)229

- Righezza, M., see Chrétien, J. R. 609(1992)261
Rowe, R. C., see Wren, S. A. C. 609(1992)363
Rozing, M. J. M., see Stäb, J. A. 609(1992)195
Rubiolo, P., see Bicchi, C. 609(1992)305
Sachse, J.
 Identification and determination of mellein in cultures of the fungus *Septoria nodorum* (Berk.) by thin-layer and high-performance liquid chromatography 609(1992)349
Saitoh, K., Kashiwa, R., Tada, R., Kiyohara, C. and Suzuki, N.
 High-performance thin-layer chromatographic mobility of porphyrins and their copper complexes on different adsorbents 609(1992)341
Schumann, U., see Kraus, A. 609(1992)277
Sheehan, T., see Lai, F. 609(1992)173
Siemens, K. and Zawistowski, J.
 Determination of *Penicillium roqueforti* toxin by reversed-phase high-performance liquid chromatography 609(1992)205
Simonyi, M., see Fitos, I. 609(1992)163
Singhal, R. P., Hughbanks, D. and Xian, J.
 Separation of dideoxyribonucleosides in trace amounts by automated liquid chromatography and capillary electrophoresis 609(1992)147
Smith, K. D., see Davies, M. 609(1992)125
Smolková-Keulemansová, E., see Snopek, J. 609(1992)1
Snopek, J., Jelinek, I. and Smolková-Keulemansová, E.
 Chiral separation by analytical electromigration methods (Review) 609(1992)1
Soják, L., Ostrovský, I., Kubinec, R., Kraus, G. and Kraus, A.
 Separation and identification of all isomeric *n*-nonadecenes by capillary gas chromatography on a mesogenic stationary phase with Fourier transform infrared and mass spectrometric detection 609(1992)283
Sollinger, S., Levsen, K. and Emmrich, M.
 Determination of trace amounts of carboxylic acids in ambient air by capillary gas chromatography-mass spectrometry 609(1992)297
Stäb, J. A., Rozing, M. J. M., Van Hattum, B., Cofino, W. P. and Brinkman, U. A. T.
 Normal-phase high-performance liquid chromatography with UV irradiation, morin complexation and fluorescence detection for the determination of organotin pesticides 609(1992)195
Stoppini, G., see Gazzani, G. 609(1992)391
Stuppner, H., Sturm, S. and Konwalinka, G.
 Capillary electrophoretic analysis of oxindole alkaloids from *Uncaria tomentosa* 609(1992)375
Sturm, S., see Stuppner, H. 609(1992)375
Sukrasno, , see Zarate, R. 609(1992)407
Suzuki, N., see Saitoh, K. 609(1992)341
Tada, R., see Saitoh, K. 609(1992)341
Taga, M., see Kaneta, T. 609(1992)369
Tanaka, S., see Kaneta, T. 609(1992)369
Tang, Y., see Feng, Z. 609(1992)187
Toribio, F., see Martínez-Lara, E. 609(1992)141
Tribet, C., Gaboriaud, R. and Gareil, P.
 Determination of C₈-C₂₀ saturated anionic and cationic surfactant mixtures by capillary isotachopheresis with conductivity detection 609(1992)381
Tsoupras, G., see Bicchi, C. 609(1992)305
Ulisse, R., see Qian, J. 609(1992)269
Van Hattum, B., see Stäb, J. A. 609(1992)195
Visy, J., see Fitos, I. 609(1992)163
Vučković, G., Miljević, D., Janjić, T. J. and Čelap, M. B.
 Salting-out thin-layer chromatography of transition metal complexes. I. Investigation of the behaviour of mixed aminocarboxylato cobalt(III) complexes on silica gel 609(1992)427
Wainer, I. W., see Kaliszan, R. 609(1992)69
Walter, H., Raymond, F. D. and Fisher, D.
 Erythrocyte partitioning in dextran-poly(ethylene glycol) aqueous phase systems. Events in phase and cell separation 609(1992)219
Wang, H., Gen, T., Fu, R., Zhu, J., Wei, X., Li, H. and Liu, J.
 Gas chromatographic separation of polycyclic aromatic hydrocarbons on a mesomorphic copolysiloxane stationary phase 609(1992)414
Wei, X., see Wang, H. 609(1992)414
Welch, C. J. and Pirkle, W. H.
 Progress in the design of selectors for buckminsterfullerene 609(1992)89
Wenclawiak, B., see Paschke, T. 609(1992)333
Winzor, D. J., see Booth, C. K. 609(1992)83
Wren, S. A. C. and Rowe, R. C.
 Theoretical aspects of chiral separation in capillary electrophoresis. II. The role of organic solvent 609(1992)363
Xian, J., see Singhal, R. P. 609(1992)147
Yeoman, M. M., see Zarate, R. 609(1992)407
Yoshida, H., see Kaneta, T. 609(1992)369
Zarate, R., Sukrasno, and Yeoman, M. M.
 Application of two rapid techniques of column chromatography to separate the pungent principles of ginger, *Zingiber officinale* Roscoe 609(1992)407
Zawistowski, J., see Siemens, K. 609(1992)205
Zgonnik, V. N., see Belenkii, B. G. 609(1992)355
Zhou, F.-X., Krull, I. S. and Feibush, B.
 9-Fluoreneacetyl-tagged, solid-phase reagent for derivatization in direct plasma injection 609(1992)103
Zhu, J., see Wang, H. 609(1992)414

Errata

corrected 26 Oct 92/AP.

J. Chromatogr., 595 (1992) 103–111

Please note that the Azlactone Resin from 3M used in this article is not a commercially available resin.

J. Chromatogr., 606 (1992) 103–111

Page 103, 2nd column, 7th line from the bottom: “Theoretixcal” should read “Theoretical”.

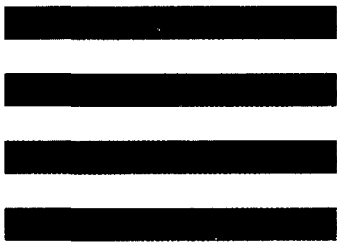
Page 105, eqn. 4b: “ $\chi_L \cdot \frac{\partial T}{\partial r}$ ” should read “ $\chi_L \cdot \frac{\partial T^-}{\partial r}$ ”.

Page 105, 1st column, 9th line from the bottom: “in ref. 8” should read “in ref. 10”.

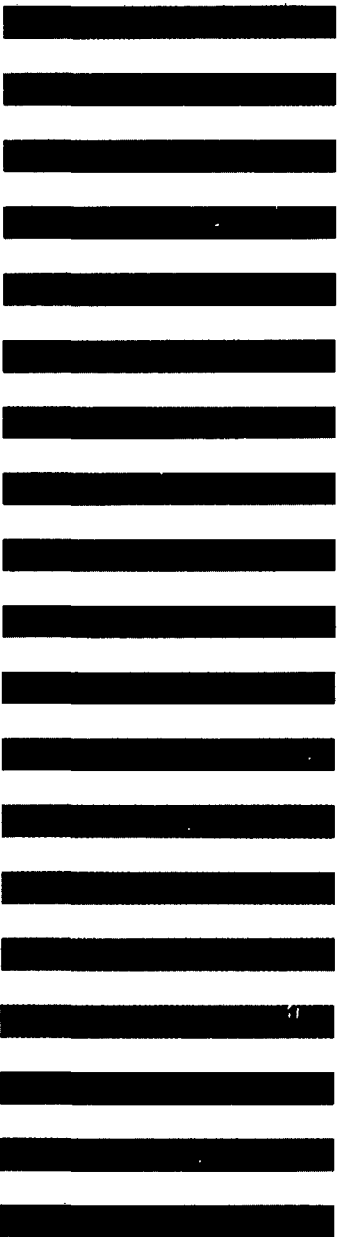
Page 107, 1st column, last sentence: this sentence should be deleted.

J. Chromatogr., 606 (1992) 133–135

Page 134, 1st column, 2nd line from the bottom: “ $-\text{CH}_2\text{CH}_3$ ” should read “ $-\text{CH}_2\text{CH}_3$ ”.



Instructions to Authors



JOURNAL
of
CHROMATOGRAPHY
INCLUDING ELECTROPHORESIS AND OTHER SEPARATION METHODS
BIOMEDICAL APPLICATIONS

SYMPOSIUM VOLUMES

Elsevier Science Publishers B.V.
Desk-Editorial Office *Journal of Chromatography*:
P.O. Box 330, 1000 AH Amsterdam, Netherlands
Sara Burgerhartstraat 25, 1055 KV Amsterdam, Netherlands
Tel. + 31-20-5862793
FAX + 31-20-5862304
Telex 10704 espom



ELSEVIER
AMSTERDAM - LONDON - NEW YORK - TOKYO

General

The *Journal of Chromatography* publishes papers on all aspects of **chromatography, electrophoresis** and related methods. Contributions consist mainly of research papers dealing with chromatographic and electrophoretic theory, instrumental developments and their applications.

Biomedical Applications. This section, which is under separate editorship, deals with the following aspects: developments in and applications of chromatographic and electrophoretic techniques related to clinical diagnosis or alterations during medical treatment; screening and profiling of body fluids or tissues related to the analysis of active substances and to metabolic disorders; drug level monitoring and pharmacokinetic studies; clinical toxicology; forensic medicine; veterinary medicine; occupational medicine; results from basic medical research with direct consequences in clinical practice.

Symposium volumes. This publication, which is under separate editorship, publishes proceedings of symposia on chromatography, electrophoresis and related methods.

Types of contributions

The following types of papers are published in the *Journal of Chromatography* and the section on *Biomedical Applications*: Regular research papers (full-length papers), Review articles, Short Communications and Discussions. Review articles are invited or proposed in writing to the Editors, who welcome suggestions for subjects. An outline of the proposed Review should first be forwarded to the Editors for preliminary discussion prior to preparation. Short Communications are usually descriptions of short investigations, or they can report minor technical improvements of previously published procedures: they reflect the same quality of research as full-length papers, but should preferably not exceed five printed pages. Discussions (one or two pages) should explain, amplify, correct or otherwise comment substantively upon an article recently published in the journal.

Submission of an article is understood to imply that the article is original and unpublished and is not being considered for publication elsewhere.

Upon acceptance of an article by the journal, the author(s) will be asked to transfer the copyright of the article to the publisher. This transfer will ensure the widest possible dissemination of information.

Submission of papers

The preferred medium of submission is on disk with accompanying manuscript (see *Electronic manuscripts* below).

Manuscripts in English (**four** copies, as well as a set of reproducible figures, are required) should be submitted to:

for the *Journal of Chromatography*:

Editorial Office
JOURNAL OF CHROMATOGRAPHY
P.O. Box 681
1000 AR Amsterdam, Netherlands

for the *Biomedical Applications* section:

Dr. K. Macek
The Editor of
JOURNAL OF CHROMATOGRAPHY,
BIOMEDICAL APPLICATIONS
P.O. Box 681
1000 AR Amsterdam, Netherlands

Manuscripts for the SYMPOSIUM VOLUMES section (*three* copies are required) should be submitted during the symposium concerned. After the symposium, correspondence should be sent by *regular air mail (NOT by registered, special delivery of private mail services)* to the Editor handling the corresponding proceedings, *i.e.*, either:

Dr. E. Heftmann
Editor of
JOURNAL OF CHROMATOGRAPHY,
SYMPOSIUM VOLUMES
P.O. Box 928
ORINDA, CA 94563, USA

or
Dr. Z. Deyl
Editor of
JOURNAL OF CHROMATOGRAPHY,
SYMPOSIUM VOLUMES
Institute of Physiology
Czechoslovak Academy of Sciences
Videnská 1083
14220 PRAGUE 4-Krc
Czechoslovakia

English linguistic improvement, if appropriate, is provided as part of the normal editorial process.

Every paper must be accompanied by a letter from the senior author, stating that he/she is submitting the paper for publication in the *Journal of Chromatography*.

Manuscripts

Manuscripts should be typed in **double spacing** on one side of consecutively numbered sheets of paper of uniform size. A 2-cm margin should be left on each side, an easily readable font (12 pt.) should be chosen, and (in case of computer-processed manuscripts) a letter-quality printer or equivalent should be used. The manuscript should be preceded by a sheet of manuscript paper carrying the title of the paper and the name, full postal address and FAX number of the author to whom correspondence is to be addressed. As a rule,

papers should be divided into sections, headed by caption (*e.g.* Abstract, Introduction, Experimental, Results, Discussion). All illustrations, photographs, tables, etc. should be on separate sheets. **Four** copies of the complete manuscript (with illustrations and tables attached to each copy) should be submitted (for *Symposium Volumes* only: *three* copies).

Electronic manuscripts

Electronic manuscripts have the advantage that there is no need for the rekeying of text, thereby avoiding the possibility of introducing errors and resulting in reliable and fast delivery of proofs.

The preferred storage is a 5.25- or 3.5-in. disk in MS-DOS format, although other systems are welcome, *e.g.*, Macintosh (in this case, save your file in the usual manner, do not use the option "save in MS-DOS format"). Your disk and (**exactly matching**) printed version (printout, hardcopy) should be submitted together to the accepting editor or Editorial Office. In case of revision, the same procedure should be followed such that, on acceptance of the article, **the file on disk and printout are identical**. Please specify the type of computer and word-processing package used (do not convert your textfile to plain ASCII). Ensure that the letter "l" and digit "1" (also letter "O" and digit "0") have been used properly, and format your article (tabs, indents, etc.) consistently. Characters not available on your word processor (Greek letters, mathematical symbols, etc.) should not be left open but indicated by a unique code (*e.g.* gralpha, @, #, etc., for the Greek letter α). Such codes should be used consistently throughout the entire text. Please make a list of such codes and provide a key. Do not allow your word processor to introduce word splits and do not use a "justified" layout. Please adhere strictly to the general instructions on style/arrangement and, in particular, the reference style of the journal. Further information may be obtained from the Publisher.

Title

The title of the paper should be concise and informative. Since titles are widely used in information retrieval systems, care should be taken to include the key words. The title should be followed by the authors' full names, academic or professional affiliations, and the address of the laboratory where the work was carried out. If the present address of an author is different from that mentioned, it should be given in a footnote. Acknowledgements of financial support are not to be made in a footnote to the title or name of the author, but should be included in the Acknowledgements at the end of the paper.

Abstract

All articles should have an abstract of 50–100 words which clearly and briefly indicates what is new, different and significant. No references should be given.

Introduction

Every paper must have a concise introduction that mentions what has been done before on the topic, with appropriate references, and that states clearly what is new in the paper now submitted.

Experimental

The Experimental section should contain sufficient information for others to repeat the Experiments. Whereas general conditions can usually best be specified in the Experimental section, it is often better to give specific details in the figure captions. Appendix 1 lists what should typically be specified.

Tables and illustrations

Although appropriate tables and illustrations contribute to a clear and concise presentation of results, they should not merely repeat data already given in the text.

Tables should be typed (in double spacing) on separate pages, and numbered in Roman numerals according to their sequence in the text. A brief descriptive heading should be given above each table. Below the heading the experimental conditions should be described. The layout of the tables should be given serious thought, so that the reader can grasp quickly the significance of the results.

Figures should be submitted in a form suitable for reproduction, either drawn in Indian ink on drawing or tracing paper, or as sharp prints [either photographic (glossy) prints or prints from a high-resolution laser printer]. All axes of graphs and chromatograms should be clearly labelled, with full quantitative data, or equivalent information should be provided in the legend. Please note that any lettering should also be in a form suitable for reproduction. Lettering (which should be kept to a minimum) and spacing on axes of graphs should be such that numbers, etc., remain legible after reduction in size. One reproducible copy and three photocopies are required. The figures should preferably be of such a size that the same degree of reduction can be applied to all of them. The size of the figures should preferably not exceed the size of the text pages. Simple straight-line graphs (such as calibration lines) are not acceptable, because they can readily be described in the text by means of an equation or a sentence. Claims of linearity should be supported by regression data that include slope, intercept, standard deviations of the slope and intercept, standard error and the number of data points; correlation coefficients are optional. Standard symbols should be used in line drawings; the following are available to the typesetters and can also be used in the legends:

○ ● □ ■ △ ▲ ◇ ◆ + × ▽ ▼

Photographs should have good contrast and intensity. Sharp, glossy photographs are required to obtain good halftones. References to the illustrations should be included in appropriate places in the text by Arabic numerals and the approximate position of the illustration should be indicated in the margin of the manuscript. Each illustration should have a caption, all the *captions* being typed (with double spacing) together on a *separate sheet*.

If structures are given in the text, the original drawings should be provided.

Coloured illustrations are reproduced at the author's expense, the cost being determined by the number of pages and by the number of colours needed.

The written permission of the author and publisher must be obtained for the use of any figure already published. Its source must be indicated in the legend.

Nomenclature, symbols, abbreviations and units

Widely accepted symbols, abbreviations and units (SI) should be used. If there is any doubt about a particular symbol or abbreviation, the full expression followed by the abbreviation should be given the first time it appears in the text. Abbreviations used in tables and figures should be explained in the captions. In general, the recommendations of the International Union of Pure and Applied Chemistry (IUPAC) should be followed and attention should be given to the recommendation of the Analytical Chemistry Division in the journal *Pure and Applied Chemistry* (see also *IUPAC Compendium of Analytical Nomenclature, Definitive Rules*, 1987). Appendix 2 gives a conversion table for the non-SI units most frequently used and in Appendix 3 the abbreviations and symbols that may be used without definition are given. Decimal points should be indicated by full stops. All decimal numbers smaller than unity should include a leading zero (e.g. 0.11).

References

References should be numbered in the order in which they are cited in the text, and listed in numerical sequence on a separate sheet at the end of the article. The numbers should appear in the text at the appropriate places in square brackets. In the reference list, periodicals [1], monographs [2], multi-author books [3], and proceedings [4] should be cited in accordance with the following examples:

- 1 D. P. Ndiomu and C. F. Simpson, *Anal. Chim. Acta*, 213 (1988) 237.
- 2 T. Paryjczak, *Gas Chromatography in Adsorption and Catalysis*, Wiley, Chichester, 1986.
- 3 M. Saito, T. Hondo and Y. Yamauchi, in R. M. Smith (Editor), *Supercritical Fluid Chromatography*, Royal Society of Chemistry, London, 1988, Ch. 8, p. 203.
- 4 F. I. Onushka and K. A. Terry, in P. Sandra, G. Redant and F. David (Editors), *Proceedings of the 10th International Symposium on Capillary Chromatography, Riva del Garda, May 1989*, Hüthig, Heidelberg, 1989, p. 415.

Abbreviations for the titles of journals should follow the system used by *Chemical Abstracts*. Articles not yet published should be given as "in press" (journal should be specified), "submitted for publication" (journal should be specified), "in preparation" or "personal communication". The *Journal of Chromatography; Journal of Chromatography, Biomedical Applications* and *Journal of Chromatography, Symposium Volumes* should be cited as *J. Chromatogr.*

Dispatch

Before dispatch of the manuscript please check that the envelope contains four copies of the paper complete with references, legends and figures. One of the sets of figures must be the originals suitable for direct reproduction. Please also ensure that permission to publish has been obtained from your institute.

Proofs

One set of proofs will be sent to the author to be carefully checked for printers' errors. Corrections must be restricted to instances in which the proof is at variance with the manuscript. We shall be obliged to make a charge for all "extra corrections" at a rate in accordance with their cost to us.

To ensure the fastest possible publication, proofs are sent to authors by *air mail* and must be returned to the publisher also *by air mail*. If this is not done, the article will be passed for publication with house correction only. Proofs may also be returned by FAX; the FAX number of *Journal of Chromatography* is: 31 (Netherlands) -20 (Amsterdam) -5862304.

Reprints

Fifty reprints of Full-length papers, Reviews, Short Communications and Discussions will be supplied free of charge. Additional reprints can be ordered. The order form containing price quotations will be sent to the authors together with the proofs of their article.

Subscription orders

Subscription orders should be sent to Elsevier Science Publishers B.V., P.O. Box 211, 1000 AE Amsterdam, Netherlands. The *Journal of Chromatography* and the *Biomedical Applications* section can be subscribed to separately. Indexes can also be ordered separately. Write to the Marketing Manager, Chemistry, at the above address for more details.

Appendix 1: Experimental conditions to be specified

General

Chemicals. Supplier (+ city/town, state, country) and degree of purity of all less common chemicals; EC number of enzymes; optical purity of enantiomers.

Equipment. Model and manufacturer (+ city/town, state, country) of commercial instruments (e.g. chromatographs and detectors). For instruments that are not commercially available, sufficient detail (or a reference) should be given to allow others to construct their own instrument. Detection parameters (e.g. type, wavelength, attenuation, linearity range, limit of detection at a specified signal-to-noise ratio).

Sample preparation. Application papers should contain full details (or a reference) of the method of sample preparation. For centrifugation steps, give details of *g* value and time. Injection device and volume and concentration of the injected sample should be specified.

Column liquid chromatography

Column. Column dimensions (length × internal diameter), manufacturer and location, packing material (for non-commercial columns or columns that are not widely used the chemical composition should be specified), particle diameter, pore diameter, column temperature.

Mobile phase. Complete and unambiguous description of the mobile phase composition or procedure for its preparation; pH; flow-rate; gradient programme.

k' values. When reporting *k'* values, the method for determining the hold-up time (t_0) must be described.

Gas chromatography and supercritical fluid chromatography

Column. In addition to the parameters mentioned for column liquid chromatography, specify type of column (packed, capillary, etc.) support material, film thickness of the stationary phase, and surface modification, if applicable.

Carrier gas. Type, purity, flow-rate or inlet pressure (bar or MPa).

Temperature. All relevant temperatures (or temperature programmes) should be detailed.

Planar chromatography

Chamber. Internal dimensions, manufacturer and location, saturation, temperature, humidity.

Thin layer or paper. Manufacturer and location, material, dimensions, type (laboratory-prepared or commercially precoated) and thickness of layer, additives (fluorescent indicator, binder), position of starting line, development mode, method of activation.

Solvent. Composition of solvent, monophasic or upper or lower phase of two-phase mixture, total volume.

Sample. Application method, size of spot or streak, solvent and amount of solute and volume of solution applied.

Detection. Spray reagent, wavelength, details of colours, R_f values.

Electrophoresis

Matrix. For example, cellulose acetate, agarose, polyacrylamide; gel concentration; percentage cross-linker; dimensions and material of tube, sheet, etc., surface modification, length between column inlet and detector, temperature.

Buffers. Complete and unambiguous description of buffers used, pH and how the pH was set or adjusted.

Other. Injection method, voltage, current. In electropherograms, anode and cathode should be indicated.

Appendix 2: Conversion table for the non-SI units most frequently used

The use of some non-SI units has been accepted for practical reasons; to this category belong units for time (min, h), volume (l), pressure (1 bar = 10^5 Pa), temperature (°C), energy (1 eV \approx $160\,219 \cdot 10^{-21}$ J), mass (1 u \approx $1.66053 \cdot 10^{-27}$ kg) and activity (1 Ci = $3.7 \cdot 10^{10}$ Bq). This journal also accepts Å (= 0.1 nm). Concentration should formally be expressed in mol dm⁻³ or mol l⁻¹, but the symbol *M* is accepted; normality (*N*) should not be used, however. The frequently used “daltons” are not compatible with the SI system—the relative molecular mass (M_r) should be given as a value only (dimensionless). Gravitational force must be expressed in *g*; rpm is not allowed for centrifugation (but it is, e.g., for Vortex mixing). The table below summarizes some conversion factors; to obtain the value in SI units, the value in non-SI units should be multiplied by the factor.

Physical quantity	Type of conversion	Factor
Length	in. → cm	2.54
	ft. → cm	30.4801
Area	in. ² → cm ²	6.451626
Mass	lb. → kg	0.45359237
Volume	gallon (USA) → l	3.785332
	gallon (UK) → l	4.54609
Pressure	atm → Pa	101 325
	mmHg or Torr → Pa	133.322
	mmH ₂ O → Pa	9.80665
	kp cm ² → Pa	98 066.5
	lbs. in. ⁻² or p.s.i. → Pa	6894.76

Other frequently used non-SI “units” are ppm, ppb and ppt. When used in this journal, the American billion (10^9) and trillion (10^{12}) are meant. The use of ppm, ppb and ppt is *only* permitted if they refer to weight/weight or volume/volume ratios; they should **not** be used for weight/volume ratios. The first time such a “unit” appears in an article, it should be indicated whether it refers to weight/weight or to volume/volume.

Appendix 3: Abbreviations and symbols that may be used without definition

Abbreviations and symbols should not be used in article titles. Please note that most abbreviations should only be used in combination with a value, or in structural formulae.

Abbreviations

A, C, G, T	adenine, cytidine, guanine, thymine
Ac, OAc	acetyl, acetate
A/D	analog-to-digital
ADP, AMP, ATP, and similar nucleoside phosphates	adenosine 5'-di-, -mono-, triphosphate, etc.
a.c.	alternating current
amino acids	standard 3- and 1-letter codes
AU	absorbance units
BET	Brunauer–Emmett–Teller
b.p.	boiling point
Bu	butyl
cpm	counts per minute
CE	capillary electrophoresis
d, m, p, r, t (in nucleosides/ nucleotides/ nucleic acids)	deoxy, messenger, phosphate, recombinant/ribosomal, transfer
d.c.	direct current
DDD, DDT, DDE	di-, trichloro-bis(chlorophenyl)ethane, -ethylene
DEAE	diethylaminoethyl
DNA, DNase	deoxyribonucleic acid, deoxyribonuclease
Dns, dansyl	5-dimethylaminonaphthalene-1-sulphonyl
DOPA	3,4-dihydroxyphenylalanine
dpm	disintegrations per minute
EC	enzyme commission numbering system
EDTA	ethylenediaminetetraacetate, -acetic acid
equiv.	equivalent
Et	ethyl
FS	full scale
FT	Fourier transform
GC, GLC, GSC	gas chromatography, gas-liquid chromatography, gas-solid chromatography
HP...	high-performance...
I.D.	internal diameter
IgG	immunoglobulin G
i.p.	intrapertitoneal
IR	infrared
I.S.	internal standard
I.U.	international unit
i.v.	intravenous
LC	liquid chromatography
LD	lethal dose
Me	methyl
m.p.	melting point
MS	mass spectrometry
NAD, NADH (NADP, NADPH)	nicotinamide-adenine dinucleotide (phosphate)
NMR	nuclear magnetic resonance
O.D.	outer diameter
Ph	phenyl
Pr	propyl
PTFE	poly(tetrafluoroethylene)
RNA, RNase	ribonucleic acid, ribonuclease
RP....	reversed-phase....
rpm	revolutions per minute
R.S.D.	relative standard deviation (preferred over coefficient of variation)
S.D.	standard deviation
TLC	thin-layer chromatography
Tris	tris(hydroxymethyl)aminomethane
u	atomic mass units (reference to mass of ¹² C; preferred over a.m.u./amu: reference to mass of ¹⁶ O)

UV	ultraviolet
vol., v/v	volume, volume/volume
Vis	visible
wt., w/w	weight, weight/weight

Symbols

A	absorbance
α	separation factor
d_p	particle diameter
ϵ	molar absorptivity
ΔG^0	standard Gibbs free energy
ΔH^0	enthalpy
H	plate height
J	coupling constant
K	equilibrium constant
k'	capacity factor
λ	wavelength
M_r	(relative) molecular mass
N	number of plates
n	number of determinations
η	viscosity
p, P	probability or pressure
$p...$	negative logarithm of... (as in pH, pI, pK _a)
r	correlation coefficient
R	molar gas constant
R_f	distance travelled by spot / distance travelled by solvent front
R_M	$\log (1/R_f - 1)$
R_s	resolution
ΔS^0	entropy
S/N	signal-to-noise ratio
T	temperature
t	time
t_0	retention time of unretained compound
$t_R (t'_R)$	(corrected) retention time
V_0	retention volume of unretained compound
$V_R (V'_R)$	(corrected) retention volume

PUBLICATION SCHEDULE FOR 1992

Journal of Chromatography and *Journal of Chromatography, Biomedical Applications*

MONTH	O 1991–M 1992	J	J	A	S	O	N	D
Journal of Chromatography	Vols. 585–600	602/1 + 2 603/1 + 2 604/1	604/2 605/1 605/2 606/1	606/2 607/1 607/2	608/1 + 2 609/1 + 2			
Cumulative Indexes, Vols. 551–600		^a						
Bibliography Section	610/1	610/2			611/1			611/2
Biomedical Applications	Vols. 573–577/1	577/2	578/1 578/2	579/1	579/2 580/1 + 2	^b		

^a Cumulative Indexes will be Vol. 601, to appear early 1993.

^b The publication schedule for further issues will be published later.

INFORMATION FOR AUTHORS

(Detailed *Instructions to Authors* were published in Vol. 609, pp. 439–445. A free reprint can be obtained by application to the publisher, Elsevier Science Publishers B.V., P.O. Box 330, 1000 AH Amsterdam, The Netherlands.)

Types of Contributions. The following types of papers are published in the *Journal of Chromatography* and the section on *Biomedical Applications*: Regular research papers (Full-length papers), Review articles, Short Communications and Discussions. Short Communications are usually descriptions of short investigations, or they can report minor technical improvements of previously published procedures; they reflect the same quality of research as Full-length papers, but should preferably not exceed five printed pages. Discussions (one or two pages) should explain, amplify, correct or otherwise comment substantively upon an article recently published in the journal. For Review articles, see inside front cover under Submission of Papers.

Submission. Every paper must be accompanied by a letter from the senior author, stating that he/she is submitting the paper for publication in the *Journal of Chromatography*.

Manuscripts. Manuscripts should be typed in **double spacing** on consecutively numbered pages of uniform size. The manuscript should be preceded by a sheet of manuscript paper carrying the title of the paper and the name and full postal address of the person to whom the proofs are to be sent. As a rule, papers should be divided into sections, headed by a caption (*e.g.*, Abstract, Introduction, Experimental, Results, Discussion, etc.). All illustrations, photographs, tables, etc., should be on separate sheets.

Abstract. All articles should have an abstract of 50–100 words which clearly and briefly indicates what is new, different and significant. No references should be given.

Introduction. Every paper must have a concise introduction mentioning what has been done before on the topic described, and stating clearly what is new in the paper now submitted.

Illustrations. The figures should be submitted in a form suitable for reproduction, drawn in Indian ink on drawing or tracing paper. Each illustration should have a legend, all the *legends* being typed (with double spacing) together on a *separate sheet*. If structures are given in the text, the original drawings should be supplied. Coloured illustrations are reproduced at the author's expense, the cost being determined by the number of pages and by the number of colours needed. The written permission of the author and publisher must be obtained for the use of any figure already published. Its source must be indicated in the legend.

References. References should be numbered in the order in which they are cited in the text, and listed in numerical sequence on a separate sheet at the end of the article. Please check a recent issue for the layout of the reference list. Abbreviations for the titles of journals should follow the system used by *Chemical Abstracts*. Articles not yet published should be given as "in press" (journal should be specified), "submitted for publication" (journal should be specified), "in preparation" or "personal communication".

Dispatch. Before sending the manuscript to the Editor please check that the envelope contains four copies of the paper complete with references, legends and figures. One of the sets of figures must be the originals suitable for direct reproduction. Please also ensure that permission to publish has been obtained from your institute.

Proofs. One set of proofs will be sent to the author to be carefully checked for printer's errors. Corrections must be restricted to instances in which the proof is at variance with the manuscript. "Extra corrections" will be inserted at the author's expense.

Reprints. Fifty reprints will be supplied free of charge. Additional reprints can be ordered by the authors. An order form containing price quotations will be sent to the authors together with the proofs of their article.

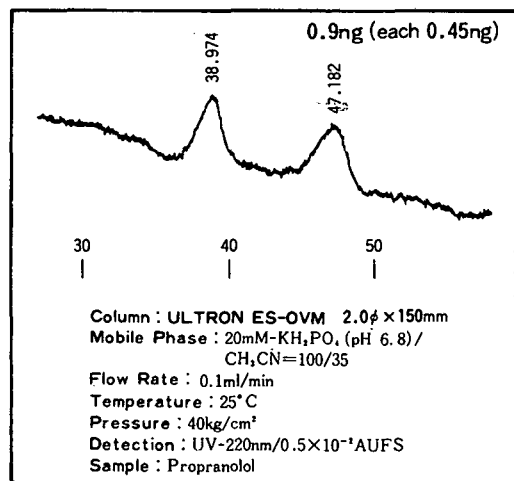
Advertisements. The Editors of the journal accept no responsibility for the contents of the advertisements. Advertisement rates are available on request. Advertising orders and enquiries can be sent to the Advertising Manager, Elsevier Science Publishers B.V., Advertising Department, P.O. Box 211, 1000 AE Amsterdam, Netherlands; courier shipments to: Van de Sande Bakhuizenstraat 4, 1061 AG Amsterdam, Netherlands; Tel. (+31-20) 515 3220/515 3222, Telefax (+31-20) 6833 041, Telex 16479 els vi nl. *UK:* T. G. Scott & Son Ltd., Tim Blake, Portland House, 21 Narborough Road, Cosby, Leics. LE9 5TA, UK; Tel. (+44-533) 753 333, Telefax (+44-533) 750 522. *USA and Canada:* Weston Media Associates, Daniel S. Lipner, P.O. Box 1110, Greens Farms, CT 06436-1110, USA; Tel. (+1-203) 261 2500, Telefax (+1-203) 261 0101.

The most useful chiral separation column, ULTRON ES-OVM, for enantiomeric drugs.

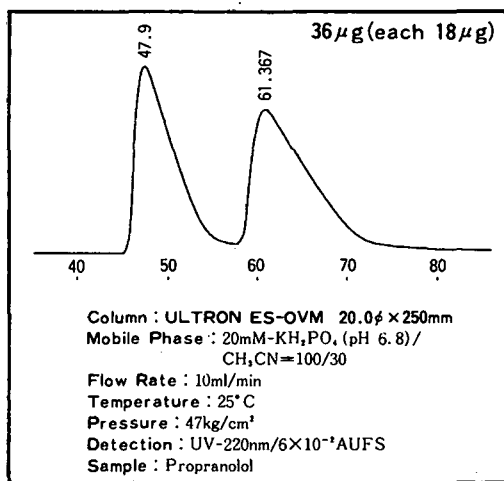
Substance	Rs	Substance	Rs	Substance	Rs
Acetylpheneturide	2.74	Disopyramid	2.04	Nisoldipine	2.36
Alimemazine	6.06	Eperisone	1.15	Nitrendipine	1.80
Alprenolol	1.09 ¹⁾	Ethiazide	1.42	Oxazepan	2.65 ²⁾
Arotinolol	1.95	Fenoprofen	0.80	Oxprenolol	1.38
Bay K 8644	5.92	Flurbiprofen	1.27	Pindolol	2.04
Benproperine	3.27	Glutethimide	1.36	2-Phenylpropionic acid	0.80
Benzoin	8.41	Glycopyrronium	1.73	Pranoprofen	0.63
Biperiden	3.17	Hexobarbital	1.70	Prenylamine	0.86
Bunitrolol	3.08	Homochlorcyclizine	3.04	Profenamine	3.31
Bupivacaine	1.26	Hydroxyzine	2.15	Promethazine	1.42
Chlormezanone	6.48	Ibuprofen	1.72	Propranolol	1.24
Chlorphenesin	2.23	Ketoprofen	1.37	Terfenadine	2.22
Chlorpheniramine	2.36	Lorazepam	2.55 ²⁾	Thioridazine	0.72
Chlorprenaline	2.34	Mecizine	3.71	Tolperisone	1.50
Cloperastin	2.85	Mepenzolate	1.40	Trihexyphenidyl	5.16
Dimethindene	4.33	Mephobarbital	1.70	Trimipramine	3.69
1,2-Diphenylethylamine	1.74	Methylphenidate	1.13 ¹⁾	Verapamil	1.49

NOTE: 4.6×150mm column at room temp. except¹⁾ 6.0×150mm at room temp. and²⁾ 6.0×150mm at 10°C

From trace analysis for metabolites



to preparative scale



SHINWA CHEMICAL INDUSTRIES, LTD

50 Kagekatsu-cho, Fushimi-ku, Kyoto 612, JAPAN

Phone: 80-75-621-2360 Fax : 80-75-602-2660

Please contact in United States of America and Europe to :

Rockland Technologies, Inc. 538 First State Boulevard, Newport, DE 19804, U.S.A.

Phone : 302-633-5880, Fax : 302-633-5893

This product is licenced by Eisai Co., Ltd.